SPECIAL PUBLICATION 2013-SP2

MECHANISMS OF NITROGEN REMOVAL IN SPRING-FED RIVERS

Mechanisms of Nitrogen Removal in Spring-Fed Rivers

Final Report to the St. Johns River Water Management District

March 2011

Matthew J. Cohen[1], James B. Heffernan[2], Andrea Albertin[1], Robert Hensley[1], Megan Fork[2], Chad Foster[1], Larry Korhnak[1]

1 – University of Florida, School of Forest Resources and Conservation

2 – Florida International University, Department of Biology

TABLE OF CONTENTS

Acknowledgements

This project would not have been possible without the assistance of numerous individuals and agencies. We thank our collaborators on two of the research elements (Dr. Brian Katz of USGS on Element #6 and Ray Thomas of UF on Element #8). We also gratefully acknowledge the permission to perform this research granted by the Florida Department of Environmental Protection State Parks and the US Forest Service for access to sites in Ocala National Forest. We particularly want to thank Ms. Kim Davis, owner of Gilchrist Blue Springs, one of our spring study sites, and homeowner on the Santa Fe River at our main station location, who allowed us regular access to both. Detailed comments that enriched the work were provided by Rob Mattson, Dr. Erich Marzolf and Dr. Dave Toth on an earlier draft of this report. Finally, we acknowledge the St. Johns River Water Management District for the funds to carry out this work and the dedication to springs protection that made that funding a priority in challenging economic times.

Executive Summary

Massive N enrichment in the Upper Floridan Aquifer (Aquifer) over the last 50 years is one of the most significant management challenges facing Florida's water resources. Enrichment from a variety of sources including lawn and crop fertilization, septic tanks and sprayfields, animal agriculture (concentrated animal feeding operations), and enhanced atmospheric deposition has led to concentrations in the Aquifer that greatly exceed pre-development conditions. Florida's karst geology contributes to high vulnerability to nitrate enrichment in particular, and evidence that nitrate concentrations have increased nearly ubiquitously across the state is unequivocal; numerous groundwater wells now exceed EPA regulatory standards (10 mg NO_3-N/L) for human health, and concentrations at spring vents are as much as 100 times or more enriched over background levels. This project was designed to understand the fate and consequences of elevated N delivery to springs, quantify the processes that affect N attenuation there, and contrast processes occurring in spring fed rivers with those occurring in blackwater rivers. This report summarizes findings from a 2-year study.

The study was developed to address one core question: **What are the mechanisms and magnitudes of N removal in spring fed rivers?** This is the foundational question of the research, and was addressed using a variety of methods and across springs spanning a gradient of concentrations and size. At the heart of our approach is the high resolution (sub-hourly) measurement of nitrate concentrations using a new breed of UV sensor over extended river deployments from which we obtain estimates of assimilatory N removal (i.e., plant demand). Using mass balance techniques, we estimated dissimilatory removal (denitrification) by difference, allowing temporal separation of total N removal into component processes. Using the same sensors, but deployed to measure nitrate concentrations at much higher resolution (i.e., 0.5 Hz or 1 measurement every 2 seconds), we obtained detailed longitudinal concentration profiles from which additional estimates of N removal were obtained that allowed spatial separation of N removal. Links to metabolism offered confirmatory evidence of this segmentation of assimilatory and dissimilatory demand. To address this primary question, we determined that it was first necessary to understand the hydraulic properties of these rivers, and this posed an additional question on that topic: **What are the hydraulic properties of spring-fed karst rivers?** We posed this question because the biogeochemical processing of N depends fundamentally on how river water interacts and exchanges with the sediments and other benthic habitats, and the hydraulic properties of these rivers were almost wholly unknown. Finally, because not all of the rivers in Florida have the same clear water attributes that make them ideal for the methods utilized in this work, we explored the extension of the

methods to black water rivers: **How does N processing in blackwater rivers compare to spring runs?** We addressed this question by applying the same suite of methods used in spring rivers to waters made colored by the high concentration of tannic and fulvic acids (hereafter dissolved organic carbon or DOC). The rationale for this question is that most of the rivers in Florida are blackwater systems, and accurate prediction of N fate and transport requires process-specific rate estimates for these rivers.

Results obtained in addressing these core questions spawned additional questions during the course of the research that are also addressed here. We identified 3 additional areas of research that were executed under the current contract and that address questions that arose during it.

1) **Aquifer denitrification**. By way of context, we report that the proposed methods for the direct measurement of open channel denitrification were unsuccessful for reasons that we outline in the report in detail. We briefly outline why below. However, during execution of this method, we obtained numerous measurements of dissolved N_2 gas along with ancillary measurements at numerous spring vents. A pattern consistent with aquifer denitrification began to emerge, and given the long-standing assumption that denitrification does not occur in the Floridan Aquifer, we pursued that question to a notable conclusion. The result is a section in this report synthesizing the available evidence for denitrification in the Floridan.
2) **Isotopic indicators of N mass removal mechanisms.** The literature is now increasingly rich with observational studies regarding the use of dual isotopes of nitrate to understand riverine processing. We surmised that no study systems were as conducive to use of these techniques than Florida's springs, because of their stability in discharge, chemistry and temperature. As such, we implemented an initial investigation of changes in isotopic composition in time and space in the Ichetucknee River. Initial results were enormously interesting, and we pursued this line of investigation further; one chapter of this report documents findings from that effort.
3) **Alexander Springs N Dynamics.** The Alexander Springs Creek system is among the most important springs river systems in the state because it among the only ones that has high primary production and background levels of nitrate. The algal mat that has developed in that system is also unparalleled in our sampling efforts. When we deployed sensors in this system, we got results that were completely inverted to the expectations built by very consistent patterns across all other rivers. That is, the nitrate signal rose during the day and fell at night, completely out of phase with the nitrate signals in other spring run streams we studied. After ascertaining that the signal was indeed real, and subsequently discovering that the same pattern

was observed in Silver Glen springs (another low nitrate system), we were forced to consider what might create such a dramatic shift in nitrate dynamics, particularly since estimates of N demand by the algal mat over that upper 500 m of river are very close to the entire N flux discharged at the spring vent. To address this set of questions, we initiated a field campaign to sample water, seston, isotopes and field chemistry in the river, algal mat and vent over 2 days (day and night samples). One chapter of this report is dedicated to that analysis, which revealed several critically important observations about the nature of N limitation in springs.

We have organized the results of this report into 8 reporting elements that capture a broad array of methods and inferences about N dynamics in Florida's rivers. A short summary of the major findings is captured below for each element.

Element 1 – Karst River Hydraulics

To evaluate the hydraulic properties of each of the rivers in this study (ranging in discharge from 0.9 to 16.9 m^3/s), we used a pulse injection of a conservative fluorescent dye tracer (Rhodamine WT), with an injection point as far upstream towards the spring vent as was practical. Dye breakthrough was evaluated at two downstream locations using continuous submersible fluorometers that can detect Rhodamine at concentrations below 0.2 parts per billion. The sensors were placed at the most downstream location, and at a location partway down the river at which geomorphic changes in the channel geometry were evident from measurements obtained from 10 lateral transects. Injections were typically done at night, and fluorometers were placed in the river several hours prior to injection and for 24 hours following the injection. Analysis of the breakthrough curves using standard and modified advection-dispersion-transient storage models as well as moment analyses permitted estimation of residence times, velocity distributions, effective channel and hyporheic storage zone areas, and vegetation effects on river hydraulics (with vegetation measurements obtained from transects and longitudinal underwater photo interpretation). There are 4 main findings from this work:

1) The morphology of the river channels is generally very deep for rivers of this discharge, compared with rivers elsewhere of comparable magnitude. This suggests different mechanisms of channel formation in these rivers than the fluvial processes that dominate in other settings. This is particularly true of the lower reach of Ichetucknee and the Silver River system. One explanation may be that these channels follows fractures and conduits in the underlying

limestone, and are deep because they are partially controlled by surface collapse processes. The channel cross section occupied by vegetation varied from 0 (downstream at Weeki Wachee and upstream at Rock Springs Run) to over 70% (Mill Pond Springs, Gilchrist Blue Spring run). The larger rivers had, on average, vegetation in 25%, 31% and 43% of the channel cross section for Rainbow, Silver and Ichetucknee, respectively. Measured sediment cross sections averaged 2 times larger than the channel cross section (range from 0.27 to 4 times the channel area), but low sediment hydraulic conductivity (mean ± SD = 5.6 ± 3.2 m/d) generally implied limited longitudinal water movement through the hyporheic zone.

2) Despite their karst bed, these rivers typically exhibit relatively little transient storage and very high dye recovery efficiency (96-105%) compared to rivers elsewhere. This suggests that a) the downstream flow gaging appears highly accurate, b) that water losses are minimal despite gage measurements to the contrary at Ichetucknee River, and c) that concerns about the dye adhering to organic sediments is of minimal concern here. Moment analysis revealed median residence times that range from 19 minutes (Mill Pond Springs run) to over 11 hours (Rainbow River). This quantity is dependent on reach length, so the nominal velocity is a more informative metric across sites. This quantity varied from 0.03 m/s (Gilchrist Blue) and 0.07 m/s in upper Alexander Springs Creek to over 0.25 m/s (lower reach of the Ichetucknee) and 0.27 m/s (upper reach of Rock Springs Run). In almost all cases, the upper river reaches (Rock Springs was an exception) had lower velocities (by a factor as much as 4) than the lower rivers, suggesting geomorphic breaks that may be ecologically important. The median velocity was strongly a function of benthic vegetation cover.

3) In most cases, the standard single storage advection-dispersion-transient storage model fit the data poorly; the primary error was in predicting the long low concentration tail present in many of the rivers. Only Weeki Wachee and Mill Pond Springs, and the downstream reaches of Gilchrist Blue Springs Run and Rainbow Rivers were best fit by a single transient storage zone. The parameters of the two fitted zones are suggestive of one large slow exchange zone and one smaller faster exchanging zone. We tested the hypothesis that the two storages were arranged in series (with the fast zone interacting with the river, and the slow zone interacting with the fast zone) instead of in parallel and found strong evidence to support this. We conclude that the first zone is broadly indicative of plant beds and the second of mineral sediments. The dimensions of the first transient storage zone fitted from the breakthrough curve were strongly correlated with the vegetation frontal area (i.e. cross section occupied by SAV), while the second

was most strongly correlated with the sediment cross sectional area, though the slope of that line suggests that only a small fraction of the sediment cross-section is hydraulically active.

4) An opportunistic test of breakthrough dynamics in response to changing vegetation was made possible by contrasting benthic vegetation conditions in Gilchrist Blue Springs run. Under high vegetation conditions, prior to summer when recreational impacts reduce SAV cover, the median residence time was extended by roughly 40%, and a much longer tail was evident. More importantly, the model that best fit the breakthrough curve under the poorly vegetated condition contained a single transient storage zone. This supports the contention that vegetation is an essential component of transient storage. We infer that SAV (submersed aquatic vegetation or benthic aquatic plant beds) in these river systems plays a three-fold role in regulating solute transport. First, they are responsible for direct assimilation. Second, they supply the organic substrate that microbes use in other heterotrophic transformations (e.g., denitrification). Third, they extend the residence time of water in the river which increases the likelihood of solute contact with favorable redox conditions for processes like denitrification. As such, these findings support restoration of diverse and structurally complex aquatic plant beds.

Element 2 – Ecosystem Metabolism and Diel Nitrate Variation

This is the core element of this report. In this section, we report on our measurements of N dynamics in 9 spring run streams spanning short term (8-16 day) deployments; a longer deployment (365 days) in Ichetucknee is also reported. Our objective was to understand the mass loss of N in these rivers, the mechanisms of that loss, and the controls on those mechanisms. Our approach is fundamentally a mass balance, but initiated at very high temporal resolution; using a fully submersible UV nitrate analyzer (SUNA) we measured nitrate concentrations in each river at every 15 minutes. We estimated assimilation based on integration of the diel variation in the observed signal, with nitrate high at night and low during the day, a pattern which was observed at all rivers except Alexander. Denitrification was estimated by difference between total N removal (based on measured upstream input concentrations) and assimilation; we neglect other heterotrophic N removal because generous assumptions of its magnitude suggest that it is very small. This yield estimates, on a day-by-day basis, of N assimilation at the ecosystem scale and denitrification at the ecosystem scale. We coupled to these nitrate estimates measurements of ecosystem metabolism (gross primary production and ecosystem respiration), from which we can also estimate the C:N ratio of integrated ecosystem production, and coupling of C and N

elemental cycles in these river ecosystems. Several methodological assumptions were made to implement this method. First, lateral dilution is assumed to be minimal. The method is relatively robust to small volumes of water with nitrate concentrations similar to the river, but large fluxes of water with markedly different concentration will be interpreted by this method as higher (in the case of dilution) or lower (in the case of enrichment) denitrification. Second, the method assumes that all of the diel variation can be ascribed to assimilation, and that the breakthrough curve of concentration declines in response to assimilation occurs within one 24 hour period. That is, if the effect of yesterday's assimilation is still affecting concentrations today, the method will underestimate assimilation. Hydraulic information from the previous element confirm that the latter assumption is plausible; the former assumption is also supported (because of high % mass recovery of conservative dye), but cannot be validated without additional measurements of longitudinal changes in discharge. There are seven key findings from this portion of the work.

1) **The method is an exciting new tool for understanding riverine N use**, and is comparatively low cost in comparison to other methods that would provide similar information. Further refinements are possible, but the basic outline of a monitoring implementation is now clear, and would permit vastly improved evaluation of ecosystem status and trends. The cost of the sensor package that permits both N and C metabolism is ca. $32,000; at that cost, we contend that integration into springs monitoring should be a priority. Some of the inferences that are possible and their relevance to restoration and management are outlined in the subsequent conclusions.
2) **Spring rivers are major sinks for nitrogen.** We observed mass loss between 2% and 40% of the vent water flux (i.e., what comes in from the springs) over relatively short study reaches. Removal is strongly a function of vent flux, with the highest fluxes least affected, as expected. However, the strong association between vent water flux and removal efficiency permit identification of rivers that are particularly effective at N removal, and ones that perform that service less than expected. Alexander Springs Creek and Silver Glen removes much less N (as a percentage of flux) than would be expected (implying significant internal N recycling), while Rainbow River removes much more. Total mass removal averaged 0.57 g $N/m^2/d$, and ranged from 0.2 (Rock Springs) to over 1.2 (Rainbow). These removal rates speak to a remarkable N removal capacity of these river, the loss of which would dramatically affect downstream ecosystems

3) **Mass removal is dominated by denitrification**. Across springs, the N mass loss due to denitrification was 80% of the total (74 – 92%), with an order of magnitude range from 1130 (Rainbow) to 155 (Rock Springs) mg $N/m^2/d$. The lowest fraction of removal due to assimilation (the balance, ca. 20%, of total removal) was observed on Rock Springs and Juniper Creek, which are net heterotrophic rivers because of significant shading effects over the stream channel. Denitrification is strongly positively associated with GPP ($r^2 = 0.85$), a finding that suggests both that autochthonous production is the fuel for denitrification and that that process is limited, at least broadly, by the availability of carbon.
4) **Ecosystem respiration shows significant temperature sensitivity**. While the finding is expected based on metabolic theory (with remineralization of organic carbon to yield energy modeled as a function of temperature) the magnitude of this effect in spring run streams, where temperature variation (in this case, specifically variation in the nighttime temperature) is very modest, was surprising. Notably, the effect was only observed during winter time deployments, presumably because summer nighttime temperatures are approximately the same as vent water temperatures, making other attributes more important for regulating respiration. The slope of the fitted line between respiration and temperature across all rivers varied between 1 and 3 g $O_2/m^2/d$ per degree C, suggesting that a unit change in temperature can have a fairly large effect on respiration. One sentinel reason to be aware of this association is that a consequence of global warming will likely be an increase in the recharge temperature to the aquifer. Significant shifts in that recharge temperature may be sufficient to tip the springs towards net heterotrophy, with potentially significant ecologically effects.
5) **Elemental coupling.** C:N ratios at the ecosystem scale reveal key attributes of the autotrophic community in springs. The method used in this study offers the first glimpse of elemental coupling for primary production at the integrated ecosystem scale. Indeed, because river ecosystems are comprised of multiple autotrophs (vascular macrophytes, macro- and microalgae), all with different elemental ratios and turnover times, identifying the composite ecosystem C:N ratio was not possible. We measured these based on gross primary production (from diel oxygen dynamics), from which we estimated net primary production on a molar C basis assuming autotrophic respiration is 0.5 GPP. The molar rate of N assimilation is obtained from inference of the mass assimilation rate. The C:N values that we obtained from the rivers ranged from 11.8 (Juniper Creek) to 43 (Rainbow River). These values are broadly consistent with the C:N ratios of primary producers, with algal taxa typically on the lower end of the range

(ca. 10-15) and vascular plants ranging from 20 to 60. Note that we do not know the C:N ratio of the particular organisms in each river (that is part of ongoing work across the state) so no quantitative inference should be drawn about any of the values. Qualitatively, however, we conclude that Juniper Creek is dominated by microflora and other low C:N autotrophs, and that Rainbow is heavily dominated by higher C:N taxa (primarily vascular macrophytes). Indeed, there was broad qualitative correspondence between the C:N values obtained and the relative contribution of benthic algae to the autotroph community. Rainbow had very little algal cover throughout the entire reach we studied (high C:N), Silver, Ichetucknee and Gilchrist Blue springs had modest evidence of algal cover, particularly in the upper river for the two former sites (moderate C:N) and Rock Springs and Juniper Creek were algal dominated or apparently bare and presumably dominated by microflora (low C:N). We draw this inference tentatively, but suggest that if it holds under further scrutiny, the C:N ratio may be a uniquely integrative metric of ecosystem condition that lends insight into the status and trends of the primary producer community in these systems; a deeper appreciation of ecosystem phenology and other natural variation will be required to optimize the use of this metric. Of particular interest in this regard is the finding that the ecosystem C:N ratio is a statistically significant positive correlate of nitrate concentration. This is counter-intuitive because expectations are that if N were limiting primary production, higher availability of N should lend a competitive advantage to taxa that require more N per unit production, thus creating a negative association with concentration. The positive association, and the absence of any association when one point (Juniper Creek) is removed, strongly suggests that variation in nitrate concentration has no effect on the composition of the autotrophic community.

6) **Evidence for light limitation and limited evidence of N limitation**. We evaluated the association between insolation at nearby weather stations (as much as 25 km away) and GPP on a day-by-day basis, and observed a statistically significant positive association in all cases. The fit of the line varied ($r = +0.54$ to $+0.93$, mean = $+0.71$), as did the best fit parameters, suggesting that light exerts variable impacts depending on unquantified ecosystem attributes like shading, aspect and light attenuation by water. N limitation is widely asserted for these ecosystems, and invoked as the explanation for observed changes in composition and cover of autotrophs, particularly benthic filamentous algae. Because of the central importance of the N enrichment narrative in springs restoration activities, we explored this hypothesis somewhat formally. First, we observed no association between GPP and nitrate, which suggests that concentration alone

doesn't offer insight about the ecosystems capacity to fix C. However, there was a significant positive relationship between U_a (assimilation of nitrate) presumably, at least in part, because assimilation could not be inferred from the diel nitrate signal at Alexander Springs Creek or Silver Glen Springs. In considering evidence for N limitation (i.e., as opposed to light limitation) in these ecosystems, we considered metrics of mass flux vs. ecosystem demand to evaluate thresholds of limitation. Because the direct ratio of mass flux-to-demand is strongly dependent on the reach length, we adopted a metric that is independent of length that we call the autotrophic uptake length; this metric describes the reach length required for autotrophs to remove the mass flux present at the upstream boundary, ignoring any internal recycling. Short lengths indicate more likely N limiting conditions. The results were striking. Autotrophic uptake lengths ranged from less than 1500 m for Alexander and Silver Glen (the autotrophic demand was, in these cases, estimated from GPP and stoichiometry) to over 410,000 m in Rainbow River and nearly 700,000 m in the Santa Fe River. The average length, excluding Alexander and Silver Glen, was 364,000 m. In short, the reach lengths necessary to remove N at the present concentrations are dramatically longer than the reach lengths of the rivers, suggesting that the autotrophs cannot exhaust their N supply over the physical lengths of the rivers. We further explored the autotrophic uptake length assuming a historical nitrate concentration (50 µg/L or 0.05 mg N/L) and the same autotrophic demand per area as was observed under contemporary conditions (i.e., assuming these systems have always been as productive as they are today, and that the aggregated C:N ratios of the primary producer communities have not markedly decreased). The effect, as expected, dramatically shortens the uptake lengths; the mean length was 16,500 m, and ranged from 2,600 m in Gilchrist Blue spring run to over 32,000 m in Juniper Creek; Rainbow, Silver, and Ichetucknee had background autotrophic uptake lengths of 10,000, 22,000 and 16,000 m, respectively. While there is no published threshold in this metric to delineate N limited from N sufficient ecosystems, unpublished data from a survey of streams from across North America suggest that somewhere between 2,600 and 5,700 m is the range of autotrophic uptake lengths at which demonstrable N limitation occurs. Using this number, and background levels of nitrate, we can estimate that Rock Springs Run and Gilchrist Blue would be close to N limited at 0.05 mg N/L, and Rainbow River would be borderline (at roughly twice the threshold value). This implies that if the restoration goal is to reestablish N limitation, concentrations would need to be far more dramatically reduced than current proposals suggest. Conversely, it seems reasonable to conclude that N limitation may not have been the natural

condition of these ecosystems, even under background conditions, and reductions in N, though critical to pursue as a broad water quality goal and for variety of associated water quality benefits, may not restore the composition and productivity of these spring ecosystems.

7) **Strong indirect elemental coupling.** We observed consistent coupling between the magnitude of denitrification and gross primary production, both at the seasonal scale and at the inter-day scale. That is, day-to-day changes in GPP reverberate through the N cycle in these rivers such that cloudy days that yield low GPP depress the magnitude of denitrification the following day. The most parsimonious explanation for this is that the fixation of labile organic carbon is the fuel necessary for the denitrifiers, though the strength of the short-term coupling is surprising. The slope of these associations were consistently around 20:1, suggesting that a unit change in GPP (g $O_2/m^2/d$) yields a 20 mg $N/m^2/d$ change in denitrification, or about a 4-10% drop. Given the large magnitude of GPP variation in response to cloud cover and or seasonal changes in photoperiod, this implies a major shift in N removal capacity.

Element 3 – Longitudinal Nitrate Variation

The UV nitrate analyzer used in this work was, in the last section, used at a single point documenting the diel changes in nitrate concentration. Another application that is new and relevant to springs monitoring and understanding is deployment over space in a synoptic survey of concentrations along the length of each river. We explored this approach in some detail in 8 rivers across north Florida; most overlap with previous work, but one was not done because of logistical constraints (Gilchrist Blue) and one additional river was done (Weeki Wachee). Longitudinal transects (down the length of the stream channel, following the thalweg) were done on most rivers at the start and end of the diel deployments (Element 2) with the sensor configured to collect a nitrate measurement every 2 seconds. A logging GPS, measuring x-y location every 5 seconds, was used to determine the spatial location of each measurement, and to reconstruct the longitudinal removal profiles. The results include highly detailed longitudinal profiles of nitrate concentration, and moving average estimates of N removal from that longitudinal profile and channel geometry at each location (derived from previous work presented in Element 1). We draw three primary conclusions from this work.

1) In all rivers except Alexander Springs Creek, the profile of nitrate is declining with distance downstream, consistent with N removal via both denitrification and assimilation. Transects were run in the morning, suggesting that most of the removal is due to denitrification because assimilation peaks in the early to late afternoon. The signal is somewhat noisy, primarily due to

sensor noise, but also potentially due in part to actual local-scale mixing dynamics wherein eddies carrying water up from the benthic sediments is depleted in nitrate compared to water moving downwards. The extent to which the short range signal is real or an artifact of the sensor is, at this time, unknown.

2) A 100-point moving average over reaches that do not exhibit major dilution signals (as was observed on the upper Ichetucknee and Santa Fe) permitted estimates of removal. There was substantial spatial variation in that quantity, potentially indicative of variation in hyporheic exchange or benthic assimilation. Mean reach-length values ranged from 0.10 in Rock Springs Run to 0.85 in Rainbow River. These rates were broadly consistent with estimates of removal from the diel method ($r = +0.91$), but the slope of the line indicates that the diel method yields higher values (slope = 1.48 for total removal, 1.35 for denitrification alone). The most likely explanation for the differences is that the starting point of the longitudinal transects was lower in the river (far below where we estimated that the various spring vents had coalesced), and that the concentration used for the diel method was from higher up the river. Further work (#3 below) would help establish the appropriate boundary condition for the diel method.
3) This longitudinal method is strongly subject to the assumption that no lateral dilution occurs. This assumption is supported by the hydraulic measurements (Element 1) but is not conclusive. Any dilution would be interpreted as removal by this method, and similarly, inputs of water more N rich than the river would create negative removal estimates. We propose a sequence of stable solute injection experiments to determine the longitudinal discharge dynamics of these rivers; absent that critical information about the source of water from the various spring vents (and diffuse discharge), any mass balance approach to removal (or metabolism) will have some degree of uncertainty.

Element 4 – Open Channel and Sediment Assay Denitrification Estimates

Direct measurement of denitrification in flowing water has recently become possible by observing patterns of dissolved N_2 gas in the water column; modeling the gas concentration based on physical conditions (temperature and excess air, obtained for other dissolved gases) and reaeration dynamics has allowed several researchers to estimate per area flux rates. We applied these methods in spring runs, but were forced to reject this method for this setting for two primary reasons. First, the water coming out of the spring vent is significantly disequilibrated with the atmosphere in both N_2 and Ar (an inert gas

tracer of physical processes). As such, a large component of the longitudinal changes in gas concentrations are controlled by poorly constrained physical processes (i.e., reaeration). Moreover, even in the springs where denitrification flux has been estimated to be very large, the unusually deep morphology of these rivers means that the benthic N_2 production rate exerts a relatively small effect on the water column N_2 concentration. Either one of these confounding effects could be overcome, but together they create such an uncertain inference that we chose not to perform the regular quantitative analyses. That said, we report the data from longitudinal profiles that are strongly consistent with significant N_2 production. Note that this signal is of comparable magnitude to what we'd expect based on our mass balance estimates of denitrification, but very noisy.

Because this component of the research was prematurely discontinued, we pursued two lines of similar inquiry. The first focuses on aquifer denitrification; during the measurements of open channel denitrification, we collected numerous spring vent samples as upstream boundary conditions. A persistent pattern indicative of denitrification began to emerge and, in collaboration with Dr. Brian Katz at the US Geological Survey, we compiled the most complete data set for evaluating this question. Our findings are summarized in Research Element #6; in short, there is evidence of large and spatially variable denitrification in the Upper Floridan, and this has highly significant implications for how we develop inference of N sources from isotopic evidence.

The second area was development of a new method for evaluating denitrification potential. These assays work based on measuring N_2 production in the overlying water in a sealed sediment-water incubator. The method has several advantages over existing methods: it is very fast (with results emerging within hours); it relies on the very high precision measurements possible with a membrane inlet mass spectrometer (MIMS); it measures the direct endpoint of denitrification rather than some intermediary (e.g., the acetylene block) or enzymes associated with the process (e.g., denitrogenase enzyme activity). Results from this trial run suggest ambient denitrification rates that are consistent with our observed rates based on ecosystem mass balance, and were highest in Alexander Springs Creek (1.3 µg N/g sediment/hr) and lower in Silver and Ichetucknee (0.3 and 0.2 µg N/g sediment/hr, respectively). Moreover, experimental additions of nitrate (N), dextrose (C), and their combination suggest that denitrification in the Silver and Ichetucknee River sediments are strongly limited by nitrate (a finding consistent with isotopic evidence presented in Research Element #5), and that sediments in Alexander Springs Creek are not limited by either C or N. We believe that this new method holds

significant promise for evaluating river sediments, and are working to extend these measurements to blackwater systems where C availability may be higher but lability considerably lower.

Element 5 – Isotopic Inference of N Removal Mechanisms in Ichetucknee River

Dual stable isotopes of nitrate (^{15}N and ^{18}O, reported in reference to the mass of the lighter isotopes, ^{14}N and ^{16}O, and indexed to globally accepted standards) are increasingly used to understand the sources and processes that regulate aquatic nitrogen dynamics. We implemented a series of isotope measurements in the Ichetucknee River, selected because it has the longest record of diel nitrate variation, and has well bounded spring inputs because of the presence of USGS gages at 6 of the main springs. We implemented both longitudinal and diel measurements of isotope values, and used these to test the hypothesis that isotopes can be used to separate the N removal processes between assimilation and denitrification. There are two ways that was expected to work. First, isotope fractionation (whereby a process selects preferentially for the lighter isotope) was expected to be higher for denitrification than for assimilation, leading to regular diel variation because plant uptake occurs only during the day. Second, the coupling of O and N isotopes was expected to vary between processes, with uptake by plants fractionating both elements equally (i.e., plot of N vs. O isotopes yields a line with slope = 1.0), while denitrification fractionates the N more than that O (yielding a line with slope of 0.5 when N isotopes are reported on the x-axis); the slope resulting from the mixture was expected to be indicative of the relative prevalence of each process. The results were striking, and altogether unexpected.

1) Fractionation of N was larger during the day (when denitrification and assimilation are occurring), and smaller at night, contrary to our expectations. Moreover, the fractionation factor, a measure of the degree of fractionation, was low (between -2 and -6‰ during the day, roughly 1‰ less negative at night) compared to previous published studies, which have reported fractionation due to denitrification at -15 to -30‰.
2) Diel variation in isotope values was marked, with higher isotope values during the day than at night. The implication is that assimilation has very high fractionation, and in fact, based on N mass balance (as in Element 2) during the 24-hour study period, varied dramatically over the course of the day from -25 to -2‰. Variation of this magnitude is highly unlikely, and suggests instead that the river exhibits significant diel variation in denitrification rates, presumably in response to the availability of oxygen inhibiting the degree to which surface sediments are

thermodynamically suitable for denitrifiers; covariant effects on the availability of labile DOC may also play a role in this diel variation. Further supporting this contention is marked counter clockwise hysteresis in the relationship between nitrate concentrations and isotope values, suggestive of highly dynamic N processing rates.

3) Over all time scales, and for both diel and longitudinal data, the coupling of N and O isotopes followed a 1:1 line, in spite of strong mass balance evidence that denitrification dominates N removal in this river. Lab culture data also confirm that under some circumstances, the coupling due to denitrification may be 1:1, not the theoretically derived and broadly supported 1:2 that we expected.
4) Both the low fractionation and the 1:1 isotope coupling may suggest that denitrification in the Ichetucknee is limited by the rate at which nitrate can diffuse downwards into the sediments to reach zones favorable for denitrifiers. Such 1:1 coupling usually indicates assimilatory removal (i.e., algae) but the well constrained mass balance estimates for this system make ascribing all the observed removal to assimilation highly unlikely; moreover, we observed 1:1 coupling in the vent water isotope measurements where autotrophic assimilation is not plausible. Experimental evidence suggests that isotope coupling for denitrification can be very close to 1:1 though the conditions that control that remain unclear. We argue that this system is diffusion limited because of strong evidence from nested wells that suggests that hydraulic gradients are towards the river throughout its length (i.e., it is a gaining river), and because the hydraulic conductivities and riverine hydraulic gradients are generally low. Diffusion limitation is consistent with isotope coupling, because fractionation is due to the diffusion process rather than the denitrification process (which proceeds to completion), and with the marked diel variation in denitrification observed in the river, which varies in response to the availability of oxygen in the surface sediments. The isotope data therefore suggest that denitrification is nitrate limited, in stark contrast to the findings above that suggest C limitation. We reconcile these apparently contradictory observations by suggesting that labile carbon availability ALSO controls the depth of oxygen diffusion in this system, with high GPP creating favorable conditions for denitrification shallower in the sediment profile. As such, days with low GPP will fix less carbon, which will allow oxygen to diffuse further into the sediment, and inhibit denitrification. This conclusion, though clearly speculative, may be salient to this and other rivers where we seek to understand what controls N removal.

5) While the two expectations articulated above were not observed, and indeed we conclude that dual isotopic inference is not a straightforward tool to separate N removal, we also conclude that isotopic inference lends remarkable integrative clarity to riverine N processes. As costs for these kinds of measurements have fallen nearly 5-fold in the last 3 years, they should be included in the list of analytes that are useful for aquatic ecosystem monitoring.

Element 6 – Floridan Aquifer Denitrification Estimates

Our efforts to directly quantity denitrification using open channel estimates of N_2 production were unsuccessful, principally because of the depth and discharge geometry of these rivers. Discharge and channel geometry combine to make the dynamics of N_2 production a small signal, potentially bi-directional (ie.., N_2 may be degassing and being produced over some length below a spring vent) and therefore extremely sensitive to reaeration estimates and instrument noise, both of which we were unable to overcome in this work. However, in order to bound those estimates we required good dissolved gas measurements at the spring vents, which exhibited N_2 enrichment above and beyond what would be expected from recharge temperature and excess air entrainment alone. This suggests aquifer denitrification, a process long thought to not occur in the organic carbon-poor Floridan Aquifer. Since the riverine estimates were confounded, we focused instead on spring vents, and expanded the study to over 111 measurements at 61 spring vents, as well as augmenting these measurements with those previously obtained from around the State; recharge temperature was corrected using Ar concentrations, and excess air entrainment was fixed using Ne concentrations where available, and a simple model relating springshed size and characteristics where it was not. The key findings of that effort are summarized below:

1) We observed excess N_2 suggestive of denitrification, in most of the spring vents, with excess N_2 concentrations ranging from -0.7 to 3.5 mg N_2/L (mean = 0.82 ± 0.83 mg N_s/L). Inference that this is denitrification is further supported by the fact that there was a strong correlation between excess N_2 and DO (negative association), with a sharp break at 2 mg DO/L.
2) Estimates of denitrification rates based on excess N_2 measurements in the springs range from 0 to 97% of the inferred recharge nitrate concentration. Across all springs, 34% of the original nitrate was present in the water in excess N_2 form, suggesting a massive and previously unknown depletion of nitrate in the aquifer. Volumetric removal rates were low compared to

other aquifers (2.75 µmol/m^3/d), consistent with the low substrate availability in the Floridan. Areal rates were also low compared to the global average (3-49 kg N/ha/yr), with a mean rate across springs of 1.22 kg N/ha/yr; 20% of springs, however, had areal estimates above that global average. Denitrification may be fueled by particulate OM in the matrix, may occur exclusively at the Floridan water table (where DOC entry is higher), or may be occurring in response to the availability of other substrates (reduced Fe and reduced S) that have been shown to replace OM as a substrate for some chemoautotrophic denitrifiers.

3) Isotopic evidence (^{15}N and ^{18}O) also support denitrification in the Floridan, with springs isotope values ranging from -0.3 to 23.9‰, and covarying with DO. From the isotope values at the spring vent, and the progression of denitrification (based on the excess N_2 in the water vis-à-vis the inferred recharge nitrate), fractionation factors were determined. Values were low compared to other groundwater studies, consistent with a largely oxic aquifer. More importantly, dual isotope coupling (^{15}N vs. ^{18}O) was consistent with denitrification in other aquifers, exhibiting a strong positive covariance with a fitted slope of 1:1.7.
4) The presence of denitrification in the aquifer, and its effects on the isotopic signal of the nitrate at the spring vent, confound inference of sources based on isotope values alone. Across a broad population of springs, isotopic evidence has been used to conclude that over 20% of springs are sourced principally from organic sources (e.g., septic tanks, animal feed lots) given isotope values in excess of 9‰, and that over 50% of springs had mixed fertilizer and organic nitrate sources (in excess of 6‰). Back-calculating the isotope values for the source nitrate based on denitrification fractionation yields a different story, however, with only 5.5% of sites exceeding 9‰ and 26% exceeding 6‰. In other words, denitrification in the aquifer has induced systematic changes in nitrate isotope values that appear like organic sources. We conclude that nitrate sources to the aquifer are, with few exceptions (Wakulla Springs is one) overwhelmingly dominated by fertilizer sources. One particular example merits additional attention: Wekiwa Springs, which has high isotope values that have been interpreted as a an organic source actual appears to have high rates of aquifer denitrification, and the back-calculated source of nitrate is consistent with a dominant contribution from fertilizers.

Element 7 - Nitrogen Cycling in the Alexander Springs Creek

1) Diel variations in nitrate concentrations in Alexander Springs Creek are inverted as compared to other spring-fed rivers in Florida; peak nitrate concentrations occur during the day, while concentrations are lowest at night. Despite having the lowest nitrate concentration of any first magnitude spring in Florida (mean of 0.07 mg/L), a continuous benthic mat dominated by the filamentous green alga, *Hydrodictyon* sp., covers 24,000 m^2 of the bottom of the spring run.
2) We found the system to be highly productive, with a mean GPP of 15 g $O_2/m^2/d$. The average mass of N coming out of the spring vent was 17 kg/day, average algal mat N demand was 7 kg/day, and total mass removal of N along the river run was also 7 kg/day. The fraction of the algal mat recycled to meet N demand varied on a daily basis (due to variation in GPP),and ranged from 0% to 61%.
3) Higher N_2:Ar concentrations at night than during the day both within the algal mat and overlying water column, as well as enriched $\delta^{15}N$ and $\delta^{18}O\text{-}NO_3$ of water within the algal mat, suggest that denitrification does occur at night (most likely in the algal mat/sediment interface as well as the sediment)and is a primary mechanism for nitrogen removal along the river run. During the day, high dissolved oxygen (DO) concentrations within the algal mat likely impede denitrification by increasing the depth at which it can occur in the mat and sediment.
4) We hypothesized that spikes in nitrate (or lack of expected draw-down) during the day could be explained by nitrification adding nitrate back into the water column and/or by the assimilation of large amounts of internally recycled N (and therefore less uptake than expected during the day). We found little evidence of nitrification within the benthic mat, however, and conclude that a large portion of benthic mat N demand is met through the internal recycling of N.
5) A large amount of seston (dominated by masses of *Hydrodictyon* sp.with other macrophytes and terrestrial organic carbon interspersed) is exported downstream each day and shows a distinctly diel pattern, with export increasing exponentially from 12 pm to 6 pm, which coincides with peak DO concentrations in the algal mat and overlying water column, and then dropping down again by early morning. We calculated that a total dry mass of 368 kg/day, or 1% of the standing benthic mat, is exported daily, although this is likely an overestimate. However, since we assumed that the seston captured in the net was representative of the entire channel cross-sectional area.

Element 8 – Method Application in Blackwater Rivers

The original intent of this study was to apply these methods to springs, and establish their future applicability to blackwater rivers. The primary consideration is that the nitrate sensors that are at the heart of the method are optical sensors, and, as such, are sensitive to optical interferences such as turbidity and dissolved organic carbon. The latter, specifically a problem in Florida's blackwater rivers, actually occludes the variation in transmittance due to variation in nitrate because the optical absorbance in the range of nitrate activity (200-230 nm) is very strong. As such, at some physical threshold algorithmic corrections for DOC are not possible: there is actually no signal to interpret. We sought to establish where this occurs along a gradient of DOC concentrations using a laboratory experiment that examined sequential dilutions of high DOC water (50 mg C/L) from the Santa Fe River crossed with matrix spikes of nitrate to achieve a range of concentrations (0.05, 0.1, 0.2, 0.5 and 1.0 mg N/L). The spectral response and the prediction accuracy and precision were our focal outputs. There are three primary conclusions from this effort:

1) The interference of DOC is strongly evident in spectral transmittance signatures, with samples obtained from highly tannic water locations exhibiting muted transmittance across the entire spectrum. As such, we can infer that the sensor will categorically not produce reasonable results in the most blackwater locations.
2) Based on the sequential dilution experiment, we determined that the error (precision and accuracy) of the SUNA nitrate predictions were compromised (i.e., untenable for the purposed of implementing the diel method) above 12.5 mg C/L. While the predictions at each concentration were still reasonably accurate, the precision fell off dramatically at high DOC suggesting that oversampling (i.e., obtaining many more measurements) might help. These results need to qualified in that we contend that for the purposes of applications that do not require the accuracy necessary for the diel method (i.e., simply evaluating daily trends with storms and seasons), adequate accuracy may be obtained at higher DOC concentrations than 12.5 mg C/L. The error rates for the low DOC water were consistently lowest (ca. 0.004 mg N/), and increased monotonically to 0.06 mg N/L at the highest DOC levels.
3) Methods to chemically attenuate DOC are ongoing, and include resin capture, and oxidant addition (e.g., persulfate) and/or irradiation to break chromophoric groups that occlude light. These are showing preliminary promise, and may ultimately permit the utilization of these sensors in a black water context. Until then, the method is likely confined to clear waters.

Research Element #1 – Karst River Hydraulics

Abstract

Riverine hydraulics are an essential foundation to understanding ecological processes because flowpaths, residence times and longitudinal dispersion affect the rates of solute processing and the concentrations observed downstream as a result of those processes. We implemented a pulsed tracer technique to 8 spring-fed rivers ranging in discharge from 0.9 to 15.5 m^3/s. Along each river, we measured channel geometry, including water and sediment depth as well as the cross sectional area of the channel obstructed by vegetation, at 8 to 10 transects spaced evenly along the entire study reach. While a pulsed technique cannot be used to establish longitudinal variation in discharge (as a plateau injection can), it does yield a distribution of velocities, residence times, and dispersion. We used Rhodamine WT, a fluorescent dye, for this work, and placed high sensitivity fluorometers at two downstream locations. The bottom sensor was placed as far down river as was feasible given sampling logistics and lateral inputs, and the upper sensor was placed at an observed breakpoint in channel morphology. Most of the rivers have shallower and broader upper channels than lower channels, a surprising finding and one that may speak the evolution of channel geometry in a karst setting. Residence times varied substantially with discharge, but all exhibited significant transient storage. We observed strong evidence that an exponential distribution of residence times is inadequate for describing these rivers; adding a further transient storage zone to the standard advection-dispersion-transient storage models greatly improved model fit vis-à-vis the observed dye breakthrough curves. We inferred this from the elongated concentration tails that were poorly fit by the standard model, but much more effectively fit by a two-storage model. The implication is that a small but important fraction of the water is spending much longer than the median residence time in the river. Despite this second longer transient storage, mass recovery in all rivers was high (near 100%) based on USGS gage measurements near the downstream fluorometer. This means that the fraction of water that resides in the system for longer than the deployment is negligible. This is relevant to later portions of this report because it means that almost all of the water does not spend longer than 24 hours in the river reach. This is relevant to the diel mass balance efforts described in Element 2.

We also evaluated riverine hydraulics and observed a strong effect of benthic submerged aquatic vegetation on residence times. A repeated deployment at Gilchrist Blue Spring Run before and after removal of hydrilla (*Hydrilla verticillata*) illustrated the magnitude of that effect. The implications of this additional channel drag and transient storage are significant because measurements of sediment hydraulic conductivity and the geometry of the transient storage zones suggest that river sediments exchange water with the channel relatively little. In short, it is likely that vegetation has the capacity to elongate hydraulic residence times in these systems, and residence time is directly linked to solute processing dynamics. We argue from these lines of evidence that submerged aquatic vegetation plays direct and indirect roles in riverine nitrogen processing. First, the plants directly assimilate N for their metabolic needs, removing it from the water column and storing it in organic form. Second, the plants supply the carbon that fuels dissimilatory N removal (we return to this concept in the next section in detail). Third, they induce transient storage, yielding prolonged contact time between the water and sediment reactive zone, potentially leading to greater N processing. The importance of this last function of SAV is documented in this section.

Introduction

Solute Transport as a Driver of Nutrient Cycling

River networks have long been viewed as conduits, routing nutrients off the terrestrial landscape to downstream receiving bodies such as lakes and estuaries, however recent studies are now recognizing lotic systems as major sinks for nutrients as well. Most research on riverine nutrient dynamics has been performed on smaller headwater streams (Tank et al. 2008). While headwater streams have been shown to be hotspots for nutrient uptake (Peterson et al. 2001), studies have also shown that a significant amount of nutrient uptake within river networks occurs in fifth order or larger reaches, despite the fact that these make up only a small portion of the entire length (Seitzinger et al. 2002). The solute transport properties of the river system are one of the primary mechanisms controlling the nutrient spiraling process (Newbold et al. 1982). Therefore, as a prerequisite to understanding nutrient uptake and retention, we must first understand the physical and biological characteristics of river systems that control their solute transport properties, particularly in larger rivers.

The study of solute transport dynamics began in smaller, first and second order, pool and riffle type mountain streams (Day 1977, Bencala et al. 1983, Bencala et al. 1990, D`Angelo et al. 1993), and only recently have these efforts been expanded to larger river systems (Laenen et al. 2001). Few of these studies (Harvey et al. 2003, Goosef at al. 2007) have looked at the effects of vegetation and channel geomorphology on the solute transport properties.

North Florida features the highest abundance of artesian springs anywhere in the world, with over thirty first magnitude (>2.8 m/s^2 mean annual discharge) springs (Scott et al. 2004). Discharge, water chemistry, temperature and available sunlight remain relatively constant from season to season, making spring-fed rivers excellent model ecosystems, the closest approximation to chemostats as can be found in nature. Additionally, spring-fed rivers have certain properties that minimize or eliminate many of the factors that make solute transport studies so difficult in other types of large river systems. The point source nature and minimal tributaries greatly simplifies the process of quantifying lateral inputs and outputs. Despite the fact that numerous metabolism studies have been performed in spring-fed rivers (Odum 1957a, Odum 1957b, Knight 1983, Heffernan et al. 2010a), to date no studies have attempted to quantify the solute transport properties that are one of the primary drivers of the metabolic processes being studied.

Advection, Dispersion and Storage Equation

To quantify solute transport properties, the one-dimensional advection dispersion and storage (ADS) equation is commonly used (Bencala et al. 1983a, S.S.W. 1990, Runkle 2007). The ADS equation relates the rate of change in solute concentration to the advective, dispersive and storage properties of the stream. The rate of change in solute concentration at a given location within the channel equals the negative velocity (Q/A) multiplied by the longitudinal concentration gradient plus the dispersion coefficient (D) multiplied by the longitudinal rate of change in the longitudinal concentration gradient plus the storage exchange coefficient (α) multiplied by the concentration gradient between the storage zone and the channel.

$$\frac{\partial C}{\partial t} = -\frac{Q}{A}\frac{\partial C}{\partial x} + D\frac{\partial^2 C}{\partial x^2} + \alpha(C_S - C) \qquad \text{(Eq. 1-1)}$$

A second equation relates the rate of change in concentration within the storage zone to the storage exchange coefficient multiplied by the ratio of channel cross sectional area to storage zone cross sectional area multiplied by the concentration gradient between the channel and the storage zone.

$$\frac{\partial C_S}{\partial t} = \alpha \frac{A}{A_S}(C - C_S) \qquad \text{(Eq. 1-2)}$$

A major shortcoming of the traditional ADS equation, apart from the fact that it is a partial differential equation and requires a finite difference approach to solve, is that the very nature of the single storage zone ADS equation implicitly results in any curve having an exponential residence time distribution (RTD). Recent studies have shown that an exponential residence time distribution does a poor job of fitting the tail ends of actual breakthrough curves (particularly when concentrations are viewed in Log-space) and a non-exponentially distributed model, such as a power-law may be more realistic (Haggerty el al. 2002, Gooseff et al. 2003). Despite their small size relative to the bulk of the breakthrough curve, these longtime scale pathways are of particular importance because they represent the pathways that are hydraulically distinct from the channel, and those along which significant biogeochemical processing is likely to occur.

It is highly likely that two or more storage zones with different spatial and temporal characteristics exist within the same river reach (Castro et al. 1991, Choi et al. 2001). Including multiple storage zones within the ADS equation would allow for a non-exponential residence time distribution. The ADS equations can be modified so that the channel concentration equation has an additional storage exchange term.

$$\frac{\partial C}{\partial t} = -\frac{Q}{A}\frac{\partial C}{\partial x} + D\frac{\partial^2 C}{\partial x^2} + \alpha_1(C_{S1} - C) + \alpha_2(C_{S2} - C) \quad \text{(Eq. 1-3)}$$

$$\frac{\partial C_{S1}}{\partial t} = \alpha_1 \frac{A}{A_{S1}}(C - C_{S1}) \quad \text{(Eq. 1-4)}$$

$$\frac{\partial C_{S2}}{\partial t} = \alpha_A \frac{A}{A_{S2}}(C - C_{S2}) \quad \text{(Eq. 1-5)}$$

However, there is also the possibility that rather than interacting directly with the channel, the second storage zone interacts with the first storage zone. A particularly relevant example in the case of spring-fed rivers would be vegetation bed storage overlying hyporheic storage. In this case, the ADS equations would be modified so that the channel concentration equation remains the same as in the single storage zone case, however the first storage zone equation has an interaction with the second storage zone term added.

$$\frac{\partial C}{\partial t} = -\frac{Q}{A}\frac{\partial C}{\partial x} + D\frac{\partial^2 C}{\partial x^2} + \alpha_1(C_{S1} - C) \quad \text{(Eq. 1-6)}$$

$$\frac{\partial C_{S1}}{\partial t} = \alpha_1 \frac{A}{A_{S1}}(C - C_{S1}) + \alpha_2(C_{S2} - C_{S1}) \quad \text{(Eq. 1-7)}$$

$$\frac{\partial C_{S2}}{\partial t} = \alpha_A \frac{A}{A_{S2}}(C_{SA} - C_{S2}) \quad \text{(Eq. 1-8)}$$

The physical representation of each of these storage zone configurations is shown in Figure 1-1 below. Panel A depicts a single storage zone model, Panel B depicts a two storage zone model with both storage zones interacting with the advective channel, and Panel C depicts a two storage zone model with one storage zone interacting with the advective channel and the second storage zone interacting with the first storage zone.

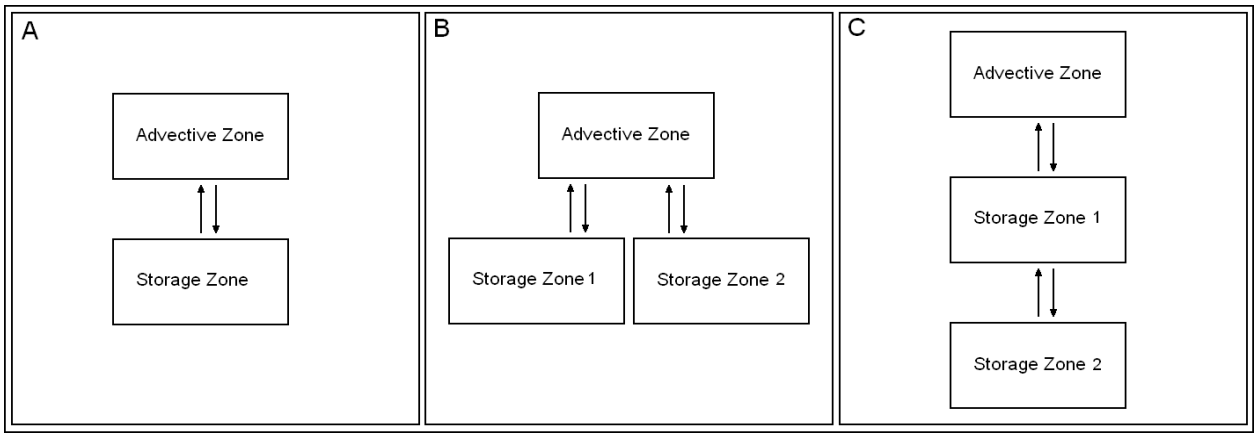

Fig.1-1. Comparison of different storage zone configurations.

Hypotheses

Before even testing the hypotheses regarding vegetative and geomorphic controls on solute transport, we intend to test the suitability of the multiple configurations of the solute transport model discussed above. Because addition of a second storage zone allows for a non-exponential distribution, we expected that the two storage model will result in a better fit of the breakthrough curves. Additionally, because the two storage zones in series better represents the physical structure we observe in these rivers (vegetation beds overlying hyporheic zones), we expected that the two storage zones in series configuration will outperform the two storage zones in parallel configuration.

Going back to the more classical velocity prediction equations (Manning 1890), it is apparent that vegetative and geomorphological characteristics of the channel will affect the solute transport properties. Recent studies using tracer release methods have confirmed this (Harvey et al. 2003, Goosef at al. 2007).

Florida's spring-fed rivers are incredibly productive, and support dense submerged macrophyte beds (Odum 1957a, Canfield et al. 1988, Hoyer et al. 2004). It was expected that vegetation will act as a control on the mean velocity. This relationship is predicted my manning's equation. We also expect that vegetation will act as a control on the magnitude of dispersion. Numerous flume studies have shown that vegetation acts as an obstruction, creating dispersion through turbulence and a non-uniform lateral velocity profile (Nepf et al. 1997, Nepf et al. 1999, Lightbody 2006). This principle should be

observed in natural rivers as well, and therefore the dispersion coefficient obtained from the ADS model was expected to be positively correlated with the amount of vegetation present.

It was expected that channel geometry also acts as a control on the magnitude of dispersion. Shear stress separation due to friction between the water and the benthic surface is a significant cause of dispersion (Taylor 1954, Elder 1959). As the hydraulic radius (normalized for discharge) decreases, a greater fraction of the flow will be in contact with the bed surface, increasing the shear stress and the magnitude of dispersion. As the channel area (normalized for discharge) decreases, a greater fraction of the flow will also be in contact with the bed surface and the same effects of shear stress on dispersion should be observed. Additionally, both Manning's equation and the continuity equation state that channel area is a major factor determining the mean velocity. As the mean velocity increases, the uniformity in the vertical velocity profile will decrease and the magnitude of dispersion will increase. It was therefore expected that the dispersion coefficient obtained from the ADS model will correlate with both the normalized hydraulic radius and the mean velocity.

Finally, we expect that dense vegetation beds and hyporheic sediments will both act as transient storage zones. It was therefore expected that the storage zone cross sectional areas from the ADS model will correlate with the measured vegetation frontal area and the benthic sediment cross sectional area.

Methods

River Characterization

Nine spring-fed rivers in north central Florida were chosen for the study. The study sites were: Alexander Springs Creek, Gilchrist Blue Spring, Ichetucknee River, Juniper Creek, Mill Pond Spring, Rainbow River, Rock Springs Run, Silver River, and Weeki Wachee River (Fig. 1-2). These sites vary by over an order of magnitude in discharge, an order of magnitude in mean width, and display a wide range of vegetative cover, ranging from almost totally vegetated to completely bare.

To quantitatively characterize river geomorphic and vegetative properties, numerous transects were run across each river, perpendicular to the flowpath. The total number of transects per river ranged from three for shorter spring runs up to ten or more for the largest rivers. Water depth, velocity, vegetation height and underlying sediment depth were recorded at 2-3 meter increments along each transect. These data were used to calculate the channel cross sectional area (A_C), channel hydraulic radius (R), discharge (Q), predicted velocity (Q/A_C) vegetation frontal area (A_V), and benthic sediment cross sectional area (A_B) for each transect. At three locations within each transect the vertical hydraulic conductivity (K) of the benthic sediments was determined by performing a falling head slug test using a two-inch diameter PVC well, open on only the bottom and inserted 10 cm into the benthic sediments.

Tracer Release and Breakthrough Analysis

For the tracer release, each river was partitioned into two reaches with the upstream and downstream boundaries of these reaches chosen based on morphological or vegetative differences observed during river characterization. The tracer release occurred at the upstream end of the upstream reach, and tracer monitoring stations were located at the downstream end of each reach.

The tracer release consisted of a single pulse of Rhodamine WT (Keystone Aniline Corporation, Chicago, IL), a conservative dye that fluoresces at 580 nm under light at 550 nm. The total mass of tracer released was determined by targeting a downstream peak concentration of 20 µg/L based on historically measured discharge and expected dispersion over the combined upstream and downstream reach length. Tracer breakthrough was measured at the downstream end of each reach using a Turner Design (Sunnyvale, CA) C3 fluorometer. The fluorometers were calibrated using a two-point curve with 0 µg/L and 10 µg/L standards. The fluorometers were set to sample every minute, and were allowed to

Fig.1-2. Study sites for river hydraulics (this research element) and diel metabolism and N removal (Research Element #2). Note that Weeki Wachee was a study site for river hydraulics, not for diel metabolism, while Silver Glen was a site for diel metabolism but not for river hydraulics. Shown for each river are the locations of the dye injection, locations of the downstream sensor deployments (both fluorometers for this work and nitrate sensors for Element #2 work) and locations of lateral transects where channel geometry, vegetation,n and sediment cross-sectional area were measured.

collect data until it was reasonable to assume all the tracer had been transported through the system. This varied from a few hours in smaller systems to a full day or more in larger rivers.

The first step in analyzing the breakthrough curve was to filter out any interference caused by dissolved organic carbon (DOC). Because DOC may fluoresce at the same wavelength as Rhodamine WT, it can cause the fluorometer to overestimate tracer concentrations. To correct for this potential source of error, baseline readings of DOC and Rhodamine WT were taken using the same fluorometer before the tracer release. A simple linear regression was performed to determine the relationship between the two and the overestimation of Rhodamine WT concentrations were subtracted out from the total during the actual tracer test.

Next, moment analysis was performed on each breakthrough curve. Integrating to calculate the area under the breakthrough curve and multiplying this value by the discharge yields the mass of tracer recovered (Kadlec and Knight 1996). The mass recovered divided by the mass injected upstream yields the fractional mass recovery. Calculating the mass recovery is important for several reasons. It is useful in verifying that the measured discharge value is correct, the fluorometers were properly calibrated, and that any DOC interference was filtered out properly. More importantly, it verifies that the fluorometer was left in place long enough to capture the entire "tail-end" of the breakthrough curve.

Another value determined using moment analysis is the mean residence time. Dividing the first moment of the breakthrough by the total area under the curve yields the centroid of the curve (Kadlec and Knight 1996). This centroid is the mean residence time (τ).

The length (L) of each reach was determined by measuring the distance from the upstream boundary to downstream boundary along the center of the channel using aerial images. The mean velocity (u) of each reach was calculated by dividing the reach length by the mean residence time.

$$u = \frac{L}{\tau} \qquad \text{(Eq. 1-9)}$$

Advection, Dispersion and Storage Model

Because of the difficulty of solving the partial differential equation containing spatial and temporal derivatives, it is usually easiest to solve the advection dispersion and storage equation by estimating the spatial derivatives using a finite difference approach (Runkel 1998). Each reach can be

broken up into a finite number of segments (n). The length of each segment (Δx) is equal to the total reach length divided by the number of segments.

$$\Delta x = \frac{L}{n} \quad \text{(Eq. 1-10)}$$

The concentrations within each segment can then be solved for, and the process iterated over a finite time step (Δt). The discrete form of the ADS equations are shown below:

$$C_{t,x} = \left[C_{t-1,x} + \left(-\frac{Q}{A}\right)\left(\frac{C_{t-1,x+1}-C_{t-1,x-1}}{2\Delta x}\right) + D\left(\frac{(C_{t-1,x+1}-C_{t-1,x})-((C_{t-1,x}-C_{t-1,x-1})}{\Delta x^2}\right) + \alpha\left(C_{St-1,x-1} - C_{t-1,x}\right)\right] * \Delta t \quad \text{(Eq. 1-11)}$$

$$C_{St} = \left[C_{St-1} + \alpha\left(\frac{A}{A_S}\right)(C_{t-1} - C_{St-1})\right] * \Delta t \quad \text{(Eq. 1-12)}$$

The concentration at the current time and segment is therefore a function of the concentration at that segment during the previous time step, the upstream segment concentration during the previous time step, and the upstream segment concentration at the current time step. Using Microsoft Excel (2007), a spreadsheet model was created which solves for the concentration in each segment during each time from concentrations in the appropriate adjacent cells.

Plotting the concentration in a given segment with respect to time creates a modeled breakthrough curve for that location. The modeled breakthrough curves for the segment locations corresponding to the fluorometer locations for each river were plotted side by side with the actual breakthrough curves from the tracer tests. The initial boundary concentrations in the upstream-most segment, and each of the coefficients (Q, A, D, α, and A_S) are variables which determine the position and shape of the modeled breakthrough curves. The initial boundary concentrations were known based on the mass of tracer released and the measured river discharge. While both the discharge and channel cross sectional area were measured, the channel cross sectional area was left as an unknown to see if it would converge on the measured channel area or a smaller value reflecting the displacement effects of the vegetation bed volume. This decreased the unknowns which determine the shape of the modeled breakthrough curve to four coefficients (A, D, α, and A_S). By using the solver function in Excel to minimize the sum of squared errors between the modeled breakthrough curve and the actual breakthrough curve from the tracer test, the optimal coefficients for each reach were determined.

The addition of a second storage zone will increase the number of unknowns in the model by two: a second storage zone cross sectional area (A_{SB}) and a second exchange coefficient (α_B). The addition of these variables is likely to improve the fit of the model to the measured breakthrough curve. Therefore, to determine whether adding additional variables to improve the model fit was justified, the Akaike information criterion was used. The Akaike information criterion uses the residual sum of squares (RSS), the number of parameters (k) and the number of observations (n) to calculate the Akaike information criterion (AIC), which ranks models according to their accuracy while penalizing the number of parameters (Akaike 1974). If the single storage zone model had a lower AIC it was used over the two storage zone model.

$$\mathrm{AIC} = 2\mathrm{k} + \mathrm{n} * \ln(\mathrm{RSS}) \qquad \text{(Eq. 1-13)}$$

Statistical Regressions

To determine which vegetative and morphologic properties control the solute transport properties, regressions were performed and P-values were calculated to see if there was a statistically significant correlation between the optimized model coefficients for each river reach and the measured vegetative and morphologic properties for that particular reach.

To address the hypothesis that vegetation controls the magnitude of dispersion, the dispersion coefficient from the ADS model was regressed against the measured vegetation in both absolute terms (measured vegetation frontal area) and relative terms (percentage of the total channel cross-sectional area obstructed by vegetated).

To address the hypothesis that the channel geometry controls the magnitude of dispersion, the dispersion coefficient from the ADS model was regressed against the mean hydraulic radius normalized to the discharge (R/Q). The reasoning behind this is that with a smaller hydraulic radius, more of the flow will be in contact with the bed surface creating more dispersion. The dispersion coefficient was also regressed against the mean velocity, the reasoning being that channel cross sectional area is a major factor controlling the velocity, and a higher mean velocity will result in greater shear stress and a greater variation in the vertical velocity profile.

To address the hypothesis that transient storage was primarily due to vegetation beds and that sediment storage was negligible, the storage zone cross-sectional area from the ADS model was regressed against the measured vegetation frontal area, the benthic cross-sectional area, and the sum

of the vegetation and benthic cross-sectional area. The relative ratio of the measured vegetation frontal area to the benthic cross sectional area, the measured hydraulic conductivity of the sediments, the hydraulic residence time of the tracer, and the mass recovery of the tracer were also subjectively taken into consideration in the examination of the hypothesis.

Results

There was an order of magnitude difference in discharge values across rivers, with the discharge values ranged from 0.9 m^3/s to 16.8 m^3/s. Within rivers however, there was very little variation in discharge, as expected. There was a great deal of variation in vegetative and geomorphological characteristics, both across rivers and between reaches within a single river. The mean channel cross-sectional area ranged from 4.1 m^2 to 106.2 m^2, the mean channel hydraulic radius ranged from 0.4 m to 2.2 m, the mean width ranged from 8.0 m to 67.5 m.

The vegetative characteristics across rivers varied greatly, ranging from almost completely vegetated to completely bare (96% of the channel area obstructed by vegetated to 0% obstructed). Within rivers, the degree of vegetation remained fairly constant, with Alexander Creek and Rock Springs Run being the major exceptions.

Table 1-1. Summary of mean measured vegetative and geomorphological characteristics.

River Reach	L (m)	Q (m^3/s)	A_C (m^2)	R (m)	W (m)	A_V (m^2)	A_B (m^2)	K (m/d)
Alexander Creek US	1300	3.8	33.7	1.0	34.6	4.1	55.6	4.4
Alexander Creek DS	1800	4.5	46.4	0.8	62.8	22.7	82.8	4.0
Gilchrist Blue Springs US	140	0.9	26.7	1.0	28.0	25.9	27.1	2.7
Gilchrist Blue Springs DS	210	1.1	10.8	0.6	18.8	7.4	27.1	2.7
Ichetucknee River US	1800	6.5	33.2	0.7	62.6	17.3	86.4	4.6
Ichetucknee River DS	2500	6.5	31.3	1.2	24.0	10.7	19.4	5.4
Juniper Creek US	1700	1.3	4.1	0.5	9.0	0.2	16.3	4.2
Juniper Creek DS	1000	1.9	10.2	1.0	9.8	0.00	19.9	8.1
Mill Pond Spring	160	0.9	4.8	0.4	10.8	3.2	8.7	-
Rainbow River US	1500	14.7	106.2	1.5	65.7	32.6	28.4	6.1
Rainbow River DS	4250	16.8	65.9	1.4	47.8	12.4	20.7	4.6
Rock Springs Run US	700	1.3	5.2	0.6	8.0	0.00	11.8	15.4
Rock Springs Run DS	2300	1.3	23.6	0.6	35.3	13.2	47.4	4.0
Silver River US	1550	14.5	101.9	2.2	47.1	34.0	114.3	4.2
Silver River DS	5300	15.5	71.3	2.2	30.9	20.7	63.2	3.5
Weeki Wachee River US	1300	3.1	15.0	0.6	21.5	1.5	48.1	5.6
Weeki Wachee River DS	2000	3.1	8.8	0.8	12.0	0.00	26.6	9.6

The benthic sediment cross-sectional area ranged from 8.7 m^2 to 114.3 m^2. Benthic cross-sectional area ranged from 27% up to 398% as large as the channel cross-sectional area. The vegetative frontal area was smaller than this underlying benthic cross sectional-area in all cases except the upstream reach of Rainbow River (where it was only slightly larger). A summary of the measured vegetative and geomorphic characteristics is shown below in Table 1-1. A sample of cross-sectional profiles from the Ichetucknee River is shown below in Fig. 1-3. For this figure, transects 5 and 6 are located in the downstream reach, while transects 8 and 9 are located in the upstream reach. Note how the differences in hydraulic radius and channel width evident in the figure are reflected in the mean values presented in the table.

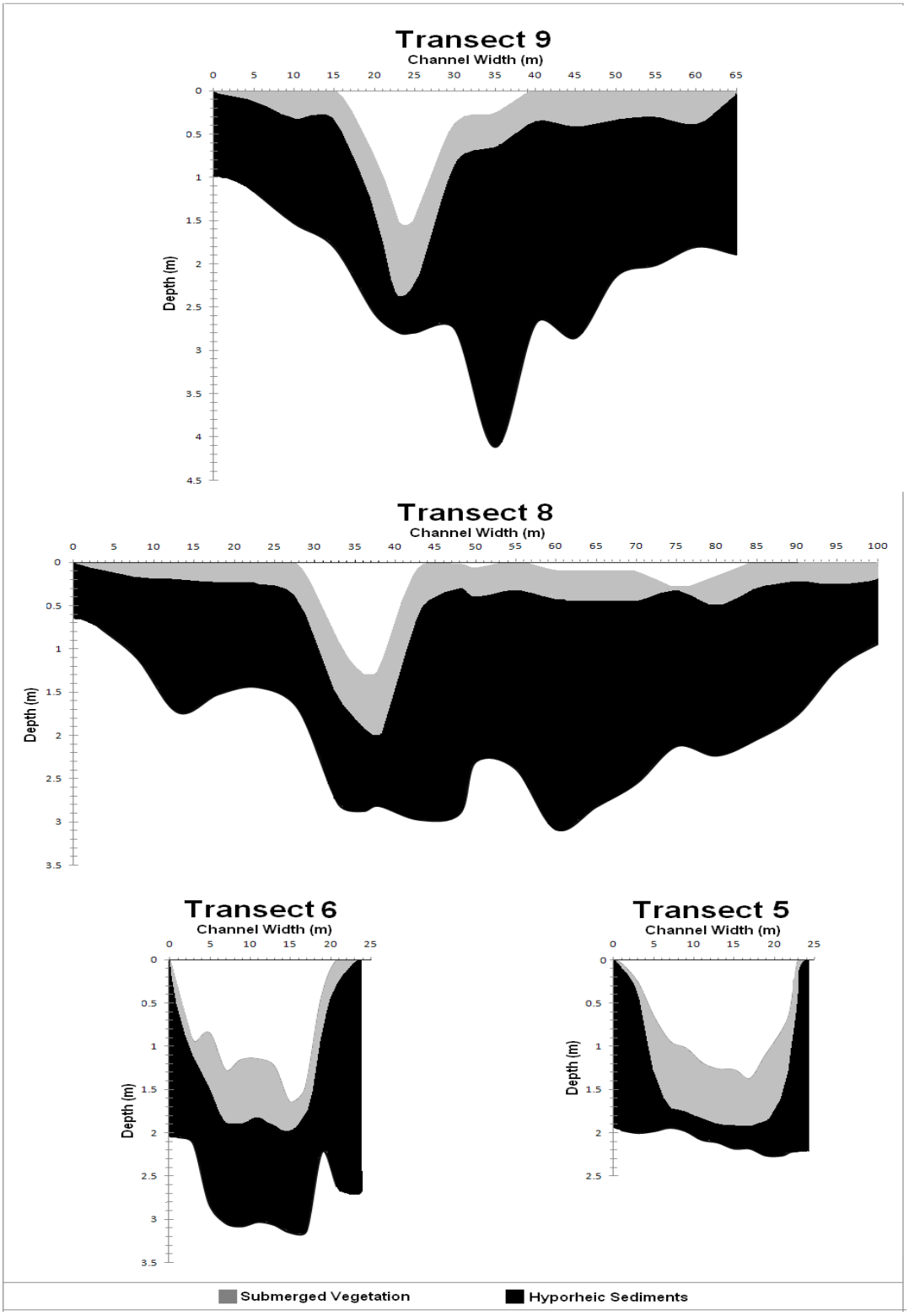

Fig. 1-3. Sample cross-sectional profiles of the Ichetucknee River.

A summary of the data derived from moment analysis of the breakthrough curves is shown below in Table 1-2. The mean residence time ranged from 19 minutes to 685 minutes. The mean residence time alone is somewhat meaningless however, because each reach is a different length. Dividing the reach length by the mean residence time gives the mean velocity, which ranged by nearly an order of magnitude, from 0.03 m/s to 0.28 m/s. The mean velocity correlated strongly with the expected mean velocity calculated by dividing the discharge by the channel area. Mass recovery was uniformly high, suggesting that there is little evidence of major mass loss between the injection and downstream locations. However, this does not preclude significant lateral inputs since the upstream discharge values are generally quite uncertain; this has major implications in subsequent sections.

Table 1-2. Summary of breakthrough curve moment derived data. DS and US refer to downstream and upstream fluorometer stations, respectively.

River Reach	Recovery (%)	τ (min)	u (m/s)
Alexander Creek US	99.89%	294	0.07
Alexander Creek DS	100.15%	314	0.10
Gilchrist Blue Springs US	104.54%	86	0.03
Gilchrist Blue Springs DS	99.10%	59	0.06
Ichetucknee River US	100.24%	193	0.16
Ichetucknee River DS	99.68%	168	0.25
Juniper Creek US	99.58%	172	0.16
Juniper Creek DS	99.46%	135	0.12
Mill Pond Spring	99.21%	19	0.14
Rainbow River US	98.93%	387	0.06
Rainbow River DS	97.45%	298	0.24
Rock Springs Run US	100.46%	43	0.27
Rock Springs Run DS	79.48%	418	0.09
Silver River US	99.65%	157	0.16
Silver River DS	96.08%	456	0.19
Weeki Wachee River US	99.26%	125	0.17
Weeki Wachee River DS	101.32%	118	0.28

The Akaike Information Criterion values for each of the Advection dispersion and Storage models is shown below in Table 1-3. The values indicate that for the downstream reach of Gilchrist Blue Spring, Mill Pond Spring, the downstream reach of the Rainbow River and the downstream reach of the Weeki Wachee River, a single storage zone model was justified. For all other cases, the two storage zones in series model was justified. It should be noted that in all the cases where a single storage zone was justified based on the AIC, addition of a second storage zone in either configuration did not improve the squared error of the fit. For comparison between the two storage zones in parallel or two storage zones in series (because the number of parameters remains the same) only the absolute squared error matters, and the AIC values simply reflect this.

Table 1-3. Summary of AIC values.

River Reach	Single Storage	Two Stor. (Parallel)	Two Stor. (Series)
Alexander Creek US	5782	4051	**3932**
Alexander Creek DS	2102	2106	**1545**
Gilchrist Blue Springs US	3611	3615	**2837**
Gilchrist Blue Springs DS	**898**	1721	902
Ichetucknee River US	5082	4620	**4400**
Ichetucknee River DS	4221	2723	**2568**
Juniper Creek US	7836	7236	**6098**
Juniper Creek DS	5068	2972	**2551**
Mill Pond Spring	**1124**	1128	1128
Rainbow River US	4314	4318	**4066**
Rainbow River DS	**4318**	4624	4322
Rock Springs Run US	5735	5375	**5375**
Rock Springs Run DS	3493	1737	**1734**
Silver River US	8919	7648	**7646**
Silver River DS	5584	2729	**2116**
Weeki Wachee River US	4236	4240	**3134**
Weeki Wachee River DS	**1464**	2660	1468

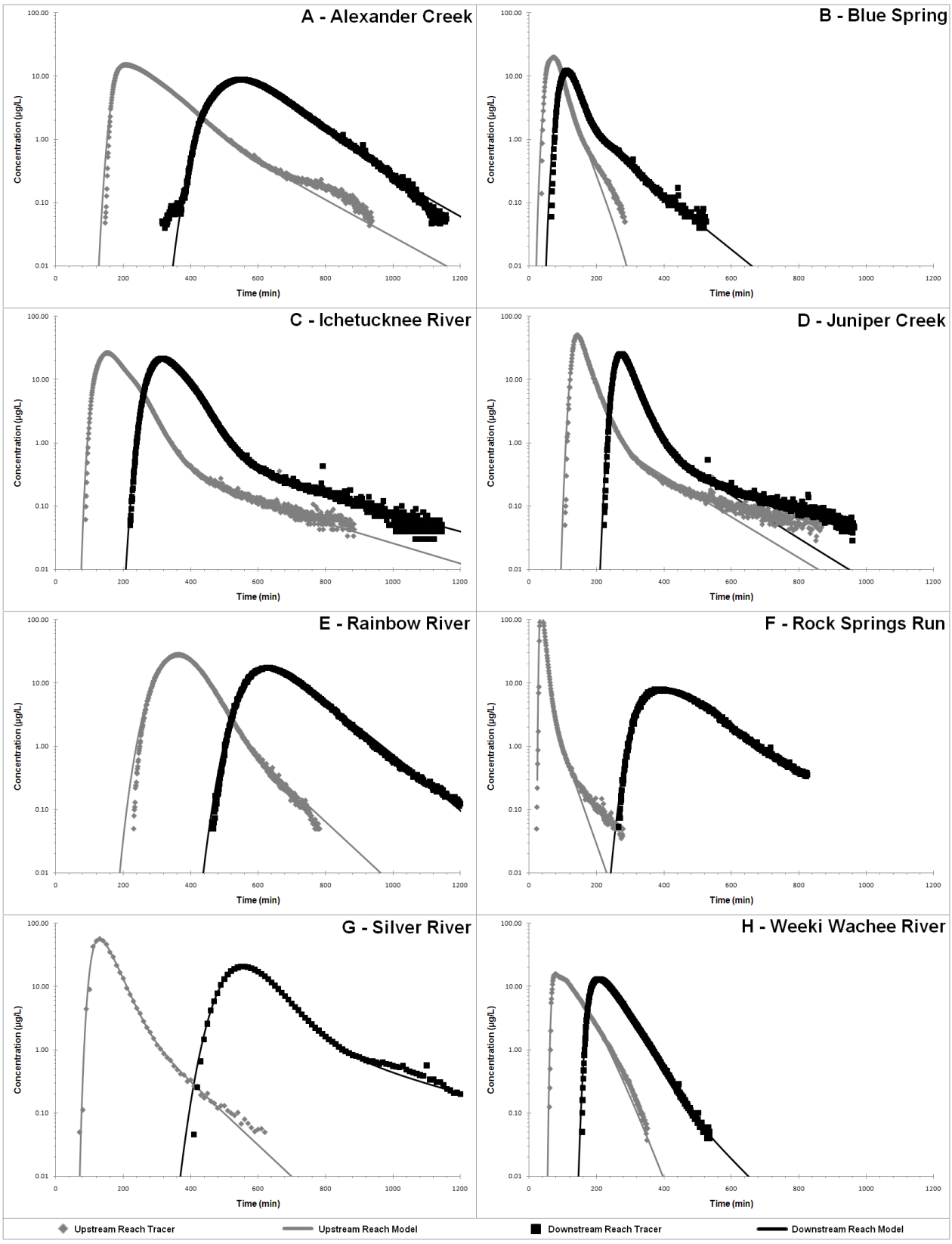

Fig. 1-4. Fitted breakthrough curves viewed in Log-space. Note the variable presence of long tails.

The breakthrough curves, and the fitted Advection, Dispersion and Storage model curves are shown in Figure 1-4. The curves are shown in Log-space. Note the long tails of the breakthrough curves, which occur at low enough concentrations so as not to be immediately apparent when viewing the curves in normal-space. The tails are of particular interest because they are indicative of water taking much longer flowpaths than the bulk of the water being advected down the main stream channel.

These flowpaths play a crucial role in nutrient cycling. In many cases, using a single storage zone model with an exponential residence time distribution significantly under-represented these tails. Addition of the second storage zone with a smaller exchange coefficient (i.e., a longer turnover time) significantly improved the curve fit. A summary of the Advection, Dispersion and Storage model coefficient for each river reach is shown in Table 1-4. The model channel cross-sectional area correlated very strongly with the measured channel cross-sectional area ($P<0.001$). It should be noted that this was not a linear fit, and that the model cross-sectional area was approximately 86% of the measured cross-sectional area, which indicates that transport is only occurring only in a subset of the total channel.

Table 1-4. Summary of ADS model coefficients.

River Reach	A ($m^{2)}$	D (m^2/s)	A_{S1} ($m^{2)}$	α_1 (s^{-1})	A_{S2} ($m^{2)}$	α_2 (s^{-1})
Alexander Creek US	31.0	0.62	14.5	0.00032	8.3	0.00017
Alexander Creek DS	41.7	2.81	1.7	0.00009	1.3	0.00010
Gilchrist Blue Springs US	16.1	0.04	14.2	0.00218	3.6	0.00010
Gilchrist Blue Springs DS	11.6	0.70	7.7	0.00012	-	-
Ichetucknee River US	25.4	7.79	5.4	0.00012	3.4	0.00002
Ichetucknee River DS	21.7	5.30	1.9	0.00010	1.8	0.00004
Juniper Creek US	5.4	1.04	1.7	0.00087	0.9	0.00029
Juniper Creek DS	10.5	0.39	1.7	0.00044	1.8	0.00004
Mill Pond Spring	5.8	0.99	0.8	0.00015	-	-
Rainbow River US	124.0	3.36	9.1	0.00006	5.9	0.00007
Rainbow River DS	53.0	0.00	13.1	0.00007	-	-
Rock Springs Run US	2.8	2.21	1.3	0.00419	0.6	0.00108
Rock Springs Run DS	10.6	1.28	5.2	0.00020	8.9	0.00002
Silver River US	57.7	1.81	23.9	0.00066	11.5	0.00016
Silver River DS	57.0	2.16	17.1	0.00029	10.1	0.00004
Weeki Wachee River US	8.9	3.55	5.3	0.00057	2.0	0.00020
Weeki Wachee River DS	8.3	4.22	0.7	0.00014	-	-

The model dispersion coefficient was negatively correlated with the hydraulic radius normalized for discharge (P=0.033). The model dispersion coefficient did not however correlate with the vegetation cross sectional area (P=0.681) or with the fraction of the channel vegetated (P=0.750) as expected. It should be noted that there was some correlation (albeit very weakly) between the dispersion coefficient and the mean velocity (P=0.131) and at the same time, the mean velocity was negatively correlated with the fraction of the channel vegetated (P=0.024). This concept will be revisited in detail in the discussion section, but this may suggest that while the obstructive properties of vegetation may induce dispersion, vegetation also decreases the velocity (as predicted by Manning's equation) which results in less shear stress separation, and ultimately less total dispersion.

The cross-sectional area of the primary model storage zone correlated with both the measured vegetation frontal area (P=0.005) and the measured benthic sediment cross-sectional area (P=0.026). The cross-sectional area of the secondary model storage zone also correlated with both the measured vegetation frontal area (P=0.015) and the measured benthic sediment cross-sectional area (P=0.006). The strongest correlation however, was between the sum of model storage cross-sectional areas and the sum of the vegetation frontal area and underlying benthic sediment cross-sectional area (P=0.002).

At Gilchrist Blue Spring, an opportunity arose to conduct a second tracer test. The initial tracer test, reported in the results above, was conducted under almost completely vegetated conditions. This secondary test was conducted under very low vegetation conditions (primarily as a result of recreation activities, the vegetation within Gilchrist Blue Springs changes dramatically throughout the seasons). A comparison of the resulting breakthrough curves from the downstream reach is shown below in Figure 1-5. Note how the mean residence time for the high vegetation breakthrough curve is much longer than for the low vegetation conditions (145 minutes versus 105 minutes). Also note how the tail of the high vegetation breakthrough curve is much more pronounced than for the low vegetation conditions. This is indicative of a higher degree of transient storage.

In the case of very low vegetation conditions the best fit model was a single storage some model. This is in contrast to the high vegetation conditions when a two storage zone model was the best fit. A comparison of the model coefficients for the best fit model under high and low vegetation conditions at Gilchrist Blue Spring is shown below in Table 1-5.

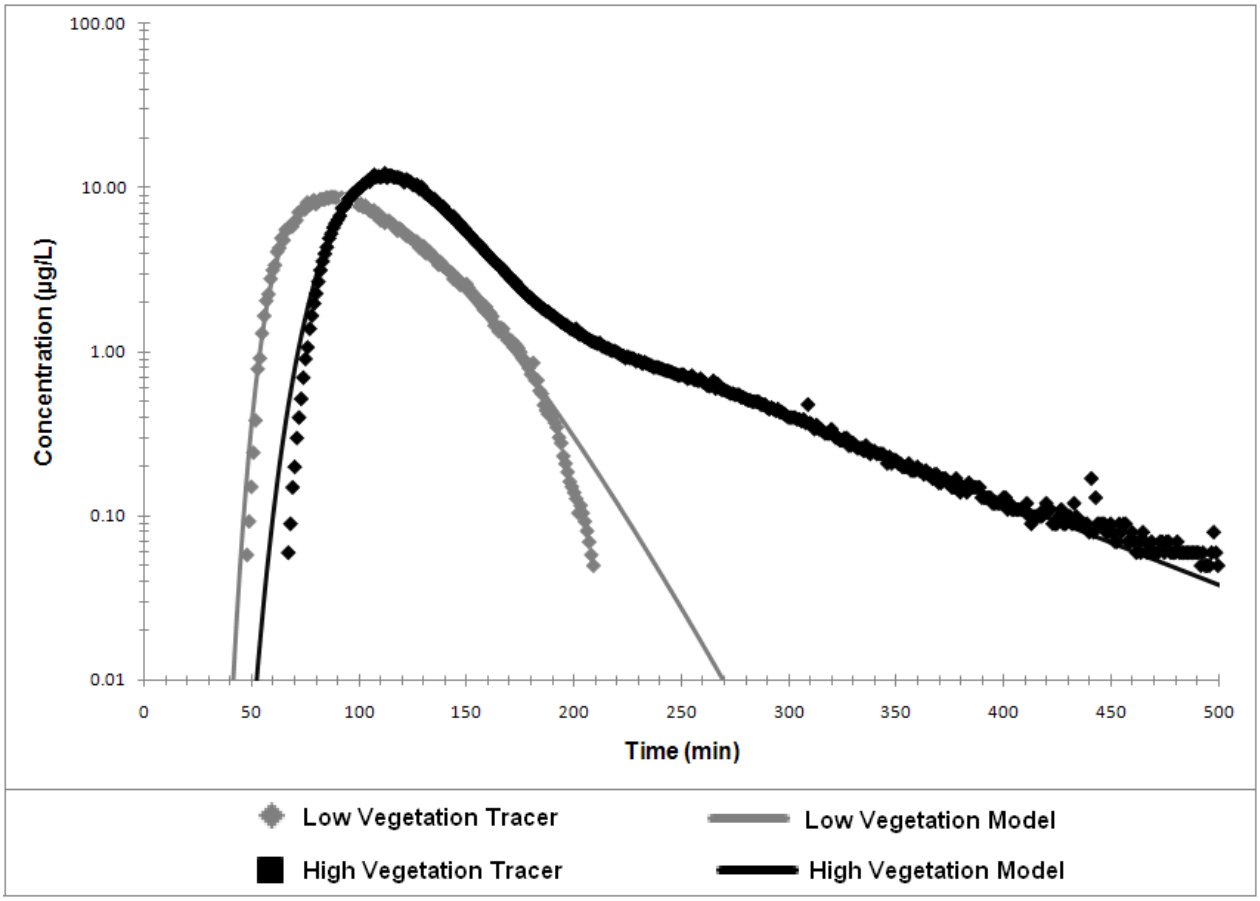

Fig. 1-5. Comparison of breakthrough curves for Gilchrist Blue Springs under varying vegetative conditions. Note the long tail for the highly vegetated condition that is absent under lower vegetation conditions.

Table 1-5. Comparison of ADS coefficients for Blue Spring under varying vegetative conditions.

River Reach	A ($m^{2)}$)	D (m^2/s)	A_{S1} ($m^{2)}$)	α_1 (s^{-1})	A_{S2} ($m^{2)}$)	α_2 (s^{-1})
Gilchrist Blue Spring High	20.26	0.40	4.31	0.00006	3.59	0.00001
Gilchrist Blue Spring Low Veg.	16.02	0.33	9.70	0.00091	-	-

Discussion

When viewing the curves in Log-space, it was immediately apparent that while the best fit curve from the single storage zone model very accurately fit the bulk of the data points, it systematically underrepresented the long tails of the data set. While the bulk of the data set represents the majority of the flow, from a biogeochemical cycling perspective we are not particularly interested in this water, as it is simply being advected down the thalweg of the channel with a small amount of dispersive action. We are particularly interested in the tails however, which while representing only a small portion of the total flux, represent water taking much longer flowpaths. These flowpaths are likely to include areas where significant biogeochemical processing is likely to occur, such as dense vegetation beds and hyporheic zones. Additionally, because this water spends much more time in the system (several times longer than the mean residence time) it is subject to biogeochemical processing for a longer period of time. Therefore, because these long tails are so important to understanding biogeochemical processing, properly fitting them should be a major consideration, even though they make up a small fraction of the total flow.

By its very nature, a solute transport model based on the classical advection, dispersion and storage equation with only a single storage zone will always result in an exponential distribution of residence times (Gooseff et al. 2003). Previous studies have found actual stream residence times to be more of a power-law rather than exponential distributions (Haggerty et al. 2002, Gooseff et al. 2003). Addition of a second storage zone allows for alternative distributions and was therefore expected to improve the model fit.

In all but four cases (downstream reach of Gilchrist Blue Spring, Mill Pond, downstream reach of Rainbow River, and downstream reach of Weeki Wachee River), the addition of a second storage zone to the solute transport model improved the fit of the model curve. When viewing these exceptions in log space, it is apparent that their tails appear linear, without major inflection, explaining why they can be fit by a single storage zone model (though not what particular attributes of the rivers themselves cause this distribution). In all cases where addition of a secondary storage zone improved the fit of the model, the AIC value justified this addition.

In all the cases where addition of a secondary storage zone was justified, the two storage zones in series always resulted in a better fit (and better AIC since the number of variables was the same) over the two storage zones in parallel. This reflects the likely nature of the real storage zones of the river, hyporheic

sediments underlying vegetation beds. Water in the hyporheic sediments does not interact directly with the channel, but must pass in and out of the vegetation beds.

In the case of Gilchrist Blue Spring, where tracer tests were conducted under contrasting vegetative conditions, it was found that under low vegetative conditions a single storage model sufficed, while under high vegetative conditions addition of a second storage zone improved the fit the curve. This implies that vegetation is indeed acting as a transient storage zone with hydraulic properties distinct from the hyporheic storage zone.

In addition to testing model configuration and providing the first systematic survey of geometric, vegetative and hydraulic properties of spring fed rivers, this study also tested hypotheses about the role these features play in regulating riverine hydraulics. The results indicate that both channel geomorphology and vegetation greatly influence the magnitude of advection, dispersion and storage in these rivers, the combination of which determines the overall residence time. Vegetation in particular appears to be an especially important control on the mean residence time.

Manning's Equation predicts that vegetation would decrease the mean velocity (Manning 1890, Manning 1895), and this study appears to confirm this by finding that the percentage of the channel cross sectional area obstructed by vegetation strongly correlated with the mean velocity ($P=0.024$). This effect was also observed directly by the decrease in mean velocity and increase in mean residence time in Gilchrist Blue Spring under varying vegetative conditions. In addition to simply adding shear stress, this study showed that vegetation also influences residence time by acting as transient storage zones. This inference is drawn partly from the finding that vegetation cross sectional area was strongly correlated with the model predicted storage cross sectional area ($P=0.005$). However, several other observations also indirectly support this conclusion.

The mass recovery alone also has implications for the type of storage which is occurring. Near total mass recovery occurred in every tracer test (range was from 95 – 105%). Many previous studies using Rhodamine WT have failed to get complete mass recovery, and this is partially due to the fact that Rhodamine WT is not perfectly conservative, having a tendency to sorb to sediments (Smart et al. 1977, Bencala el al. 1983b, Sabatini et al. 1991). Another reason for failure to achieve total mass recovery has been attributed to long time scale storage (such as within hyporheic sediments) and release over extended periods at concentrations below the detection limit of the fluorometer. The fact that this study achieved near total mass recovery, coupled with the observation that hydraulic conductivities of

the benthic sediments were relatively low (<10 m/day), may indicate that hyporheic sediment storage in these rivers may be only limited to the first few centimeters. This implies that the majority of transient storage in these rivers is occurring in vegetation beds.

From a management perspective, the determination that vegetation density greatly affects residence times have several important implications in regards to the maintenance or restoration of submerged aquatic vegetation in spring-fed rivers. In the last fifty years, many springs have seen nitrate concentrations increase by an order of magnitude over historic concentrations due to anthropogenic activities (Katz et al. 2001, Stevenson et al. 2007). Insofar as residence time is one of the major factors determining the magnitude of nutrient removal within a reach, it would appear that a high vegetation density should be a management target. Vegetation may have direct effects on nitrogen cycling (through assimilation), first-order indirect effects (by providing the carbon which drives denitrification) and second-order indirect effects by extending the residence time so that more assimilation and denitrification may occur. Unfortunately, over this same time period, many of these systems have seen a precipitous drop in the abundance of submerged aquatic vegetation (Frazer et al. 2006).

In conclusion, as anthropogenic activities continue to increase nutrient loads of both surface and groundwater, the role of river systems as sinks for these nutrients has become ever more apparent. If we are to understand and predict the ecological implications of this increased loading both in the rivers themselves and their downstream receiving bodies, we must be able to accurately predict the transport properties and ultimate fates of nutrients in these systems. A prerequisite to developing an effective model of nutrient transport and metabolism is to first determine the morphological and vegetative mechanisms which control the solute transport properties of these systems. Determining these relationships in spring-fed river is critical, not only because these particular systems are in immediate peril due to increased nutrient loading, but also because they make excellent model analogs for rivers in general. Understanding the mechanisms which control the hydraulic properties in these systems is an important early step in the ongoing process of determining these mechanisms in a more general sense for large rivers everywhere.

Research Element #2 – Ecosystem Metabolism and Diel Nitrate Variation

Abstract

We applied the diel nitrate variation method to short term (8 – 16 days) deployments in 8 rivers to assess N assimilation and denitrification. A longer deployment in Ichetucknee (365 days) was also used to evaluate seasonal patterns in those quantities. Each deployment consisted of one or two stations at which we installed a UV nitrate sensor capable of very high temporal resolution measurements (1 per minute was our standard), and a multi-parameter sonde capable of commensurate resolution measurements of dissolved oxygen, pH, specific conductance and temperature. Marked diel variation in all parameters was observed at nearly all sites, with nitrate variation resulting in high concentrations at night, and low concentrations during the day; the exception was Alexander Springs Creek, where nitrate variation was inverse to the typical pattern (i.e., it was high during the day and low at night), suggesting markedly different patterns of N cycling in that river. Inference of N assimilation was made by computing the mass flux implied by daytime depression of nitrate concentrations compared with nighttime concentrations. Denitrification was estimated by difference between the total N removal (vent water inputs vs. downstream mass flux) and assimilation, computed on a 15-minute time step. We assumed for this work that vent water nitrate concentrations are constant over the deployment, and that denitrification is constant over each 24 period. Diel variation in oxygen in response to photosynthesis was inverse (high during the day, low at night), and allowed us to estimate ecosystem metabolism (gross primary production – GPP, and respiration – R), subject to air-water reaeration rates inferred from patterns of evening dissolved oxygen changes. GPP was generally high (> 8 g $O_2/m^2/d$) in these springs, though Rock Springs Run and Juniper Creek were lower, and generally carbon neutral (i.e., P ~ R). N assimilation rates varied widely, but were generally between 30 and 120 mg $N/m^2/d$. In all springs, this was a small fraction of total N removal between the spring vent and the measurement locations, with denitrification making up between 75 and 90% of the observed removal. The fraction of assimilation and denitrification was basically constant across seasons in the Ichetucknee River. We observed strong positive associations between net primary production and N assimilation from which we estimated the C:N ratio of ecosystem assimilation. Values ranged from a low of 11:1 in Juniper Creek to a high of 44:1 in Rainbow River, and were broadly consistent with the relative prevalence of SAV vs. algae in the river at the time of deployment, with high SAV sites generally exhibiting higher C:N ratios. We also observed strong positive associations between light intensity and GPP, consistent with the notion that these systems are light limited. However, the fitted slopes of the lines differed markedly between rivers, suggesting significant site level control over that relationship. During all of the winter deployments, we observed a strong positive association between nighttime water temperature and

ecosystem respiration; this relationship disappeared in the summer when spring water temperatures are highly uniform at night. The implications of this on expectations of ecosystem response to changes in recharge temperature (e.g., with changing climate controls) are significant because the slope of the relationship is consistently higher than might be expected by the temperature sensitivity of heterotrophic organic carbon remineralization alone. Finally, in almost every case, we observed evidence of strong short term positive coupling between primary production and denitrification. This C to N coupling effect is likely via indirect pathways; the most parsimonious explanation is that days with high GPP yield highly labile organic carbon that fuels denitrification the next day. Across springs, the slope of that association suggests that a unit change in GPP yields a 3-10% change in denitrification. Inverted patterns of nitrate variation in Alexander Springs Creek, a low nitrate spring with vent water inputs of 0.06 mg/L and extremely high GPP (ca. 15 g $O_2/m^2/d$) were interpreted as suggestive of autotrophic N limitation. Further analysis of this inference is provided in Research Element 7. Based on the patterns of diel nitrate variation observed in all other rivers (which suggests that the ecosystem autotrophs are acquiring N only during the day), the relatively small fraction of total N removal that arises due to assimilation, and the strong links between light and GPP, we conclude that these ecosystems are not currently N limited, that many would not have been N limited under historic nitrate concentrations, and that enormous declines in nitrate concentrations would be necessary to induce limitation.

Introduction

Ecosystems require nutrients in proportion to their metabolic needs. A direct connection exists between the rates of autotrophic production and nutrient assimilation/transformation, and this connection is at the heart of any understanding of nutrient limitation and how changes in ecosystem structure and function occur when that limitation is alleviated via anthropogenic addition of excess nutrients. Specifically, when a nutrient is scarce compared to ecological metabolic requirements, it may constrain primary production, over time selecting for a suite of autotrophs that are conservative with respect to that elemental requirement. Changes in nutrient availability that alter the limitation status of an ecosystem can have dramatic effects on the composition of the autotrophs in the system, and consequently alter the entire food web.

In addition to direct coupling between ecosystem metabolism and nutrient processing, there is a link between heterotrophic processes and nutrient cycling. Remineralization of organic carbon itself requires nutrients, sometimes at supply rates different than what is required for autotrophic production. In the particular case of the nitrogen cycle, on which the work herein focuses, there is the additional pathway of nutrient removal when nitrate is used as a terminal electron acceptor during organic carbon remineralization, a process known as denitrification.

River ecosystems process nitrogen to a substantial degree (Alexander et al. 2000, Ensign and Doyle 2006, Wollheim et al. 2006). Mass loading to watersheds is reduced somewhere near 75% during coalescence and delivery to the sea (Boyer et al. 2004). This can occur in response to assimilatory removal (i.e., plant uptake of N) or dissimilatory removal (i.e., denitrification). While there is a growing quantitative basis for understanding the rates of N processing in lotic systems, this understanding is largely based on work conducted in small streams (headwater and 2^{nd} order streams, typically less than 200 L/s). Large rivers, like those formed when 1^{st} and 2^{nd} magnitude springs emerge from the Floridan Aquifer, are less well understood, because the standard measurements for process-specific understanding in rivers are logistically constrained to small discharge (e.g., due to the costs of isotope dosing experiments). Moreover, few lotic systems are as productive as spring-fed rivers, which implies that assimilatory removal rates are expected to be high.

The documented increase in nitrate concentrations in the Upper Floridan Aquifer is a source of considerable management concern (FSTF 2000, Mattson et al. 2006), principally because of the perceived link between nitrate enrichment and algal proliferation (Stevenson et al. 2007), but also for

associated risks to fish and invertebrates at very high concentrations (Guillette and Edwards 2005, Mattson et al. 2006). Background levels of ca. 0.05 mg/L (50 µg/L) have been exceeded 100 times or more in many springs, and the consequences of this N enrichment are thought to be significant. While historically we have viewed freshwater ecosystems as generally limited by phosphorus, there is evidence to suggest that N limitation, co-limitation, sequential limitation and other complex nutrient stimulatory effects are present in inland waters (Elser et al. 2007). Estuarine and nearshore coastal waters are generally thought to be N limited (though numerous exceptions exist), making the attenuation of N through rivers a priority for water quality management of these ecosystems. Early studies of springs metabolism (Odum 1957) observed strong evidence of light limitation, suggesting that primary production is not controlled by the availability of either N or P. More recent work suggests that N enrichment may not lead inexorably to the accumulation of algal biomass (Stevenson 2004, Heffernan et al. 2010a), but the consequences of N enrichment on these lotic ecosystems may be manifest along other ecological pathways such as saturation of denitrification potential, potential inhibitory effects on primary production (WSI 2008), and possible ecotoxicological effects on spring fauna (Guillette and Edwards 2005, Mattson et al. 2006). Moreover, because of the enrichment of N in many springs, any mechanisms of N removal in spring runs becomes enormously valuable to downstream ecosystems, in terms of preventing N eutrophication effects downstream. Our overarching goal with this work is to determine how spring run streams use nitrogen (principally as nitrate-N), and thus explore the following 4 objectives:

1) Quantify direct and indirect links between ecosystem metabolism and N removal.
2) Evaluate evidence for ecosystem nutrient limitation in observed patterns of assimilation.
3) Evaluate the controls on the magnitude of assimilatory and dissimilatory removal.
4) Quantify the C:N ratio of ecosystem primary production within spring ecosystems as a means for determining the dominant primary producers.

Methods

The core methods for this work are applied uniformly across a number of study streams to ascertain rates of primary production, N assimilation, and denitrification. First, we describe the study sites and sensor deployment locations. The methods to determine in-stream metabolism are well developed in the scientific literature, and are offered in brief. We do pay particular attention to the assessment of

the reaeration rate for oxygen diffusion since we use a less common method to determine this, and because inference of ecosystem metabolism is so strongly sensitive to this parameter. A new method, developed in spring ecosystems, for determining nitrogen assimilation and, via mass balance between inputs and outputs, also dissimilatory removal, is described in greater detail. Finally, methods exploring the coupling between C and N are outlined.

Study Sites

We deployed *in situ* sensor arrays to draw inference about both C and N dynamics in 8 stream systems (Fig. 2-1), many of them more than once (Table 2-1). With the exception of the Santa Fe River, all of them are spring-fed ecosystems measured during periods of clear water (i.e., not during flooding events, which introduce highly colored floodwaters to many of these systems). For each of the rivers (again with the exception of the Santa Fe) we previously obtained detailed hydraulic information (Element #1 – Riverine Hydraulic Properties) from which we could describe the nominal residence time of water in the study reaches, the benthic area contributing to observed single-station diel variation in solute chemistry, and median water velocity. In previous work, we showed that there are distinct geomorphic reaches within these rivers, with a general trend towards broader and shallower upper reach channels, and deeper, narrower lower reach channels (citation). For the initial deployments (on Alexander, Rainbow, Silver and Ichetucknee), a sensor package (see below) was deployed at the downstream location that integrates the entire river from the spring vent; in later deployments (all rivers), sensor packages were placed at two locations, demarcated based on geomorphic of vegetative discontinuities. Our analysis here is confined to direct metabolism and N removal measurements at both upstream and downstream stations; the specific metabolic and N removal rates in the reach between the upstream and downstream sondes is, for simplicity, inferred by difference between two single station estimates rather than using the two-station approach.

All of the rivers with the exception of Gilchrist Blue Spring run have existing USGS flow gages that were active at the time of the deployment; at Gilchrist Blue, we manually measured discharge during the deployment using the USGS flow-velocity method (Buchanan and Somers 1969). The hydrology of these spring fed rivers can be relatively complex, with reaches of substantial water gain and some reaches where existing flow data suggest water loss (e.g., the lower Ichetucknee). All subsequent methods (metabolism and N removal dynamics) depend on accurate water fluxes, and we made the assumption that measured flows are accurate. This is particularly important for estimating denitrification because that flux is enumerated by difference between input mass flux (water flux * input concentration) and

output mass flux (ignoring the diel variation due to assimilation). Since water inputs from unknown/unmeasured spring vents were not quantified, even in the Ichetucknee River system where 6 of the head springs are gaged, and the various head spring inputs may vary in nitrate concentrations, we used the measured upstream nitrate concentration at night as the input boundary condition, recognizing that our estimates of denitrification are strongly sensitive to this assumption.

Weather data (air temperature, solar insolation, rainfall) were obtained from nearby Florida Automated Weather Station (fawn.ifas.ufl.edu) records, in each case, within 25 km of spring vent.

Sensor Deployment

Each deployment consisted of two sensors. The first measured basic water chemistry (water temperature, specific conductance, pH, dissolved oxygen). In each case, we used a fully deployable YSI6920, which has on-board power and data storage capability. This sonde uses optical DO measurements that have been shown to be more stable for extended deployments, and less subject to bio-fouling. A copper-guard was used on each sonde to preclude algal colonization, and a wiper on the optical DO sensor ensures limited bio-fouling over the 2-3 week deployment periods used here. We routinely obtained measurements every hour, but for smaller river systems increased the sampling intensity to every 15 minutes.

The second sensor is a Submersible UV Nitrate Analyzer (SUNA) made by the Satlantic Corporation (Halifax, Nova Scotia) (Fig. 2-2). This sensor uses UV light attenuation to determine nitrate concentrations, a method similar to the laboratory standard method based on second derivative UV spectroscopy. In low-color waters, these sensors are exceedingly accurate, and permit high-resolution temporal sampling rates (up to 0.5 Hz). Prior to field deployment of these sensors, we applied a battery of laboratory tests to determine the accuracy and precision, and an outline of the results of this effort are presented in this chapter (see below) as evidence in support of the utilization of these sensors. Their principle of operation (nitrate absorbs UV light at ca. 220 nm) makes them extremely resistant to calibration drift, but quite sensitive to bio-fouling. We used a copper guard over the sensor gap, and wrapped the sensor in 100 µm Nitex mesh to prevent animal colonization (e.g., caddisflies and midges). Because the SUNA requires off-board power and data storage, deployment required data and power cables attached to the sensor at all times. An Acumen data logger was used to write data files to flash memory cards from the machine output, and deep-cycle marine batteries were sufficient to supply continuous power for the 2-3 week deployments. Sensors were run in “polled” mode where they are

Table 2-1 – Summary of sites, deployment dates (all in 2010) and duration, hydrologic and water quality measurements during the deployment, sensor locations, and measured channel attributes for each deployment presented here. See Figure 1-2 for sensor and transect locations.

					Upstream Station				Downstream Station			
Site	Start Date	Duration	Flow (m^3/s)	Input NO_3 (mg/L)	Latitude (NAD 1983)	Longitude (NAD 1983)	Length (m)	Mean Width (m)	Latitude	Longitude	Length (m)	Mean Width (m)
Silver	1/15/10	16 days	14.2	1.36	n.a.	n.a.	n.a.	n.a.	29°12'36.61"	-81°59'30.27"	6850	35
Silver	10/6/10	9 days	15.5	1.38	29°12'17.49"	-82° 01'45.10"	1550	47	29°12'36.61"	-81°59'30.27"	5300	31
Rainbow	2/19/10	14 days	16.1	1.68	n.a.	n.a.	n.a.	n.a.	29° 3'23.38"	-82°26'44.64"	5750	52
Rainbow	10/18/10	10 days	17.2	1.68	29°05'14.86"	-82°25'39.59"	1900	65	29° 3'23.38"	-82°26'44.64"	4050	48
Alexander	4/3/10	6 days	2.8	0.07	29°05'03.27"	-81°34'39.32"	550	54	n.a.	n.a.	n.a.	n.a.
Alexander	8/27/10	12 days	2.8	0.07	29°05'03.27"	-81°34'39.32"	550	54	n.a.	n.a.	n.a.	n.a.
Alexander	9/18/10	13 days	2.8	0.07	29°05'03.27"	-81°34'39.32"	550	54	n.a.	n.a.	n.a.	n.a.
Rock	12/2/10	14 days	1.3	1.36	28°45'34.70"	-81°29'43.31"	700	8	28°46'27.72"	-81°30'6.70"	2300	35
Juniper	11/11/10	11 days	1.3	0.08	29°10'58.31"	-81°41'50.47"	1700	9	n.a.	n.a.	n.a.	n.a.
Gilchrist	4/16/10	20 days	0.91	1.88	29°49'56.14"	-82°40'54.90"	340	13	n.a.	n.a.	n.a.	n.a.
Ichetucknee	1/8/10	362 days	8.3	0.59	29°57'53.14"	-82°45'42.86"	1800	63	29°57'10.82"	-82°47'8.82"	2500	24
Santa Fe	11/13/10	10 days	18.7	1.1	29°50'58.26"	-82°42'56.09"	11250	38	n.a.	n.a.	n.a.	n.a.
Silver Glen	4/6/11	15 days	2.6	0.05	29°14'54.67"	-81°38'05.60"	920	60	n.a.	n.a.	n.a.	n.a.

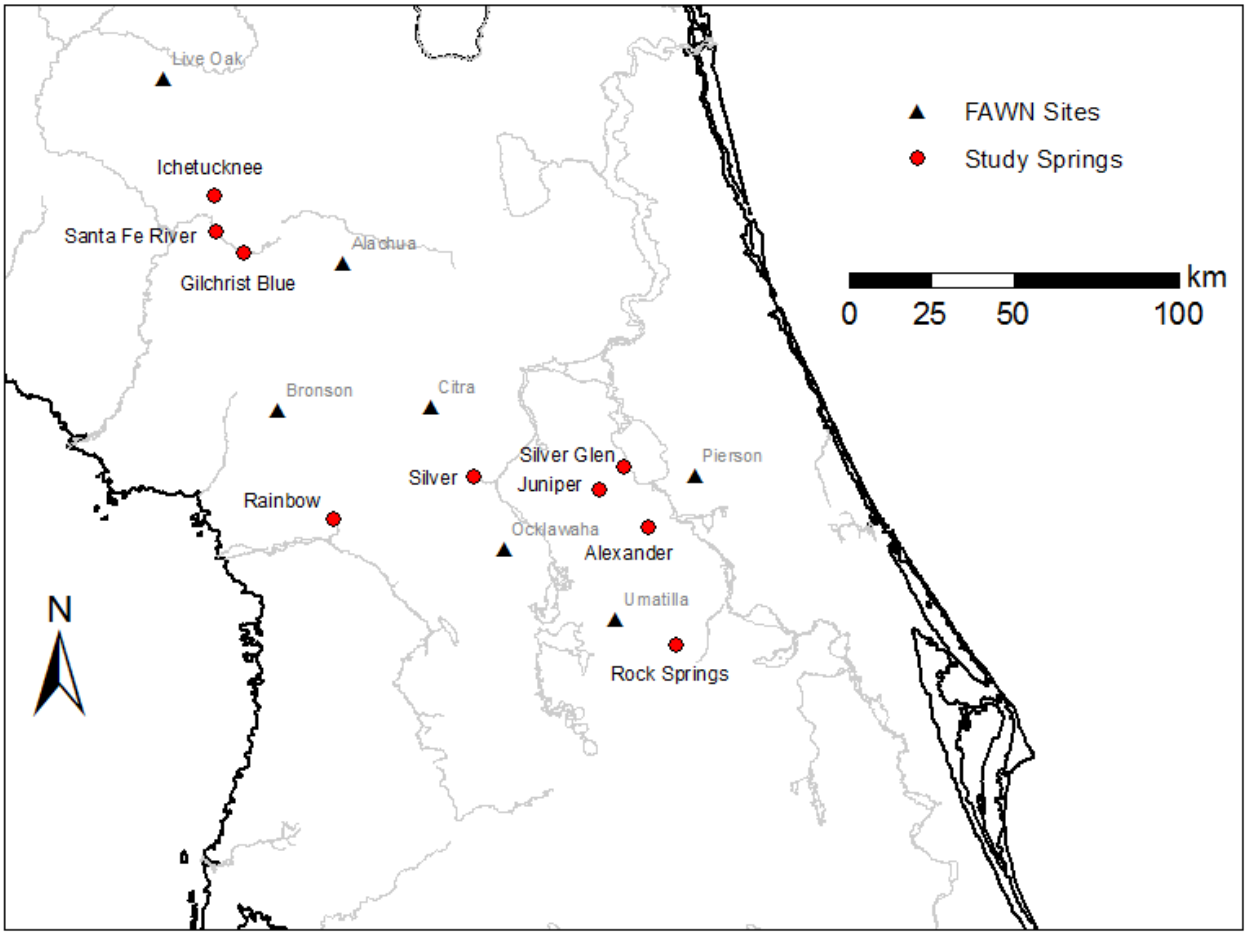

Fig. 2-1 – Location of the primary study sites for river metabolism and N removal dynamics. Also shown are the locations of nearby continuous weather stations (Florida Automated Weather Network) from which air temperature, rainfall and solar insolation date were obtained.

powered on for 20 seconds every 15 minutes, during which they collect 10 nitrate concentrations. We analyzed the average of these 10 measurements in each case. We selected a higher resolution sampling rate (i.e., 15 minutes instead of 1 hour) to minimize the impacts of sensor noise; sampling rates in the polled mode could be increased to ca. 5 minutes without impacting sensor temperature. Both sensors were deployed in the advective zone of the river channel by lashing them to fixed base materials; in most cases a submerged log was identified to which the sensors could be discreetly attached. Sensors were carefully located to ensure that they sampled the flowing water, and to preclude the confounding effects of bubbles on the SUNA; the latter was prevented by placing the sensors with the sensor gap facing just off downward, and with the sensor oriented with flow. Only one instance of vandalism occurred during deployments for this project (August in Rainbow Springs), during which the cable that held the SUNA was cut and the sensor was dropped into the mud.

Fig. 2-2 – Photograph of the Satlantic Submersible UV Nitrate Analyzer (SUNA). Data communications occur via the port to the upper left; the sensor requires off-board power and data storage, and is therefore tethered during the entirety of each deployment. The UV-lamp irradiates across the 1-cm gap 1/3rd down the sensor, passing through the ambient fluid; no flow cell was used during our deployments. A copper guard was inserted in the sensor gap to preclude biofilm development. In addition, the sensor was wrapped in Nitex mesh to prevent benthic invertebrate colonization. Power and data cables were reinforced using garden hoses to prevent impacts from turtles and other herbivores. (Photo Credit: www.satlantic.com/photos/513000_Plastic%20SUNA.jpg)

Sensor Testing

The SUNA presents a new and exciting tool for water quality testing, but it requires a rigorous examination to ensure that it is sensitive to the natural variations present in the field. To test this capacity, we developed a laboratory experiment in which the SUNA was deployed in continuous mode (sampling once every 2 seconds in water with systematically varying nitrate concentration created by pumping nitrate standard or deionized water into the vessel where the SUNA was deployed. We tested the SUNA under several configurations of simulated diel variation, ranging in both the amplitude of simulated diel variation, and the baseline concentration (i.e., the mean). Results from three experiments are shown here to demonstrate the sensor noise (Fig. 2-3). Note that the manufacturer reports a sensor accuracy of ca. 0.028 mg/L, but we observed much greater accuracy. The three experiments are 1) baseline 0.5 mg/L, amplitude of variation 0.05 mg/L, 2) baseline 0.125 mg/L,

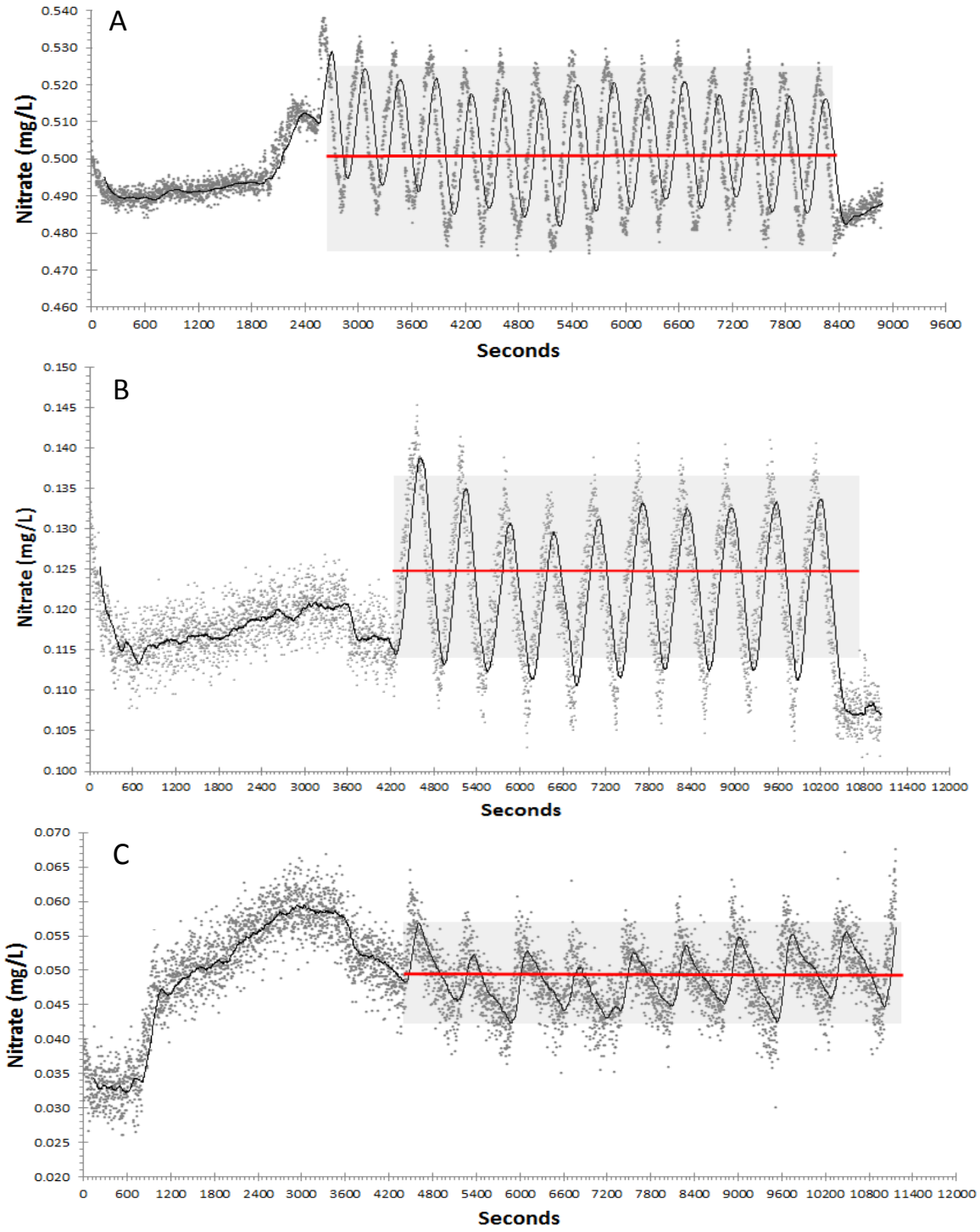

Fig. 2-3 – Summary of laboratory tests to evaluate SUNA performance; measurements were taken at maximum sensor resolution (0.5 Hz). All tests simulated diel variation of varying magnitude (0.05, 0.025, 0.015 mg/L) and at varying baseline concentrations (0.5, 0.125, 0.05 mg/L) by sequentially dosing the tank with nitrate standard (1.0, 0.25 and 0.1 mg/L) or deionized water. The black line is the 30 point <u>lagging</u> moving average provided to visualize mean behavior. Data during the 1-hour SUNA start-up phase when lamp temperature equilibrates should be ignored, and should be considered during future deployments (the first 24 hours of sampling at 15-minute intervals may be of insufficient accuracy.)

amplitude 0.03 mg/L, and 3) baseline 0.05 mg/L, amplitude 0.015 mg/L. Based on observed sensor performance, we proceeded with field deployments highly confident in the resulting data obtained from these sensors; note in particular the performance at low concentration (50 µg/L) with low diel variation (15 µg/L) (Fig. 2-3c). We note that other SUNA users around the country have reported some important temperature effects on sensor performance (B. Pellerin, personal communication); we do not address these here because of the thermal stability of the spring systems in which the sensors are deployed. Applications in other rivers (e.g., where temperatures can vary over 10 degrees or more) may require additional sensor testing to ensure reliable results.

One of the implications from these simulated diel data is that sensor sampling rate is an important predictor of process inference accuracy. As with all methods, there is some intrinsic measurement error associated with the sensor, and this error can confound rate inference if the sampling rate is too short. The sampling rate here (1 every 2 seconds) and the timing of simulated diel variation (wavelength is ca. 12 minutes) corresponds to a sampling rate over 24 hours of once every 15 minutes, which we selected for all deployments in this study. Higher resolution sampling rates for smaller or more dynamic systems may be necessary, but greater sampling intensity is offset by sensor temperature effects that may start to arise at sampling periods shorter than 5 minutes.

Metabolism

We calculated gross primary production (GPP) and ecosystem respiration (R) in units of g $O_2/m^2/d$ for each day of our deployments using the single-station method in all cases (Odum 1956, Bott 1996). The integration area, estimated for single-station deployments, was not used except for the Santa Fe River because the upstream benthic area contributing to river metabolism is constrained by the geometry of the river between the spring-vent and the sensor location.

Reaeration is the most uncertain parameter in metabolism measurements. We estimated the reaeration constant on a daily basis from the relationship between declining DO concentration at night and the changes in the saturation deficit. Specifically, reaeration (K, in units of hr^{-1}) is the slope of the line relating the DO change (mg/L/hr) to the saturation deficit (mg/L) during the period when photosynthesis has ceased for the day, and oxygen levels are declining to their nighttime levels (at which respiration and reaeration are in balance; Fig. 2-4). Fitted lines on a daily basis were generally extremely strong ($r^2 > 0.95$), with exceptions on days with nighttime rainfall. While K values varied little over the deployment period in each spring or even between deployment periods on the same spring, they varied

substantially between springs. In the Ichetucknee River, where we collected a year of data rather than just 2 weeks, reaeration shows a significant response to stage (presumably due to lower velocity during the high stage backwater flood observed), but very little seasonal variation.

To estimate the C:N ratio of primary production required estimating the net C assimilation implied by the gross production estimates in oxygen units. We assumed autotrophic respiration was 50% of GPP (Hall and Tank, 2003), and converted the resulting NPP rate from O_2 to C based on the 32:12 ratio of molecular weights. Based on previous estimates that suggest trivial heterotrophic nutrient demand (Heffernan and Cohen 2010), we neglected any nutrient uptake due to gross heterotrophic assimilation.

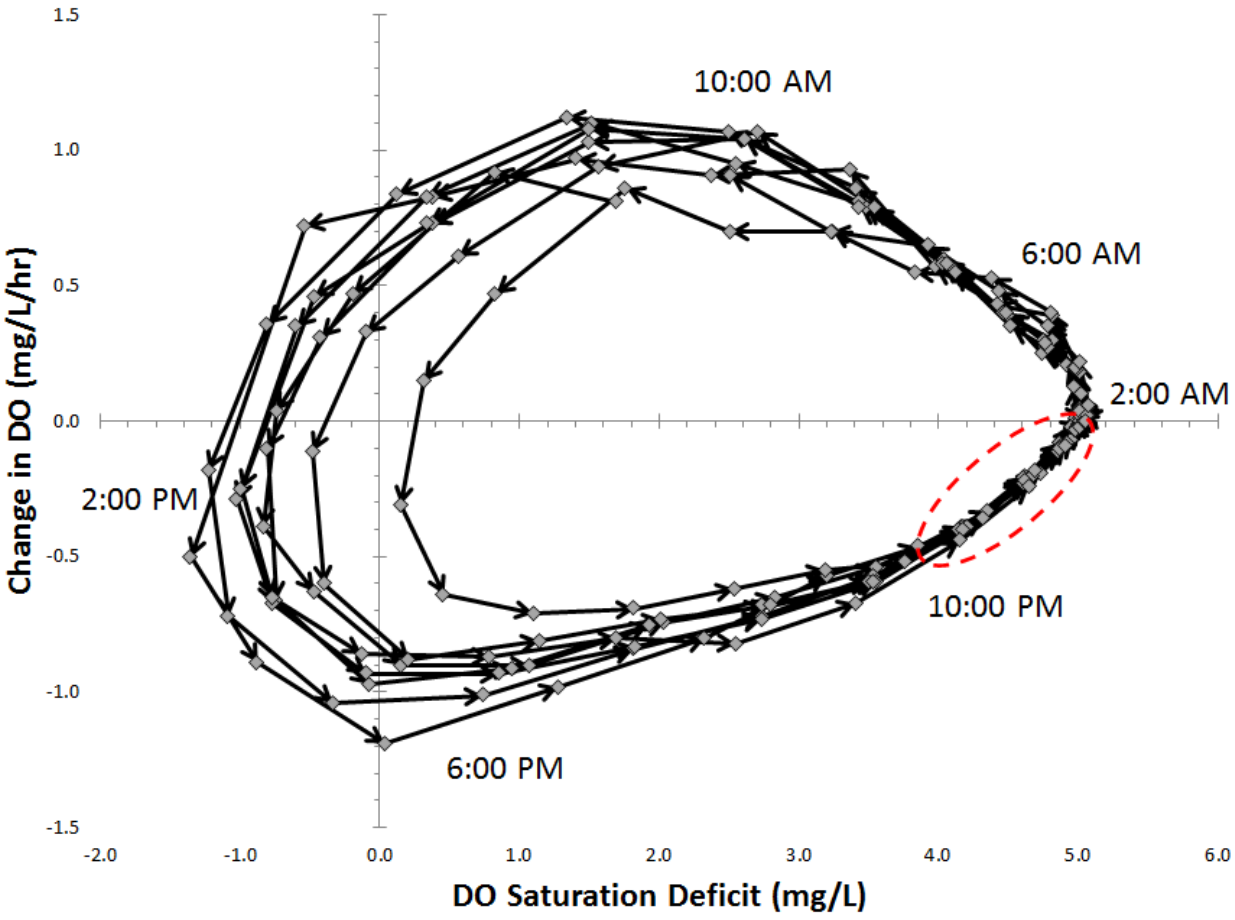

Fig. 2-4 – Example of estimation of K (reaeration rate in units of hr^{-1}) from a bi-plot of the dissolved oxygen saturation deficit (mg/L; x-axis) and the subsequent change in DO (mg/L/hr; y-axis). Reaeration is estimated from the slope of the fitted line during the period of day when photosynthetically derived dissolved oxygen is reequilibrating with the atmosphere (dashed red oval). These data, from the Ichetucknee River over a period of 8 days yield a mean K value of 0.53 hr^{-1}. Times-of-day are approximate.

N Removal – Assimilation and Denitrification

The method for estimating N removal via assimilation is based on diel variation in nitrate concentrations. Nitrate (measured as NO_3^-N using the UV method – APHA 4500-NO3-B) is the overwhelmingly dominant form of N in all the systems studies (DON is generally low and NH_4^+ is generally below detection), so the ecological system acquires its nitrogen in that form. Note that for this work we assume that rooted plants acquire most of their nutrients from foliar uptake, a finding supported by isotopic evidence (De Brabandere et al. 2007) and the absence of transport mechanisms other than diffusion through the plants as with emergent or terrestrial species. Diel variation in solute concentrations can be attributable to other mechanisms (e.g., metal solubility due to photolytic oxidation and reduction reactions), but these mechanisms are presumed small for riverine nitrogen processing. Moreover, the magnitude of diel variation in other solutes is extremely small compared to the observed diel variation in nitrate (de Montety et al. 2011), suggesting an overwhelming dominance of biological processes in that signal.

Based on previous work (Heffernan and Cohen 2010) that developed this method, daily N assimilation was estimated based on the extrapolation of nighttime baseline NO_3 concentrations (Fig. 2-5b). Other configurations of the algorithm to estimate assimilation are plausible (e.g., interpolating between nighttime maxima – Fig. 2-5a), but substantial inter-day variation in the nighttime baseline (that is, the maximum nighttime concentration reflecting conditions when assimilation is presumed zero) make that approach problematic. Specifically, day-to-day variation in the nighttime baseline concentration is apparently due to variation in denitrification, and this variation (and the controls on it) is obscured by peak-to-peak interpolation. This extrapolated baseline suggests that the changes in the nighttime baseline occur rapidly, and at night, rather than uniformly throughout the 24 hours between peaks, an assumption with important implications for what controls variation in denitrification. The algorithm for estimating N assimilation is thus:

$$U_A = \frac{Q}{A}\sum(C_0 - C_t) \qquad \text{Eq. 2-1}$$

where Ua is the autotrophic uptake (assimilation in g N/m^2/d), Q is river discharge (m^3/15 minutes), A is the horizontal benthic area upstream of the sensor (m^2), and C_0 and C_i are the baseline and observed nitrate concentrations, respectively (g/m^3). The summation is made over all 15 minute segments.

We reiterate that the formulation for inferring N assimilation from Eq. 2-1 assumes that nighttime assimilation is zero. This could be violated if primary producers are sufficiently N limited that nighttime assimilation is advantageous, or if flowpaths through the river system take longer than 24 hours (i.e., such that the removal signal is spread over more than a day, requiring modeling to better understand the signal). Based on hydraulic measurements in each of these systems, we reject the latter as unlikely (the longest mean residence time for any system studied is 11 hours – Table 1-2). The former is more interesting, and is the subject of subsequent investigation. We simply note here that the presence of diel variation may be diagnostic of N saturation, arising because plants can obtain the necessary N for their metabolic requirements at the time they are acquiring bicarbonate from the water column; additional metabolic investment may be needed to acquire N when photosynthesis is not active. In other words, diel variation may not occur in N limited systems because the autotrophs there are investing additional energy to acquire nutrient resources at night.

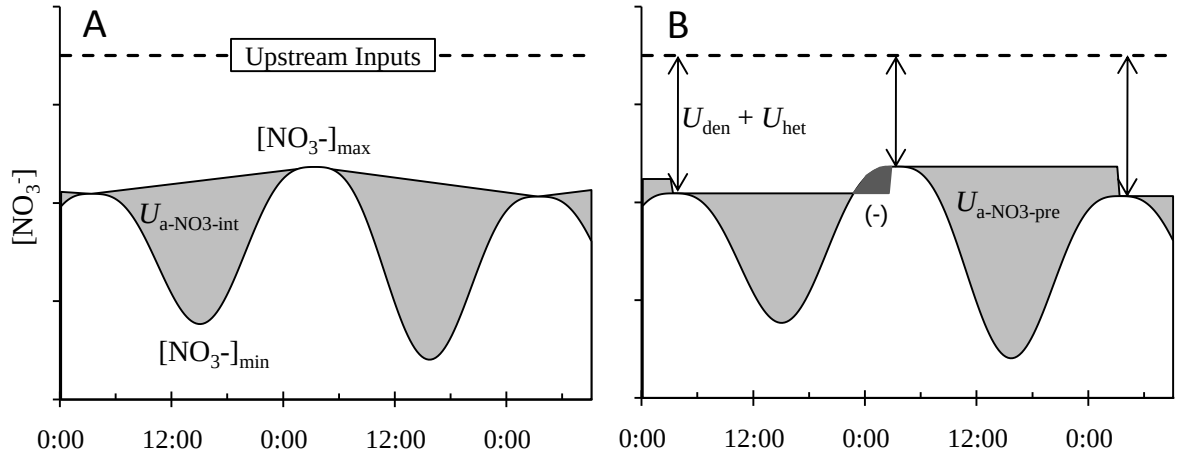

Fig. 2-5 – (after Heffernan and Cohen 2010) Alternative schemes for estimating autotrophic demand (U_a) from observed diel variation in nitrate concentrations. A) Interpolation of nighttime maxima and integration of the area between the interpolation line and the observed concentration and B) Extrapolation of the prior nighttime maxima and similar integration. The methods differ primarily in how they deal with day-to-day variation in the nighttime baseline, which has been interpreted as changing rates of denitrification (U_{den}). The upstream inputs are generally considered fixed over any two week deployment. Heterotrophic assimilation (U_{het}) is assumed negligible. For all deployments in this work, we used the extrapolated baseline method (B).

Denitrification is estimated using mass balance at the 15-minute time scale. Since all diel variation is ascribed to autotrophic uptake, the remaining N loss (i.e., the difference between observed concentrations and the flow-weighted input concentration) is ascribed to heterotrophic removal. As

discussed above, we neglect direct heterotrophic uptake based on prior work that suggested it is small, leaving the balance of removal due to dissimilatory pathways (denitrification). We note that dissimilatory nitrate reduction to ammonia (DNRA) is likely small because of the absence of an ammonium accumulation signal, but cannot be ruled out as a secondary mechanism. Chemoautotrophic denitrification pathways (e.g., those that use reduced iron or sulfur as the electron donor) are plausible contributors to the overall dissimilatory flux, but cannot be parsed from the heterotrophic pathway using this method. The overall denitrification flux is computed as follows:

$$U_{Den} = \frac{Q}{A}\sum(C_B - C_0) \qquad \text{Eq. 2-2}$$

Where U_{den} is the denitrification flux (g N/m^2/d), Q is river discharge (m^3/15 minutes), A is the benthic area of the river contributing to the flux, and C_B and C_0 are the flow-weighted input concentration emerging from the aquifer and the nighttime baseline nitrate concentrations (g/m^3), respectively. As with assimilation, the summation to arrive at daily denitrification occurs over all 15 minute segments in a 24 hour period. The start and end time of that 24 hour period depends subtly on the river hydraulics. In all but the two largest rivers, developing the integration over 24 hours starting at midnight each day is sufficient. However, in Rainbow and Silver Rivers, the longer hydraulic residence time means that the signal of daytime assimilation is consistently observed until approximately 3:00 am, meaning that for these rivers, the diel integration starts at that time each day. Errors that accrue from neglecting this are relatively small.

Data Analysis

After estimating GPP, R, NPP, U_a and U_{den} for each day of each deployment, we sought to understand the degree to which these values were associated and predictable. We first sought to relate NPP and U_a (both on a molar basis), from which we can obtain an estimate of the C:N ratio of overall ecosystem metabolism. These were compared qualitatively with measurements of C:N from field samples of algae and submerged aquatic vegetation (SAV) that suggest low ratios for the former (ca. 12:1) and higher ratios for the latter (ca. 30:1). Where a system falls within that range may be suggestive of the relative importance of different autotroph guilds in overall ecosystem productivity.

Second, we sought to relate observations of GPP to solar insolation, and R to water temperature. The expectations for both are strong positive associations since these systems have been shown previously (Odum 1957a) to be light limited, and because respiration, as a heterotrophic process, should be sensitive to temperature variation, albeit slight in these systems.

We also sought to predict dissimilatory heterotrophic removal (denitrification). The mechanisms that might regulate denitrification are temperature (since the process is heterotrophic), and the availability of organic carbon. Previous work (Heffernan and Cohen 2010) showed a strong indirect coupling between heterotrophic removal and GPP, with denitrification on any given day strongly correlated with GPP the previous day. This was interpreted to mean that the availability of labile organic carbon (e.g., root exudates and recently senesced material) controls short term variability in denitrification; indeed, that work estimated that approximately 35% of the variation in denitrification was due to day-to-day variation in GPP.

Results

A summary of the deployment lengths on each river is shown in Table 2-1. For each deployment we reporta summary of the metabolism measurements (gross primary production, respiration). Table 2-2 gives a summary of the observed mean reaeration for each deployment with the exception of Ichetucknee, which was more variable because of the longer deployment period; reaeration estimates for that river are graphically shown separately. For each station on each deployment in each river, we show 4 graphs:

1) Summary of raw observed data (nitrate, temperature, dissolved oxygen, radiation and rainfall)

2) Graph summarizing parameters necessary for inference of N removal (i.e., assimilation and denitrification based on nighttime baseline concentrations and flow-weighted input concentrations)

3) Daily summary of GPP and R, and U_a and U_{den}, and

4) Summary of the interrelationships between ecosystem variables for the period of deployment (NPP vs. U_a, on a molar basis from which the C:N ratio of ecosystem metabolism can be estimated, GPP vs. solar radiation, R vs. water temperature, and ΔGPP vs. ΔU_{den}, to explore indirect coupling between GPP and denitrification.

The special case of the Ichetucknee River is also presented with the same scheme, but additional details are relevant. Specifically, because the deployment was over 300 days (with large periods during which the sensors either failed or were used for other tasks), the patterns of GPP, R and nitrogen processing with season and discharge can be explored.

Another special case, discerned only after several deployments there, is Alexander Springs Creek and Silver Glen Springs. At that site, the pattern of diel variation in nitrate concentration exhibited in the other spring run streams (i.e., lower during the day, higher at night) was not observed; the special conditions that lead to this inversion of the pattern in Alexander Springs Creek are of particular interest because they suggest a threshold in the diel variation pattern that is consistent with N limitation at that site. A much more detailed examination of the N dynamics in that spring run stream system are presented in Research Element #8.

Deployment 1: SILVER RIVER – January 2010

The first Silver River deployment occurred in January 2010, and lasted 16 days. The dual sensor package was deployed only at the downstream location, so the integration is over the entire benthic region from the main vent to near the confluence with the Ocklawaha. The reaeration constant averaged 0.44 hr^{-1} over the entire period, with a standard deviation of 0.05 hr^{-1}. Because of uncertainty introduced by 4 instances of rainfall during the night or early morning hours, when K is estimated on this river, we used an average K of 0.44 hr^{-1} for all days.

A summary of the field chemistry observed during the deployment (Fig. 2-6) shows marked diel variation in nitrate, with high values during the early morning (between 3:00 and 6:00 am) from which the baseline nitrate value was determined. The shape of the curves, with short nighttime baseline duration, suggests that this river is relatively close to violating one of the methodological assumptions (i.e., that residence times are sufficiently short to permit allocating all diel removal to one day's assimilation). Measured median residence time in this river is over 600 minutes (Table 1-2), and a long breakthrough curve tail (Fig 1-3) suggests that ca. 10% of the water has residence time greater than 12 hours, which means that water reaches the downstream location around the time that we estimate the baseline concentration. Further modeling work will be needed to ascertain when the assimilation (as well as the metabolism) measurements are confounded by this longitudinal storage. Similarly marked variation in temperature and DO were observed, and these appear to qualitatively parallel the inter-day temporal dynamics of N removal. Solar radiation and rainfall are also shown, and there is evidence of significant

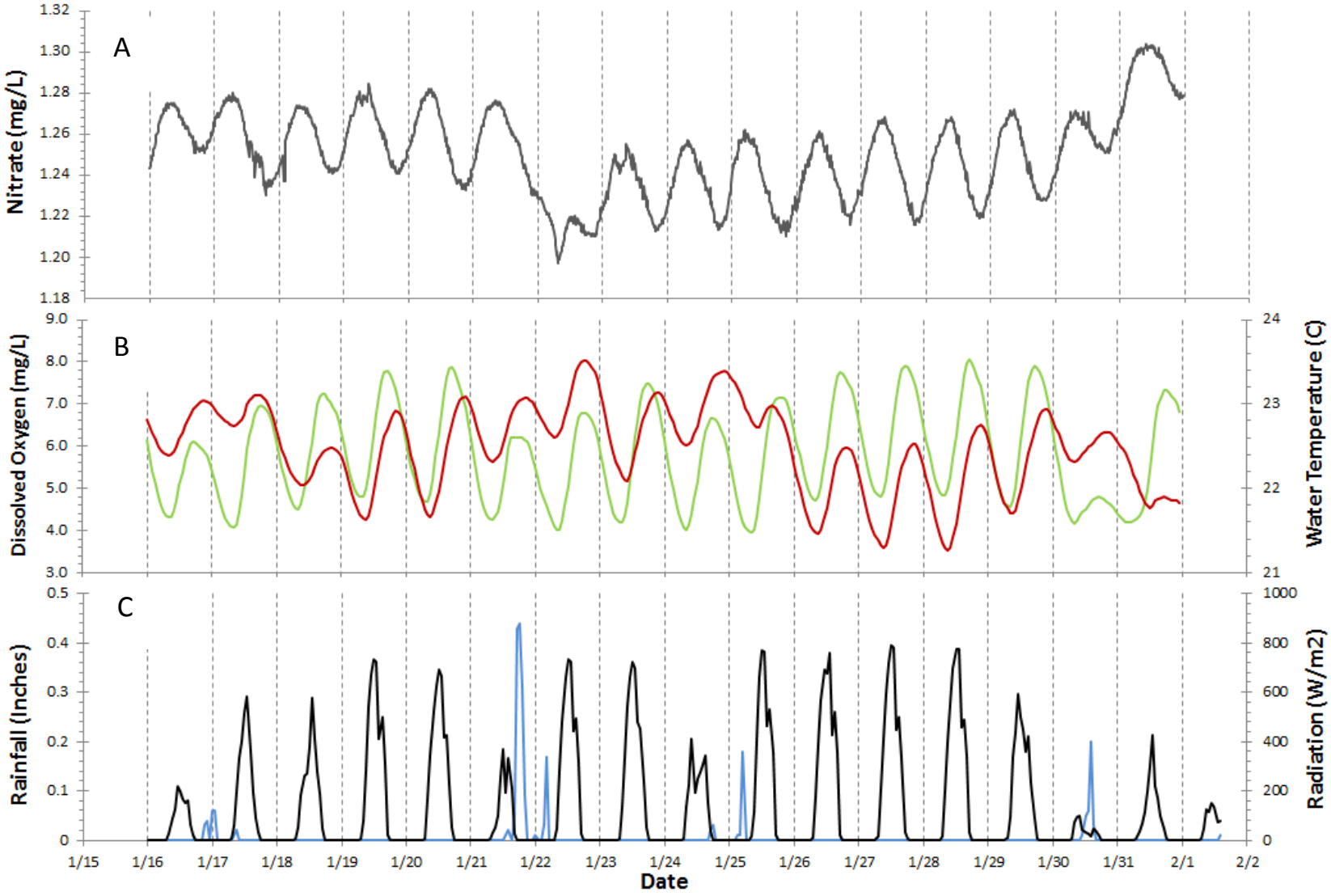

Fig. 2-6 - Diel variation in nitrate (grey line), dissolved oxygen (green line), water temperature (red line), radiation (black line) and rainfall (blue line) for Silver River during a January 2010 deployment.

water contribution to the river during the rain event on Jan. 21st that limits the utility of the nitrate assimilation method on that and the subsequent day. Another cloudy day (Jan. 30th) was followed by a dramatic increase in the baseline nitrate concentration, consistent with the indirect C and N coupling observed previously in the Ichetucknee River (Heffernan and Cohen 2010).

Inference of N removal based on this diel variation and longitudinal concentration declines is presented in Fig. 2-7. Shown are the raw nitrate observations, the estimated baseline concentrations (i.e., mean nighttime values, averaged from 3:00 to 5:00 am) and the input concentration measured using the SUNA at dawn at the point where the various source springs are fully mixed (the 1200 m station). This value, 1.36 mg/L, is consistent with recent water quality measurements in the various springs, and suggests a substantial N removal due to denitrification, since we ascribe all differences between the nighttime maximum and the input concentration to denitrification. Two aspects of this inference are notable.

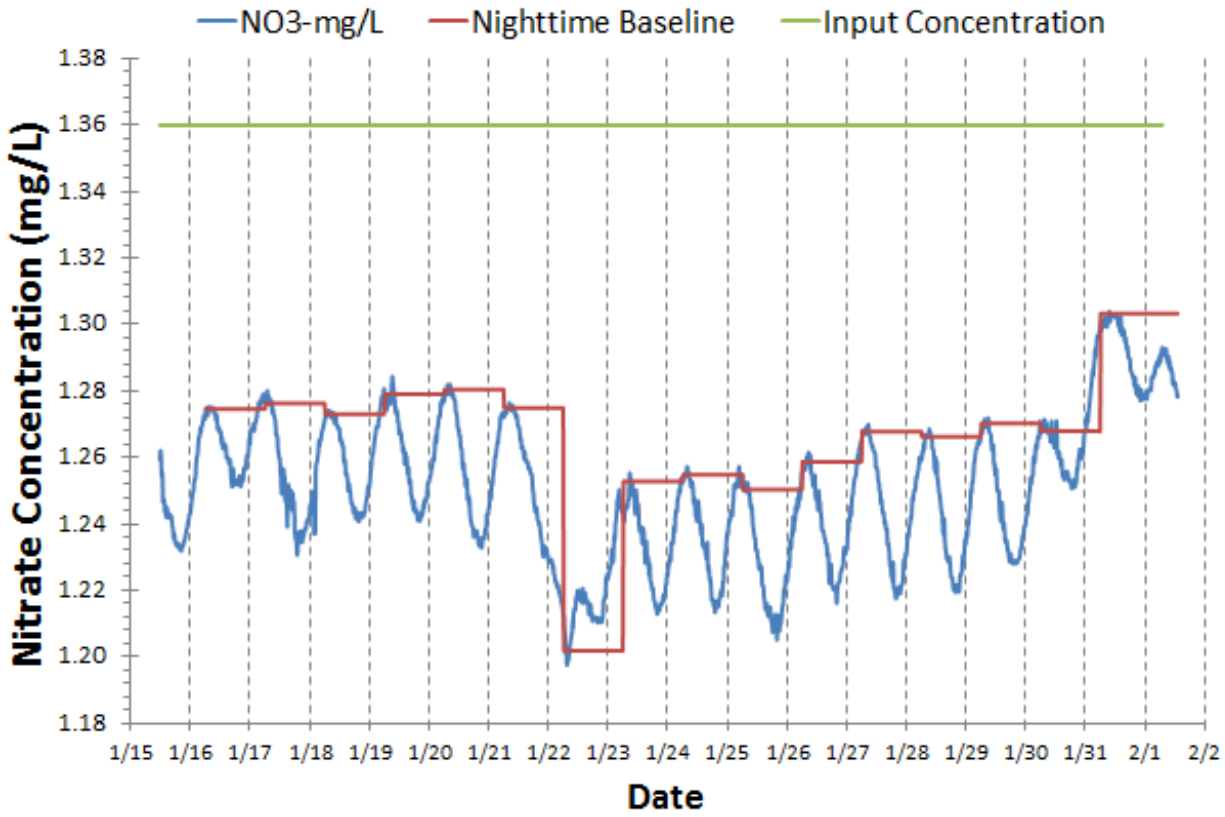

Fig. 2-7 – Summary of N removal mechanism inference. Assimilatory removal is estimated based on diel variation in nitrate (blue line) referenced to a nighttime baseline value (red line). Note that N removal was not estimated on 1/22 and 1/23 because these days did not exhibit typical diel variation patterns due to intense rainfall leading to stormwater dilution. Dissimilatory removal is estimated as the mass loss between upstream input concentrations (green line) and the nighttime baseline; that is, denitrification is assumed constant over the course of each 24-hour period. Day-to-day variation in the nitrate baseline is explored below.

First, the magnitude of denitrification is strongly sensitive to the magnitude of this flow weighted input concentration, as all mass balance estimates are. Second, and most importantly, this method cannot readily distinguish between denitrification and dilution. There are many springs in the Silver system, and if this means lateral inputs of low nitrate water into the channel upstream of our measurements, it will be interpreted as denitrification. This speaks to the critical need to accurately establish flow patterns in these rivers using independent methods of flow assessment to those used by the USGS. Our hydraulic studies, previously presented, yield high recovery rates (always more than 95%), which suggests this problem is comparatively small, but we propose that reported denitrification be viewed as upper bounds of actual rates, which may be lower due to unquantified inflow of low-nitrate water.

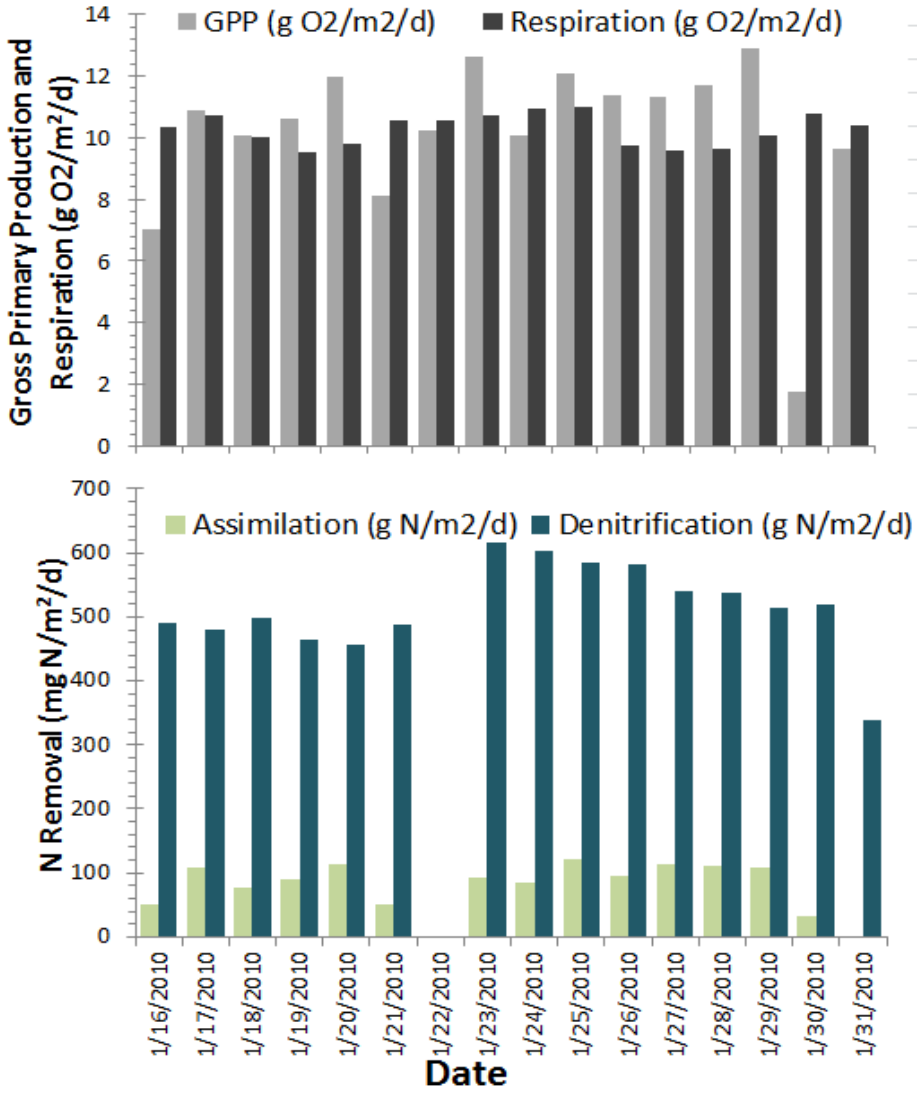

Fig. 2-8 – Summary of January 2010 deployment at Silver River showing estimates of gross primary production and respiration (top panel) and assimilatory and dissimilatory N removal (bottom panel).

The observed GPP and R values are strongly consistent with previous studies of the Silver River during this period of the year (Fig. 2-8) (Munch et al. 2004); GPP averaged 10.1 g $O_2/m^2/d$, and R averaged 10.3 g $O_2/m^2/d$. We observed the river to be carbon neutral for the period of record (P:R averaged 0.99), but that most days P:R was slightly higher than 1; on one day (Jan 30th) the P:R ratio fell to 0.16. Day-to-day variation in assimilation and denitrification were also evident (note that we did not estimate U_a on 1/21 and 1/22 and didn't estimate U_{den} on 1/22), but the general trend is a mean of 89 mg $N/m^2/d$ for U_a and 514 mg $N/m^2/d$ for U_{den}. This value, though high compared to most rivers, is entirely plausible for a river with high benthic production and nitrate availability (Laursen and Seitzingger 2002, McCutchan and Lewis 2008); notably it is nearly 3 orders of magnitude higher than the globally averaged background rate for denitrification of 0.95 mg $N/m_2/yr$ (Seitzinger et al. 2006), underscoring the special role of spring run streams in the N cycle in river drainages in Florida. The rate of denitrification observed here is also comparable to the rate observed previously in the Ichetucknee River (Heffernan and Cohen 2010). Overall this suggests that assimilation is a small fraction of the total N removal (ca. 15%), a finding consistent with the contention that N is not currently limiting primary production in the river; we revisit the idea of historical N limitation at the end of this research element. While diel variation in nitrate (which average ca. 50 µg/L) may suggest that similar productivity would be limited at estimated historical concentrations (which are between 50 and 100 µg/L), ecosystem responses to lower N concentrations (including non-diel assimilation dynamics that become advantageous under conditions of lower supply) may lead to N sufficiency under all conditions. Further work in this area, particularly in light of observations (see Research Element #7) at Alexander Springs is needed.

The observed GPP coupling to N assimilation is extremely strong in this deployment (Fig. 2-9a). The slope of the line (between molar uptake rates of C and N) suggests that the molar C:N ratio of ecosystem production is ca. 20 for this river, a value at least qualitatively consistent with a mixture of algal (C:N ~ 12) and vascular plant (C:N ~ 30) production; if we take the mean across days, the C:N ratio is 25.1. A more detailed analysis of C:N ratios across deployments is presented later in this section.

As expected, GPP is strongly a function of solar insolation (Fig. 2-9b); the curvilinear relationship was surprising, but may suggest a saturating effect of increasing light intensity. We note that the low GPP value at left has enormous leverage on the fitted line, and that a linear fit is optimal if that point is omitted. Also notable is the observation that ecosystem respiration is a strong function of nighttime minimum water temperature (Fig. 2-9c); while this is expected for a heterotrophic process, the strength and magnitude of the association is surprising. It suggests, for example, that a 1 degree change alters

the respiration rate in the ecosystem by nearly 10%. Since the system is highly thermally buffered, this effect is modest over all, but may signal an important effect of global climate change insofar as the recharge temperatures, and thus vent water temperatures, may be increased by climate change.

Finally, we observed strongly significant evidence of indirect coupling between primary production and dissimilatory N removal. Fig. 2-9d shows how day-to-day changes in GPP impact changes in U_{den} on the following days. The slope of the line (14.9) suggests that a unit change in GPP accounts for a ca. 3% change in U_{den}. The fitted line is strongly leveraged by the data point from Jan 30th, but is still statistically significant (p = 0.007) without it, and with a similar slope.

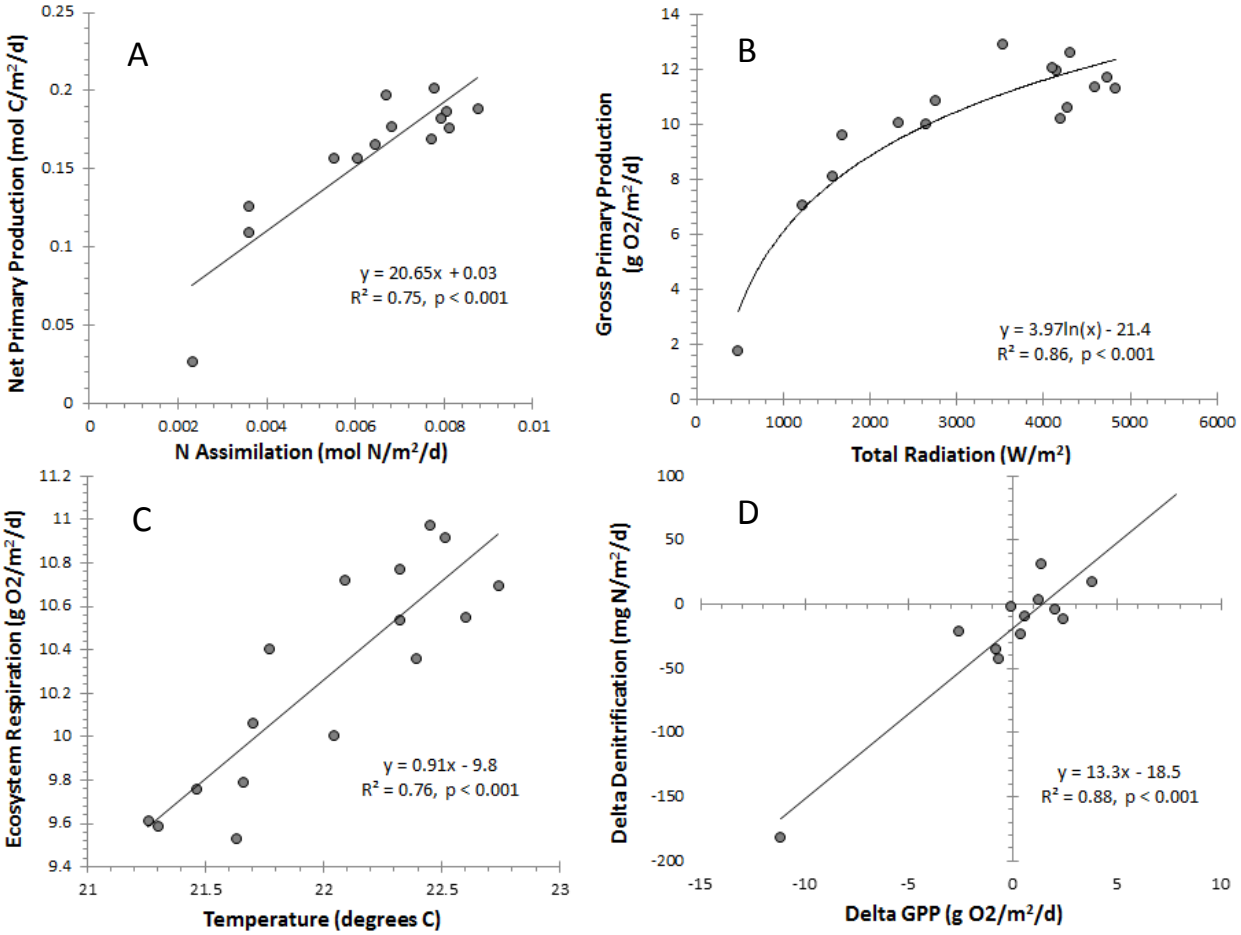

*Fig. 2-9 – Summary of interrelated elements of ecosystem C and N metabolism. A) Relationship between N assimilation and C assimilation (assuming net primary production = 0.5 * gross primary production) on a molar basis. The fitted slope indicates the C:N stoichiometry of ecosystem metabolism is ca. 20:1. B) Relationship between GPP (in g $O_2/m^2/d$) and incoming solar radiation (W/m^2), with a natural log best fit line. C) Relationship between ecosystem respiration (g $O_2/m^2/d$) and minimum daily water temperature (degrees C). D) Strong inter-day coupling of gross primary production and heterotrophic N removal (denitrification), showing that day-to-day changes in GPP (in g $O_2/m^2/d$) explain almost 90% of the observed day-to-day changes in estimated denitrification (mg $N/m^2/d$).*

Deployment 2: Rainbow River – February 2010

Our second deployment occurred in the Rainbow River in February 2010, and lasted 13 days. The raw observations from that deployment (Fig. 2-10) indicate strong diel nitrate variation that is out of phase to dissolved oxygen production. The input nitrate concentration was 1.68 mg/L indicating the magnitude of N removal in this river (200-250 μg/L). Temperature variation is modest (ca. 2 degrees) and slightly dispersed compared to DO, indicating the thermal mass of the river water. The shape of the temperature response is somewhat asymmetric, which may reflect differences in water residence time between upper and lower river reaches. Solar radiation and rainfall from the nearby Brooksville FAWN station are also shown, and suggest that there was marked variation in insolation over the study period associated with 4 rain events. Note the dramatic increase in insolation between the January deployment at Silver and this deployment (mean = 4800 W/m^2 for this deployment vs. 3200 W/m^2 for the Silver deployment).

During this deployment, the reaeration constant averaged 0.56 hr^{-1}, but was more variable among days (SD = 0.1 hr^{-1}) than we observed in other rivers. Some of that variation appears to be in response to weather events, with rainy and cloudy days exhibiting reduced reaeration rates, and sunny days showing higher rates. This short duration deployment is insufficient to establish any practical predictor of reaeration, so we used the deployment period mean for all days (0.56 hr^{-1}).

Inference of N removal based on diel variation is summarized in Fig. 2-11; shown are the input concentration (measured using the SUNA at dawn below the confluence of the suite of source springs), the nighttime baseline estimated each day from the concentration between 3:00 and 5:00 am, and the actual observations. There is strong evidence of nighttime baseline variation that is explored further below. There are several anomalous periods that remain unexplained. In particular, there is a large drop in nitrate concentrations just after midnight on the 25th of February. There also appears to be some evidence of a failure of the nitrate concentration to plateau each 24 hours, shown by the highly rounded and very late nighttime peaks, which are brief and compared to what was observed in other rivers (including the Silver). The median residence time in Rainbow River is slightly longer than the Silver River (11.5 hours) and a fairly significant fraction of the water resides in the river long enough to affect the following days N removal and DO dynamics. As such, we recommend that future deployments in the Rainbow River identify a station upstream of our downstream station to minimize this effect; we discovered this potential issue before proceeding to a second deployment in Rainbow (October 2010).

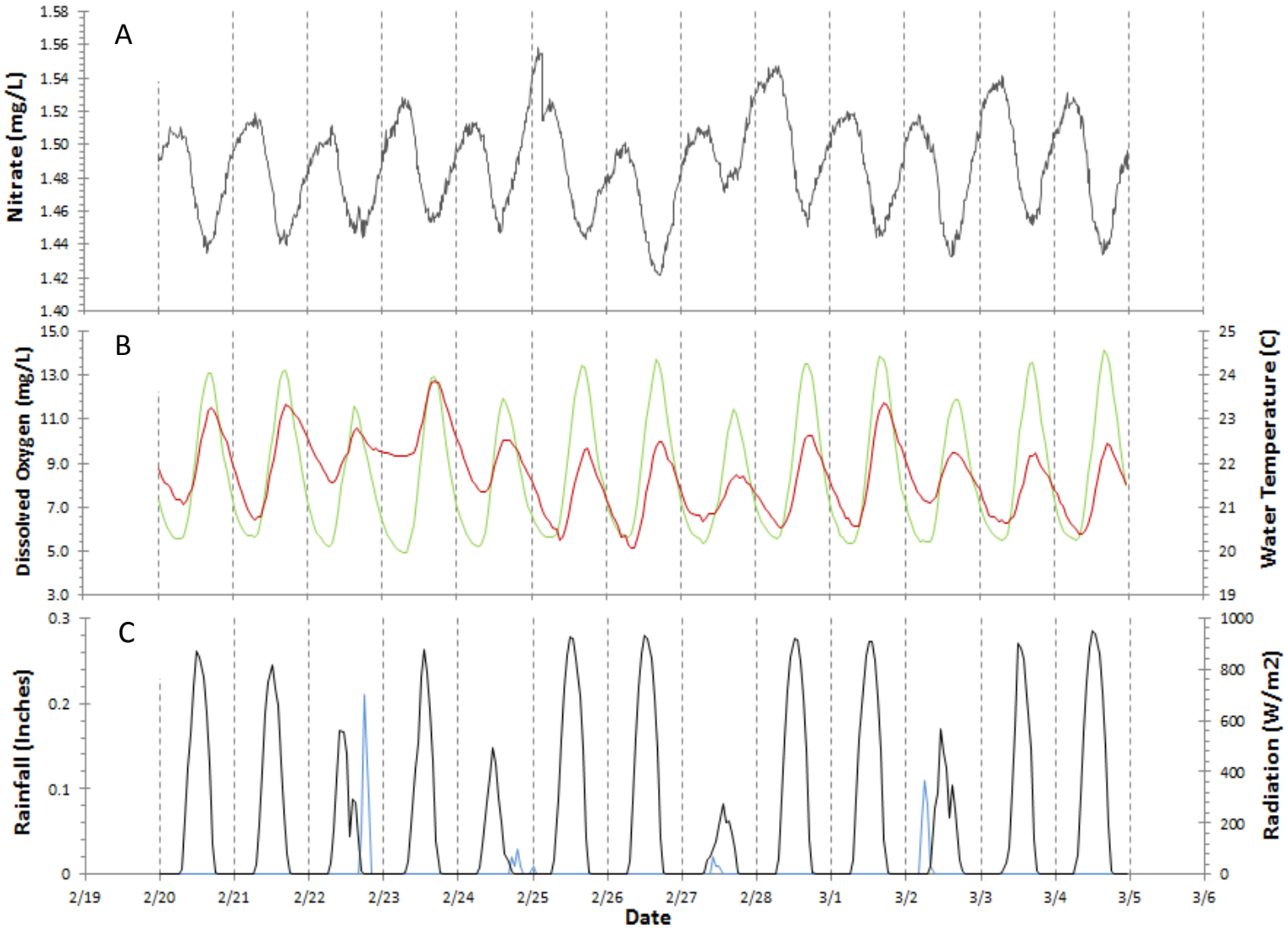

Fig. 2-10 - Diel variation in nitrate (grey line), dissolved oxygen (green line), water temperature (red line), radiation (black line) and rainfall (blue line) for Rainbow River during a February 2010 deployment. Vertical dashed lines are at midnight every 24 hours.

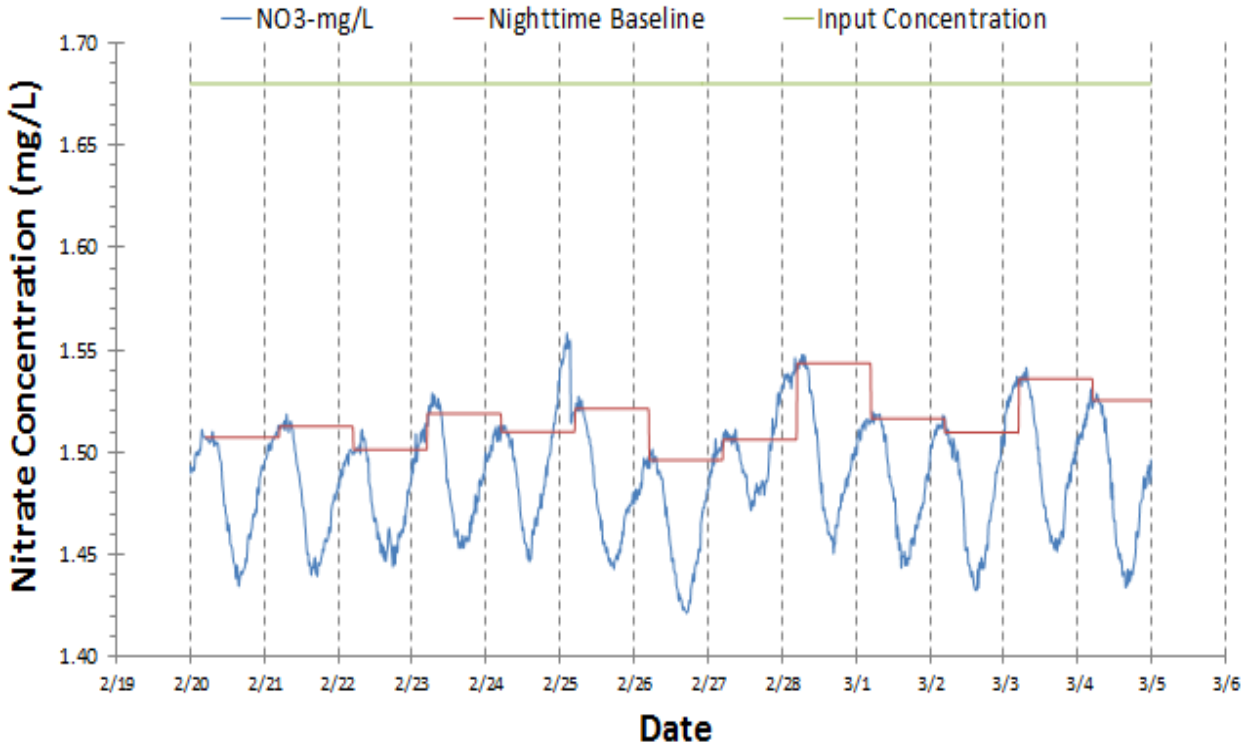

Fig. 2-11 – Summary of N removal mechanism inference from Rainbow River, February 2010. Assimilatory removal is estimated based on diel variation in nitrate (blue line) referenced to a nighttime baseline value (red line). Dissimilatory removal is estimated as the mass loss between upstream input concentrations (green line) and the nighttime baseline; that is, denitrification is assumed constant over the course of each 24-hour period. Day-to-day variation in the nitrate baseline is explored below.

A summary of the estimated gross production, respiration, assimilation and denitrification for each day during the deployment is shown in Fig. 2-12. For this deployment, respiration was very nearly constant, but GPP was variable and much larger than R. Indeed, the P:R ratio estimated during this period averaged 1.8. While there is some uncertainty about the reaeration rate, this high P:R ratio may be typical of more highly productive days during the spring season. Indeed the phenology of spring river primary production appears to peak during the spring, when leaf occlusion of light is reduced prior to leaf-out during March and April. This pattern is strongly present in the Ichetucknee, but in that system, respiration tracks GPP much more closely. Further deployments in Rainbow (in October 2010) will allow us to establish if high P:R during this deployment is a deployment or site anomaly.

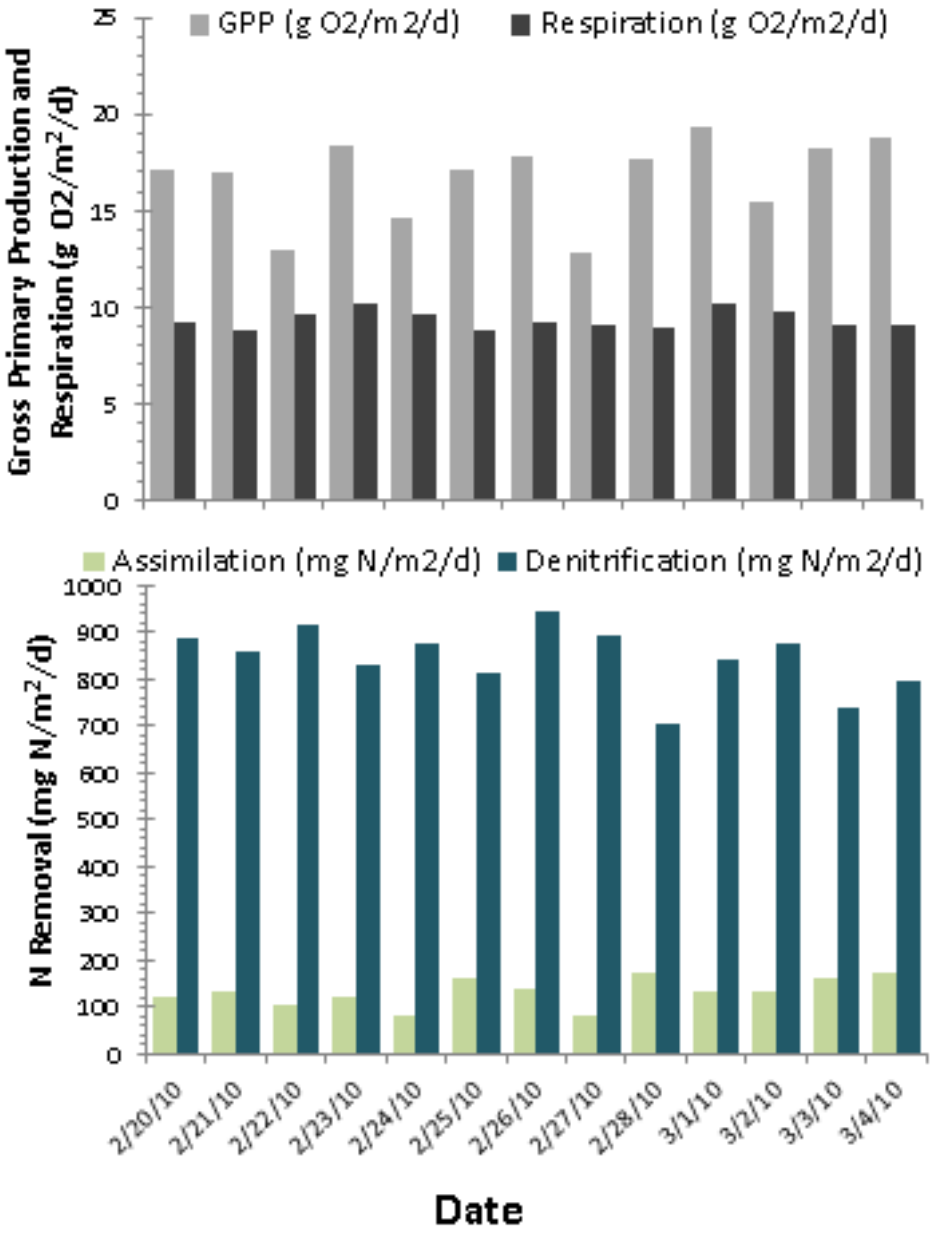

Fig. 2-12 – Summary of February 2010 deployment at Rainbow River showing estimates of gross primary production and respiration (top panel) and assimilatory and dissimilatory N removal (bottom panel).

Day-to-day variation in assimilation and denitrification is relatively large. As with Silver and other rivers, assimilation is a small fraction of total removal (14% on average) despite a comparatively high mean areal U_a rate of 132 mg N/m^2/d. The reason is a remarkably high denitrification rate (over 840 mg N/m^2/d), 50% higher that was observed on the Silver River a month earlier. The combined removal of nearly 1 g N/m^2/d is higher than has been previously observed in other spring fed rivers.

Examining the deployment length variation in N vs. C coupling (Fig. 2-13a) suggests a slightly weaker association than was observed in Silver River, though it is still statistically significant ($p < 0.001$; Fig. 2-13a). Moreover, the slope of the fitted line where the intercept is allowed to be non-zero is very small, and not representative of the mean C:N ratio estimated across days, values of which are near 28:1, which is the slope of the fitted line when the intercept is set to 0. The reason is unclear; the implication is that N assimilation varies more than C assimilation over the range of observed values, which may be due to higher intrinsic error rates in the N assimilation estimation method than are present in the C metabolism calculations. Variation in C:N ratio with GPP is predicted by stoichiometric theory (Sterner and Elser 2002); specifically we would expect higher C:N ratios at high GPP in response to the saturation of N demand by chloroplasts and other protein rich cellular structures, and continued investment in energy storing compounds (long-chain polysaccharides). However, that would suggest a best fit line during this high GPP deployment that is greater than the no-intercept line. Note that the resulting C:N ratio is higher than Silver River (ca. 22:1), which may be consistent with reduced algal cover in the Rainbow system compared with the Silver system.

The relationship between solar insolation and productivity follows a logarithmic relationship as it did in the Silver River (Fig. 2-13b), with best fit parameters that are remarkably comparable. Likewise the association between minimum water temperature and ecosystem respiration is similar to what was observed at Silver (Fig. 2-13c), with the exception that the incremental influence of a 1 degree change is slightly larger in Rainbow, for reasons that are unclear.

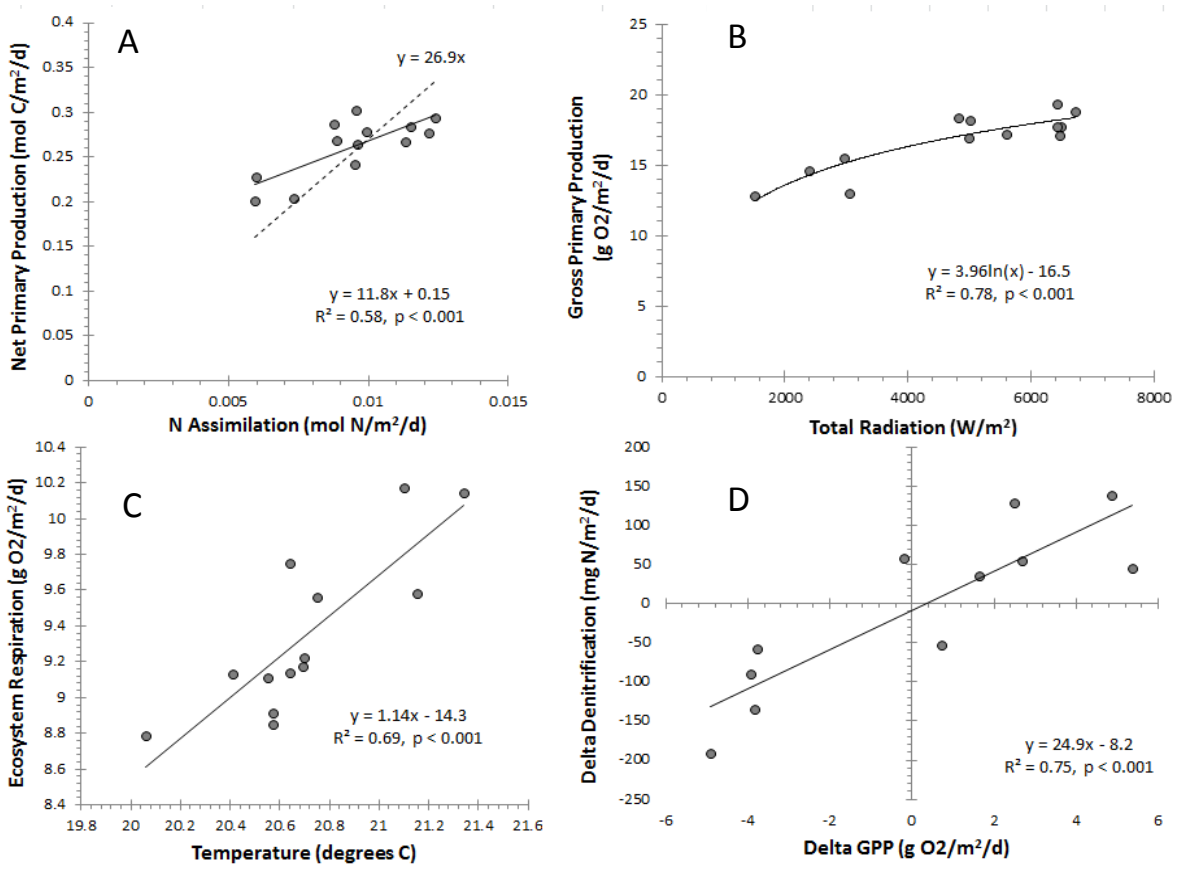

*Fig. 2-13 – Summary of interrelated elements of ecosystem C and N metabolism from Rainbow River, February 2010. A) Relationship between N and C assimilation (assuming net primary production = 0.5 * gross primary production) on a molar basis. The fitted slope of the dashed line (intercept forced through 0) indicates C:N stoichiometry of ecosystem metabolism is ca. 27:1. B) Relationship between GPP (in g $O_2/m^2/d$) and incoming solar radiation (W/m^2), with a best fit line. C) Relationship between ecosystem respiration (g $O_2/m^2/d$) and minimum daily water temperature (degrees C). D) Strong inter-day coupling of GPP and heterotrophic N removal (denitrification), showing that day-to-day changes in GPP (in g $O_2/m^2/d$) explain 75% of the observed day-to-day changes in estimated denitrification (mg $N/m^2/d$).*

The indirect GPP vs. U_{den} coupling is also strongly evident in the Rainbow system (Fig. 2-13d) as it is in Silver and as was previously observed in Ichetucknee. A 1 g $O_2/m^2/d$ change in GPP leads to a 25 mg $N/m^2/d$ change in U_{den}, a 3% change. Overall, this means that a substantial fraction of the denitrification occurring in the Rainbow River is based on very recently fixed organic carbon.

Deployment 3: Alexander Springs Creek – March 2010

Alexander Springs Creek is an important study site for all springs research because it is one of the few springs in Florida that continues to exhibit background nitrate concentrations of ca. 0.05 mg/L (50 µg/L). As such, ecosystem behavior under conditions at that system, which is among the only "reference"

springs that also has a well-lit and well-protected run (Juniper Creek is also low N but is highly shaded along much of its length, and Silver Glen Spring run is heavily impacted by recreational activities). Interestingly, some of the most extensive algal mat development is observed in the upper 600 m of Alexander Springs Creek, which has been interpreted as one line of evidence countering N enrichment as the fundamental cause of algal accumulation in spring run streams (Heffernan et al. 2010b).

Reaeration in Alexander Springs was highly stable over the deployment period at a mean value of 0.39 hr^{-1} and a standard deviation of 0.05 hr^{-1}. While the nominal velocity is Alexander was relatively slow (0.07 m/s) compared to other spring fed rivers, it was somewhat surprising to see such a low reaeration rate given the broad shallow channel morphology that characterizes the upper reach (500 m long).

An examination of high resolution chemical measurements in Alexander Springs Creek reveals a pattern that is a striking departure from the other spring run stream systems in this study (Fig. 2-14). While there continues to be marked diel variation in dissolved oxygen and temperature, indicative of a highly productive ecosystem, the diel nitrate variation is inverted compared to the other study streams. Nitrate peaks at the same time as oxygen, and declines to a nighttime low that is ca. 30 µg/L below the spring vent concentration (which was measured at 0.06 mg/L). This striking inversion of the expected diel nitrate variation is the subject of considerable additional attention in this report (e.g., see Element #6 on isotopic evidence for mechanisms of N removal in that system).

In addition to inverting the expected nitrate variation, there is evidence to suggest that there are days when the river is actually exporting MORE N than it receives from the vent water during the mid-afternoon. There are several plausible (and not exclusive) explanations for this reversal; we carefully ruled out the possibility of sensor time stamp error with further deployments that resulted in the same signal. A first explanation is that oxygenation of the water column during the day inhibits denitrification, leading to nitrate export at higher rates. A second explanation is that oxygen stimulates nitrification of ammonium (a process carried out by obligate aerobes) during the day. We can rule out vent water varying diurnally based on measurements from other springs (M. Cohen, unpublished data). One important implication of this nitrate reversal is that our method for inferring assimilation will not work here. Fig. 2-15 shows a graph like what has been previously produced which simply illustrates

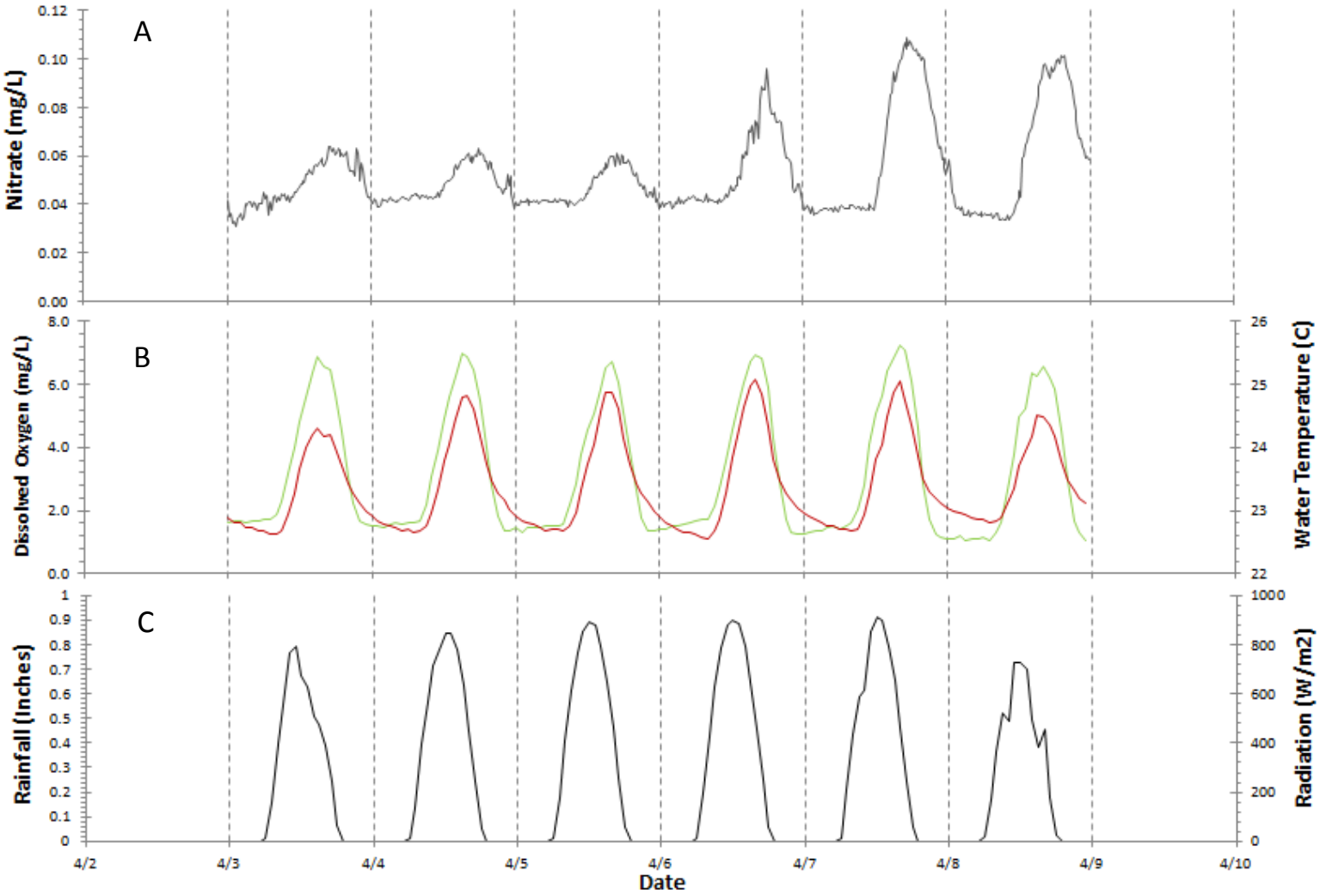

Fig. 2-14 - Diel variation in nitrate (grey line), dissolved oxygen (green line), water temperature (red line), radiation (black line) and rainfall (blue line) for Alexander Springs Creek during an April 2010 deployment. Vertical dashed lines are at midnight every 24 hours. Note the striking departure from patterns in other rivers in the nitrate variation which is now coincident with oxygen as opposed to nearly perfectly out of phase. Also note the increase in daytime nitrate on the last two days of the deployment; at this time we have no explanation for inter-day variation.

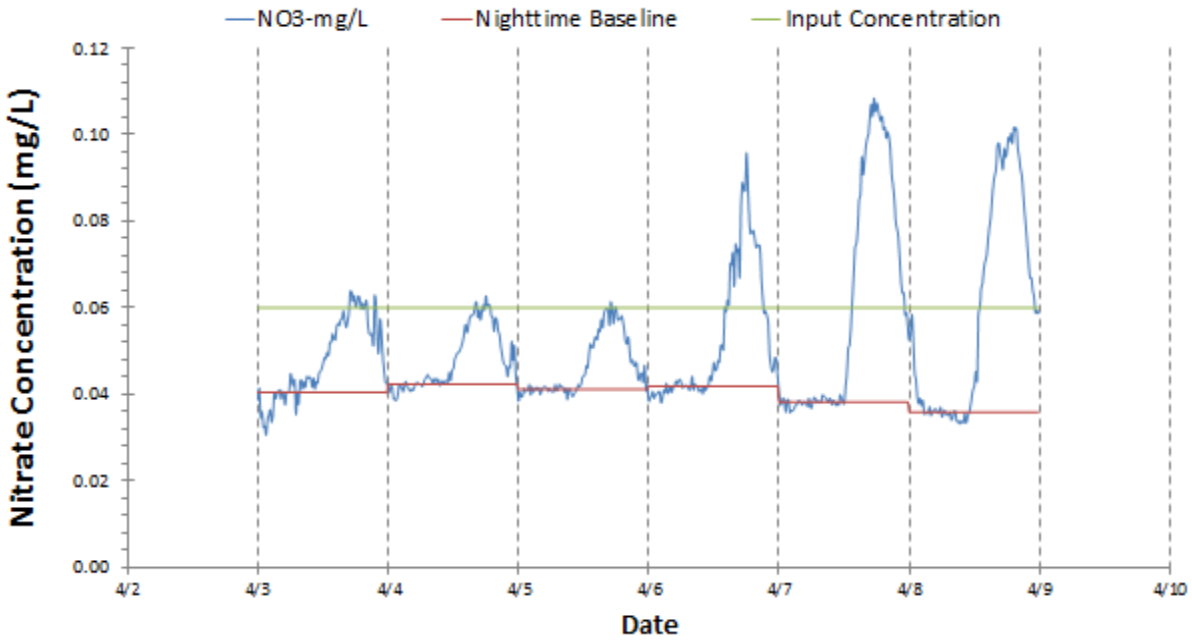

Fig. 2-15 – Summary of N removal inference from Alexander Springs Creek, April 2010. Assimilatory removal is typically estimated based on diel variation in nitrate (blue line) referenced to a nighttime baseline value (red line), but in this case this inference is not possible (or rather, it yields negative numbers). Likewise, dissimilatory removal is estimated as the mass loss between upstream input concentrations (green line) and the nighttime baseline; that is, denitrification is assumed constant over the course of each 24-hour period. While results that arise from both methods are problematic in this case, where diel variation is inverse to expectations, the total mass removal (green line minus blue line) is still informative, and is used later to estimate the magnitude of internal N recycling in the algal mat.

why this is the case; the nighttime baseline concentration against which daytime measurements are compared to yield assimilation is actually lower than those daytime values, yielding negative assimilation estimates. Similarly, the actual downstream nitrate concentration occasionally exceeds the vent concentration, making estimates of denitrification equally problematic. In short, the method as previously applied won't work. One preliminary explanation that we revisit below is that this ecosystem is nitrogen limited, and consequently the algal mat is acquiring N all day long rather than only during the day. It may be that there are physiological costs to N acquisition at night that leads plants to assimilate N only during the day when that nutrient is abundant. In this system, where N loading is low and primary production is high, the primary producers may not have that luxury. Consequently, the nighttime drop in nitrate compared with the vent (blue vs. green line in Fig. 2-15) is the combined effects of assimilation, denitrification and inhibited nitrification. Disentangling these elements of the nitrogen cycle in this river, and the broader implications for our understanding of lotic N limitation make this spring run stream a profoundly useful study system.

We estimated GPP and R, and report those values in Fig. 2-16. The river appears to be net autotrophic (mean P:R = 1.09) with high GPP (mean = 16.8 g $O_2/m^2/d$). Assuming a C:N ratio of the algal tissue of 12.5:1 (a value which we subsequently measured and is very close the actual values in the *Hydrodictyon* spp. algal mat), this means that the autotrophic N demand is between 8 and 9 kg N/d over the entire algal mat (300,000 m^2), which is remarkably close to the N flux from the spring vent (14.7 kg N/d); the resulting flux:demand ratio averages 1.7 over this deployment. While there is no coherent theory in the literature for when along a gradient of flux:demand an ecosystem becomes N limited, a lotic ecosystem that requires 50% or more of incident N flux from upstream is likely to be N limited. For comparison, the same ratio (which is admittedly confounded by reach length) in the Silver River requires less than 3%.

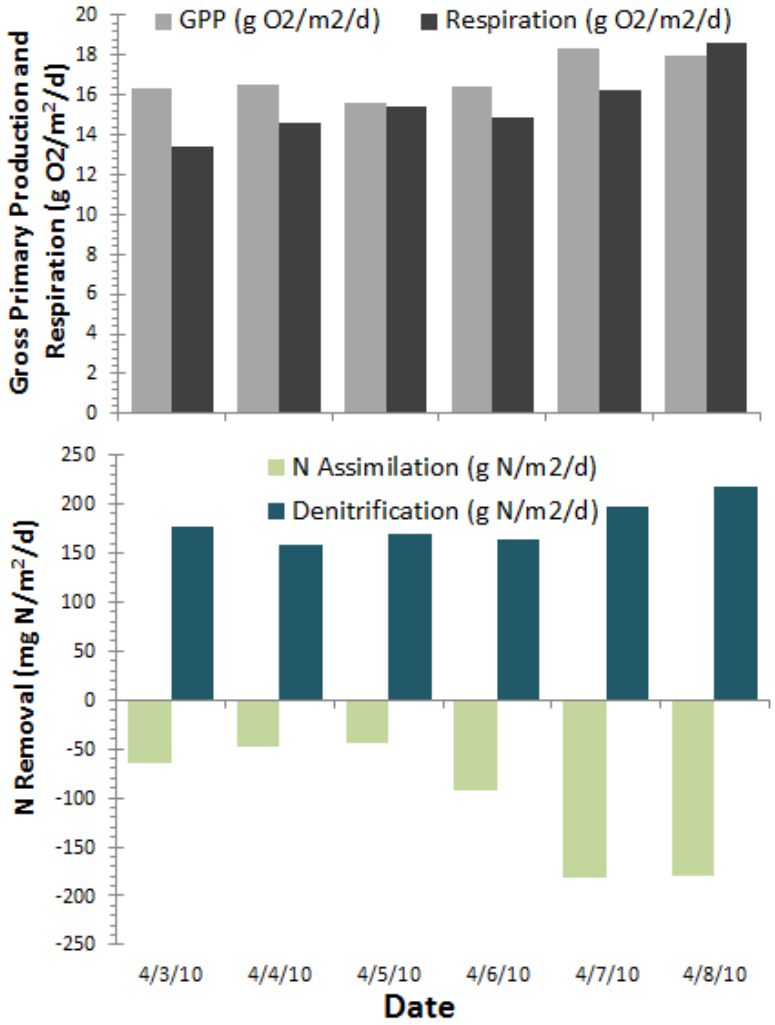

Fig. 2-16 – Summary of April 2010 deployment at Alexander Springs Creek showing estimates of gross primary production and respiration (top panel) and assimilatory and dissimilatory N removal (bottom panel). Note that the estimates of N removal are confounded by the inversion of the diel nitrate signal. However, the total mass removal (sum of light and dark green bars) is itself informative.

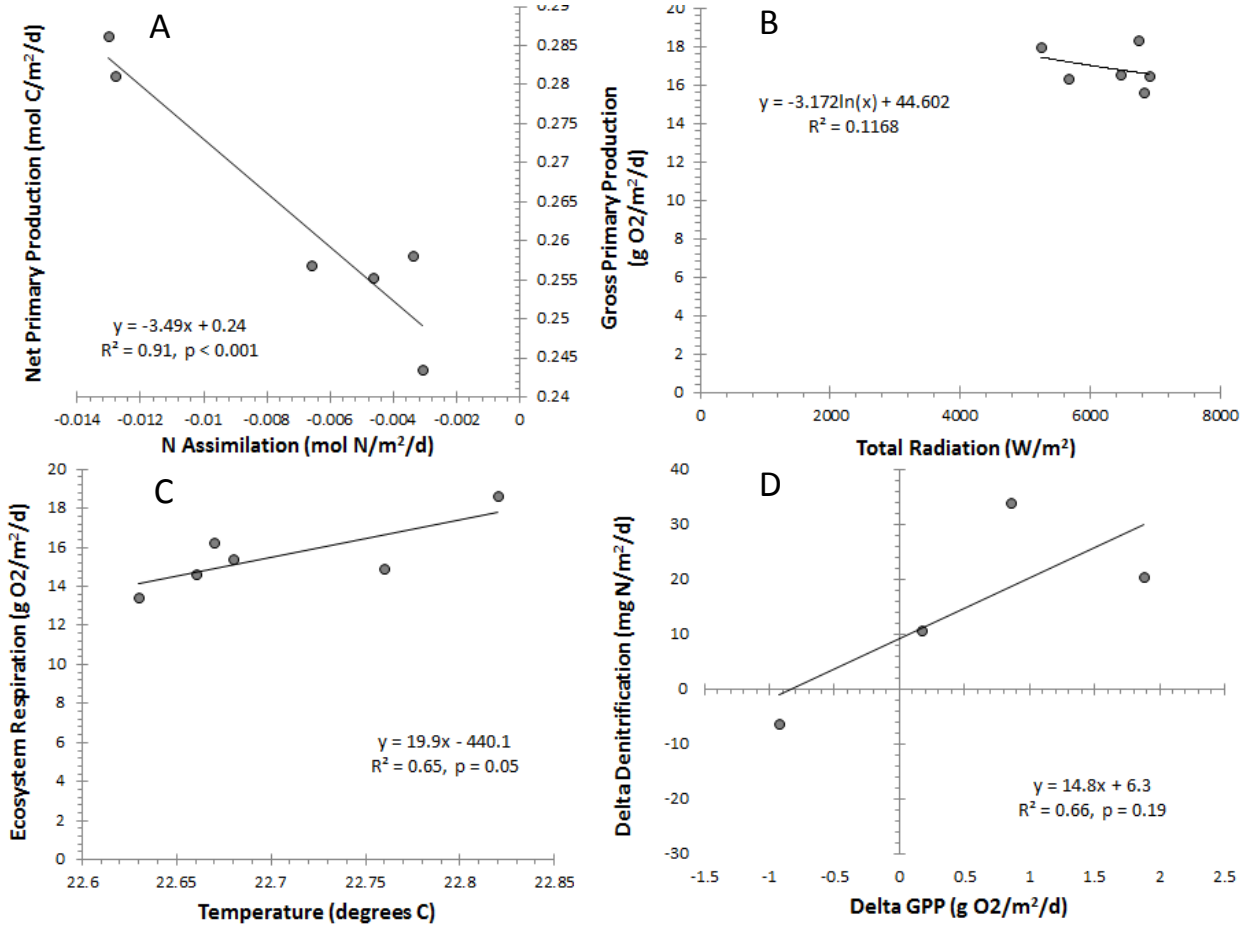

*Fig. 2-17 – Summary of interrelated elements of ecosystem C and N metabolism from Alexander Springs Creek, April 2010. A) Relationship between N and C assimilation (assuming net primary production = 0.5 * gross primary production) on a molar basis. While we cannot draw inference in the standard way from this graph (because the diel nitrate signal is inverted, yielding negative assimilation estimates) we note that the statistically significant relationship between NPP and diel N removal suggests that the magnitude of the nitrate peaks are somehow proportional to the magnitude of production, but DO NOT suggest the assimilation mass. B) Relationship between GPP (in g $O_2/m^2/d$) and incoming solar radiation (W/m^2), with a best fit line. C) Relationship between ecosystem respiration (g $O_2/m^2/d$) and minimum daily water temperature (degrees C). D) Despite the absence of a typical diel nitrate signal, we still observe suggestive (though not statistically significant due to low power) inter-day coupling of GPP and heterotrophic N removal (denitrification), indicating that day-to-day changes in GPP (in g $O_2/m^2/d$) explain 66% of the observed day-to-day changes in estimated denitrification (mg $N/m^2/d$).*

While the assimilation estimates are not reasonable for this system (they are negative; Fix. 2-17a), that diel variation continues to be a statistically significant function of GPP suggests that primary production still controls the amplitude of diel variation, even if that effect is not mechanistically related to autotrophic uptake. One explanation for the strong negative association (that is, where GPP increases,

the magnitude of diel variation actually decreases) may reflect the manner in which oxygen produced from GPP mediates other parts of the N cycle (e.g., by enhancing nitrification and inhibiting denitrification; see Research Element #7).

The association between incident radiation and primary production was far weaker in this deployment, possibly because radiation was high and constant throughout (Fig. 2-17b). It remains unclear whether a global GPP vs. radiation line should hold, particularly since the radiation estimates are not made directly on site. Suffice it to say, the absence of a significant association may suggest that light effects on primary production are saturated in this river and something else (e.g., N) limits GPP. One supporting observation for this observation is that much of the N demand in the algal mat is apparently satisfied from internal recycling pathways, and, as such, day-to-day controls on productivity derive from internal N supply mechanisms. We return to this discussion in a later section.

The relationship between temperature and respiration is still positive (Fig. 2-17c), but the parameters are highly implausible suggesting that the relationship may be spurious; the slope of 19 suggests that for each unit change on temperature there is a commensurate 19 g $O_2/m^2/d$ change in respiration, which is impossible. Given the extremely narrow range of nighttime temperatures, it seems reasonable to reject this relationship; one potential explanation is massive biofouling that occured towards the end of this deployment, which may have interfered with local DO dynamics around the sensor.

Finally, despite the fact that denitrification estimates are problematic using the standard method, there still appears to a positive though not significant association between the day-to-day variation in GPP and the associated day-to-day variation in the nighttime baseline concentration (Fig. 2-17d). While the relationship is not statistically significant, because there are only 4 data points (from 6 days), the orientation and parameters of the effect are strikingly similar to what has previously been observed.

Deployment 4: Ichetucknee River – January 2010 – January 2011

The Ichetucknee River is a special case deployment for this study; we have been monitoring the downstream station at Ichetucknee (at the US 27 bridge) for over a year now. Despite several extended blocks during which sensors failed (in every case battery or data logger attachment failures), we still can report on over 184 days of diel nitrate variation, 300 days of oxygen metabolism, and over 150 days with both on the same day. Regular sampling at the spring vents allows us to estimate with high precision

the flow weighted inputs to the system, and a continuous gage at the US 27 bridge allows us to estimate the hydrologic flows accurately. This unprecedented data set allows deep insight into the controls on spring river N metabolism, and offers a useful comparison to shorter term deployments implemented at all the other rivers studied for this work. Here we report a summary of this year of measurements, and some of the insights about coupling of C and N that have been obtained from this work.

Fig 2-18 shows the raw data from the extended deployment; the top panel shows both the density of gaps (particularly severe for the nitrate record) and the flow weighted inputs. There is marked diel variation on all days, and clear seasonality in both the baseline concentration (i.e., the nighttime maxima) and the amplitude of variation. Of particular interest is the period during mid-February when the river was back-flooded (due to flooding on the downstream Santa Fe River) such that stage was 7-8 ft higher than typical (dashed line, center panel). During this period, river flow was reduced substantially, and residence times lengthened such that assumptions about ascribing 24 hour deviations from the nighttime baseline may be problematic. A striking period of variation in baselines was observed during July of 2010 in response to a period of high rainfall and cloud cover, followed by a period of clear skies, and then by another period of lower insolation.

The dissolved oxygen and temperature records are not identical, suggesting that primary production does not display the same seasonal patterns as terrestrial ecosystems; maximum DO variation is observed in spring (March, April, May) while maximum above-canopy insolation and temperatures are observed between June and August; we note that the composition of the floodplain forest includes numerous deciduous trees, which may explain the phenology of GPP in this system. Also notable is the stability of nighttime temperatures during the summer, and much greater magnitude of nighttime temperature variation during the non-summer months. Finally, insolation and rainfall over the period of record are shown, with the relatively wet spring, normal (wet) summer and dry fall clearly evident.

As with other rivers, the reaeration rate dominates uncertainty in metabolism estimates. The method we used allowed us to empirically measure the K value on each day, and this information is summarized in Fig. 2-19. Two elements of this graph are particularly striking. First, the reaeration is relatively constant around 0.5 hr^{-1} for most the year, though some interesting changes accompany variation in discharge in August and December. Second, the reaeration constant drops during the high stage event in February (to ca. 0.2 hr^{-1}). Note that the model fit (r^2; brown triangles) is above 0.9 in 95% of the cases, and generally exceeds 0.95. This suggests that there are days on which the method does not

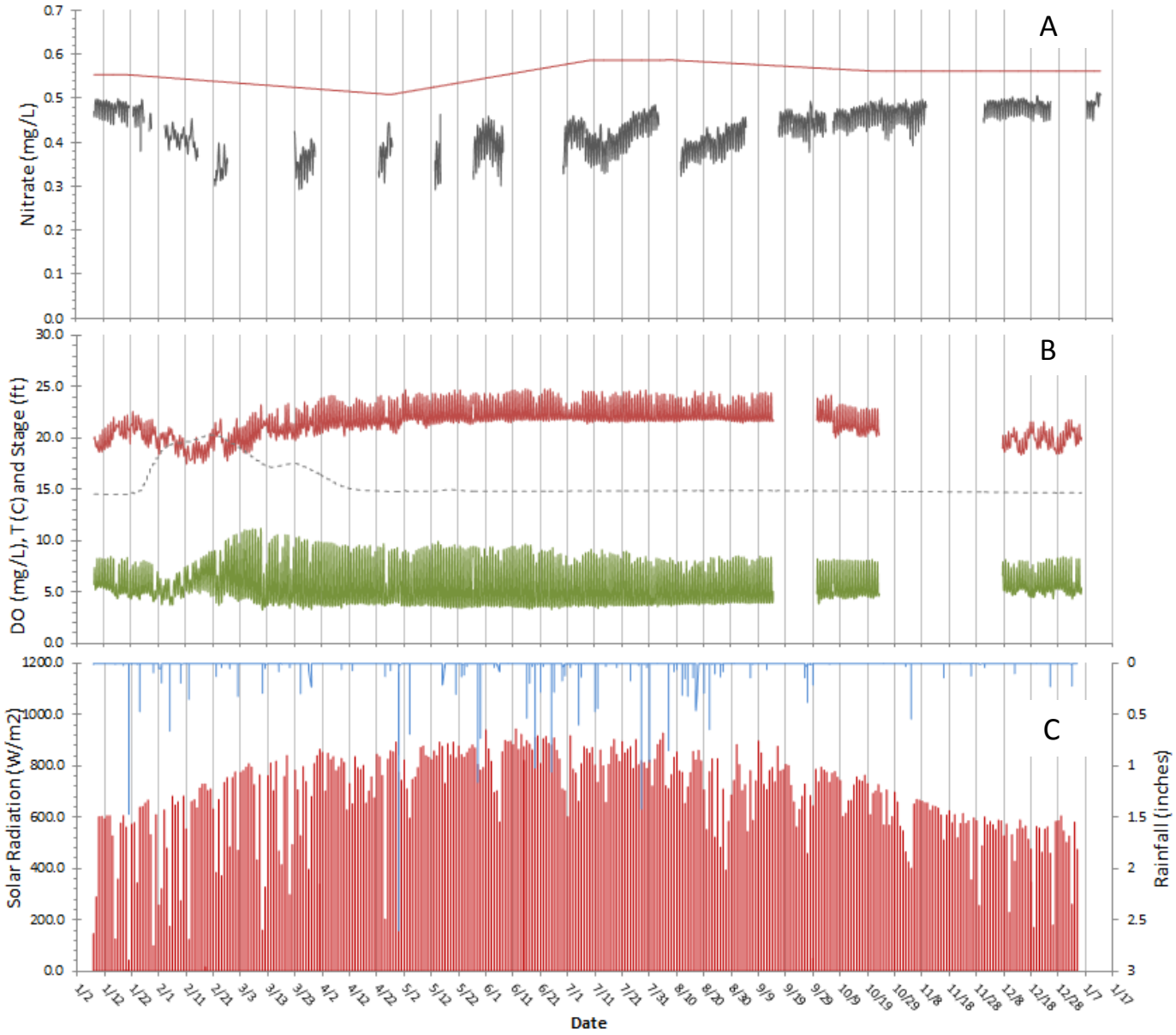

Fig. 2-18 – Raw data from the Ichetucknee River long term deployment showing A) nitrate concentrations at the US 27 bridge (mg/L, black line) as well as flow-weighted inputs (mg/L, red line); B) dissolved oxygen (mg/L, green line), stage (ft NGVD1929, dashed line) and water temperature (degrees C, red line), and C) nearby weather data showing solar radiation (W/m^2, red line) and rainfall (inches, blue line)

work (and a running average should be used), but that generally it delivers a robust integrated estimate of gas exchange between the river and atmosphere. Comparisons using dissolved gas tracers (e.g., SF_6 or propane) would confirm the adequacy of the method. Note that the period or record average discharge at US27 is 8.3 m^3/s, which is slightly less than the longer term average of 8.5 m^3/s since 2002 (range = 3.5 to 15.7 m^3/s).

The resulting estimates of GPP and R show a strong seasonal variation that is linked to photoperiod, canopy shading, and river discharge/stage (Fig. 2-20). GPP was low at the start (ca. 6 g $O_2/m^2/d$) and climbed markedly after the flood in February to a peak GPP of over 20 g $O_2/m^2/d$ in late March. For the remainder of the study period, GPP declined almost monotonically to values around 8 g $O_2/m^2/d$ in December of 2010. Respiration was also seasonally variable, and showed a much more marked response to the February high-stage event (because of the associated changes in reaeration). There is a notable symmetry to the GPP and R values over the study period (note that R is reported in negative units for figure clarity). We explore this statistically below.

On the second panel in Fig. 2-20, we show the estimates from the diel variation method for assimilation and denitrification. As with GPP and R, there is a striking seasonality to both measurements, assimilatory removal highest (ca. 130 mg $N/m^2/d$) in the period from April to June, and declining thereafter to a winter value around 60 mg $N/m^2/d$. Likewise, denitrification is highest in the late spring (between 800 and 1100 mg $N/m^2/d$), declining dramatically to a winter minimum of between 500 and 650 mg $N/m^2/d$. While the seasonal variation in assimilation is clearly expected based on the variation in GPP, the associated seasonal variation in denitrification once again reinforces the idea that primary production and denitrification are indirectly coupled via the effect of GPP on the availability of labile carbon to fuel the process. The fractional contribution to N removal from assimilation is 14.4%, and the variation around this value is small (SD = 4.4%). In short, denitrification dominates N removal in this river, as has been observed for the other rivers.

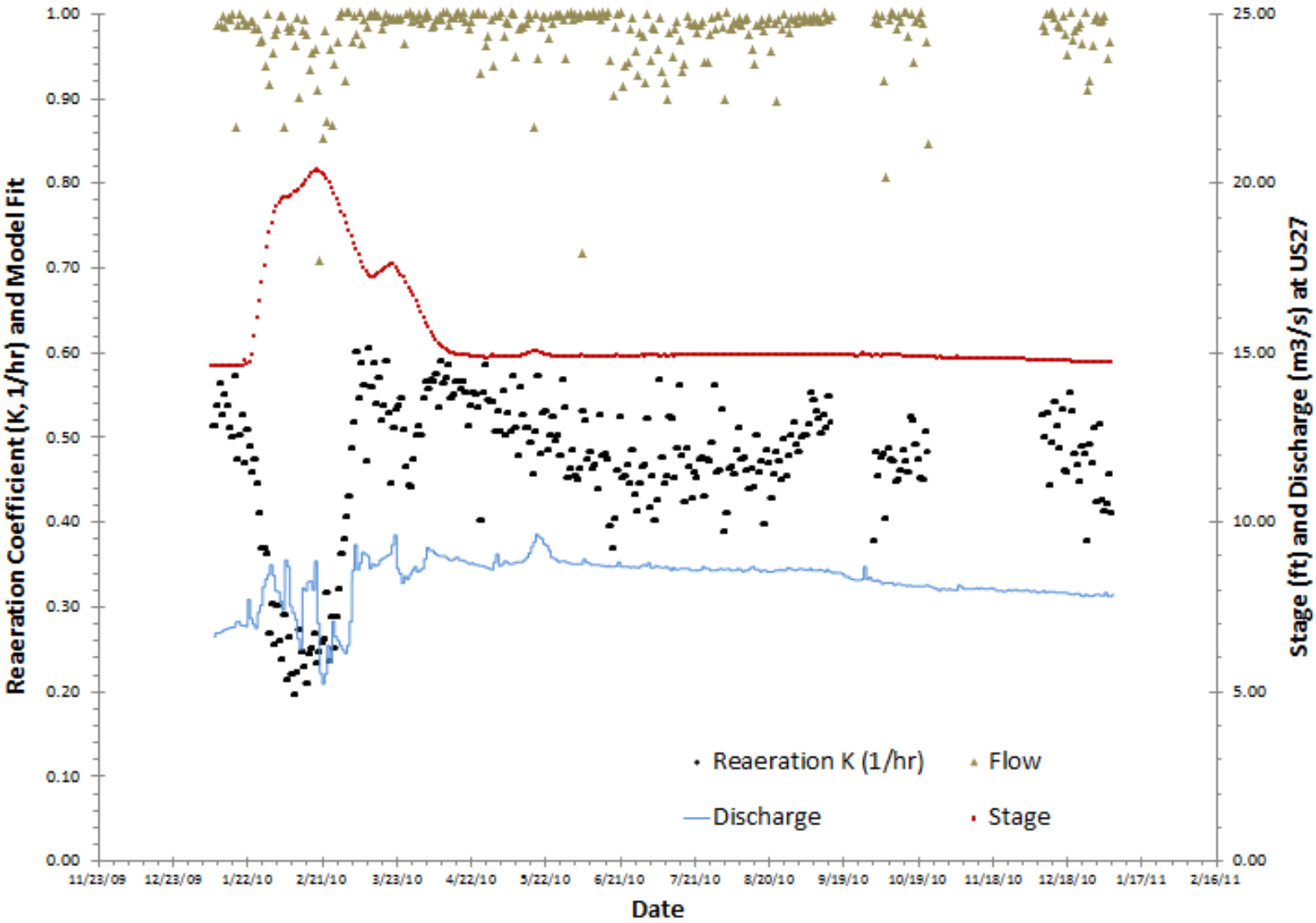

Fig. 2-19 – Results from the Ichetucknee River long term deployment showing the estimated reaeration constant (K, hr^{-1}) for each day (black dots). Also shown are river discharge (m^3/s) and stage (ft) at the US 27 bridge, as well as an estimate of goodness of fit (r^2) for estimating K from nighttime DO dynamics.

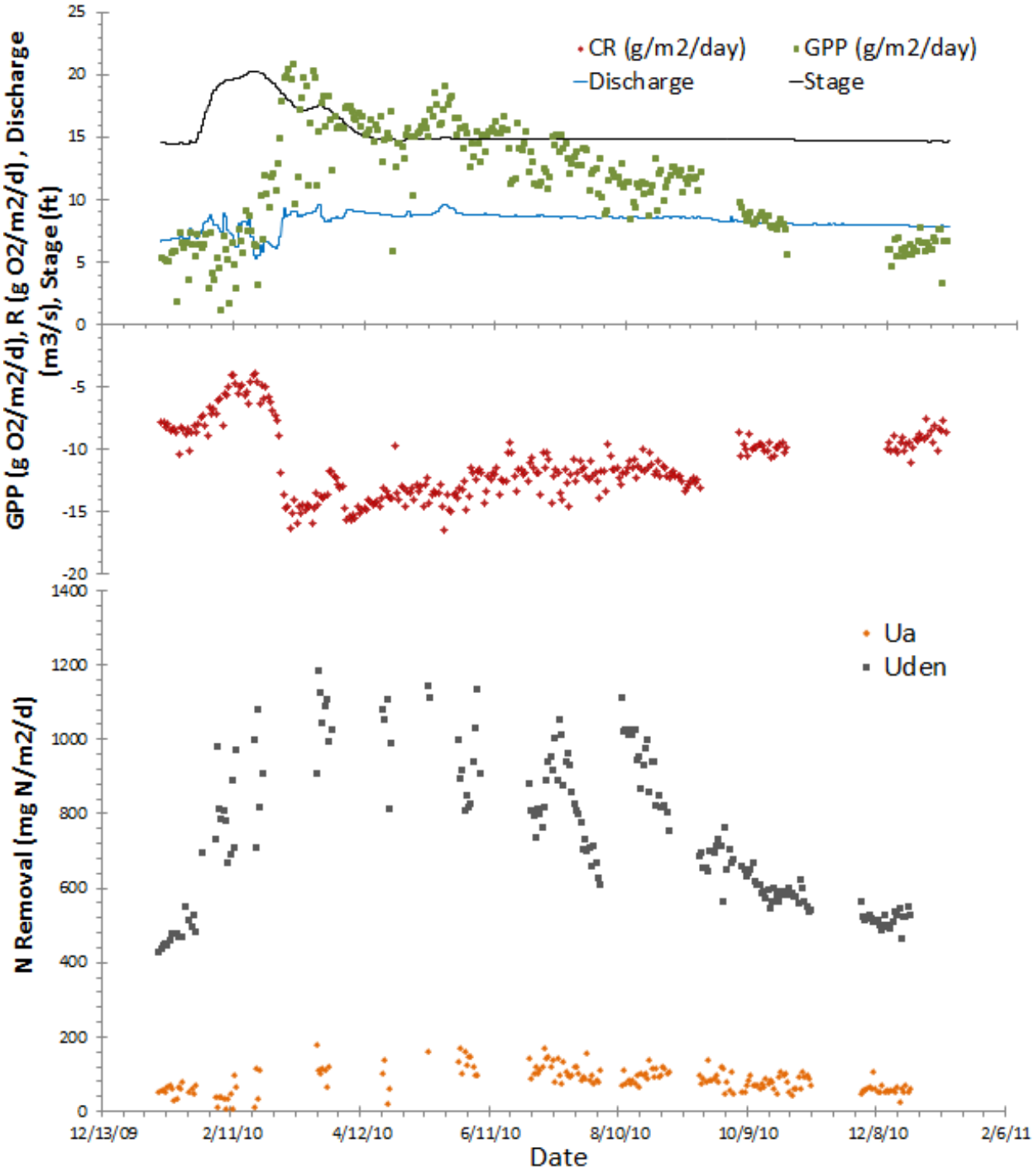

Fig. 2-20 – Results from the Ichetucknee River long term deployment showing A) riverine GPP and R (g $O_2/m^2/d$), discharge (m^3/s) at the US 27 bridge, and stage (ft) at the same location over the period of record. Note that R is reported in negative units for figure clarity. B) Estimates of denitrification and N assimilation for the same period (mg $N/m^2/d$).

Analysis of process coupling is more statistically powerful in this data set (Fig. 2-21). As with Rainbow and Silver, there is a strong covariance between NPP and U_a (Fig. 2-21a), with the fitted slope equal to 25.4; this value is the C:N ratio of primary production in this system. Seasonal and structural variation in this quantity is explored below. We interpret this to mean that primary production in this river system is generally dominated by vascular plants, a finding consistent with observations of the dominance of submerged aquatic vegetation in this river.

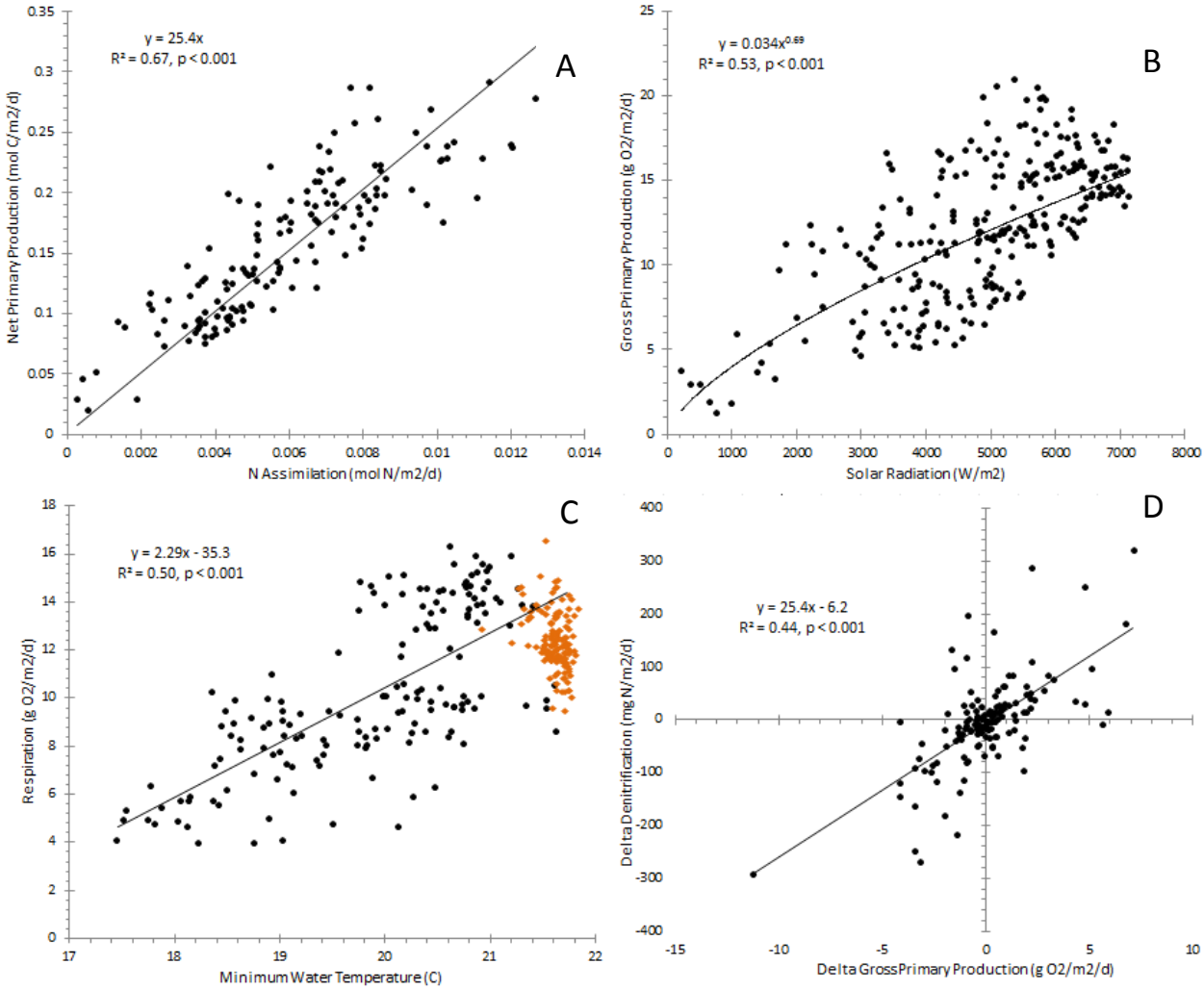

Fig. 2-21 – Results from the Ichetucknee River long term deployment showing A) Molar rate of C fixation (mol C/m^2/d) vs. estimate N assimilation (mol N/m^2/d). Slope of the line is the mean C:N ratio of ecosystem metabolism over the period or record. B) Association between incident radiation (W/m^2) and gross primary production (g O_2/m^2/d) showing strong but saturating relationship. C) Respiration (g O_2/m^2/d) vs. mean minimum temperature (degrees C), showing both winter dates (black dots) and summer dates (orange dots); linear fit is for winter only. D) Coupling of primary production and denitrification, showing how day-to-day changes in GPP (g O_2/m^2/d) result in concomitant changes in denitrification (mg N/m^2/d) the following day.

As with other rivers, there is strong concordance between light and GPP (Fig. 2-21b); a power function was the best fit, but scatter in the data mean that linear and logarithmic fits are equally plausible. This relationship is consistent with light limitation of ecosystem productivity, but also suggests that at the high end of insolation values, there is considerable scatter. This may be because insolation data are obtained from an open space (Alachua FAWN site), and therefore fail to capture the phenological effects of canopy closure in early summer. Similarly, distance of the FAWN site (ca. 20 km away) from the river means that local thunderstorms may not be uniform, and days with high insolation at the FAWN site may not be as sunny at the river. Continuous irradiance measurements at the springs would benefit the accuracy of this association, particularly because longitudinal changes in channel morphology make for distinct light environments; even without those, it is clear that light controls GPP. Our confidence in the presence of light saturation (implied by the power function) is low because the sensor measurements are a poor proxy for actual light conditions along the river; in other words, shading during the high insolation months is as plausible an explanation for the observed behavior as is light saturation.

Respiration is expected to be temperature sensitive; Fig. 2-21c shows that this is the case, but only for the winter observations (black dots); remarkable thermal stability during the summer (orange dots) occludes any temperature sensitivity, making variation in respiration much more a function of the estimated reaeration rate and/or labile carbon availability than temperature. Notably, the best fit line for the winter temperature-respiration relationship has a slope parameter that is much larger than has been previously observed (2.3 vs. 0.9 – 1.1). This could suggest that respiration is more temperature sensitive in this river, though the reasons for that difference are unclear, but are likely more a function of the strong covariance between GPP and R (see below) and a modest correlation between GPP and temperature; since this is the most northern site, a climatic control may also be possible. In other words, at least part of this correlation may be confounded by other factors, namely the availability of labile C for ecosystem respiration. If the strong temperature sensitivity stood up to additional scrutiny, this association would imply a large change (2.3 g $O_2/m^2/d$) for each unit change in temperature, making the Ichetucknee particularly vulnerable to changes in water recharge temperature that may be changing with global warming. Other local disturbances of note (e.g., recreational impacts on metabolism) remain largely unquantified despite recent efforts (WSI 2011).

Finally there is an unequivocal relationship between GPP and denitrification (Fig. 2-21d). The slope of the line suggests that for each unit change in GPP there is a 25 mg $N/m^2/d$ change in denitrification, which corresponds to 3-5% of the total. Given the marked variation in GPP (changes ranged from -11 to

+7 g $O_2/m^2/d$), this means that short term variation in GPP controls a substantial fraction of the variation in denitrification. Moreover, this does not capture the strong seasonal variation in U_{den} that appears correlated (Fig. 2-20) to GPP. We explored longer lag cross-correlation and found significant positive correlation at a 14-day lag, and a significant negative correlation at 9 day lag, but in each case these were barely above the white-noise background, and may be incidental. In short, the cross-correlation is the strongest on the next day, and then governed by mean seasonal variation.

Strong correspondence between GPP and R observed qualitatively in Fig. 2-20 is analyzed formally in Fig. 2-22a. There is a strongly significant positive correlation between GPP and R. This suggests that both respond to the same external driver (e.g., sunlight and temperature), but is also consistent with a direct link between recent GPP and R based on availability of labile organic carbon. Notably, the slope is significantly less than one, meaning that variation in respiration is smaller than, and potentially lags, variation in GPP. Even at zero primary production, that linear model predicts 5.2 g $O_2/m^2/d$ respiration. Fig 2-22b shows an analysis designed to test day-to-day coupling on P and R. We observe modest evidence of such short term coupling, with a statistically significant positive association. We note that the r^2 is comparatively small (7% of the variation in ΔR can be explained by variation in ΔGPP).

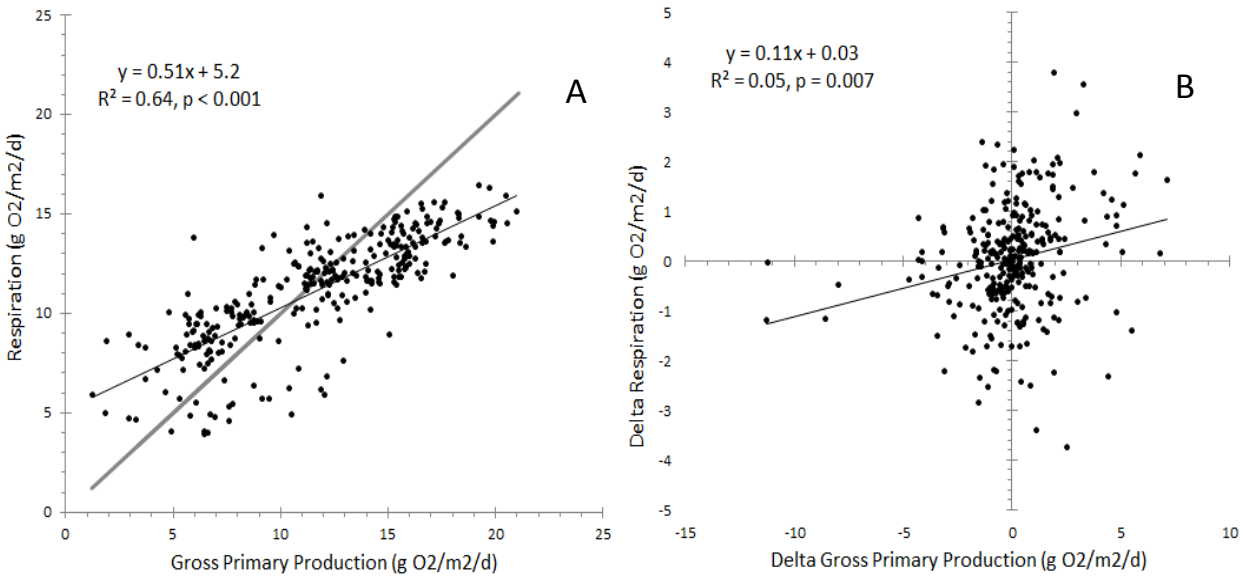

Fig. 2-22 – a) Association between GPP and R in the Ichetucknee River. Shown are instantaneous values of P and R, the best fit line, and the 1:1 line. Over the entire period, P:R is 1.1:1, but varies substantially. During periods of low GPP, baseline R remains high (intercept = 5.2 g $O_2/m^2/d$), and R varies less annually (mean ± SD: 11.1 ± 2.77 g $O_2/m^2/d$) than GPP (11.7 ± 4.3 g $O_2/m^2/d$). b) Inter-day coupling of P and R, showing weak but statistically significant positive coupling between day-to-day changes in GPP and associated changes in R.

Day-to-day variation in the C:N ratio of ecosystem metabolism is clear in Fig. 2-21a; we plotted that ratio over time to see if there are systematic patterns. What we observed (Fig. 2-23a) suggests that during the spring there is a slight tendency towards a higher C:N ratio, with lower values in the winter. However, within each month, there is significant short term variation, possibly as a result of uncertainties in the method. However, when we plot the C:N ratio vs. GPP we see modest evidence of a relationship consistent with expectations. That is, we would predict, based on how plants allocate resources, that as GPP increases, N demand can be more readily saturated and the plant begins to invest in N-poor energy storage compounds. As such, we would expect higher bulk C:N ratios at high GPP. The relationship is statistically significant at the p = 0.05 level (Fig. 2-23b) but explains only a small fraction of the variation; we present these data as warranting additional scrutiny. Controls on C:N ratios in ecosystem metabolism may also be phenological; plants and algae grow and die in relatively consistent annual patterns, and the relative abundance of these autotrophs may control the ecosystem scale production as expressed by the C:N ratio. Mechanisms to explain the significant short term variability in C:N are not yet clear, and represent an interesting avenue for basic lotic ecosystem research.

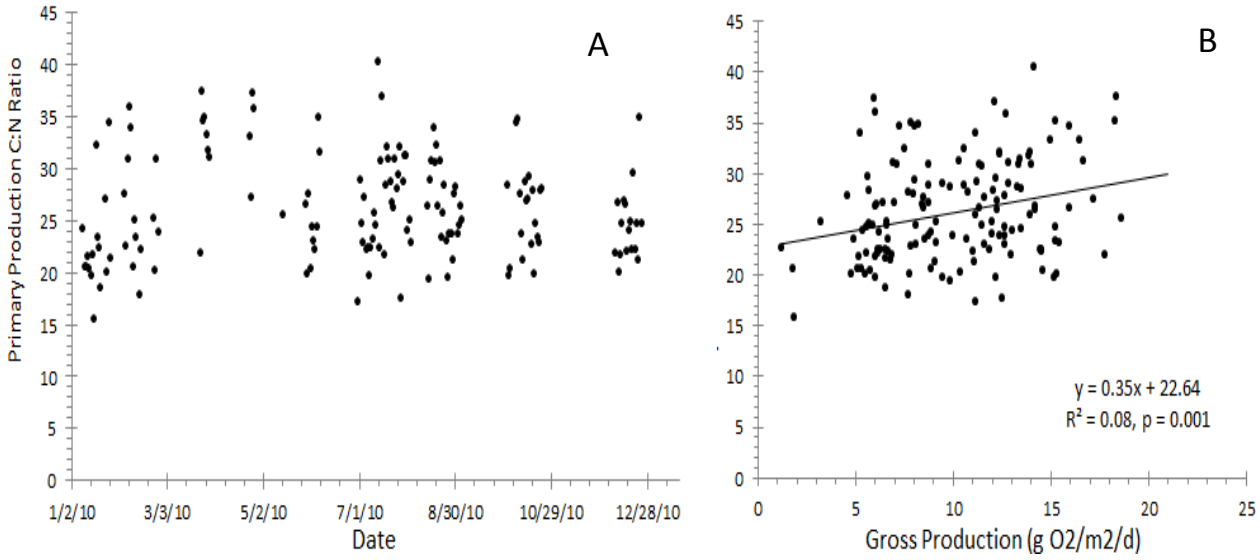

Fig. 2-23 – A) Molar ratio of primary production over time in Ichetucknee River. Overall mean C:N is 25.4 for the period of record. B) Molar ratio of primary production vs. GPP in the Ichetucknee River. The positive association suggests reduced N requirements at high primary production, consistent with physiological allocation theory.

Deployment 5: Gilchrist Blue Run – April 2010

Deployment at Gilchrist Blue Springs run in April 2010 lasted 19 days, and exhibited considerable variation in both sensor noise (high at the outset, low later in the deployment), and weather conditions (Fig. 2-24). Marked diel nitrate variation was clearly evident, with enormous drift (ca. 40 µg/L) in the nighttime baseline over the period. Because we obtained vent water concentration measurements using the SUNA only at the beginning of each deployment, we cannot rule out that the inflow concentration may have changed over the deployment, but the dynamics of that change are unknown.

Similar diel variation was observed for dissolved oxygen and temperature. Temperature exhibits odd nighttime behavior suggesting long residence time flowpaths. Hydraulic data confirm the presence of a long tail, and the geometry of the boil area (with large transient storage zones evident in the hydrilla beds) supports this explanation. Nighttime DO concentrations are high reflective of high boil DO (measured 4.4 mg/L). Note observed variation occurs over a short (350 m) narrow (20 m) run.

Weather conditions during the deployment were variable, with one extremely cloudy day (4/25) and two nights with considerable rainfall (4/30 and 5/4). Both of the rain days created strong dilution signals, presumably from direct runoff.

The reaeration rate for the period was determined as for the other springs. Values ranged between 0.44 and 0.6 hr^{-1}, with an average of 0.52hr^{-1}. Because of some uncertainty with two of the days with larger values (due in part to rain events), we used the mean value for all days of the deployment (0.52hr^{-1}).

The diel method works in this river system, but there was some uncertainty created by a shifting input baseline (Fig. 2-25). At some point during the deployment, the concentration may have shifted slightly (apparently upwards); we measured 1.9 mg/L at the outset, but using this value for the entire deployment means comparatively low denitrification rates during the middle of the deployment. If the nitrate concentration of the boil increased over the deployment (and the inputs from rainfall make such a scenario plausible) we would fail to capture that. This observation underscores the method's sensitivity to upstream boundary conditions.

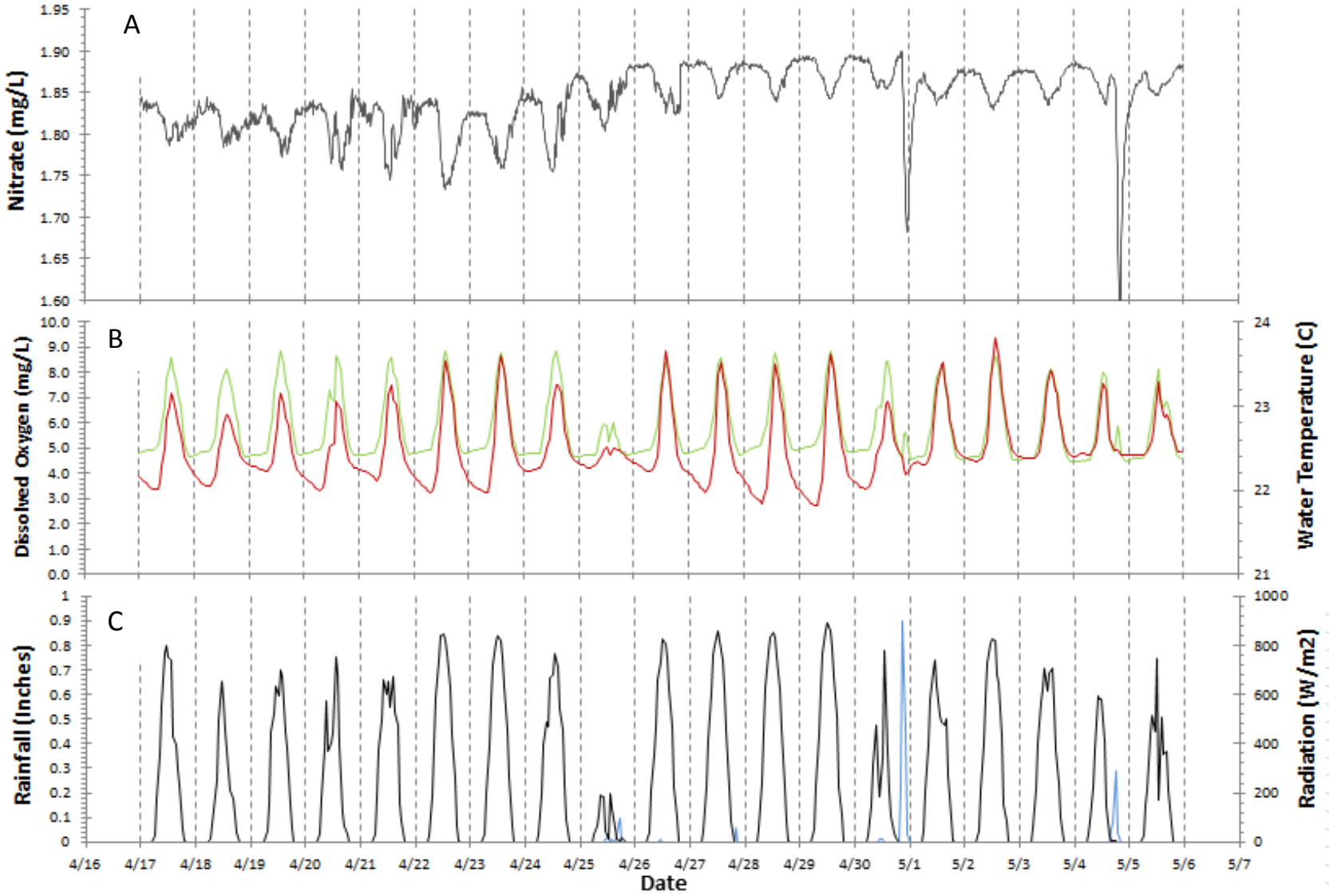

Fig. 2-24 - Diel variation in nitrate (grey line), dissolved oxygen (green line), water temperature (red line), radiation (black line) and rainfall (blue line) for Gilchrist Blue Springs run during an April 2010 deployment. Vertical dashed lines are at midnight every 24 hours.

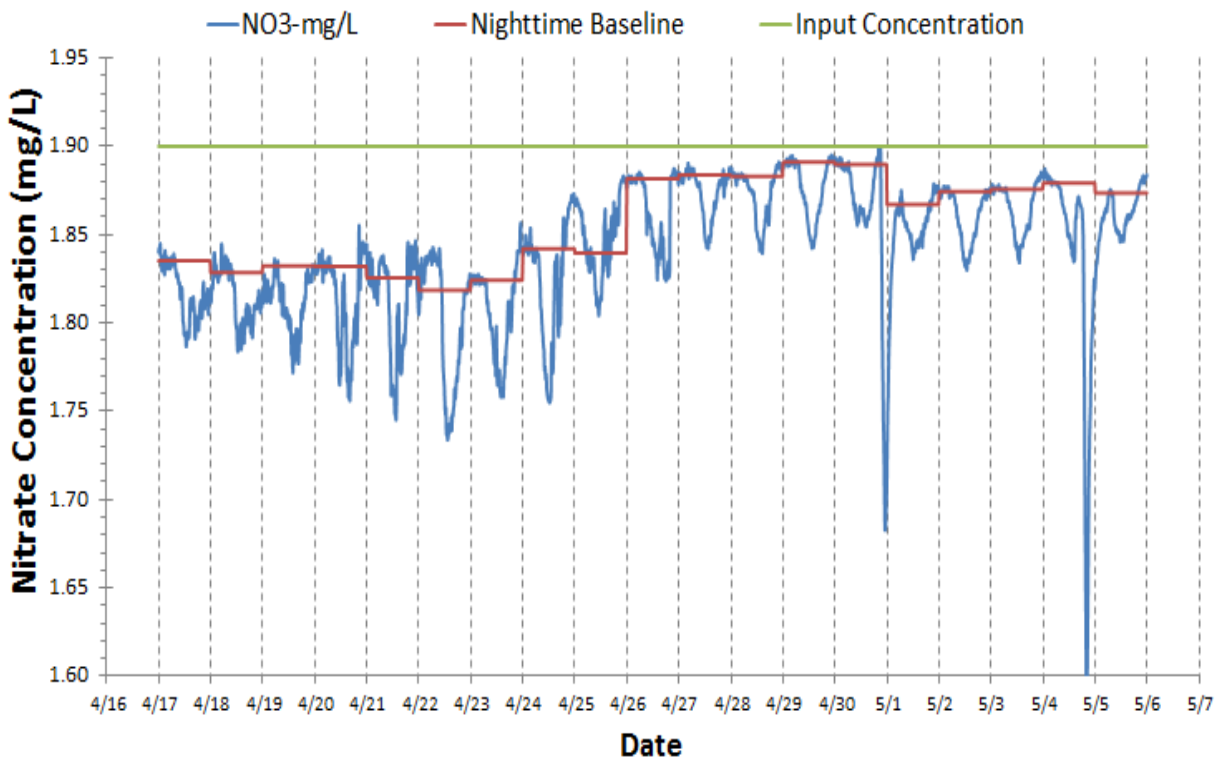

Fig. 2-25 – Summary of N removal mechanism inference. Assimilatory removal is estimated based on diel variation in nitrate (blue line) referenced to a nighttime baseline value (red line). Dissimilatory removal is estimated as the mass loss between upstream input concentrations (green line) and the nighttime baseline; that is, denitrification is assumed constant over the course of each 24-hour period. Day-to-day variation in the nitrate baseline is explored below.

A summary of system GPP and R (Fig. 2-26) indicates that the river is in metabolic balance (P:R = 0.91) except on 4/25 when GPP was dramatically reduced due to low insolation. Both P and R are extremely high (mean P = 13.7 g $O_2/m^2/d$, mean R = 15.2 g $O_2/m^2/d$) consistent with high productivity during the spring and early summer. We also note that recreational impacts on the vegetation, which can be dramatic by the end of the summer, were not yet evident at the time of this deployment. N assimilation is also high (mean U_a = 134 mg $N/m^2/d$), consistent with high GPP (Fig. 2-26). Denitrification was variable, but relatively high (mean U_{den} = 518 mg $N/m^2/d$); the range of observations was from over 900 (4/22) to around 100 mg $N/m^2/d$ (4/29). Assimilation was a slightly larger fraction of removal than in other rivers (ca. 20.1%), but still comparatively small.

Finally we present data to suggest that this smaller spring run (Q = 1.07 m^3/s) shares many of the properties of the other larger spring fed rivers. Specifically, we observed a strong association between

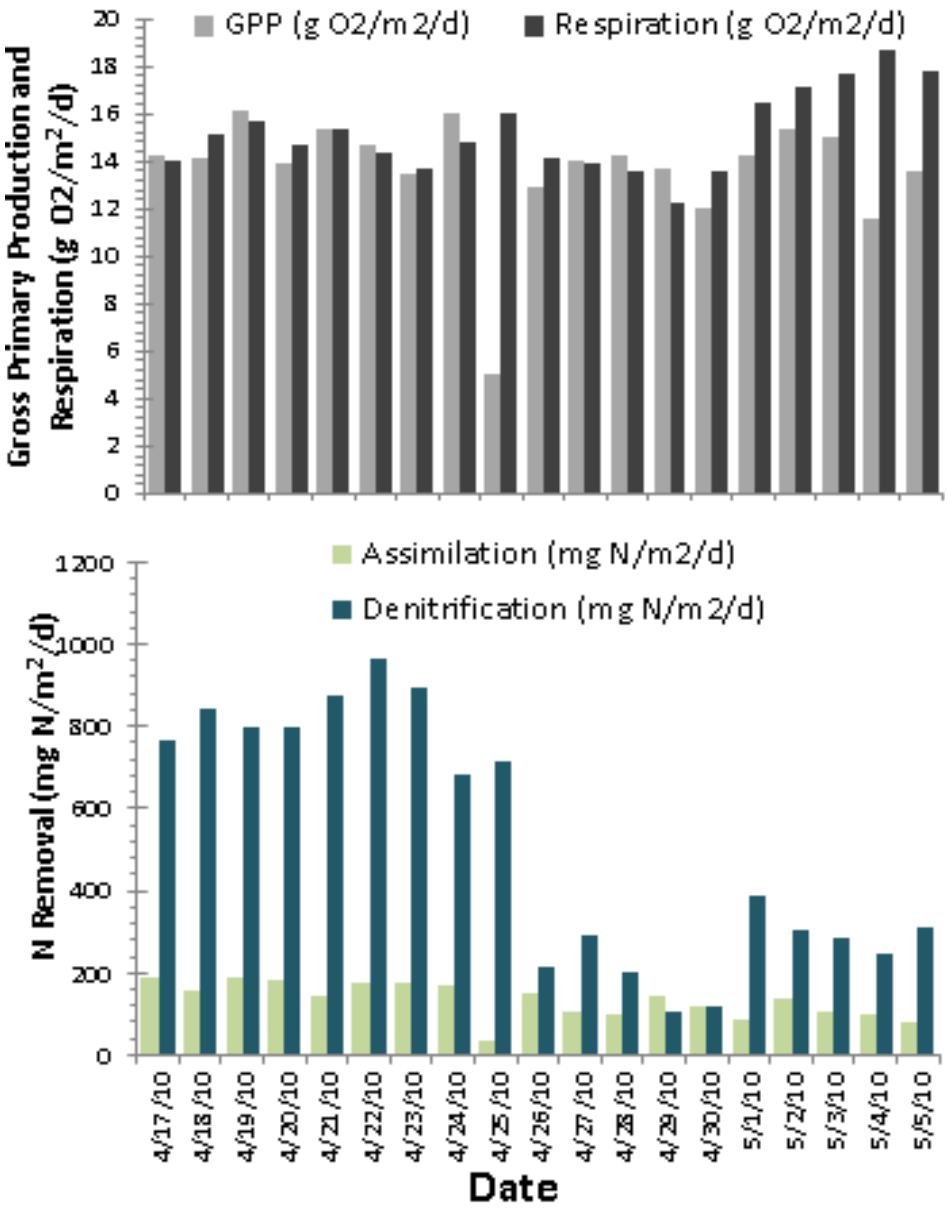

Fig. 2-26 – Summary of April 2010 deployment at Gilchrist Blue run showing estimates of gross primary production and respiration (top panel) and assimilatory and dissimilatory N removal (bottom panel).

NPP and U_a such that the mean C:N ratio of assimilation was just over 24:1 (Fig. 2-27a). We also observed strong insolation controls on GPP (Fig. 2-27b), strong temperature effects on respiration (Fig. 2-27c) and a statistically significant signal suggesting indirect coupling between GPP and U_{den} (Fig. 2-27d). This last relationship, now widely observed, suggests that a unit change in GPP results in a 27 mg $N/m^2/d$ change in U_{den}, or about a 6% change. This fractional effect is larger than in other systems. Overall, despite more shading and starkly different channel morphology, this river behaves broadly like other large N-rich spring run streams.

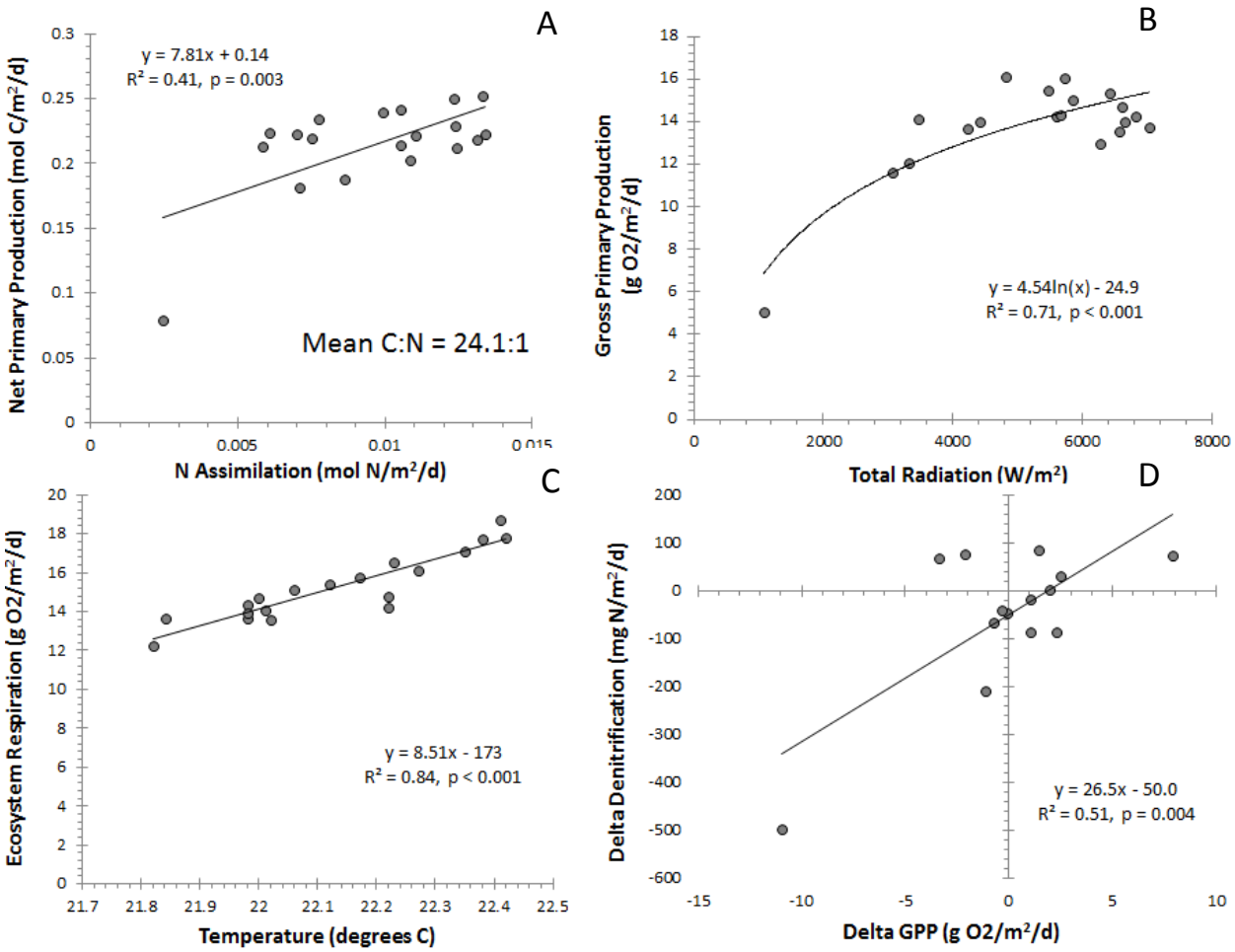

*Fig. 2-27 – Summary of ecosystem C and N metabolism from Gilchrist Blue Spring run, April 2010. A) Relationship between N and C assimilation (assuming net primary production = 0.5 * GPP) on a molar basis. The fitted slope of the dashed line (intercept forced through 0) indicates C:N stoichiometry of ecosystem metabolism is ca. 24:1. B) Relationship between GPP (in g $O_2/m^2/d$) and incoming solar radiation (W/m^2), with a best fit line. C) Relationship between ecosystem respiration (g $O_2/m^2/d$) and minimum daily water temperature (degrees C). D) Strong inter-day coupling of GPP and heterotrophic N removal (denitrification), showing that day-to-day changes in GPP (in g $O_2/m^2/d$) explain 51% of the observed day-to-day changes in estimated denitrification (mg $N/m^2/d$).*

<u>*Deployment 6: Silver River – October 2010*</u>

A second deployment on the Silver River took place in early October, 2010. During this 9 day deployment, we had sensors at both upstream and downstream locations, and present results for both of these. Note, however, for this and subsequent two-station deployments, we estimate GPP, R, U_a and U_{den} for each reach. As such, the downstream station includes the area captured by the upstream stations. Two-station approaches are entirely tenable with these sensors, but methodological details

remain under consideration. Note that the two station method compounds any sensor error by utilizing the difference between two sensors (one upstream and one downstream).

The raw data (Fig. 2-28) show substantial diel variation in both sensors. Notably, the amplitude of diel variation at upstream and downstream locations is comparable (ca. 35 μg/L), but the pattern of diel variation is markedly different, with the width of the daytime troughs much larger downstream. As with previous Silver River deployments, there is uncertainty about the hydraulics at the lower sensor location, specifically whether the daytime assimilation signal is complete before the next day's signal starts. The possibility for day-to-day carryover of the assimilation signal is consistent with the sinusoidal signal (i.e., without a persistent nighttime high). However, based on the hydraulic measurements made in the Silver River, the fraction of water with a residence time longer than 12 hours is small (<10%). As such, we proceed with the inference of assimilation for a day based on the standard method used for all the other rivers in this study. Note that any errors likely would also apply to metabolism estimates.

Similar patterns were observed with dissolved oxygen and temperature, with similar (or even lower) amplitude of diel variation downstream, but much broader shape to the diel pattern (Fig. 2-28b). During the deployment there were no days with more than trace rainfall, and insolation patterns were remarkably constant (Fig. 2-28c).

Nitrate data from the two stations also suggests substantial denitrification in the upstream reach, with the nighttime baseline dropping nearly 110 μg/L between upstream and downstream stations (Fig. 2-29). Given the magnitude of flow on the Silver River during this deployment (15.5 m^3/s), this represents a tremendous mass of N removal; the upstream boundary condition for nitrate (1.38 mg/L) was measured upstream of the 1200 m station after all of the major spring vents have entered the river. The diel method for estimating mechanisms of N loss appears highly robust for this deployment despite slightly greater instrument noise observed at the downstream station.

A summary of estimates of GPP and R for the upstream and downstream reaches (Fig. 2-30) suggests higher productivity in the upper reach (mean GPP = 20.0 g $O_2/m^2/d$), and slightly net autotrophic conditions (mean P:R = 1.21). In contrast, the entire river, integrated down to the confluence with the Ocklawaha exhibits lower productivity (mean GPP = 10.9 g $O_2/m^2/d$) and more of a balance between autotrophy and heterotrophy (P :R = 1.07). The dramatic drop in GPP may have something to do with changes in river morphology (the river is markedly wider in the upper reach than the lower), or river clarity (all spring rivers exhibit longitudinal declines in water clarity – Duarte et al. 2010). Note that

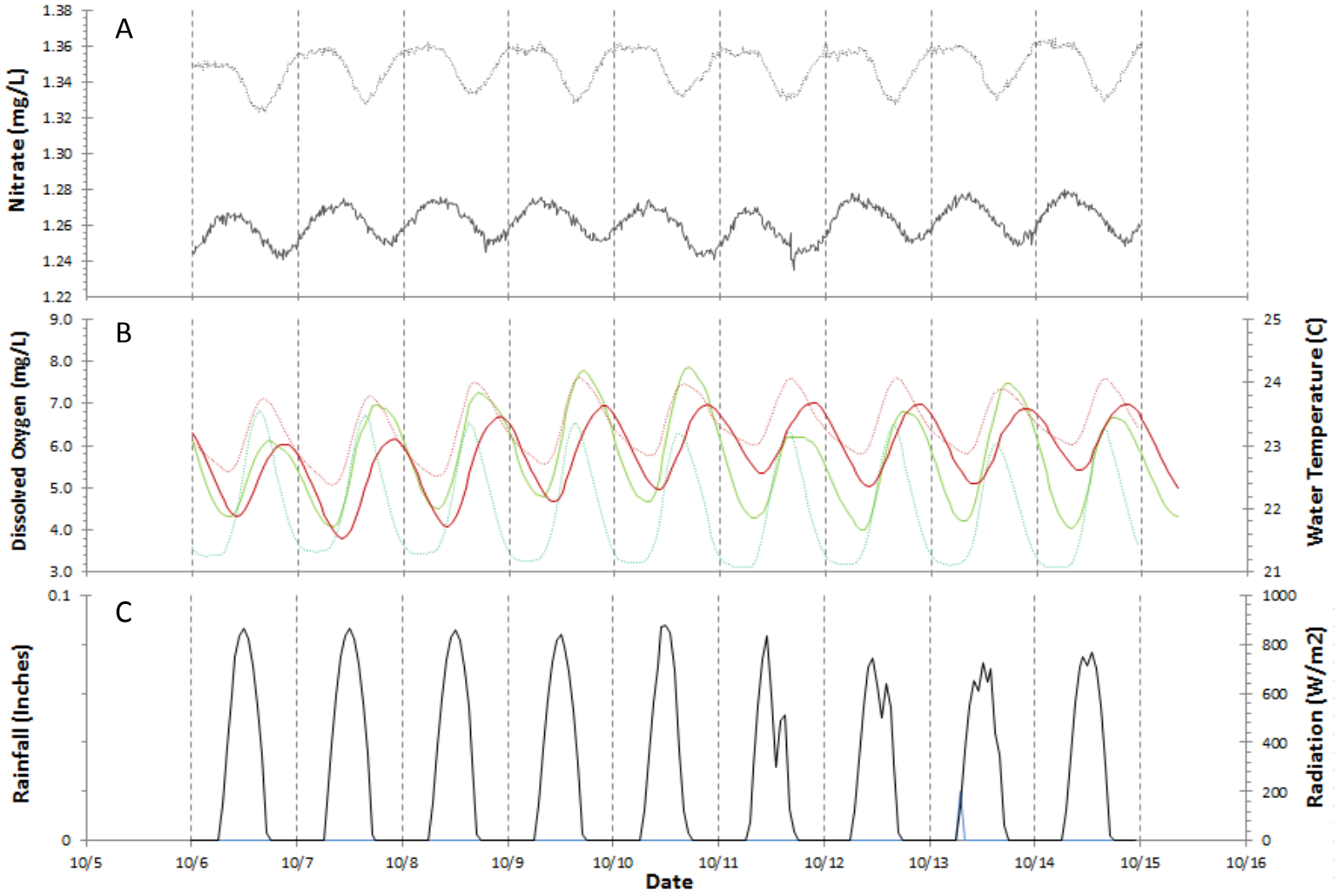

Fig. 2-28 - Diel variation in nitrate (solid grey line – downstream, dashed grey line - upstream), dissolved oxygen (sold green line – downstream, dashed green line – upstream), water temperature (solid red line – downstream, dashed red line – downstream), radiation (black line) and rainfall (blue line) for Silver River during an October 2010 deployment. Vertical dashed lines are at midnight every 24 hours.

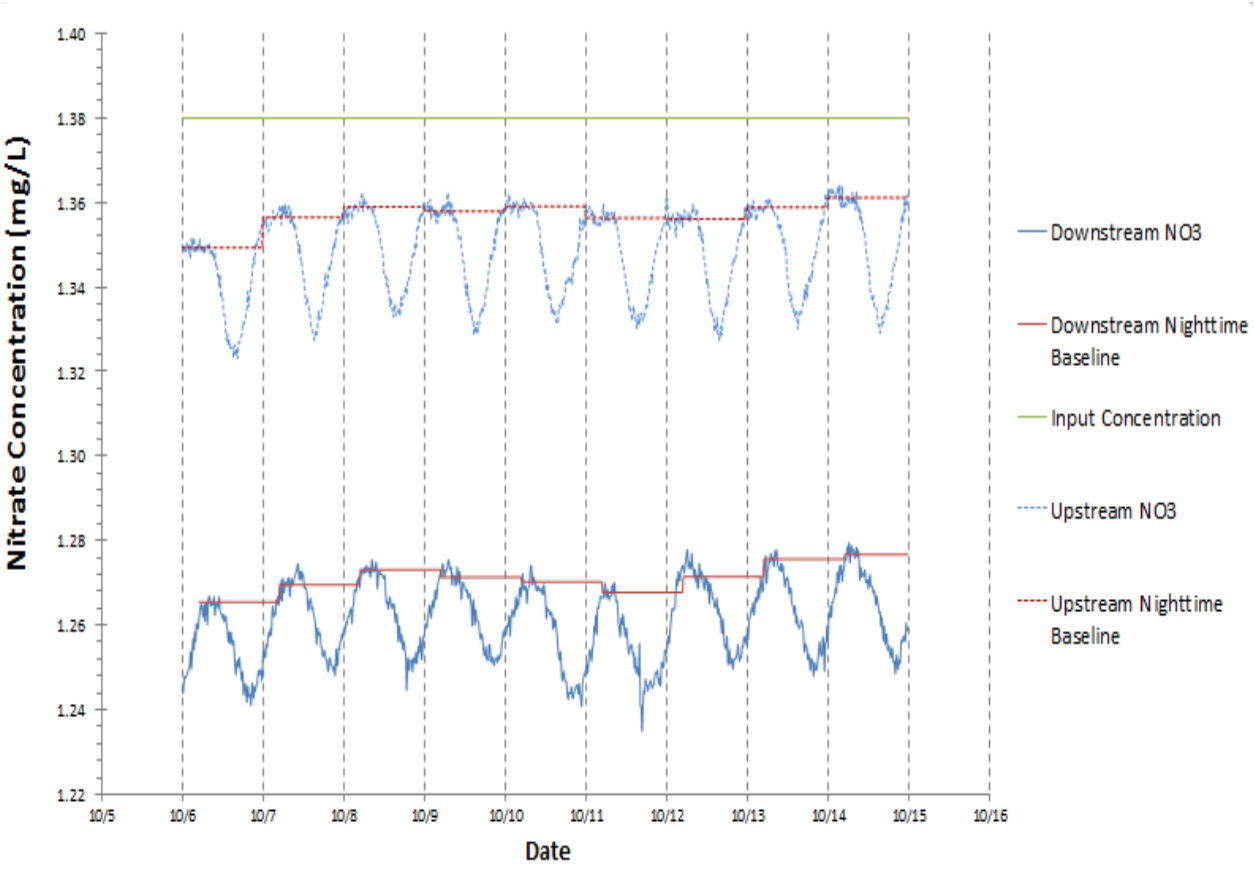

Fig. 2-29 – Summary of N removal mechanism inference for Silver River, October 2010. Assimilatory removal is estimated based on diel variation in nitrate (blue line; dashed – upstream, solid - downstream) referenced to a nighttime baseline value (red line; dashed – upstream, solid - downstream). Dissimilatory removal is estimated as the mass loss between upstream input concentrations (green line) and the nighttime baseline; that is, denitrification is assumed constant over the course of each 24-hour period. Day-to-day variation in the nitrate baseline is explored below.

these metabolism estimates are dependent on the reaeration rates for both, which averaged 0.35 hr^{-1} in the upper river and 0.42 hr^{-1} in the entire river.

A similar contrast is evident for assimilation (U_a) which averaged 122 mg $N/m^2/d$ in the upstream reach and 58 in the entire river. The estimates were remarkably consistent across the deployments with the standard deviations of 9.7 and 7.3 mg $N/m^2/d$, or roughly 10% of the mean. In contrast, U_{den} is higher in the entire river (on a per unit area basis) than in the upper river (336 mg $N/m^2/d$ upstream vs. 613 mg $N/m^2/d$ downstream). The potential reasons for this are multiple. First, because of the density of springs and seeps in the upper reach, which imply a positive potentiometric gradient (i.e., towards the

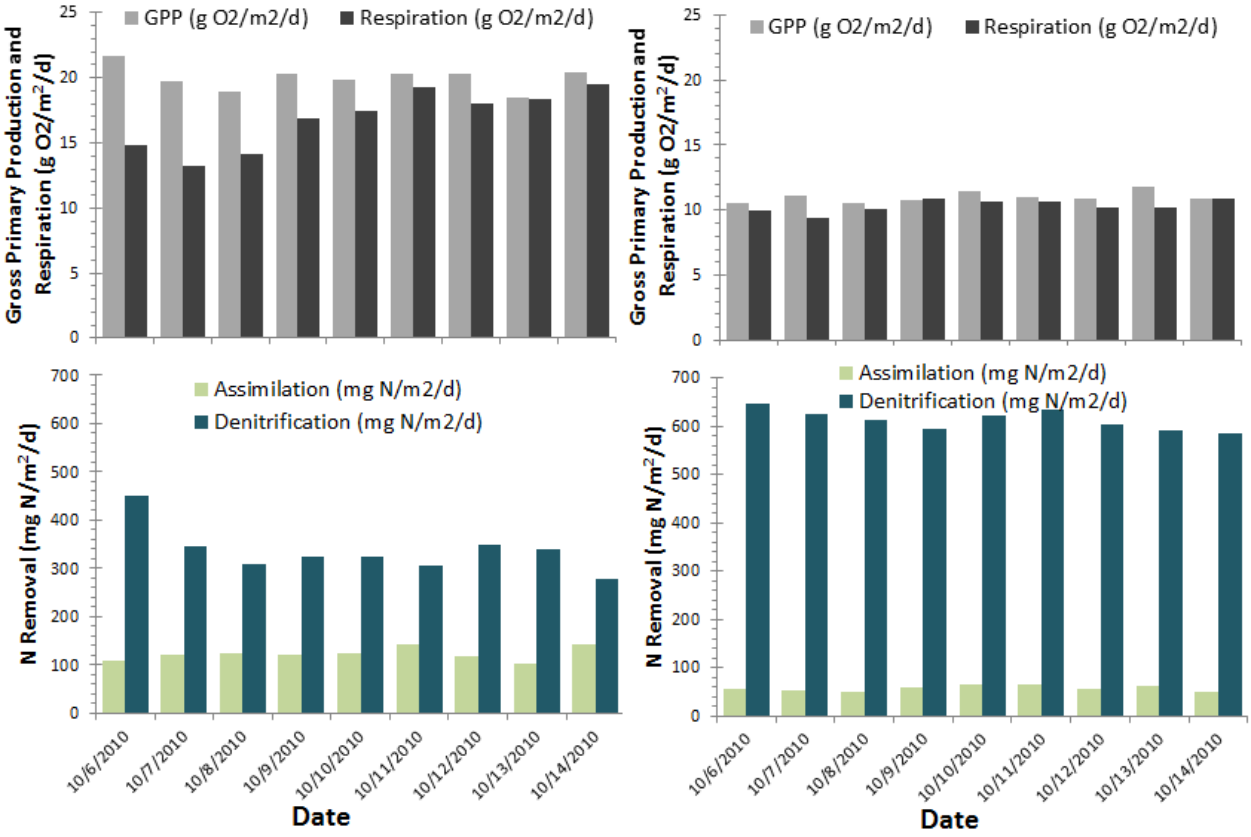

Fig. 2-30 – Summary of October 2010 deployment at Silver River showing estimates of gross primary production and respiration (top panels) and assimilatory and dissimilatory N removal (bottom panels) for both upstream (left panels) and downstream (right panels) reaches.

river) it may be more difficult for nitrate to interact with high OM low redox sediments. Further, greater interaction between the river water and the floodplain in the lower river may amplify denitrification.

As with previous deployments, we explore the direct coupling of primary production and assimilation, and observed a weak but significant positive association (Fig. 2-31a). One reason for the weak relationship may be the low range of variation during this deployment. We also note that the best fit line includes a significant positive intercept, suggesting some intrinsic non-linearity between assimilation of C and N, possibly as a function of changing stoichiometry with production rates. The best-fit line without an intercept (dashed line, Fig. 2-31a) suggests a C:N ratio of primary production of nearly 35:1 during this deployment. There was no significant association between solar insolation and GPP (Fig. 2-31b), suggesting light does not control day-to-day variation in production; note that the range of values over this short deployment are very small. As with other winter deployments, the association between nighttime water temperature and respiration is extremely strong and positive, but the slope is markedly

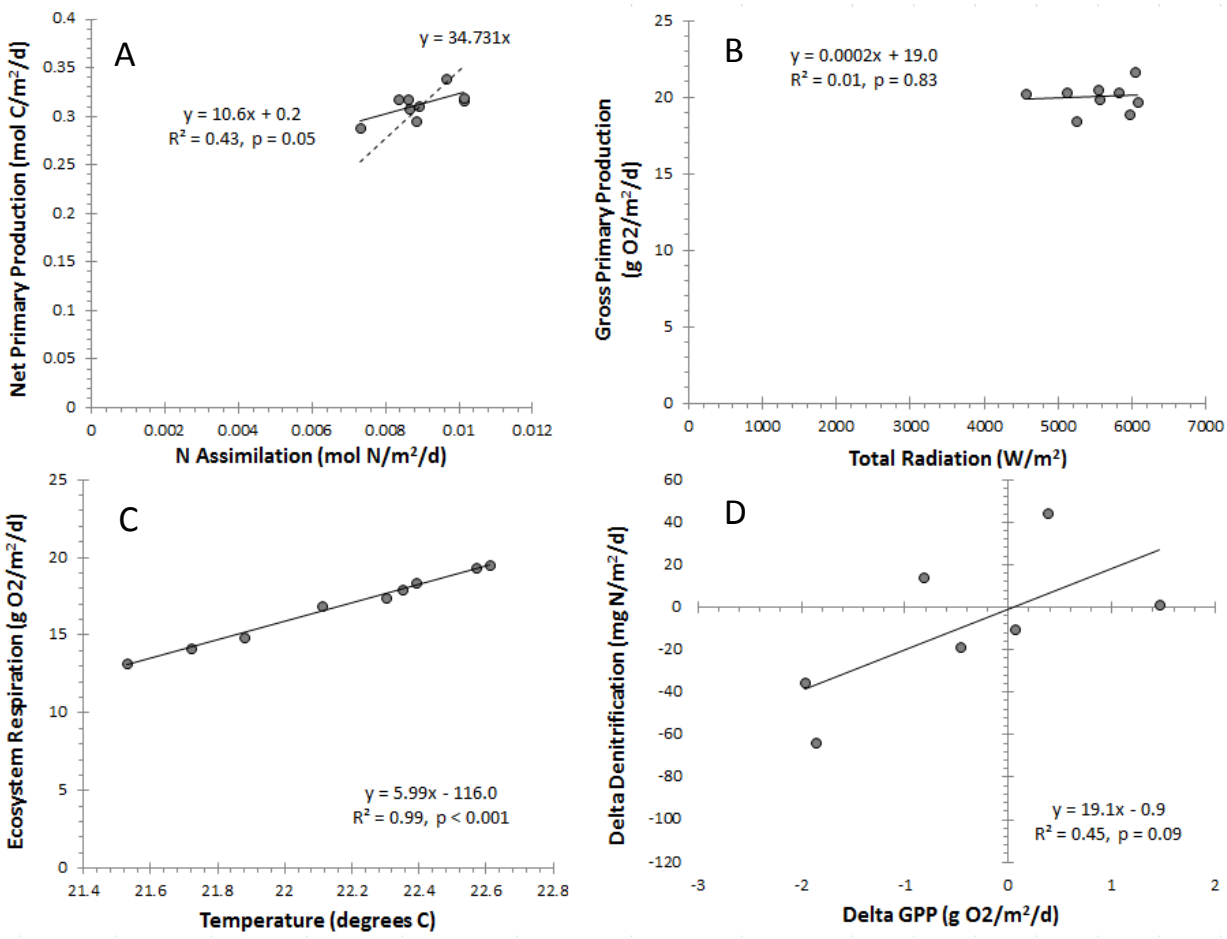

*Fig. 2-31 – Summary of interrelated elements of ecosystem C and N metabolism from the upstream station on the Silver River, October 2010. A) Relationship between N and C assimilation (assuming net primary production = 0.5 * gross primary production) on a molar basis. The mean C:N stoichiometry of ecosystem metabolism is ca. 35:1; the slope of the fitted line is different from this value because the intercept is not zero. B) Relationship between GPP (in g $O_2/m^2/d$) and incoming solar radiation (W/m^2), with a best fit line. C) Relationship between ecosystem respiration (g $O_2/m^2/d$) and minimum daily water temperature (degrees C). D) Strong inter-day coupling of GPP and heterotrophic N removal (denitrification), showing that day-to-day changes in GPP (in g $O_2/m^2/d$) explain 45% of the observed day-to-day changes in estimated denitrification (mg $N/m^2/d$).*

higher than the temperature effect observed in other spring run streams, with a 1° change in temperature changing respiration by nearly 6 g $O_2/m^2/d$ (Fig. 2-31c). The reason for this unlikely magnitude of temperature effects is unknown, but may have to do with day-to-day changes in the reaeration rate, which was notably higher on warmer days. Finally, the evidence for the indirect coupling between GPP and U_{den} observed in nearly all the deployments is modest (Fig. 2-31d); a 1 unit change in GPP results in a 19 mg $N/m^2/d$ change in U_{den} which is nearly a 7% change.

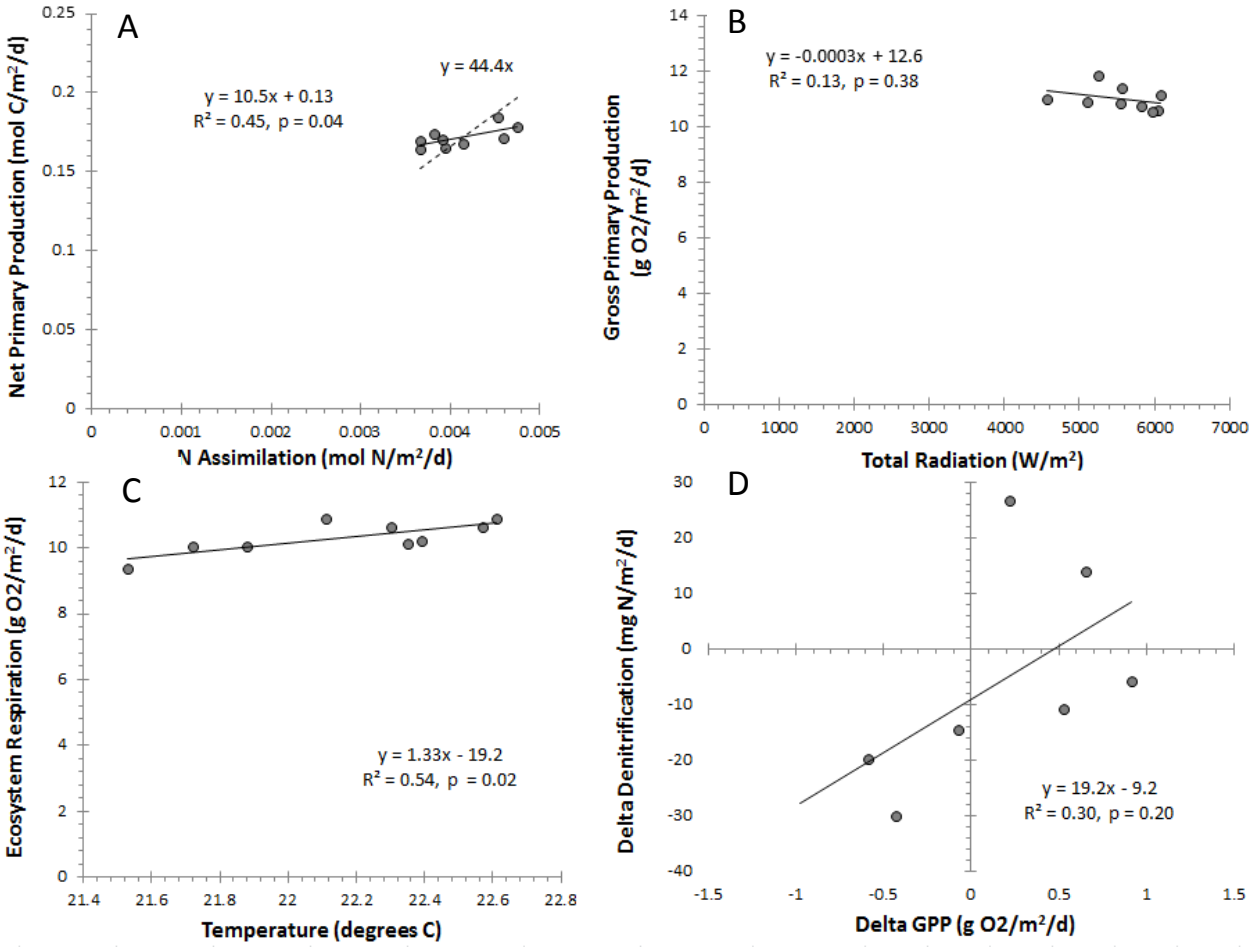

*Fig. 2-32 – Summary of interrelated elements of ecosystem C and N metabolism from the <u>downstream station</u> on the Silver River, October 2010. A) Relationship between N and C assimilation (assuming net primary production = 0.5 * gross primary production) on a molar basis. The mean C:N stoichiometry of ecosystem metabolism is ca. 44:1; the slope of the fitted line is different from this value because the intercept is not zero. B) Relationship between GPP (in g $O_2/m^2/d$) and incoming solar radiation (W/m^2), with a best fit line. C) Relationship between ecosystem respiration (g $O_2/m^2/d$) and minimum daily water temperature (degrees C). D) Strong inter-day coupling of GPP and heterotrophic N removal (denitrification), showing that day-to-day changes in GPP (in g $O_2/m^2/d$) explain 30% of the observed day-to-day changes in estimated denitrification (mg $N/m^2/d$).*

We examined the same associations in the lower river, and observed similar patterns (Fig. 2-32). There was a weak but significant positive association between NPP and U_a (Fig. 2-32a), but with a best fit line that had a large and positive y-intercept. The overall mean C:N ratio of primary production across the entire river was 44:1, which is strongly suggestive of macrophyte dominance during this period, and in stark contrast to the previous deployment where the C:N ratio of primary production was much lower. Algal and SAV phenology are mostly unknown for these rivers, though Quinlan et al. 2008 observed

seasonality to algal cover in this system, with roughly double the algal biomass in the summer. Covariance between insolation and GPP was absent or even slightly reversed (Fig. 2-32b), again likely due to the narrow range of insolation values observed during this deployment, and water temperature and respiration (Fig. 2-32c) suggest that the predicted controls on ecosystem processes in these lotic systems (i.e., that production is affected by light availability, and respiration by water temperature) are confirmed. Finally, there was no significant relationship between day-to-day changes in GPP and U_{den} (Fig. 2-32d), but the slope of the line (7.3 mg $N/m^2/d$ per g $O_2/m^2/d$ of GPP variation), while smaller than previously observed values, is suggestive of some indirect coupling. The reason the signal is weaker in the downstream than upstream, and weaker during this deployment than during previous deployments is unknown, but may have to do with the low range of variation observed in weather conditions during this deployment. Longer deployments would likely reveal the annual phenology of this river.

Deployment 7: Rainbow River – October 2010

A similar two-station deployment was done at the Rainbow River in October of 2010, with sensors deployed for 9 days. During this deployment, we observed marked diel nitrate variation (Fig. 2-33a), with strong evidence of longitudinal removal, with the downstream concentrations lower than upstream concentrations by almost 150 µg/L. In this case, diel variation was markedly higher in the downstream (ca. 70 µg/L) than in the upstream (ca. 40 µg/L), and the geometry of the curves were different, with much broader troughs in the downstream case, as would be expected from hydraulic dispersion effects. Slightly noisier downstream concentrations may be driven by differences in sensors or may be a result of complex mixing and eddy dynamics in the river.

Similarly, we observed diel variation in DO and temperature (Fig. 2-33b), with variation in the downstream significantly higher than in the upstream. Rainbow is unusual in one respect, in that the vent water DO concentrations are high (ca. 6 mg O_2/L) which means that the nighttime DO levels are actually higher upstream than downstream. The duration of the nighttime lows in both parameters is further confirmatory that the differences in the patterns of the upstream and downstream nitrate signals is due to the hydraulic dispersion effects that increase with distance downstream from the vent. Interestingly, temperature in the upper river is asymmetrical (rapid daytime increases, slow nighttime

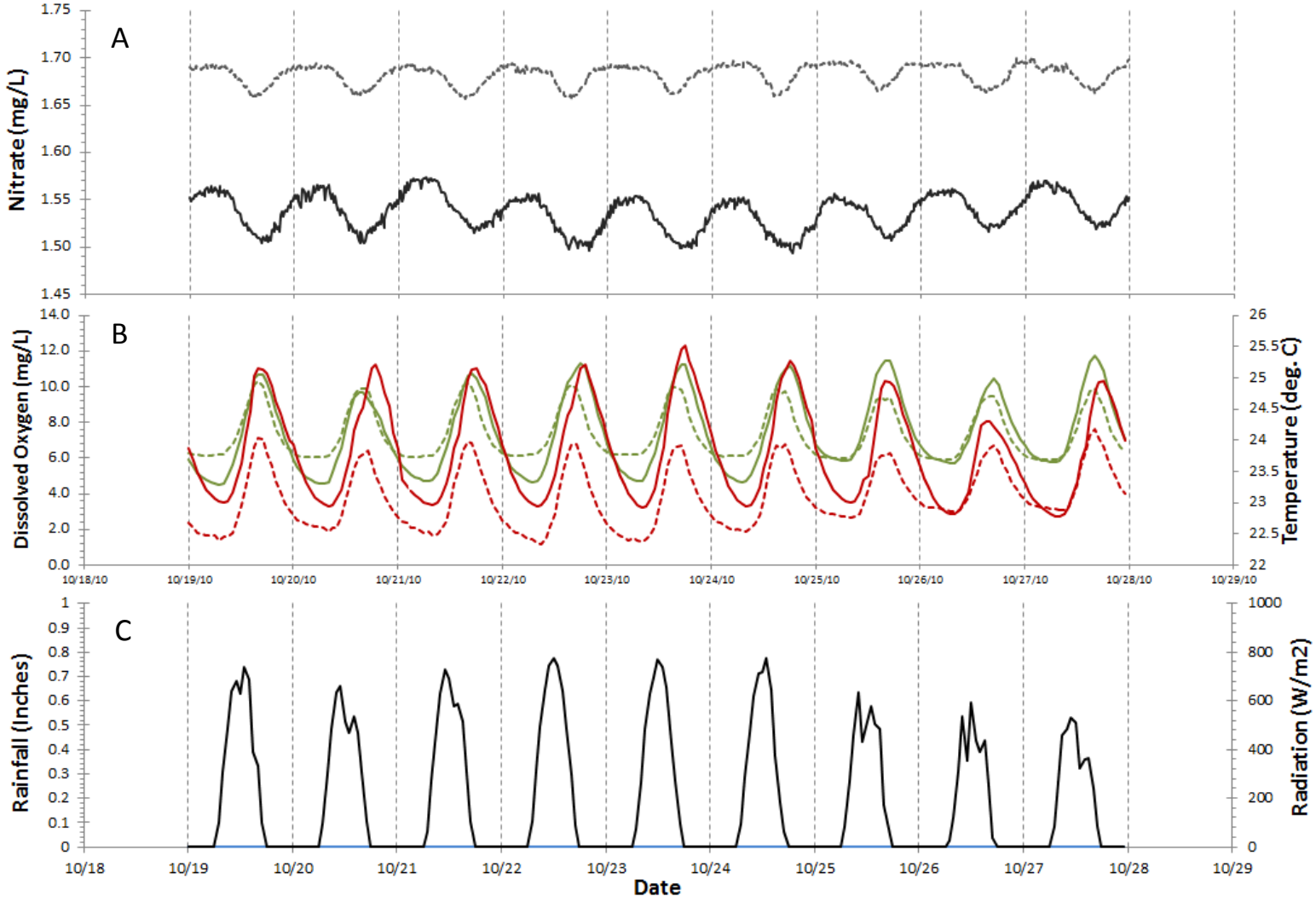

Fig. 2-33 - Diel variation in nitrate (solid grey line – downstream, dashed grey line - upstream), dissolved oxygen (sold green line – downstream, dashed green line – upstream), water temperature (solid red line – downstream, dashed red line – downstream), radiation (black line) and rainfall (blue line) for Rainbow River during an October 2010 deployment. Vertical dashed lines are at midnight every 24 hours.

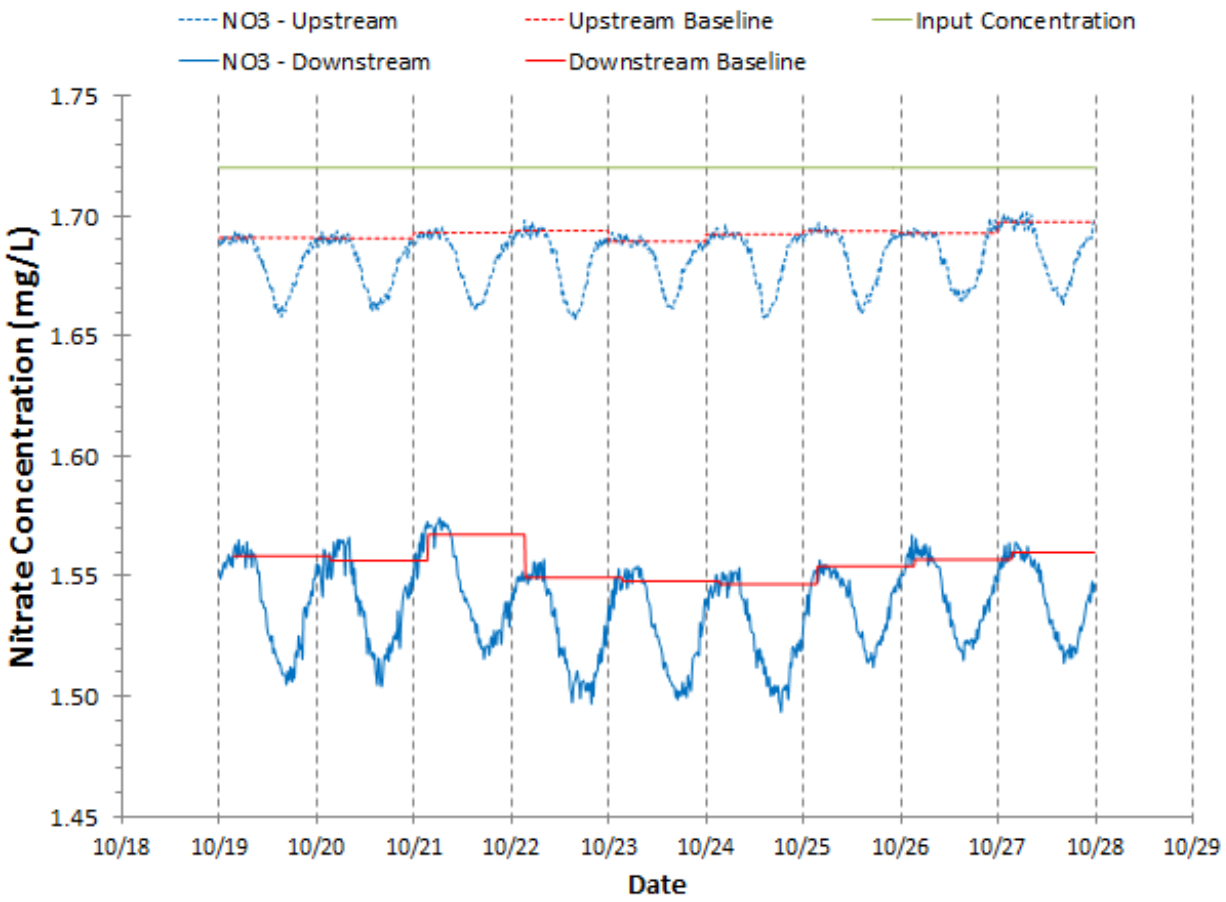

Fig. 2-34 – Summary of N removal mechanism inference for Rainbow River, October 2010. Assimilatory removal is estimated based on diel variation in nitrate (blue line; dashed – upstream, solid - downstream) referenced to a nighttime baseline value (red line; dashed – upstream, solid - downstream). Dissimilatory removal is estimated as the mass loss between upstream input concentrations (green line) and the nighttime baseline; that is, denitrification is assumed constant over the course of each 24-hour period. Day-to-day variation in the nitrate baseline is explored below.

declines), while the lower river is nearly perfectly symmetrical. The reason for this difference is unknown, but may arise in response to complex vent water mixing dynamics in the upper river versus more straightforward longitudinal dispersion and mixing in the lower river. During the deployment, we observed relatively little variation in solar radiation, and no rainfall (Fig. 2-33c).

Diel nitrate variation means that the method used elsewhere can be implemented here at both stations. Fig. 2-34 summarizes the input concentration, measured at a location several hundred meters above K.P. Hole Park, which we used as the baseline (and constant) input to estimate the mass balance. Nighttime baseline concentrations (red lines) are estimated each night, and extrapolated for the entire 24-hr period; changes in this baseline imply changes in denitrification (U_{den}). The nighttime baseline

concentration at the upstream location was easy to estimate because the river stayed at or near that concentration for several hours. However, in the downstream location, the nighttime baseline was more transient, presumably because of hydraulic dispersion effects; we estimated that baseline between 3:00 and 4:00 am.

Estimates of GPP and R are strongly affected by estimates of reaeration. During this deployment, reaeration averaged 0.49 hr^{-1} in the upstream and 0.56 hr^{-1} in the entire river; standard deviations were relatively high for the lower river (0.16 hr^{-1}) but much lower for the upper river (0.07 hr^{-1}). Because of the uncertainty in the lower river, we used the average deployment value for all days (0.49 hr^{-1})

Estimates of GPP and R for both stations are shown in Fig. 2-35. Both suggest high levels of primary production (mean GPP = 25.6 and 21.0 g $O_2/m^2/d$ for the upstream and downstream stations, respectively) and respiration (mean R = 16.9 and 12.3 g $O_2/m^2/d$ for the upstream and downstream stations, respectively). In both locations, the P:R ratio suggests relatively strong and consistent net autotrophy (mean P:R = 1.51 and 1.72:1 for the upstream and downstream stations, respectively). Curiously, R is constant in the upstream location over the deployment, but clearly declining over that same period in the downstream location, perhaps in response to cooler air temperatures. Longer term deployments at each of these rivers would be necessary to determine if this decoupling of upper and lower rivers is a common or persistent phenomenon.

Estimates of N removal are also variable day-to-day and between stations. Assimilation is higher in the upstream than downstream locations (mean U_a = 106 and 117 mg $N/m^2/d$ for upstream and downstream, respectively), consistent with observed differences in gross production. However, denitrification is much higher for the river as a whole than for the upstream location (mean U_{den} = 443 and 1130 mg $N/m^2/d$ for upstream and downstream stations, respectively. The denitrification rate in the lower river is the largest observed for any river studied here, but is still within the range of plausible denitrification values observed using open channel methods in shallow highly productive rivers elsewhere (e.g., McCutchan and Lewis 2006). Reasons for the marked jump in U_{den} rates between the upper and lower river are not well understood; the river is geomorphically relatively similar along the entire run, but in a way that would create the expectation of lower U_{den} in the lower river (i.e., same depth but 20 m narrower in the lower river). Further research using this method will be required to establish geomorphic and longitudinal controls on denitrification, and, crucially, to effectively distinguish between denitrification and dilution by obtaining high precision tracer-based estimates of discharge along the entire length of the river.

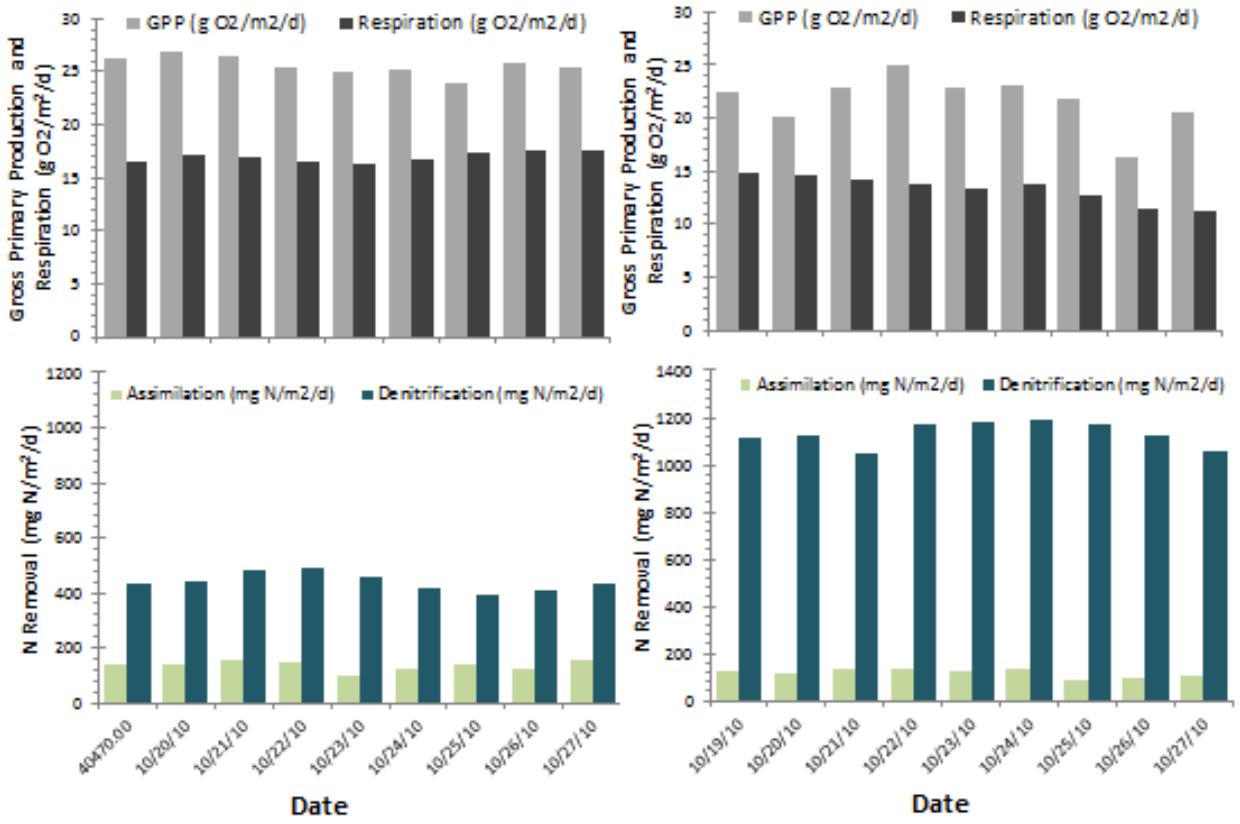

Fig. 2-35 – Summary of October 2010 deployment at Rainbow River showing estimates of gross primary production and respiration (top panels) and assimilatory and dissimilatory N removal (bottom panels) for both upstream (left panels) and downstream (right panels) reaches.

As with other deployments we sought to evaluate the C:N ratio of primary production. A strong positive covariance between NPP and U_a was observed for both upstream and downstream reaches (Fig. 2-36a and Fig. 2-37a), and the C:N ratio for uptake was similar (53.9 and 39.5:1), and strongly suggestive of a dominance by vascular plants. We note that the fitted slopes for both regression lines were lower than this value because both imply large positive y-intercept values (that is, a rate of NPP at which N assimilation is zero). The short duration of the deployment makes it hard to discern if there is some systematic variation in C:N ratio with GPP or some other factor, as was observed with the Ichetucknee system. The C:N values are likely too high for even plausible attribution to vascular plants; alternative explanations that may merit investigation are 1) the long residence hydraulics of this river leading to signals from sequential days overlapping and 2) violations of the assumption of constant denitrification over the course of a day-night cycle. Exploration of these possibilities is ongoing.

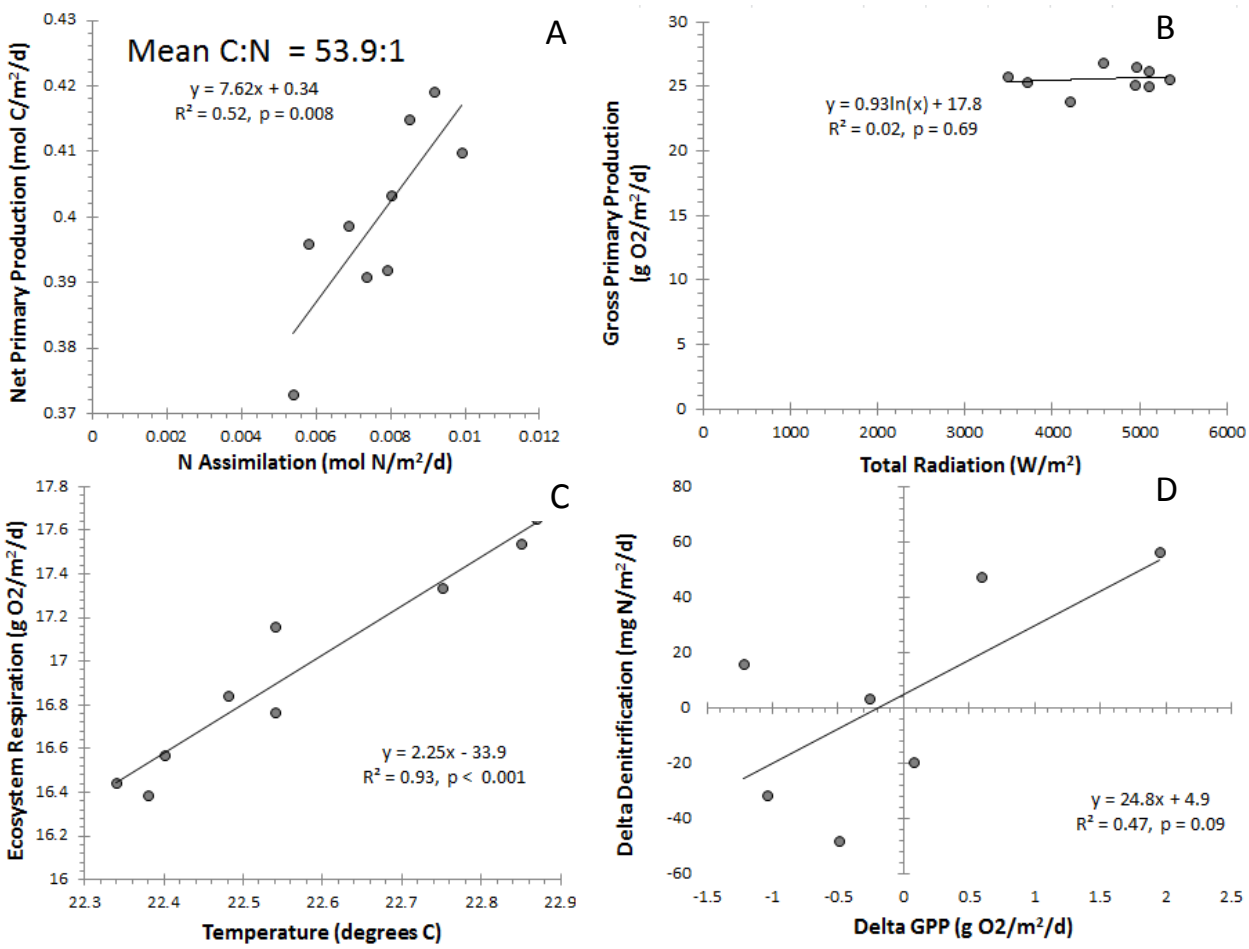

*Fig. 2-36 – Summary of interrelated elements of ecosystem C and N metabolism from the upstream station on the Rainbow River, October 2010. A) Relationship between N and C assimilation (assuming net primary production = 0.5 * gross primary production) on a molar basis. The mean C:N stoichiometry of ecosystem metabolism is ca. 53:1; the slope of the fitted line is different from this value because the intercept is not zero. B) Relationship between GPP (in g $O_2/m^2/d$) and incoming solar radiation (W/m^2), with a best fit line. C) Relationship between ecosystem respiration (g $O_2/m^2/d$) and minimum daily water temperature (degrees C). D) Strong inter-day coupling of GPP and heterotrophic N removal (denitrification), showing that day-to-day changes in GPP (in g $O_2/m^2/d$) explain 47% of the observed day-to-day changes in estimated denitrification (mg $N/m^2/d$).*

Similarly, as with previous deployments, there is a significant positive association between insolation and GPP, though that effect was slightly clearer for the upper river (Fig. 2-36b) than for the lower river (Fig. 2-37b), for reasons that are not clear. Evidence to support light limitation of primary production is absent, despite a relatively large range of insolation values. As with other winter time deployments, there was a tremendously strong association between nighttime water temperatures and respiration

(Fig. 2-36c and 2-37c); the slope of both upstream and downstream fitted lines suggest that a unit change in temperature has an enormous effect on respiration (2.3 and 3.6 g $O_2/m^2/d$ for upstream and downstream, respectively), beyond what would be expected based on heterotrophic metabolic sensitivity to temperature in other settings. The reason for this acute sensitivity of respiration is still unknown, but implications in light of climate change on these ecosystems are profound.

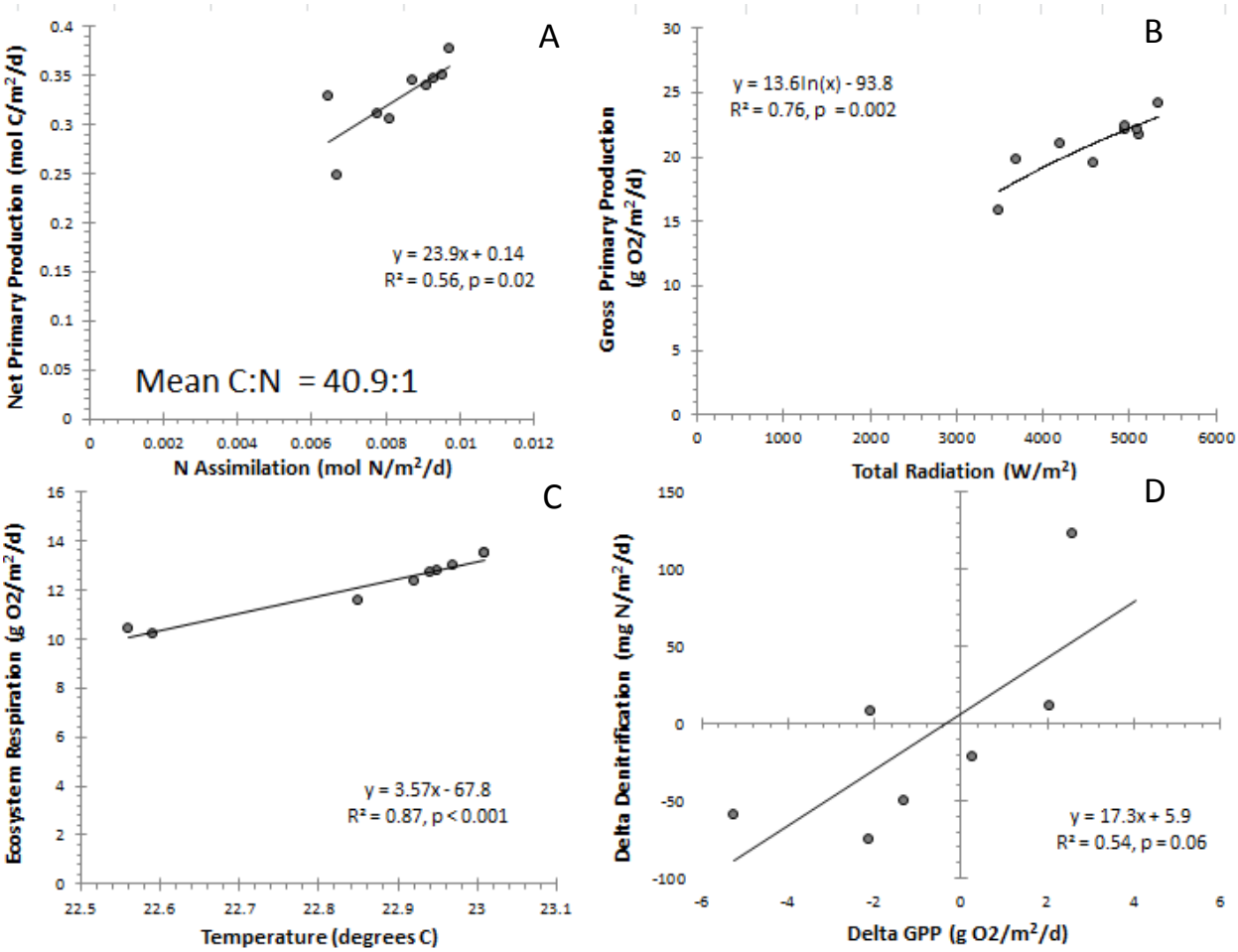

*Fig. 2-37 – Summary of interrelated elements of ecosystem C and N metabolism from the <u>downstream station</u> on the Rainbow River, October 2010. A) Relationship between N and C assimilation (assuming net primary production = 0.5 * gross primary production) on a molar basis. The mean C:N stoichiometry of ecosystem metabolism is ca. 40.9:1; the slope of the fitted line is different from this value because the intercept is not zero. B) Relationship between GPP (in g $O_2/m^2/d$) and incoming solar radiation (W/m^2), with a best fit line. C) Relationship between ecosystem respiration (g $O_2/m^2/d$) and minimum daily water temperature (degrees C). D) Strong inter-day coupling of GPP and heterotrophic N removal (denitrification), showing that day-to-day changes in GPP (g $O_2/m^2/d$) explain 54% of observed day-to-day changes in denitrification (mg $N/m^2/d$).*

Finally, as with previous deployments, there appears to be some weak statistical evidence of day-to-day indirect coupling of primary production and denitrification (Fig. 2-36d and 2-37d) suggesting that denitrification is at least partly driven by very recently-produced organic carbon. The signal is slightly weaker during this deployment than has been observed in deployments in other rivers, partially due to the low levels of day-to-day metabolism variation. The slope of the fitted lines in both upstream and downstream cases are similar, and suggest that a unit change in primary production changes denitrification by 15-17 mg $N/m^2/d$, or about 4% of upstream denitrification.

Deployment 8: Alexander Springs Creek – September 2010

The Alexander Springs Creek continues to be a setting of considerable research interest, both because it is among the only springs in the state that has nitrate concentrations at the presumed background concentrations historically found in the Floridan, and because it exhibited diel variation in nitrate inverse to that exhibited by other spring run streams. In this deployment, we installed the sensors at the upstream location (not, however, at the downstream location that on each previous deployment was confounded by tannic water inputs) for 13 days. The last 3 days of that deployment, we initiated a series of additional measurements of water chemistry, isotope chemistry and organic carbon export that is described in a subsequent section (Research Element #7); the intent of that was to understand the N demand of the primary production occurring over this relatively short (ca. 500 m) reach, and discern more clearly evidence that this system is N limited.

The raw data from the deployment, shown in Fig. 2-38, show the same inverse diel variation in nitrate as was previously observed. Moreover, the observations are suggestive of very high rates of primary production (with diel DO amplitudes greater than 5 mg O_2/L), which simply underscores the curious nitrate observations. Note that concentrations are generally at or below the vent water input (measured repeatedly during the latter part of this deployment at 0.07 mg N/L) suggesting that the reach is removing N, but at a time when other rivers shut off assimilation. Diel variation in temperature and insolation are similar to what has been observed elsewhere. We note that there were 4 cloudy days during this deployment, and 2 relatively significant rainfall events (9/23 and 9/28).

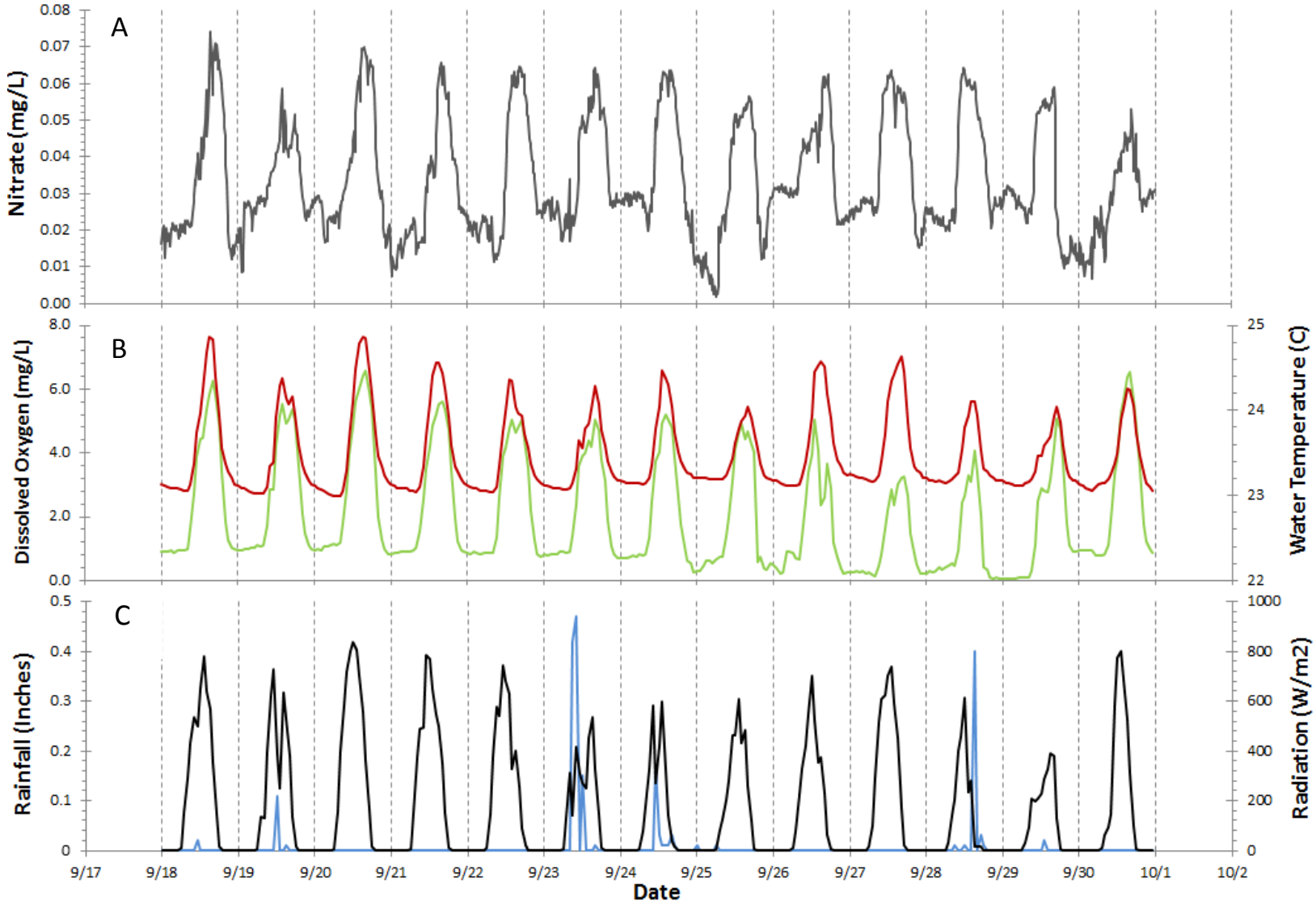

Fig. 2-38 - Diel variation in nitrate (grey line), dissolved oxygen (green line), water temperature (red line), radiation (black line) and rainfall (blue line) for the Alexander Springs Creek during September 2010 deployment. Vertical dashed lines are at midnight every 24 hours.

The inversion of the diel pattern is more clearly displayed in Fig. 2-39 which suggests that the nighttime baseline is less than the daytime maximum, implying a negative assimilation rate. Note also the fact, previously mentioned, that the concentrations observed are almost always less than the vent input concentration. We know of no additional sources of water or nitrate over the length of this river, and thus interpret these observations as something induced by the thick algal mat present across almost the entire study reach. Note that the total mass removal between the vent and the measurement site can be estimated based on the concentration difference between the vent (green line) and the measurements (blue line); this quantity cannot be partitioned between assimilation and denitrification, but is a useful upper bound estimate on assimilatory removal that can be used as a benchmark against which stoichiometric assessments of N demand from oxygen metabolism can be compared.

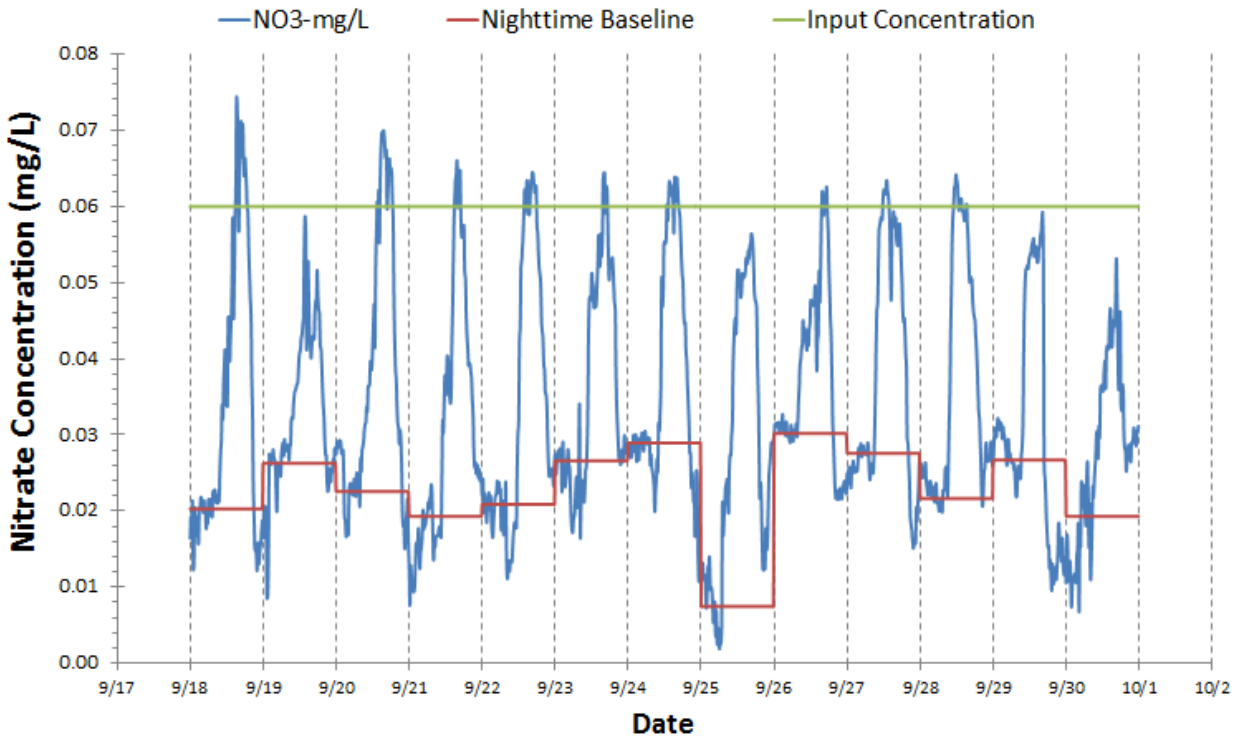

Fig. 2-39 – Summary of N removal mechanism inference for the Alexander Springs Creek in September of 2010. Assimilatory removal cannot be estimated based on diel variation because nitrate (blue line)during the day is higher than the nighttime baseline value (red line). Estimates of total removal based on the mass loss between upstream input concentrations (green line) and the observed concentrations cannot be partitioned between denitrification and assimilation using the assumptions made elsewhere, but do provide a useful benchmark against which to compare other estimates of assimilatory demand (i.e., from oxygen metabolism measurements assuming a C:N ratio of the algal productivity of 12.5:1).

The mean reaeration coefficient for the deployment period was 0.37 hr^{-1}, comparable to other deployments in this river. The resulting estimates of primary production and respiration suggest (Fig. 2-

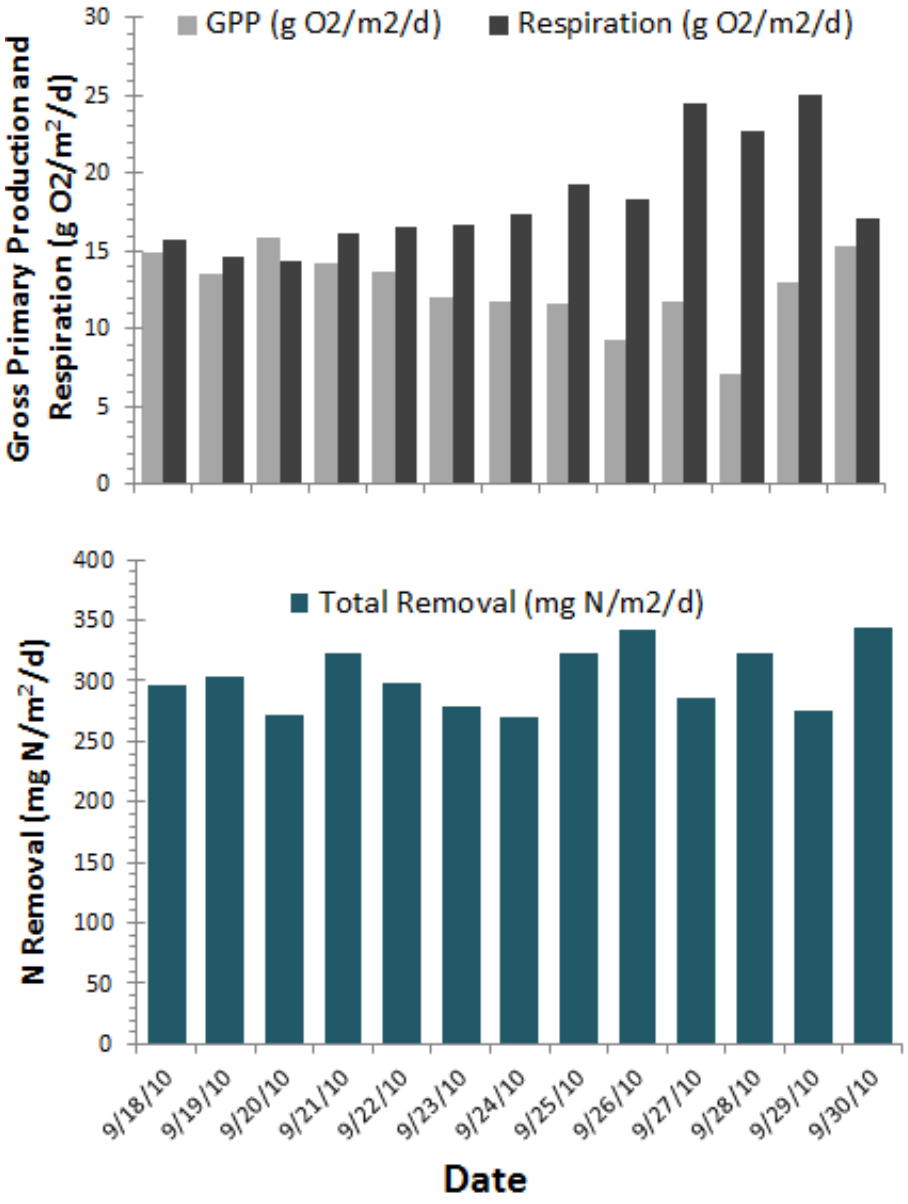

Fig. 2-40 – Summary of September 2010 deployment at Alexander Springs Creek showing estimates of gross primary production and respiration (top panel) and total N removal (bottom panel). Note that estimates of total N removal include both denitrification and assimilation, rates of which cannot be partitioned in this system because diel nitrate variation is inverse to what has been observed elsewhere. We use the total N removal as an upper bound on algal mat assimilation, recognizing that denitrification is almost certainly occurring in this system because dissolved oxygen levels get very low at night.

40a), surprisingly, a slightly net heterotrophic system, with marked increase in P:R during the period between 9/24 and 9/28. The systems P:R ratio averaged 0.71:1, and got as low as 0.31:1. This is surprising because there is relatively little evidence of allochthonous organic carbon delivery to the system; which is very broad and has relatively small amount of emergent herbaceous standing biomass. However, the mass of the algal mat is tremendous, and it is not implausible that the mat itself goes through periods of net autotrophy and net heterotrophy. Also notice that the GPP rates are quite large, averaging over 13 g $O_2/m^2/d$ over the deployment. Estimates of assimilation and denitrification executed in the standard way yield negative plant uptake values and modest denitrification rates.

Therefore, we report only the total N removal based on the deviation between the vent water inputs and downstream outputs, integrated over each 24-hour period Figure 2-40b). This value, which ranges from 270 to 340 mg $N/m^2/d$ represents a upper bound of assimilation. We return to the implications of this in a later section. In brief, if we estimate assimilation using an alternative approach based on stoichiometry and oxygen metabolism for all three deployments at Alexander Springs (for one of which, August 2010, data are not presented) we can estimate the ratio of flux out of the vent to ecosystem demand. Fig. 2-41 shows the demand as a percentage of the vent flux, and suggests that the values for all three deployments average over 50%; that is the flux:demand ratio is less than 2:1. By way of comparison, over the much longer reach of the Silver River, this value is 55:1; that is there is 55 times more N emerging from the vent than is needed to supply all of the autotrophic demand over the upper 6,500 m of that river. While there is no theoretical threshold for when N limitation occurs, ongoing research (Sean King, Ph.D. student University of Florida, personal communication) supports an interpretation of these values for Alexander Springs as diagnostic of N limitation. This contention motivates an entire section dedicated to efforts to understand N dynamics in this river system, particularly in light of the tremendous algal mat that has developed there.

Finally, while we don't expect the same association patterns as observed at other river sites, we explored relationships between NPP and U_a (despite the latter being negative); Fig. 2-42a suggest a negative association that is statistically significant. Previous deployments here showed a similar negative association (e.g. Fig. 2-17 from April 2010) suggesting that the magnitude of diel variation is somehow linked to the magnitude of primary production (Fig. 2-42a). The most likely explanation is an indirect effect of the magnitude of daytime oxygen production via effects on other aspects of

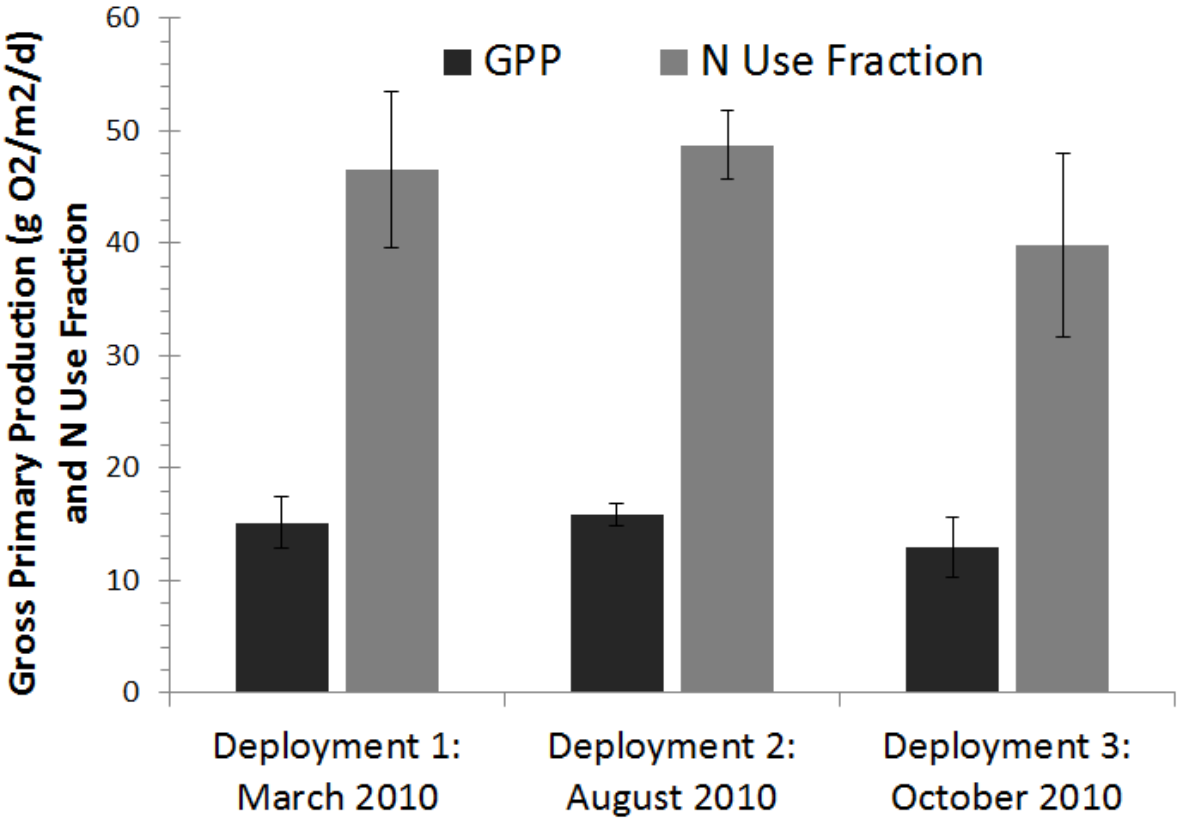

Fig. 2-41 – Summary values of GPP and fractional N demand (N demand by autotrophs as function of vent water delivery, obtained based on O_2 metabolism and a C:N ratio of 12.5:1) for three deployments at Alexander Springs Creek. For comparison, the flux:demand ratio for the Silver River is ca. 55:1.

the N cycle in this system (i.e., increasing nitrification and inhibiting denitrification). This conclusion is tentative, but few other explanations fit.

Links between insolation and GPP are positive and significant, a curious finding if we operate under the assumption that the primary production in this system is N limited. However, we explore the possibility in the separate research element on Alexander Springs that the algal mat has enormous capacity to buffer N delivery via internal recycling pathways, potentially creating a condition where the river can be broadly N limited but still respond to day-to-day variation in solar inputs. The link between respiration and water temperature is weak and non-significant (fig. 2-42c), and the parameterization of that relationship is untenable, suggesting that extremely small variation yields very large changes in respiration. This non-significant relationship and enormous slope may arise because the actual variation in nighttime water temp is vanishingly small (0.2 degrees).

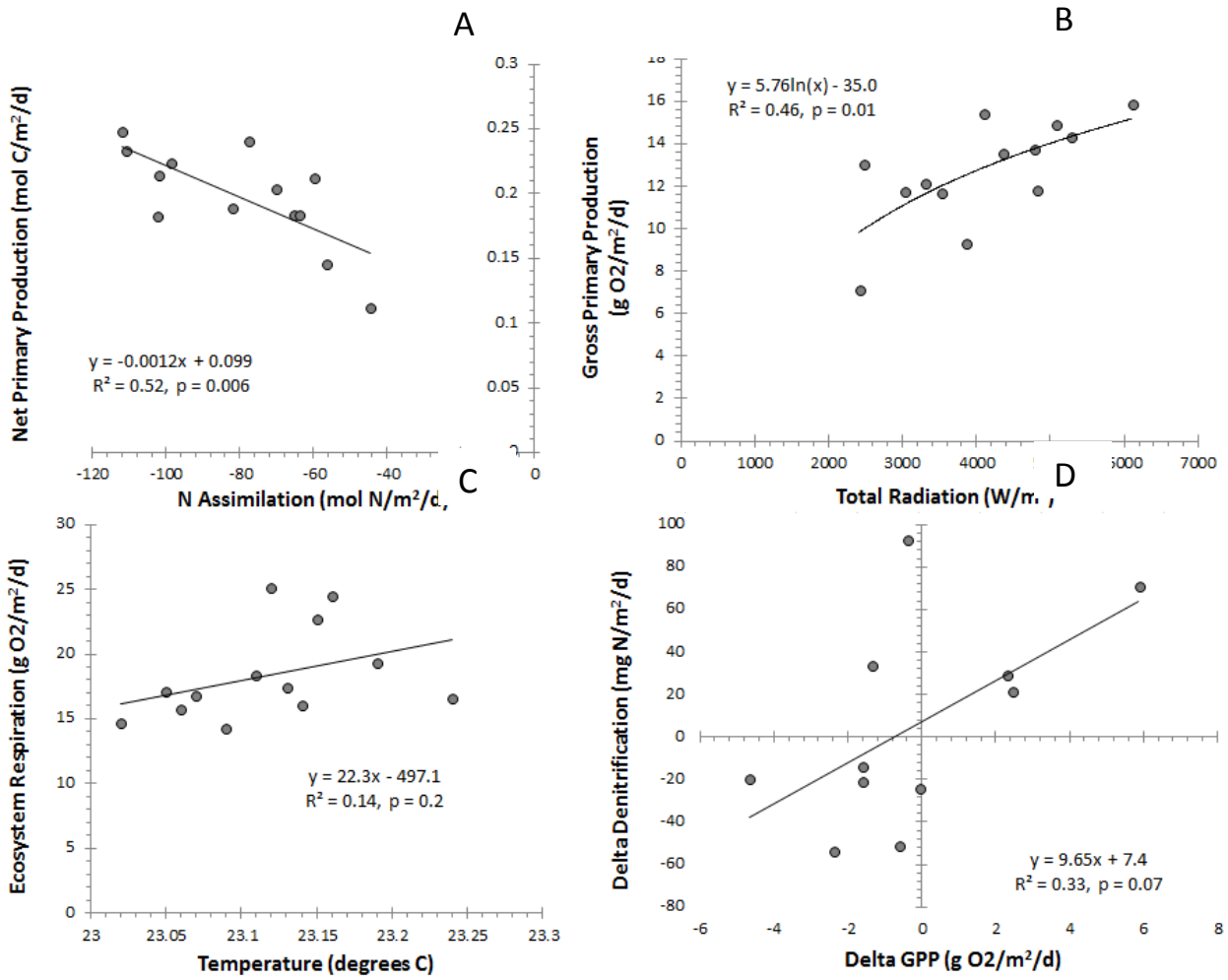

*Fig. 2-42 – Summary of interrelated elements of ecosystem C and N metabolism from the Alexander Springs Creek, September 2010. A) Relationship between N and C assimilation (assuming net primary production = 0.5 * GPP) on a molar basis. U_a estimates are negative because of inverted diel nitrate variation; however, the magnitude of diel N excursion was still statistically significantly associated with primary production. B) Relationship between GPP (g $O_2/m^2/d$) and solar radiation (W/m^2), with a best fit line. C) Relationship between respiration (g $O_2/m^2/d$) and minimum water temperature (C). D) Modest inter-day coupling of GPP and denitrification, showing day-to-day changes in GPP (in g $O_2/m^2/d$) explain 33% of observed day-to-day changes in estimated denitrification (mg $N/m^2/d$). Note that denitrification estimates are confounded by inverted diel variation, and as such are not reflective of that process alone.*

Finally, we observed a weak association between variation in GPP and variation in the estimate of denitrification (Fig. 2-42d). Since that latter estimate is confounded, and is more an estimate of depth of the nighttime trough compared to the vent, we interpret this to mean that more productive days are followed by deeper nighttime troughs, which likely reflects increases in assimilation as well as denitrification.

Deployment 9:- Santa Fe River – November 2010

The Santa Fe River alternates between a runoff-fed blackwater river (at average and higher flows) and a spring run stream (at low flows). Consequently, this river presents significant challenges for the application of the approach used in this section. Specifically, high DOC confounds measurement of nitrate by the UV sensor, and the density of samples necessary to enumerate diel variation is otherwise not feasible. In Section #8 we report on the DOC sensitivities of the SUNA as a way of describing the conditions under which this method would be useful. However, during November of 2010 an extremely dry late summer and fall led to the Santa Fe River running clear, fed entirely by springs along the lower river (i.e., between the River Rise and the Suwannee). We used that opportunity to examine patterns of N removal in that river system, albeit under unusual circumstances. The central motivation for this effort comes from the question of whether the recalcitrant carbon available to blackwater rivers can fuel the same rates of denitrification as the much more labile autochthonous carbon available in springs. We note, however, that during the clear-water period on the Santa Fe River, numerous beds of SAV and benthic algae were evident, and the carbon derived from that recent production may affect any inference made about the intrinsic capacity of this blackwater river to provide N removal services.

The deployment took place for 10 days during mid-November, and the sensors were deployed at the USGS gaging station half-way between the river-rise and the Suwannee (Santa Fe River near Ft. White, Station #02322500, hereafter referred to as the 2500-station); note that this location is several river miles upstream of the confluence with the Ichetucknee. Flow at the time of the deployment was 660 cfs, and was dominated by discharge from Ginnie (ca. 200 cfs), Poe (ca. 90 cfs), Gilchrist Blue (ca. 40 cfs) and River Rise (ca. 270 cfs). Other named springs (e.g., Rum Island, Lilly) are relatively small; there are also numerous small unnamed spring vents along that run. It is crucial to point out that we do not have a well constrained estimate of the upstream nitrate concentration from which to implement the denitrification portion of the method; we estimated an upstream boundary condition of 1.1 mg N/L based on historic measurements, but this value is little better than an educated guess. The raw observed data are presented in Fig. 2-43.

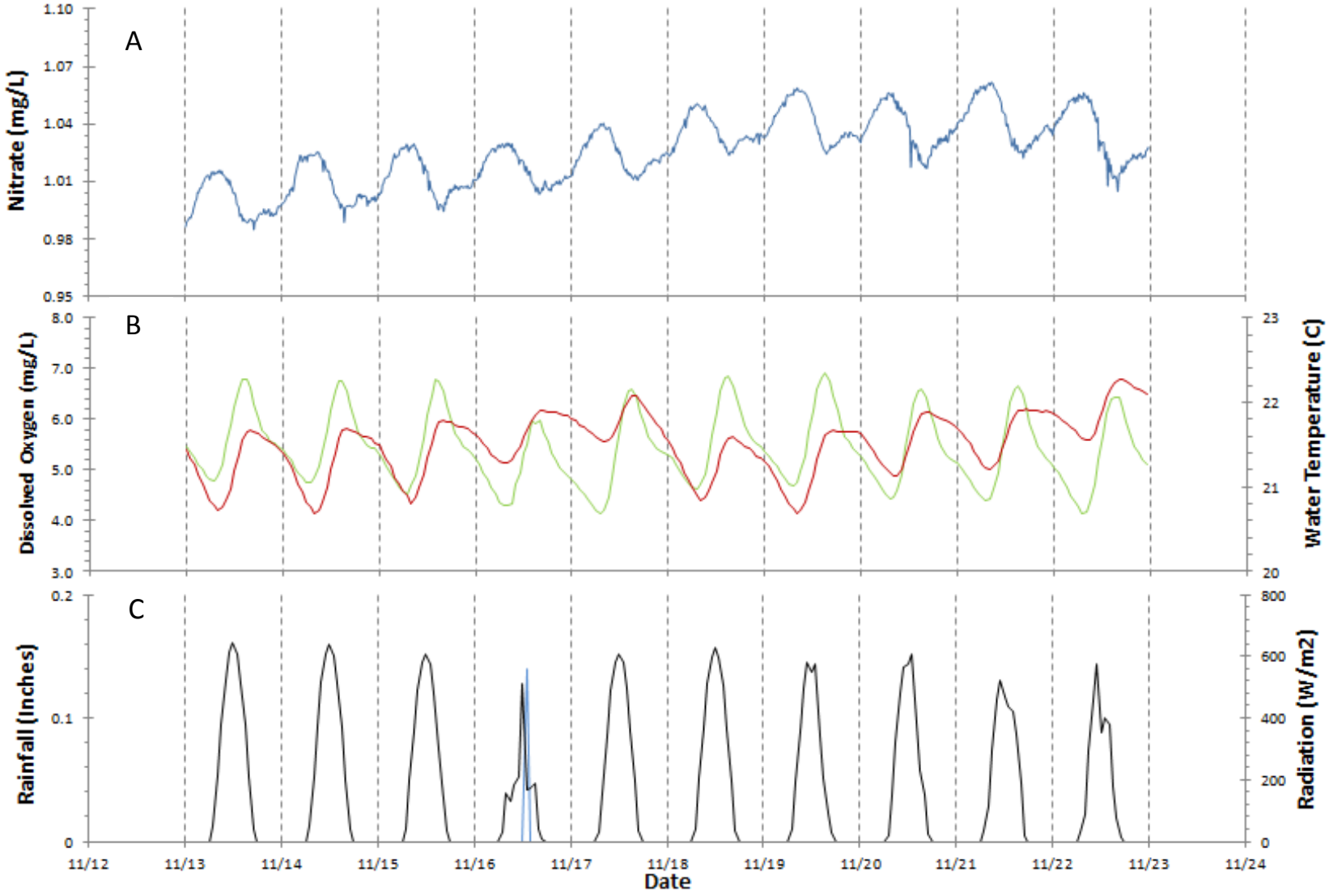

Fig. 2-43 - Diel variation in nitrate (grey line), dissolved oxygen (green line), water temperature (red line), radiation (black line) and rainfall (blue line) for the Santa Fe River during a November 2010 deployment. Vertical dashed lines are at midnight every 24 hours.

A striking diel pattern, consistent with what has been observed in other rivers, is evident in the Santa Fe during this low discharge period (Fig. 2-43a). The mean nitrate concentration (ca. 1.0 mg/L) is influenced by Poe, Ginnie and Blue that have concentrations higher than this, and the River Rise which is generally lower (ca. 0.5 mg N/L). The diel variation is structured at two time scales, with clear diel variation but also a late evening smaller cycle that is regular enough to consider real. One explanation for this has to do with the different travel times of water between the springs and the 2500-station; since the springs are situated all along the lower Santa Fe, and some (particularly Gilchrist Blue) are themselves creating diel patterning, discrete residence times of different sources of water may explain this observation. We also note a strong upward trend in the nitrate concentration over time that may be related to declines in flow from the River Rise as contributions from the Upper Basin (at the River Sink, which are low in nitrate) decline over this period.

Diel variation in temperature and oxygen also exhibit patterns suggestive of complex riverine mixing dynamics. The marked asymmetry in the temperature and DO profiles over 24 hours (steep rising limbs, more shallow falling limbs) suggests that O_2 enrichment due to primary production in the tributary spring runs is delivered to the 2500-station after the DO from in-stream processes, creating a long tail to the diel time series. There was a highly regular pattern to radiation delivery, underscoring the clear dry conditions that prompted these unusual circumstances in the first place. There was a trace amount of rain on 11/16, but no evidence of anything except a temperature effect.

The prerequisites for implementing the diel method are clearly met (Fig. 2-44). The diel variance occurs in the expected direction and is coherent. That said, the nighttime nitrate peak occurs near 6:00 am, meaning that water that has been acted upon by assimilation is arriving at the 2500-station 12 hours after sundown the previous day. If the residence time for some of the water is longer than 12 hours, and we have no data to suggest that this is a negligible fraction, then the assimilatory signal blends from one day to the next, and requires more sophisticated hydraulic modeling to untangle the downstream signal; note that a two-station approach to these data (i.e., as opposed to the single station method applied throughout), would obviate this problem. Since we lack the basic hydraulic data for this river that we have for the others, we proceed with the full estimation of assimilation and denitrification as though day-to-day carry-over of assimilation is negligible. Note, however, that this will tend to reduce the estimate of N assimilation (both by truncating the uptake duration AND lowering the nighttime baseline concentration) and, as such, the emergent C:N ratios of primary production may be lower than they actually are.

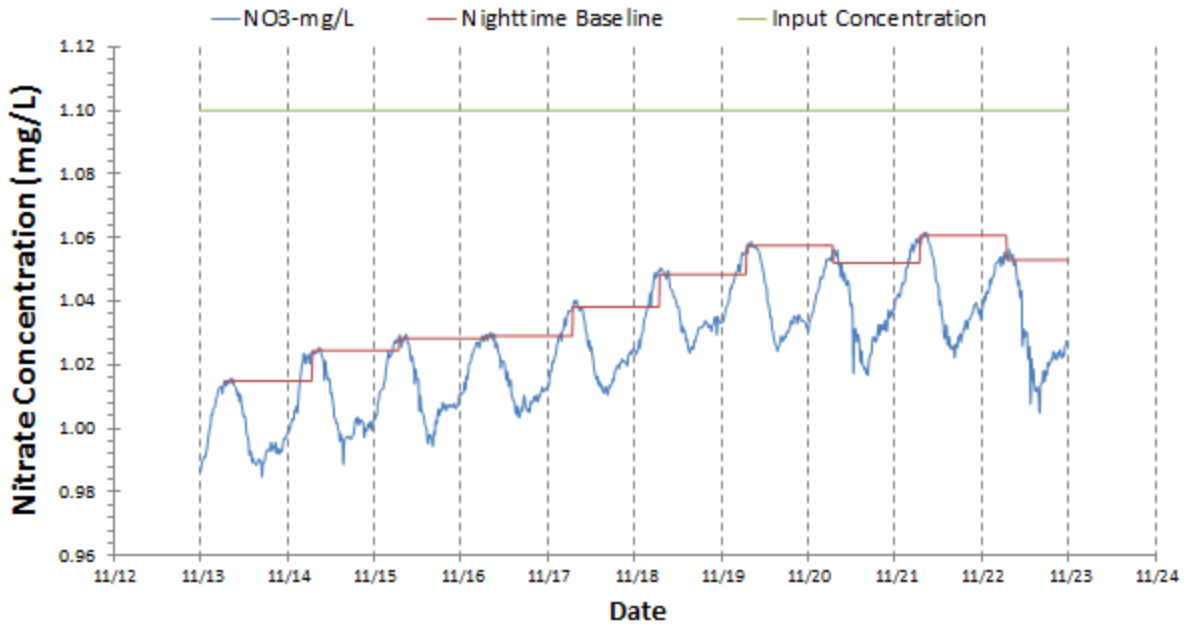

Fig. 2-44 – Summary of N removal mechanism inference for the Santa Fe River in November of 2010. Assimilatory removal is estimated based on diel variation in nitrate (blue line) referenced to a nighttime baseline value (red line). Dissimilatory removal is estimated as the mass loss between upstream input concentrations (green line) and the nighttime baseline; that is, denitrification is assumed constant over the course of each 24-hour period. Day-to-day variation in the nitrate baseline is explored below.

A summary of primary production and respiration in the Santa Fe during the deployment period is contingent on estimates of reaeration. We estimated K to be between 0.16 and 0.31 hr^{-1} (average = 0.24 hr^{-1}) over the deployment period. The mean value was used to estimate GPP and R (Fig. 2-45), which suggest that the Santa Fe is weakly net autotrophic during the period (P:R = 1.06:1) and that primary production is relatively modest. Note that the integration distance for this application of the single station method (where there is no fixed input point) was estimated based on the river velocity and reaeration rate (D = 3*v/K, where v is velocity and K is the reaeration rate). We used a total river length of 11.2 km for this work, with a mean river width of 35 m (a benthic area of 33.7 ha). Over that area, GPP and R are both relatively low for the river, perhaps reflecting the short time available for dense SAV communities to establish following declines in river color. This is consistent with the relatively low diel variation in DO observed.

Day-to-day variation in assimilation is small, with U_a averaging 67 mg $N/m^2/d$; low variation is expected given the small variation in weather conditions during the deployment. Denitrification estimates are highly uncertain because of poorly constrained upstream boundary conditions; we estimate an average rate of 288 mg $N/m^2/d$, with the rate falling monotonically throughout the deployment as the baseline

nitrate concentration climbs. Overall, as with other spring-fed rivers, the estimate of assimilation is a small fraction of the total N removal (ca. 19% overall). We strongly urge caution, however, in extrapolating this finding to periods when the Santa Fe is more tannic because of the role of labile autochthonous organic carbon. We would predict that internal C fixation would be greatly reduced under dark-water conditions, and one of the sentinel observations of this study is that recent GPP is critically important for fueling denitrification.

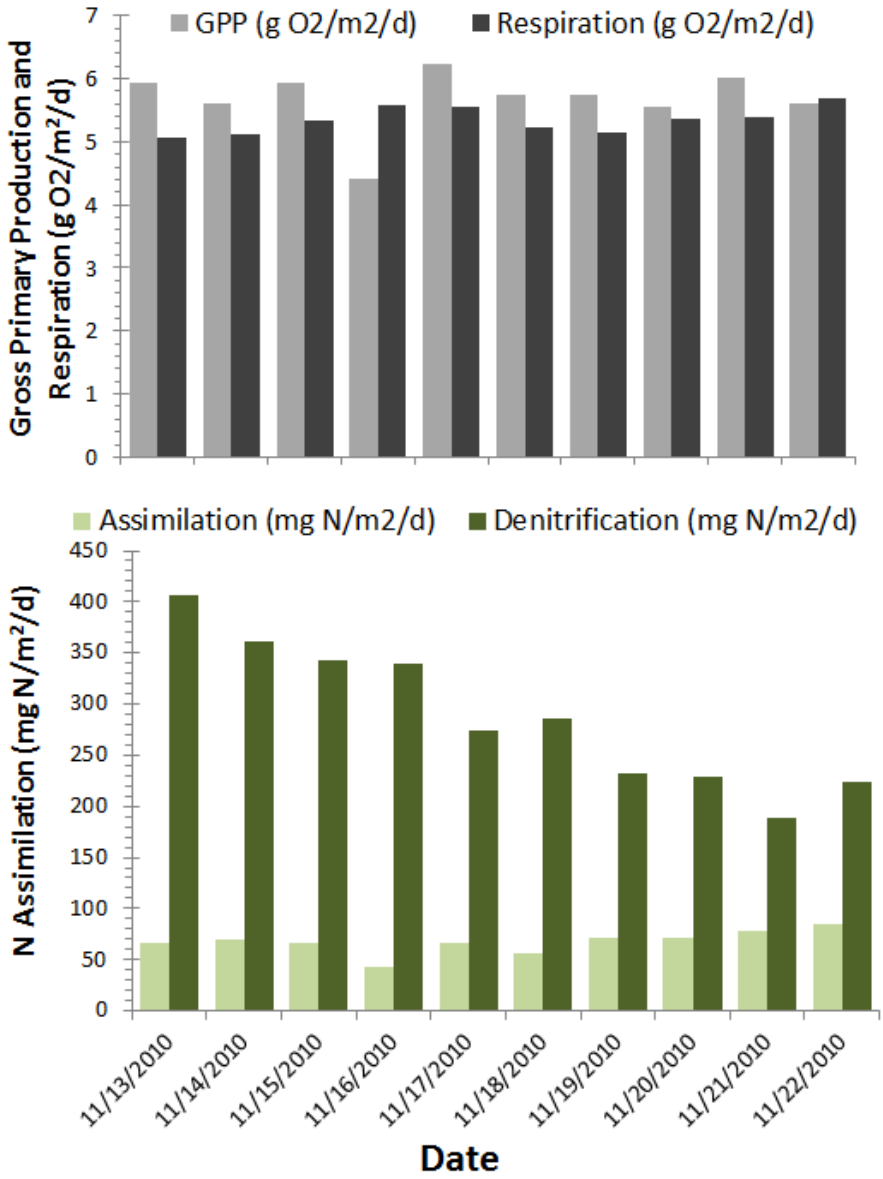

Fig. 2-45 – Summary of November 2010 deployment at the 250—station of the Santa Fe River showing estimates of gross primary production and respiration (top panel) and assimilatory and dissimilatory N removal (bottom panel). Note that estimates of denitrification are highly uncertain because of poorly constrained upstream input concentrations

We explore the same patterns of association as we did in other rivers in the Santa Fe. We observed, for example, a strong positive association between primary production and N assimilation (Fig. 2-46a), with a derived C:N ratio of ecosystem metabolism of 18.8:1, possibly suggesting a greater fractional contribution of algae and benthic biofilms to overall primary production than in other rivers. This would be consistent with the brief time for community establishment between periods when the tannic content of the river preclude high rates of primary production.

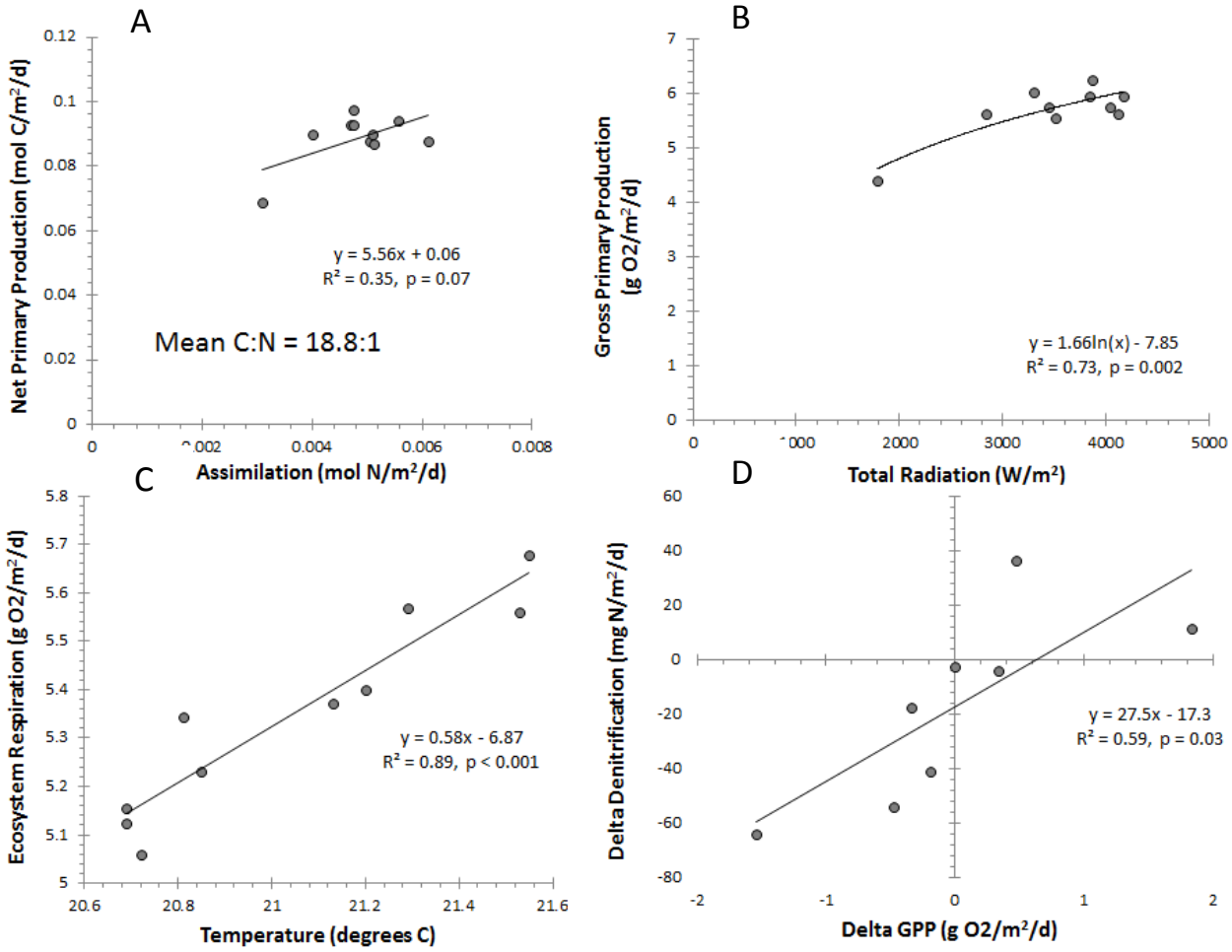

*Fig. 2-46 – Summary of interrelated elements of ecosystem C and N metabolism from the Santa Fe River, November 2010. A) Relationship between N and C assimilation (assuming net primary production = 0.5 * gross primary production) on a molar basis. The mean C:N stoichiometry of ecosystem metabolism is ca. 19:1; the slope of the fitted line is different from this value because the intercept is not zero. B) Relationship between GPP (in g $O_2/m^2/d$) and incoming solar radiation (W/m^2), with a best fit line. C) Relationship between ecosystem respiration (g $O_2/m^2/d$) and minimum daily water temperature (degrees C). D) Moderate inter-day coupling of GPP and heterotrophic N removal (denitrification), showing that day-to-day changes in GPP (in g $O_2/m^2/d$) explain 59% of the observed day-to-day changes in estimated denitrification (mg $N/m^2/d$).*

We also observed strong covariance between incident radiation and GPP (Fig. 2-46b), and between the nighttime water temperature and respiration (Fig. 2-46c). The latter relationship has a smaller slope than other similar relationships, suggesting less temperature sensitivity to respiration (0.58 vs. 0.9 – 2.3 in other rivers); whether high levels of recalcitrant OM in this river system has a role to play in this difference is unknown.

Finally, as with nearly all other rivers in this study, there is a strong day-to-day indirect coupling between changes in GPP and attendant changes in denitrification (Fig. 2-46d). While the magnitude of denitrification is uncertain, these changes are less subject to that uncertainty, and further suggest that recent autochthonous production is the driver of denitrification. Indeed, the slope is nearly 30, suggesting that a unit change in GPP yields nearly a 10% change in denitrification. This underscores the importance of not extrapolating these findings to a more general behavior of black-water rivers. This labile OM is simply not produced in the same quantities in the river when tannic acids occlude light to the benthic surface, and in the absence of that recent primary production, it is entirely unclear what levels of U_{den} can be expected. Refinements of the method that allow application in blackwater systems (the subject of a subsequent section of this report) may allow deeper insight into what the decline in N removal rates are under more typical conditions in the Santa Fe, and other similar rivers.

Deployment 10 – Juniper Creek November 2010

Juniper Creek is of particular interest because, like Alexander Springs, it is a low nitrate system, and unlike Alexander Springs, it does not appear to be as biologically productive, at least in the upper river where it is well shaded. We deployed sensors at two locations, one upstream (ca. 1700 m from the boil) and another further downstream (ca. 3300 m from the boil). Data from the lower sensor were unusable because of high levels of color accumulated from riparian swamps, and are not reported here. Raw data from the upstream location are shown in Fig. 2-47, and exhibit marked diel variation in nitrate, DO, and temperature. Of particular significance is the observation that nitrate varies in the same direction as other rivers, and NOT as in Alexander Springs Creek. This suggests that diel method is appropriate for this system, possibly indicating the absence of N limitation in this highly shaded spring run.

Patterns of diel variation for DO and temperature were distinctly asymmetrical (steeper leading than receding edge) which was observed in the Santa Fe River. This may be a function of Fern Hammock Springs as a major tributary with its own spring run (which feeds in above our upstream station) or the numerous sand boils that contribute groundwater along the channel downstream of the headspring.

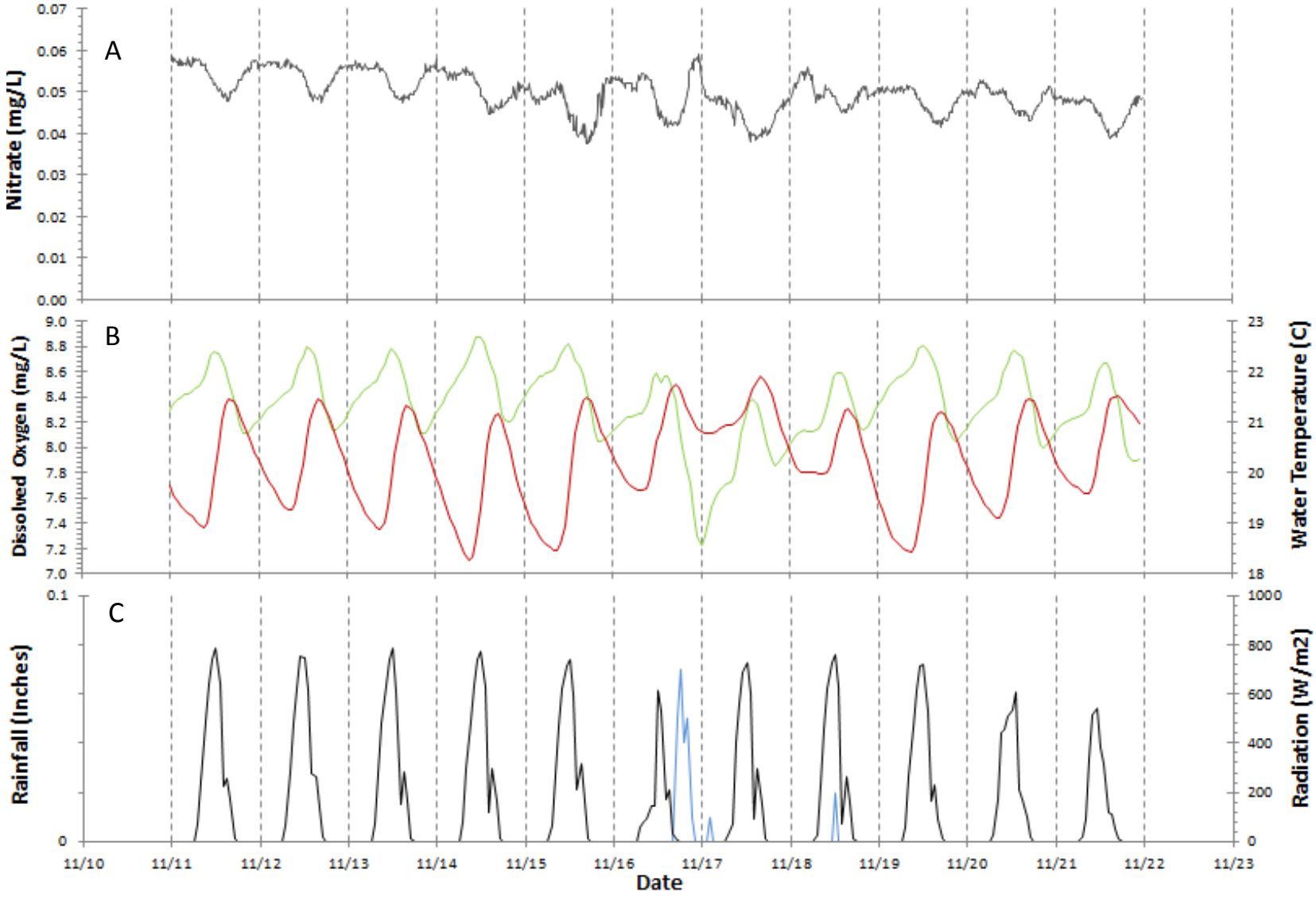

Fig. 2-47 - Diel variation in nitrate (grey line), dissolved oxygen (green line), water temperature (red line), radiation (black line) and rainfall (blue line) for Juniper Creek during a November 2010 deployment. Vertical dashed lines are at midnight every 24 hours.

A major oxygen depletion event occurred on 11/16 in response to a modest rainfall event, perhaps as a result of the mobilization of water from the adjacent swamps.

The nitrate curve, which is noticeably noisier than other rivers presumably because of the low concentration (ca. 0.07 mg/L) has long night-time plateaus suggesting that the hydraulics of this river meet the basic assumption of 24-hour removal ascribed to a single day. The input baseline at the spring vent was measured as 0.08 mg/L, suggesting that both assimilation and denitrification are occurring in this system (Fig. 2-48). There were two days on which the assimilation estimates were problematic (11/15 with a noisy baseline, and 11/17 where a rain event changed the concentration for a short period). We excluded these two dates in subsequent analyses.

Estimates of GPP in this system are dependent on reaeration, which averaged 0.52 hr^{-1} across the deployment, with a range from 0.50 to 0.53; despite the relative constancy of this value, we used the mean reareation value throughout.

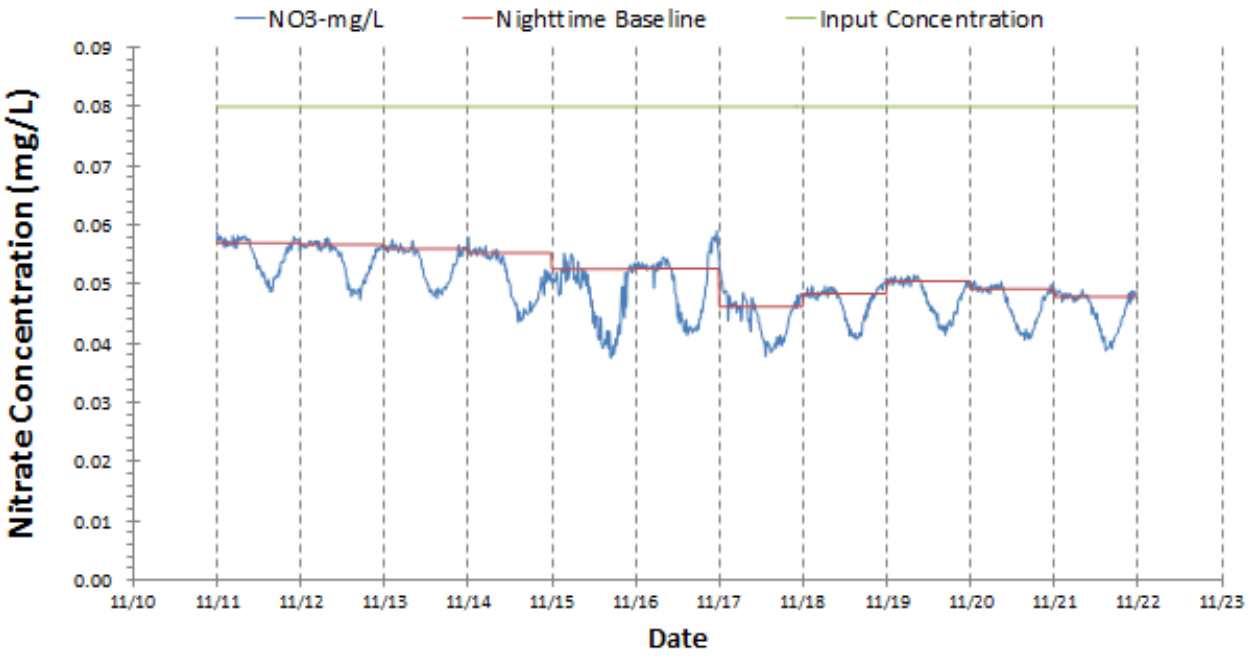

Fig. 2-48 – Summary of N removal mechanism inference for Juniper Creek, November 2010. Assimilatory removal is estimated based on diel variation in nitrate (blue line) referenced to a nighttime baseline value (red line). Dissimilatory removal is estimated as the mass loss between upstream input concentrations (green line) and the nighttime baseline; that is, denitrification is assumed constant over the course of each 24-hour period. Day-to-day variation in the nitrate baseline is explored below. Note that the nitrate variation in this low nitrate system is in the same direction as other higher nitrate rivers, in stark contrast to the observed diel variation in Alexander Springs.

Estimates of GPP and R for the deployment (Fig. 2-49) suggest that Juniper in this upper reach is net heterotrophic (P:R = 0.62), and GPP values are low (1.9 g $O_2/m^2/d$). This is consistent with the sand bottom and low density of algae and vascular plants, as well as the dense shade over the entire reach. Maintenance of net heterotrophy in this river is probably accomplished by regular allochthonous organic

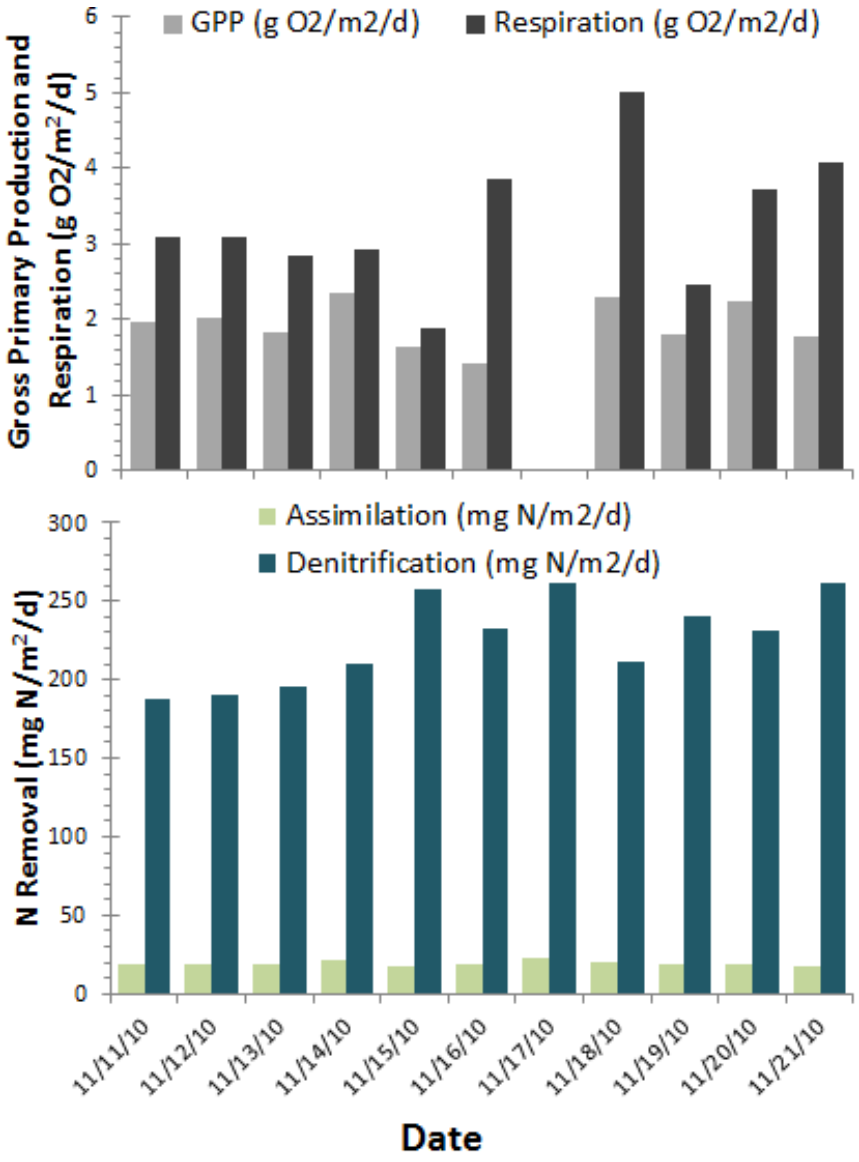

Fig. 2-49 – Summary of November 2010 deployment at Juniper Creek showing estimates of gross primary production and respiration (top panel) and assimilatory and dissimilatory N removal (bottom panel). Note that GPP and R values for 11/17 were omitted because of storm induced depression of DO (presumably from enhanced lateral inflows from the littoral swamps).

carbon delivery from the trees that shade the river, as well as bank seepage of water rich in dissolved organic carbon (DOM). Evidence for the latter was observed in the longitudinal accumulation of color over the lower reach of the river, and the generally tannic nature of the river much farther downstream.

N removal was low as well, with N assimilation averaging 19 mg $N/m^2/d$ and denitrification averaging 226 mg $N/m^2/d$. We note that the latter is, like all such estimates, subject to uncertainty because of the concentration of the inputs, and because of the confounding effects of dilution on the mass balance. As such, this might best be viewed as an upper bound estimate of the denitrification mass flux.

NPP covaries modestly with N assimilation estimates (Fig. 2-50a); the relationship is positive and statistically significant, but suggests a large y-intercept that we cannot explain. However, it does yield a C:N ratio (22.3:1) for primary production that is similar or slightly lower than values observed in other rivers dominated by vascular plants. GPP was a weak function of insolation (Fig. 2-50b), though one reason for the weaker than expected association is the presence of a dense canopy that may make the system more sensitive to when the insolation is high rather than simply the total amount (i.e., because of canopy gap effects). The relationship between nighttime water temperature and respiration was very strong, as it has been for all non-summer deployments (Fig. 2-50c); the slope of the line is consistent with other rivers, but suggests an extremely large relative effect in this low metabolism river. Finally, the day-to-day indirect coupling between GPP and denitrification (Fig. 2-50d) is strongly significant. Note however, that the entire range of GPP variation in the river moves U_{den} only by about 20%, suggesting that other sources of carbon may be actively maintaining high U_{den} levels even where autochthonous organic carbon availability is varying. The slope of the ΔGPP vs. ΔU_{den} line is markedly larger than other rivers studied, perhaps reflecting the relative paucity of labile C in this well shaded river.

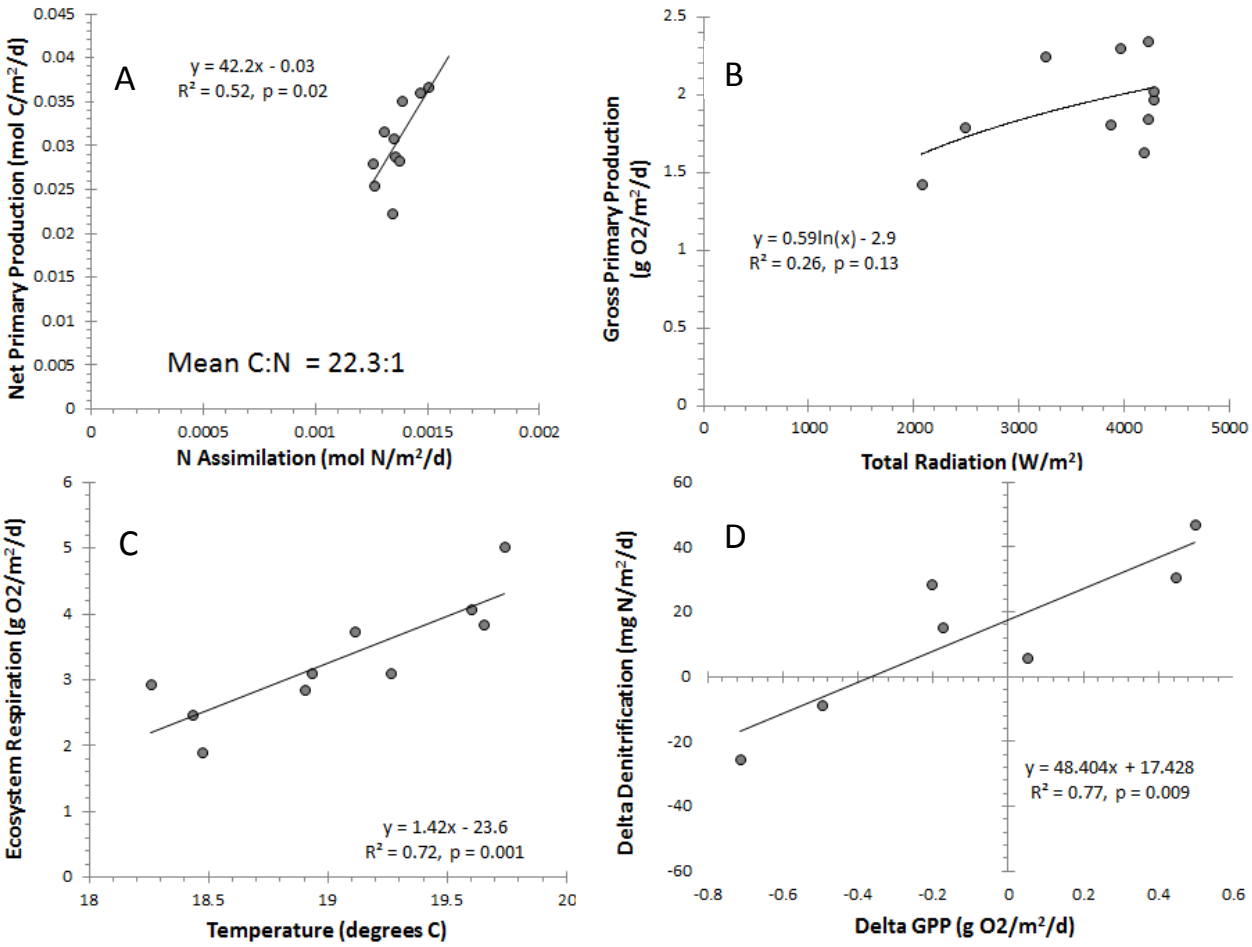

*Fig. 2-50 – Summary of ecosystem C and N metabolism from Juniper Creek, Nov. 2010. A) Relationship between N and C assimilation (assuming net primary production = 0.5 * gross primary production) on a molar basis. Mean C:N stoichiometry of ecosystem metabolism is ca. 22.3:1; note that this is different than the fitted line because the intercept is not zero. B) Relationship between GPP (in g $O_2/m^2/d$) and incoming solar radiation (W/m^2), with a best fit line. C) Relationship between ecosystem respiration (g $O_2/m^2/d$) and minimum daily water temperature (degrees C). D) Strong inter-day coupling of GPP and heterotrophic N removal (denitrification), showing that day-to-day changes in GPP (in g $O_2/m^2/d$) explain 77% of the observed day-to-day changes in estimated denitrification (mg $N/m^2/d$).*

<u>*Deployment 11: Rock Springs Run – December 2010*</u>

For this portion of the research, our final deployment was in Rock Springs Run, with sensors deployed at two locations, one relatively far upstream near the downstream boundary of at the Orange County park, and the other much further downstream in the reach of the river where channel morphology gets much deeper and broader, with attendant changes in velocity. Over the period of the deployment, which occurred in early December 2010, photoperiod was short making comparisons of GPP to other rivers somewhat challenging. Despite that caveat, the raw data suggest obvious diel nitrate variation, with

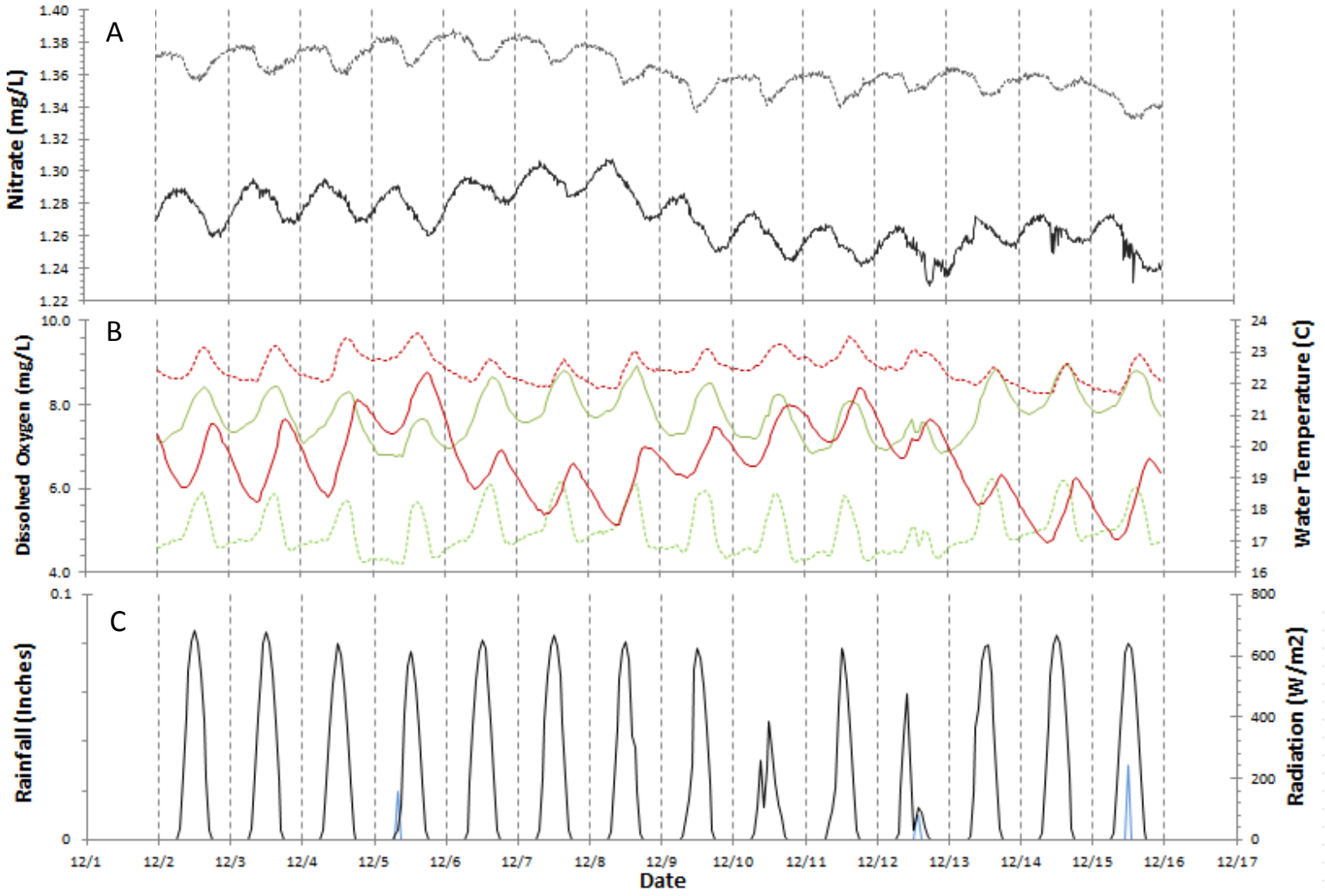

Fig. 2-51 - Diel variation in nitrate (solid grey line – downstream, dashed grey line - upstream), dissolved oxygen (sold green line – downstream, dashed green line – upstream), water temperature (solid red line – downstream, dashed red line – downstream), radiation (black line) and rainfall (blue line) for Rock Springs Run during a December 2010 deployment. Vertical dashed lines are at midnight every 24 hours.

daytime troughs and nighttime peaks, and typical variation in both dissolved oxygen and temperature (Fig. 2-51). There were two cloudy days during the deployment (12/10 and 12/12) and there was a clear oxygen response, but no clear nitrate response. The temperature and DO variation is markedly elongated in the lower river, as would be expected due to longitudinal hydraulic dispersion.

The diel nitrate method can be implemented here, but the upstream nitrate concentration measured at the spring vent results in several days in the upper river when denitrification is actually negative (Fig. 2-52). Much higher magnitude of denitrification is implied by the dramatic station-to-station drop, though as with other rivers, this cannot be readily disentangled from lateral inputs of low nitrate water. There is evidence of some systematic variation in the baseline; both upstream and downstream stations vary in the same way, with high nitrate levels during the first half of the deployment, and lower levels for the second half. It is unknown whether this is due to variation in the vent inputs, or synchronized changes in ecosystem processes. Also notable is the dramatic differences between upstream and downstream

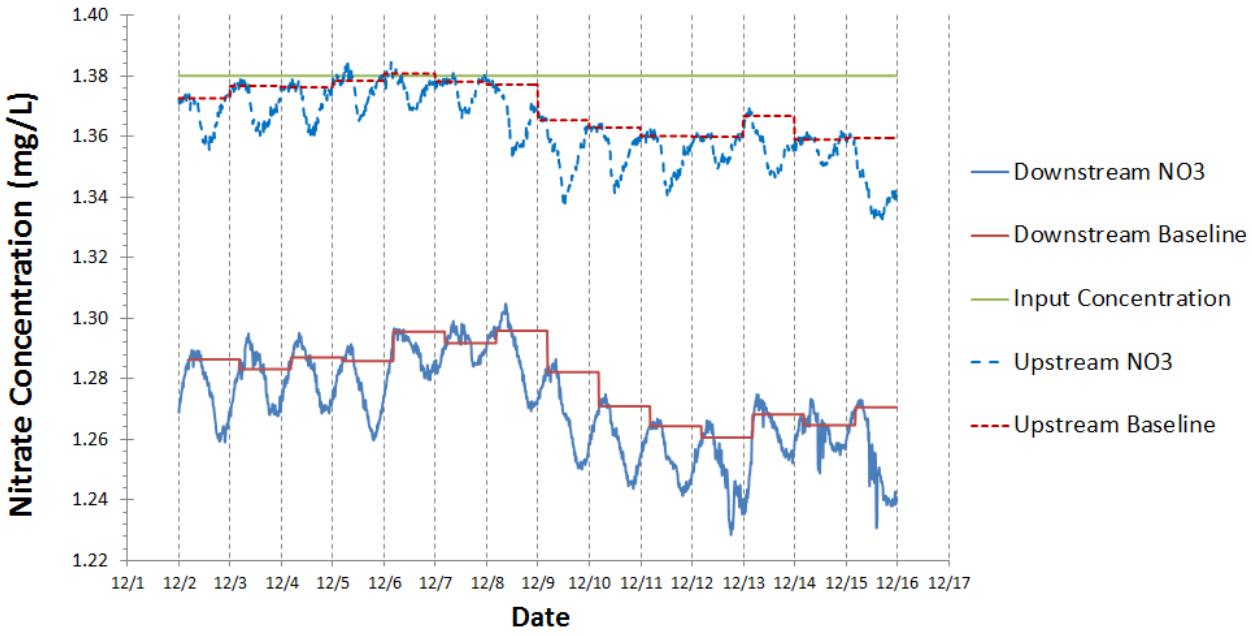

Fig. 2-52 – Summary of N removal mechanism inference for Rock Springs Run, December 2010. Assimilatory removal is estimated based on diel variation in nitrate (blue line; dashed – upstream, solid - downstream) referenced to a nighttime baseline value (red line; dashed – upstream, solid - downstream). Dissimilatory removal is estimated as the mass loss between upstream input concentrations (green line) and the nighttime baseline; that is, denitrification is assumed constant over the course of each 24-hour period. Day-to-day variation in the nitrate baseline is explored below. Note that variation in the spring vent concentration, which may explain the global pattern, is unknown for this deployment

nitrate signals with regard to the diel amplitude, which was ca. 20 µg/L in the upstream station and more than double that in the downstream station, in addition to being more longitudinally dispersed (i.e., shorter duration nighttime baseline concentrations. Overall N removal appears to be on the order of 10% over the reach.

The reaeration constants used for the deployment varied dramatically between the upper and entire river reaches. The upstream reach, which has much higher velocities, had an average K of 0.66 hr^{-1} over the deployment, ranging from 0.61 to 0.72, with the low value during the cloudy day on 12/12. In contrast the lower river, which includes the upper section, had an integrated reaeration rate of 0.40 hr^{-1}, with a range between 0.35 and 0.46 hr^{-1}.

The resulting estimates of GPP and R for both upstream and downstream runs are shown in Fig. 2-53. Notably, both productivity and respiration are much higher in the upper river (5.8 and 3.3 g $O_2/m^2/d$, respectively), and decline substantially for the entire river estimate (1.9 and 2.4 g $O_2/m^2/d$, respectively),

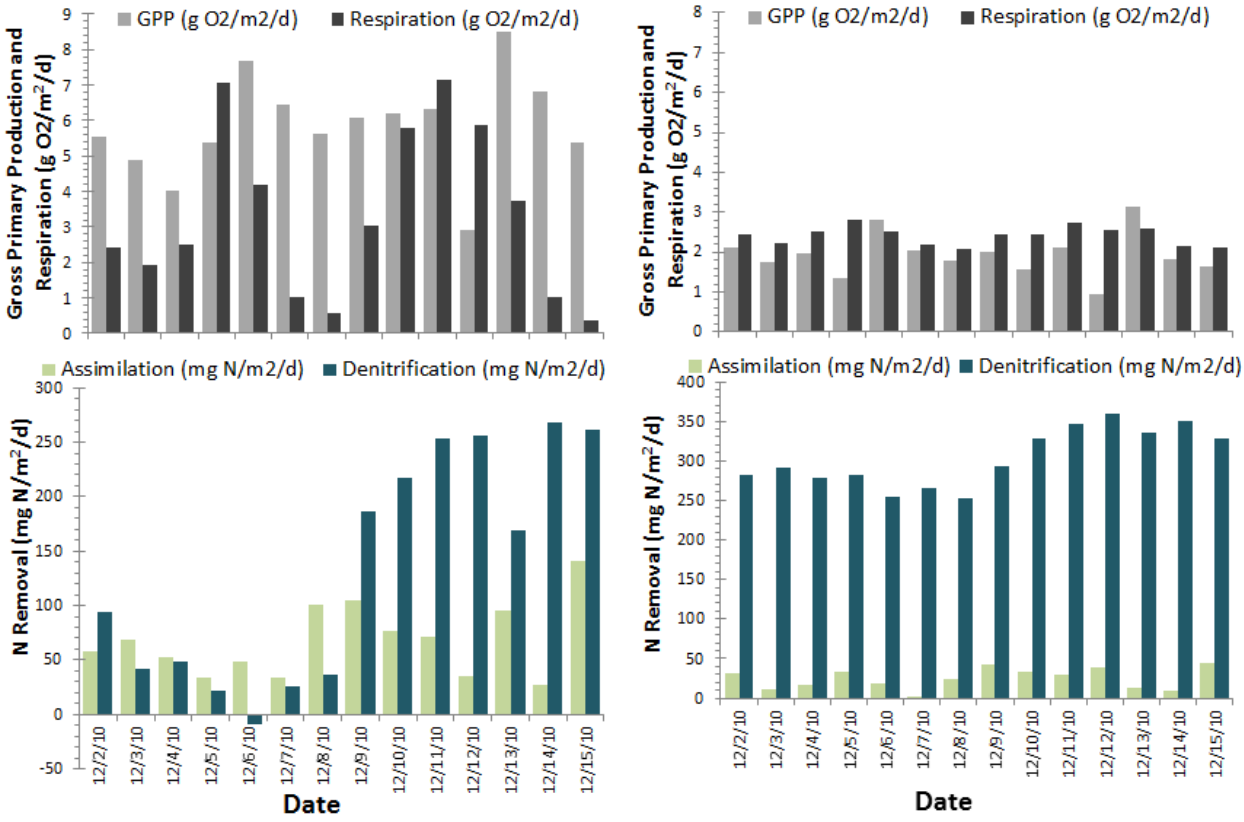

Fig. 2-53 – Summary of December 2010 deployment at Rock Springs Run showing estimates of gross primary production and respiration (top panels) and assimilatory and dissimilatory N removal (bottom panels) for both upstream (left panels) and downstream (right panels) reaches.

suggesting that GPP and R of the lower reach is even lower (since the upper reach is included in the entire river estimate. The river is also basically metabolically neutral, with P:R ratios in both upper and lower stations near 1 (0.80 for the downstream and 1.75 for the upstream sondes). The reason for such dramatic differences in productivity between upper and lower rivers is unknown, but longitudinal increases in water color may explain part of that signal.

A similar analysis of assimilation (U_a) and denitrification (U_{den}) between the upper and lower river suggest striking differences as well (Fig. 2-53). As might be expected based on patterns of primary production, assimilation estimates are higher in the upper (67 mg N/m^2/d) than the lower (25 mg N/m^2/d) river. However, given the upstream concentrations observed 1.38 mg N/L), the estimated denitrification in the upper river is small and, on some dates, negative (mean U_{den}= 133 mg N/m^2/d). Downstream, the denitrification estimate is much more consistent and larger (mean U_{den} = 303 mg N/m^2/d), and dwarfs assimilation, which represents less than 10% of the total removal. The large change in U_{den} around 12/9/2011 is best explained by variation in the headspring concentration, but we have no empirical data to support that, and the headspring concentration that was measured at the start and finish of the deployment was the same. Note that the hydraulics of Rock Springs Run are quite complex, with significant channel braiding and potential for lateral inputs, as well as bank hardening in the headspring area in the County Park. All of these features may affect the estimates of denitrification, as may modest variation in vent water concentrations over the period of the deployment. The plausibility of this latter explanation is supported by the strong temporal similarities between the two denitrification patterns, which might not be the case if there are time varying lateral inputs.

The typical assessment of process rate associations reveals several notable findings (Fig. 2-54). First, the association between NPP and U_a is weak (non-significant) in the upper river. The resulting C:N ratio is a comparatively low 23:1, suggestive of mixed autotrophic production, and consistent with relatively high algal cover observed during deployments. Second, we observed a positive but non-significant association between light and GPP; we surmise that the relationship is not significant primarily because of shading effects on this relatively narrow reach of the river (see Fig. 2-1 for study site maps). The association between nighttime water temperature and respiration was strong, as has been observed for all winter-time deployments across rivers. Finally, despite the relatively modest magnitude of denitrification in this upper river segment, we continue to see a statistically significant coupling between inter-day changes in GPP and associated changes in U_{den}. The slope of this line is comparable to other systems, suggesting that a unit change in GPP results in a 14 mg N/m^2/d change in U_{den}.

Similar associations in the lower river (Fig. 2-55) result in the unexpected observation that NPP and U_a are negatively associated, though this association is not statistically significant. The reason for this is entirely unclear, though it may have something to do with heterotrophic N demand. The C:N ratio of primary production over the entire deployment is 21:1, but is highly variable, as would be expected given the inverted association of NPP and U_a (range of C:N = 5 to 40:1). Other associations are more typical. We observed a marginally significant relationship between light and GPP with best-fit parameters comparable to what was observed for the upper river. The association between water

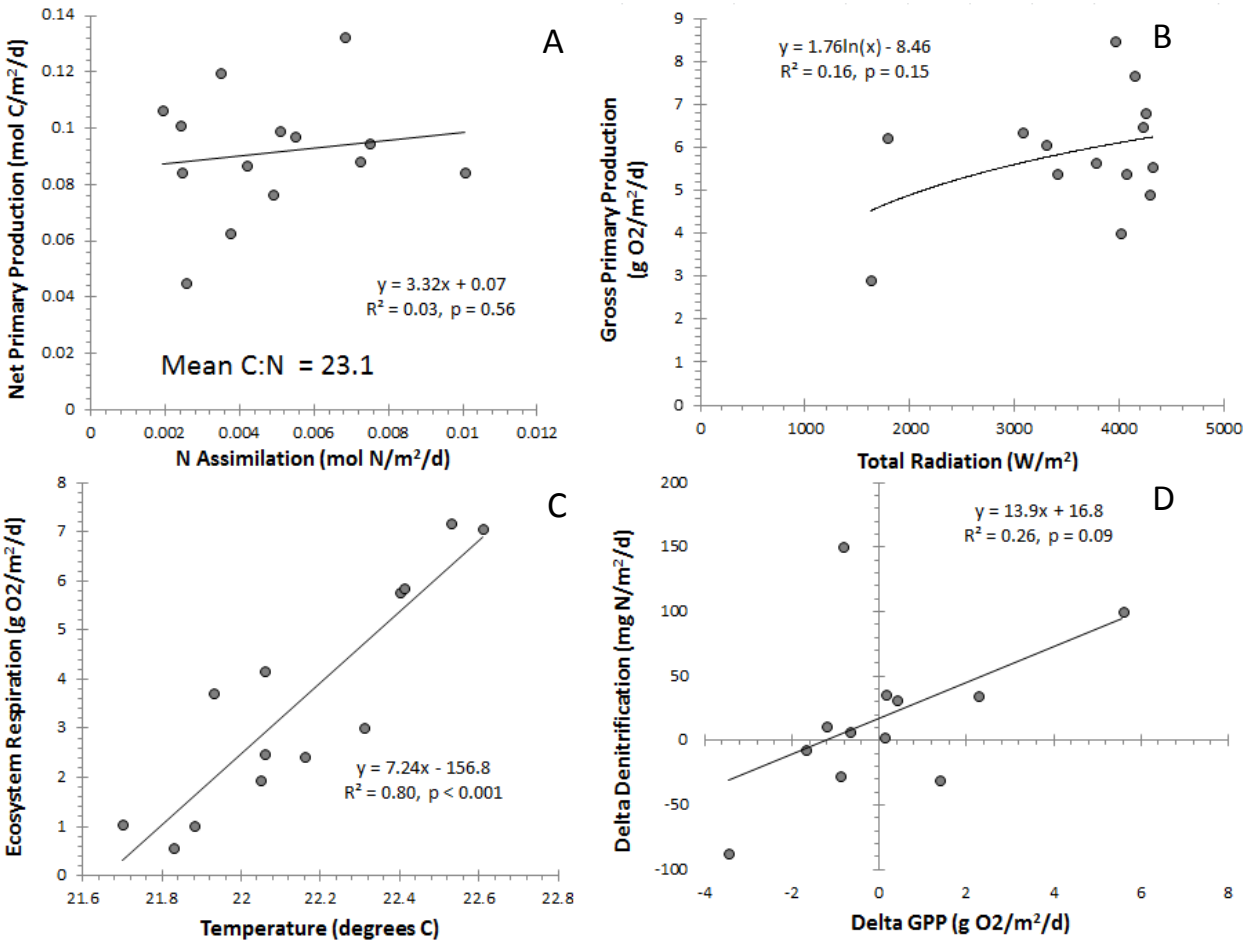

*Fig. 2-54 – Summary of interrelated elements of ecosystem C and N metabolism from upstream Rock Springs Run, December 2010. A) Relationship between N and C assimilation (assuming net primary production = 0.5 * gross primary production) on a molar basis. The mean C:N stoichiometry of ecosystem metabolism is ca. 21.3:1; note that this is different than the fitted line because the intercept is not zero. B) Relationship between GPP (in g $O_2/m^2/d$) and incoming solar radiation (W/m^2), with a non-statistically significant best fit line. C) Relationship between ecosystem respiration (g $O_2/m^2/d$) and minimum daily water temperature (degrees C). D) Modest but significant inter-day coupling of GPP and heterotrophic N removal (denitrification), showing that day-to-day changes in GPP (in g $O_2/m^2/d$) explain 26% of the observed day-to-day changes in estimated denitrification (mg $N/m^2/d$).*

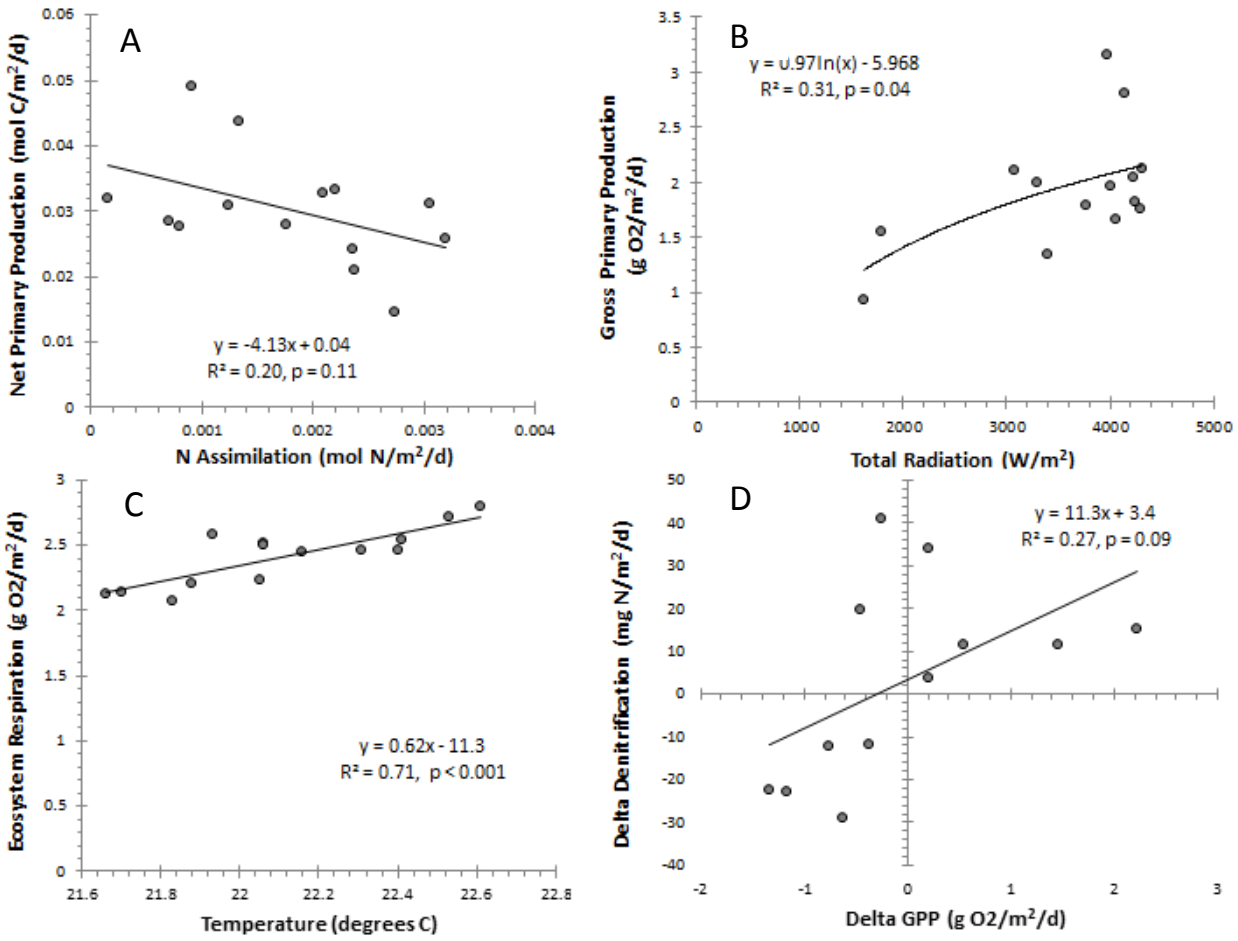

*Fig. 2-55 – Summary of interrelated elements of ecosystem C and N metabolism from Rock Springs Run, December 2010. A) Negative relationship between N and C assimilation (assuming net primary production = 0.5 * gross primary production) on a molar basis; the reason for this inversion in the expected direction of the association is unclear. The mean C:N stoichiometry of ecosystem metabolism is ca. 15:1; note that this is different than the fitted line because the intercept is not zero, and that this mean value has a tremendous range (5 – 40:1) over the deployment. B) Relationship between GPP (in g $O_2/m^2/d$) and incoming solar radiation (W/m^2), with a best fit line. C) Relationship between ecosystem respiration (g $O_2/m^2/d$) and minimum daily water temperature (degrees C). D) Modest inter-day coupling of GPP and heterotrophic N removal (denitrification), showing that day-to-day changes in GPP (in g $O_2/m^2/d$) explain 27% of the observed day-to-day changes in estimated denitrification (mg $N/m^2/d$).*

temperature and respiration was particularly strong, though the magnitude of the effect was smaller in the entire river than in the upper river by an order of magnitude. Spatial and temporal variation in this respiration-temperature association is an area of future research, since the effect is ubiquitous but with variable magnitude. Finally, as with the upper river, there is evidence of an indirect association between GPP and U_{den} with a slope consistent with other rivers and the upper Rock Springs Run reach.

Deployment 12: Silver Glen Springs Run – April 2011

After the completion of the main project deployments, we became particularly curious about what controls the pattern of diel variation between high and low N concentration rivers. The observed signal at Alexander Creek Run, which is inverted from all the other signals observed in this work, was tentatively ascribed to N limitation; the proposed underlying mechanism of inverted diel variation is that assimilation occurs at all times (not just the daytime) in N limited ecosystems, and the diel variation (increase in N during the day) is due to O_2 inhibition of denitrification. Silver Glen spring run is another low N concentration spring (vent water was measured at 0.05 mg N/L) with a reasonably long run for which the methods used here may be applicable. We deployed the sensors at a downstream location (ca. 920 m below the main vent) on April 7th, 2011, and monitored water quality for 13 days; the last three days of the deployment were unusable because of biofouling (algal detritus) so we report in Fig. 2-56 the raw data for the first 10 days only.

Notably, the diel variation in nitrate follows the SAME pattern as was observed in Alexander Creek, and opposite to all other systems, including the low N and low GPP Juniper Creek. Overall, there is apparent net removal, with the concentration at the downstream location almost always lower than the vent water concentration. During the day, however, and contemporaneous with the peak in dissolved oxygen concentrations, the nitrate levels in the water are effectively equal to the vent concentrations. Diel variation in temperature and dissolved oxygen are typical of a well lit and highly productive aquatic ecosystem, and during the period of record there was no rainfall and highly regular insolation (measured at the nearby Pierson FAWN station). As with Alexander Creek, the inference of assimilation and denitrification doesn't work here because of the inverted diel signal (Fig. 2-57). However, we do note that there is significant net N removal (ca. 30% of the vent flux).

A summary of the ecosystem metabolic and nutrient uptake estimates for Silver Glen are shown in Fig. 2-58. The reaearation estimate for this river was reliably predicted by the nighttime regression method, and averaged 0.46 hr^{-1} over the period of deployment. The Silver Glen ecosystem is metabolically neutral, with P:R averaging 0.96 over the deployment. GPP was high (mean 11.4 g $O_2/m^2/d$) consistent with the well lit conditions. The total benthic area (55,200 m^2) was more than sufficient to detect both ecosystem metabolism and nutrient uptake. As mentioned above, we are unable to partition N removal into autotrophic and denitrification fluxes because of the inverted diel signal, but we can estimate the net N removal flux (Fig. 2-58, lower panel). Interestingly, the net N removal is relatively low (mean =

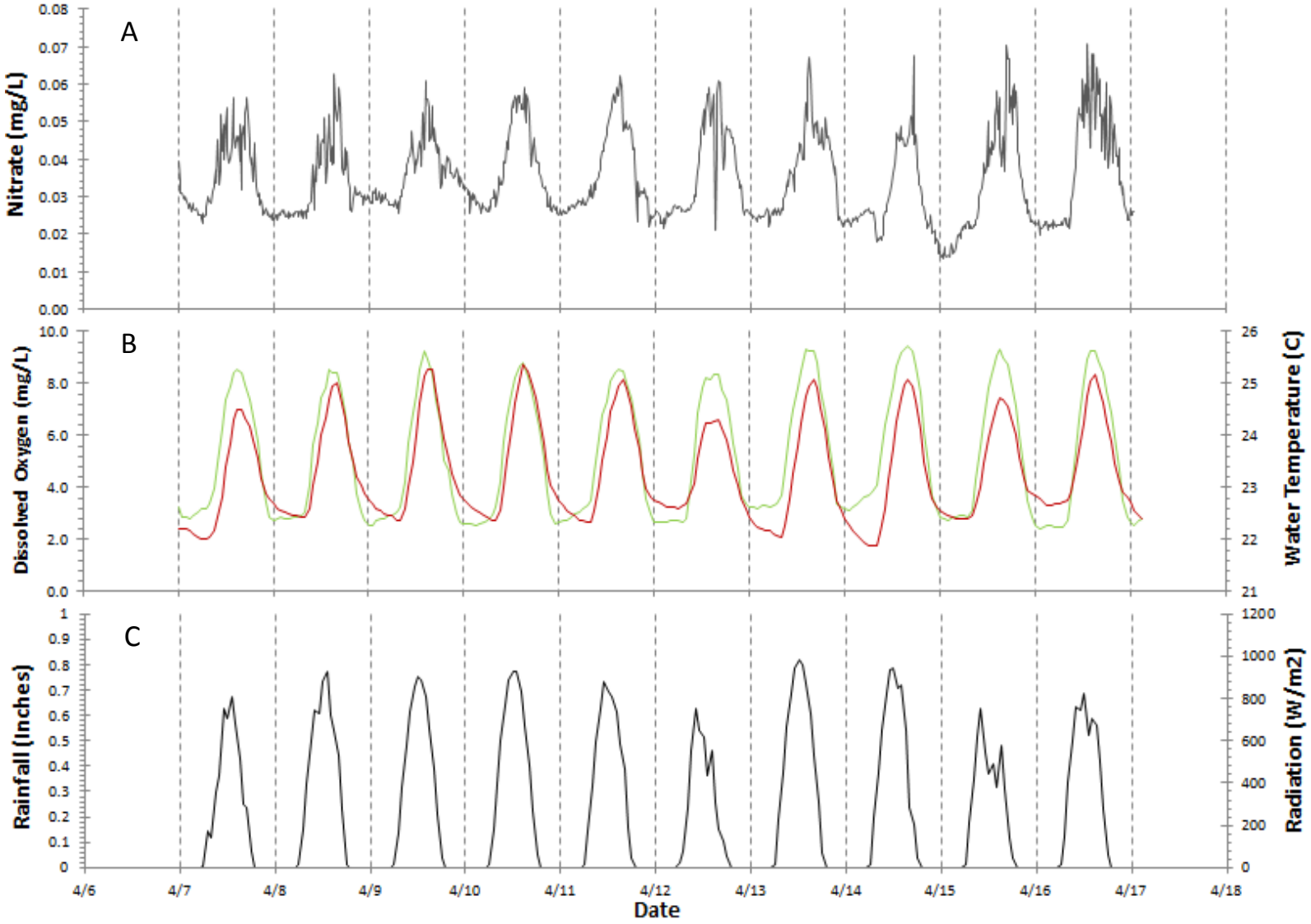

Fig. 2-56 - Diel variation in nitrate (grey line), dissolved oxygen (green line), water temperature (red line), radiation (black line) and rainfall (blue line) for the Silver Glen Springs during April 2011 deployment. Vertical dashed lines are at midnight every 24 hours.

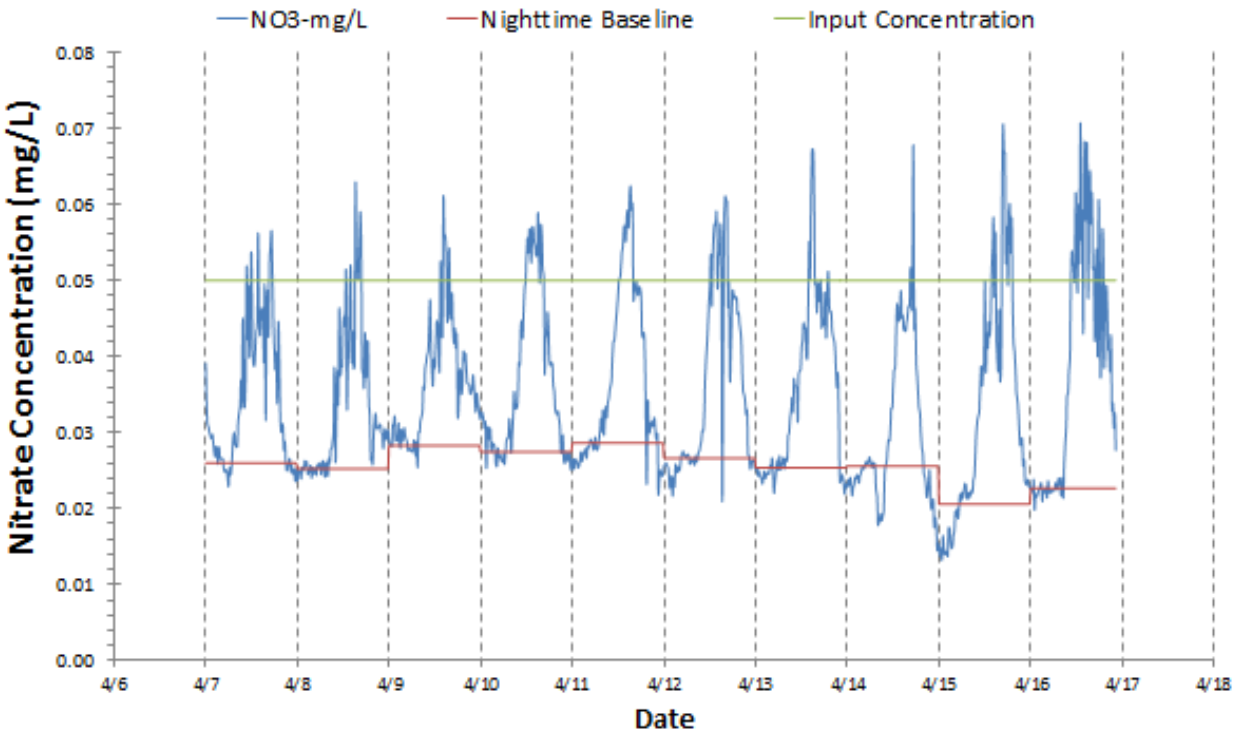

Fig. 2-57 – Summary of N removal mechanism inference for the Silver Glen Springs in April of 2011. Assimilatory removal cannot be estimated based on diel variation because nitrate (blue line) during the day is higher than the nighttime baseline value (red line). Estimates of total removal based on the mass loss between upstream input concentrations (green line) and the observed concentrations cannot be partitioned between denitrification and assimilation using the assumptions made elsewhere, but do provide a useful benchmark against which to compare other estimates of assimilatory demand (i.e., from oxygen metabolism measurements assuming a C:N ratio of the algal productivity of 12.5:1).

60.2 mg N/m^2/d) compared with other rivers. Moreover, given the high GPP and an assuming a C:N ratio of 12.5:1 (typical of algal taxa dominant in the Silver Glen system), the imputed autotrophic demand is very large (197 mg N/m^2/d) compared to the net removal flux, suggesting that internal recycling is a critical component of ecosystem N demand in the low concentration setting. We revisit these types of calculations in Research Element #7 in Alexander Creek.

Finally, we present the summary figures from Silver Glen Springs. As with Alexander, the relationship between GPP and N assimilation is negative (Fig. 2-59A) though not statistically significant; this occurs as a consequence of diel signal inversion. That the magnitude of the diel variation remains correlated with primary production is consistent with the idea that the magnitude of daytime inhibition of denitrification is proportional to how much oxygen is produced (i.e., GPP). As such, we use the association as tentative confirmation that most of the diel pattern is due to denitrification dynamics, and that assimilatory demand must be relatively constant over the day. Unlike some of the other rivers,

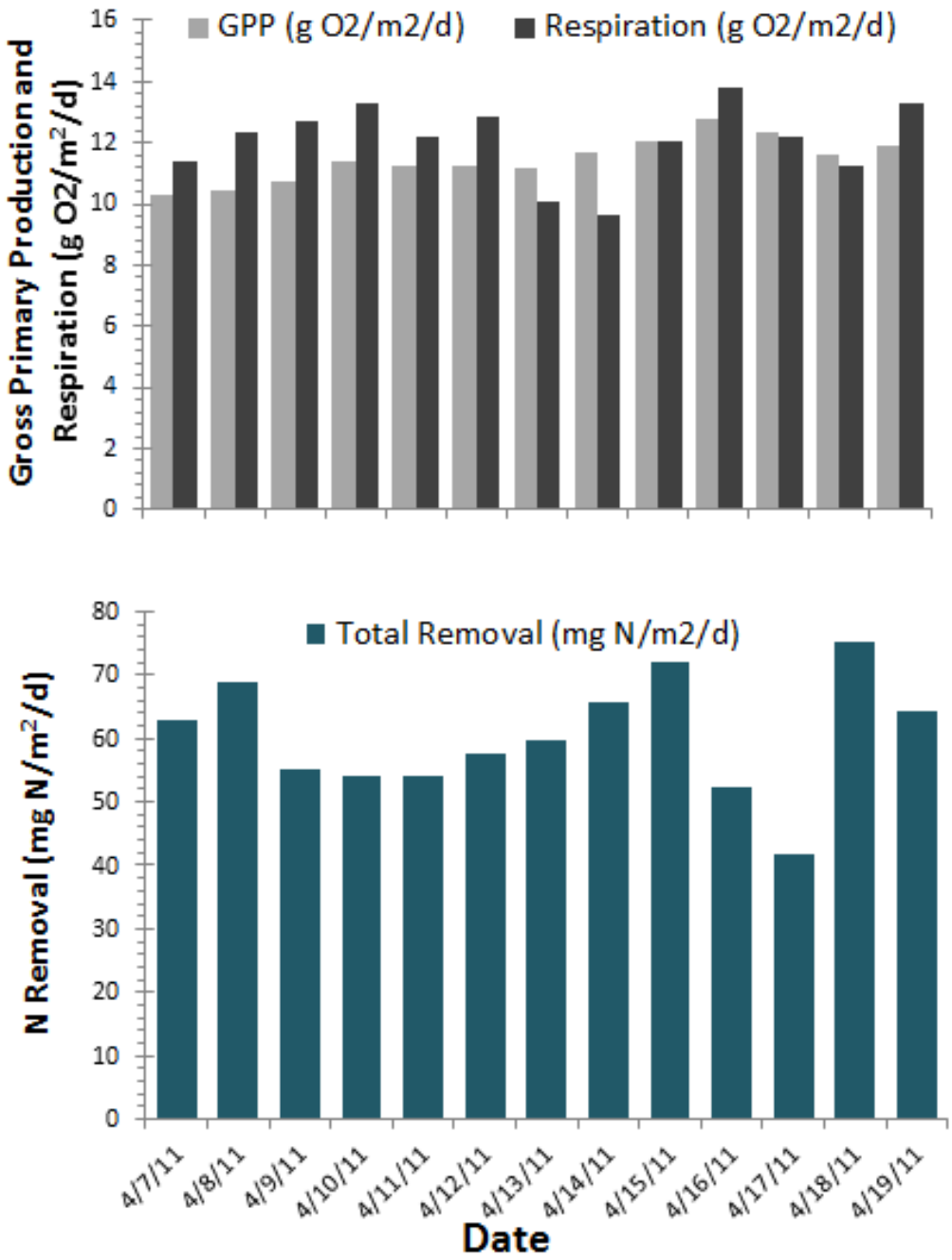

Fig. 2-58 – Summary of April 2011 deployment at Silver Glen Springs showing estimates of gross primary production and respiration (top panel) and total N removal (bottom panel). Note that estimates of total N removal include both denitrification and assimilation, rates of which cannot be partitioned in this system because diel nitrate variation is inverse to what has been observed elsewhere. We use the total (net) N removal as an upper bound on net algal mat assimilation, recognizing that denitrification is almost certainly occurring in this system because dissolved oxygen levels get very low at night.

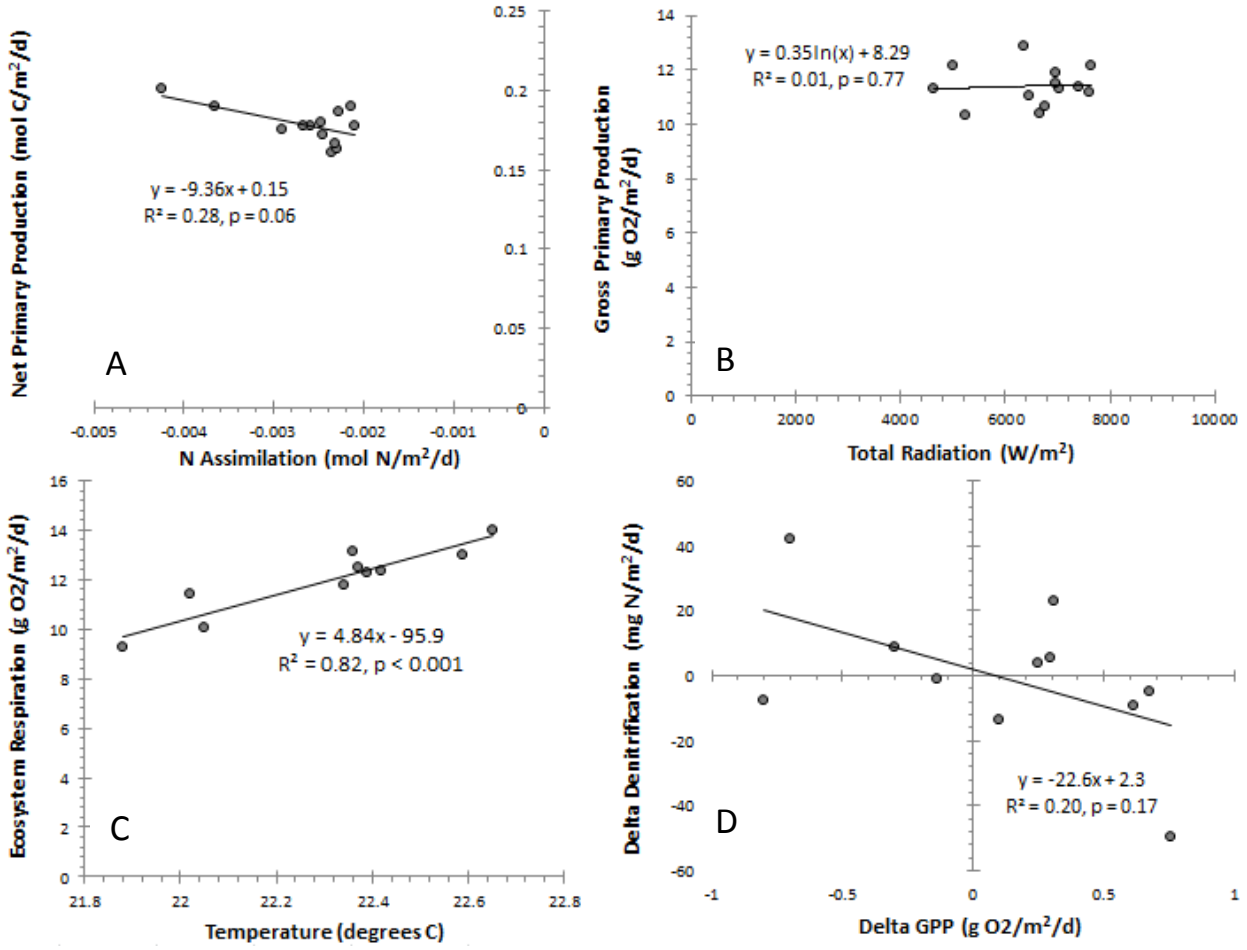

*Fig. 2-59 – Summary of interrelated elements of ecosystem C and N metabolism from the Silver Glen Spring, April 2011. A) Relationship between N and C assimilation (assuming net primary production = 0.5 * GPP) on a molar basis. U_a estimates are negative because of inverted diel nitrate variation; however, the magnitude of diel N excursion was still statistically significantly associated with primary production. B) Relationship between GPP (g $O_2/m^2/d$) and solar radiation (W/m^2), with a best fit line. C) Relationship between respiration (g $O_2/m^2/d$) and minimum water temperature (°C). D) Inter-day coupling of GPP and denitrification was not evident in this system. Note that denitrification estimates are confounded by inverted diel variation, and as such are not reflective of that process alone.*

there was no association between measured insolation and GPP, perhaps because of light saturation effects at these high insolation rates. What was significant, and was observed on other systems, was a strong association between respiration and temperature; the slope of the line (4.84 g $O_2/m^2/d$ for each degree change in minimum temperature) suggests larger than expected sensitivity to temperature. Finally, we noted no association between day-to-day changes in denitrification and commensurate changes in primary production; that association was observed in nearly all other systems, and its absence here is not well understood.

Synthesis

The findings of this section focus on estimating the rates of two mechanisms of N removal, assimilation and denitrification. To interpret the N removal mechanisms in an ecosystem context, we also obtained measurements of metabolism (gross primary production and respiration). We report the summary statistics for each of the deployments in Table 2-2. There are two important caveats that need to be considered for this work. First, each of the deployments took place at different times of the year, and this makes a direct comparison challenging. Despite the chemical and discharge constancy of these systems, there is pronounced seasonal variation in processes, responding to variation in light, ambient air temperature, rainfall patterns, and the phenological dynamics of the elements of the autotrophic AND heterotrophic communities. This means that even ratios (like C:N) may have seasonal dynamics that would confound a direct comparison between deployments in different rivers at different times. That said, broad patterns of high or low assimilation or denitrification are very likely to be maintained based on the relative constancy of the Ichetucknee River data for which a longer period of measurement exists. Second, there are several important hydraulic assumptions embedded in this analysis. First and foremost is that we cannot discern, based on these data, whether mass loss we observed between the vent and the nighttime baseline concentration, which we attribute to denitrification, is actually a dilution signal. We have reason to believe that the importance of dilution is relatively low, based on

*Table 2-2 (next page) – Summary of diel nitrate variation deployments showing metabolism measurements (upper panel) and N removal estimates (lower panel). On the upper panel, K is the reaeration rate (hr^{-1}), GPP is gross primary production and R is ecosystem respiration (both in g $O_2/m^2/d$), P:R is the ratio of production to respiration, GPP vs. Sun Fit is the goodness of fit (r^2) between solar insolation and GPP over the deployment, and the T vs. R slope is the slope of the line relating ecosystem respiration and nighttime water temperature. On the lower panel, assimilation (U_a) and denitrification (U_{den}) are reported in mg $N/m^2/d$), % U_a is fraction of total removal that is due to assimilation, total flux is the vent water mass flux reported on a per unit area basis (mg $N/m^2/d$), $S_{w,a}$ is the autotrophic uptake length (distance to remove boundary inputs of N via autotrophic assimilation, a measure of N limitation with smaller values indicating more limiting conditions) for each river estimated for current and historical nitrate delivery conditions (assuming historical concentrations of 0.05 mg N/L), C:N is the mean estimate of the C:N ratio of ecosystem metabolism, and the fit (r^2) and slope of the line relating changes in GPP and changes in U_{den} are shown. The * at Alexander Springs Creek and Silver Glen Springs denote that assimilation and denitrification estimates are obtained differently than other systems. Assimilation is derived from GPP, assumed 50% autotrophic respiration and a C:N ratio of 12.5:1. Denitrification is actually TOTAL net N removal. These differences from other systems are necessary because of inversion in diel nitrate signal that preclude inference about riverine N removal used for all the other rivers.*

				Metabolism					
River	**Location**	**Date**	**Duration**	**K (hr-1)**	**GPP**	**R**	**P:R**	**GPP vs. Sun Fit**	**T vs. R Slope**
Silver	Downstream	15-Jan	16 days	0.45	10.1 ± 2.7	10.3 ± 0.5	0.99 ± 0.28	0.86	0.91
Silver	Upstream	6-Oct	9 days	0.35	20.0 ± 0.9	16.9 ± 2.3	1.21 ± 0.18	0.01	5.99
Silver	Downstream	6-Oct	9 days	0.42	10.9 ± 0.4	10.3 ± 0.5	1.07 ± 0.07	0.13	1.33
Rainbow	Downstream	19-Feb	14 days	0.56	16.8 ± 2.1	9.3 ± 0.4	1.79 ± 0.24	0.78	1.14
Rainbow	Upstream	18-Oct	10 days	0.49	25.6 ± 0.9	16.9 ± 0.5	1.51 ± 0.07	0.02	2.25
Rainbow	Downstream	18-Oct	10 days	0.62	21.0 ± 2.4	12.3 ± 1.2	1.72 ± 0.17	0.76	3.57
Alexander	Upstream	3-Apr	6 days	0.39	16.8 ± 1.1	15.5 ± 1.8	1.09 ± 0.09	0.11	19.90
Alexander	Upstream	18-Sep	13 days	0.37	12.4 ± 2.4	18.5 ± 3.7	0.71 ± 0.24	0.46	22.30
Silver Glen	Upstream	7-Apr (2011)	10 days	0.46	11.4 ± 0.7	11.9 ± 1.3	0.97 ± 0.12	0.01	4.84
Rock	Upstream	2-Dec	14 days	0.66	5.8 ± 1.4	3.3 ± 2.4	3.82 ± 4.23	0.16	7.24
Rock	Downstream	2-Dec	14 days	0.40	1.9 ± 0.6	2.4 ± 0.2	0.80 ± 0.22	0.31	0.62
Juniper	Upstream	11-Nov	11 days	0.52	1.9 ± 0.3	3.3 ± 0.9	0.62 ± 0.16	0.26	1.42
Gilchrist	Downstream	16-Apr	20 days	0.52	13.7 ± 2.9	15.2 ± 0.8	0.91 ± 0.20	0.71	8.51
Ichetucknee	Downstream	8-Jan	362 days	0.47	11.7 ± 4.3	11.1 ± 2.8	1.04 ± 0.29	0.53	2.29
Santa Fe	Downstream	13-Nov	10 days	0.24	5.7 ± 0.5	5.3 ± 0.2	1.07 ± 0.11	0.73	0.58

		N Removal								GPP vs. U_{den}	
River	**Location**	**U_a ($mg/m^2/d$)**	**U_{den} ($mg/m^2/d$)**	**% U_a**	**Total Flux ($mg\ N/m^2/d$)**	**% Flux Removed**	**$S_{w,a}$ (m) Current**	**$S_{w,a}$ (m) Historical**	**C:N**	**Fit**	**Slope**
Silver	Downstream	89.1 ± 27.6	514.4 ± 69.8	14.60%	6960	8.7%	535051	19917	25.2 ± 5.5	0.88	13.30
Silver	Upstream	122.1 ± 13.4	336.0 ± 48.4	26.70%	25369	1.8%	322041	11583	35.2 ± 2.8	0.45	19.10
Silver	Downstream	57.5 ± 5.8	613.4 ± 21.4	8.60%	7708	8.7%	918309	34784	42.0 ± 3.3	0.30	19.20
Rainbow	Downstream	132.2 ± 29.6	843.6 ± 68.5	9.40%	7816	12.5%	339949	10133	28.4 ± 4.7	0.75	24.90
Rainbow	Upstream	106.9 ± 20.8	442.6 ± 35.3	19.50%	20216	2.7%	359303	8405	53.9 ± 9.7	0.47	24.80
Rainbow	Downstream	117.1 ± 16.9	1130.2 ± 52.1	9.40%	8350	14.9%	410007	12213	39.5 ± 4.5	0.54	17.30
Alexander	Upstream	291.4 ± 25.7*	61.6 ± 49.7*	-	570	10.9%	1132	809	-	-	-
Alexander	Upstream	224.1 ± 22.1*	299.2 ± 24.1*	-	570	37.0%	1400	1000	-	-	-
Silver Glen	Upstream	197.3 ± 13.6*	60.2 ± 9.1*		203	30.2%	945	945	-	-	-
Rock	Upstream	67.7 ± 33.2	133.7 ± 106.0	33.60%	27278	0.7%	282044	12103	23.4 ± 13.3	0.26	13.90
Rock	Downstream	25.8 ± 12.0	302.3 ± 38.3	7.80%	1697	19.3%	205316	5850	22.2 ± 14.9	0.27	11.30
Juniper	Upstream	19.3 ± 1.5	225.5 ± 28.2	7.90%	587	41.7%	52000	32842	22.2 ± 2.6	0.77	48.40
Gilchrist	Downstream	134.0 ± 45.9	517.9 ± 273.2	20.60%	33442	1.9%	84853	2653	24.1 ± 5.8	0.51	26.50
Ichetucknee	Downstream	83.1 ± 33.9	522.0 ± 197.2	13.70%	7052	8.6%	212144	16065	26.2 ± 5.0	0.44	25.40
Santa Fe	Downstream	67.5 ± 11.6	288.3 ± 71.4	18.90%	4157	8.6%	693912	31730	18.8 ± 2.6	0.59	27.50

work presented previously (Research Element #1) suggesting 100% mass recovery for injected dye based on USGS discharge measurements. However, the massive density of small vents, the existence of unnamed larger springs and the general complexity of a karst channel make this assumption an important one to test in future research. As such, the denitrification estimates provided here can be viewed as an upper bound. Note, however, that if the lateral inputs are actually *higher* than the river water, then the denitrification estimate will be low. Across nearly all spring fed rivers we have observed the common pattern of highest concentrations at the vent, and declining concentrations in spring inputs with distance downstream. The reason for this trend is unknown, but it implies that the most likely condition is that lateral inputs along the spring run will tend to be lower than the river, and this would contribute to dilution.

Synthesizing, we explore 7 attributes of the method and the inference from these spring ecosystems.

1. **Method Application:** The diel nitrate variation method, made possible by the use of high resolution nitrate sensors, is a significant new tool for understanding how spring run streams process nitrogen, and should therefore be considered as a tool for evaluating restoration performance. In addition to providing insight into how ecosystems are using nitrogen (and changes that might ensue as concentrations change), the sensors provide a relatively low cost way of evaluating water quality at a resolution that is 4 orders of magnitude more frequent than typical sampling, and that permits assessment of status and trends that can account for sampling artifacts created by significant diel variation. Springs are an ideal study system for developing an understanding of rivers more broadly because the ecosystem mass balance is simplified by the relatively stable discharge and chemistry at the vent, particularly over the length of the sensor deployments utilized here. Further refinements of the method will come from the inference from two-station approaches (in the same way as the two-station method is used in many ecosystem metabolism studies), longer term deployments, and use in various enrichment dosing experiments (i.e., to monitor reactive solute breakthrough; Covino and McGlynn 2010). Our recommendation is that all spring run streams subject to regulatory interventions (e.g., TMDL, MFL) be assessed using this relatively low cost technology; the entire sensor package (SUNA, YSI, power, data loggers, cables) used in this work costs $32,000 each.

2. **Mass Loss of N:** Spring run streams act as significant sinks for nitrogen. Over relatively short reaches (the longest in this study was just over 6 kilometers) we observed between 2 and 50% of the vent water N removed. In the Silver, Rainbow and Ichetucknee River systems, the value is near 10% of

the mass flux, which, given the mass delivery at the vent represents a large loss of N. The highest values (near 50% of the vent flux removed) are at the Alexander and Juniper systems, where low concentrations in the vent water permit higher removal efficiencies, in the latter case despite relatively low removal rates on a per unit area basis. A power relationship between removal efficiency and input mass flux per unit area yields a strong association ($r = 0.85$, $\%Removal = 16.5*Flux^{-0.63}$, $p < 0.001$; Fig. 2-60). This could guide assessment of rivers that are providing removal service at or above expectations; note that Alexander Springs (points below the line just below 15% efficiency) achieves lower than predicted removal efficiency (presumably because of internal recycling within the large *Hydrodictyon* spp. mat present at that site; see later sections), while Rainbow River achieves higher efficiency than predicted (both points significantly above the line near 15% efficiency are Rainbow). Note however that removal reported as an efficiency is principally controlled by the vent concentration, and should not be interpreted to mean that springs with low efficiency are not functioning appropriately.

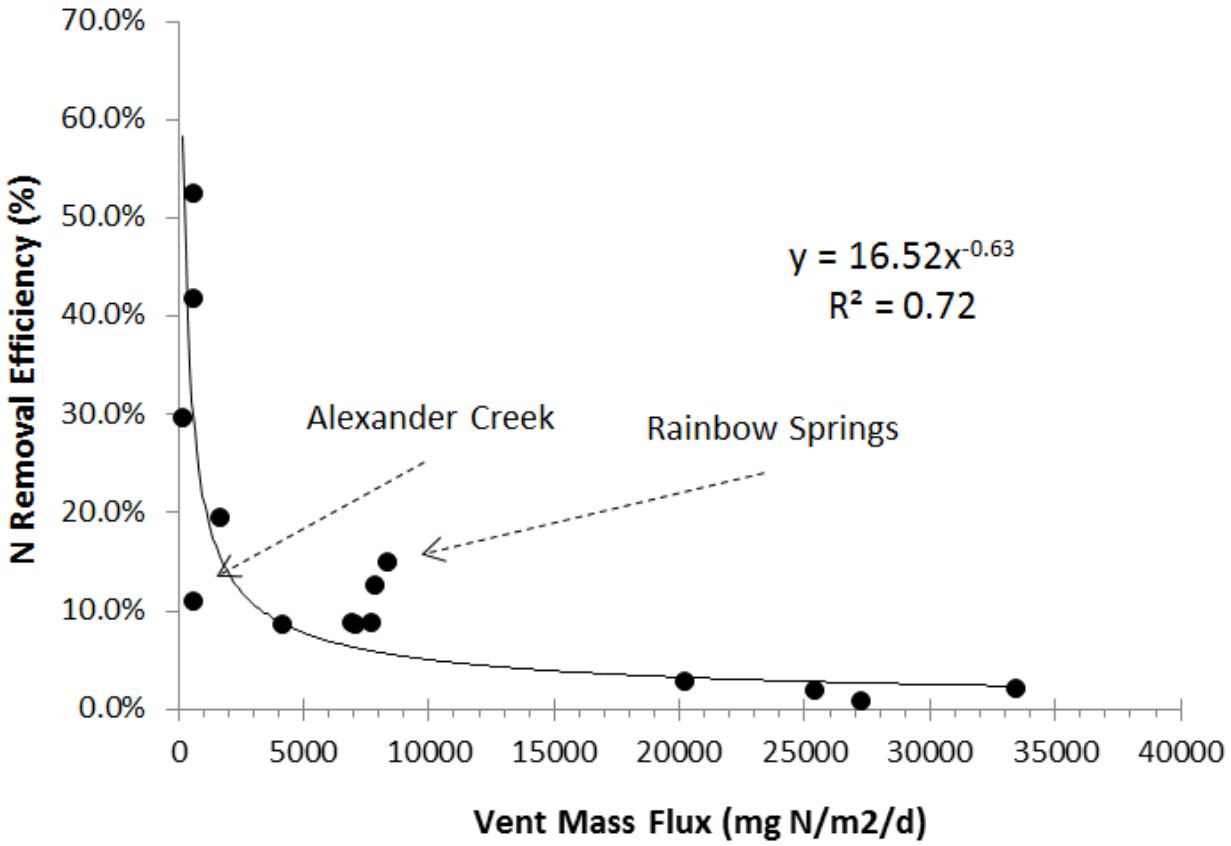

Fig. 2-60– Vent mass flux of N vs. total N removal efficiency. The one site significantly below the line is at Alexander Springs, while the two sites significantly above the prediction line are at Rainbow Springs.

3. **Dominated by Denitrification:** Nitrogen removal from spring run streams is dominated by denitrification across almost all systems, with over 80% of the removal from the vent to the downstream stations controlled by what are apparently heterotrophic processes (range 67 – 92%). The range of denitrification rates is large, with Rainbow exhibiting the highest rates at over 1,130 mg $N/m^2/d$, and Rock Springs Run an order of magnitude lower (133 mg $N/m^2/d$). Variation in assimilation is approximately equal, ranging from 135 mg $N/m^2/d$ in Rainbow to 19 mg $N/m^2/d$ in the upper part of Juniper Run. We note that the lowest fraction contribution from assimilation (Rock and Juniper) are also the systems in which metabolism is clearly net heterotrophic, and possibly influenced by lateral inputs water rich in dissolved organic carbon. Denitrification is strongly coupled to GPP; while this can be thought of as the direct effects of C fixation providing fuel for the process, the strength of the association, particularly after removing two upstream reach sites that are low for reasons not yet well understood, is striking (Fig. 2-61; $r^2 = 0.84$). Assuming a molar C:N stoichiometry of denitrification of 5:4, the slope of the line (43 mg N per g O_2) suggests that roughly 10% of primary production is being utilized as substrate to fuel denitrification, a surprisingly large fraction of the total fixed C.

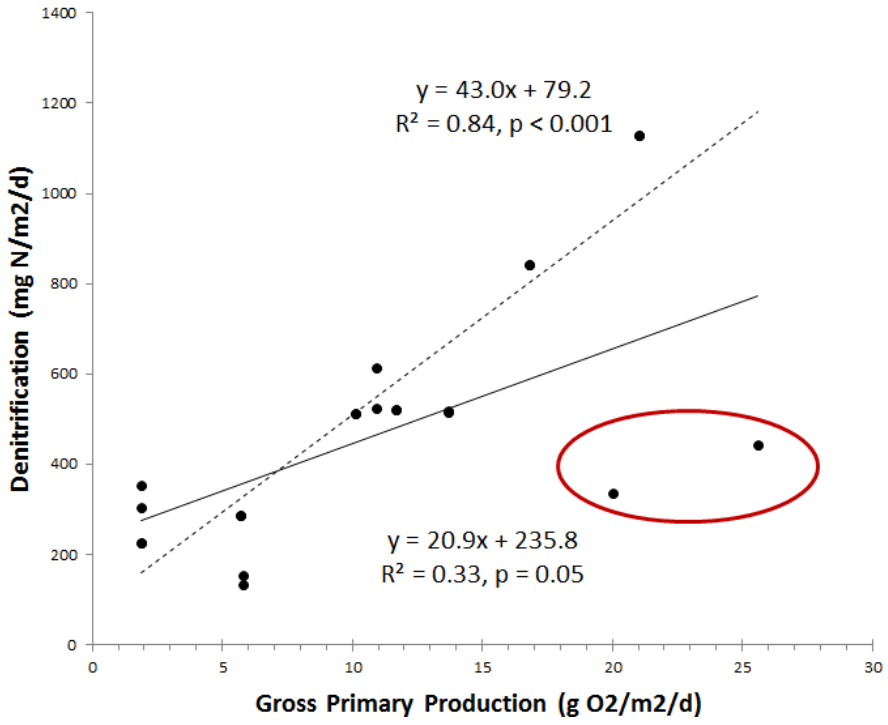

Fig. 2-61 – Relationship between denitrification (U_{den}) and gross primary production across rivers. The two outliers removed to yield the dashed line fit are both for upper river sites (Silver and Rainbow), which may not achieve the same level of denitrification as the rest of the river because of stronger hydraulic gradients (precluding water entering the sediments from the river) or because of reduced labile C availability.

4. **Temperature Sensitivity:** Ecosystem respiration is strongly a function of temperature. Omitting the two Alexander Springs Creek deployments, which yield numbers that are too large to be reasonable, we observed a remarkably consistent link between temperature and respiration for all the winter deployments. Only the summer data in Ichetucknee fails to exhibit this strong association, likely because the nighttime temperatures during the summer months are almost exactly the vent water levels, so there is effectively no variation. While an association between respiration and temperature is to expected, the magnitude of the effect is surprising. Over the entire suite of rivers, we infer that a unit change in temperature yields a change in respiration of 1-5 g $O_2/m^2/d$. This has major implications for the C balance of these ecosystems with changing climate (spring vent temperature is, in part, an integrated measure of average air temperatures at the time of recharge), potentially tipping them towards net heterotrophy. A potential consequence is the systematic decline in stored organic matter, which would have large, but fairly unpredictable, consequences on ecosystem function.

5. **Elemental Coupling of Ecosystem Production:** The magnitude of diel variation is strongly linked to gross primary production in almost all rivers, and the simultaneous inference of C and N assimilation gives a new tool for assessing the stoichiometry of primary production. Further work in this regard is needed, but the results here across study streams support the contention that the ecosystem-scale C:N ratio is commensurate with the relative importance of low C:N autotrophs (principally algae) vs. high C:N autotrophs (i.e., submerged aquatic vegetation). Specifically, Rainbow River has low algal cover and very high C:N, Silver, Gilchrist Blue and Ichetucknee have intermediate algal cover and intermediate C:N, and Rock has high algal cover and low C:N. Juniper Creek has relatively low C:N, and primary production in that system may be dominated by benthic microflora since large algal mats and beds of relatively sparse SAV are present in the study reach. If this qualitative inference holds under further scrutiny, we contend that the C:N ratio of metabolism may be a useful indicator of ecosystem change, with declines in the value indicating an increasing role of algae in primary production, and also potentially of changing relative importance over seasons (i.e., the life history and phenology of algae and macrophyte growth would be expressed in a longer time series of C:N ratios. Note that this index provides insight in the comparative productivity NOT just cover or biomass. Increasing C:N ratio of primary production may be useful as a restoration performance measure. However, before that can happen, a deeper appreciation of intra- and inter-annual variation is needed, particularly since our long term Ichetucknee data suggest some ecosystem phenology (e.g., markedly higher productivity in the spring, intra-annual variation in algal cover). Across systems, we observed the C:N ratio to be weakly positively associated with nitrate

(Fig. 2-63c), and assimilation. These findings are unexpected, and suggest that primary producers trend towards high C:N ratios in high nitrate and high uptake systems. We note that the systems that are high nitrate also tend to be high productivity (specifically Gilchrist Blue and Rainbow), a fact that may lead one or the other association to be confounded. The only low nitrate sites that are also high productivity are Silver Glen and Alexander Springs, and those sites exhibit highly unusual diel nitrate variation that prevents direct estimation of assimilation; specifically, these sites are not included in Fig. 2-62c, though measurements of tissue C:N concentrations in both locations supports the same trend since they both are dominated by algal taxa with C:N of ca. 10-12:1.

Light vs. N Limitation: The springs evaluated showed some evidence of light limitation, a finding consistent with all previous studies of spring run stream metabolism (e.g., Odum 1957a). More than half the springs exhibited statistically significant positive association between GPP and total insolation on a day-to-day basis; the rest were not significant, though generally had a positive slope. Note that the insolation estimates are from nearby weather stations, some as far as 25 km away, and numerous issues may confound the day-to-day covariance between that measured insolation and GPP in the river, including variable shading, and spatial variation in cloud cover and rainfall (which may make observations at the station different than what was experienced at the river). This is particularly true at Juniper, Gilchrist Blue and Rock Springs, where shading effects are more likely because of the narrow channel geometry. Moreover, many of the deployments where non-significant GPP vs. light associations were observed were short and had relatively constant weather (e.g., Silver Glen, the 2nd Silver deployment). Overall, there was strong across-springs evidence of light limitation (Fig. 2-62), particularly when the known confounding effect of high channel shading (particularly at Juniper and Rock Springs) was removed. The presence of a saturating effect at high insolation may suggest limitation by some other constituent (e.g., bicarbonate), or may arise from the use of a distant climate monitoring station for this work. Future work will include on-site measurements of incident radiation to obviate the assumption that measurements made as far as 30 km away are applicable.

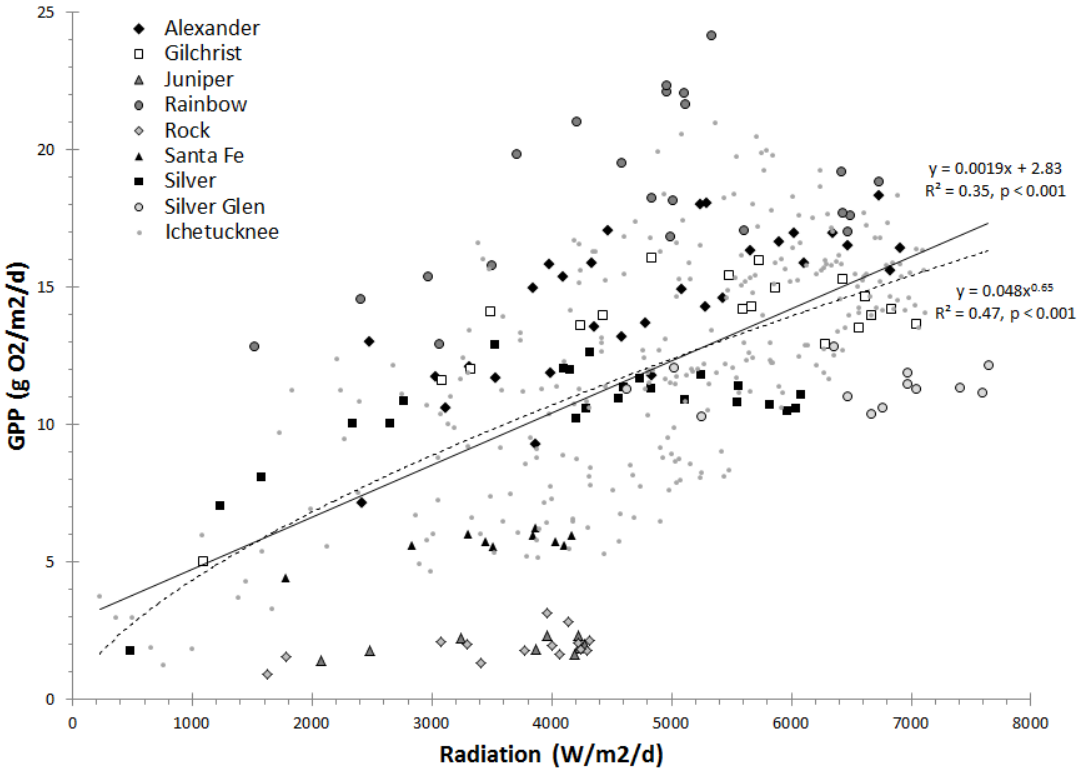

Fig. 2-62. Global analysis of the association between gross primary production and solar inputs. A linear function (the best fit functional form for ALL the data) was strongly significant; when Rock Springs and Juniper Springs were omitted because of the confounding effects of high shade, a power function that explained nearly half the variation was the best fit functional form.

Consistent with the general inference that spring run ecosystems are light limited is the absence of a correlation between GPP and nitrate concentrations; the association is positive but not statistically significant (Fig. 2-63a). Of particular importance to that graph is the observation of extremely high GPP in two of lowest N concentration systems (Silver Glen and Alexander Springs Creek). As we discuss below, there is evidence to suggest that these systems are indeed N limited, and satisfy their enormous N demand from internal recycling. Note also that these systems are heavily, albeit qualitatively for this work, dominated by algae as the main primary producer.

Interestingly, there is a statistically significant positive association between U_a (mean assimilation rate) and the nitrate concentration across springs (Fig. 2-63b). The association between U_a and nitrate concentration is odd and requires explication because we also observed that GPP and U_a are almost perfectly correlated (r = +0.89). This is particularly true because of experimental evidence that suggests that increased nitrate concentrations (i.e., 9 mg N/L) modestly inhibited rooted macrophyte growth

(Boedeltje et al. 2005), which we'd expect would lead to reduced assimilation at higher concentration, opposite what we observed. This assimilation vs. concentration association, with some qualitative evidence of saturation of U_a at high GPP consistent with models of autotrophic nutrient demand (Fig. 2-63d), suggests that covariance of U_a with other proxy variables may be mediated by effects on GPP. Moreover, in the Ichetucknee, where input nitrate concentrations are effectively constant, U_a values vary between 4 and 177 mg N/m^2/d, suggesting that other variables clearly control the vast majority of variation in assimilation rates. That said, further investigation of the impacts of nitrate concentrations on U_a are warranted. One explanation for the association between nitrate and U_a is that higher nitrate prompts higher uptake rates, but this is contradicted by the absence of a direct association between GPP and nitrate, and also a weak positive association between nitrate and the ecosystem C:N ratio (Fig. 2-63c). A more likely explanation is that the assimilation estimates do not include values from Alexander Springs, which is a high GPP/low nitrate system (the upper left most two sites on the GPP vs. nitrate graph; Fig. 2-63a). This provides the Juniper Creek system, a low GPP and therefore low N assimilation system, abundant leverage. The model without that point included is not statistically significant, and when the three deployments at Alexander and Silver Glen are included (where, crucially, assimilation is based on measured stoichiometry rather than diel nitrate variation) the sign of the association reverses (though the resulting negative slope is not significant). Additional study sites and repeated deployments under varying seasonal conditions will establish the durability of this finding.

Several other lines of evidence counter the contention that most of the springs are currently N limited (Alexander and Silver Glen being perhaps the notable exceptions). First, there was a weak but positive association between nitrate and C:N, which suggests that under higher nitrate conditions, ecosystem primary production is dominated by high C:N ratio autotrophs (e.g., SAV). The expectation from N limitation theory is that increased N availability would lead to dominance by low C:N species that have higher N demand per unit biomass production (Sterner and Elser 2002). The C:N ratio of assimilation appears significantly correlated with assimilation (Fig. 2-63e, when two outlier points that are the upper reaches of Silver and Rainbow Rivers are omitted), a finding suggestive of saturation of N demand, but also potentially confounded by the fact that the high assimilation systems were also generally low in algal cover at the time of sampling (particularly Rainbow and Gilchrist Blue). While this study was not designed to evaluate this question, and therefore is unable to control for several important confounders (notably spring size), we can reliably infer that higher nitrate concentrations across springs is not systematically associated with a change in primary producer biomass towards low C:N taxa.

In considering evidence for N limitation (i.e., as opposed to light limitation) in these ecosystems, we considered metrics of mass flux vs. ecosystem demand to evaluate thresholds of limitation. Because the direct ratio of mass flux-to-demand is strongly dependent on the reach length, we adopted a metric that is independent of length that we call the autotrophic uptake length ($S_{w,a}$); this metric describes the reach length required for autotrophs to remove the mass flux present at the upstream boundary, ignoring any internal recycling. We define $S_{w,a}$ as follows: $S_{w,a} = (Q * C) / (w * U_a)$, where $S_{w,a}$ is the uptake length in meters, Q is the discharge in m^3/d, C is the nitrate concentration in g/m^3, w is the mean river width (m) and U_a is the benthic area assimilation rate in g $N/m^2/d$. Short lengths indicate more likely N limiting conditions; the available supply of mineral N is reduced and taken up more readily from the water column. The results were striking. Autotrophic uptake lengths ranged from <1,500 m for Alexander and Silver Glen (where autotrophic demand was estimated from stoichiometry) to over 410,000 m in Rainbow River and nearly 700,000 m in the Santa Fe River. The average length, excluding Alexander, was 367,000 m. In short, the reach lengths necessary to remove N at the present concentrations are dramatically longer than the reach lengths of the rivers, suggesting that the autotrophs do not approach exhaustion of their N supply over the physical lengths of the rivers. We further explored the autotrophic uptake length assuming a historical nitrate concentration (50 µg/L or 0.05 mg N/L) and the same autotrophic demand per area as was observed in this study. The effect, as expected, dramatically shortens the uptake lengths; the mean autotrophic uptake length was 16,500 m, and ranged from 2,600 m in Gilchrist Blue Springs to over 33,000 m in Juniper Creek; Rainbow, Silver, and Ichetucknee had background autotrophic uptake lengths of 10,100, 18,000 and 19,700 m, respectively (Fig. 2-64). While there is no published threshold of this metric to delineate N limited from N sufficient ecosystems, data from one survey of streams from across North America suggest that the value is likely between 2,500 and 5,700 m (95% confidence intervals around the mean; S. King, unpublished manuscript). Likely the threshold in sensitivity of ecological production to nitrate will occur at lengths somewhat shorter than this. Using this threshold, and background levels of nitrate, we can estimate that Gilchrist Blue may be N limited at 0.05 mg N/L, and Rainbow River and Rock Springs Run would be borderline. This implies that if the restoration goal is to reestablish N limitation, concentrations would need to be far more dramatically reduced than current proposals suggest (e.g., 15 ppb in Silver, 29 ppb in Rainbow, and 17 ppb in Ichetucknee). Conversely, it seems reasonable to infer that N limitation may not have been the natural condition in these ecosystems (i.e., Odum 1957), even under background conditions, and reductions in N, though critical as a broad water quality goal, may not alter composition and productivity of these ecosystems.

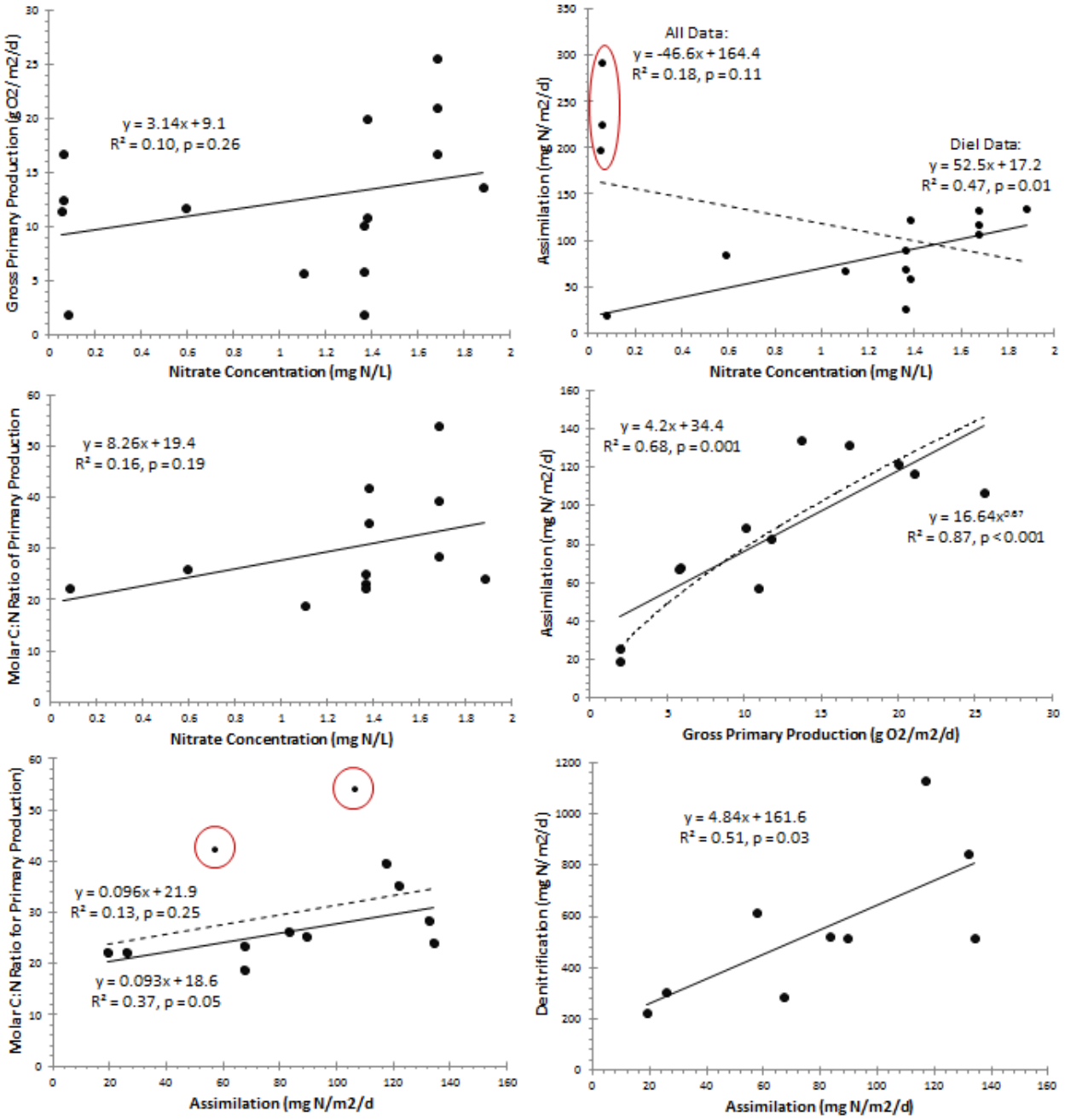

Fig. 2-63 – Associations across springs. A) Nitrate vs. gross primary productivity, B) nitrate vs. autotrophic N assimilation (U_a) without (solid) and with (dashed) the Alexander Springs Creek and Silver Glen Springs (red circle) included (note that U_a for these two systems was estimated from tissue stoichiometry NOT diel nitrate variation), C) nitrate vs. molar C:N ratio of primary production, D) GPP vs. U_a, showing both a linear and power fit, E) U_a vs. primary production C:N stoichiometry (including regression with [solid] and without [dashed] outlier points on the upper Silver River and upper Rainbow River), and F) U_a vs. U_{den} (site means).

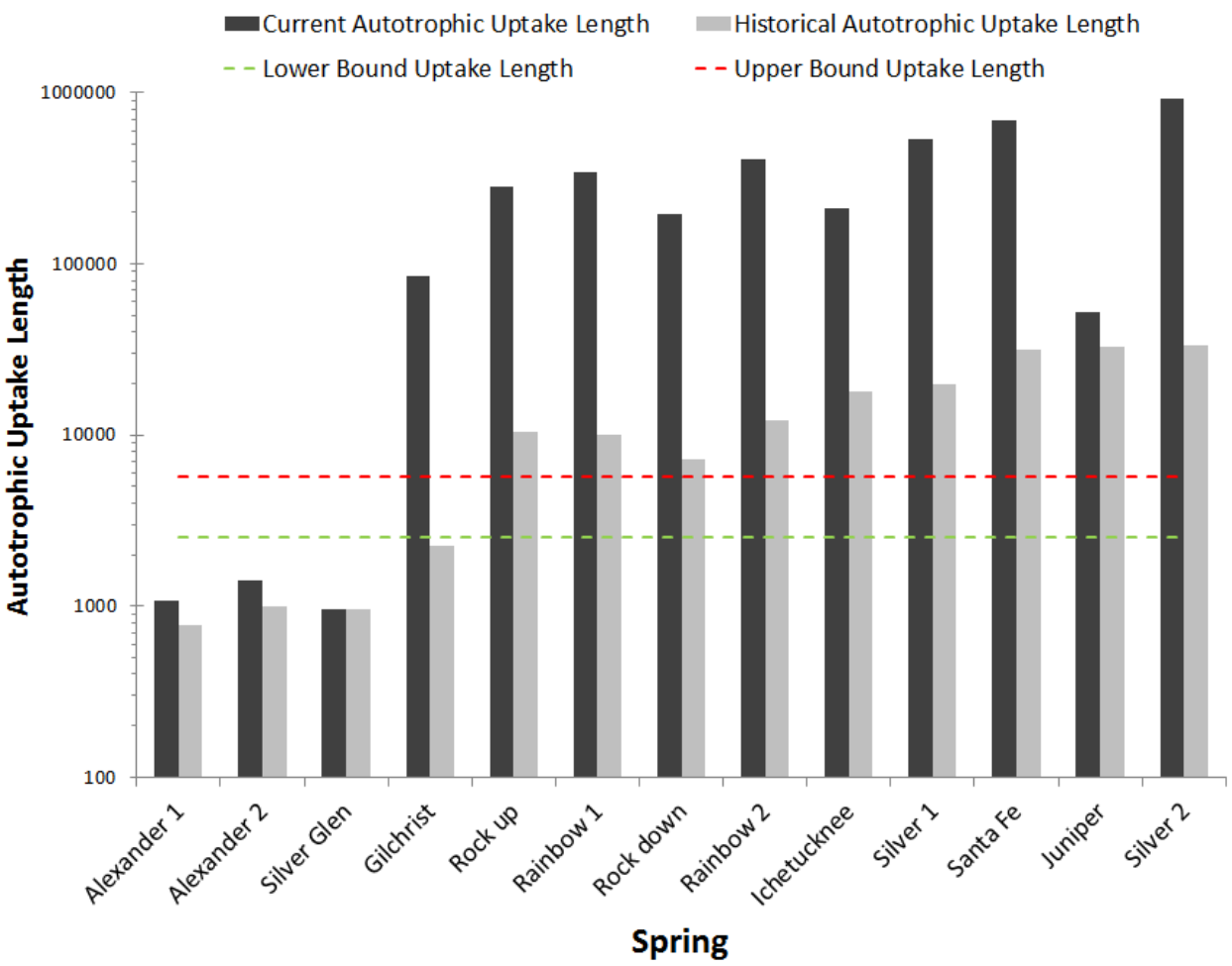

Fig. 2-64 – Summary of autotrophic uptake length (a measure of N limitation in lotic ecosystems) for springs under current and historical (0.05 mg N/L) nitrate input concentrations. Autotrophic uptake length values between 2,500 (dashed green line) and 5,700 m (dashed red line) are the best estimates of where nutrient limitation occurs (S. King, unpublished data).

6. **Indirect Elemental Coupling:** Perhaps the most consistent outcome of this work is the strong inter-day link between GPP and denitrification. A longer term link between denitrification and primary production observed in Ichetucknee is expected; GPP fixes carbon that is the substrate for denitrifiers, so higher values should broadly correspond to periods of high U_{den}, assuming there is some substrate limitation in the system. However, the strong day-to-day coupling that was first observed in Ichetucknee (Heffernan and Cohen 2010) is repeated regularly across the study streams, suggesting that the degree of substrate limitation for denitrification is both broadly present, and highly dynamic. Overall, day-to-day changes in GPP yield commensurate day-to-day changes in U_{den} such that a unit change in GPP (i.e., 1 g $O_2/m^2/d$) yields a change of 22 mg $N/m^2/d$ in U_{den}. Given that the mean rate of denitrification across springs is 480 mg

$N/m^2/d$, this day-to-day variation in response to a unit change in GPP corresponds to a 4% shift. Given that a cloudy day can depress GPP by as much 7 g $O_2/m^2/d$ in the larger, more productive rivers, this represents a large change in N removal capacity. The mechanism for this coupling has been that recent GPP yields low molecular weight organic compounds that are the ideal fuel for denitrifiers, whereas bulk organic matter is less labile. In a later section, we explore isotopic evidence for what controls denitrification, and observe a more complex story (specifically, that denitrification is limited by diffusion rates into the sediments); we reconcile these two observations (C limitation invoked here, diffusion limitation from the isotope evidence) by arguing that changes in the availability of labile C alters the depth that nitrate must diffuse into the sediments to reach locations with redox conditions favorable for denitrification. That is, reduced C availability on and after cloudy days exacerbates diffusion limitation, depressing denitrification overall. This indirect coupling suggests some management relevant considerations. First, the presence of rooted vegetation that deliver labile C from the roots to the upper sediments is critical for the denitrification process; add to that effect the observation that SAV alters hydraulic residence times to create some fraction of water that spends much longer in the river system than the median residence time in the river channel. This implies that there are two key ways in which vegetation management affects N removal dynamics of rivers: (1) Because denitrification is the dominant, and the only permanent removal pathway, efforts to restore plant beds should result in significant downstream water quality protection. (2) Measurements of water quality need to account for both time of day (because of relatively large diel variation) but also the weather and seasonal context, since observations of concentration can vary by 20 μg/L or more (Fig. 2-44 for the Santa Fe River, Fig. 2-25 for Gilchrist Blue Springs, Fig. 2-52 for Rock Springs Run, and Table 2-1 for comparisons between Silver River deployments) depending on when samples are obtained and in covariation with flow (as has been observed in the Wekiva Springs system; Mattson et al. 2006).

Research Element 3 – Spatially-Disaggregated Loading and Removal from High Resolution Longitudinal Nitrate Variation

Abstract

River ecosystems remove N along two primary pathways, assimilation and denitrification, and estimates of these processes are generally made by: a) isolating portions of the river bottom from ambient conditions to estimate flux rates; b) extracting sediments to estimate rate potentials; or c) evaluating integrated removal rates over some relatively large benthic area using temporal measurements at a single location. Here we present a new method that offers insight into the spatial variation in N removal rates along a river. It is based on extremely high resolution measurements of nitrate made possible by advances in UV analyzers that can obtain optical measurements of nitrate at 0.5 Hz (that is, 1 sample every 2 seconds). We evaluated longitudinal transects for 8 rivers, many of them twice, and extracted benthic removal rates from variation in nitrate concentration and known channel geometry. Rates varied widely between rivers, and conformed well ($r = 0.94$, slope = 0.97) with estimates obtained for the same river using the diel variation method (Research Element #2). We note that the method as implemented here computes only a bulk removal rate, and that further refinements, namely day vs. night transects, would be necessary to decompose assimilation from denitrification. Moreover, we discuss some limitations of the method. Of particular importance is the fact that this method (and indeed any such mass balance method) cannot readily distinguish between removal and dilution. While we have reason to believe that dilution effects due to diffuse seepage are relatively small, we discuss a set of tracer-based discharge measurements that would be necessary to more accurately describe longitudinal variation in discharge.

Introduction

Nitrogen removal in rivers is a process that is spatially uneven in response to variation in benthic plant cover, which controls assimilation, sediment-water exchange, which controls denitrification, and channel morphology, which affects both. One of the prevailing methodological questions in aquatic ecosystems ecology is the extent to which integrated measurements such as primary production and nitrogen removal can be decomposed to better understand the rich spatial context of the lotic landscape. To date, few methods have been available to address spatial variation in process rates at the ecosystem scale; most focus on isolating a small part of the benthic surface and evaluating mass balance under conditions that are, of necessity, different than the open-channel conditions of the lotic ecosystem. Other methods such as sediment denitrification assays are enormously useful for understanding the constraints on process (e.g., C or N limitation), but provide only estimates of potential rates because the specific redox and hydraulic conditions of any particular sediment sample are lost when the material is removed.

In stream ecology there has been a tension between Eulerian sampling of processes, wherein samples are collected from a point and used to draw integrated inference about processes occurring in some area upstream, and Lagrangian sampling, where a parcel of water is followed as it travels through the system, changing as it goes. For the most part, Lagrangian sampling of ecosystem process rates has been constrained by sampling density; that is, the sampling requirements are prohibitive for sufficiently dense measurement of longitudinal changes in water chemistry from which it would be possible to discern spatial variation in process rates. However, for longitudinal N processing, the emergence of new optical sensors based on UV absorbance offer a new tool to bring to bear on the question of spatial variation in lotic ecosystem solute processing rates. Specifically, the Submersible UV Nitrate Analyzer (SUNA; Satlantic Corporation, Halifax, Nova Scotia) used in the previous section to obtain very high resolution Eulerian samples can similarly be used to obtain heretofore unprecedented spatial resolution of water chemistry from which spatial disaggregated process rates can be inferred. This section of the report documents a new method for longitudinal sampling using these sensors in “continuous” mode, in which measurements are made every 2 seconds, for spatial resolution of lotic ecosystem process rates. Our hypothesis is that longitudinal rates of removal will compare with rates observed in the previous section using Eulerian sampling, and that they will reveal spatial variation in removal rates that may eventually point to hot-spots in the rivers systems for N removal.

Methods

Longitudinal transects were run down each river in a canoe; efforts were made to stay in the river thalweg to ensure maximum mixing, but the nature of these karst rivers (complex bottom topography in areas, multiple spring vents) and the long mixing lengths due to low velocities meant that any measurements are subject to some geographic uncertainty. A Submersible Ultraviolet Nitrate Analyzer (SUNA) (Satlantic, Halifax, Nova Scotia) was used to record nitrate concentrations every 2 seconds. The SUNA is highly accurate at detecting large differences in nitrate concentrations (0.0001 mg/L N), but because samples were taken at such frequent intervals, the expected point-to-point variation in nitrate concentration was small resulting in a fair amount of "noise" in the data. To compensate for this, a running average of 100 points was used for all subsequent calculations.

A handheld GPS unit (DeLorme, Yarmouth, ME) recorded the location of the canoe every 5 seconds. The GPS data were interpolated into 2 second intervals, and each location was matched to its corresponding nitrate concentration; the SUNA clock and GPS clock were synchronized prior to each transect to ensure positional accuracy of each measurement. The GPS data was converted from degrees into Universal Transversal Mercator (spatial units of meters), and the Pythagorean Theorem was used to calculate the distance traveled between each of the points. The benthic area of each point was estimated based on channel widths obtained from previous work (Element #1) or from GIS aerial images. Aerial images showing the location of each river reach modeled are shown in Figs. 3-1 through 3-10.

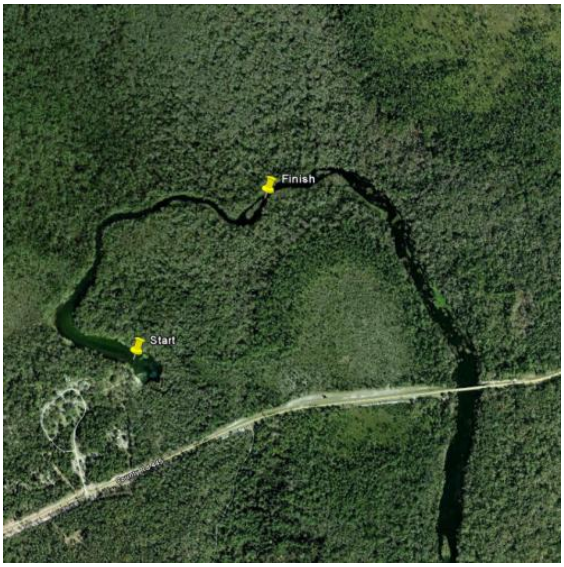

Figure 3-1. Map of Alexander Creek showing starting and ending point of the longitudinal transects. The total transect length was approximately 1,200 m. (Image Source: Google Earth).

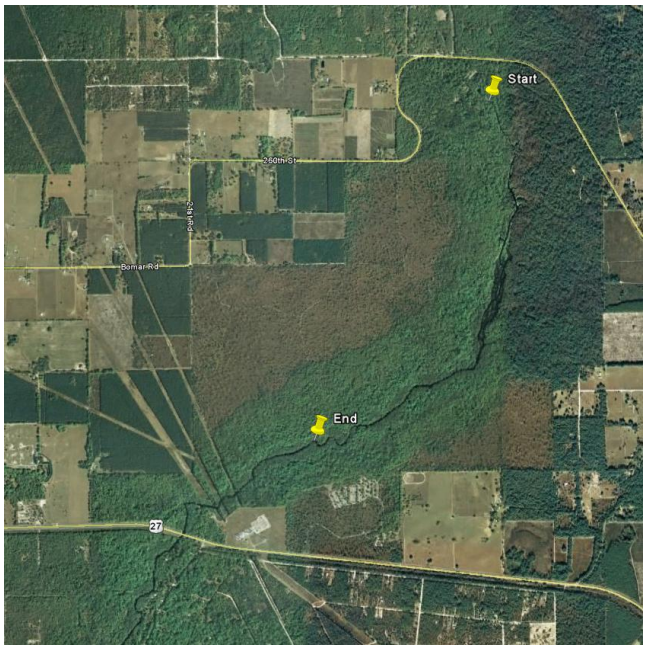

Figure 3-2. Map of Ichetucknee River showing starting and ending point of the longitudinal transect. The total transect length was approximately 4,000 m. (Image Source: Google Earth).

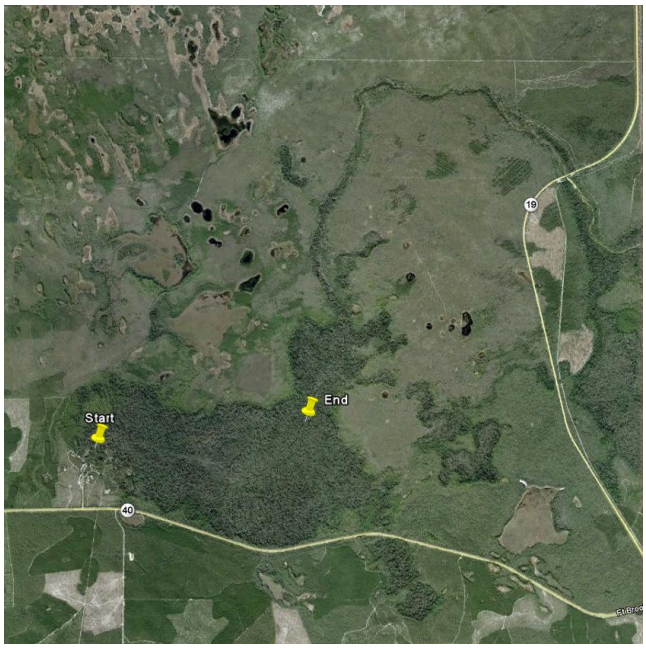

Figure 3-3. Map of Juniper Creek showing starting and ending point of the longitudinal transects. The total transect length was approximately 3,000 m. (Image Source: Google Earth).

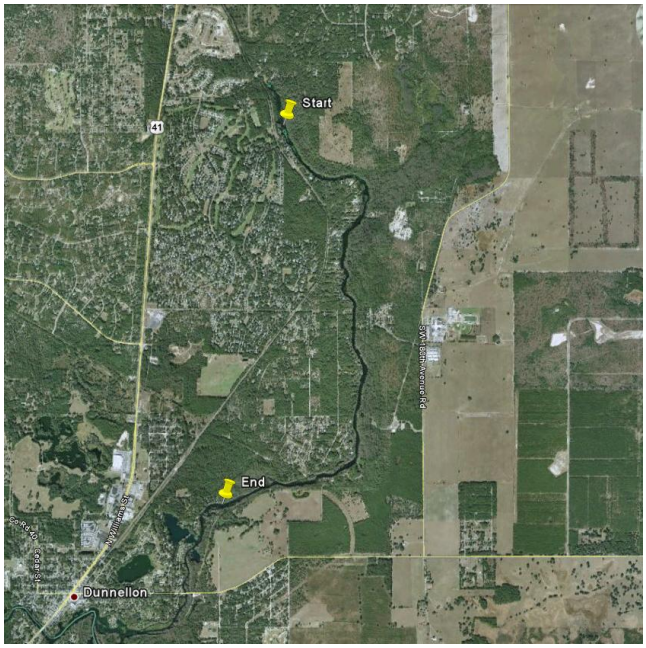

Figure 3-4. Map of Rainbow River showing starting and ending point of the longitudinal transects. The total transect length was approximately 6,500 m. (Image Source: Google Earth).

Figure 3-5. Map of Rock Springs Run showing starting and ending point of the longitudinal transects. The total transect length was approximately 3,000 m. (Image Source: Google Earth).

Figure 3-6. Map of Upper Reach of Santa Fe River showing starting and ending point of the longitudinal transect. The total transect length was approximately 9,500 m. (Image Source: Google Earth).

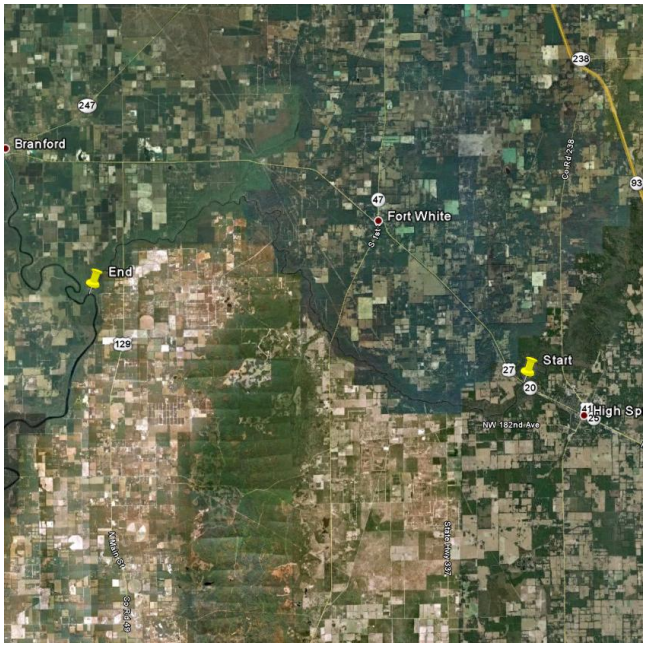

Figure 3-7. Map of Lower Reach of Santa Fe River showing starting and ending point of the longitudinal transect. The total transect length was approximately 35,000 m. (Image Source: Google Earth).

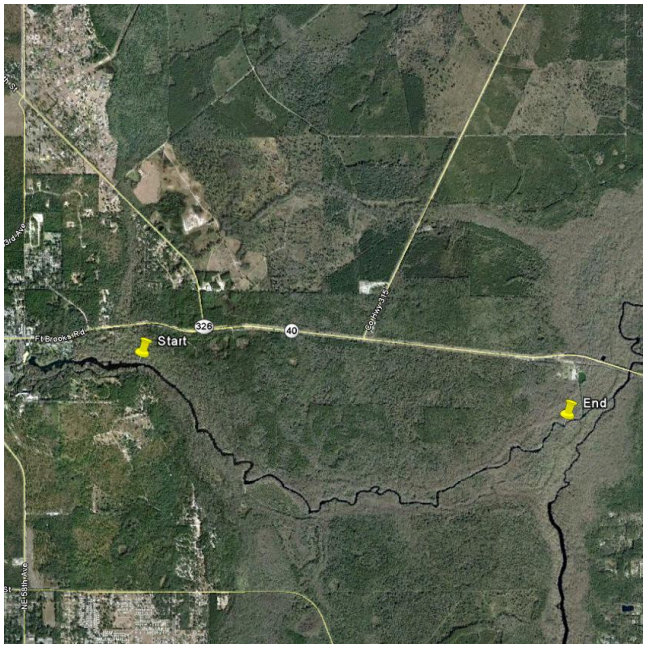

Figure 3-8. Map of Silver River showing starting and ending point of the longitudinal transects. The total transect length was approximately 6,500 m. (Image Source: Google Earth).

Figure 3-9. Map of Silver Glen showing starting and ending point of the longitudinal transects. The total transect length was approximately 1,000 m. (Image Source: Google Earth).

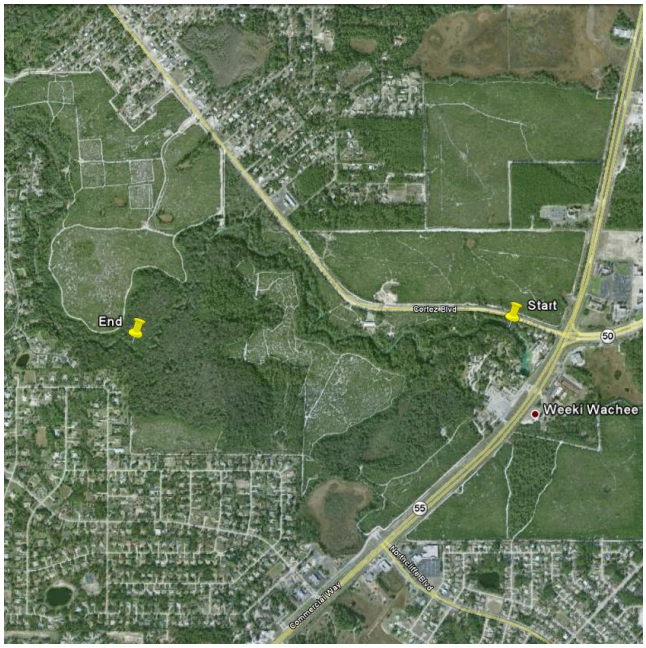

Figure 3-10. Map of Weeki Wachee River showing starting and ending point of the longitudinal transect. The total transect length was approximately 3,000 m. (Image Source: Google Earth).

The nitrate concentrations and corresponding distances traveled between each point were imported into a spreadsheet created using Microsoft Excel (2007). The distance traveled was multiplied by the width of the river to calculate the benthic surface area of that particular "cell". The mass flux of nitrate into and out of this cell was calculated by multiplying the upstream and downstream nitrate concentrations by the flow rate of the river. The difference in mass flux rate into and out of the cell was divided by the benthic surface area of the cell to calculate the nitrate loss rate of that particular cell. Note again that these estimates were smoothed by using running averages of nitrate concentrations since the magnitude of the point-to-point signal is small compared to instrument noise. Note also that what we refer to as noise in this section may well be, at least in part, real natural variation induced by the particulars of eddies in the river, with upward fluxing water depleted of nitrate compared with downward fluxing water because of the overwhelming dominance of the benthos in riverine N removal.

Because transects were run in both the upstream to downstream and downstream to upstream directions (i.e. with and against the current), and the velocities within and across rivers vary, the distance traveled in each 2 second interval varied. This, coupled with the fact that the channel width is variable, resulted in variation in the size of each individual cell. To compensate for this, when calculating the mean loss rate of the entire river, the loss rate of each individual cell was weighted based

on its benthic surface area relative to the whole river benthic surface area. Note that we assumed constant discharge along each longitudinal transect, an assumption that requires additional vetting, but that was necessary for this purpose; the method cannot distinguish between longitudinal removal of nitrate and dilution from water of lower concentration. We explicitly omitted or controlled for river sections where known point sources discharge, but the karst nature of these rivers makes it challenging without careful tracer-based discharge estimates to discriminate between removal and dilution. A screenshot of the spreadsheet used for estimating removal rates is shown below in Fig. 3-11.

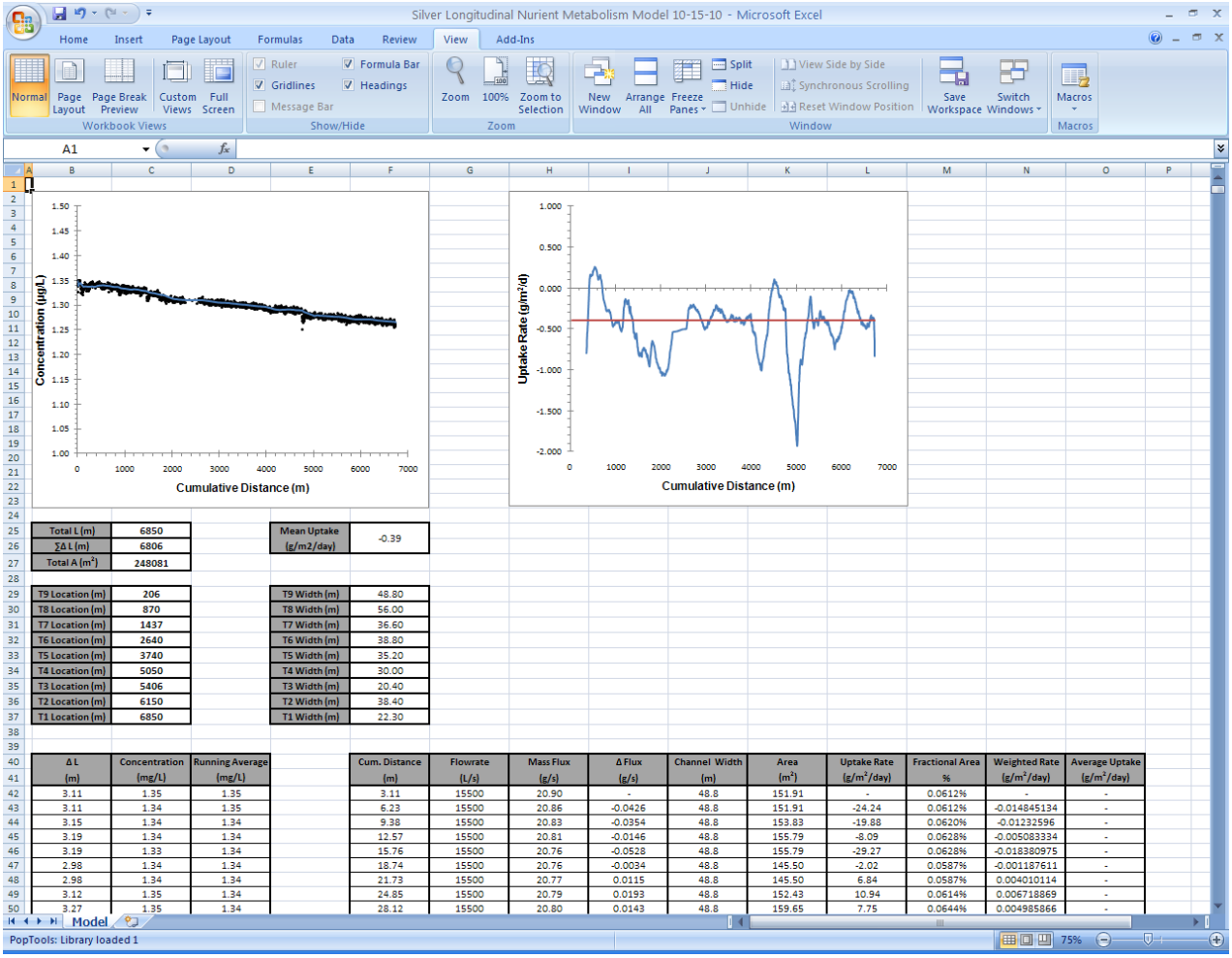

Figure 3-11. Screenshot of Microsoft Excel Longitudinal Metabolism Spreadsheet. Shown are the river parameters (widths at each transect, discharge), the raw nitrate concentration (upper left figure), the computations of removal and the resulting longitudinal patterns in removal (upper right figure).

Results/Discussion

For nearly all rivers, we observed systematic declines in longitudinal nitrate concentrations, but with strong spatial variation in the geometry of that removal. In systems like the Santa Fe and Ichetucknee that have large, discrete spring inputs, the method was somewhat challenging to implement without highly accurate discharge information, which is generally not available. In one river, Alexander, the longitudinal profile was inverse to what was observed elsewhere, in much the same way that the diel signal was also inverted (Research Element #2). Figures 3-12 through 3-20 present the longitudinal nitrate profiles and the uptake rate profiles for the rivers studied. In the case where multiple transects were conducted on the same river, these profiles are shown adjacent to one another.

The top panels of each figure show the longitudinal nitrate profiles, with zero distance being the most upstream location (usually the spring pool). The black dots represent the individual SUNA measurements, and the blue line is the 100 point moving average. Note that the 100 point running average is only shown on the reaches it was used to calculate the mean uptake rate. The bottom panels of each figure show the uptake rate profiles for the rivers studied. The blue line represents the loss rate at that particular location, while the red line represents the mean loss rate of the entire river. Consequently, the red line should approximately bisect the blue line.

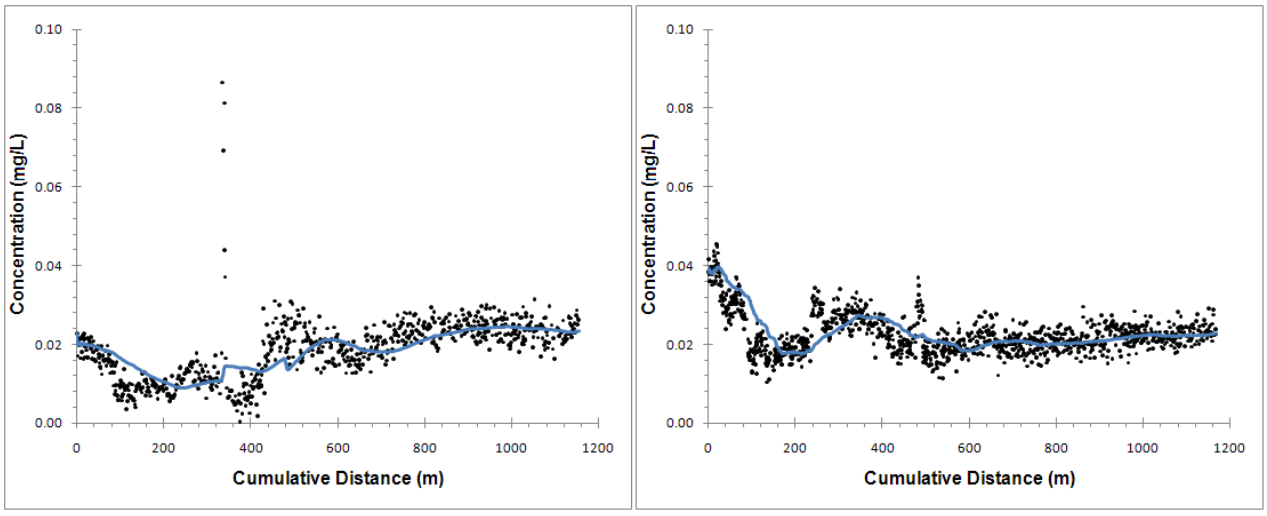

Figure 3-12. Longitudinal nitrate concentration profile for Alexander Creek on August 26, 2010 (Left) and September 8, 2010 (Right). Note there are no uptake rate profiles. The reason for this will be discussed later. Note that the upstream point (0 m) is below the main vent by ca. 100 m.

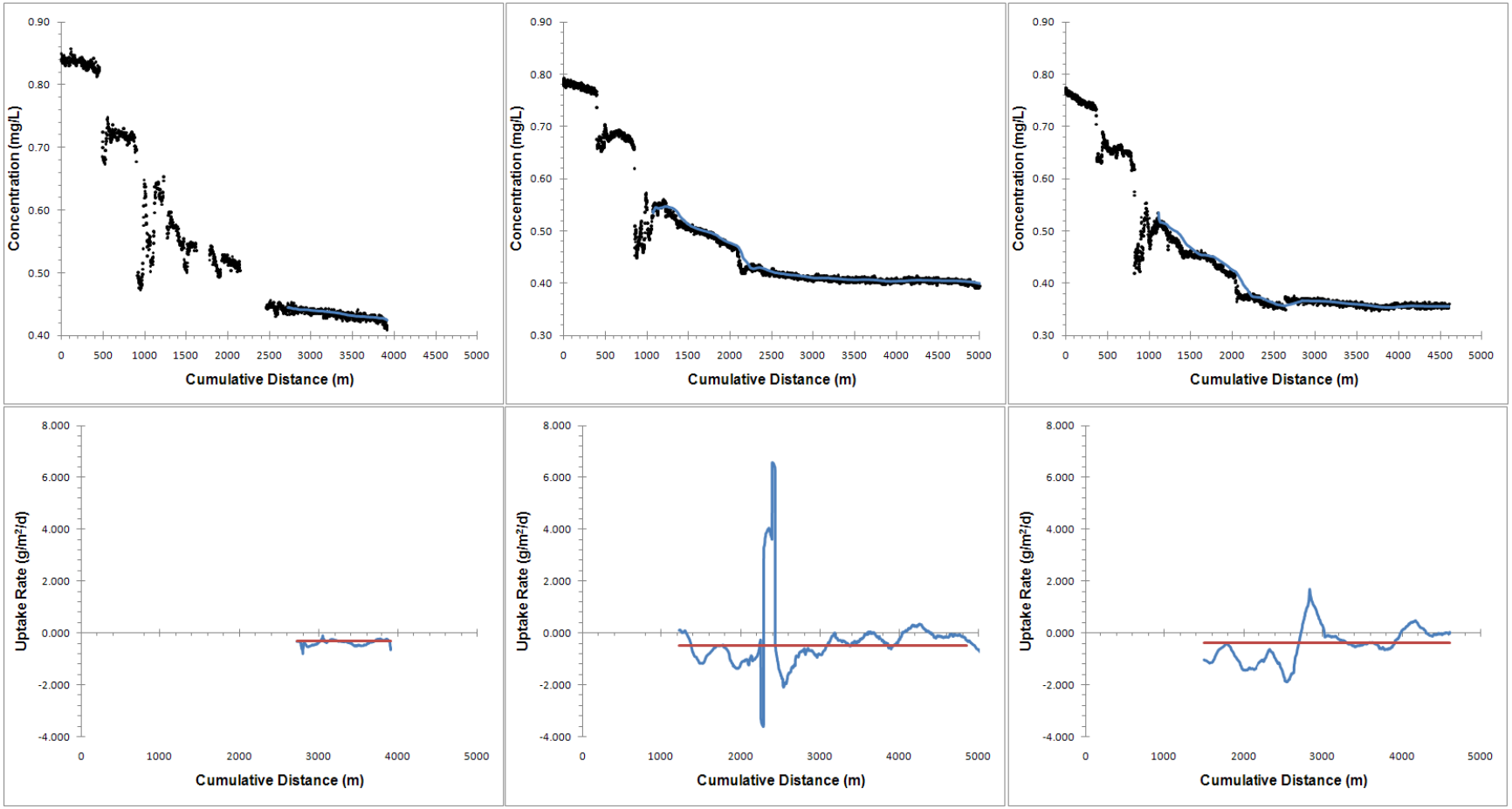

Figure 3-13. Longitudinal nitrate concentration profile (Top) and loss rate profile (Bottom) for Ichetucknee River on March 18, 2010 (Left), March 21, 2011 morning (Center) and March 21, 2011 afternoon (Right) . The large drops in the data are the result of spring inputs. The large break in the March 18, 2010 data is due to equipment malfunction. Note the loss rate has only been calculated for the downstream reach which has continuous data (last 1,500 m).

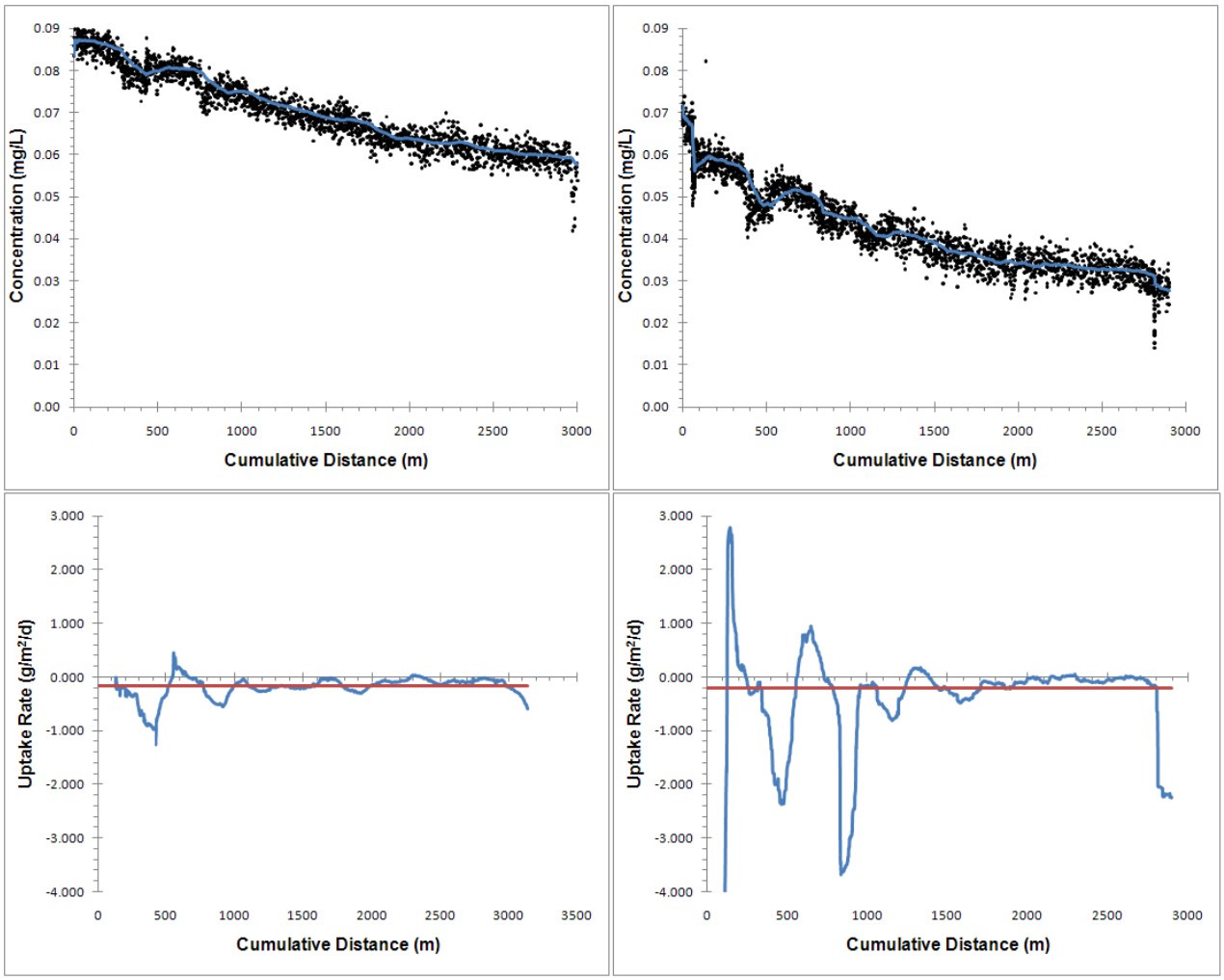

Figure 3-14. Longitudinal nitrate concentration profile (Top) and loss rate profile (Bottom) for Juniper Creek on November 10, 2010 (Left) and November 22, 2010 (Right).

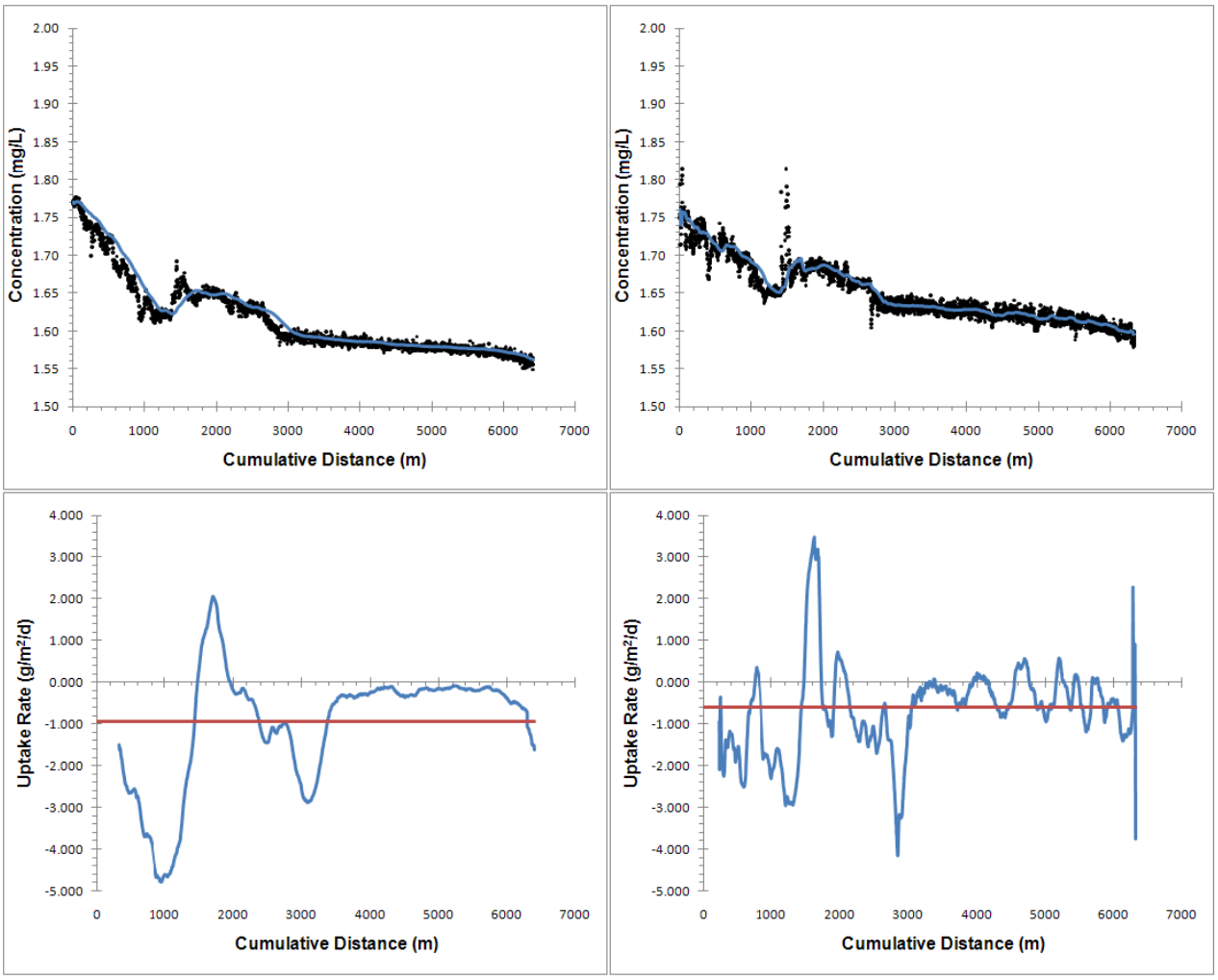

Figure 3-15. Longitudinal nitrate concentration profile (Top) and loss rate profile (Bottom) for Rainbow River on October 18, 2010 (Left) and October 28, 2010 (Right).

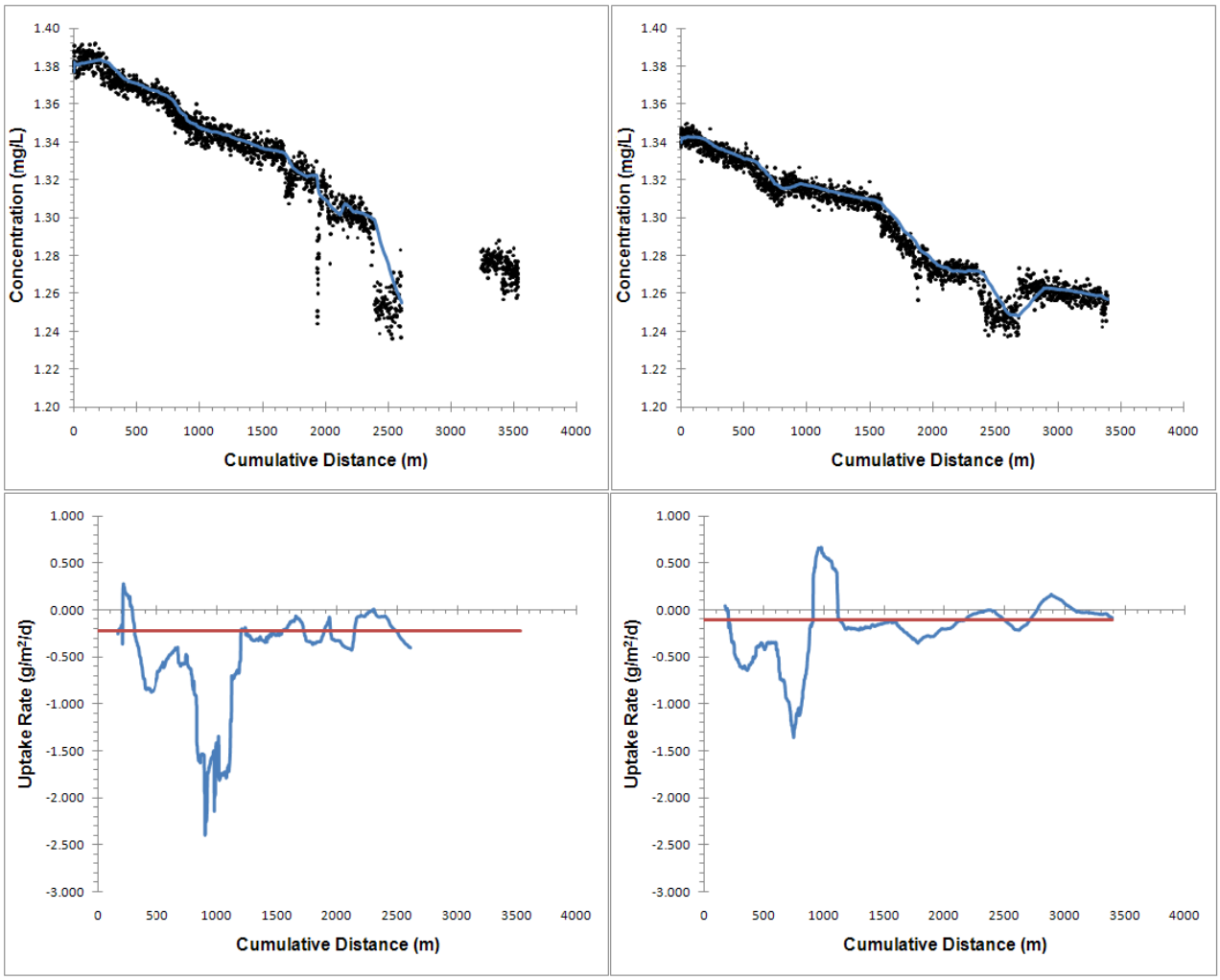

Figure 3-16. Longitudinal nitrate concentration (Top) and loss rate (Bottom) for Rock Springs Run on Dec. 1, 2010 (Left) and Dec. 16, 2010 (Right). The data break on the left is due to equipment malfunction.

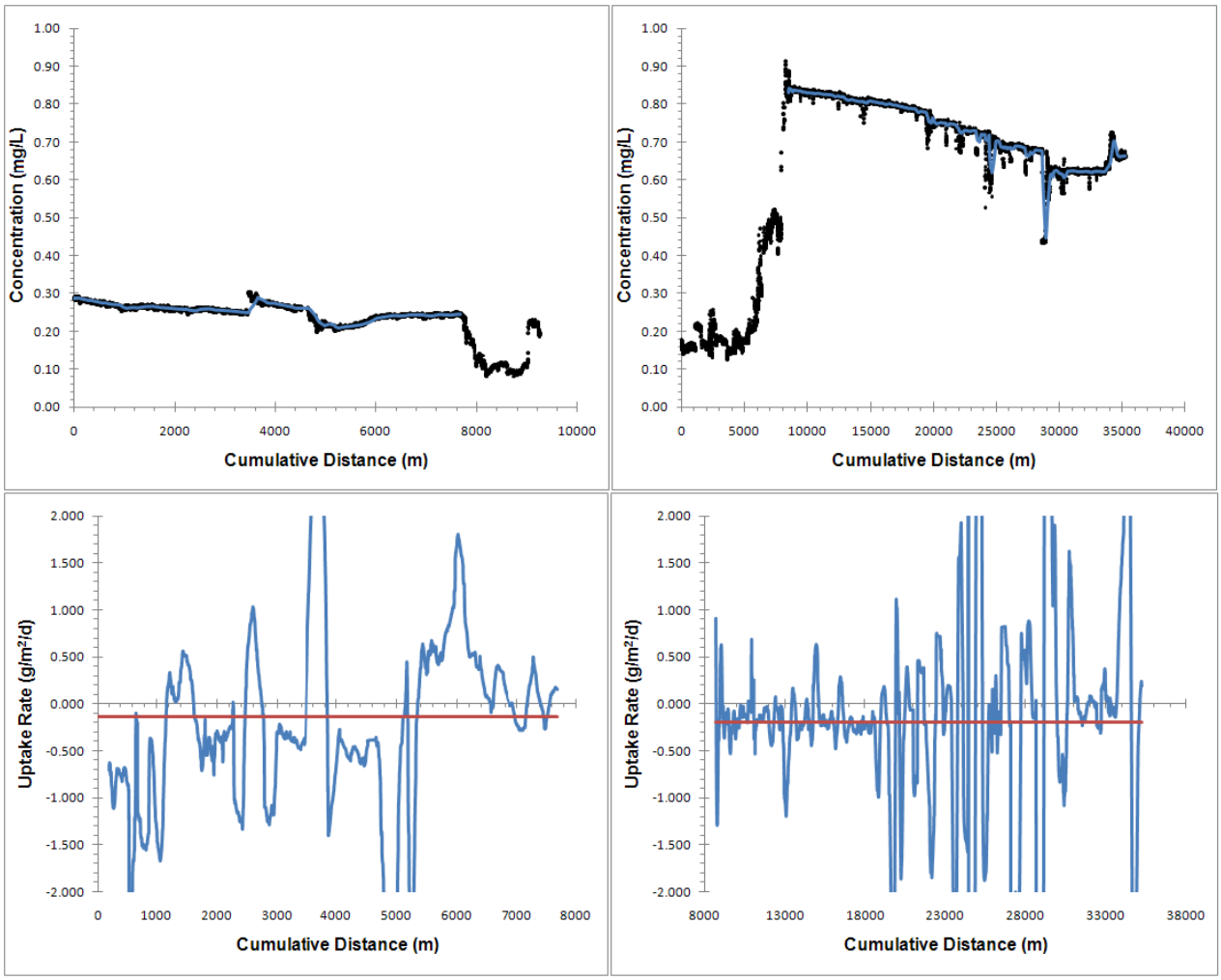

Figure 3-17. Longitudinal nitrate concentration profile (Top) and loss rate profile (Bottom) for Santa Fe River. The Upper reach data from November 17, 2010 is on the left and the Lower reach data from November 18, 2010 is on the right.

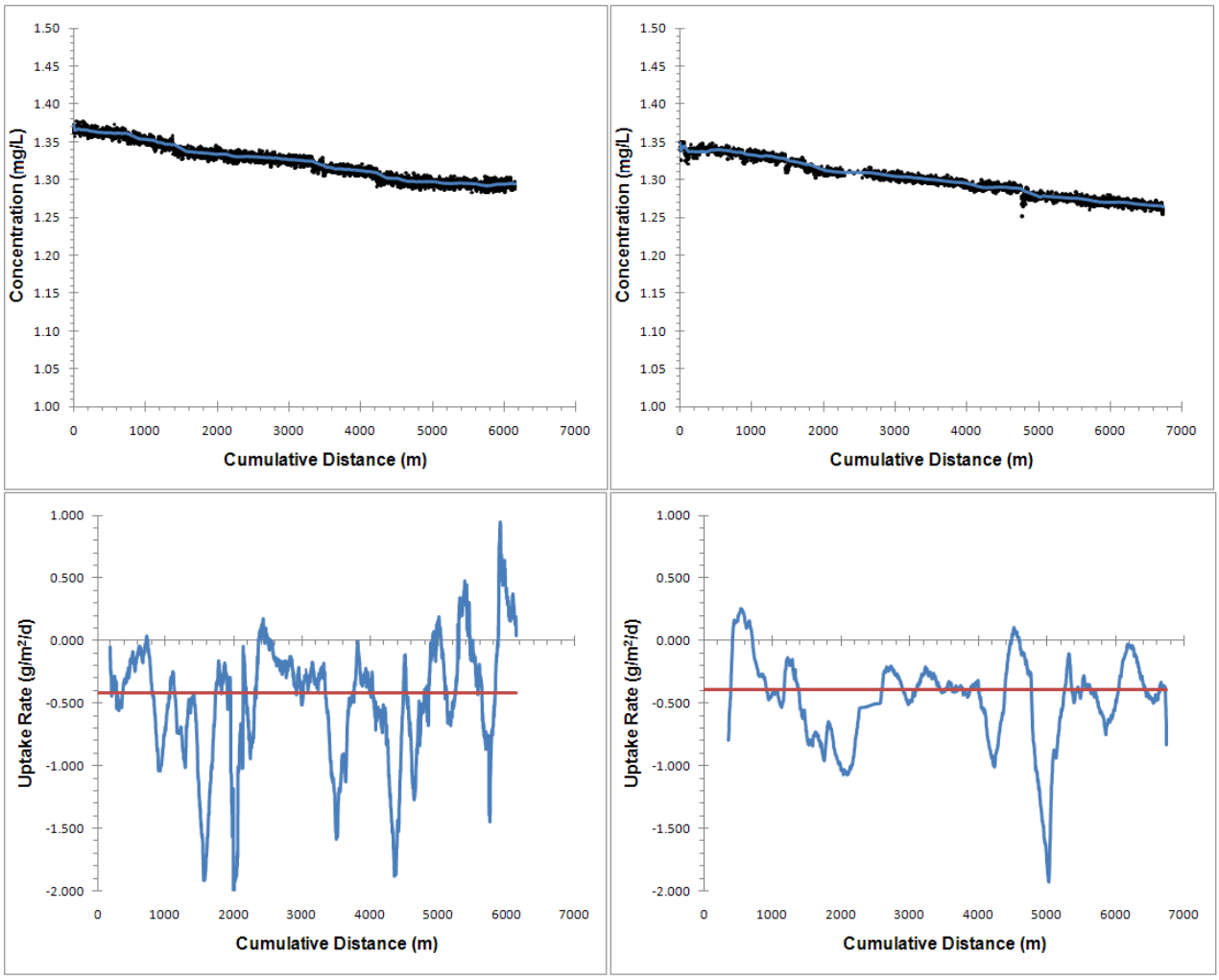

Figure 3-18. Longitudinal nitrate concentration profile (Top) and loss rate profile (Bottom) for Silver River on October 5, 2010 (Left) and October 15, 2010 (Right).

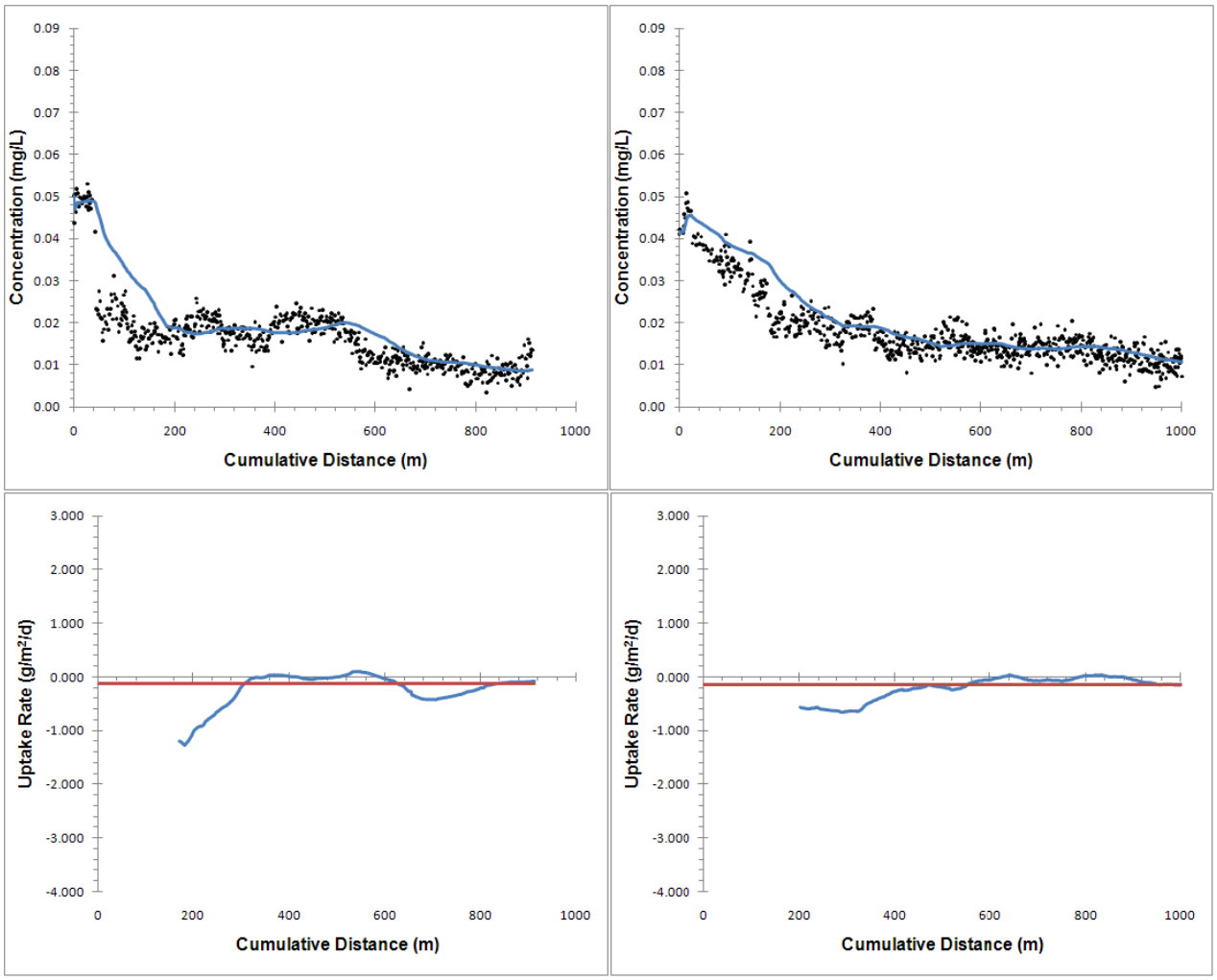

Figure 3-19. Longitudinal nitrate concentration profile (Top) and loss rate profile (Bottom) for Silver Glen on April 6, 2011 (Left) and April 21, 2011 (Right).

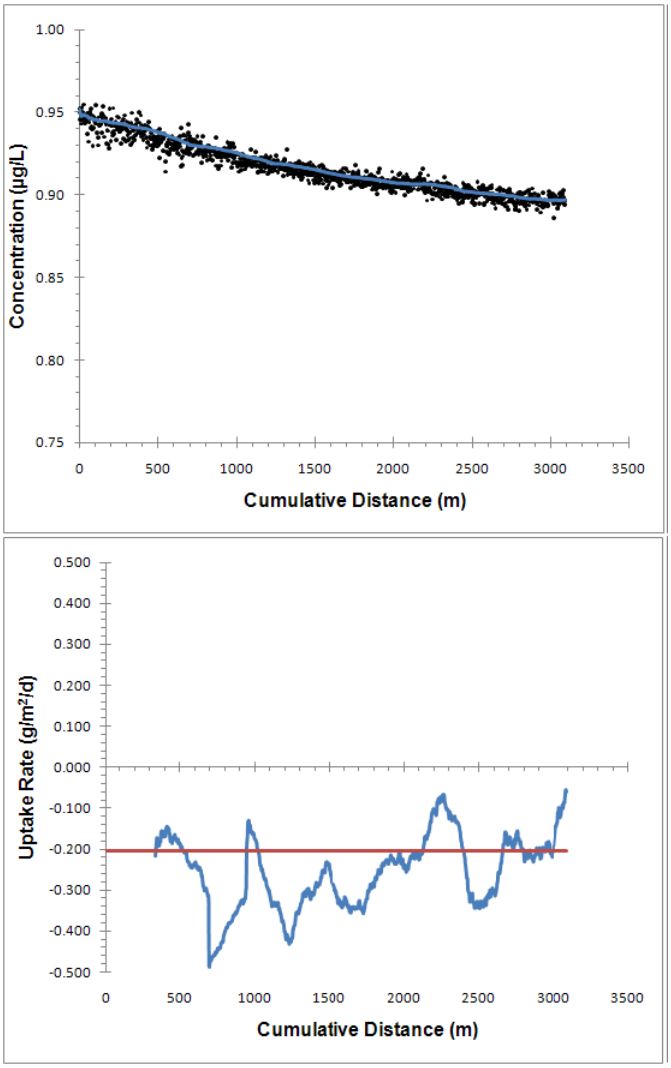

Figure 3-20. Longitudinal nitrate concentration profile (Top) and loss rate profile (Bottom) for Weeki Wachee River on January 27, 2011.

The calculated loss rates for each of the rivers are listed in Table 3-1. Note the range in loss rates, ranging over almost an order of magnitude. Also note the similarity between mean loss rates measured in the same river but on different days. Also shown in the table are the estimated uptake rates calculated using the diel method (Element #2). The uptake rates incorporate assimilation and denitrification; future implementation of this method should seek to acquire longitudinal profiles during the day and night to determine localization of both processes.

Table 3-1. Mean Loss Rates.

River	Date	Loss Rate ($g/m^2/day$)	Total Uptake Rate ($g/m^2/d$)	U_a ($g/m^2/d$)	U_{den} ($g/m^2/d$)
Alexander Creek	8-26-10	N/A	N/A	N/A	N/A
Alexander Creek	9-8-10	N/A	N/A	N/A	N/A
Ichetucknee (Lower Reach)	3-18-2010	0.31	0.41*	0.073	0.335
Ichetucknee (Lower Reach)	3-21-2011 AM	0.49	0.41*	0.073	0.335
Ichetucknee (Lower Reach)	3-21-2001 PM	0.37	0.41*	0.073	0.335
Juniper Creek	11-10-2010	0.17	0.24	0.019	0.226
Juniper Creek	11-22-2010	0.20	0.24	0.019	0.226
Rainbow River	10-18-2010	0.85	0.57-1.25	0.117	1.13
Rainbow River	10-28-2010	0.56	0.57-1.25	0.117	1.13
Rock Springs Run	12-1-2010	0.23	0.21-0.38	0.032	0.355
Rock Springs Run	12-16-2010	0.10	0.21-0.38	0.032	0.355
Santa Fe (Upper Reach)	11-17-2010	0.13	0.34	0.067	0.288
Santa Fe (Lower Reach)	11-17-2010	0.20	0.34	0.067	0.288
Silver River	10-5-2010	0.42	0.46-0.58	0.055	0.525
Silver River	10-15-2010	0.39	0.46-0.58	0.055	0.525
Silver Glen	4-6-2011	0.13	N/A	N/A	N/A
Silver Glen	4-21-2011	0.14	N/A	N/A	N/A
Weeki Wachee River	1-27-2011	0.20	N/A	N/A	N/A

** - Removal data for the lower reach is estimated from a short term deployment during which sensors were placed at the top and bottom of the lower reach (data not previously shown)*

An alternative simplified method for estimating the loss rate using the longitudinal profile was also experimented with. Rather than calculating the loss rate as the weighted sum of the loss rates of individual benthic compartments, this method simply uses the overall slope of the longitudinal nitrate

profile. The slope of the best-fit linear trend line (in units of mg/L/m) is multiplied by the flow and divided by the mean channel width to estimate the loss rate. An advantage of this method is that its simplified nature decreases the potential for human error in the calculation. A disadvantage is that changes in loss rate indicative of removal hotspots (or dilution from spring inputs) are not as apparent. Rivers can however be quickly broken into reaches with different flows and widths as shown for Ichetucknee in the figure (3-21) and table (3-2) below.

Note that the slope based estimations of mean loss compare very favorably with compartment method estimations. For the combined reach 3 and 4 the compartment model estimated a mean loss rate of 0.49 g/m^2/day in the morning and 0.37 g/m^2/day in the afternoon. Averaging the estimated loss rates of reaches 3 and 4 obtained from the slope method results in a mean loss rate of 0.44 g/m^2/day in and 0.47 g/m_2/day respectively (although for a precise comparison, a weighted average based on their contributing area should be performed).

Research Element #4 – Open Channel and Sediment Assay Denitrification Estimates

Abstract

Direct measurement of denitrification in flowing water has recently become possible by observing patterns of dissolved N_2 gas in the water column; modeling the gas concentration based on physical conditions (temperature and excess air, obtained for other dissolved gases) and reaeration dynamics has allowed several researchers to estimate per area flux rates. We applied these methods in spring runs, but were forced to reject this method for this setting for two primary reasons. First, the water coming out of the spring vent is significantly disequilibrated with the atmosphere in both N_2 and Ar (an inert gas tracer of physical processes). As such, a large component of the longitudinal changes in gas concentrations are controlled by poorly constrained physical processes (i.e., reaeration). Moreover, even in the springs where denitrification flux has been estimated to be very large, the unusually deep morphology of these rivers means that the benthic N_2 production rate exerts a relatively small effect on the water column N_2 concentration. Either one of these confounding effects could be overcome, but together they create such an uncertain inference that we chose not to perform the regular quantitative analyses. That said, we report the data from longitudinal profiles that are strongly consistent with significant N_2 production. Note that this signal is of comparable magnitude to what we'd expect based on our mass balance estimates of denitrification, but very noisy.

Because this component of the research was prematurely discontinued, we pursued two lines of similar inquiry. The first focuses on aquifer denitrification; during the measurements of open channel denitrification, we collected numerous spring vent samples as upstream boundary conditions. A persistent pattern indicative of denitrification began to emerge and, in collaboration with Dr. Brian Katz at the US Geological Survey, we compiled the most complete data set for evaluating this question. Our findings are summarized in Research Element #6; in short, there is evidence of large and spatially variable denitrification in the Upper Floridan, and this has highly significant implications for how we develop inference of N sources from isotopic evidence.

The second area was development of a new method for evaluating denitrification potential. These assays work based on measuring N_2 production in the overlying water in a sealed sediment-water incubator. The method has several advantages over existing methods: it is very fast (with results emerging within hours); it relies on the very high precision measurements possible with a membrane inlet mass spectrometer (MIMS); it measures the direct endpoint of denitrification rather than some intermediary (e.g., the acetylene block) or enzymes associated with the process (e.g., denitrogenase enzyme activity). Results from this trial run suggest ambient denitrification rates that are consistent

with our observed rates based on ecosystem mass balance, and were highest in Alexander Springs Creek (1.3 μg N/g sediment/hr) and lower in Silver and Ichetucknee (0.3 and 0.2 μg N/g sediment/hr, respectively). Moreover, experimental additions of nitrate (N), dextrose (C), and their combination suggest that denitrification in the Silver and Ichetucknee River sediments are strongly limited by nitrate (a finding consistent with isotopic evidence presented in Research Element #5), and that sediments in Alexander Springs Creek are not limited by either C or N. We believe that this new method holds significant promise for evaluating river sediments, and are working to extend these measurements to blackwater systems where C availability may be higher but lability considerably lower.

Introduction

High frequency nutrient measurements have been used to quantify the magnitude and mechanisms of nutrient removal in river ecosystems (Heffernan and Cohen 2010). This approach uses diel variation to partition nitrate removal between autotrophic assimilation, denitrification, and heterotrophic assimilation. Estimates of autotrophic assimilation using diel NO_3^- variation are supported by strong relationships of these estimates with gross primary production and associated predictions of autotrophic demand. Estimates of heterotrophic N demand suggest that this process contributes negligibly to N removal (Heffernan at al. 2010). Based on the insufficiency of assimilatory process, the preponderance of N removal in spring-fed rivers of Florida has been attributed to denitrification (Research Element #2). However, this inference has not been supported to date by methodologically-independent estimates of dissimilatory N removal (i.e. denitrification). Alternative explanations for apparent N removal include underestimation of assimilatory processes or unaccounted dilution of river NO_3^- concentrations by groundwater inputs. The primary objective of the study described in this section is to corroborate mass-balance estimates of denitrification from long-term and high frequency nitrate time series of NO_3^- in the Ichetucknee River. To that end, we used measurements of dissolved nitrogen and argon gases (N_2 and Ar) to estimate N_2 gas saturation and physical reaeration, and denitrification (Laursen and Seitzinger 2002, McCutchan et al. 2003). In addition, we used laboratory sediment assays to provide an additional, independent estimate of denitrification and to assess the potential limitation of this process by organic carbon or NO_3^- availability.

Methods

Laboratory Sediment Assays

We collected sediments for laboratory denitrification assays from the Alexander Springs Creek, Silver River, and Ichetucknee River. Sediment samples from the Alexander Springs Creek were collected at the 6 sampling stations described in Research Element 7 on the second day of intensive diel study (September 2010). Sediments from the Silver River were collected from 7 stations along the entire length of the river and from 10 stations along the length of the Ichetucknee River in October 2010.

From each sampling location, we collected approximately 1 kg of benthic sediment using a hand inserted polycarbonate coring device to a consistent depth of 10 cm. At least three replicate samples for each

vegetation class (present or absent) were collected at each study stream, and stored on ice until returned to the laboratory. A YSI 556 sonde equipped with an optical or Clark DO probe was used to collect dissolved oxygen (DO), pH, specific conductivity and temperature at the time of sediment sampling.

Upon return to the laboratory, sediments were stored at 4°C until assays were performed. Sediments were brought to room temperature overnight in order to allow microbial communities to acclimatize and regain activity before analysis (Herrman et al. 2008), and sediment was homogenized in collection bags before being split for the denitrification assay.

Nutrient amendments were used to assess limitation of denitrification by the availability of organic carbon and NO_3^-. Nutrient amendment solutions for denitrification assays consisted of four treatments: Control (0; distilled water with nitrate added to measured background levels for each system), nitrate (N; 1 mmol nitrate solution), carbon (C; 1 mmol dextrose solution), and carbon-nitrate (CN; 1 mmol each nitrate and dextrose solution).

We added approximately 100 g of wet, homogenized sediment to 300 mL BOD bottles, excluding particles too large to fit into the neck of the bottle. For samples that did not contain enough sediment (~80 g) to complete assays as above, we added approximately 30 g wet, homogenized sediment to 60 mL BOD bottles, and completed the experiment in the same way. Two sets of each treatment were constructed, with one set measured at time zero (T0) and one set measured at time 6 hours (T6). Treatment solutions were added at room temperature using a siphon to minimize contact with the atmosphere, and were overfilled so that air was excluded. We placed the glass stoppers and inverted the bottles several times to remove any air pockets from the sediment. Bottles were then be partially refilled from the bottom to remove bubbles.

We used membrane inlet mass spectrometry (MIMS) to measure changes in N_2 concentration (as outlined below for open channel measurements). MIMS measures dissolved gases directly from water samples, avoiding problems associated with the acetylene block technique, which is generally used for conducting denitrification assays (Groffman et al. 2006). T0 measurements were made immediately by directly sampling supernatant water using the MIMS intake. These measurements were then subtracted from the T6 measurements to determine the increase in N_2 over the incubation period.

Sediments from denitrification assays were dried at 50C, and water volume in each replicate determined by mass difference. Sediment mass was calculated as the difference between dried mass and the mass

of individual assay bottles when empty (determined prior to each experiment). A subsample from each replicate was combusted to at 500C, and organic carbon (as ash-free dry mass [AFDM]) determined by mass loss.

We calculated denitrification rates on a sediment mass specific basis based on measured changes in N_2 concentration, water volume, and sediment dry mass. We used two-way ANOVA to evaluate the effects of dextrose and nitrate amendments on denitrification rate. We estimated denitrification on an areal basis from measured mass-specific rates assuming a sediment bulk density of 2 g/cm^3 and a depth of 10 cm.

Open channel estimates of denitrification

Field sampling

On May 6, 2010 we sampled dissolved gases and measured field water quality parameters at 11 stations along the Ichetucknee River and at each of the 5 major springs (Ichetucknee, Blue Hole, Devil's Eye, Mission, Mill Pond) in conjunction with isotopic and nutrient sampling. At each station, we collected 3 replicate dissolved gas samples in 300 ml BOD bottles using a peristaltic pump, and measured field water chemical parameters (dissolved oxygen (DO), temperature, specific conductance, and pH) from spring vents using a YSI 556 sonde equipped with an optical DO probe. Nutrient analysis was done using EPA standard methods for nitrate (EPA 353.2, Cd reduction), and performed at Florida International University. Dissolved gas samples were stored under ice water until analysis within 36 hours; water samples were frozen until analysis.

Sample analysis

We measured dissolved N_2 and Ar using a Membrane Inlet Mass Spectrometer (MIMS)[1] within 36 hours of collection, over which period our storage protocol exhibited negligible atmospheric contamination. The membrane inlet mass spectrometer was equipped with a copper reduction column heated to 600 °C to remove O_2 and reduce interference with N_2 measurements. Standards for N_2 and Ar concentration consisted of atmosphere-equilibrated deionized water in 1 L spherical vessels incubated and stirred in high-precision water baths (± 0.01 ºC) at their respective temperatures (10, 15, and 20 ºC) for at least 24 hours prior to analysis. Gas concentrations in each standard were calculated using temperature-solubility formulas without salinity correction (Table 4-1). Signal strength for samples and standards was

determined as the mean value of the 1st minute following signal stabilization. To account for instrument drift, we ran complete standard curves every 6-8 samples and applied interpolated parameter values from adjacent standard curves (r^2 = 0.99-1.00) to estimate gas concentrations in each sample. A fourth standard equilibrated with pure N_2 gas served as an external source QC.

Table 4-1. Parameter values for determination of solubility-temperature relationships for Ne, Ar, and N_2 gas.

Coefficient	Ne	Ar	N_2
A_0	2.18156	2.79150	6.42931
A_1	1.29108	3.17609	2.92704
A_2	2.12504	4.13116	4.32531
A_3	0	4.90379	4.69149

Modeling denitrification

We estimated denitrification via a Lagrangian model of physical and biological processes influencing N_2 gas concentrations in a parcel of water as it moves downstream, based on data fit with observations at longitudinal sampling stations (according to the procedures of Laursen and Seitzinger 2002). For characterization of hydrologic characteristics and channel dimensions, we divided the Ichetucknee River into 10 reaches bounded by our sampling stations. Sampling stations were situated just upstream of inflow from major springs, so that hydrologic and chemical characteristics were reasonably homogenous within each reach. We used spring discharge measurements and channel dimensions from Hensley et al. (in review) to estimate parcel dimensions (width, length, depth) and residence time within each reach. Using the equations of Laursen and Seitzinger (2002), we used [Ar] at the upstream and downstream end of each reach to estimate reach-specific physical atmospheric exchange coefficients. These were converted to atmospheric exchange coefficients for N_2 based on the indexing approach of Gulliver et al. (1990). Upstream concentrations of N_2 and atmospheric exchange coefficients were used to estimate expected N_2 concentrations at the bottom of each reach, and differences between these predicted values and observed N_2 concentrations were used to estimate denitrification rates within each reach. We also used previous estimates of denitrification from mass balance (Heffernan and Cohen 2010, Heffernan et al. 2010a) to determine predicted N_2 concentrations from those studies assuming spatially invariant denitrification equal to 0.77 g N /m2 /d.

Results and Discussion

Laboratory Sediment Assays:

Sediments from all three rivers exhibited net production of N_2 in laboratory incubations. In Alexander Springs Creek, we observed high variability in N_2 production, and controls had the highest rate of

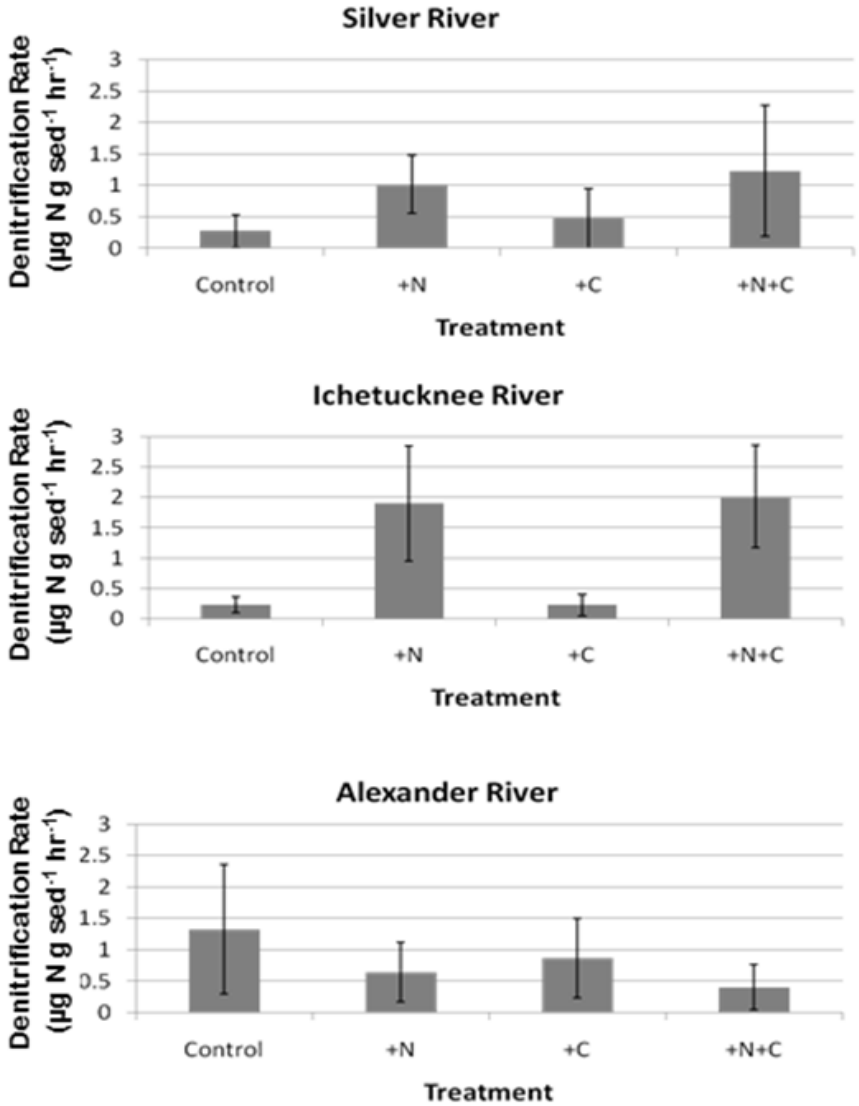

Figure 4-1. Results of laboratory denitrification assays for sediments from Silver River (upper panel), Ichetucknee River (middle panel), and Alexander Springs Creek (lower panel). In Alexander Springs Creek, we observed no significant effects of C or N amendment, but N addition resulted in higher rates of denitrification in both Silver and Ichetucknee Rivers (statistical results reported in Table 4-1). Rates from controls were used to estimate areal denitrification for Ichetucknee and Silver Rivers, and were comparable to mass balance estimates (see Section 3). Evidence for N limitation is supportive of diffusion-limitation mechanism invoked to explain diel and longitudinal isotope dynamics in the Ichetucknee River (Element #5).

denitrification. Highly variable Ar concentrations in these samples indicate that this variability likely results from contamination of some samples with atmospheric N_2. Neither N nor C additions influenced observed N_2 production in Alexander sediments.

In Silver and Ichetucknee River, addition of NO_3 stimulated 4- and 10-fold increases in denitrification rate, respectively (Figure 4-1; Table 4-2 through 4-4). Addition of labile C as dextrose had no effect on denitrification, either singly or in combination with N amendments. This is consistent with isotopic dynamics that indicate N limitation of denitrification via diffusion-limitation of supply to sediments.

Denitrification rates in control treatments for Ichetucknee and Silver Rivers were ca. 0.2 µg N g sed^{-1} hr^{-1}. Assuming bulk density of soil of 2 g/cm^3, and an active denitrifying layer of 10 cm, these mass specific rates correspond to rates of 1.1 and 1.3 g N/m_2/d in the Ichetucknee and Silver River, respectively. These rates are slightly greater than estimates based on ecosystem mass balance (0.77 g N/m^2/d; Heffernan et al. 2010a) in the Ichetucknee. The similarity of estimates provides support for inference of denitrification from long-term and high-frequency N mass balance studies in spring fed rivers.

Table 4-2. Results of Analysis of Variance (ANOVA) assessing effects of C and N amendments on denitrification in Alexander Springs Creek. Note that estimates are for control treatment(s) in each case, such that negative estimates indicate increased rates of denitrification in response to amendment.

Tests of Between-Subjects Effects

Dependent Variable: Ln(denitrification)

Source	Type III Sum of Squares	df	Mean Square	F	Sig.
Corrected Model	.528	3	.176	.733	.540
Intercept	7.704	1	7.704	32.064	.000
C	.131	1	.131	.545	.466
N	.423	1	.423	1.762	.194
C * N	.001	1	.001	.004	.953
Error	7.689	32	.240		
Total	16.535	36			
Corrected Total	8.218	35			

Parameter Estimates

Dependent Variable: Ln(denitrification)

					95% Confidence Interval	
Parameter	B	Std. Error	t	Sig.	Lower	Upper
Intercept	.292	.185	1.576	.125	-.085	.669
[C=.00]	.132	.242	.545	.589	-.360	.624
[N=.00]	.229	.247	.927	.361	-.274	.732
[C=.00] * [N=.00]	-.020	.330	-.060	.953	-.693	.653

Table 4-3. Results of Analysis of Variance (ANOVA) assessing effects of C and N amendments

on denitrification rate in the Ichetucknee River. Note that parameter estimates are for the control treatment(s) in each case, such that negative parameter estimates indicate increased rates of denitrification in response to amendment.

Tests of Between-Subjects Effects

Dependent Variable: Ln(denitrification)

Source	Type III Sum of Squares	df	Mean Square	F	Sig.
Corrected Model	6.083[a]	3	2.028	11.222	.000
Intercept	13.274	1	13.274	73.463	.000
C	.007	1	.007	.040	.842
N	6.034	1	6.034	33.397	.000
C * N	.012	1	.012	.066	.799
Error	6.685	37	.181		
Total	26.541	41			
Corrected Total	12.768	40			

Parameter Estimates

Dependent Variable:LnDen

Parameter	B	Std. Error	t	Sig.	95% Confidence Interval	
					Lower Bound	Upper Bound
Intercept	.984	.128	7.676	.000	.724	1.243
[C=.00]	-.061	.186	-.326	.746	-.437	.316
[N=.00]	-.802	.186	-4.318	.000	-1.178	-.426
[C=.00] * [N=.00]	.068	.266	.256	.799	-.470	.607

Open Channel Estimation:

N_2 and Ar concentrations in each spring vent were well in excess of atmospheric equilibrium. Concentrations of these dissolved gases generally declined longitudinally, with punctuated increases associated with spring inputs. Atmospheric exchange coefficients estimated from Ar ranged from 0.04 to 0.64, but both the highest of those estimates and the greatest divergence of observed and modeled data occurred in the Rice Marsh reach of the Ichetucknee River between Blue Hole and Devil's Eye Spring, where mixing of inputs from these springs is almost certainly incomplete (Figure 4-2a). Previous studies (Heffernan and Cohen 2010a) have estimated k_{O2} (Element #2) as ranging from 0.3 to 0.5 based on diel variation of O_2. Reaeration coefficients of N_2 and Ar are generally similar to those of O_2; the

results of this study thus suggest either far more variable reaeration than previously assumed, or indicate high uncertainty in gas flux estimates based on complex hydrologic mixing.

Table 4-4. Results of Analysis of Variance (ANOVA) assessing effects of C and N amendments on denitrification rate in the Silver River. Note that parameter estimates are for the control treatment(s) in each case, such that negative parameter estimates indicate increased rates of denitrification in response to amendment.

Tests of Between-Subjects Effects

Dependent Variable:LnDen

Source	Type III Sum of Squares	df	Mean Square	F	Sig.
Corrected Model	.990[a]	3	.330	1.765	.182
Intercept	5.624	1	5.624	30.071	.000
C	.010	1	.010	.055	.817
N	.975	1	.975	5.211	.032
C * N	.023	1	.023	.123	.729
Error	4.301	23	.187		
Total	11.161	27			
Corrected Total	5.292	26			

Parameter Estimates

Dependent Variable:LnDen

Parameter	B	Std. Error	t	Sig.	95% Confidence Interval	
					Lower Bound	Upper Bound
Intercept	.638	.163	3.904	.001	.300	.976
[C=.00]	.019	.231	.084	.934	-.459	.498
[N=.00]	-.322	.231	-1.395	.176	-.801	.156
[C=.00] * [N=.00]	-.117	.334	-.350	.729	-.807	.573

Longitudinal patterns of N_2 gas concentrations were generally consistent with the occurrence of denitrification, especially in the upper half of the Ichetucknee River, as observed N_2 concentrations were typically greater than those predicted based on physical processes alone (Figure 4-2b). Reach-specific estimates of denitrification ranged from <0 to 1.23 g N /m2 /d. However, uncertainty associated with measurement of N_2 concentration, mixing dynamics, and reaeration coefficients is extremely high, especially when compared to the small divergence expected to result from mass-balance derived

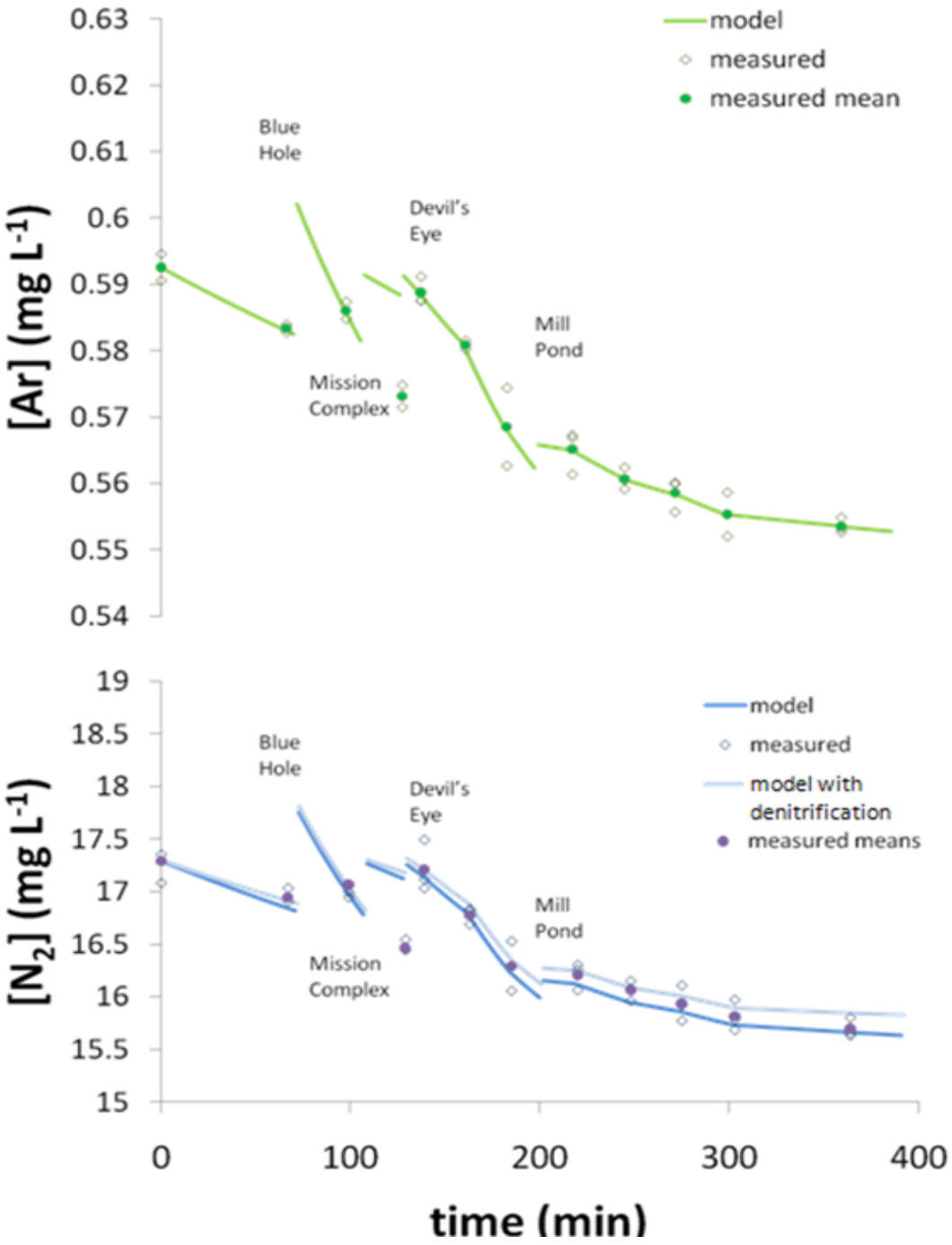

Figure 4-2. Longitudinal changes in (upper panel) Ar and (lower panel) N_2 concentration in the Ichetucknee River, 6 May 2010. In the upper panel, upstream and downstream concentrations of Ar in each reach were used to estimate physical reaeration coefficients. We used these estimates to predict N_2 concentrations in the absence of denitrification (lower panel – dark blue line), and to predict N_2 concentrations based on previous mass-balance estimates of denitrification (lower panel – light blue line). While observed N_2 concentrations generally exceed predictions from physical processes alone, uncertainty in both observed and predicted values is large enough to warrant caution in the inference of denitrification from these data.

estimates of denitrification (Figure 4-2b). Thus, open-channel approaches to estimation of denitrification neither increase confidence in previous estimates, nor do they contradict those findings.

Estimation of denitrification from open channel approaches is generally most robust in shallow, slow-moving channels where denitrification rates are high, reaeration rates can be precisely estimated, and where groundwater inputs are minimal (McCutchan 2003). The suitability of this approach to studies of N cycling in spring run streams is thus somewhat unclear. The approach might yield results with greater precision in smaller spring run streams, or those with NO_3^- concentrations that are more enriched than those observed in the Ichetucknee River. Correspondence between mass balance and open-channel estimates of denitrification in such systems would increase confidence in mass balance from other systems such as the Ichetucknee, but the likely success of such efforts is difficult to predict.

Research Element #5 – Isotopic Inference of N Removal Mechanisms in the Ichetucknee River

Abstract

Longitudinal and diel measurements of dual isotope composition ($\delta^{15}N$ and $\delta^{18}O$) in nitrate (NO_3^-) were made in the Ichetucknee River, a large (ca. 8 m^3 s^{-1}), entirely-spring fed river in north-central Florida, to determine whether isotopic variation can decouple assimilatory and dissimilatory removal, rates of which are well constrained in this system. Specifically, in comparing nitrate concentrations and isotope composition during the day (assimilation + denitrification) and night (denitrification only) we predicted: a) significant daytime declines in total fractionation due to the low fractionation expected for assimilation; and b) systematic variation in isotope coupling of $\delta^{15}N_{NO3}$ and $\delta^{18}O_{NO3}$ between 1:1 (assimilation) and 2:1 (denitrification). Five daytime longitudinal transects showed consistent NO_3^- removal (25-35% of inputs) and modest isotopic fractionation ($^{15}\varepsilon_{total}$ between -2 and -6‰). Fractionation during two pre-dawn transects was consistently lower (by ca. 1‰) than the preceding day, suggesting higher fractionation for assimilation than for denitrification. Total fractionation was negatively associated with discharge, flow-weighted nitrate concentration, total N removal, and the fractional water loss in the lower river. Despite mass balance estimates that denitrification represents 80% of total N removal, N and O isotopes from longitudinal and diel sampling consistently showed 1:1 coupling (i.e., correlation slope) except during a brief pre-dawn period when the isotopes were apparently decoupled. Hourly samples on two dates at a downstream location showed significant diel variation in NO_3^- concentration (60 to 90 µg N/L) and isotope composition ($\Delta\delta^{15}N$ of -0.7‰ to -1.6‰). While total fractionation differed between day and night only on one date, diel variation in fractionation estimated for assimilation by assuming constant denitrification was implausibly large ($^{15}\varepsilon$ = -2 to -25‰), suggesting that the fractionation and removal due to denitrification is unlikely to be diurnally constant. Pronounced counter-clockwise hysteresis in the hourly relationship between NO_3^- and $\delta^{15}N$ further illustrates the presence of previously undescribed diel variation in N isotope processing dynamics. Together, weak fractionation, diel isotope vs. NO_3^- hysteresis, and consistent 1:1 isotope coupling is interpreted as an indication that denitrification is limited by NO_3^- diffusion into the benthic sediments (i.e., rather than occurring along hyporheic flowpaths). While this study observed marked temporal and spatial variation in isotope composition, consistent fractionation and isotope coupling among N removal processes precludes using dual isotope measurements to decompose removal in this system.

Introduction

Amplification of the global nitrogen (N) cycle at least 2-fold during the 20th century (Galloway et al. 2004) has had deleterious effects on lakes, stream and river ecosystems (Dodds 2006), estuaries (Smith 2006) and, in some areas, human and animal health (Townsend et al. 2003). While there has been a marked increase in nitrogen export to the coastal ocean (ca. 65 Tg total N yr^{-1}; Seitzinger et al. 2005), the load applied to watersheds is substantially larger, indicating an estimated river network N removal efficiency near 75% (Van Breeman et al. 2002). This important water purification process is distributed unevenly in space and time (McClain et al. 2000), with removal occurring both in channels (Laursen and Seitzinger 2004) and riparian zones (Sebilo et al. 2003, Lowrance et al. 1995), via assimilatory and dissimilatory pathways, and varying with environmental drivers (oxygen, discharge, light, temperature, organic carbon concentrations) and stream order (Alexander et al. 2000, Peterson et al. 2001, Seitzinger et al. 2002). To predict and manage watershed N removal requires understanding rates, mechanisms and controls of N loss, which in turn necessitates methods that can be applied uniformly across stream order, geography and with sufficient intensity to capture natural variation.

Techniques for process-specific measurements of lotic N processing have focused on low-order streams (Tank et al. 2008); solute and isotope dosing studies (Hall et al. 1998, Mulholland et al. 2000) have yielded rates of and controls on N removal (assimilatory vs. dissimilatory pathways; Böhlke et al. 2004, Mulholland et al. 2009) and nitrification (Hamilton et al. 2001). Similar advances have lagged in higher order stream systems, primarily because of prohibitive costs of isotopic enrichment work at this larger scale. Studies of N processing in high discharge systems that have been done (e.g., Tank et al. 2008) have used enrichment dosing techniques that draw inference from total removal of injected solutes that do not partition removal pathways; moreover, the logistics of large-volume dosing experiments constrains their utility for understanding removal variation in response to environmental or geomorphic controls.

Natural stable isotope abundances are increasingly used for discerning the sources and transformations of N (Kendall 1998, Battaglin et al. 2001, Sebilo et al. 2006, Kendall et al. 2007), offering a synoptic tool from which river processes can be inferred in low- and high-order systems alike. In particular, dual isotope measurements of nitrate ($\delta^{18}O_{NO3}$ and $\delta^{15}N_{NO3}$) have recently been applied to detecting variation in sources (Pellerin et al. 2009), rates and locations of denitrification (Sebilo et al. 2003, Chen et al. 2009), nitrification (Sebilo et al. 2006) and assimilation (Battaglin et al. 2001, De Brabandere et al. 2007, Deutsch 2009). Since both dissimilatory and assimilatory removal pathways operate, and vary in their

relative importance and absolute magnitude at diel, seasonal, and event spatial scales, robust isotopic discrimination between pathways that can be discerned from simple synoptic sampling would greatly aid efforts to understand N processing in large rivers.

We sought to use dual isotopes to decompose removal mechanisms in the spring-fed Ichetucknee River in north Florida where thermal, discharge and chemical stability along with high primary production yield coherent ecosystem-scale signals (e.g., diel nitrate variation) that permit well constrained estimates of both assimilatory and dissimilatory N removal (Heffernan and Cohen 2010). We assessed whether $\delta^{15}N$ and $\delta^{18}O$ measured longitudinally (on different days and nights) and diurnally could discriminate N removal pathways, and whether repeated measures reveals controls on fractionation.

While there are processes other than removal (primarily nitrification) that affect riverine nitrate isotopes, we focused on pathways of N removal, particularly biotic assimilation, which is intrinsically transient but may be significant at diel, seasonal or inter-event time scales, and denitrification, which reduces nitrate to N_2 gas which evades to the atmosphere. Two lines of evidence were proposed to discriminate between dissimilatory and assimilatory removal: differential coefficients of ^{15}N enrichment, and differential coupling of ^{15}N and ^{18}O enrichment.

Strong isotopic enrichment of nitrogen (reported as $^{15}\varepsilon$, units of ‰; Mariotti et al. 1981) and oxygen ($^{18}\varepsilon$) isotopes in nitrate has been documented during denitrification, increasing the mass fraction of ^{15}N and ^{18}O in the residual nitrate pool ($^{15}\varepsilon$ ~ -11 to -30‰, ^{18}O ~ -6 to - 18‰; Sebilo et al. 2006). This range, typical of groundwater isotope enrichment, may not apply in surface water systems, particularly where denitrification is nitrate limited (e.g., where diffusion limits benthic denitrification - Sebilo et al. 2003; in low-redox wetland settings - Lund et al. 2000). Generally, however, high rates of riverine enrichment have been observed (e.g., $^{15}\varepsilon$ of -6 to -20‰ in Ruehl et al. 2007, -14.8‰ in Chen et al. 2009). More modest though highly variable enrichment has been observed in response to assimilation ($^{15}\varepsilon$ = 0 to -27‰ in Fogel and Cifuentes 1993) with fractionation declining with increased growth and decreased nutrient availability (Battaglin et al. 2001). Some studies (Lund et al. 2000, Søvik and Mørkved 2008) assume zero fractionation due to assimilation, which may hold for emergent vascular plants dominant in their study sites (though $^{15}\varepsilon$ of -4.4‰ were estimated in riparian wetlands; Dhondt et al. 2003), but is unsupported for most aquatic systems. Montoya and McCarthy (1995) found higher fractionation in diatoms ($^{15}\varepsilon$ of -9 to -12‰) than for other phytoplankton ($^{15}\varepsilon$ of -0.9 to -3.2‰) suggesting that identity of the dominant primary producer is highly relevant to ecosystem-scale fractionation. Notably, one study of vascular plants (SAV) and epiphytic algae in a similar spring-fed river (de Brabandere et al. 2007)

observed $^{15}\varepsilon$ between -0.9 to -3.2‰, and no differences between primary producers. Based on these broad differences in fractionation, and assuming that assimilation occurs during the day and denitrification is diurnally constant, we hypothesized that diel variation in isotope fractionation and nitrate flux could be used to decompose removal processes. We predicted greater longitudinal removal of nitrate, the overwhelmingly dominant form of N loaded to our study site (Heffernan et al. 2010), during the day (assimilation + denitrification), but reduced fractionation during nighttime conditions because of greater denitrification fractionation. Similarly, we predicted diel variation in $^{15}\varepsilon$ would show a trough at peak assimilation, when $\delta^{15}N$ is enriched and nitrate depleted under night conditions.

A second mode of discriminating N removal pathways focuses on differences in isotopic coupling (i.e., $\delta^{15}N_{NO3}$ vs. $\delta^{18}O_{NO3}$) between assimilation and denitrification. Fractionation occurs in the same direction for both processes, with heavy isotope enrichment of the residual nitrate pool, but isotope coupling, measured as the slope of the $\delta^{15}N_{NO3}$ vs. $\delta^{18}O_{NO3}$ association, differs. Specifically, during assimilation the slope is reported to be 1:1 (i.e., $^{15}\varepsilon = {}^{18}\varepsilon$; Granger et al. 2004), while the slope for denitrification is 1:2 (i.e., $^{15}\varepsilon = 2 * \varepsilon^{18}$; Lehmann et al. 2003). Most studies reporting 1:2 coupling were for groundwater (Aravena and Robertson 1998, Böttcher et al. 2000), but both Ruehl et al. (2007) and Chen et al. (2009) provide supporting evidence for this mode of inference in rivers. Recent experimental evidence (Granger et al. 2006) suggests uniform 1:1 coupling during denitrification with both freshwater and marine denitrifiers. As such, the conditions under which 1:2 coupling occurs remains an important uncertainty. The study by Ruehl et al. (2007) is noteworthy in that they used ancillary evidence to confirm that other removal mechanisms (dilution, assimilation) cannot explain longitudinal depletion; as such, their observation of 1:2 isotope coupling for denitrification is particularly robust. As such, we expected isotope coupling would approach a 1:2 slope at night when denitrification is dominant, while the mixed removal process during the day would exhibit a slope between 1:1 and 1:2.

Using these lines of inference to decompose N removal processes is predicated on two assumptions. First is that diel variation in nitrate concentration, and consequently in nitrate isotopes, is due to variation in assimilation. That is, we assumed denitrification was constant over each day, fractionation due to denitrification is constant, and assimilation is zero at night. Heffernan and Cohen (2010) report significant inter-day variation in denitrification, but used correlative evidence to conclude that within-day mass flux variation is negligible. Further, N assimilation estimated from diel nitrate variation was consistent with GPP stoichiometry and biomass turnover only when autotrophic uptake was assumed zero at night. Second, lateral water inputs of unknown isotopic composition are minimal. Despite

piezometric (M. Kurz, unpublished data) and conservative solute (de Montety et al. 2011) data from the river that suggest diffuse lateral inputs in the upper reaches, total springs discharge is generally higher (by 10-20%) than measured downstream flows. We assumed the Ichetucknee is a losing river in its lower reach, simplifying inference of longitudinal processing.

Factors controlling temporal variation in fractionation are essential for interpreting synoptic measurements. Measures of input nitrate concentrations, discharge (inputs and river water loss), and N removal, along with dual isotope inference, allow enumeration of covariates with fractionation. Several studies have examined temporal variation in fractionation. Ruehl et al. (2007) report strong discharge dependence on both N removal (reduced at higher discharge) and fractionation (greater at higher discharge). Similarly, Chen et al. (2009) report seasonal variation in fractionation due to denitrification, with fractionation increasing under high load conditions and in response to temperature and discharge. Our expectations in this stable spring-fed river system were that fractionation would increase with discharge due to increased interaction with hyporheic and riparian sediments, and decrease at lower concentrations and with greater N removal signaling more complete processing of the available nitrate.

Methods

Study Site

The Ichetucknee River is an entirely spring-fed tributary of the Santa Fe River and part of the Suwannee River basin in North Florida, USA. The 770 km^2 springshed recharges water to the Upper Floridan Aquifer, which discharges to 6 major spring vents where the carbonate aquifer is unconfined (Fig. 5-1; Scott 1998). Daily discharge of the six major springs and the Ichetucknee River at US 27 is available since Feb 2002, over which time flow has varied only 3-fold; low discharge variability, and the absence of episodic scouring of accumulated organic material, is one reason spring rivers are useful model systems. Over that period, downstream discharge at US27 has averaged 8.6 m^3/s, ~11% less than the combined flow of the springs (9.6 m^3/s); we note, however, that diffuse groundwater inputs in the upper river may still be significant even though the lower river below the spring inputs is a losing river.

Channel morphology and chemistry change over the 8-km length of the river in response to sequential mixing of spring vents. Within 1 km of the Ichetucknee head spring (median annual discharge = 1.3 $m^3 s^{-1}$), the river is fed by water from Blue Hole (3.6 $m^3 s^{-1}$) and Cedar Spring (0.3 $m^3 s^{-1}$), followed by Mission Springs (2.6 $m^3 s^{-1}$) and Devil's Eye spring (1.4 $m^3 s^{-1}$) (Fig. 5-1). To this point, the river is narrow (mean

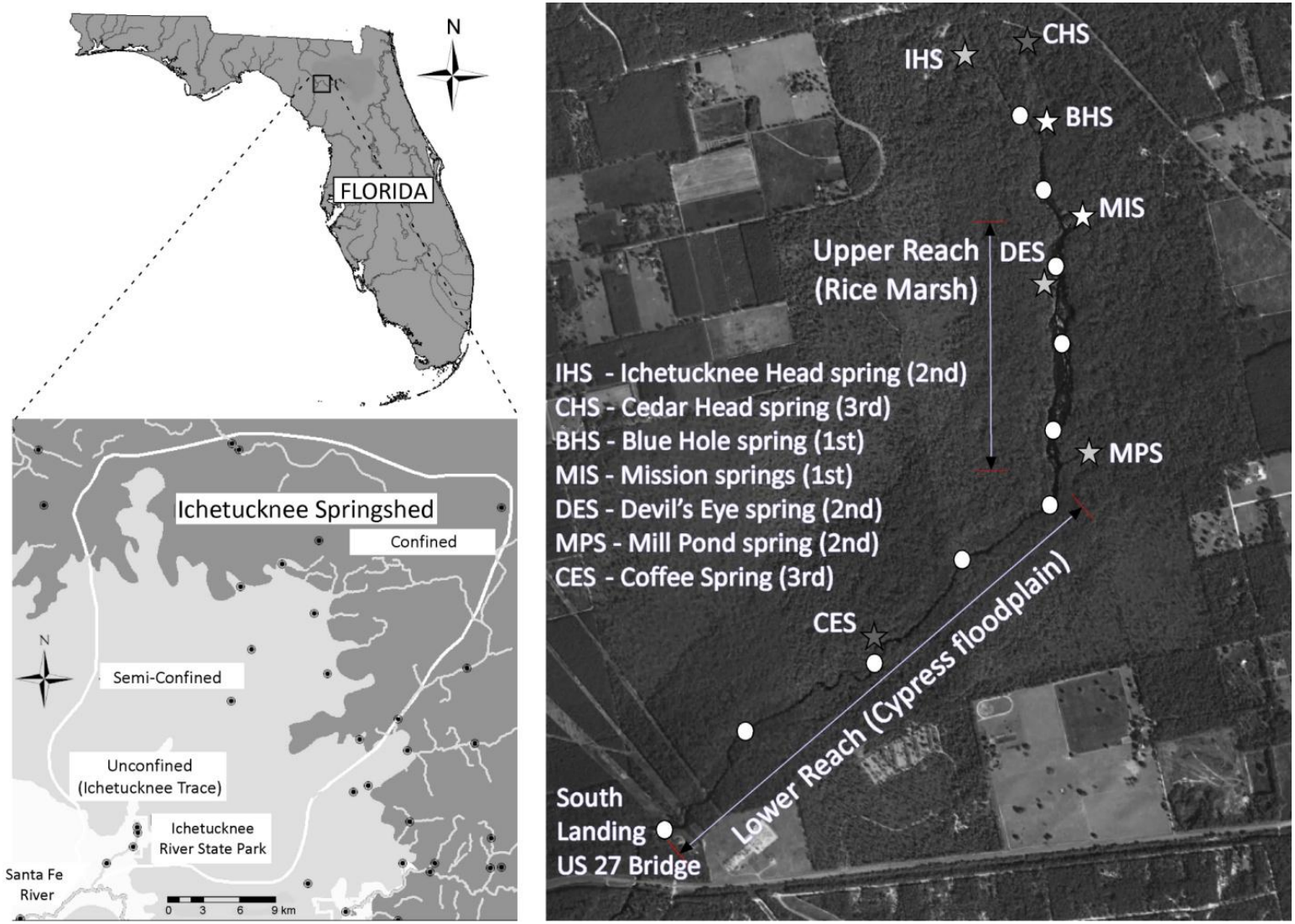

Fig. 5-1. Study site showing the springshed (770 km^2) in Columbia County, Florida, the six springs (stars) that feed the Ichetucknee River, longitudinal sample locations (n = 10, white circles with the upstream site as #1) and downstream diel sampling location (at US27 bridge). Distinct morphologic zones (shallow/wide upper; deep/narrow lower) are marked.

width = 15 m), shallow (mean depth = 0.75 m) and slow moving (mean velocity = 0.16 m s^{-1}). Over the next 1000 m, the river passes through an area known as the Rice Marsh, where the river channel widens substantially (mean width= 65 m). Flow is primarily routed through a deeper (mean depth = 1.0 m) thalweg that is 20-25 m wide, but is also evident braiding throughout a shallower (mean depth = 0.4 m) highly vegetated zone that remains wetted during all but the most extreme low flow periods. At the end of the Rice Marsh, two more springs (Grassy Hole: 0.2 m^3 s^{-1}, and Mill Pond: 0.8 m^3 s^{-1}) enter the river, and the channel narrows substantially (mean width = 24 m), deepens (mean depth = 1.2 m) and velocity increases (mean velocity = 0.25 m s^{-1}). The channel is confined by a wide floodplain (75-200 m) that is inundated episodically by backwater effects of stage variation in the downstream Santa Fe River, 8-km from the headspring; the boundary of Ichetucknee River State Park at the US 27 bridge, 5-km from the headspring, is the downstream extent of this study. The mean residence time of water in the river (between Blue Hole Spring and the downstream location) is 6 hours, and conservative tracer breakthrough curve analysis suggests that less than 5% of the water resides in the river longer than 9 hours (Hensley 2010).

Water chemistry varies across springs due to different contributing areas, flowpaths and residence times, but remains remarkably constant over time within springs (Martin and Gordon 2000). Elevated nitrate-N concentrations, up to 16 times reported background levels (ca. 0.05 to 0.1 mg/L), are found in all springs, but are particularly significant in Ichetucknee, Cedar Head and Blue Hole (0.77, 0.82, 0.70 mg/L, respectively), with Mission, Devils and Mill Pond somewhat lower (0.52, 0.55, 0.41 mg/L, respectively), but still elevated above background. Based on isotopic and mass balance evidence, mineral fertilizer, likely applied to row-crop agriculture, pasture and managed forests, is the principal N source (Katz et al. 2009); the springshed also includes Lake City (pop. 10,000), and many septic tanks in the adjacent unincorporated areas of Columbia County. Monthly water chemistry measurements over 15 months between 2007 and 2008 showed a mean coefficient of variation for [NO_3] of 7% across springs and autocorrelation at 1 month lag of +0.82, supporting our assumption of constant boundary inputs over any given sampling event.

Previous work in this system indicated that denitrification dominates N removal (Heffernan et al. 2010a, Heffernan and Cohen 2010). High resolution mass balance based on the flow-weighted upstream nitrate concentrations from the springs (measured monthly) and observed diel variation in downstream river concentrations (measured hourly) were used to estimate daily assimilation and denitrification (Heffernan and Cohen 2010). These values aligned well with long-term mass balance calculations using

archival samples (obtained from EPA STORET) and multiple methods to estimate autotrophic demand from gross primary production. All methods suggest that denitrification comprises between 75 and 85% of observed longitudinal N removal (20-year mean total removal = 0.77 g N /m2 /d; Heffernan et al. 2010a). Heffernan et al. (2010a) note that assimilated N is either exported as particulate organic carbon, likely a relatively small flux based on river suspended material concentrations, or remineralized to nitrate since: 1) dissolved TKN is low and constant along the entire study reach and; 2) ecosystem storage in this hydrologically-invariant river is assumed to be continuously near equilibrium. Nitrification rates have not been measured directly in this system. Seasonal variation in assimilatory and dissimilatory N removal rates was similar across seasons (Heffernan and Cohen 2010), suggesting strong coupling between rates of organic carbon production and heterotrophic mineralization.

Field Sampling

Filtered water samples were collected from each of the 6 springs monthly between March 2007 and March 2008, and then again during the spring and fall of 2009. Water samples were also collected from a longitudinal transect consisting of 10 fixed locations (Fig. 5-1) in the early afternoon (between 2:00 pm and 4:00 pm) on 5 different days (September 2007, March 2008, March 2009, October 2009 and November 2009). Pre-dawn samples were collected at each station the morning following day-time sampling in October 2009 and November 2009. Measurements of pH, dissolved oxygen, and temperature were obtained using a YSI field sonde (YSI 650, Yellow Springs OH) that was calibrated prior to each field day.

Water samples were also collected hourly over a 24-hour period using an ISCO 6700 auto-sampler at the downstream location (US 27 bridge) on two occasions (March 2009, November 2009). Discrete samples were collected by hand at the start and finish of each 24-hour period to control for sampling device or holding time effects; based on evidence of contamination, a third day (October 2009) of hourly samples was excluded from further analysis.

All water samples for NO_3 and dual isotope ($\delta^{15}N$ and $\delta^{18}O$) composition were collected in acid-washed 150-mL brown polyethylene bottles and frozen until analysis. Measurements of NO_3 were made within 28 days using second-derivative UV spectroscopy (Aquamate UV-Vis spectrometer); interference from color was minimal as these waters are naturally low in UV-absorbing dissolved organic carbon. Because springs discharge at different locations along the upper river, the expected concentrations assuming

mixing-only were computed based on the flow weighted average concentration from springs that discharge upstream of each sampling location; longitudinal removal was evaluated using this quantity.

Isotope Measurements

Nitrate isotopes were measured at the University of Florida, Department of Geological Sciences, using the bacterial denitrifier method (Sigman et al. 2001, Casciotti et al. 2002) whereby nitrate was quantitatively converted to N_2O by the bacteria *Pseudomonas aureofasciens*. The $\delta^{15}N$ and $\delta^{18}O$ of the N_2O produced was measured on a Thermo Delta-Plus XP isotope ratio mass spectrometer using the GasBench interface and a continuous flow of helium. Isotopic composition was reported using the δ notation relative to air (for ^{15}N) and VSMOW (Vienna Standard Mean Ocean Water, for ^{18}O). International ^{15}N standard (IAEA-N3 $\delta^{15}N$ = +4.72‰) and ^{18}O standards (USGS-34 = -27.9 ‰,, USGS-35 = +25.5‰) were included in each batch along with laboratory duplicates to estimate overall analytical precision of ±0.2‰ for $\delta^{15}N$ and ±0.6‰ for $\delta^{18}O$.

The expected flux-weighted isotopic composition at each sampling location assuming mixing only was computed based on daily gage estimated discharge, and measured nitrate concentration and isotopic composition of each spring during that month (not necessarily on our sampling date). Low temporal variation in spring nitrate concentrations ($CV_{\delta 15N}$ = 4%, 4%, 5%, 4%, 4%, and 19% for Head, Cedar, Blue, Mission, Devils and Mill Pond, respectively, over 18 monthly samples) and isotope composition ($CV_{\delta 15N}$ = 3%, 7%, 3%, 2%, 4%, and 13%, respectively) supported using this asynchronous input data.

Data Analysis

The slope of the best-fit line from ordinary least squares (OLS) regression between the natural logarithm of NO_3 remaining in the water column (i.e., $Ln([NO_3]_i/[NO_3]_0)$, where $[NO_3]_i$ is the concentration at downstream location i and $[NO_3]_0$ is the flow-weighted input concentration) vs. isotope abundances compared to flux-weighted inputs ($\Delta\delta^{15}N$) was used to determine enrichment factors ($^{15}\varepsilon$ and $^{18}\varepsilon$ for nitrogen and oxygen in nitrate, respectively; Mariotti et al. 1981). Linear coupling between $\delta^{15}N$ and $\delta^{18}O$ was evaluated using OLS to obtain slope estimates, tested for significant deviation from 1.0, and goodness-of-fit. Associations between inferred enrichment factors and environmental covariates (day vs. night, total springs discharge, longitudinal water loss, longitudinal N loss, flow-weighted nitrate

inputs) were also evaluated. Total N removal was estimated from the longitudinal decline in nitrate mass, assuming that water lost from the river between the springs and the downstream sampling location experienced the same decline in nitrate concentration as was observed in water remaining in the channel. These total loss rates compared favorably with values previously calculated (Heffernan et al. 2010a, Heffernan and Cohen 2010). Further, on the two days when both day and night (pre-dawn) longitudinal transects were sampled, denitrification was estimated from pre-dawn removal. Assimilatory fractionation was estimated based on the additional mass removal during the day, assuming denitrification rates are diurnally constant, and the observed day vs. night change in isotope values (i.e., $\Delta\delta^{15}N$ between night and day).

Diel isotope coupling was evaluated over 24 hours and for both day and night segments on two days; a third day of samples were obtained (Oct. 2009), but were omitted from this study because of apparent autosampler contamination. The first day (March 2009) was cloudy while the second (Nov 2009) was sunny; cloud cover was expected to affect both primary production that day and denitrification the next day (Heffernan and Cohen 2010). Hourly variation in total isotope enrichment was determined as the difference between springs inputs of nitrate and isotope abundance vs. downstream observations. These values were compared to estimates from simultaneous longitudinal transects. For diel time-series, the component of isotope enrichment due to denitrification ($^{15}\varepsilon_{den}$) was estimated from total $^{15}\varepsilon$ values observed between 10:00 pm and 7:00 am (i.e., when assimilation is negligible). Mass loss due to denitrification was estimated from the same time period, and both denitrification removal and fractionation were initially assumed constant. Assimilation was estimated from additional daytime mass removal; fractionation due to assimilation ($^{15}\varepsilon_a$) was estimated from the difference between isotope values expected with denitrification alone ($^{15}\varepsilon_{den}$) and observed hourly isotope values during the day.

Results

Springs inputs to the Ichetucknee were remarkably constant (Table 5-1) over the study period. Flow varied between 7 and 8.5 m^3/s, while monthly measurements of flow weighted nitrate concentration varied between 0.61 and 0.56 mg/L and flux-weighted isotopic composition varied between 5.4 and 6.5‰ (for $\delta^{15}N$) and 8.1 and 11.3 ‰ (for $\delta^{18}O$) (Table 5-1; solid lines in Fig. 5-2B-H). The coefficient of variation was less than 10% for individual springs attributes (temperature, pH, conductivity, nitrate, $\delta^{15}N$, and $\delta^{18}O$) except for dissolved oxygen, (CV of 21% across springs), and $\delta^{15}N$ in Mill Pond spring (CV

= 13%). In short, upstream boundary conditions are constant, which permits use of spring vent conditions measured within 10 days of diel and longitudinal sampling events as upstream inputs. Modest differences in the nitrate and isotope contribution of the various springs, principally driven by temporal variation in discharge (Table 5-1), are evident in subtle shifts in the shape of solid lines denoting flow-weighted nitrate and flux-weighted isotope inputs (Fig. 5-2B-H).

Longitudinal samples show marked and consistent depletion of nitrate and enrichment of ^{15}N (Fig. 5-2B-H; black circles are observed nitrate, grey diamonds are observed $\delta^{15}N$). An important component of

Table 5-1. Summary of Ichetucknee springs inputs during the study period.

	Sep-07	Mar-08	Mar-09	Oct-09	Nov-09	Sep-07	Mar-08	Mar-09	Oct-09	Nov-09
Spring	Flow ($m^3 s^{-1}$)					[NO3] (mg N/L)				
Ichetucknee	1.30	1.36	1.27	1.42	1.45	0.78	0.82	0.75	0.84	0.82
Cedar	0.15	0.14	0.15	0.16	0.15	0.83	0.83	0.82	0.82	0.76
Blue Hole	3.11	2.91	2.72	2.18	2.15	0.72	0.68	0.67	0.64	0.63
Mission	2.43	2.63	2.26	2.49	2.46	0.49	0.50	0.48	0.45	0.45
Devils Eye	1.44	1.22	1.33	0.99	0.98	0.49	0.50	0.45	0.48	0.47
Mill Pond	0.62	0.82	0.59	0.59	0.57	0.37	0.35	0.37	0.25	0.25
River @ US27†	7.58	8.43	7.13	7.30	7.02	0.61	0.59	0.57	0.56	0.55
Spring	$\delta^{15}N_{NO3}$ (‰)					$\delta^{18}O_{NO3}$ (‰)				
Ichetucknee	3.8	3.7	3.2	3.2	3.5	9.2	9.3	5.7	5.7	5.3
Cedar	3.7	3.7	3.8	3.1	3.6	9.5	9.7	6.4	5.7	4.9
Blue Hole	4.3	4.2	4.2	4.3	4.3	10.2	9.0	6.6	6.7	6.0
Mission	6.8	6.8	7.2	8.4	8.3	13.5	12.4	10.3	11.3	11.2
Devils Eye	7.3	6.8	9.6	10.9	11.7	13.4	12.4	11.5	15.3	14.9
Mill Pond	7.3	8.3	12.5	17.5	17.1	13.4	14.5	14.2	13.4	13.5
River @ US27†	5.3	5.2	5.7	6.0	6.0	11.3	10.6	8.2	8.5	8.5
Spring	DO (mg/L)					Temperature (C)				
Ichetucknee	4.8	4.1	3.9	4.2	3.8	22.8	21.9	21.8	21.8	21.7
Cedar	3.7	3.1	3.2	3.1	3.2	22.0	21.7	21.4	21.7	21.6
Blue Hole	2.2	1.8	1.8	2.3	2.0	21.8	21.7	21.8	21.8	21.8
Mission	2.0	0.5	0.7	0.5	0.5	22.1	21.9	22.0	21.8	21.8
Devils Eye	-	0.7	0.9	0.4	0.4	-	22.0	21.9	21.7	21.8
Mill Pond	0.4	0.5	0.5	0.3	0.4	22.1	21.9	22.1	21.9	21.9
River @ US27†	2.0	1.5	1.6	1.7	1.6	22.1	21.8	21.9	21.8	21.8

† - chemical concentrations for the river @ US27 are flow weighted (for NO_3, dissolved oxygen and temperature) and flux-weighted inputs (for isotope values), not observations.

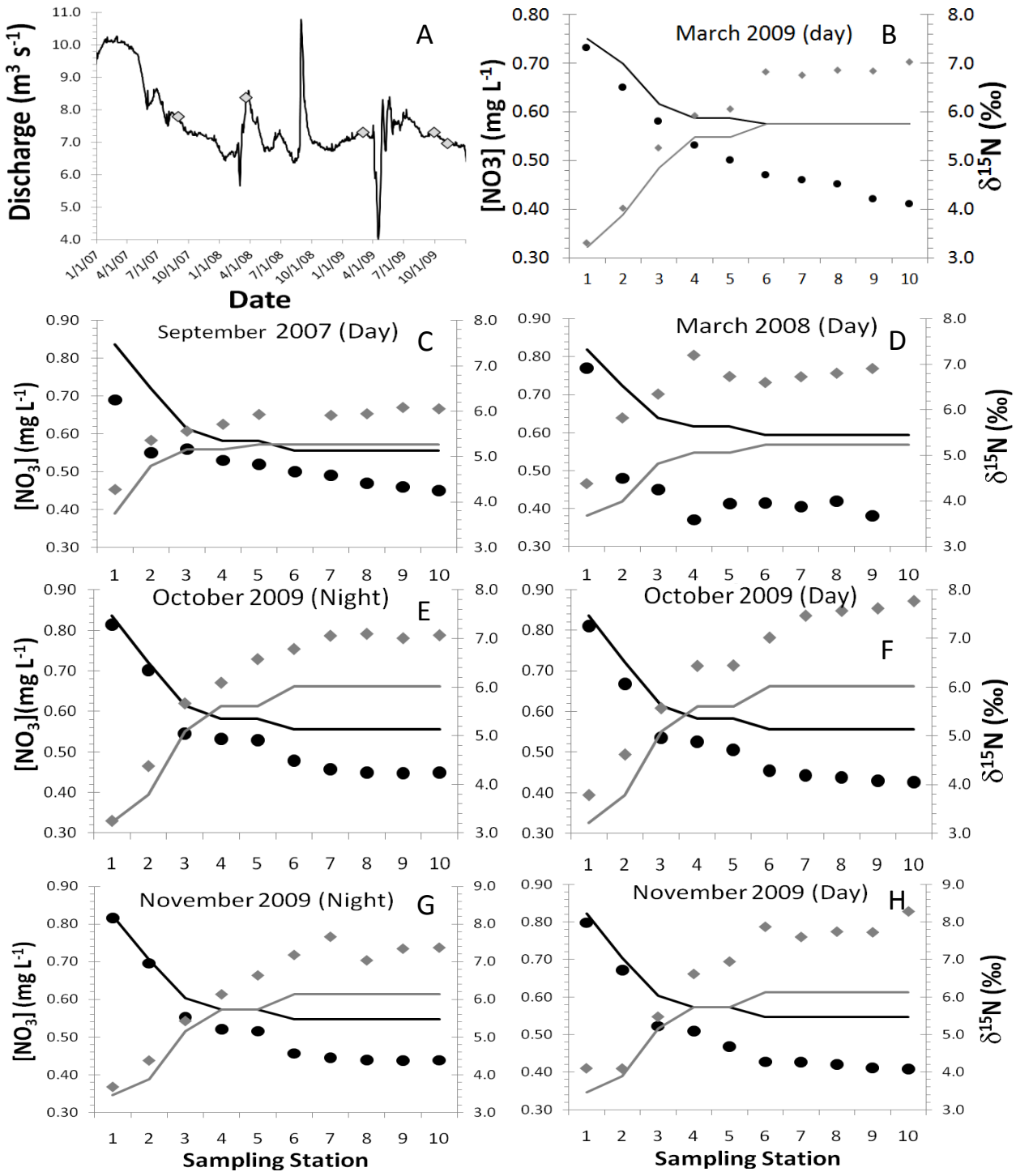

Fig. 5-2. Measured downstream discharge (A, black line) showing longitudinal sampling events (grey diamonds); hourly sampling was done in March and November 2009. Longitudinal changes in [NO_3^-] (black circles) and $\delta^{15}N$ (grey diamonds) are shown from 7 events (5 day, 2 night, B - H). Springs inputs assuming mixing only are shown for [NO_3^-] (black line) and $\delta^{15}N$ (grey line); deviation between observations and this line indicate biological processing.

the general trend observed across all 7 longitudinal transects (5 days, 2 nights) of declining nitrate concentrations and increasing ^{15}N composition arises from the spatial arrangement of springs, with the highest nitrate concentrations and lowest $\delta^{15}N$ values in the upper springs; however, biological activity clearly causes deviations from values expected based on mixing (e.g., solid lines, Fig. 5-2). Removal and isotope enrichment appear to be modestly reduced when comparing adjacent night and day sampling events in October 2009 (Fig. 5-2E, F) and November 2009 (Fig. 2G, H).

Total nitrogen removal was between 27% (October 2009) and 35% (March 2008) over the entire study reach during the day (Fig. 5-2). Given measured discharge on each day, this corresponds to a range in total removal between 8.8 kg/hr (1.1 g /m2/hr) in March 2008 and 5.5 kg/hr (0.75 g /m2/hr) in October 2009. Nighttime removal observed in October and November 2009 suggests that denitrification accounts for 78 and 76% of total removal (0.59 and 0.60 g /m2/hr), respectively, consistent with long-term mass balance estimates of the relative contributions of assimilation (19%) and denitrification (81%) to overall removal (Heffernan et al. 2010a). Based on longitudinal profiles, most nitrate removal occurred between stations 3 and 6, which is in the broad, shallow Upper Reach (Fig. 5-1).

Isotopic enrichment with N removal (Fig. 5-2 B-H) suggests fractionation. Estimated enrichment factors ($^{15}\varepsilon$; fitted line slopes) for the 5 daytime transects varied between -1.92‰ (Sept. 2007) and -5.82‰ (Nov. 2009) (Fig. 5-3 A and B). Intercept values were statistically different from zero only for September 2007 and March 2008 when longitudinal removal was unusually strong in the upper river (Stations 1-3; Fig. 5-2C and 5-2D, respectively). Enrichment was less pronounced for night transects than on the preceding day (by 2 and 1.5‰ in October and November 2009, respectively; Fig. 5-3B); concordance between fractionation factors for samples collected in the day and those in the night one month apart is particularly striking. Comparison of day and night transects suggests that fractionation due to assimilation is, unexpectedly, higher than denitrification. Assuming fractionation and removal due to denitrification is constant, assimilation is estimated to be 5.8 and 7.7% of the total N flux for October and November transects, respectively. Based on $\Delta\delta^{15}N$ of 0.75 and 0.56‰ between day and night transects, we estimated assimilatory fractionation ($^{15}\varepsilon_A$) to be -9.38 and -9.33‰, markedly higher than the estimated values for denitrification (-3.38 and -4.32‰ for October and November; Fig 5-3B).

Isotopic coupling, the slope of the line relating $\delta^{15}N$ and $\delta^{18}O$, was indistinguishable from 1 for all longitudinal transects, including those done at night in October and November 2009 (Fig. 5-4). Given previous mass balance estimates suggesting the dominant role of denitrification in N removal in this river, particularly for the two night-time sampling events, the evidence does not support the predicted

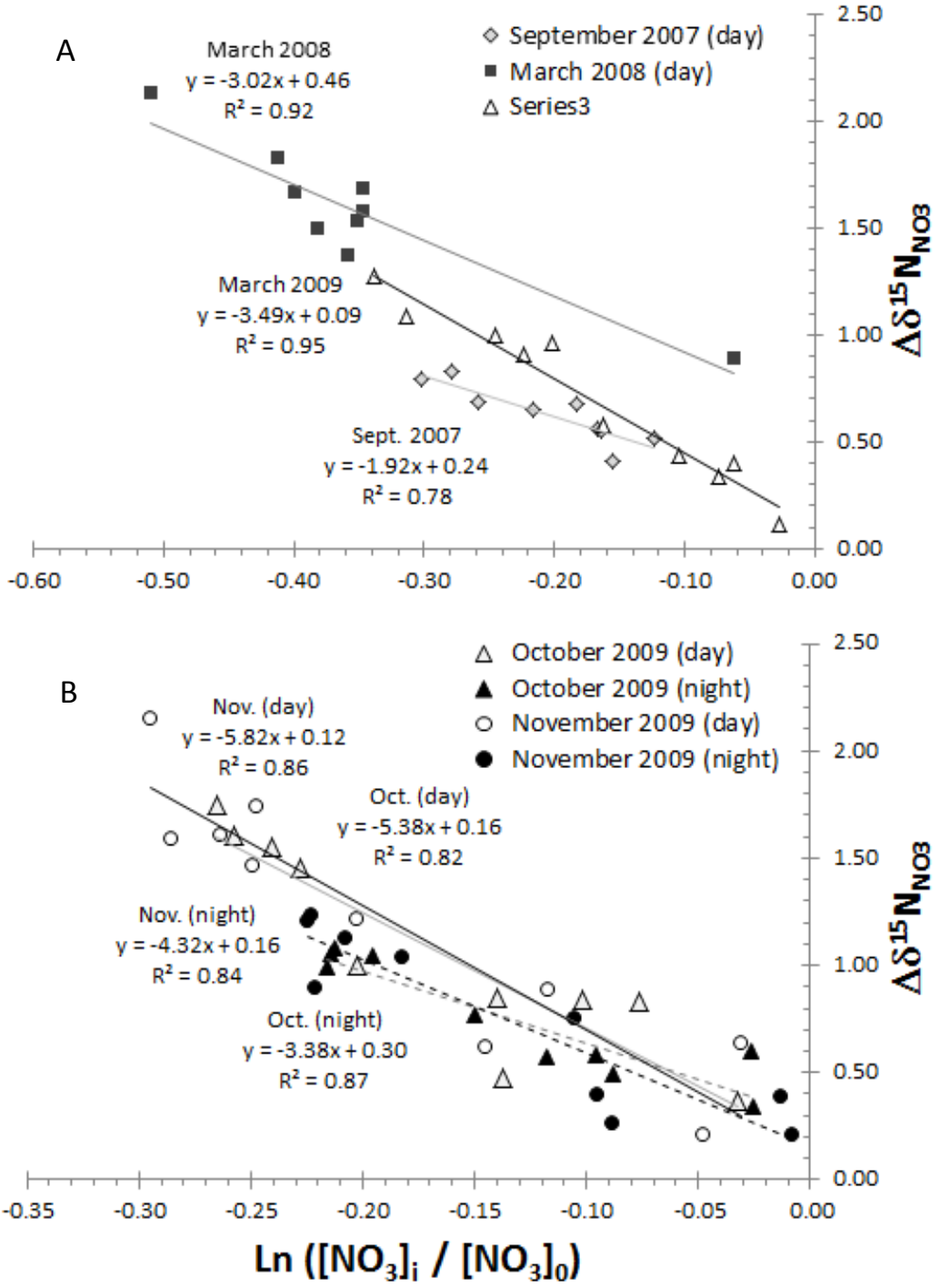

Fig. 5-3. Isotope enrichment ($\Delta\delta^{15}N$ between observations and flux-weighted springs inputs) of residual NO_3^- from 7 longitudinal sampling events (5 day – solid lines, 2 night – dashed lines); fitted slopes are enrichment factors (ε^{15} in ‰).

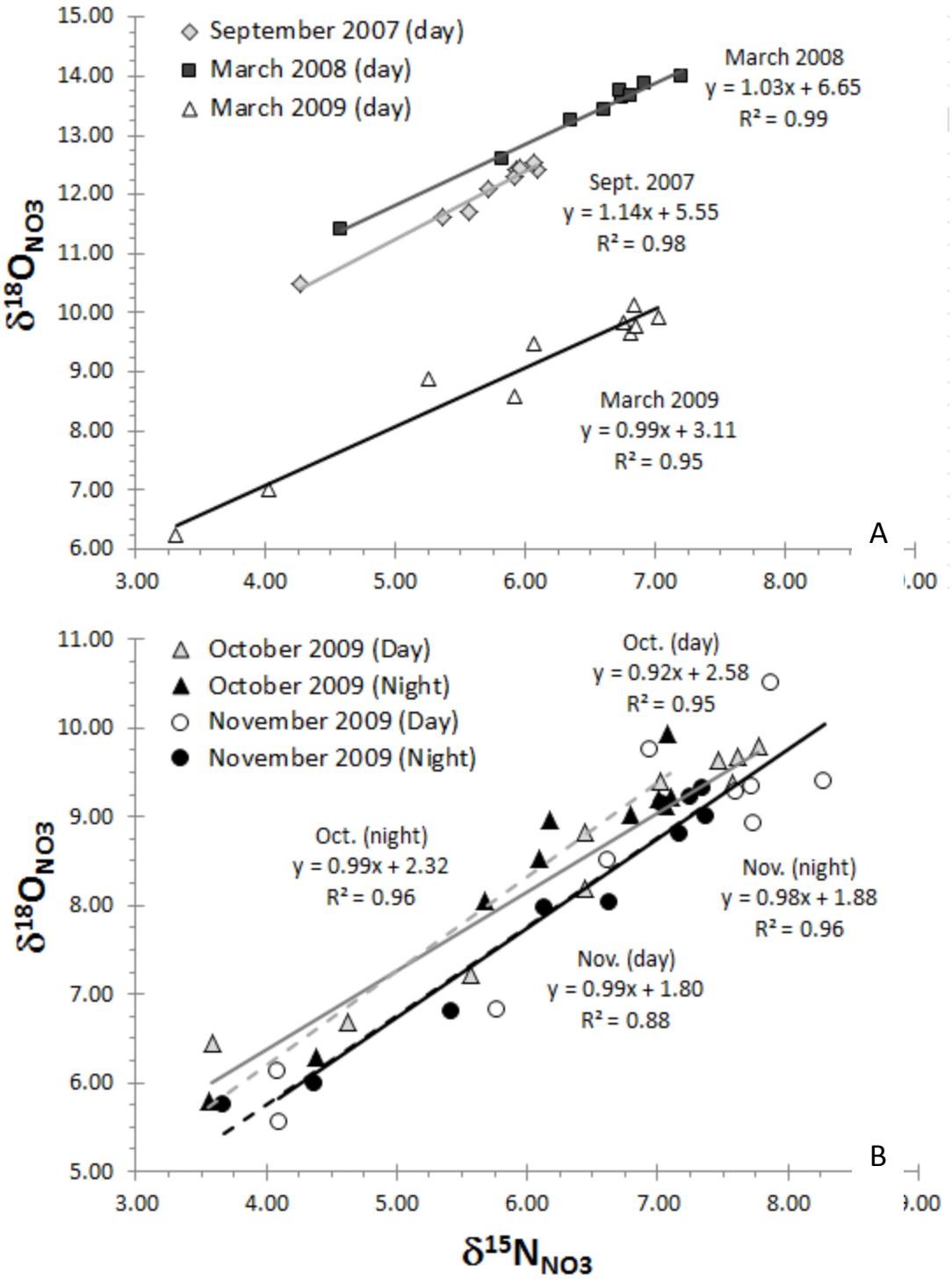

Fig. 5-4. Dual isotope coupling (slope of $\delta^{15}N$ vs. $\delta^{18}O$) from longitudinal transects (5 day – solid lines and 2 night – dashed lines).

1:2 coupling observed in other rivers with denitrification. There was evidence of variation in the intercept values among sampling periods, with March 2008 and September 2007 exhibiting higher $\delta^{18}O$ values than other sampling events. These elevated $\delta^{18}O$ values are consistent with monthly spring vent sampling data that suggest higher input values during that period. The cause of variation in $\delta^{18}O$ that is independent of variation in $\delta^{15}N$ in the spring vent water is unknown, but may reflect variation in nitrate source loading, particularly given that the two periods of high $\delta^{18}O$ are also the periods of highest discharge (Fig. 5-2A).

Temporal variation in longitudinal fractionation suggests control by environmental drivers may be important. As shown above, there was evidence of a time-of-day effect (Fig. 5-5A) with greater fractionation during the day, when both assimilation and denitrification are acting, than at night when only denitrification is occurring. We observed a strong correlation between the enrichment factor and flow-weighted nitrate inputs (Fig. 5-5B) suggesting that as input nitrate concentration increases, fractionation decreases; note, however, that the range of flow-weighted concentrations was small (0.54 to 0.61 mg/L) and was nearly perfectly correlated with total springs discharge ($r = +0.96$, $p < 0.01$). Hydrologic conditions also appear to control fractionation (Fig. 5-5C), with increasing springs discharge negatively associated with isotope enrichment (i.e., higher fractionation under conditions of lower flow). At the same time, fractionation increased as the proportion of water lost during passage through the lower reach decreased (from less than 10% loss to roughly a 5% gain). Finally, we noted that fractionation decreased as total N removal increased (Fig. 5-5D).

Hourly sampling at the most downstream location revealed significant diel variation in isotope abundances that was approximately out of phase with diel variation in nitrate concentrations (Fig. 5-6). Diel variation in $[NO_3]$ yields estimates (Heffernan and Cohen 2010) of autotrophic assimilation of 0.14 and 0.09 g $N/m^2/d$ in March (Fig. 5-6A) and November (Fig. 5-6B) 2009, respectively. This estimate of assimilation is subtracted from total N removal, estimated by difference between hourly downstream concentrations and the flow-weighted input concentrations, to yield denitrification estimates of 0.61 and 0.42 g $N/m^2/d$ in March and November, respectively. Values of $\delta^{15}N$ and $\delta^{18}O$ at the downstream location were always higher than the flux-weighted inputs from the springs ($\delta^{15}N = 5.81$ and 6.09‰, $\delta^{18}O = 8.27$ and 7.73‰ in March and November, respectively), but values were markedly higher during the day when both assimilation and denitrification were occurring. Diel patterns in $\delta^{15}N$ and $\delta^{18}O$ appear synchronous (Fig. 5-6), but with lower temporal autocorrelation in the $\delta^{18}O$ signal.

While dual isotope coupling (slope of $\delta^{15}N$ vs. $\delta^{18}O$) was slightly below 1:1, this deviation was statistically significant only for March ($p = 0.03$, Fig. 5-7A). There was some evidence that nighttime slopes were shallower than the daytime slopes, consistent with movement towards 1:2 coupling, but this difference was not statistically significant. The strength of isotope coupling (r^2) was also stronger in the daytime. We note that parsing isotope values and coupling based on day and night defined by sunrise and sunset may be confounded by the hydraulic residence time in the river (ca. 6-8 hours; Hensley 2010). An 8-hour moving window analysis of isotope coupling revealed greater variation in slopes (0.4 to 1.1 in March, 0.4 to 0.9 in November), with evidence of lower slopes in the early morning (ca. 5 to 10 am),

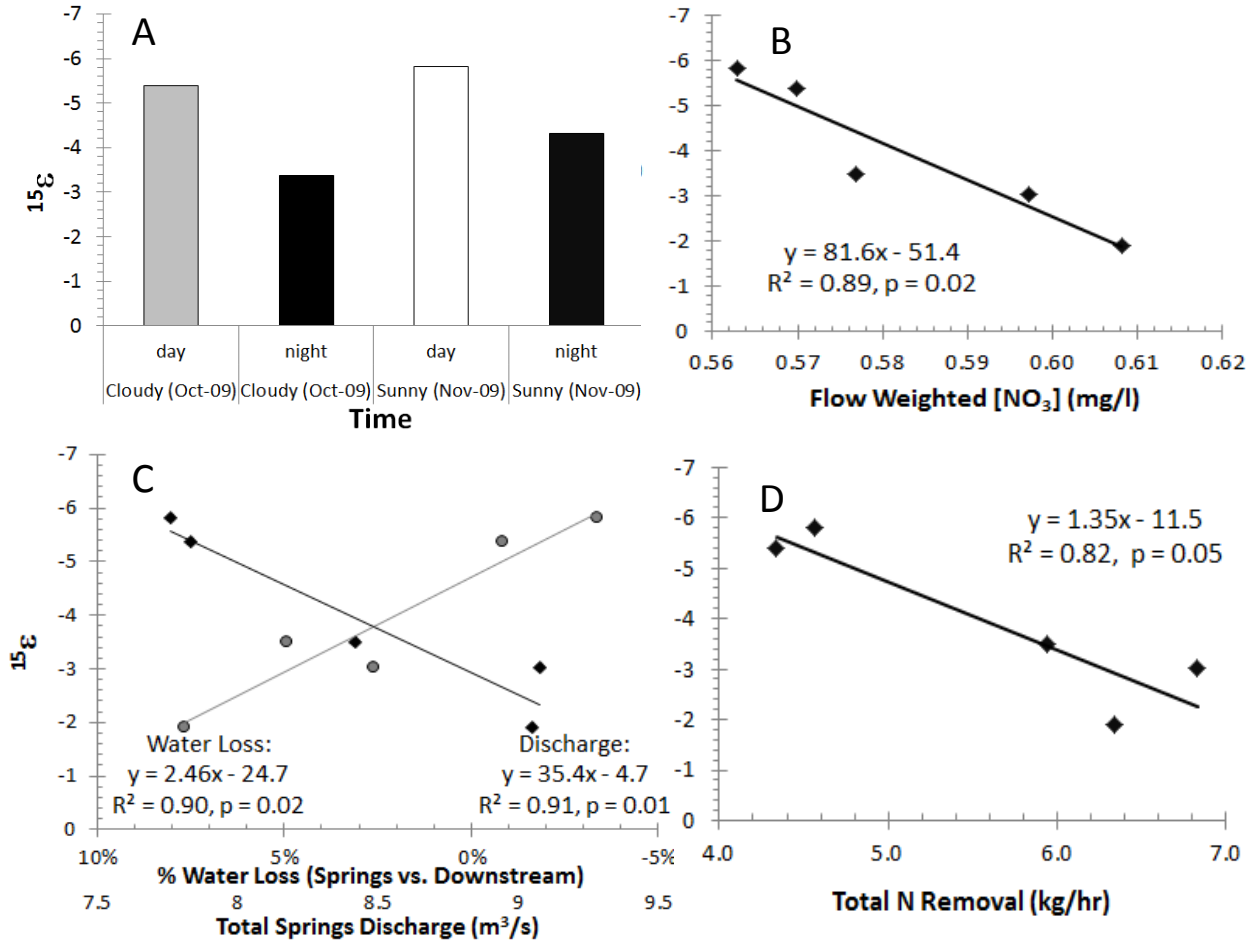

Fig. 5-5. Controls on longitudinal ^{15}N fractionation including A) time of day, B) flow-weighted springs NO_3 inputs, C) combined spring discharge (black diamonds) and fractional water loss (grey circles) lower reach), and d) total riverine N removal. Effects in B, C, and D are for daytime transects only.

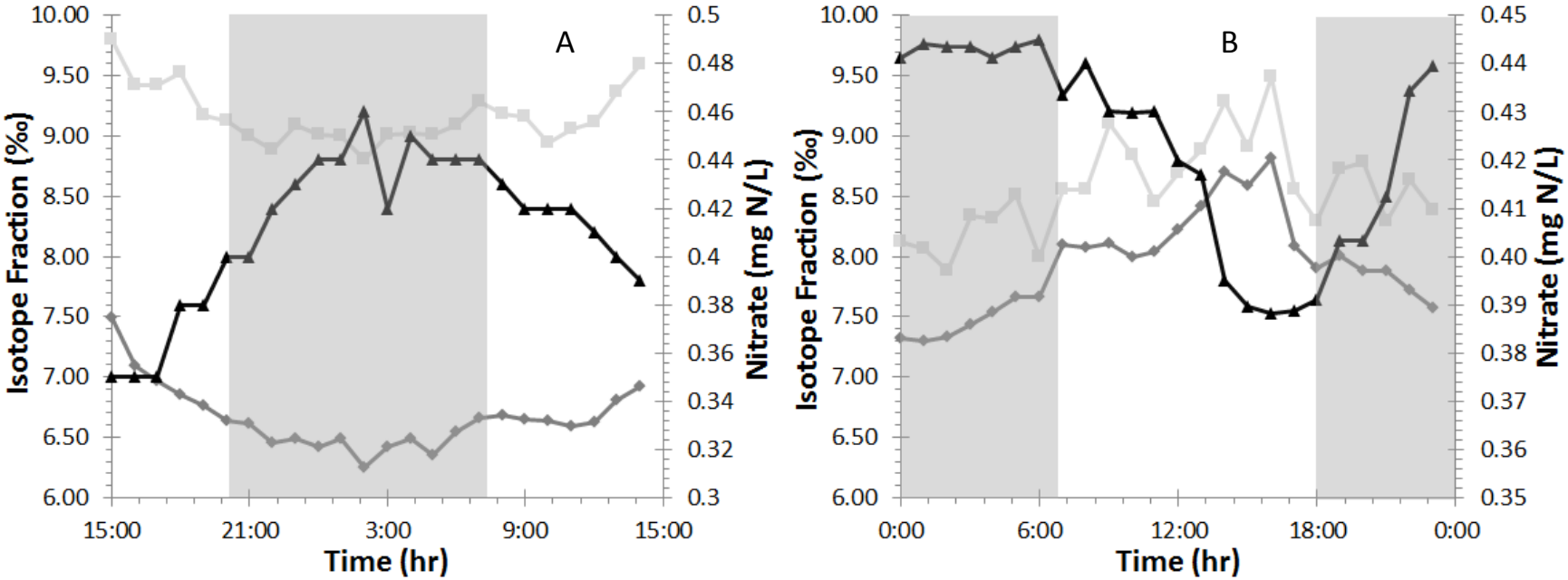

Fig. 5-6. Diel variation in [NO_3] (black line), $\delta^{15}N$ (dark grey line) and $\delta^{18}O$ (light grey line) for a) March and b) November 2009. Shaded areas denote night-time.

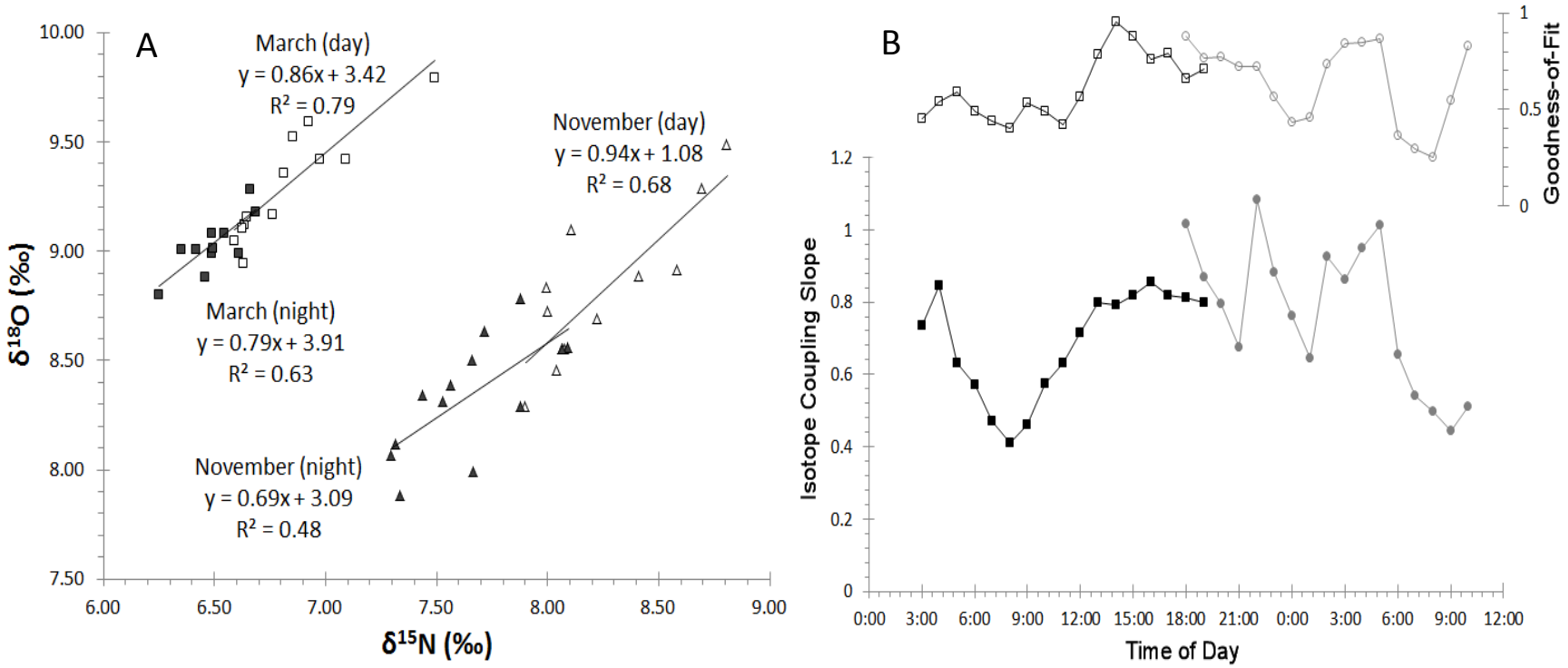

Fig. 5-7. A) Isotope coupling for March and November 2009, partitioned by day and night. Combined slopes are significantly below 1 (p = 0.03) for March, but not November (p = 0.12); slopes were not significantly different between day and night on either date. B) Moving window (8-hour) analysis of isotope coupling and goodness-of-fit for March (circles) and November (squares) 2009.

accompanied by evidence of decoupling (low goodness-of-fit r^2 values) (Fig. 5-7B) during the night-to-day transition. Evidence for strengthened coupling during the day is present in the November data (squares), but not as clearly for the March data (circles). However, because each slope is derived from only 8 measurements, none of the values were significantly different from 1:1.

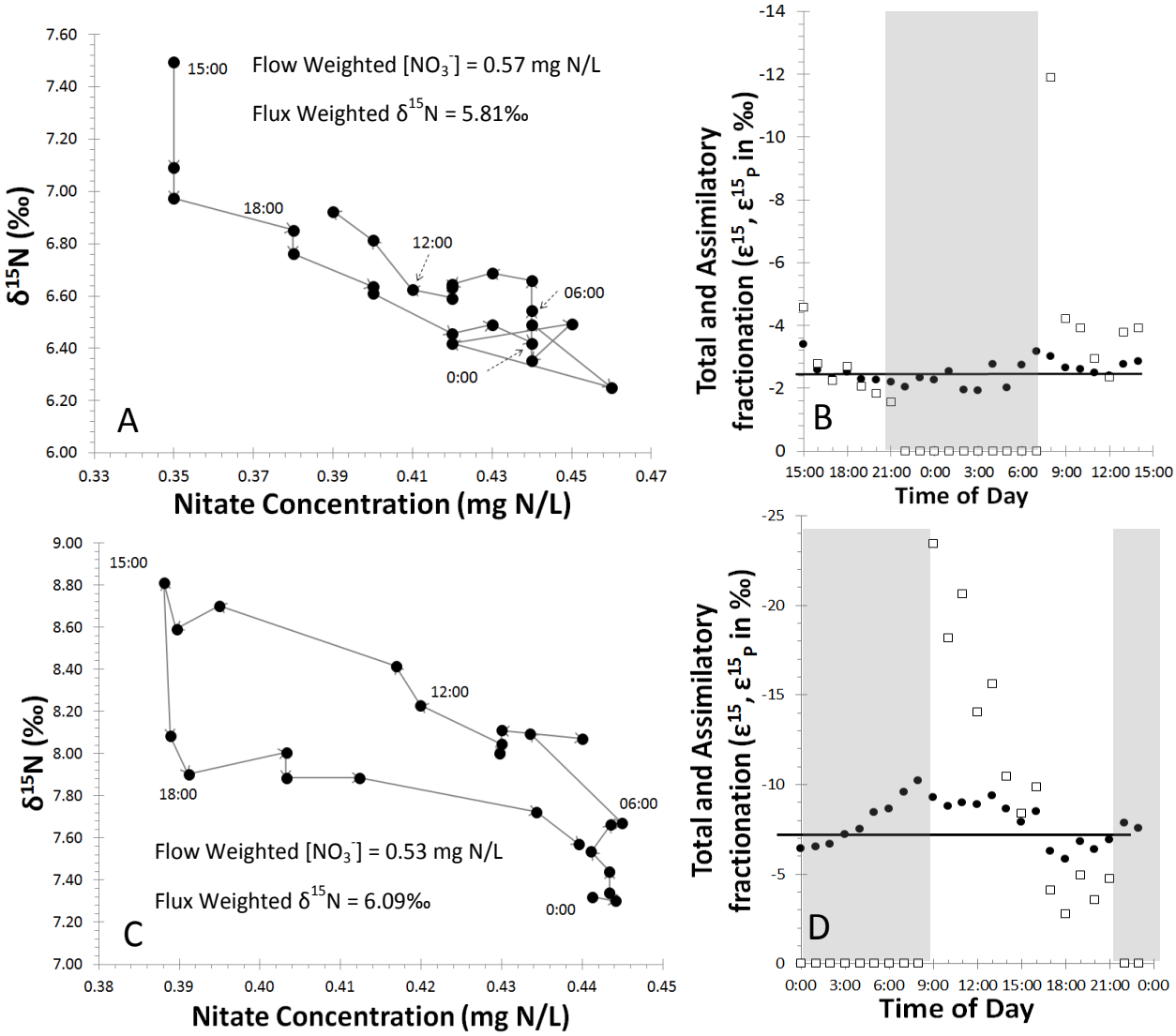

Fig. 5-8. Diel variation in isotope values and [NO_3] (A and C, for March and November 2009, respectively). Springs inputs (flow-weighted [NO_3^-] and flux-weighted $\delta^{15}N$) are shown for each date. Total fractionation (black dots, in B and D, from March and November 2009, respectively) at night (grey areas) was used to estimate denitrification fractionation (horizontal black lines). Assuming constant denitrification fractionation implies significant variation in assimilatory fractionation (white squares) that drops over the course of the day.

A negative temporal correlation between [NO_3] and isotope composition was significant in both March ($\delta^{15}N = 9.2 – 6.2*[NO_3]$; $r^2 = 0.76$; $p < 0.001$) and November ($\delta^{15}N = 13.2 – 12.3*[NO_3]$; $r^2 = 0.36$; $p = 0.002$), with evidence of significant counter clockwise hysteresis (Fig.5-8A and 5-8C). An estimate of total fractionation obtained hourly using a two-point removal curve (between the springs and the downstream observations) indicates low and effectively constant fractionation throughout the day in March 2009 (black circles; Fig. 5-8B), and much higher fractionation with significant diel variation in November 2009 (black circles; Fig. 5-8D); note that instantaneous fractionation factors should be interpreted accounting for the ca. 4-6 hour residence time in the river. Imputing the fractionation due to assimilation based on the assumptions of constant denitrification (i.e., diel variation in concentration is due to temporal variation in assimilation), constant denitrification fractionation, and zero assimilation at night yields highly variable estimates that suggest strong diel variation ranging from -1.8 to -12.1‰ in March 2009 (white squares, Fig. 5-8B) and from -2.7 to -24‰ in Nov. 2009 (white squares, Fig. 5-8D).

Discussion

Consistent boundary inputs (flow, chemistry, temperature), high levels of primary production, and well constrained nutrient and water mass balance make the Ichetucknee River a useful model system for investigating longitudinal and diel nitrate isotope dynamics. Other rivers where longitudinal dual isotope measurements have been obtained (Battaglin et al. 2001, Ruehl et al. 2007, Pellerin et al. 2009, Deutsch et al. 2009, Miyajima et al. 2009, Chen et al. 2009) are generally subject to greater variation in sources and internal processes due to weather and management (e.g., dam releases, irrigation return flows) making inferences more complex. In addition to modest variation in source chemistry, total discharge and the relative contribution from each spring, estimates from this study of N removal mechanisms (i.e., between assimilation, ca. 20% of removal, and denitrification, the remaining 80%) align with previously published estimates (Heffernan et al. 2010a), suggesting that internal variation in the relative importance of total N removal pathways is exceedingly low. We note, however, that the magnitude of daytime total N removal varied substantially (0.58 to 1.11 g N /m2 /d, or 27 – 35% of N inputs) over the study period.

Isotopic fractionation was observed for all sampling events (5 day, 2 night) along a longitudinal transect, regardless of time of day or season. Controls on longitudinal fractionation are different than has been observed in other rivers. We observed a modest range in total enrichment factors ($^{15}\varepsilon$ from -1.9 to -

5.8‰), which was significantly correlated with hydrologic drivers (e.g., total flow and longitudinal river losses; Fig. 5-6C), flow-weighted input nitrate concentrations (Fig. 5-6B) and total N removal (Fig. 5-6D). Other studies (de Brabandere et al. 2007, Ruehl et al. 2007, Chen et al. 2009) have observed temporal variation in riverine fractionation, either in response to hydrologic control or season. However, our findings generally run counter to the expectations that: a) increasing discharge would be associated with an increase in enrichment factors due to greater contact with reactive riparian sediments and/or increased hyporheic exchange as well as increased nitrate availability, and; b) that higher N concentrations would be associated with increased fractionation due to greater N availability (implying, contrary to Heffernan and Cohen, 2010, that denitrification is N limited). Both flow and the flow-weighted input [NO_3] were negatively associated with fractionation, though we contend that the modest range of input concentrations as well as the extremely strong association ($r = +0.96$, $p < 0.01$) of input concentrations with discharge, likely make the latter correlation spurious. The range of discharge conditions sampled was small (< 15% of the mean), suggesting that additional sampling under other flow conditions may be warranted. However, because these systems are characterized by low input variation at annual and even decadal scales, we predict that these relationships are robust. Heffernan et al. (2010a) report a significant positive covariance between N removal and discharge from an analysis of archival data, a finding confirmed here ($r = +0.96$, $p = 0.007$).

The most likely explanation for the observed patterns of fractionation, and the generally low levels of fractionation overall, is that the dominant removal process (i.e., denitrification) is controlled by benthic diffusion rates. Sebilo et al. (2003) showed that riparian denitrification exhibited high rates of fractionation ($^{15}\varepsilon$ = -18‰), consistent with observations from the groundwater literature (e.g., Bottcher et al. 1990, Aravena and Robertson 1998, Fukada et al. 2003) and laboratory culture (Granger et al. 2008), because of well mixed conditions that preclude nitrate limitation of the process. In contrast, fractionation in riverine sediments, where nitrate enters primarily via diffusion exhibited much lower fractionation rates ($^{15}\varepsilon$ = -4‰) (Sebilo et al. 2003); similarly, low fractionation has been observed in wetland settings where advective nitrate delivery is limited (Lund et al. 2000, Søvik and Mørkved 2008).

In the Ichetucknee River, where sediment hydraulic conductivity is low (< 5 m/d; Hensley 2010) and hydraulic gradients weak, hyporheic water exchange is limited and nitrate delivery to the anaerobic sediments is likely to be dominated by diffusion. If diffusion is the rate limiting step for N removal, fractionation would be small, and would presumably respond to the direction of the hydraulic gradient. During periods of high discharge, which in this river occurs in response to elevated groundwater

elevations, not surface drainage, the hydraulic gradient is more strongly towards the river (i.e., gaining conditions), which would in turn limit diffusion into the sediments and lower fractionation, as observed (Fig. 5-5C); we note that conditions in other rivers would likely be reversed, where periods of high discharge correspond with hydraulic gradients out of the river because river flows respond to precipitation more rapidly than do groundwater levels. Note also that isotope fractionation is significantly associated with the percentage of water loss along the lower part of the study reach, with greater enrichment occurring when the river is either in hydrologic steady state (i.e., flow is conserved) or slightly gaining (Fig. 5-5C). Low enrichment occurs when there is longitudinal water loss, a condition under which water may be advected into the hyporheic zone, but then lost from the system.

Further evidence supporting the control of hydraulic gradients on fractionation is the observation that longitudinal isotope enrichment and N removal are not spatially coincident; we observed nitrate removal primarily in the upper river (black dots vs. black lines; Fig. 5-2), concordant with previous observations (Heffernan et al. 2010a), a pattern that was at least qualitatively similar to longitudinal isotope patterns. The upper river, to station #6, is generally gaining, with major spring inputs laterally, which means isotope fractionation can act on the river nitrate pool and result in a classical Rayleigh distillation signal. The lower river becomes losing under most flow regimes implying hydraulic gradient that advects water into the hyporheic sediments, which may be more conducive to fractionation. At the same time, however, that water may be lost to the groundwater, which results in a potentially reduced impact on the river water residual nitrate pool. Further sampling of sediment porewater would be needed to discern whether this is in fact the case.

The proposed mechanism of diffusion limitation of fractionation would also be consistent with a negative association between fractionation and total N removal; as conditions become more favorable for denitrification (i.e., more available carbon as substrate; Heffernan and Cohen 2010), that process proceeds to completion at those sites where the combination of conditions (i.e., low redox, bioavailable organic carbon and consistent nitrate delivery) are met, minimizing fractionation. We are unable to explain the strong association between flow-weighted input concentrations and fractionation (Fig. 5-5B) on the basis of this mechanism, however, reinforcing our contention above that this may be a spurious association. With only 5 data points and little natural variation, the causal significance of any observed association is difficult to discern robustly.

An alternative explanation for the strong discharge-enrichment factor association is that the contribution of diffuse inputs as a fraction of discharge is a function of discharge. De Montety et al.

(2011) report that the chloride budget for the Ichetucknee cannot close without invoking a diffuse lateral contribution of ca. 1.3 m^3/s of water that is chemically similar to Mill Pond (the most downstream spring discharging between stations #5 and #6; Fig. 5-2). Notably, this water is also generally enriched in ^{15}N and ^{18}O; if, during periods of low flow, this unaccounted for source is of increased significance as a fraction of flow, the longitudinal pattern in isotope values would appear similar to fractionation. With the data obtained here, we cannot reject this outright, but we note two aspects of the longitudinal isotope data that do limit the likelihood of this scenario. First, the chemical characteristics of the springs are relatively constant and spatially discrete (i.e., each spring has a unique chemistry) at annual and even decadal time scales, implying that the additional water similar to Mill Pond would be discharged in approximately the same location. There is no evidence from the longitudinal profiles of a consistent isotopic discontinuity that would support a relatively discrete and large unaccounted for source of water, particularly during the latter three transects when the $\delta^{15}N$ values for Mill Pond were extremely high; we note that in March 2009, and November 2009 there is evidence of a spike in ^{15}N near Mill Pond, but enrichment factors estimated without those points are identical to those with them. Second, the fractional contribution of Mill Pond, discharge of which would presumably co-vary with the unaccounted for source of water, is constant (ca. 8.3%) and unassociated with total discharge or flow-weighted input [NO_3]. We conclude that even if this unaccounted for source of water is present, its effect on spatial and temporal patterns of isotopic composition are minimal.

Variation in fractionation between day and night ran contrary to our expectations. We expected stronger fractionation due to denitrification, and thus a decrease in total fractionation during the day, when N is removed by the combination of assimilation and denitrification. Instead, we observed greater daytime fractionation, implying that fractionation due to assimilation is higher than denitrification. While diffusion-limited denitrification can explain low denitrification fractionation, the magnitude of the daytime isotopic enrichment over nighttime levels indicates assimilatory fractionation in excess of -6‰. This value is substantially larger than previous studies in a similar spring-fed river (de Brabandere et al. 2007) where modest plant fractionation (ca. -2 to -3‰) was inferred based on differences between water column nitrate and plant tissue N isotope ratios. Observed fractionation is also at the high end of the range observed for marine phytoplankton (-2.2 to -6.2‰; Needoba et al. 2003) and benthic algae in springs (-1 to -6‰; Albertin et al. *in press*). Further experimental work to constrain the timing and magnitude of plant N assimilation and fractionation is clearly needed, particularly for macrophytes that dominate production in these systems (Odum 1957, Duarte and Canfield 1990).

The observation that diel isotope variation was slightly higher on and after a highly productive (i.e., sunny) day (ca. 1.7‰, Fig. 5-6B), than on and after a highly overcast day earlier in the year (ca. 0.7‰; Fig. 5-6A) may be linked to a previous inference (Heffernan and Cohen 2010) of strong day-to-day coupling between primary production and denitrification. In short, increased availability of labile organic carbon following days with high GPP may cause greater oxygen reduction in the sediments, thereby enhancing denitrification (i.e., by reducing the depth to which nitrate must diffuse to encounter suitable redox conditions). Increasing the duration of hourly isotopic measurements to span multiple days with varying GPP would help confirm this; the experimental set-up of Sebilo et al. (2003) to evaluate diffusive vs. advective environments modified to include substrate additions would help refine this inference. We note, however, that nitrogen removal (3.7 vs. 5.4 kg N/hr) and diel nitrate variation (0.05 vs. 0.11 mg/L) were actually both larger on the cloudy day; we previously observed similar seasonal dynamics of N removal (spring > fall) in the Ichetucknee (Heffernan et al. 2010).

We observed 1:1 dual isotope coupling in both longitudinal and diel sampling, which is inconsistent with the 1:2 coupling expected for a system where N removal is dominated by denitrification (Lehmann et al. 2003). The basis for the expected association between $\delta^{15}N$ and $\delta^{18}O$ is primarily the groundwater literature (Bottcher et al. 1990, Aravena and Robertson 1998) as well as theoretical modeling studies (Lehmann et al. 2003); however, several river studies (Battaglin et al. 2000, Ruehl et al. 2007, Chen et al. 2009) have reported evidence of 1:2 isotope coupling due to denitrification. In contrast, however, laboratory measurements of denitrification by respiratory denitrifiers support 1:1 coupling under both fresh and sea-water conditions (Granger et al. 2008). Deutsch et al. (2009) observed 1:1 coupling in the Elbe River, but interpreted this to indicate dominance of N removal by assimilation. Our data, combined with the laboratory culture findings of Granger et al. (2008) suggest that process inference from the slope of the isotope coupling line may be confounded, though the reasons remain unclear. One possible explanation for the observed differences in slope is that dual isotope fractionation under advective conditions occurs differently than under diffusive conditions. As discussed above, fractionation is reduced substantially when nitrate is supplied to denitrifiers via diffusion (Sebilo et al. 2003), but the effects of diffusion limitation on $\delta^{18}O$ fractionation remains unknown. The Ichetucknee River, by virtue of low hydraulic gradients and the absence of episodic scouring events, has a anomalously large accumulation of fine benthic sediments, which may create hydraulic conditions where diffusion is unusually important to sediment nitrogen dynamics. One consequence may be isotopic coupling dominated by diffusion fractionation, whereas in coarser grained or higher gradient systems, advection

controls solute delivery to anoxic sediments resulting in isotope coupling dominated by denitrification fractionation.

Diel variation in isotope coupling reveals a more complex story. Systematic diel variation in dual nitrate isotope fractions has not, to our knowledge, previously been described, though studies in other rivers have observed large though largely unpatterned variation (Pellerin et al. 2009). Aggregated measurements partitioned by day and night, defined by sunrise and sunset on each day, suggest that 1:1 coupling is ubiquitous. Modest departures from 1:1 slopes at night were not-significant, but an 8-hour moving window analysis revealed a short period in the early morning for both 24-hour sampling events when the slope dropped considerably. Notably, however, this occurred at the same time as strong declines in goodness of fit (r^2), meaning that none of the slopes could statistically be distinguished from 1:1. In this river system, decoupling cannot plausibly be explained as a change in source because of the extremely stable input chemistry and absence of additional tributaries. One potential explanation may be that the early morning period is naturally one of reduced isotope variation, and the signal of decoupling (i.e., reduced goodness of fit) is due to the increased importance of measurement error. We note the autocorrelation appears stronger for $\delta^{15}N$ than for $\delta^{18}O$ (Fig. 5-7), in line with observed analytical precision (0.2 and 0.6‰ for $\delta^{15}N$ and $\delta^{18}O$, respectively).

Nitrification is another mechanism that could induce dual nitrate isotope decoupling because oxygen and nitrogen are derived from different sources (Sebilo et al. 2006, Wankel et al. 2007). The ^{15}N of nitrification-derived nitrate originates in ammonium, with modest fractionation, but the ^{18}O comes from either dissolved oxygen ($\delta^{18}O$ ranging from -24‰ to -12‰ with diel variation in primary production) or water ($\delta^{18}O$ between -4 and 0‰) ($1/3^{rd}$ and $2/3^{rds}$, respectively; Mayer et al. 2007); Sebilo et al. (2006) report $\delta^{18}O_{NO3}$ after nitrification of approximately 3‰. In the Ichetucknee, where ammonium accumulation in the water column is negligible (Heffernan et al. 2010a) and net assimilation is assumed slightly positive (i.e., uptake > remineralization) because of longitudinal accumulation of particulate OM, the isotopic effect of nitrification on ^{15}N of nitrate is likely neutral because the process proceeds to completion. Ambient values of $\delta^{18}O_{NO3}$ remain between 8 and 10‰ in the Ichetucknee at all times (Fig. 5-6), suggesting that systematic lightening of $\delta^{18}O_{NO3}$ is not occurring. Moreover, nitrification is expected to be enhanced during the day when pH, DO and temperature are high (Warwick 1986), but the observed decoupling occurs when these parameters are consistently at their lowest values (Fig. 5-7B).

Despite strong evidence of diel variation in isotope ratios for both ^{15}N and ^{18}O that is approximately out of phase with diel nitrate variation (Fig. 5-6), fractionation exhibited diel variation only in one case (November 2009; Fig. 5-8D). Moreover, the direction of diel fractionation was opposite our expectations, suggesting autotrophic fractionation greater than denitrification. Total fractionation has been used to back-calculate assimilatory fractionation based on the assumption that fractionation due to denitrification is constant (Dhondt et al. 2003). Our findings challenge the assumption of diurnally constant denitrification rates and fractionation for the Ichetucknee River system. As discussed above, literature evidence suggests assimilatory fractionation is generally small, and we know of no studies that report significant diel variation in that fractionation. However, the assumption of constant denitrification requires invoking enormous daytime variation in plant fractionation, ranging monotonically from highly discriminating in early morning (-12 and -25‰ in March and November 2009, respectively) to weakly discriminating in late afternoon (-2 and -4‰) (Fig. 5-8B and 5-8D).

If we reject the implied magnitude and variation in assimilatory fractionation as implausible, then the remaining explanation for the observed diel variation in isotope values is that the magnitude of and/or fractionation due to denitrification is not a constant. Above, we reasoned that denitrification is diffusion limited, and during the day DO produced in the water column will also diffuse into the benthic sediments, increasing the effective depth to which nitrate must diffuse to reach favorable redox conditions for denitrification. As such, we might expect both a quantitative reduction in denitrification rates during the day, as well as qualitative changes with increased diffusion limitation during the day, which would presumably act in the direction of reducing fractionation. One implication is that our inference of N assimilation, based on the assumption that plant uptake is the source of diel variation, is an underestimate.

One of the most intriguing observations in this work is diel hysteresis in the relationship between nitrate removal (concentration) and isotope ratios ($\delta^{15}N_{NO3}$). The hysteresis occurs counter-clockwise (i.e., nitrate changes lagging isotopic changes), with evidence, particularly from the November 2009 sampling (Fig. 5-8C), of 4 diel stages: 1) early morning increases in $\delta^{15}N_{NO3}$without a commensurate change in nitrate removal, 2) a rapid decline in nitrate through mid-day with modest isotopic effects, 3) a late afternoon decline in $\delta^{15}N_{NO3}$, again without a change in nitrate, and 4) an nighttime increase in nitrate concentration without an isotopic effect. While the evidence for this pattern is weaker in the March 2009 sampling (Fig. 5-8A), the timing and topology of the pattern is still evident. There are several explanations that can be invoked. The first is that fractionation due to assimilatory removal, which

drives diel nitrate variation, is highly variable, as discussed above; the magnitude of that variation is depicted in Figs. 5-8B and 5-8D. We tentatively reject that possibility, based mostly on the unprecedented magnitude of the diel variation in fractionation that would be implied. Another plausible explanation is that diel variation in fractionation due to denitrification is much larger than assumed. We note that during phase 1 (pre-dawn to early morning), the nitrate concentration remains constant, but fractionation increases (i.e., isotope values are generally increasing). This is consistent with diffusion limited denitrification because during this period reduced DO concentrations in the water column limit the depth to which nitrate must diffuse to reach favorable redox conditions. Likewise, during phase 3 (late afternoon to early evening), nitrate concentrations vary little, but fractionation decreases, consistent with greater diffusion limitation in response to increased water column DO concentrations (peak at ca. 3:00 p.m.). Further testing in both controlled conditions and in other rivers is needed to determine if diffusion control is responsible for this phenomenon and whether that effect is general to rivers with low hydraulic conductivity sediments.

Overall, our results suggest dual nitrate isotope measurements cannot readily deconvolve assimilatory and dissimilatory removal pathways in the Ichetucknee, at least based on the two expected lines of evidence. Isotope coupling consistently follows 1:1 during both day and night, meaning that expected diel variation in coupling was not useful for partitioning processes. Similarly, differences in fractionation rates between uptake and denitrification, which were expected to be large, were not observed. We attributed deviation from both expectations to how denitrification occurs in this system, specifically that diffusion limitation and oxygen inhibition may be important regulators of isotopic fractionation. The generality of this potential control on environmental isotope dynamics, the observed discharge quantity and quality controls on whole-ecosystem fractionation, and the inference of diel hysteresis and implications for non-constant dissimilatory N removal are findings that merit further scrutiny in these and other rivers.

Research Element #6 – Floridan Aquifer Denitrification Estimates

(with Dr. Brian Katz, USGS – Tallahassee)

Abstract

Aquifer denitrification is a potentially large and poorly constrained component of regional and global nitrogen (N) budgets (Seitzinger et al. 2006), and can confound N source inference based on isotopic signatures (Kendall and Elliott 2007). Using dual noble gas tracers (Ne, Ar) to generate physical predictions of N_2 gas concentrations for 112 observations from 61 Upper Floridan Aquifer (UFA) springs, we show that excess N_2 is highly variable in space and inversely correlated with dissolved oxygen (O_2). Negative relationship between O_2 and $\delta^{15}N_{NO3}$ across a larger dataset of 113 springs, well-constrained isotopic fractionation coefficients, and strong ^{15}N:^{18}O isotope coupling further support inferences of denitrification in this uniquely organic-matter-poor system. Despite relatively low average rates, denitrification accounted for 32% of estimated aquifer N inputs across all sampled UFA springs. Back-calculations of source $\delta^{15}N_{NO3}$ based on denitrification progression suggest that isotopically-enriched nitrate (NO_3^-) in many springs of the UFA reflects groundwater denitrification rather than urban- or animal-derived inputs.

Introduction

Anthropogenic increases in reactive nitrogen (N) availability have wide-ranging consequences including eutrophication of aquatic systems. Denitrification, which reduces NO_3^- to N_2 gas, mitigates this enrichment by returning N to long-residence-time atmospheric pools, and is an important component of the nitrogen cycle at local, regional, and global scales. Although once thought to occur only via the oxidation of simple organic compounds, NO_3^- reduction can involve multiple electron donors and end products (Burgin and Hamilton 2007). Patchy and ephemeral distribution, diverse reaction modes, and challenges of direct measurement of N_2 all contribute to persistent high uncertainty in local, regional, and global estimates of denitrification, particularly in groundwaters (Davidson and Seitzinger 2006).

Existing studies of aquifer denitrification are limited in number and in spatial and temporal coverage, and are potentially biased by preferential study of aquifers with high rates of denitrification, and by frequent measurement as NO_3^- loss rather than N_2 production (Green et al. 2008). Studies that do measure N_2 directly typically rely on assumed values of either recharge temperature or excess air entrainment to estimate biologically-derived N_2. The relatively limited number of directly-measured aquifer denitrification rates nonetheless span several orders of magnitude, and associated reductions in NO_3^- range from negligible to complete (Green et al. 2008). The extent to which these outcomes vary in space and time within individual aquifers is poorly understood.

Besides mitigating downstream N fluxes, groundwater denitrification alters the isotopic composition of residual NO_3^- pools, with potential consequences for inference of N sources. Despite pleas for caution (Kendall and Elliott 2007), observed $\delta^{15}N_{NO3}$ are commonly used to infer N sources and guide management and policy related to point and non-point inputs (Fogg et al. 1998, USGS 2003, Harrington et al. 2010). Dual isotopic tracers ($\delta^{15}N_{NO3}$ and $\delta^{18}O_{NO3}$) of NO_3^- allow inference of processes and greater separation of confounded sources, and have recently been used to suggest denitrification in the UFA and other karst aquifers (Albertin et al. in press, Panno et al. 2006); however, this approach does not provide estimates of denitrification rates. While the potential effect of denitrification on isotope signatures is widely acknowledged, no studies to date have quantified its influence on source inference at the scale of a regional aquifer.

The karstic Upper Floridan Aquifer (UFA) supports the highest density of large natural artesian springs in the world (Fig. 6-1), and is a major regional and global economic resource. Throughout parts of northern Florida, the UFA is confined by low-permeability, high-clay deposits that preclude infiltration except via sinkholes; these confining layers are largely absent in the central-western portion of the state. Springs are concentrated along drainage features, especially near boundaries of confining layers.

Land use throughout the study region includes variable mixtures of row crop agriculture, urban and suburban development, and secondary forest.

Geochemistry of the UFA can be characterized as a mixture of two end members. Older water, characteristic of matrix porosity and deep flowpaths, is generally anoxic, low in NO_3^-, and enriched in minerals. Younger water characteristic of conduits and shallower flowpaths is generally oxic, enriched in NO_3^-, and sometimes subsaturated in mineral chemistry (Toth and Katz 2006). The contribution of these water sources can vary considerably among springs and over time as changes in flow drive exchange between primary and secondary porosity (including large conduits) (Martin and Dean 2001, Heffernan et al. 2010a, Heffernan et al. 2010b). Dissolved organic carbon (DOC) levels in UFA are among the lowest measured globally (Duarte et al. 2010). In conjunction with oxic conditions of many springs, low DOC undoubtedly contributes to the prevailing assumption that denitrification is negligible in this system (Katz 2004). However, denitrification in other aquifers depends on matrix-derived alternative electron donors (e.g., Fe^{2+}, H_2S) (Green et al. 2008, Schwientik et al. 2008, Torrento et al. 2010); thus concentrations of dissolved electron donors may be a poor indicator of denitrification rates.

NO_3^- concentrations in Florida springs have risen dramatically over the past half-century, and springs discharge accounts for a large proportion of the N load to estuarine and coastal waters (Pittman et al. 1997). Despite the perceived vulnerability of the UFA to nutrient enrichment, significant imbalances between inputs to North Florida landscapes and riverine export remain poorly understood (Katz et al. 2009). Landscape-scale mass balance generally suggests inorganic fertilizer as the primary source of N enrichment (Katz et al. 2009), but isotopic studies (that assumed negligible denitrification) have indicated a greater role of organic N from animal or human wastewater (Katz et al. 2001).

Our objectives are to determine the magnitude of denitrification in the Floridan Aquifer and its spatial and temporal variation; and to estimate the effect of fractionation by denitrification on $\delta^{15}N_{NO3}$ and thus apparent sources of N inputs to the UFA in Northern and Central Florida. Artesian springs (of the UFA and elsewhere) alleviate spatiotemporal limitations by integrating heterogeneity and facilitating estimates of N_2 fluxes at broad spatial scales. We collected dissolved gas and isotopic data from 33 springs of the Floridan Aquifer, and assembled more than 200 previously reported measurements from 70 additional springs (Figure 6-1). Whereas most direct measurements of aquifer denitrification rely on assumed values of either excess air or recharge temperature, our data include 36 observations of dual noble gas tracers (Ne and Ar), which permits simultaneous, direct estimation of these parameters. Approximately monthly sampling of the springs of the Ichetucknee River was used to evaluate inter-related temporal variation of O_2, and NO_3^- concentration and isotopic composition. This study of an

economically and ecologically-important groundwater system is among the most spatiotemporally- and methodologically-comprehensive assessments of denitrification in any aquifer.

Methods

Sample collection and analysis

Between June and September 2010, we sampled 33 Floridan Aquifer springs that varied in size, surficial hydrogeology, and NO_3^- and O_2 concentrations. At each spring, we measured O_2, temperature, specific conductance, and pH from spring vents using a YSI 556 sonde equipped with an optical or Clark probe. Water samples for laboratory analyses were collected using a peristaltic pump with a 5 m weighted intake tube placed as near as possible to the spring vent. We collected 3 replicate samples for nutrient and isotopic analyses in acid-washed pre-rinsed polyethylene bottles. During the synoptic survey, we collected 5 replicate field samples for dissolved gas analysis by flushing 300 ml BOD bottles 3 times, sealing with glass stopper, and capping with water-filled plastic caps to minimize exchange with atmosphere and to prevent stoppers from becoming dislodged during transport. Dissolved gas samples were stored under ice water until analysis within 36 hours; water samples were frozen until analysis.

We measured dissolved N_2 and Ar using a Membrane Inlet Mass Spectrometer (MIMS) (Kana et al. 1994) within 36 hours of collection, over which period our storage protocol exhibited negligible atmospheric contamination. The membrane inlet mass spectrometer was equipped with a copper reduction column heated to 600 °C to remove O_2 and reduce interference with N_2 measurements (Eyre et al. 2002). Standards for N_2 and Ar concentration consisted of atmosphere-equilibrated deionized water in 1 L spherical vessels incubated and stirred in high-precision water baths (± 0.01 ºC) at their respective temperatures (10, 15, and 20 ºC) for at least 24 hours prior to analysis. Gas concentrations in each standard were calculated using temperature-solubility formulas without salinity correction (Hamme and Emerson 2004). Signal strength for samples and standards was determined as the mean value of the 1st minute following signal stabilization. To account for instrument drift, we ran complete standard curves every 6-8 samples and applied interpolated parameter values from adjacent standard curves (r^2 range: 0.997-1.00; mean r^2 = 0.9997) to estimate gas concentrations in each sample. A fourth standard equilibrated with pure N_2 gas served as an external source QC. Coefficients of variation for field replicates ranged from 0.22-2.27% (mean: 0.80%; median: 0.49%).

We measured nitrate concentrations in samples from the synoptic survey and Ichetucknee River springs times series using second-derivative UV spectroscopy (APHA, AWWA, WEF 2005) using an

Aquamate UV-Vis spectrometer. Isotopic composition of nitrate ($\delta^{15}N_{NO3}$, $\delta^{18}O_{NO3}$) was measured using the bacterial denitrifier method (Casciotti et al. 2002, Sigman et al. 2001) in the Department of Geological Sciences at the University of Florida (2007-2009) or the UC-Riverside Facility for Isotope Ratio Mass Spectrometry (2010).

Previously-collected data both increased spatial coverage and in many cases provided repeated measurements of springs included in our synoptic survey (Fig. 6-1). Measurements of Ne, Ar, N_2, O_2, NO_3^-, and nitrate isotopes ($\delta^{15}N_{NO3}$, $\delta^{18}O_{NO3}$) spanning from 1997 to 2008 were obtained from published

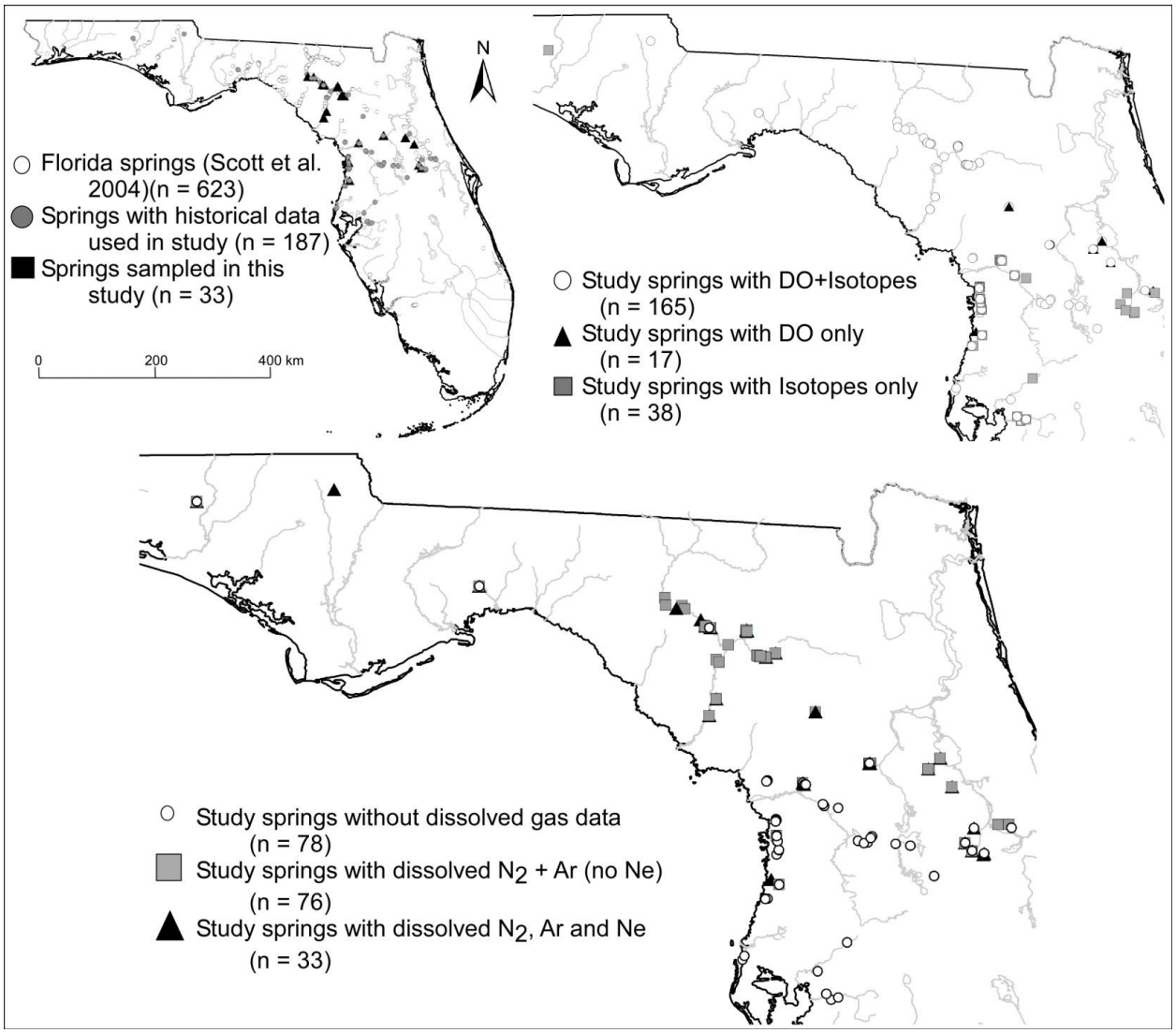

*Figure 6-1. Geographic distribution of Florida springs and observations sets used in this study. Panels illustrate (**a**) distribution of study sites (closed symbols) in comparison to distribution of all named springs, (**b**) distribution of study springs with and without isotopic measurements, and (**c**) distribution of study sites without dissolved gas data, with O_2, Ar, and N_2, and with additional observation of Ne.*

articles (Toth and Katz 2006, Katz 2004, Katz et al. 2001, Katz et al. 2004 and Knowles et al. 2010), state agency reports (Chasar et al. 2005, Katz et al. 1999, Phelps et al. 2006, Phelps 2004), and directly from researchers in cases where data were not reported directly. 36 archival observations (from 31 springs) included Ne in addition to Ar, O_2, and N_2 (and in 23 cases $\delta^{15}N_{NO3}$). In all, we assembled 112 observations of dissolved gas concentrations (O_2, Ar, N_2) from 62 distinct spring vents, of which 58 included both $\delta^{15}N_{NO3}$ and $\delta^{18}O_{NO3}$, and 34 others included $\delta^{15}N_{NO3}$ but not $\delta^{18}O_{NO3}$. Excluding the repeated measurements of the Ichetucknee River springs in 2008-2009, our data included 166 observations of $\delta^{15}N_{NO3}$ and DO and 204 total observations of $\delta^{15}N_{NO3}$. Of the 113 springs represented in the isotope data set, 14 had 4 or more instances of concurrent measurements of both O_2 and $\delta^{15}N_{NO3}$. Observations were drawn from springs in each major drainage in North and Central Florida (Fig. 6-1), and with discharges ranging from <0.01 $m^3 s^{-1}$ to 11 $m^3 s^{-1}$.

All measurements of Ne from prior studies were determined by mass spectrometry at the Lamont-Doherty Earth Observatory Noble Gas Laboratory at Columbia University. NO_3^- was generally measured using the cadmium reduction method (Wood et al. 1967). N_2 and Ar from previously published studies were measured using gas chromatography. Recent (2007 and later) measurements of $\delta^{15}N_{NO3}$ were generally conducted using the bacterial denitrifier method and included $\delta^{18}O_{NO3}$ (Sigman et al. 2001). For data prior to 2007, $\delta^{15}N_{NO3}$ was measured via combustion and mass spectrometry (Kendall and Grim 1990).

Springshed characterization

To determine hydrogeologic predictors of excess air entrainment and recharge temperature, we characterized each spring by latitude, long-term mean discharge, and springshed hydrogeology as measured by aquifer vulnerability to surface contamination (Arthur et al. 2007). We collected discharge records for each spring from online databases of the United States Geological Survey National Water Information System (waterdata.usgs.gov/nwis), Southwest Florida Water Management District (www.swfwmd.state.fl.us/data), and the St. Johns River Water Management District (floridaswater.com/toolsGISdata) where available, since these records were generally the most complete. Where continuous records were unavailable, we used the mean of discrete measurements from published studies and agency reports as our estimate of mean long-term discharge. Since discharge variability of Floridan Aquifer springs is extremely low, use of these more limited data to quantify long-term mean discharge is unlikely to have introduced significant error in subsequent analyses.

Where available, we used previously delineated boundaries (www.dep.state.fl.us/geology/programs/hydrogeology/hydro_resources.htm) to characterize springshed hydrogeology, and to estimate springshed size and location for un-delineated springs. The relationship between discharge and springshed area was determined for those springs with previously delineated springsheds ($A = Q \times 134.9$, where A is springshed area in km^2 and Q is discharge in $m^3 s^{-1}$; n =14, r = +0.79, $p < 0.001$). For springs without a delineated springshed, we estimated the contributing area based on their period-of-record discharge. We assumed each springshed was circular, and estimated the springshed orientation based on the regional drainage network such that the springshed was located with one edge at the spring vent, and the rest up-gradient from the closest river.

We used the Floridan Aquifer Vulnerability Assessment (FAVA) as a metric of springshed hydrogeologic characteristics (Arthur et al. 2007). This measure quantifies the intrinsic contamination risk of the Upper Florida Aquifer (UFA) based on local hydrogeologic conditions. Point observations of aquifer properties diagnostic of rapid recharge rates (e.g., nutrient and major element chemistry, high O_2 concentrations) comprise a data set (n = 148) on which aquifer risk was trained using a weights-of-evidence approach based on a variety of spatially extensive data layers. These included surface soil permeability, surface elevation, subsurface stratigraphy, presence of karst features (e.g., sinkholes) at the surface, thickness of the intermediate aquifer system that regulates hydraulic confinement of the UFA, and the potentiometric head difference between the surface and UFA interpolated from a regional well network. Posterior contamination probabilities were classified as “less vulnerable”, “vulnerable” and “most vulnerable”. None of the springsheds in this study contained more than 3% of their area in the less vulnerable category, so we used the fraction of each springshed area delineated as most vulnerable, typically more than 75% of the area, as a predictor in our model of excess air entrainment.

Estimation of excess air, recharge temperature, and excess N_2

We used Ne and Ar concentrations to determine recharge temperature (T_{rec}) and excess air (A_{ex}) in the subset (n = 36) of springs for which measurements of both gases were available. We estimated these parameters for each observation by simultaneously solving the following equations for those parameters using the Solver function in Microsoft Excel:

$$\mathrm{Ne}]_{obs} = k_{\mathrm{Ne}} \cdot \ \mathrm{Ne}]_{Trec} + A_{\mathrm{ex}} \cdot P_{\mathrm{Ne}} \quad (1)$$

$$\mathrm{Ar}]_{obs} = k_{\mathrm{Ar}} \cdot \ \mathrm{Ar}]_{Trec} + A_{\mathrm{ex}} \cdot P_{\mathrm{Ar}} \quad (2)$$

where k_{Ne} and k_{Ar} are coefficients for unit conversion of Ne and Ar from nmol kg^{-1} (for Ne, k = 0.02) or µmol kg^{-1} (for Ar, k = 0.04; for N_2, k = 0.028) to mg/L; P_{Ne} and P_{Ar} are the mass proportion of Ne

($1.818 \bullet 10^{-5}$) and Ar ($9.34 \bullet 10^{-3}$) in the atmosphere; and $[Ne]_{Trec}$ and $[Ar]_{Trec}$ are the concentrations of those gases at the recharge temperature as determined by:

$$\ln([\mathrm{Ne}]_{Trec}) = \mathrm{A}_0 + \mathrm{A}_1\mathrm{T}_\mathrm{S} + \mathrm{A}_2\mathrm{T}_\mathrm{S}^2 + \mathrm{A}_3\mathrm{T}_\mathrm{S}^3 \quad (3)$$

$$\ln([\mathrm{Ar}]_{Trec}) = \mathrm{A}_0 + \mathrm{A}_1\mathrm{T}_\mathrm{S} + \mathrm{A}_2\mathrm{T}_\mathrm{S}^2 + \mathrm{A}_3\mathrm{T}_\mathrm{S}^3 \quad (4)$$

where T_S is determined as:

$$\mathrm{T}_\mathrm{S} = \ln\left(\frac{298.15 - T_{rec}}{273.15 + T_{rec}}\right) \quad (5)$$

and A_0-A_3 are compound specific solubility constants (Table 6-3).

Among this set of springs with Ne data, estimated T_{rec} ranged from 15-22ºC, was overwhelmingly determined by Ar rather than Ne (Fig. 6-2 **a,b**), and varied significantly as a function of latitude (Fig. 6-2**c**). The observed latitudinal variation in T_{rec} is much greater than variation in mean annual air temperature, and likely reflects regional variation in timing of precipitation and infiltration.

A_{ex} ranged from 1.0-2.7 ml/L and was overwhelmingly determined by Ne rather than Ar (Fig. 6-2**a,b**). Based on multiple regression analysis, mean discharge over the period of record (Q_{POR}) and springshed vulnerability were strong predictors of excess air (Fig. 6-2**d**). Palm springs, whose springshed had no land in the 'most vulnerable' category and was the only value less than 50%, was excluded from this analysis. We used this statistical relationship to estimate A_{ex} in springs for which Ne data were not available, then solved for recharge temperature in those springs using Eq. 1.

We used estimates of T_{rec} and A_{ex}, whether direct or modeled statistically, to determine N_2 concentrations that would be observed based only on those physical processes ($[N_2]_{phys}$), without any biological N_2 production. Specifically, we calculated expected N_2 concentrations using the same temperature-solubility relations described in Eq. 1 through 5, but parameterized for N_2:

$$[N_2]_{phys} = k_{\mathrm{N2}} \cdot [N_2]_{Trec} + A_{\mathrm{ex}} \cdot P_{\mathrm{N2}} \quad (6)$$

where k_{N2} is 0.028; P_{N2} is 0.78084 and $[N_2]_{Trec}$ is the concentration of N_2 at recharge temperature as determined by:

$$\ln([N_2]_{Trec}) = \mathrm{A}_0 + \mathrm{A}_1\mathrm{T}_\mathrm{S} + \mathrm{A}_2\mathrm{T}_\mathrm{S}^2 + \mathrm{A}_3\mathrm{T}_\mathrm{S}^3 \quad (7)$$

where T_S is given in Eq. 5 and N_2-specific values for the A_0-A_3 are given in Table 6-1. We estimate the magnitude of denitrification ($[N_2]_{den}$) for each sampling date and time as the difference between observed N_2 concentrations and concentration predicted by physical processes:

$$[N_2]_{den} = [N_2]_{obs} - [N_2]_{phys} \quad (8)$$

To test the hypothesis that $[N_2]_{den}$ reflects the magnitude of denitrification, we used regression analyses to evaluate the relationship between $[N_2]_{den}$ and dissolved O_2. We used both linear and logarithmic

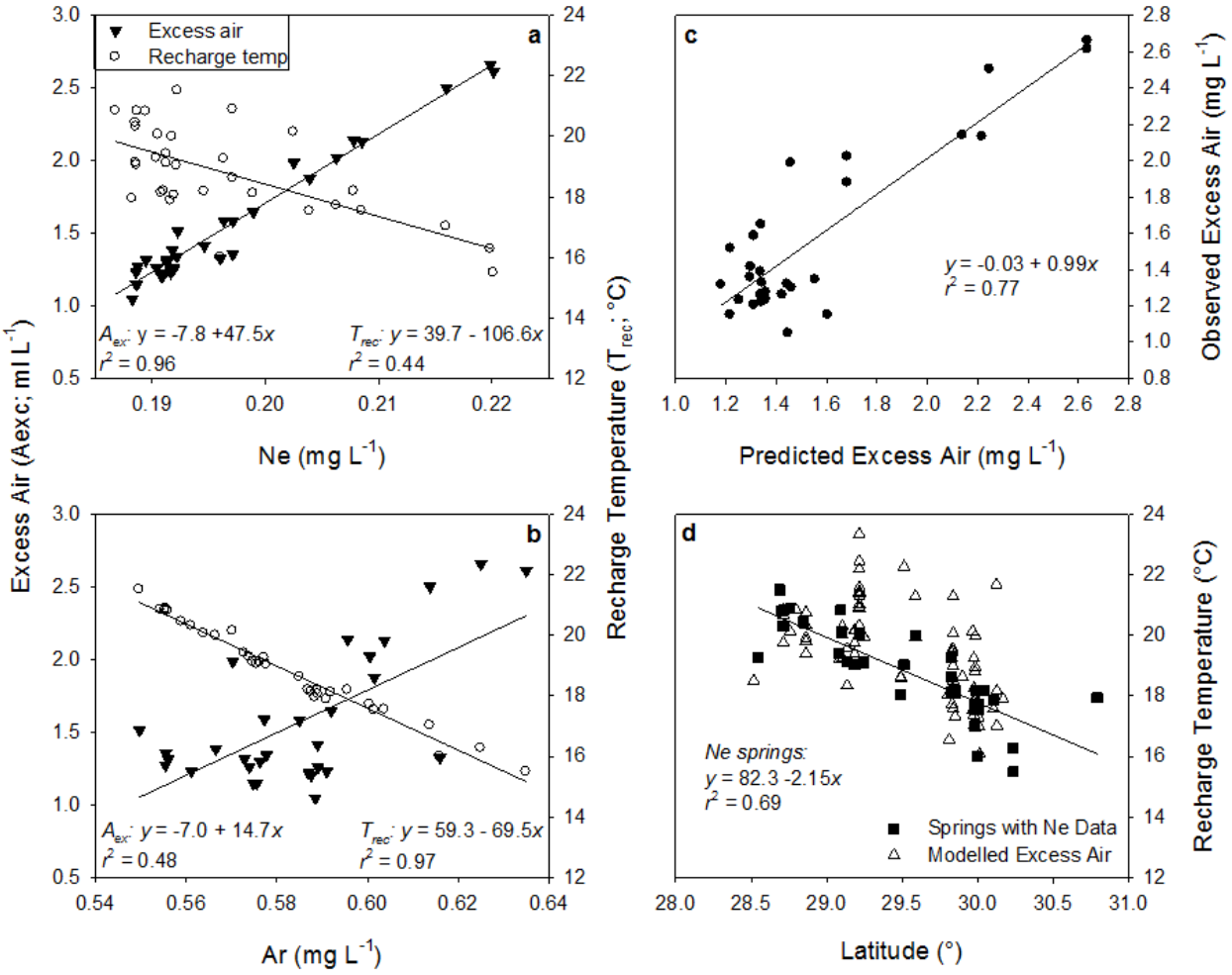

*Fig. 6-2. Geochemical indicators (**a**,**b**) and springshed predictors (**c**,**d**) of excess air (A_{exc}) and recharge temperature (T_{rec}) in Florida springs. (**a**) Ne concentrations are the overwhelming determinant of A_{exc} estimates, and only weakly correlated with T_{rec}; (**b**) Ar concentrations had relatively small influence on A_{exc} estimates, but a high degree of influence over estimates of T_{rec}. These relationships permit statistical determination of excess air and robust estimation of recharge temperature for springs without Ne measurements. (**c**) A_{exc} across springs was best predicted by the combination of aquifer vulnerability (V_{aq}) and spring size as measured by mean historic discharge ($\underline{Q}_{por}$). (**d**) T_{rec} decreased with increasing latitude, a relationship that is clearer among springs for which Ne data allowed simultaneous direct estimation of A_{exc}.*

forms to predict $[N_2]_{den}$ from O_2, for the entire data set and for the subset of observations in which A_{ex} was calculated from Ne data, rather than estimated statistically. We also analyzed the relationship between mean dissolved O_2 and mean $[N_2]_{den}$ from the subset of springs for which 3 or more observations were available.

Table 6-1. Parameter values for determination of solubility-temperature relationships for Ne, Ar, and N_2 gas.

Coefficient	Ne	Ar	N_2
A_0	2.18156	2.79150	6.42931
A_1	1.29108	3.17609	2.92704
A_2	2.12504	4.13116	4.32531
A_3	0	4.90379	4.69149

To evaluate the relative precision and accuracy of $[N_2]_{den}$ estimates based on Ne and statistically modeled excess air, we calculated the mean and standard deviation of $[N_2]_{den}$ estimates for all springs with O_2 greater than 2 mg/L. Bias in estimates would cause divergence of the mean from zero, assuming that denitrification is negligible in these oxic springs (Green et al. 2008, Bohlke 2002).

Denitrification progression and isotopic fractionation

We indirectly evaluated the relationship between denitrification progression and $\delta^{15}N_{NO3}$ via analysis of relationships between dissolved O_2 and $\delta^{15}N_{NO3}$ both within and across springs, reasoning that springs with lower dissolved O_2 would have greater depletion of NO_3^- pools by denitrification than springs with higher O_2. We used both linear and logarithmic regression equations to evaluate dissolved O_2 as a predictor of $\delta^{15}N_{NO3}$ across all observations and excluding observations from the Ichetucknee time series collected between July 2007 and November 2009. Inclusion of the entire Ichetucknee data set had a minimal influence on regression parameters, so only the results from the complete (global) data set are reported here. In addition to this global analysis, we used linear regression to evaluate relationships between dissolved O_2 and $\delta^{15}N_{NO3}$ within springs for which 3 or more observations were available. We then used regression analysis to evaluate how the strength (as measured by the correlation coefficient [*r*]) and slope of these within spring relationships varied as a function of mean dissolved O_2. This analysis allowed us to evaluate whether the patterns observed in the global data set were structured by variation within or among springs.

We directly evaluated the relationship between denitrification progression and isotopic composition of NO_3^- by determining the fractionation coefficient ($^{15}\varepsilon$) for $\delta^{15}N_{NO3}$ from a cross-system analysis that included springs with dissolved gases from both our synoptic survey and previously reported data, and a separate analysis from the Ichetucknee Springs time series (of which most dates did not include dissolved gas measurements). These analyses required estimates of initial NO_3^- concentration ($[NO_3^-]_{init}$) at the time of recharge, which we estimated using different approaches for

springs with dissolved gas data and for the Ichetucknee Springs time series. For analysis of data from the synoptic survey and previous observations that included dissolved gases, we calculated $[NO_3^-]_{init}$ as the sum of $[NO_3^-]_{obs}$ and $[N_2]_{den}$. This estimate would include nitrate derived from nitrification in the vadose zone or UFA as part of $[NO_3^-]_{init}$, and assumes that denitrification is the only sink for NO_3^- (i.e., that assimilation, dissimilatory nitrate reduction to ammonium [DNRA], etc. are negligible) as indicated by concentrations of ammonium and particulate and dissolved organic nitrogen that are typically below detection limits at spring vents. Effects of these processes on $\delta^{15}N_{NO3}$ are also assumed to be zero.

Estimates of $[NO_3^-]_{init}$ allow determination of the progression of denitrification. For each observation, we calculated the proportion of nitrate remaining from the original pool $[NO_3^-]_R$ as:

$$[NO_3^-]_R = \frac{[NO_3^-]_{obs}}{[NO_3^-]_{init}} \quad (5)$$

where $[NO_3^-]_{obs}$ is measured concentration, and $[NO_3^-]_{init}$ is the initial concentration. We used linear regression to determine the isotopic enrichment factor ($^{15}\varepsilon$) for $\delta^{15}N_{NO3}$ (assuming Rayleigh distillation kinetics) as the slope of the relationship between $\delta^{15}N_{NO3}$ and $\ln([NO_3^-]_R)$ (Green et al. 2008, Mariotti 1986, Bohlke et al. 2002). We excluded springs with NO_3^- concentrations below 0.1 mg/L (Juniper, Silver Glen, and Alexander Springs) from this analysis due to the high variability of $[N_2]_{den}$ estimates relative to these lower concentrations.

For the Ichetucknee Springs times series, we calculated $[NO_3^-]_R$ for each spring and sampling date by assuming that $[NO_3^-]_{init}$ for all springs was equal to $[NO_3^-]_{obs}$ in the Ichetucknee Headspring on the same date. The first assumption implicit in this analysis is that denitrification rates in the Ichetucknee Headspring are negligible. High O_2 concentrations (mean ± SD: 4.1 ± 0.2 mg O_2/L), low values of $[N_2]_{den}$ (which averaged 0.32 mg N/L and represented minimal (<30%) depletion of the estimated original nitrate pool), and the low and temporally stable $\delta^{15}N_{NO3}$ (mean ± SD: 3.6±0.3, *n* = 16) observed in the Ichetucknee Headspring all support this assumption. The second implicit assumption, that springsheds of the Ichetucknee springs receive equivalent N loads from sources with identical isotopic signatures, is based on the relative homogeneity of land use in the Ichetucknee springshed, and the predominance of fertilizer application to improved pasture as a source of N to the watershed (Katz et al. 2009). The third assumption, that variation among springs of the Ichetucknee is driven by denitrification, is supported by strong correlations between dissolved O_2 and NO_3^- within and across these systems (Fig. 6-3**a**).

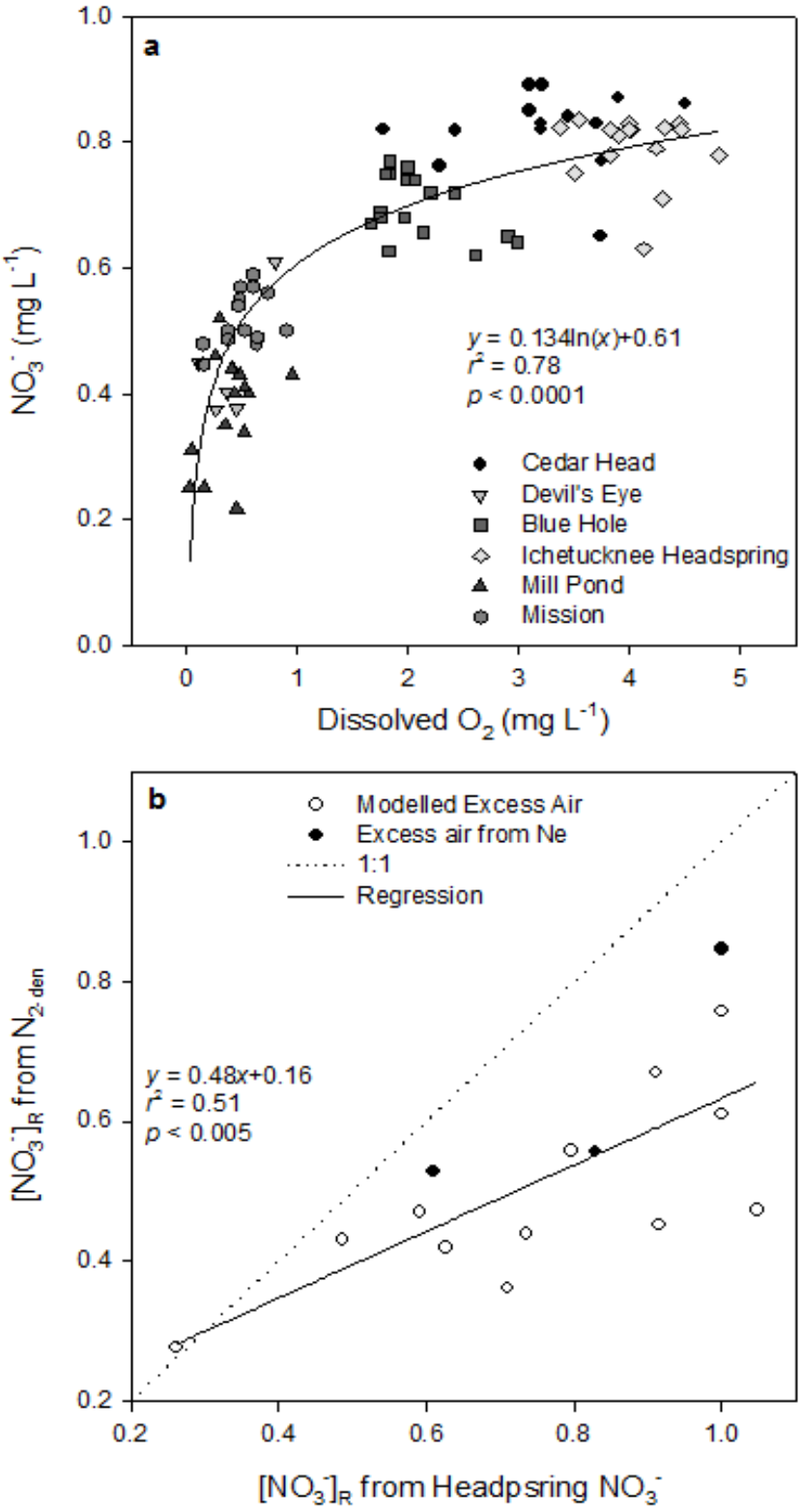

*Fig. 6-3. Denitrification as a driver of nitrate concentration in the springs of the Ichetucknee River as indicated by (**a**) correlations between dissolved O_2 and NO_3^- and (**b**) correlations between estimates of residual nitrate pools $[NO_3^-]_R$ from differences between the Ichetucknee Headspring and from direct measures of denitrification-derived N_2 ($[N_2]_{den}$).*

To further evaluate the latter two assumptions, we used $[NO_3^-]_{init}$ and $[NO_3^-]_R$ values for the springs of the Ichetucknee River on three dates when $[N_2]_{den}$ estimates were available. First, we compared $[NO_3^-]_{init}$ from the Ichetucknee Headspring with the mean value of other springs on the same date. The similarity and covariation of these values (Table 6-2) is consistent with the assumption that all springs in the Ichetucknee System receive similar N loads. In addition, we assessed the correlation between alternative estimates of $[NO_3^-]_R$, namely estimates calculated from $[N_2]_{den}$ and NO_3^- from each spring and those estimated from the differences in NO_3^- concentration between each spring and the Ichetucknee Headspring Fig. 6-3**b**). The relationship between these estimates suggests that the NO_3^- difference approach used in the analysis of the Ichetucknee Springs time series provides a more conservative estimate of the progression of denitrification than those determined using $[N_2]_{den}$, which is to be expected if denitrification has also reduced NO_3^- concentrations to a small degree in the Ichetucknee Headspring. More importantly, the correlation between these estimates is consistent with the assumption that variation in NO_3^- concentration both within and among the springs of the Ichetucknee River is driven at least in part by differences in the progression of denitrification along the flowpaths that contribute to these springs.

Table 6-2. Alternative estimates of initial NO_3^- concentration ($[NO_3^-]_{init}$) and the proportion of $[NO_3^-]_R$ remaining in springs of the Ichetucknee River for dates when direct estimates of denitrification ($[N_2]_{den}$) are available. All values are in mg N/L.

Date	Spring	NO_3^-	$[N_2]_{den}$	$[NO_3^-]_{R\text{-}NO3}$ [a]	$[NO_3^-]_{R\text{-}N2den}$ [b]	$[NO_3^-]_{init}$ [c]	Mean $[NO_3^-]_{init}$ (SD)[d]
10/24/01	Blue Hole	0.68	0.54	0.83	0.56	1.22	
	Mission	0.50	0.45	0.61	0.53	0.95	
	Headspring	0.82	0.15	1.00	0.85	**0.97**	**1.09 (0.2)**
1/30/07	Devil's Eye	0.61	0.78	0.73	0.44	1.39	
	Blue Hole	0.76	0.92	0.92	0.45	1.68	
	Mill Pond	0.52	0.72	0.63	0.42	1.24	
	Mission	0.59	1.04	0.71	0.36	1.63	
	Headspring	0.83	0.53	1.00	0.61	**1.36**	**1.49 (0.21)**
6/9/10	Devil's Eye	0.40	0.53	0.49	0.43	0.93	
	Blue Hole	0.66	0.52	0.80	0.56	1.18	
	Mill Pond	0.22	0.57	0.26	0.28	0.78	
	Mission	0.49	0.55	0.59	0.47	1.04	
	Headspring	0.82	0.26	1.00	0.76	**1.09**	**0.98 (0.17)**

[a]Calculated as the ratio of $[NO_3^-]$ in each spring relative to Headspring $[NO_3^-]$ on the same sampling date.
[b]Calculated as the ratio of $[NO_3^-]$ in each spring relative to $[NO_3^-]_{init}$ for that spring on the same sampling date.
[c]Calculated as the sum of $[NO_3^-]$ and $[N_2]_{den}$ for each sampling date
[c]Calculated from all springs other than the Ichetucknee Headspring for which data are available on each date.

Despite uncertainties underlying this analysis of the Ichetucknee time series, these estimates of $[NO_3^-]_R$ complement those based on $[N_2]_{den}$ in that estimates of $[NO_3^-]_{init}$ from the Ichetucknee time series are not influenced by error in $[N_2]_{den}$, which can be large relative to $[NO_3^-]_{obs}$. Further, variation in $\delta^{15}N_{NO3}$ among the Ichetucknee Springs is less affected by differential contributions from organic and inorganic sources as might occur in our more spatially extensive data describing dissolved gas concentrations. Finally, these data provide insight into the temporal dynamics of denitrification and its effects on $\delta^{15}N_{NO3}$, which cannot be evaluated using available data for direct estimates of denitrification.

We evaluated the ratio of ^{15}N and ^{18}O isotopic enrichment via separate regression analyses of $\delta^{15}N_{NO3}$ and $\delta^{18}O_{NO3}$ from our synoptic samples and Ichetucknee River springs time series. Because of apparent batch effects in the $\delta^{18}O_{NO3}$ measurements, we analyzed the $\delta^{15}N$-$\delta^{18}O$ relationship for pooled data separately for each sampling date. Results from the pooled regression are given later in Fig. 6-7d; regression parameters for individual sampling dates are given below in Table 6-3.

Table 6-3. Intercept (β_0), slope (β_1), and covariation strength (r^2) of $\delta^{15}N_{NO3}$- $\delta^{18}O_{NO3}$ relationships on individual dates from the Ichetucknee River springs time series.

Date	β_0	β_1	r^2
1/30/07	0.91	1.13	0.982
7/3/07	6.64	0.95	0.942
8/2/07	7.93	0.72	0.997
9/14/07	4.95	1.20	0.979
10/18/07	5.03	1.15	0.983
11/29/07	5.70	1.02	0.964
12/18/07	5.32	1.09	0.994
1/17/08	6.39	0.91	0.961
2/22/08	5.54	1.04	0.979
3/27/08	5.03	1.12	0.960
4/24/08	5.21	1.09	0.992
6/6/08	4.97	1.15	0.975
3/15/09	2.98	0.91	0.988
10/14/09	1.52	1.25	0.994
11/16/09	0.33	1.34	0.985
6/9/10	3.95	1.05	0.999
Mean	**4.52**	**1.07**	**0.980**
SD	**1.84**	**0.14**	**0.007**
Min	**0.33**	**0.72**	**0.942**
Max	**7.93**	**1.34**	**0.999**

Results and Discussion

Inter-relationships among denitrification-derived N_2 ($[N_2]_{den}$), O_2, and $\delta^{15}N_{NO3}$ all support the widespread occurrence of denitrification in the Floridan Aquifer. N_2 concentrations typically exceeded values predicted from recharge temperature and excess air (51 of 61 springs; 94 of 112 observations). $[N_2]_{den}$ ranged from -0.7 to 3.5 mg N_2/L (median: 0.67 mg N_2/L; mean ± SD: 0.82 ± 0.83 mg N_2/L), and was inversely correlated with O_2 (Fig. 6-4a). Among springs with Ne data, this relationship exhibited a sharp break at ca. 2 mg O_2/L, above which $[N_2]_{den}$ averaged 0.003 mg N_2/L (± 0.32; 2 SE); below 2 mg O_2/L, $[N_2]_{den}$ averaged 1.5 mg N_2/L (±0.33; 2 SE). Among all springs, this threshold was less distinct.

Fluxes of $[N_2]_{den}$ from UFA springs were comparable to but uncorrelated with those of NO_3^-, and the proportion of NO_3^- removed by denitrification varied among springs from 0 to as high as 97% (mean ± 2 SE: 34 ± 9%) among springs. Denitrification removed more than 75% of N inputs in 8 of 61 springs, and more than 50% in 20 of 61. Thus, within the UFA we observe variation in denitrification progression comparable to that observed across a diverse range of agriculturally-influenced aquifer environments[5]. Compared to this spatial heterogeneity, temporal variation in $[N_2]_{den}$ among springs was low (Fig. 6-5, Table 6-4). We estimate that denitrification reduced total flow-weighted NO_3^- flux from sampled UFA springs by 32%, with uncertainty in this estimate primarily driven by the representativeness of our sample of springs. Aggregate volumetric denitrification rates of 2.75 µmol/m^3/d were lower than rates obtained from direct N_2 measurements in other aquifers, but the highest values (ca. 20 µmol/m^3/d) were comparable to rates observed in more nitrate-enriched agricultural aquifers[5]. Aggregate areal denitrification for all springsheds was 1.22 kg/ha/y, with some 20% of springsheds exceeding the estimated global average for groundwater denitrification (3.49 kg/ha/y). These higher rates may indicate greater interactions between oxic, NO_3^--rich conduits and anoxic, NO_3^--poor matrix waters in some springsheds (Green et al. 2010, McCallum et al. 2008). While OM availability is the primary driver of denitrification across diverse ecosystems (Taylor and Townsend 2010), low DOC concentrations imply that UFA denitrification must either be fueled by surface-derived particulates in conduits or solid-phase electron donors (e.g., particulate organic carbon [POC], FeS_2) within the matrix (Green et al. 2008, Schwientek et al. 2008, Torrento et al. 2010).

Across 292 observations from 103 springs, $\delta^{15}N_{NO3}$ ranged from -0.3 to 23.9‰, was inversely correlated with O_2, and varied more among low-O_2 (<2 mg/L) than high-O_2 springs (Fig. 6-4b). Relationships between DO and $\delta^{15}N_{NO3}$ within individual springs varied as a function of mean O_2 concentration (Fig. 6-6). Among high-O_2 springs, temporal variation in $\delta^{15}N_{NO3}$ was small (Fig. 6-5) and

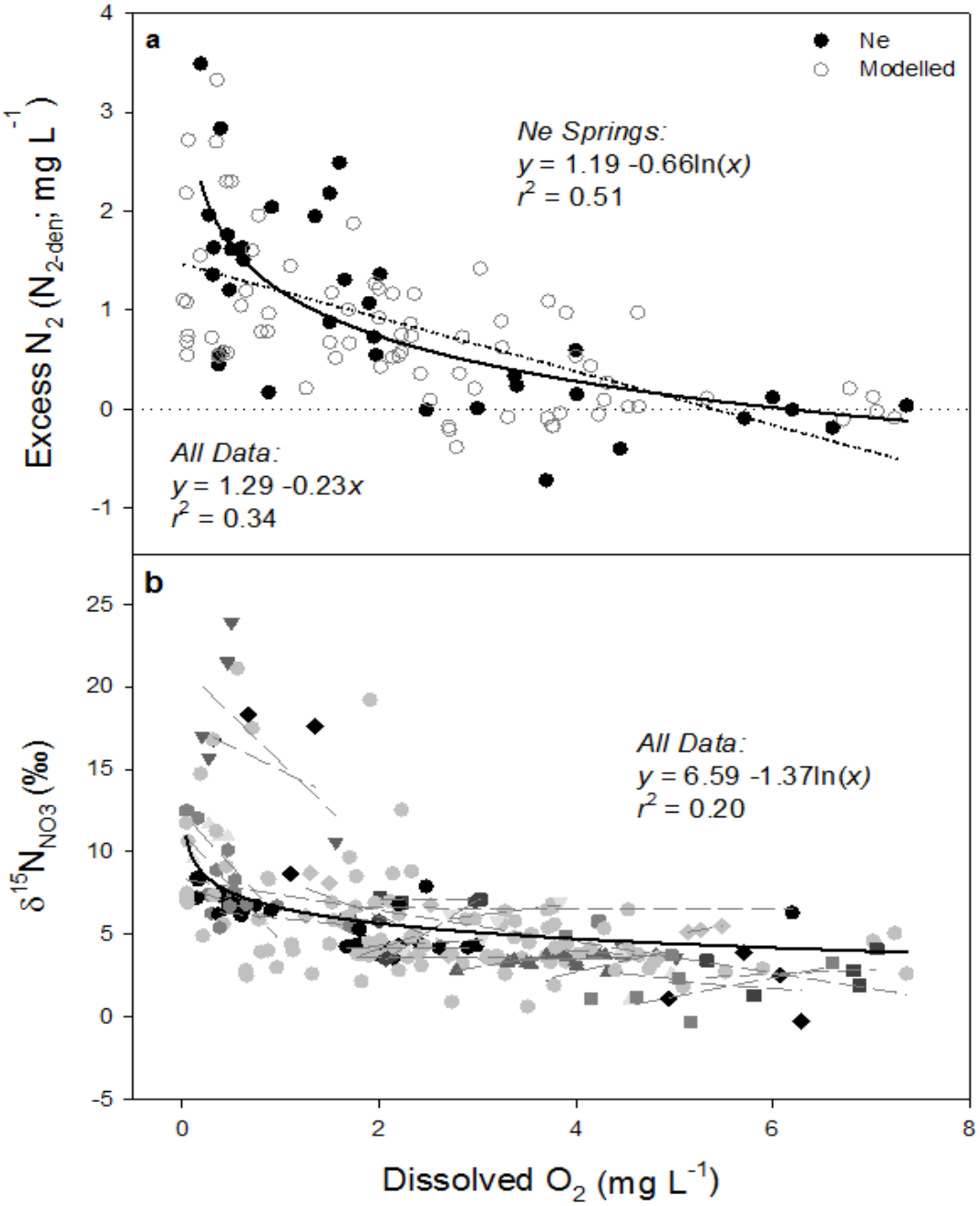

*Fig. 6-4. Dissolved oxygen as a predictor of (**a**) excess N_2 and (**b**) $\delta^{15}N_{NO3}$ in Florida springs. In (**a**), closed symbols indicate measurements of denitrification-derived N_2 ($[N_2]_{den}$) based on direct estimation of excess air and recharge temperature via Ne and Ar; best fit for Ne springs is given by the solid line. Open symbols in (**a**) indicate $[N_2]_{den}$ measurements based on modeled excess air and estimation of recharge temperature from Ar; best fit for all $[N_2]_{den}$ data are shown by the dashed line. In (**b**), light symbols indicate data from springs with 3 or fewer observations; dark symbols indicate data from springs with 4 or more observations. Lines in (**b**) are best-fit linear regressions for individual springs with four or more observations of O_2 and $\delta^{15}N_{NO3}$. Springs with high O_2 exhibit little variation in $\delta^{15}N_{NO3}$, but low O_2 springs exhibit higher variability in $\delta^{15}N_{NO3}$ that is linked to variation in oxygen concentrations. Best-fit parameters for individual springs are given in Table 6-3 and their relationship to mean dissolved O_2 is shown in Figure 6-6.*

uncorrelated with O_2, but negatively correlated with O_2 in low-O_2 springs, suggesting that denitrification accounts for much of the observed variation in $\delta^{15}N_{NO3}$. Other processes that might explain these patterns (e.g., OM loading from urban and animal N sources, variation in nitrification, or covariation of N source and age) would not explain the occurrence of excess N_2 in the UFA.

Table 6-4. Results of analysis of variance (ANOVA) to evaluate within- vs. among-spring variation in the concentration of denitrification-derived N_2 ($[N_2]_{den}$), proportional size of residual nitrate pool ($[NO_3^-]_R$), and isotopic signature of nitrate ($\delta^{15}N_{NO3}$).

Source	SSE	df	MSE	*F*	*p*
$N_{2\text{-}den}$					
Spring	44.744	15	2.983	23.367	<0.0001
Error	4.723	37	.128		
$[NO_3^-]_R$					
Spring	38634.0	15	2575.6	15.842	<0.0001
Error	5202.6	32	162.6		
$\delta^{15}N_{NO3}$					
Spring	2699.296	33	81.797	3.039	<0.0001
Error	434.824	165	2.635		

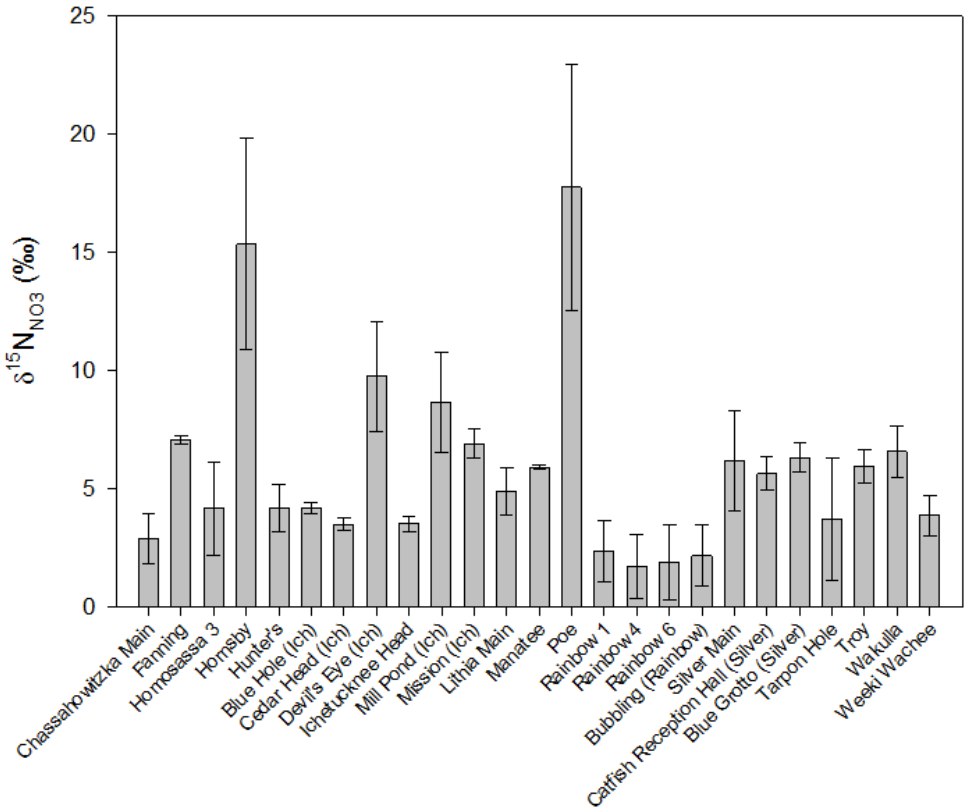

Figure 6-5. Variation in nitrate isotopic composition ($\delta^{15}N_{NO3}$) within and among springs of the Upper Floridan Aquifer. Variation among springs accounts for more than 90% of total variation in $\delta^{15}N_{NO3}$. Full results of analysis of variance are given in Table S2. Data shown are from all springs with 3 or more measurements of $\delta^{15}N_{NO3}$.

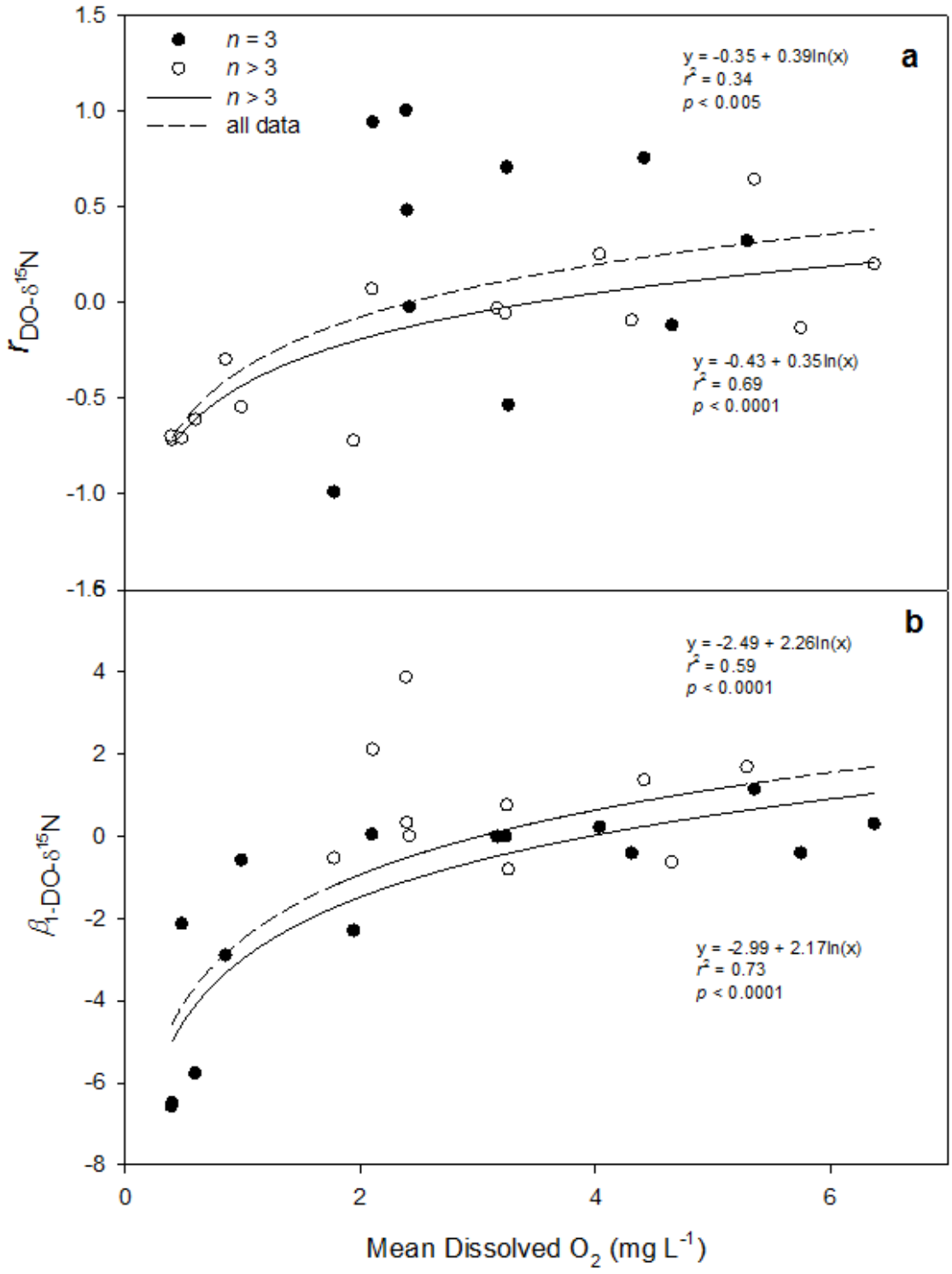

*Figure 6-6. Parameters of within-spring relationships between dissolved O_2 and $\delta^{15}N_{NO3}$ as a function of spring mean dissolved oxygen. Large negative values of both (**a**) correlation coefficient and (**b**) slope in low-O_2 springs, and their absence in higher-O_2 systems, suggest that isotopically-enriched nitrate pools are associated with old, deeply anoxic flowpaths where denitrification would be most likely to occur. Open symbols indicate springs with 3 observations of O_2 and $\delta^{15}N_{NO3}$. Closed symbols indicated springs with 4 or more observations.*

Strong relationships between the relative size of residual nitrate pools ($NO_3^-/[N_{2\text{-}den} + NO_3^-]$) and $\delta^{15}N_{NO3}$ in both the synoptic survey and Ichetucknee River time series (Fig. 6-8a,b) further suggest that variation in $\delta^{15}N_{NO3}$ in the UFA is primarily driven by denitrification. The isotopic enrichment factors for $\delta^{15}N_{NO3}$ ($^{15}\varepsilon$) are near the lower range of observed isotopic enrichment factors for denitrification, potentially indicating diffusion-constrained NO_3^- limitation of this process (Sebilo et al. 2003). The stronger relationship between denitrification progression and $\delta^{15}N_{NO3}$ for springs with Ne data vs. all springs provides additional evidence for greater precision of these estimates.

Dual isotope ($\delta^{15}N_{NO3}$:$\delta^{18}O_{NO3}$) coupling differed between the spatial survey and the Ichetucknee time series, but the slopes of both relationships are within expected ranges for denitrification. The 1:1.7 relationship across sites (Fig. 6-7c) is consistent with theoretical and empirical studies showing 1:2 enrichment by denitrification (Lehmann et al. 2003, Aravena and Robertson 1998); in contrast, the 1:1 coupling within the Ichetucknee River springs (Fig. 6-7d, Table 6-3) comports with recent laboratory studies (Granger et al. 2008) and suggests diffusion limitation of denitrification across the conduit-matrix interface in this moderately NO_3-enriched portion of the Floridan Aquifer.

Estimates of source $\delta^{15}N_{NO3}$ from denitrification progression and observed $\delta^{15}N_{NO3}$ values suggest that denitrification alters $\delta^{15}N_{NO3}$ at the regional scale. Among springs with estimates of $N_{2\text{-}den}$, nearly 20% of observed $\delta^{15}N_{NO3}$ values were greater than 9‰, and more than 50% were greater than 6‰ (Fig. 6-8c), values used in Florida and elsewhere to delineate inorganic and organic sources and mixtures thereof (Katz 2004, Bohlke 2002). Estimated $\delta^{15}N_{NO3}$ of source N (Fig. 6-8d) were much lower, with only 5.5% of observations estimated to have original source $\delta^{15}N_{NO3}$ greater than 9‰, and 26% greater than 6‰. Within the Ichetucknee River time series, differences between the distribution of observed and estimated source $\delta^{15}N_{NO3}$ were even greater (Fig. 6-8e, f). The broader applicability of these results is supported by the rarity of $\delta^{15}N_{NO3}$ values greater than 6‰ among springs with DO greater than 3 mg/L (Fig. 6-8a,b). In all three data sets, estimated source $\delta^{15}N_{NO3}$ was both lower on average and much less variable than spring water. These findings suggest that inconsistencies between isotopic and

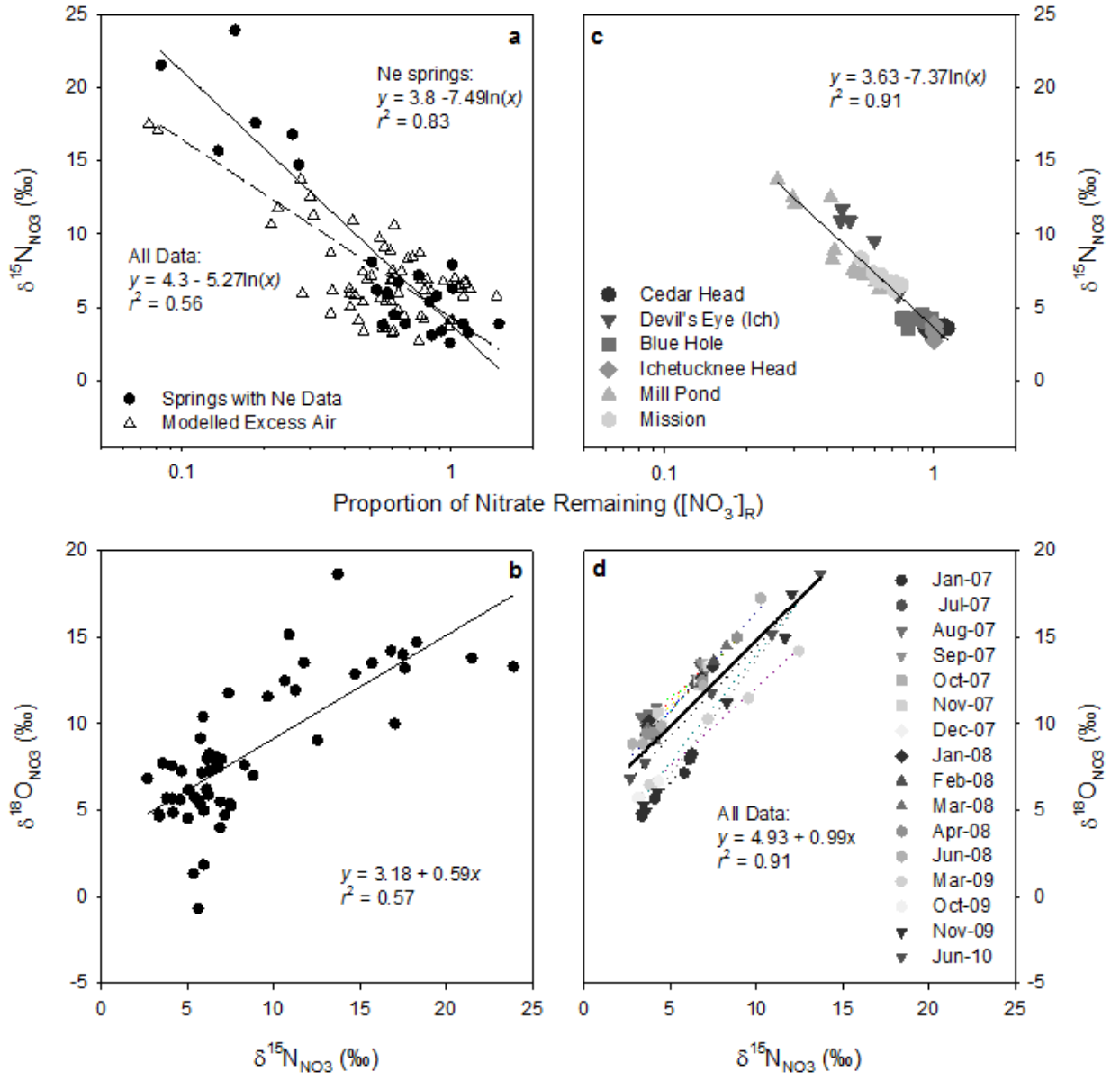

*Fig. 6-7. Effects of denitrification on isotopic composition of nitrate in Florida springs. Variation in $\delta^{15}N_{NO3}$ was strongly correlated with denitrification progression (**a**) as estimated from excess N_2 and observed nitrate concentrations across 61 springs, and (**b**) as estimated from differences between the Ichetucknee Headsprings and other springs in the Ichetucknee River. Positive correlation between $\delta^{15}N_{NO3}$ and $\delta^{18}O_{NO3}$ (**c**) across springs and (**d**) over time within the Ichetucknee system are also consistent with denitrification rather than variation in source as a driver of $\delta^{15}N_{NO3}$. Supplementary Methods and Discussion and Supplementary Fig. 6 provide additional support for inference of denitrification progression from NO_3^- concentration variation in Ichetucknee River Springs.*

mass balance estimates of N source contributions largely reflect the influence of denitrification on $\delta^{15}N_{NO3}$. Absent direct evidence for substantial organic sources for a specific spring, efforts to reduce N loading to the UFA should focus on fertilizer inputs.

The surprising importance of denitrification for N fluxes and isotopic composition in the UFA has important implications both for management of North Florida landscapes and for broader understanding of groundwater denitrification. Methodologically, this study illustrates the value of multiple lines of inference for assessing denitrification, which are strengthened by direct estimates of the physical processes that influence N_2 concentration. Significant spatial and temporal variability of denitrification within the UFA suggests that improving regional and global estimates of denitrification will require more extensive measurements in other aquifers.

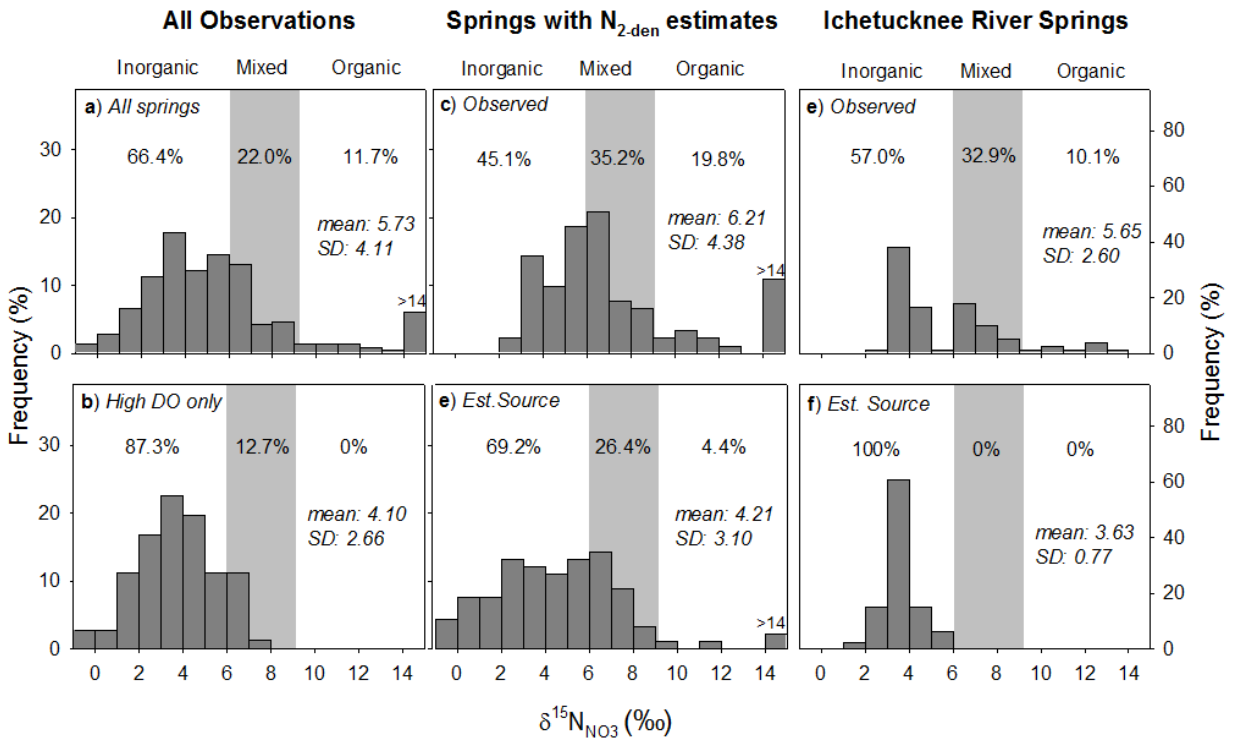

Fig. 6-8. Implications of fractionation by denitrification for inference of N sources to Florida springs. The distribution of $\delta^{15}N_{NO3}$ across all observations (A), among springs sampled for dissolved gases in this study (C) and from the Ichetucknee time series (E) all suggest meaningful contributions of organic sources (one third to one half of springs). However, $\delta^{15}N_{NO3}$ values in high DO springs (B) and source $\delta^{15}N_{NO3}$ as back-calculated from isotopic enrichment factor and denitrification progression (D, F) suggest inorganic fertilizers and soil N (from mineralized OM) as the predominant source in the overwhelming majority of springs.

Uncertainty in estimates of denitrification

Use of dual noble gas tracers (Ne, Ar) to estimate recharge temperature and excess air produced estimates that were more precise and more accurate than those derived from statistical modeling of excess air. Among springs with O_2 greater than 2 mg/L and thus presumably negligible denitrification, $[N_2]_{den}$ estimates based on dual tracers averaged 0.003 mg N/L (0.1 µmol N_2/L) with a standard deviation of 0.32 mg N/L (11.6 µmol N_2/L). For observations from high O_2 springs where Ne data were unavailable, $[N_2]_{den}$ estimates based on statistically modeled excess air averaged 0.32 mg N_2/L (11.6 µmol N_2/L) with a standard deviation of 16.8 µmol N_2/L. The greater bias and lower precision of estimates based on modeled excess air most likely reflects the variability of excess air entrainment over time among springs, but may also reflect introduction of excess air during sampling, an artifact for which our approach does not account. Nonetheless, uncertainty of our estimates compare favorably with bias (5 µmol $N_{2/L}$) and precision (SD = 22 µmol N_2/L) in a previous study of denitrification in agricultural aquifers, in which limited spatial extent permitted assumptions of constant recharge temperature within regions, and calculation of excess air from Ar concentrations (Green et al. 2008). The relatively high precision and minimal bias of $[N_2]_{den}$ estimates in this study illustrate both the value of dual isotope tracers and the utility of statistical modeling of physical processes where direct measurements are unavailable. Similar approaches will likely be necessary and useful in evaluating the spatial heterogeneity of denitrification in other aquifers.

Temporal variation in denitrification and nitrate isotopic signatures

For $[N_2]_{den}$, $[NO_3^-]_R$, and $\delta^{15}N_{NO3}$, spatial variation among springs was large compared to temporal variation within springs. Among the 16 springs with 3 or more observations (max = 5) of $[N_2]_{den}$ in our data set, over 90% of the total variation in $[N_2]_{den}$ was accounted for by spring sampled (ANOVA; Figure 6-9**a**, Table 6-4). Standard deviations within springs for $[N_2]_{den}$ ranged from 0.05 to 0.65 mg N_2/L and averaged 0.31 mg/L. Among the same set of springs, over 88% of total variation in $[NO_3^-]_R$ occurred among springs (ANOVA; Figure 6-9**b**, Table 6-4). Standard deviations within springs for $[NO_3^-]_R$ ranged from <1% to 29% and averaged 10.4%. For both variables, variation among springs was strongly correlated with mean dissolved O_2 from the same set of observations. However, variation in $[N_2]_{den}$ and $[NO_3^-]_R$ within springs was not correlated with variation within springs in dissolved O_2.

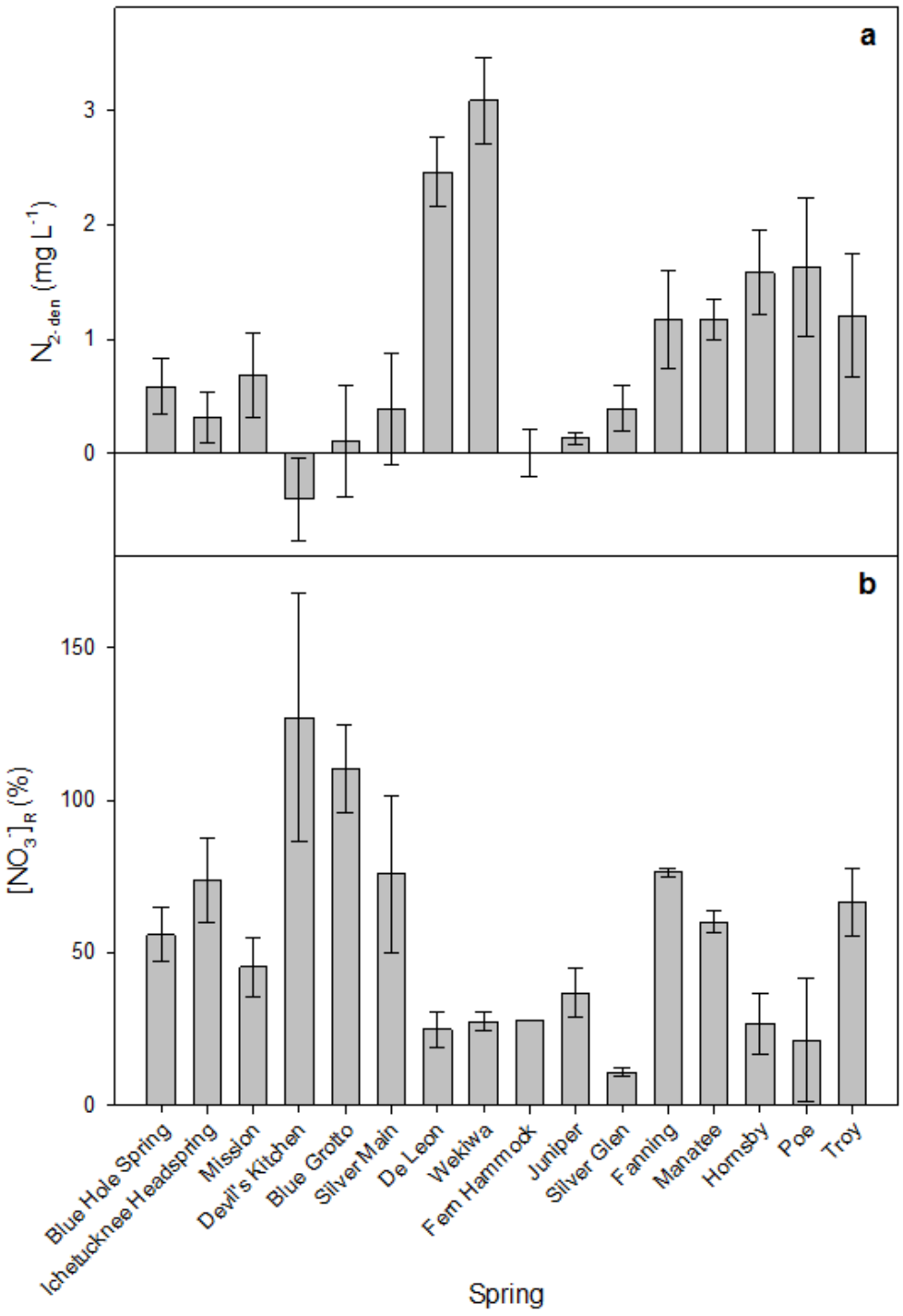

Figure 6-9. Variation in the magnitude of denitrification ($[N_2]_{den}$; panel A) and residual nitrate pools ($[NO_3^-]_R$; panel B) within and among springs of the Upper Floridan Aquifer. Variation among springs accounts for more than 90% of total variation in $[N_2]_{den}$. Full results of analysis of variance are given in Table S2. Data shown are from all springs with 3 or more estimates of $[N_2]_{den}$.

One important implication of the low within-spring variance in $[N_2]_{den}$ and $[NO_3^-]_R$ is that uncertainty in our regional estimate of the magnitude of denitrification and its effect on N loads delivered to surface waters is largely influenced by whether or not sampled springs are representative, rather than by uncertainty of estimates for individual springs. Our population of springs almost certainly oversamples large springs, since we include more than half of the first magnitude springs in northern Florida. It is unclear whether our study oversampled N rich or N poor springs, since the distribution of concentrations in small springs is not known. In light of these uncertainties, our estimate of denitrification in the Floridan Aquifer should be viewed as a first-order approximation.

Among springs with 3 or more observations (max = 18) of $\delta^{15}N_{NO3}$, 86% of the total variation in $\delta^{15}N_{NO3}$ in our data set was accounted for by variation among springs (ANOVA; Figure 6-5, Table 6-4). Standard deviations of $\delta^{15}N_{NO3}$ within individual springs ranged from 0.1 to 5.2‰ and averaged 1.4‰. Variation in $\delta^{15}N_{NO3}$ among springs was strongly correlated with mean dissolved O_2. Unlike $[N_2]_{den}$ and $[NO_3^-]_R$, variation within springs in $\delta^{15}N_{NO3}$ was also correlated with variation in dissolved O_2, particularly for low O_2 springs, which had strong, steeply negative relationships between temporal variation in $\delta^{15}N_{NO3}$ and dissolved O_2 (Figure 6-6). The apparent absence of O_2-driven variation within springs for $[N_2]_{den}$ and $[NO_3^-]_R$ is most likely attributable to low power in our data set for those variables and lower precision in estimates of $[N_2]_{den}$ (and thus $[NO_3^-]_R$) than for $\delta^{15}N_{NO3.}$

Given the strength of observed relationships across springs between denitrification progression and $\delta^{15}N_{NO3}$, the most likely explanation for within-spring $\delta^{15}N_{NO3}$-O_2 relationships is that variation in both O_2 and $\delta^{15}N_{NO3}$ reflect differential contributions of young, oxic groundwater, the isotopic signatures of which are unlikely to have been altered by denitrification, and older, anoxic groundwater, for which depletion nitrate by denitrification has produced elevated values of $\delta^{15}N_{NO3}$. Alternatively, flow variability and the resulting mixture between oxic and anoxic water masses might actually promote increased rates of denitrification[24,25]. However, the magnitude of variation in $\delta^{15}N_{NO3}$ and the necessary rates of denitrification implied by that variation make this explanation seem unlikely. Similarly, it is superficially plausible that these patterns reflect the concurrent influence of human- or animal-derived effluent on dissolved O_2 (via increased BOD) and $\delta^{15}N_{NO3}$. However, if coincident BOD and δ^{15}N-enriched NO_3^- inputs were responsible for these patterns, then high-O_2 springs would exhibit covariation between O_2 and $\delta^{15}N_{NO3}$, as is observed in low-O_2 springs. Rigorous analysis of the relationship of land use with O_2, $[N_2]_{den}$, and $\delta^{15}N_{NO3}$ is beyond the scope of this paper, but worthy of further investigation.

Research Element #7 – Nitrogen Cycling in Alexander Springs Creek

Abstract

Diel variations in nitrate concentrations at Alexander Springs Creek are the opposite of what is exhibited by other spring run streams in Florida; peak nitrate concentrations occur during the day, while concentrations are lowest at night. Despite having one of the lowest nitrate concentration of any first magnitude spring in Florida (mean 0.07 mg/L), a continuous benthic mat dominated by the filamentous green algae, *Hydrodictyon* sp., covers a 24,000 m^2 stretch of the river run. We conducted a study to discern the possible mechanisms causing the atypical diel pattern in nitrate by comparing nutrient chemistry, stable isotope composition of nitrate and N_2:Ar ratios in the spring vent, within the algal mat and in the overlying water column. We also calculated ecosystem metabolism (GPP), quantified N pools, N uptake in the river run, and the N demand of the algal mat to determine how such an extensive mat can be sustained under such low nitrate conditions. Additionally, we measured downstream export of seston.

We found the system to be highly productive, with a mean GPP of 15 g $O_2/m^2/d$. The average mass of N coming out of the spring vent was 17 kg/day, average algal mat N demand was 7 kg/day, and total mass removal of N along the river run was also 7 kg/day. The fraction of the algal mat recycled to meet N demand varied on a daily basis (due to variation in GPP), and ranged from 0% to 61%.

Higher N_2:Ar concentrations at night than during the day both within the algal mat and overlying water column, as well as enriched $\delta^{15}N$ and $\delta^{18}O\text{-}NO_3$ of water within the algal mat, suggest that denitrification does occur at night (most likely in the algal mat/sediment interface as well as the sediment)and is a primary mechanism for nitrogen removal along the river run. During the day, high dissolved oxygen (DO) concentrations within the algal mat likely impede denitrification by increasing the depth at which it can occur in the mat and sediment. We hypothesized that spikes in nitrate concentration (or lack of expected draw-down) during the day could be explained by nitrification adding nitrate back into the water column and/or by the assimilation large amounts of internally recycled nitrate (and therefore less uptake than expected during the day).We found little evidence of nitrification within the benthic mat, however, and conclude that a large portion of benthic mat N demand is met through the internal recycling of N.

Finally, a large amount of seston (dominated by masses of *Hydrodictyon* sp.with other macrophytes and terrestrial organic carbon interspersed) is exported downstream each day and shows a distinctly diel pattern, with export increasing exponentially from 12 pm to 6 pm, which coincides with peak DO

concentrations in the algal mat and overlying water column, and then dropping down again by early morning. We calculated that a total dry mass of 368 kg/day, or 30% of the standing benthic mat, is exported daily, although this is likely a gross overestimation, however, since we assumed that the seston captured in the net was representative of the entire channel cross-sectional area. But even if export is only one third of that (113 kg/day), this still represents approximately 10% of the standing benthic mat biomass.

Introduction

Diel variations in nitrate concentrations along Alexander Springs Creek are the inverse of what is observed in other spring run streams in Florida. In the Ichetucknee, Silver, Rainbow Rivers and Juniper Creek, for example, nitrate concentrations are lowest during the day due to a combination of assimilation (uptake of N by macrophytes and algae) and denitrification (by denitrifying bacteria). Nitrate concentrations are highest at night as autotroph assimilation stops or is greatly reduced and uptake occurs mainly through denitrification. Along Alexander Springs Creek, however, peak nitrate concentrations occur during the day and are sometimes higher than concentrations at the spring vent, while concentrations are lowest at night. Despite having one of the lowest nitrate concentrations of any first magnitude spring in Florida (0.07 mg/L), there is a large, continuous benthic mat composed predominantly of the filamentous green alga, *Hydrodictyon* sp. that covers 24,000 m^2 of the river run downstream of the spring pool. In addition to filamentous algae, numerous other organisms are associated with benthic mats in Florida springs, including epiphytic microalgae, bacteria and fungi (Quinlan et al. 2008; Inglett et al. 2008, A. Albertin, unpublished data).

The overarching goal of our study was to discern the possible mechanisms causing the atypical diel pattern in nitrate concentrations in Alexander Springs Creek. We had two major objectives. The first was to characterize conditions within the algal mat as compared to the spring vent and the overlying water column. Specifically, we compared dissolved inorganic nitrogen (DIN)(NO_3+ NH_4), isotopic signatures of N ($\delta^{15}N$ and $\delta\ ^{18}O$-NO_3 and $\delta^{15}N$ in algal tissue), DO and N_2:Ar ratios in these different locations. We hypothesize that uptake of nitrate during the night is due to high denitrification rates occurring in the spring run sediment, while denitrification (which requires anoxic or near anoxic conditions) is inhibited during the day due to oxygen diffusion into the sediment as a result of high DO levels in the water column, produced mainly through algal photosynthesis. We further hypothesize that nitrate concentrations peak during the day because NH_4 within the sediment and the algal mat is nitrified and moves into the overlying water column by both advective and diffusive flow.

The second major objective of the study was to determine how the large benthic mat can be sustained under such low nitrate concentrations. Specifically, we: (a) calculated GPP, N removal along the spring run and algal mat N demand, (b) quantified the total amount of N stored in the mat (algal biomass + DIN) as compared to N flux from the spring vent, (c) determined whether or not internal N cycling is required to meet N demand, and (d) quantified N export (as coarse particulate organic carbon) from the system. We hypothesize that much of the N demand of the algal mat is met through internal recycling.

Methods

Study site

Alexander Springs, a first magnitude spring with an average discharge of 3.34 m^3/s (118 ft^3/s)(Scott. et al. 2004), is located in the Ocala National Forest, Lake County, Florida. The spring pool is large (91.4 m by 78.6 m) and gives rise to a spring run stream, Alexander Springs Creek, which flows for approximately 12.9 km until it reaches the St. Johns River (Scott et al. 2004). Numerous algal species are found in the vent area, including *Lyngbya wollei*, *Vaucheria* sp., *Spirogyra* sp. and *Hydrodictyon* sp. (Stevenson et al. 2004), as well as several species of submerged and emergent aquatic vegetation, the most common being *Vallisneria americana* (Eelgrass) and *Typha* sp. (Cattail) (Bacchus and Barile 2005). The spring pool is designated for swimming and is heavily used in the summer months, causing great reductions in algal cover in all but the deepest portions of the spring pool.

Approximately 50 m downstream from the spring vent, just outside the designated swimming area, the river channel narrows to ca. 48 m and becomes shallow (0.5 to 1.0 m deep). A continuous benthic algal mat dominated by the filamentous green algae, *Hydrodictyon* sp. (Chlorophyceae) begins in this section of the river run and extends for approximately 500 m downstream, covering the great majority of the river bottom; the mat covers an area of approximately 24,000 m^2**.** Submerged, emergent and floating vegetation along this section of the river run is found primarily along the edges of the spring run channel. As swimming is not allowed in this portion of the spring run, a reduction in the extent of the benthic mat due to recreation doesn't occur.

Water and algae sample collection

An *in situ* nitrate sensor (SUNA) was deployed 550 m downstream from the spring vent at Alexander Springs Creek on three separate occasions in 2010 (Fig. 7-1). Nitrate concentrations were measured continuously at 15 minute intervals from March 3 to March 9, August 27 to September 3 and September 18 to October 1. Concurrent dissolved oxygen and water temperature were measured hourly at this same location with a YSI6920 sonde. Additional water samples were collected every two hours over a 48 hour period using an ISCO 6700 autosampler, also located approximately 550 m downstream from the spring pool, near the SUNA. Samples were collected for water column NO_3, NH_4 and $\delta^{15}N$ and $\delta\,^{18}O\text{-}NO_3$ analysis.

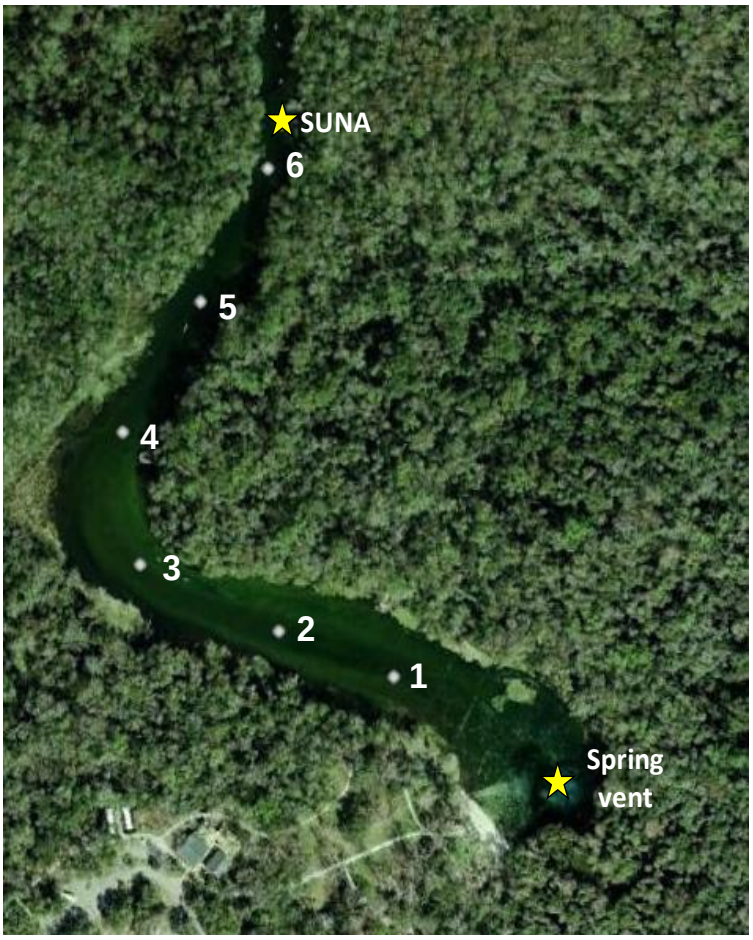

Fig. 7-1. Location of the spring vent, sampling sites (1 through 6) and the continuous nitrate sensor (SUNA) at Alexander Springs Creek.

Interstitial water samplers were used to sample water from within the *Hydrodictyon* mat as well as in the overlying water column. The samplers were deployed in the early morning and in the afternoon of September 30 and October 1, 2010. The algal mat was sampled in six sites along a downstream gradient, with each site located approximately 80 m from the other (Fig. 7-1). Sampling occurred in the general vicinity of each site (not necessarily in the exact same point). Site 1 was located approximately 90 m downstream from the vent, where the continuous algal mat begins, and Site 6 was located at the lower end of the algal mat, near the location of the SUNA, approximately 550 m from the vent.

Sampling was conducted twice a day to capture different environmental conditions within the algal mat; in most aquatic systems, photosynthesis rates and subsequent DO concentrations are low in the early morning, as compared to the afternoon, when photosynthesis rates peak and DO concentrations in the

water column are highest. Samples collected in the early morning were used as a proxy for nighttime conditions and will be referred to as “night” in all results presented. Samples collected in the afternoon were used as an indication of daytime conditions and are further referred to as “day”.

The interstitial water samplers used in our study consisted of a central 2-m-tall PVC pipe with two 30 cm-long PVC pipes attached horizontally (at right angles) (Fig. 7-2). One horizontal pipe was fixed at 10 cm from the bottom and the upper one was adjustable, so that it could be placed at 10 cm below the surface of the algal mat. Multiple holes were drilled along the length of each horizontal pipe, which was then covered with 1000 µm Nitex nylon mesh to prevent debris from clogging up the holes. Tygon tubing (0.25 inch ID) was then attached to one end of each horizontal pipe. The two Tygon tubes extended (externally) along the entire outer length of the central PVC pipe; water was sampled from these tubes.

The sampler was inserted vertically through the algal mat and then gently moved horizontally for approximately 0.5 to 1 m, so as to reach a relatively undisturbed portion of the mat. The sampler rested on the bottom of the spring run and was kept in place with a steel rod that was inserted through the central PVC pipe and hammered into the river bottom until the sampler was securely in place. While sitting in a canoe, water samples were drawn from each Tygon tube (one from each level within the algal mat) as well as from the overlying water column using a peristaltic pump with an inline 0.45-µm

Fig. 7-2. Interstitial water sampler used to collect water within the benthic algal mat and overlying water column at Alexander Springs Creek.

polycarbonate membrane filter. Water samples were first drawn from the tube corresponding to the lower portion of the algal mat (10 cm from the bottom), then from the tube corresponding to the upper portion of the algal mat (10 cm below the top of the algal mat) and finally from the overlying water column. Filtered water samples were collected for NO_3 and NH_4 concentration and for the dual-isotope analysis of nitrate ($\delta^{15}N\text{-}NO_3$ and $\delta^{18}O\text{-}NO_3$). Additionally, DO concentrations and temperature at multiple levels within the algal mat and in the overlying water column were measured at each site using a YSI 556 field probe.

After the water samples were collected, a grab sample of algae was taken from the upper portion of the mat, shaken in the water to remove any loosely attached debris, placed into a Ziploc bag and stored on ice. Algal samples were collected for % C, % N and $\delta^{13}C$ and $\delta^{15}N$ isotope analysis.

Water and algal tissue sample processing and analysis

All water and algal samples were kept on ice for 48 hrs and then transported to our laboratory at the University of Florida. Samples from the ISCO sampler were filtered (0.45-µm) in the laboratory. Water samples were stored frozen until analyzed and algal samples were rinsed with DI water, picked clean of invertebrates and debris, and stored frozen. Prior to % C and N determination and isotopic analysis, algal samples were oven dried at 50°C, picked clean of any debris initially missed, and ground and homogenized in a ball mill.

Water samples were analyzed for NO_3 concentration based on second-derivative ultraviolet (UV) spectroscopy (Simal et al. 1985) using an Aquamate UV-Vis spectrophotometer. NH_4 analysis was conducted using the NH_3 Phenate Method (Solorzano 1969). Samples for the dual-isotope analysis of nitrate ($\delta^{15}N\text{-}NO_3$ and $\delta^{18}O\text{-}NO_3$) were analyzed at the University of California Riverside using the bacterial denitrifier method (Sigman et al. 2001; Casciotti et al. 2002) in which nitrate is converted to N_2O by the bacteria *Pseudomonas aureofasciens*. The $\delta^{15}N$ and $\delta^{18}O$ of the N_2O produced was measured on a Thermo Delta-Plus XP isotope ratio mass spectrometer using the GasBench interface and a continuous flow of helium. The international standards IAEA-N3 and USGS-34 and USGS-35 were included in each analytical run and used for isotopic standardization. $\delta^{15}N$ and $\delta^{18}O$ isotope abundances are reported in δ notation relative to international standards (atmospheric air for N and Vienna Mean Standard Ocean Water (VSMOW) for O). The NO_3 concentration of many of the isotope samples was very low, resulting in a relatively high standard error in samples with the lowest NO_3 concentrations. In

summary, for 18 samples, standard errors for $\delta^{15}N$ and $\delta^{18}O$ are 0.5-0.75‰. For 20 samples, errors are ±1-2‰, and for 14 samples, the errors are ± 3‰.

Carbon and nitrogen content of algal tissues were measured by high temperature combustion on a Carlo Erba NA1500 Elemental Analyzer at the University of Florida. Carbon and nitrogen stable isotopic composition of algae was measured on a Thermo Finnigan Delta-Plus XP isotope ratio mass spectrometer using an elemental analyzer inlet system and continuous flow of He. The International Atomic Energy Association standards for sucrose and N1 were included in each run. $\delta^{13}C$ and $\delta^{15}N$ isotope abundances are reported in δ notation relative to international standards (Vienna Pee Dee Belemnite for C and atmospheric air for N).

N_2:Ar ratios within the algal mat and in the river run

Water samples for gas analyses were collected on October 1, 2010 at each site (1 through 6) using a peristaltic pump in three locations of the river run: 1) at the bottom of the algal mat (within the mat, 10 cm from sediment), 2) at the top of the algal mat (within the mat, 10 cm from the water column) and in the overlying water column. Two replicate field samples for dissolved gas analysis were collected by flushing 300 ml BOD bottles 3 times, sealing them with a glass stopper, and capping them with water-filled plastic caps to minimize exchange with the atmosphere and to prevent stoppers from becoming dislodged during transport. Dissolved gas samples were stored under ice water until analysis within 36 hours. Dissolved N_2 and Ar were measured using a Membrane Inlet Mass Spectrometer (MIMS) at Florida International University.

Diel variation in downstream export of nitrogen and carbon in seston

A 100-cm long stream drift net with a 0.44 m x 0.25 m steel frame and 500 µm Nitex nylon mesh was placed 550 m downstream from the spring vent (where the continuous *Hydrodictyon* mat ends) in order to capture coarse particulate organic carbon (i.e. masses of sloughed algae, other aquatic vegetation and invertebrates (from <1 to 1000 cm^3) exported downstream. It was placed just below the surface in the center of the river channel, facing upstream. The net was emptied every one to two hours during daylight hours. Seston was sampled from 3 pm to 5 pm on September 29, from 7 am until 6 pm on September 30 and from 6 am to 3 pm on October 1, 2010. The samples were kept on ice for 48 hrs and then transported to our laboratory at the University of Florida where they were oven dried at 50°C and ground and homogenized in a Wiley Mill. Carbon and nitrogen content of the collected CPOM were measured by high temperature combustion on a Carlo Erba NA1500 CNS Elemental Analyzer at the

University of Florida. Total seston dry mass, total C and N exported downstream and the C:N ratio of the seston were then calculated.

Algal biomass and nutrient pool calculations

We calculated the total volume (m^3) of the *Hydrodictyon* mat at Alexander Springs Creek by multiplying the total benthic area covered by the mat (24,000 m^2) by the average mat thickness (0.52 m). To estimate the total dry mass of the algal mat, we multiplied the mean dry mass (DM) of algae per unit volume by the total volume of the algal mat. As a proxy for mean DM of algae/volume, we used 3.0 mg DM/cm^3, which is the value calculated for *Vaucheria* sp. by Sickman et al. (2009) at Manatee Springs, Florida. We then multiplied the total DM of the algae by the average elemental composition of N of the algal tissue (in percent) to estimate the total mass of N in the algal mat tissue. To calculate the total mass of DIN in the interstitial water of the algal mat, we added NO_3+ NH_4 concentration for each point sampled within the mat, took the average and then multiplied it by the total volume of the algal mat. Total mass of DIN and total mass of algal tissue N were added together to get the total mass of N in the algal mat. We were not able to measure dissolved organic N.

Metabolism, N assimilation and N demand of the algal mat

We calculated gross primary production (GPP) and ecosystem respiration (R) in units of g $O_2/m^2/d$ for each day of our deployments using the single-station method (Odum 1957b). The integration area used to calculate GPP (550m length x 45 m width) was well defined by the geometry of the river and is the area between the spring vent and the sensor location.

We estimated the reaeration constant on a daily basis from the relationship between declining DO concentration at night and the changes in the DO saturation deficit; specifically, reaeration (K, in units hr^{-1}) is the slope of the line relating the DO change $(mg/L/hr)^-$ to the saturation deficit (mg/L) during the period when photosynthesis has ceased for the day, and oxygen levels are declining to their nighttime levels (at which respiration and reaeration are in balance). Fitted lines on a daily basis were generally extremely strong (r^2> 0.95), with exceptions on days with nighttime rainfall and K values varied very little over each deployment period.

To estimate the C : N ratio of primary production required estimating the net C assimilation implied by the gross production estimates in oxygen units. We assumed autotrophic respiration was 50% of GPP (Hall and Tank, 2003), and converted the resulting NPP rate from O_2 to C based on the 32:12 ratio of

molecular weights. Based on previous estimates that suggest trivial heterotrophic nutrient demand (Heffernan and Cohen 2010), we neglected any nutrient uptake due to gross heterotrophic assimilation.

The method used for estimating N removal via assimilation, based on Heffernan and Cohen (2010), does not work at Alexander Springs Creek because of the inverse diel variations in nitrate concentrations. The reasons behind this are explained in more detail in Research Element #2 of this report. In summary, assimilatory removal is typically estimated based on diel variation in nitrate referenced to a nighttime baseline value but in this case, this inference yields negative numbers. Likewise, dissimilatory removal is estimated as the mass loss between upstream input concentrations and the nighttime baseline; that is, denitrification is assumed constant over the course of each 24-hour period. While the results that arise from both methods are problematic in this case, the total mass removal (input concentration minus nitrate concentration) is still informative, and is used to estimate the internal N recycling in the algal mat.

N demand of the algal mat is based on GPP and a C:N ratio of 12.5 (estimated from GPP). The fraction of the algal mat that is recycled to meet N demand was calculated by taking the mass difference between the estimated demand and the observed removal (assimilation + denitrification), and dividing this number by N demand. The result is a lower bound for the fraction of N that has to be obtained via internal cycling, since removal also includes denitrification, which we can't calculate separately for this system.

Data analysis

The values obtained for the N_2:Ar ratios were normally distributed and were analyzed using a 2-way ANOVA using the STATISTICA software package. The values obtained for all other parameters (N_2, Ar, NO_3, NH_4, DO, temperature, $\delta^{15}N$ and $\delta^{18}O$-NO_3 and $\delta^{15}N$)were not normally distributed and were analyzed using a non-parametric ANOVA (by rank)in STATISTICA.

Results

Diel variation in nitrate concentrations and metabolism

During all three deployments of the SUNA (April, August and September 2010), nitrate concentrations were highest during the day and lowest at night, and during the March and October deployments,

concentrations during the day exceeded those of the vent water (the water discharged from the spring vent) on several days. More detailed results are presented in Research Element #2, but in summary, the average vent water nitrate concentration during all three SUNA deployments was 0.07mg $N\text{-}NO_3$/L. In April, downstream daytime peaks in nitrate (measured with the SUNA) ranged from 0.06 to 0.11 mg/L, while lowest concentrations (at night) ranged from 0.03 to 0.04 mg/L (Figure 2-15). In August, downstream daytime concentration peaks ranged from 0.045 to 0.06 mg/L and baseline nighttime concentrations ranged from 0.02 to 0.03 mg/L (figure not shown), and in October (Fig. 7-3), downstream daytime concentration peaks ranged from 0.05 to 0.07 mg/L while the lowest nighttime concentrations ranged from 0.002 to 0.03 mg/L.

Gross primary productivity and the corresponding N use fraction were remarkably high during all three deployments (Fig. 7-4). GPP in March, August and October was 15, 16 and 13 g $O_2/m^2/d$, respectively. The N use fraction (the percent of N coming out of the vent necessary to support that day's GPP) in March, August and October was 46.5, 48.8 and 39.9%, respectively. Average total removal of N (assimilation + denitrification) was 292.7 mg N/m^2/day, which when multiplied by the total area of the algal mat (24,000 m^2), results in a total N mass removal of 7 kg/day. The relationship between GPP and the daytime N enrichment (the amount of N/m^2/day) is shown in Figure 7-5 and indicates that the more oxygen is produced during the day (higher GPP), the higher the amplitude of the daytime spike in nitrate concentration. N enrichment is negative in this case because there is a spike in nitrogen concentration during the day rather than draw-down; generally, N is taken up during the day, a calculation that results in a positive number. Although the global association is not significant, the within deployment association is much stronger; the March deployment has a highly negative slope, but the August and October deployments are much closer to the same slope.

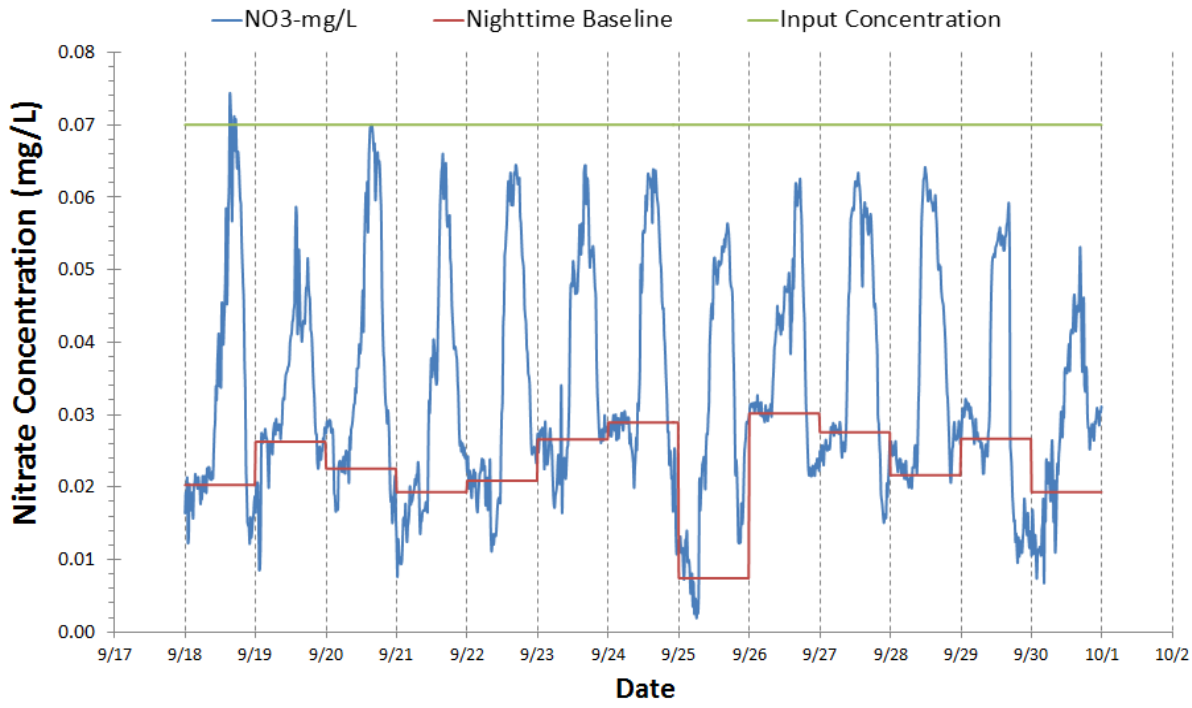

Fig. 7-3. Diel variations in nitrate concentration in the Alexander Springs Creek (approximately 550 m downstream from the vent) from September 18 to October 1, 2010. Lowest concentrations occur at night and peak during the day (vertical dashed gray lines along the x-axis indicate midnight).

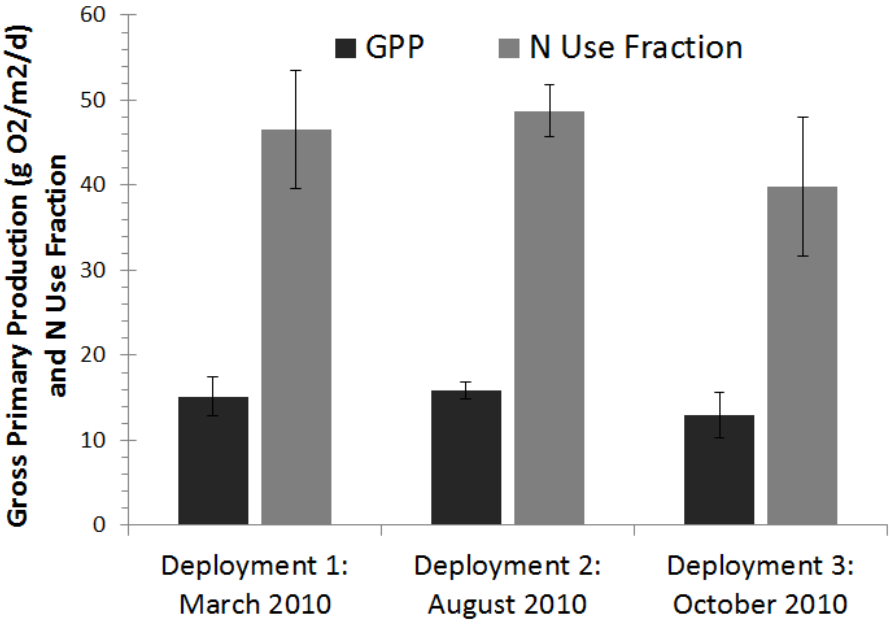

Fig 7-4. Gross primary production (GPP) and N use fraction at Alexander Springs Creek calculated for three 2-week deployments of the SUNA. The N use fraction refers to the fraction, or percent, of the nitrogen coming out of the vent that is necessary to support that day's GPP.

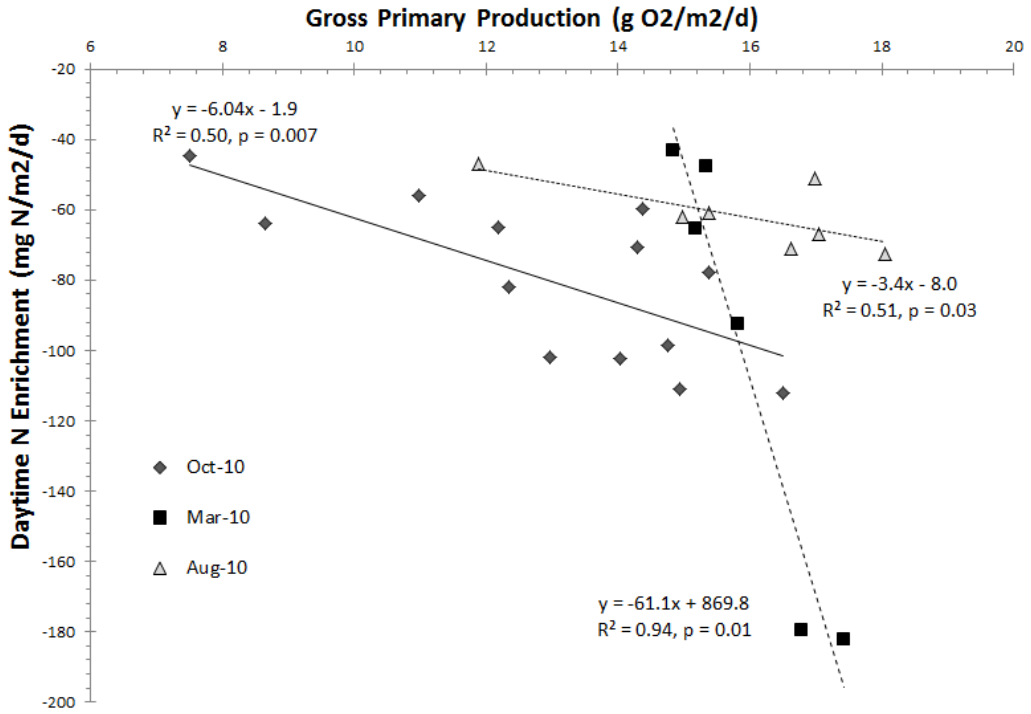

Fig 7-5. The relationship between GPP and daytime N enrichment in Alexander Springs Creek, which indicates that the more oxygen is produced during the day (higher GPP), the higher the amplitude of the daytime spike in nitrate concentration. N enrichment is negative in this case because there is a spike in nitrogen concentrations during the day; generally, N is taken up during the day, a calculation that results in a positive number.

Comparisons between water chemistry and stable isotope signatures in the spring vent, algal mat and overlying water column

The values obtained at sites 1 through 6 for nutrient chemistry, stable isotopes, dissolved oxygen and temperature were averaged to obtain mean values for location within the river run (bottom of the mat, top of the mat or in the overlying water column) rather than being analyzed on a per site basis. There were no significant differences in mean NO_3 and NH_4 concentrations ($p>0.05$) within the same location (spring vent, the top portion of the algal mat, the bottom portion of the algal mat or in the water column) from day to night (Figs. 7-6A and 6B). However, NO_3 was significantly higher ($p=0.01$) bottom of the algal mat than in the water column. Mean NO_3 concentrations in the top portion of the mat were 0.10 mg/L at night and 0.07 mg/L during the day, while in the bottom part of the mat, concentrations were 0.11 and 0.18 mg/L during the night and day, respectively. Lowest NO_3 concentrations were found in the water column (0.02 mg/L at night and 0.03 mg/L during the day). NH_4 concentrations were elevated in the bottom of the mat only and were significantly higher ($p<0.001$) than at all other locations. Mean concentrations were 0.45 mg/L at night and 0.26 mg/L during the day, while

concentrations in the top portion of the mat and in the water column and spring vent did not exceed 0.03 mg/L.

DO concentrations were significantly higher ($p \leq 0.01$) during the day than at night in the water column and both at the top and bottom of the algal mat (Fig. 7-7), and were significantly different during the day within the algal mat (top vs. bottom) ($p<0.001$); at night, significant differences were found between the water column and bottom of the mat only ($p=0.02$). As expected, DO concentrations were highest in the top portion of the algal mat and in the water column during the day due to photosynthesis (7.72 mg/L and 5.19 mg/L, respectively). DO was also surprisingly high in the bottom portions of the mat (3.23 mg/L) during the day. At night, concentrations in the water column, top and bottom of the mat dropped to 1.87, 1.78, and 1.17 mg/L, respectively. Temperatures ranged from 22.96 to 24.63°C during daytime conditions, and during the night/early morning, temperatures ranged from 22.64 to 23.37 °C , there were no significant differences in temperature between the algal mat and the overlying water column or the vent during the day ($p>0.05$).

There were no significant differences in mean $\delta^{15}N$ and $\delta^{18}O\text{-}NO_3$ between day and night values ($p>0.05$) within the same location (vent, top of the mat, bottom of the algal mat or in the water column) (Figs. 7-6C and 7-6D). Both $\delta^{15}N$ and $\delta^{18}O\text{-}NO_3$ were significantly higher during the day high within the algal mat than in the vent ($p<0.05$), but not significantly different at night. At the bottom of the algal mat, sample size was low ($n=3$) and variability between samples was high; values ranged from. However, the most enriched values of $\delta^{15}N$ and $\delta^{18}O\text{-}NO_3$ were of samples collected at the bottom of the mat; at night, $\delta^{15}N$ and $\delta^{18}O$ values were 20 and 12‰, respectively, and during the day, mean values were 13 and 9‰. Interestingly, despite more enriched values in $\delta^{15}N\text{-}NO_3$ in the interstitial waters of the algal mat as compared to the vent, the $\delta^{15}N$ of the algal tissue and spring vent were identical, 7‰ both during the day and at night. Regressions describing the linear relationship between $\delta^{15}N$ and $\delta^{18}O\text{-}NO_3$ were statistically significant within the interstitial waters of the algal mat both at night and during the day, and in the water column at night (Fig. 7-8). The linear relationship was not significant in the run at night or in the spring

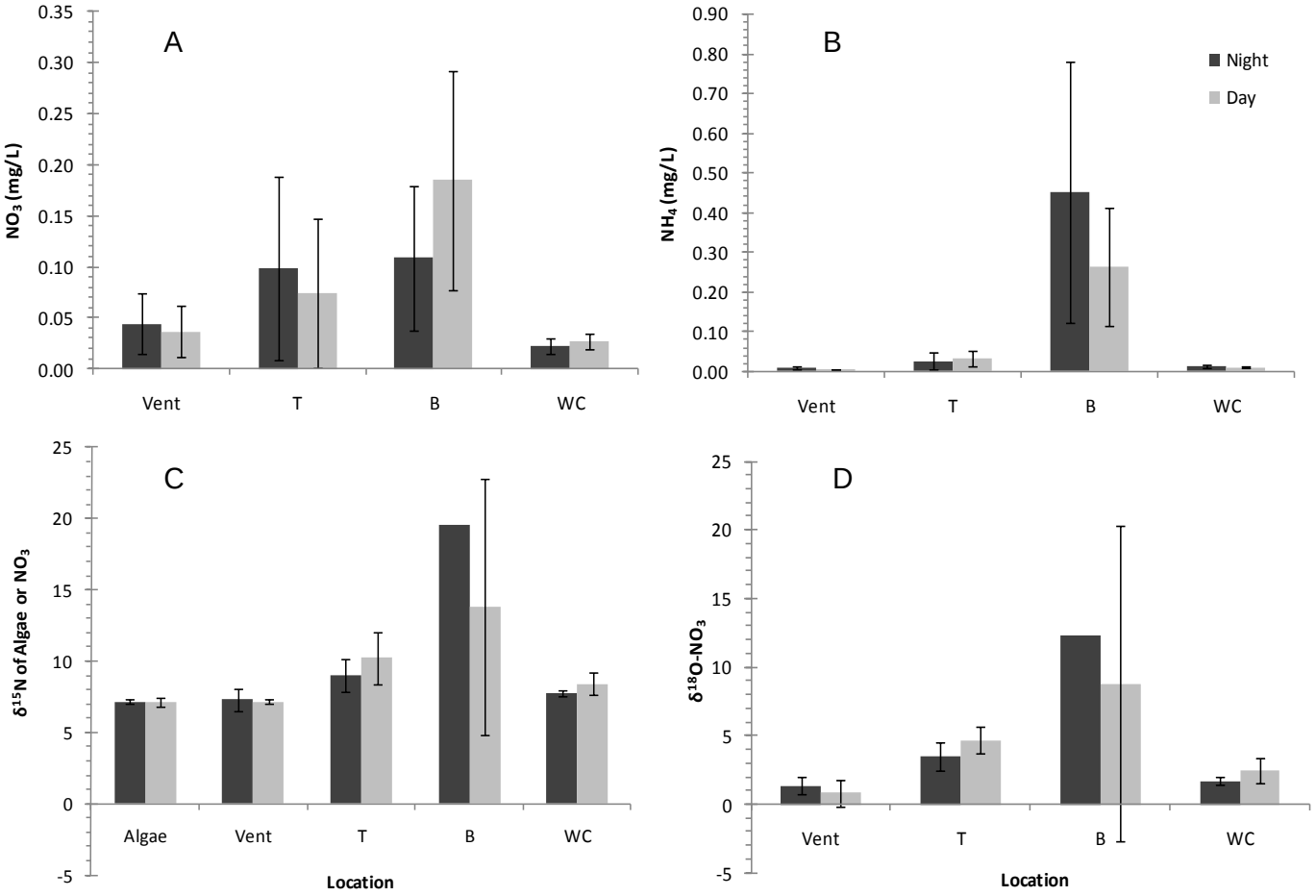

Fig. 7-6. Differences in mean day time and night time nitrate concentration (mg/L) (A), NH_4 concentration (mg/L) (B), $\delta^{15}N$ of nitrate or algal tissue (C) and $\delta^{18}O$-NO_3 (D) in different locations within Alexander Springs Creek: the spring vent, the top of the algal mat (T), the bottom of the algal mat (B) and in the water column (WC). Each value shown (except for the vent) is an average of samples taken at Sites 1 through 6 on both sampling das. Error bars are ±two standard errors.

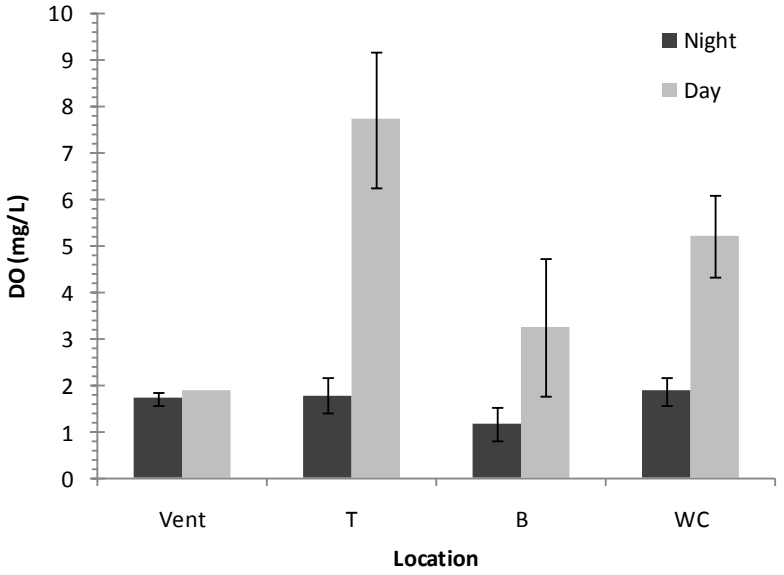

Fig. 7-7. Average day time and night time DO concentrations (mg/L) in the spring vent, the top of the algal mat (T), the bottom of the algal mat (B) and in the water column (WC) at Alexander Springs Creek. Each value shown (except for the vent) is an average of samples taken at Sites 1 through 6 on both sampling days. Error bars are ±two standard errors.

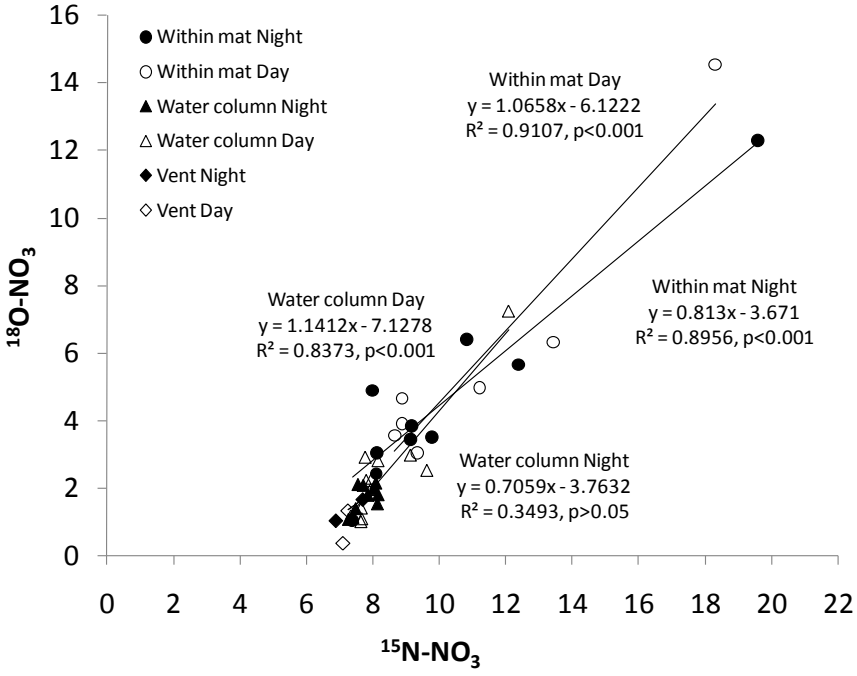

Fig. 7-8. Relationship between $\delta^{15}N$ and $\delta^{18}O\text{-}NO_3$ of water from the spring vent, the water column and within the algal mat (both the top and bottom of the mat) at the spring vent and Sites 1 through 6 along Alexander Springs Creek .

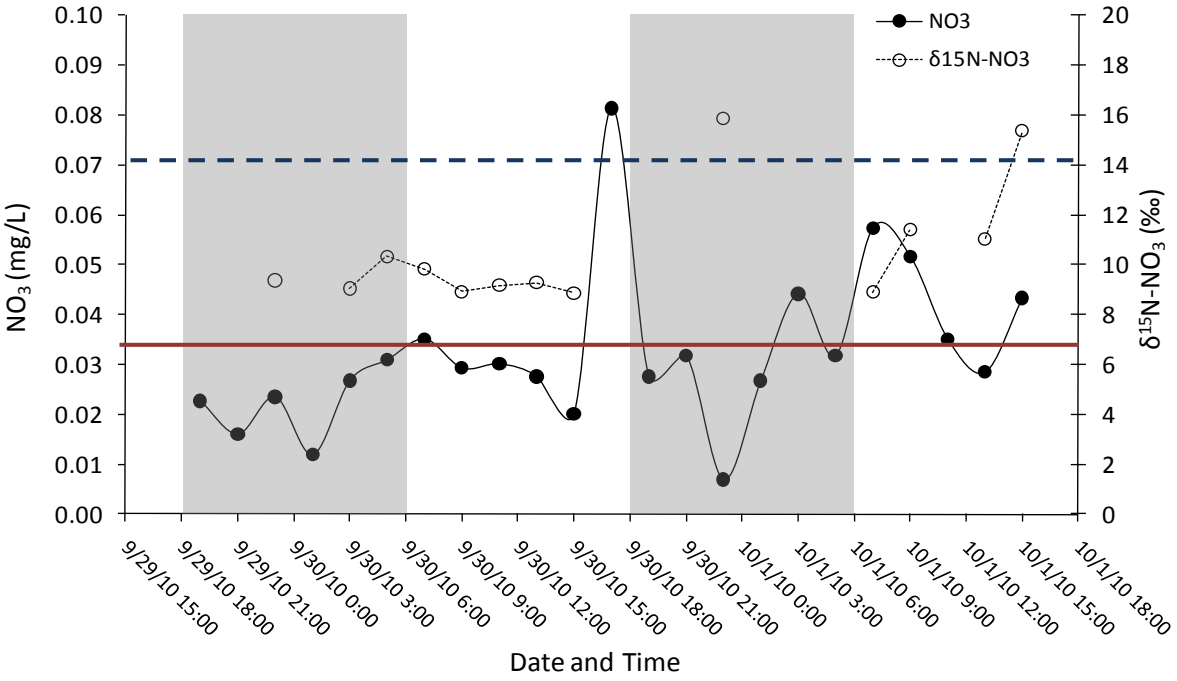

Fig. 7-9. Diel variation in nitrate concentration and δ ^{15}N-NO$_3$ of water collected with the ISCO autosampler from September 29 to October 1, 2010, approximately 550 m downstream from the vent at Alexander Springs. Nighttime hours are shaded in gray. The horizontal dashed blue line indicates mean vent nitrate concentration(0.07 mg/L) and the horizontal red solid line shows the mean δ ^{15}N-NO$_3$ coming out of the vent (7‰).

vent day or night (p>0.05), as δ^{15}N and δ^{18}O-NO$_3$ for all samples were very similar.

Nitrate concentrations and δ^{15}N-NO$_3$ of samples taken every two hours over a 48-hour period with the autosampler did not show distinct diel variations (Fig. 7-9). Nitrate was generally lowest at night, but the data were relatively noisy and did not follow a discernible pattern. δ^{15}N-NO$_3$ values were always enriched as compared to the spring vent and values varied from 9 to 16‰, while vent δ^{15}N-NO$_3$ was 7‰ (Figs. 7-6C and 7-8). However, due to very low nitrate concentrations, the measurement error associated with the isotope samples was ±1-2 ‰ for 5 of the samples and ±3 ‰ for 8 of the samples.

Nutrient pools of N and C

Nutrient pools and algal mat dimensions at Alexander Springs Creek are summarized in Table 7-1. The algal mat is enormous, covering an area of 24,000 m^2 and total volume of 12,480 m^3. The mass of N

Table 7-1 Summary of nutrient pools, demand and removal at Alexander Springs. Mass of algal tissue and seston are reported in dry weight.

Nutrient pools, demand and removal	Quantity	Units
Algal mat surface area	24,000	m^2
Average algal mat thickness	0.52	m
Total mat volume	12,480	m^3
Total mass of the mat	37,440	kg
Mass of C in the mat	13,965	kg
Mass of N in the mat	1,153	kg
DIN (NO_3+NH_4) in total mat volume	4	kg
Total N in mat (DIN+N in algal tissue)	1,157	kg
Mass of N coming out of the spring vent	17	kg/day
Total mass N removal (assimilation+denitrification)	7	kg/day
Algal mat N demand	7	kg/day
Mass of N exported as seston	9.1	kg/day
Mass of C exported as seston	79.3	g/day
Total mass exported as seston	378.1	kg/day

stored in the algal mat (algal tissue + DIN in the interstitial water of the mat) is estimated to be 1,157 kg, and is 68 times more than the mass of N discharged by the spring vent per day (17 kg). Based on GPP and the C:N ratio of 12.5, we calculated that the daily N demand of the algal mat is approximately 7 kg, which is 1.75 times more than the DIN stored in the mat (but only 0.006 % of the total N stored in the mat) and is 41% of the N discharged from the spring vent each day. Mass removal of N by the mat was also calculated to be 7 kg/d (input concentration minus nitrate concentration downstream). We calculated the fraction of the algal mat that is recycled to meet N demand by taking the mass difference between the estimated demand and the observed removal (assimilation + denitrification), and dividing this number by N demand. From September 18 to September 30, the fraction of N in the mat that had to be recycled to meet demand was highly variable and ranged from 0% to 61%.

The quantity of N exported downstream as seston at Alexander Springs Creek showed a distinctly diel pattern (Fig. 7-10) and was surprisingly high, with export increasing exponentially from 12 pm to 6 pm, which coincides with peak DO concentrations, and then dropping down again by early morning. Since we didn't sample throughout the night, however, we can't be sure that we captured peak export. The C:N ratio of the seston was low and variable, ranging from 8.6 to 20.7, with a mean of 10.4, and the majority of the material was decaying masses of *Hydrodictyon* filaments. When integrated over a 24-hr period,

the total amount of N exported per day was 9.1 kg. Total C exported was 79.3 kg/day and the total dry mass of seston exported was 378.1 kg/day; this represents approximately 1% of the total dry mass of the standing algal mat. It is imperative to note, however, that we are almost certainly overestimating the amount exported downstream since we assumed that the seston captured in the net was representative of the entire channel cross-sectional area. The more likely scenario is that there are areas with less export, e.g. lower in the water column and near the banks of the channel where flow is reduced.

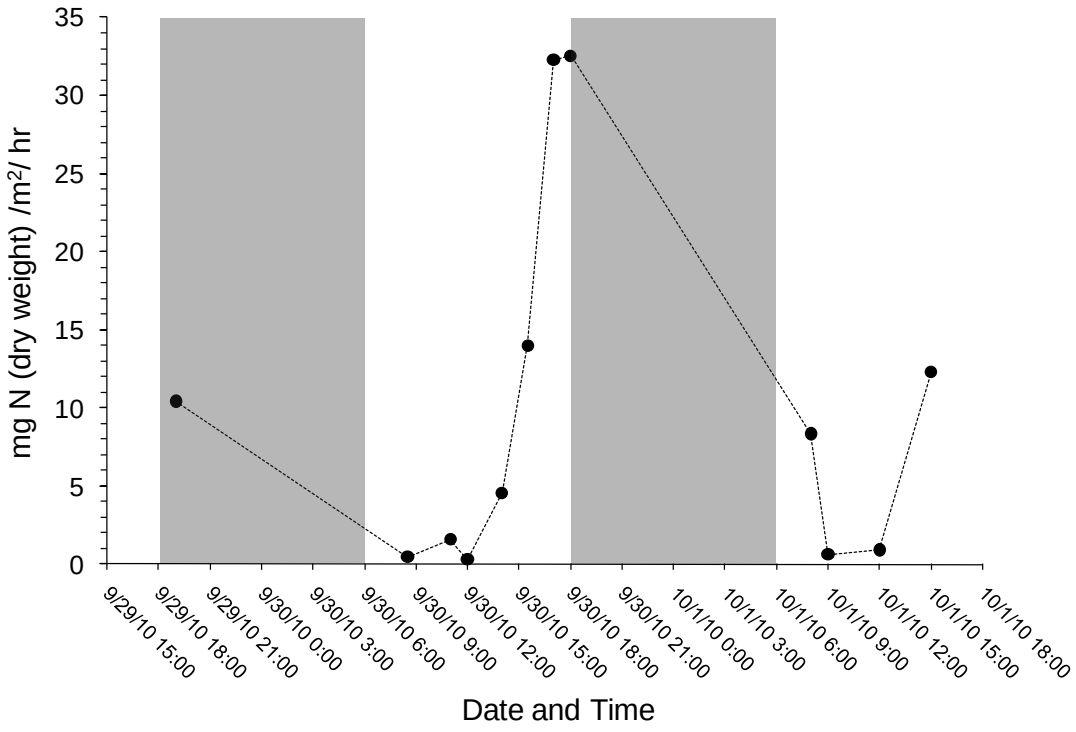

Fig 7-10. Diel variation in the amount of nitrogen exported as seston (principally sloughed masses of Hydrodictyon sp.) over the course of 48 hrs at Alexander Springs. Nighttime hours are shaded in gray. The exported N is expressed as dry mass per m^2 of the total area covered by the continuous algal mat, which is estimated to be 24,000 m^2.

N_2:Ar ratios

Mean N_2 concentrations in the spring vent were 16.65 mg/L and mean Ar concentrations were 0.57 mg/L; the mean N_2:Ar ratio was 29.57. These values are very similar to values found during the day in the spring run and in the algal mat (Figs 7-11 and 7-12). N_2, Ar and N_2:Ar ratios were significantly higher ($p<0.05$) at night than during the day in the river run (water column) and in the algal mat; this signifies that there is excess N_2 in the mat and in the water column, which is indicative of denitrification. There were no significant differences in N_2, Ar and N_2:Ar ratios and position within the spring run (bottom of the mat vs. top of the mat vs. the water column). At night, values generally increased with increasing distance from the vent, while in the day, N_2:Ar ratios decreased with increasing distance from the vent (Figs. 7-13 and 7-14).

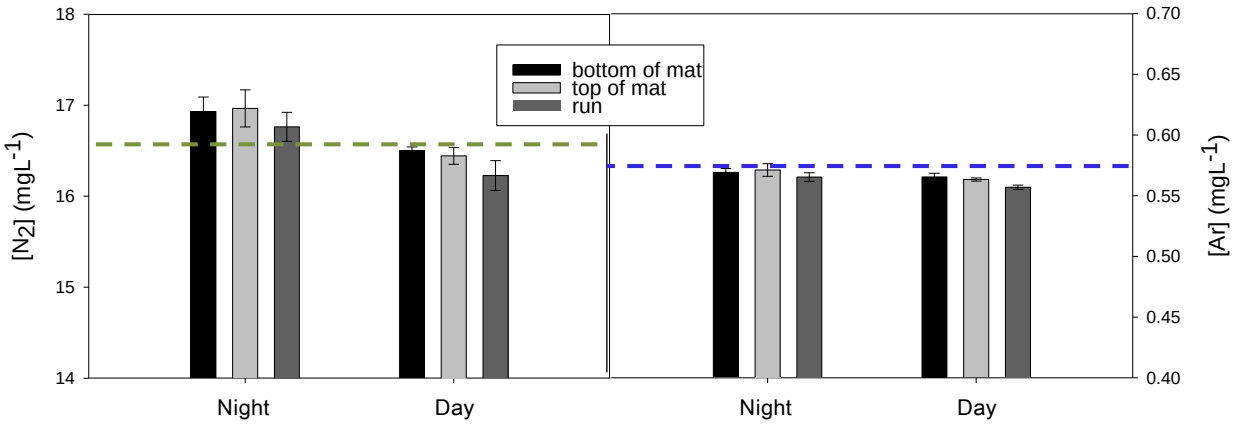

Fig. 7-11. Differences in the mean N_2 and Ar concentrations due to time of day and location. The dashed green line represents the mean vent N_2 concentration (16.65 mg/L) and the dashed blue line represents the mean vent Ar concentration (0.57 mg/L). Error bars are ± one standard error.

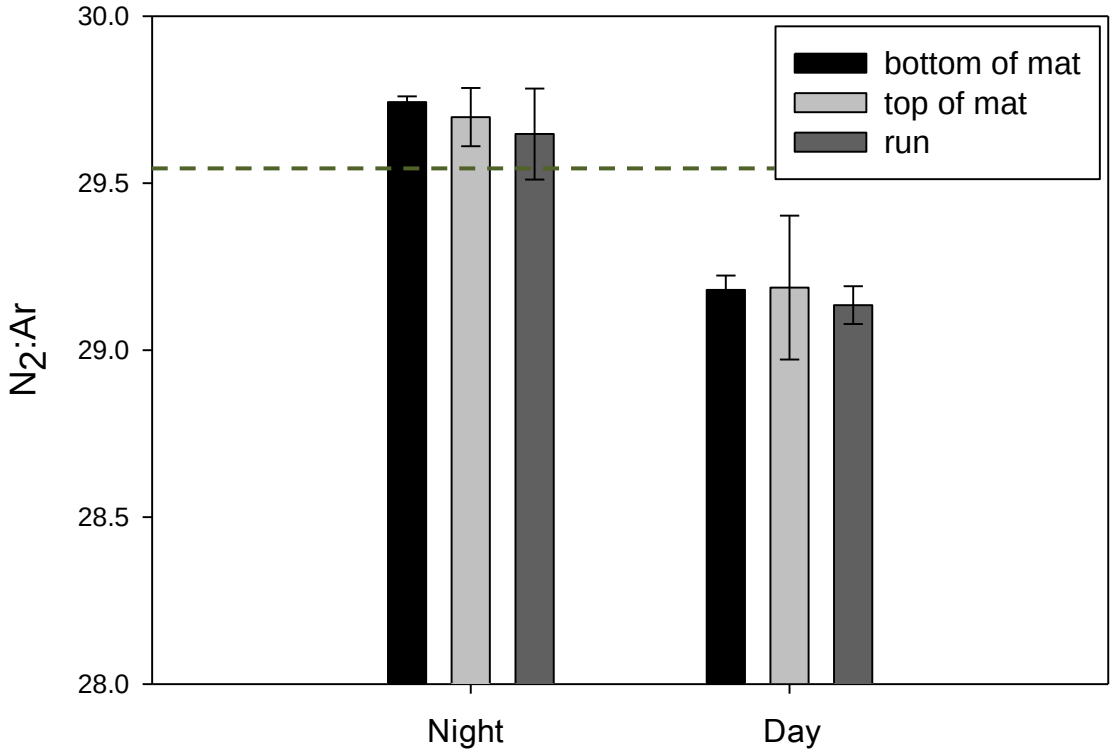

Fig. 7-12. Differences in the mean N_2:Ar ratio due to time of day and location in the river run. The dashed line represents the mean N_2:Ar ratio of the spring vent (29.57). Error bars are ± one standard error.

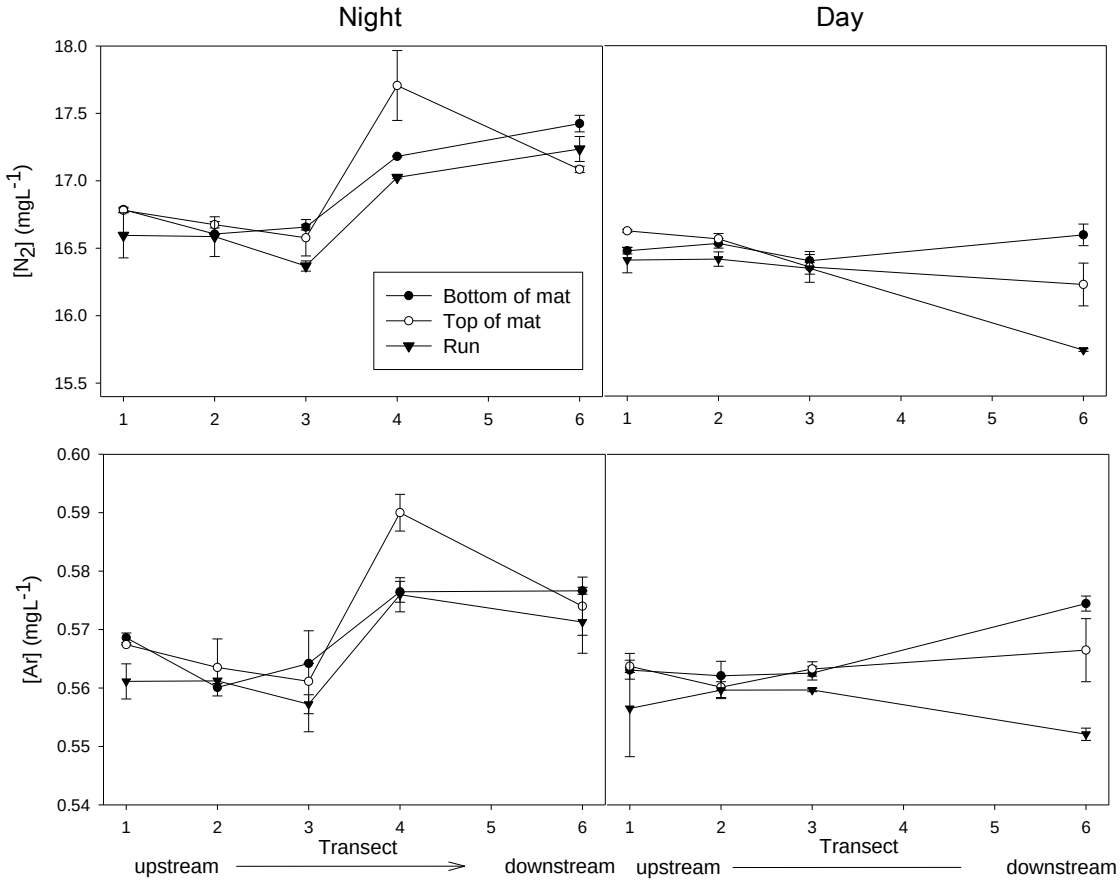

Fig. 7-13. N_2 and Argon concentrations at night and during the day at the bottom of the algal mat, at the top of the mat and in the river run, or water column. Data are shown across a longitudinal gradient.

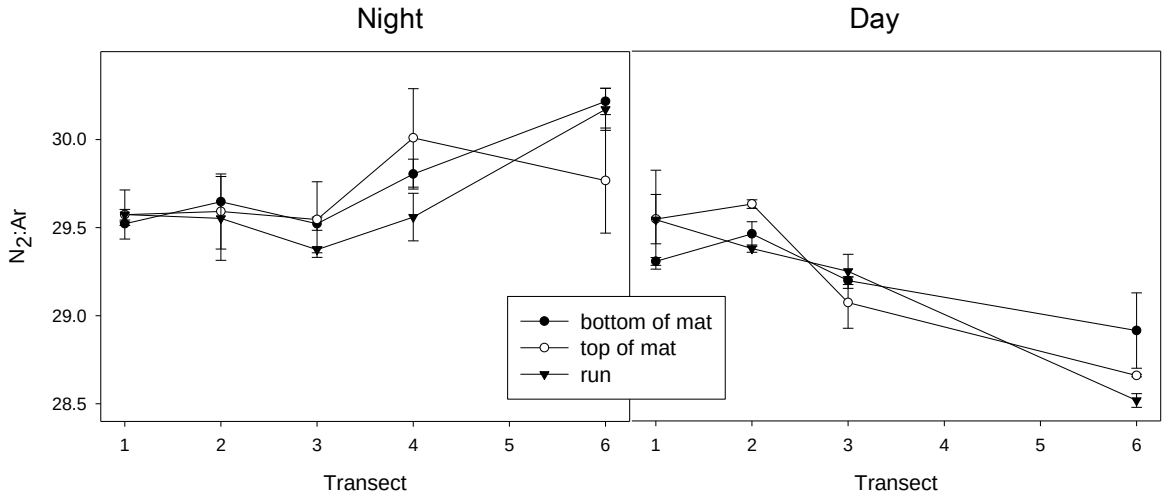

Fig. 7-14. Differences in mean night and day N_2:Ar ratio in the bottom of the algal mat, at the top of the mat and in the river run (water column).

Discussion

The overarching goal of our study was to discern the mechanisms causing the inverse diel variation in nitrate concentrations at Alexander Springs Creek; note that we also observed this pattern in Silver Glen Springs, another low nitrate system, but also one as dominated by algae as Alexander. We hypothesized that the reduction of nitrate concentrations at night was due to denitrification occurring in anoxic portions of the sediment/algal mat interface. During the day, we hypothesized that the spike in nitrate concentrations was due in large part to the inhibition of denitrification due to high DO concentrations within the mat, coupled with nitrification (re-mineralized ammonium within the benthic mat/sediment converted to nitrate). Since total N uptake during the day (the difference between nitrate concentration at the vent and nitrate concentration downriver) was relatively small (Fig. 7-3), we infer that nitrification rates must be large to replenish nitrate assimilated by the extremely large and highly productive benthic mat (mean GPP of 15g $O_2/m^2/d$). A diagram of N cycling within the benthic mat is shown in Figure 7-15.

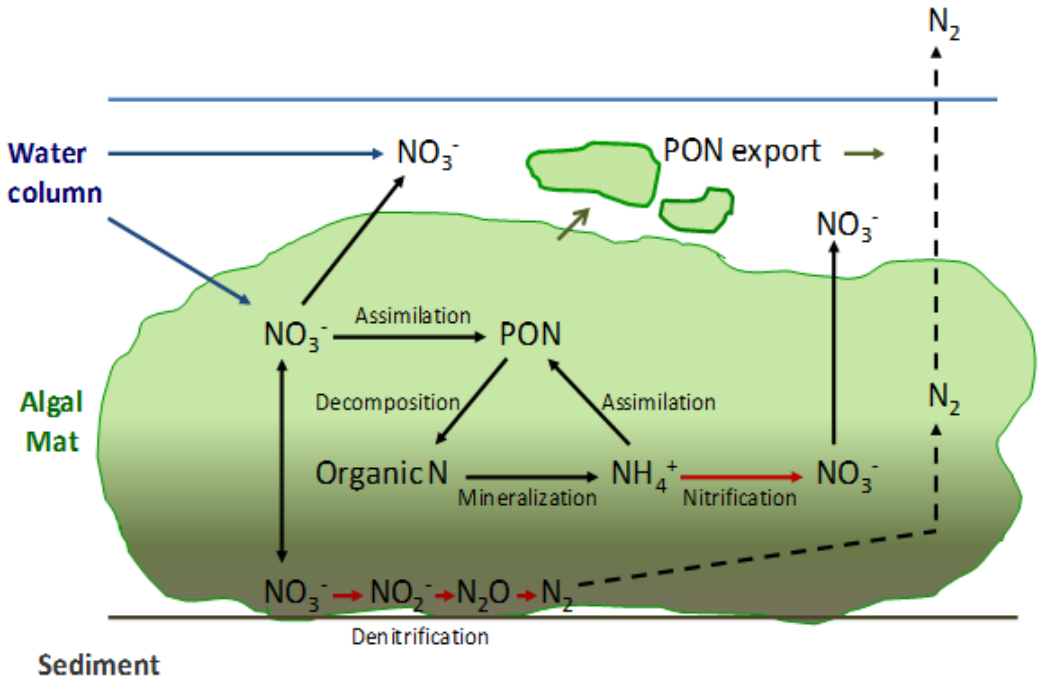

Fig. 7-15. Idealized diagram of nitrogen cycling within the benthic algal mat at Alexander Springs Creek. Red arrows indicate processes that can cause large fractionation in isotopic signatures. Denitrification often results in isotopically enriched (or heavy) residual nitrate (up to 40‰ heavier $\delta^{15}N$ than the original source), while nitrification can result in isotopically light $\delta^{15}N\text{-}NO_3$ (14 to 38‰ lighter than the original N source) (Kendall et al. 2007).

However, since the diel pattern in nitrate concentration is inverted at Alexander Springs Creek, we were unable to directly calculate nighttime denitrification rates as was done in other spring-fed rivers (see Research Element #2) and therefore assimilation vs. denitrification could not be separated. Because of this, and because we are unable to directly measure, or separate, assimilation vs. nitrification within the mat, several scenarios exist that could explain the N dynamics at Alexander Springs Creek. Two opposing extremes are discussed and evaluated below. We believe that what actually occurs is closer to the second scenario presented.

On one extreme end exists the possibility that most of the net removal during the night is actually due to assimilation rather than denitrification, and that little to no assimilation occurs during the day. Under this scenario, no internal recycling of N is needed to sustain the algal mat, and nitrate spikes during the day would be due to a little or no assimilation occurring, rather than nitrification playing a key role in replenishing nitrate concentrations in the water column. This scenario is highly unlikely, however, based on several lines of evidence.

First, although *Hydrodictyon reticulatum* (the likely species found in Alexander Springs Creek, R. Mattson, pers. communication) is known to take up nitrate both during the day and at night, nighttime assimilation is 20-25% less than daytime assimilation (Ulrich et al. 1998). *Hydrodictyon* cells have large vacuoles with the capacity to store high amounts of anions and Ulrich et al. (1998) found that as long the algal cells had enough stored energy, they were able to take up nitrogen both day and night. The algae assimilates the reduced form of N, however. The reduction of nitrate to nitrite and ammonium requires energy and therefore, the majority of nitrate uptake occurs during the day, when photosynthesis occurs.

Second, two lines of evidence indicate that denitrification is occurring at night. First, we found significantly higher N_2 concentrations and N_2:Ar ratios in the algal mat and the water column at night than during the day (Figs 7-13 and 7-14); higher N_2:Ar suggests that denitrification is occurring, as N_2 is the final product of denitrification. Additionally, at night, N_2 and N_2:Ar were higher in the algal mat and overlying water column than values in the vent water (Figs 7-13 and 7-14), further suggesting that denitrification processes occur in the sediment/algal interface. Second, we did find enriched $\delta^{15}N$ and $\delta^{18}O\text{-}NO_3$ in the mat at night (up to 20‰ and 13‰, respectively) as compared to the spring vent water (Figs. 7-8, 7-6C and 7-6D). Both the $\delta^{18}O$ and $\delta^{15}N$ of the residual nitrate increase systematically as a result of denitrification and the expected isotopic enrichment of $\delta^{18}O$ relative to $\delta^{15}N$ is 1:2 in groundwater (Kendall 1998, Chen and MacQuarrie 2005). If denitrification is diffusion limited, however,

the expected slope is closer to 1 (Sebilo et al. 2003, Granger et al. 2004). At Alexander Springs Creek, the slope of $\delta^{15}N$ vs. $\delta^{18}O$ in the algal mat at night was 0.8, which is more indicative of diffusion-limited denitrification (Fig. 7-8). Therefore, since we do have evidence of nighttime denitrification and *Hydrodictyon* sp. most likely assimilates more nitrate during the day than at night, we can be reasonably sure that this first scenario doesn't explain what we found at Alexander Springs Creek.

Under the second scenario, the opposite extreme of the first, the majority of N uptake at night is due to denitrification. During the day, denitrification is inhibited due to high DO conditions within the benthic mat, and the majority of assimilation takes place during the day. Spikes in nitrate concentration (or lack of expected draw-down) during the day could be explained by nitrification adding nitrate back into the water column, or by the assimilation of large amounts of internally recycled N; we calculated the upper bound of N recycled to meet demand at 61%.

The argument for denitrification occurring at night was discussed above and is compelling: higher N_2 concentrations and N_2:Ar ratios were found in the algal mat and the water column at night than during the day and enriched $\delta^{15}N$ and $\delta^{18}O$-NO_3 was found in the mat at night.

During the day, high DO concentrations in the algal mat and water column likely inhibit denitrification on the sediment/algal mat interface. In aquatic systems, higher dissolved oxygen concentrations in the water column as compared to the sediment results in the diffusion of oxygen into underlying sediments, inhibiting denitrification in the oxic layers (Christensen et al. 1990, Rysaard et al. 1994). We found significantly higher DO concentrations at the top and bottom of the algal mat as well as in the water column during the day (during peak photosynthesis) as compared to nighttime conditions (Figure 7-7). In the top portion of the algal mat in particular, mean DO concentrations were extremely high (7.72 mg/L), although concentrations in the bottom portion of the mat were also relatively high (3.23 mg/L), attesting to the high photosynthetic productivity of the algal mat. At Alexander Spring Creek, DO likely diffuses into the lower portions of the algal mat and sediment during the day, preventing or greatly reducing denitrification (by increasing the depth of the oxidized zone in which denitrification cannot occur). The fact that N_2 and N_2:Ar ratios are similar or lower in the algal mat and water column during the day than in the vent, and are significantly higher at night than during the day supports this argument as well. Additionally, the days with highest GPP (and therefore highest DO concentrations) were the days in which nitrate peaks in the water column were highest (Fig. 7-5), and makes it plausible that daytime DO concentrations can inhibit or greatly reduce denitrification, leading to higher nitrate concentrations in the water column during the day than at night.

We did find enriched $\delta^{15}N$ and $\delta^{18}O\text{-}NO_3$ in the algal mat and overlying water column during the day, however, which contradicts our argument that denitrification shuts down during the day. But, we don't understand the hydraulics of water movement through this mat and a possible explanation could be that the movement of residual nitrate (after denitrification processes occur) from the sediment or the bottom of the algal mat takes longer to diffuse into the upper portions of the mat and water column than N_2 gas. The enriched nitrate that we see during the day may have been processed the night before or, this may be evidence that denitrification does occur deeper in the sediment (due to DO diffusing into the sediment) even during the day, rather than completely shutting down.

In conjunction with inhibited or reduced denitrification during the day, relatively high nitrate concentrations could be explained either by high rates of nitrification or by significant internal recycling occurring within the mat. If the majority of the mineralized NH_4 within the mat was nitrified during the day, we would expect to see marked differences between daytime and nighttime NH_4 concentrations (much higher concentrations of NH_4 under nighttime conditions than during the day).However, we didn't find significant differences between day and night NH_4 within the benthic mat (Fig. 7-6B). Additionally, we didn't find evidence for nitrification in the $\delta^{15}N$ and $\delta^{18}O\text{-}NO_3$ signatures in the mat or water column. If ammonium concentrations are not limiting, nitrification generally results in isotopically light $\delta^{15}N\text{-}NO_3$ (14 to 38‰ lighter than the original N source) (Kendall et al. 2007). Under limiting conditions, all of the ammonium would be converted to nitrate and no fractionation would occur. At Alexander Springs Creek, mean NH_4 concentration (Day + Night) was significantly higher at the bottom of the mat than in any other location and even nitrate was significantly higher in the bottom portions of the algal mat than in the water column (Figs. 7-6A and 6B). Ammonium does accumulate within these mats as compared to the overlying water column and if nitrification were a major source of nitrate, we would expect to see much lighter $\delta^{15}N\text{- }NO_3$ in the mat or water column than in the vent. Instead, we found that the $\delta^{15}N\text{-}NO_3$ is either the same or is enriched as compared to the vent (Figs. 7-6, 7-8 and 7-9).

Since (1) there is little to no evidence for high rates of nitrification occurring in the benthic mat, (2) the algae assimilates most of its nitrate during the day and (3) there is relatively little mass N removal occurring during the day (Fig. 7-3), the algae has to rely heavily on internal recycling to meet N demand, possibly as high as the 61% upper bound that we calculated. The isotopic signature of the algae provides evidence for this. The $\delta^{15}N$ of the algal tissue ranged from 6-8‰ (mean 7‰) and was very similar to the $\delta^{15}N\text{-}NO_3$ of the spring vent (7‰) (Fig. 7-6C). Based on these signatures, a plausible explanation is that the algae is getting its nitrate from two sources: directly from nitrate in the overlying water column and

from the assimilation of mineralized ammonium. De Brabandere et al. (2007) found that fractionation in periphyton attached to macrophytes in the spring-fed Chassahowitzka and Homossassa rivers varied from 0.7 to 2.5 ‰ ($\delta^{15}N$ of the periphyton was this much lighter than $\delta^{15}N$-NO_3 of the water column) and they state that fractionation between algae and nitrate reported for field conditions in the literature ranges from 2.5 to 10 ‰ (multiple sources listed therein). In a regional study of spring vent pools in Florida, Albertin et al. 2011 found that algal $\delta^{15}N$ fractionation varied from 2 to 13 ‰. Therefore, the slightly lighter $\delta^{15}N$ of some of the algal tissue (6‰) than the vent $\delta^{15}N$ could be due to minimal fractionation during assimilation of vent-water nitrate. Mineralization (or ammonification) generally only causes little fractionation as well; in soils, fractionation is ±1‰ between soil organic carbon and NH_4 (Kendall et al. 2007). This also agrees with the signatures that we found in the algal tissue.

Based on the arguments and evidence presented above, we believe that the second scenario most closely explains what we found along the Alexander Springs Creek, and is as follows. The majority of N uptake at night is due to denitrification, although some assimilation by *Hydrodictyon* sp. can occur as well. During the day, denitrification is inhibited due to high DO conditions within the benthic mat and in the sediment. The majority of N assimilation takes place during the day and relatively high levels of nitrate in the water column can be explained by the assimilation of large amounts of internally recycled N, as high as 61%, rather than by relying solely on water column nitrate.

Seston export

Finally, an astounding amount of seston (made up largely of masses of *Hydrodictyon* sp. with pieces of other macrophytes and terrestrial organic carbon interspersed) flows downriver each day. We calculated that a total dry mass of 368 kg/day, or 1% of the standing benthic mat, is exported daily. A study conducted by Wetland Solutions, Inc. (2007) also measured community export (seston), both as dry mass and as organic carbon (ash –free dry weight), along Alexander Springs Creek. Unlike our study, though, they reported a net loss of export between the upper and lower transects used for measurement. It is difficult to compare both studies, however, because they were conducted in completely different reaches of the river run. The upper and lower sites used by Wetlands Solutions, Inc. were much further downstream (the upstream site was approximately 1500 m from the spring vent and the downstream site was at the CR-445 bridge), and the reach studied was dominated by SAV. Our study site was conducted much further upstream (550 m from the spring vent) in an area dominated by a continuous benthic mat, with relatively little SAV present. Even so, the amount of seston dry mass that we captured (550m from the vent) ranged from 0.29 to 33.52 g/m2/day, depending on the time in

which the seston net was sampled (data not shown), and the amount of dry mass captured in the upstream site by Wetlands Solutions, Inc. (1500m from the spring vent) ranged from 0.428 to 0.646 g/m2/day, values within the lower bound of our range. Additionally, floating seston can be trapped by SAV in the river run. Part of the reduction in seston seen further downstream may be because it gets caught in SAV as it floats downriver. We found that peak export times were in the afternoon, when photosynthesis was highest, and a possible explanation is that oxygen bubbles formed within the algal mat, helping to slough off overlying masses of algae. Although human disturbance (recreating swimmers) causes benthic mats to all but disappear in the vent pool during peak summer months, we don't believe that recreation had a significant impact on seston export during this study. We sampled in early fall, during the week (rather than on the weekend, when visitation is highest at Alexander Springs). Additionally, the seston net was placed at the downstream end of the continuous benthic mat (which covered a 24,000 m^2 area) and no swimming is allowed over this entire area. The vent pool comprises a much smaller area (7000 m^2) (Scott 2004) and was not covered by benthic mats during the time of this study; algal mats were restricted to the deeper portions of the pool, where swimmers could not stand, as well as along the edges of the pool.

Research Element #8 – Method Application in Blackwater Rivers

(with Ray Thomas, Dept. of Geological Sciences, University of Florida)

Introduction

The methods used in this work to determine riverine N cycling in clear spring-fed rivers have yet to be applied to blackwater systems. The primary constraint is the confounding effects of colored dissolved organic carbon that is photoreactive in the same deep UV region in which the nitrate sensors detect nitrate concentrations. This section describes bench-top work with the UV nitrate analyzers used in other sections to determine thresholds of DOC concentrations above which methods employed herein are no longer viable. Ongoing work at the University of Florida (Ray G. Thomas, Department of Geological Sciences) is investigating the use of chemical DOC removal techniques that may allow application in darkly tannic waters. An outline of these concepts is also presented.

The primary methodological constraint to the SUNAs is that anything that occludes light in the low UV (ca. 220 nm) will interfere with the algorithms used to infer nitrate concentrations. These include excess turbidity and colored organic carbon. In the low relief systems in Florida, the former tends not to be a problem, except where turbidity is of biological origin. Moreover, in-filtering can ameliorate this problem with too much additional field equipment (though power and maintenance demands of pumped, filtered systems can be logistically challenging). The latter, OM interferences, are more significant in our blackwater systems, and also present a more vexing corrective challenge. While resins exist that bind to OM, and a variety of oxidation agents (e.g., hypochlorite, persulfate) can be added to the water to reduce OM content, these are both expensive and potentially influence the nitrate concentration of the water (e.g., by making nitrate during oxidation). While a variety of techniques are being explored to optimally reduce OM interference, none, as yet, can reliably remove OM entirely. This section describes a sequence of matrix dilutions on high OM site water (ca. 50 mg C/L DOM) from the Santa Fe River to detect what levels of DOC are needed for reliable instrument inference of nitrate. This sets two important application bounds. First, it establishes the range of environmental conditions under which sensors can be deployed without additional chemical controls. Second, it sets a target threshold for DOC removal using the variety of means available at sites where DOC levels are too high for reliable application.

Methods

We sampled 10 L of water from the Santa Fe River near Worthington Springs during moderately high flow conditions in late 2009. We selected this site because it is among the most unimpacted blackwater

systems within easy access of Gainesville Florida, and because the DOC levels in the upper part of the Santa Fe River basin (where we sampled) are among the highest in North Florida. We established a baseline DOC concentration for the sample of 50.5 mg C/L, which is on the high side of normal for the long term average DOC concentration on the Santa Fe River, and representative of plausible conditions present on blackwater rivers throughout the Southeast.

The base water sample was diluted to 1:1, 1:3, 1:4, 1:9, and 1:19 solutions with DI water; resulting DOC concentrations were 50, 25, 12.5, 10, 5 and 2.5 mg C/L. The 50 and 25 mg/L matrices resulted in sensor errors suggesting insufficient water transmittance, and were omitted from the remaining discussion.

For each solution we assumed the background concentration was negligible; the actual concentration (measured using ion chromatography in the Hydrogeochemistry Lab, Geological Sciences, University of Florida) was 0.04 mg N/L and this value, adjusted for dilution, was included when evaluating the association between predicted and observed. To each solution we added sufficient volume of 1000 mg/L nitrate standard solution to achieve nitrate concentrations of 0.05, 0.1., 0.25, 0.5 and 1.0 mg/L (again, neglecting the internal nitrate concentration, which was corrected following the experiment).

The SUNA, running in continuous mode (i.e., 1 sample every 2 seconds) was allowed to warm up for 1 hour prior to sequential placement of the sensor in each solution for 5 minutes, progressing from low to high nitrate concentration to minimize contamination between solutions. The sensor was rinsed with DI water between solutions, and checked for interference from bubbles on the optical lens. Accuracy and precision for each solution was evaluated, and is reported as a standard deviation for precision assessment, and root-mean square error (RMSE) and mean error (ME) for accuracy assessment.

Results

To illustrate the point about DOC interference, we first present UV spectra obtained from the SUNA deployed in the field at 5 locations in the Santa Fe Basin plus deionized water (Fig. 8-1). The field sites, in order of water color are 1) a clear water site at the US27 Bridge on the Ichetucknee River, 2) a sites (2800) just upstream of the confluence of the Santa Fe with the Suwannee, which was clear at the time of sampling, but is not always this way, 3) a site just downstream of Ginnie Springs that is similarly variable, with high discharge corresponding to high color and low discharge, like at the time of sampling, resulting in low color, 3) a high color site at Worthington Springs, above the River Sink in a portion of the

basin dominated by highly tannic streams, and 5) an extremely dark water site at Station 02322700 on the Upper Santa Fe River, which drains Santa Fe Swamp (Fig. 8-1); deionized water is included as a contrast. Note two salient aspects in the contrast between the spectra. The clear water sites and DI exhibit complex variation in the spectra (largely due to the lamp intensity at different wavelengths and natural attenuation by water), and shows transmittance values that range from 500 to 20000. In contrast, the tannic water sites exhibits essentially no transmittance of the spectral features observed in clear water, and overall transmittance is more than and order of magnitude lower. Compounding the problem is the fact that transmittance in the 220-240 nm range, which is highly dynamic in the clear water sites, is completely occluded in the dark water sites. Note, this is a signal problem, not one that can be readily fixed with algorithms; that is, the problem is not one of inference (i.e., that might be improved by alternative statistical approaches), but of the complete loss of the signal that can be interpreted. Physically or chemically removing that DOC signal is an ongoing challenge, and it remains to be seen if the nitrate signal beneath can be adequately revealed or not.

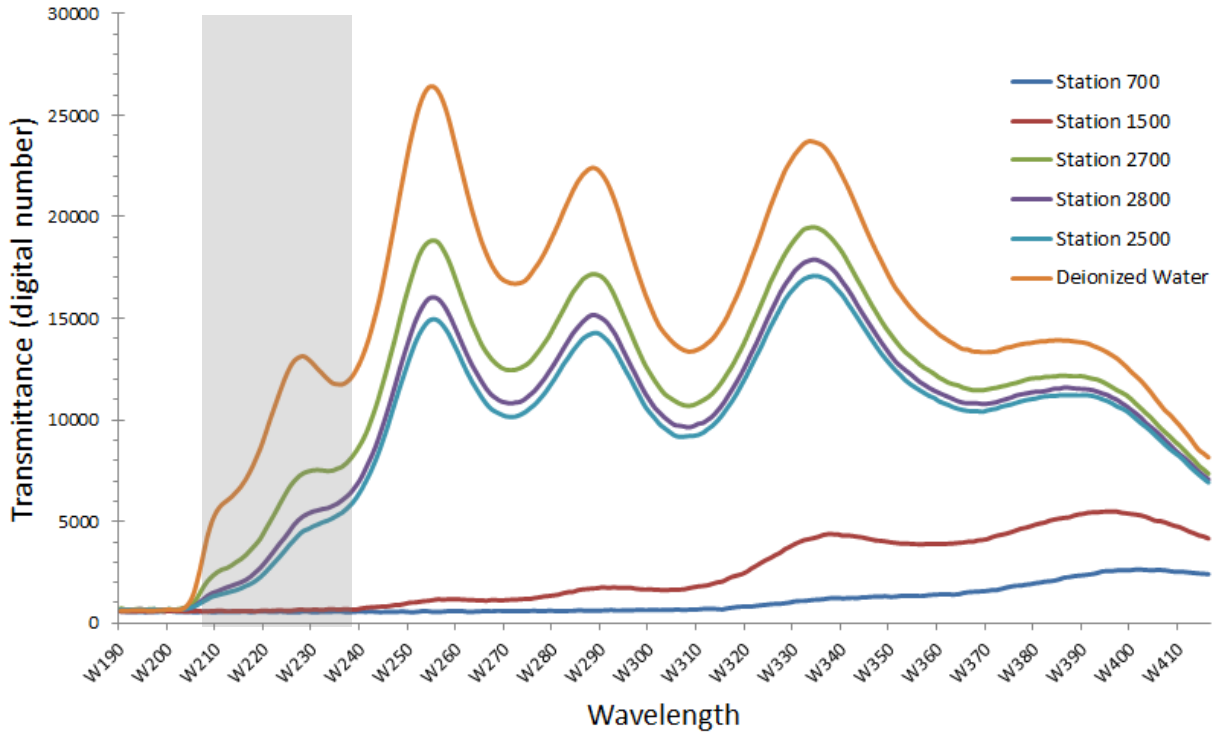

Fig. 8-1– UV spectra for water obtained from different regions of the Santa Fe River. Stations 700 and 1500 are head water reaches and have highly tannic water, while, at the time of sampling, stations 2700, 2800 and 2500 were clear spring water. Note that 2700 (Ichetucknee River) almost always has clear water while 2800 and 2500 (main stem, near the Suwannee confluence and below Ginnie Springs, respectively) vary between clear spring water at low flow and highly tannic water at high flow. Deionized water is shown for comparison. Grey area denotes spectral region of nitrate absorbance.

For the experiment wherein we explored what levels of DOC permit acceptable signals, we report the mean spectra for the ca. 10-15 minutes during which the sensor was placed in each water sample. Fig. 8-2 shows the spectrographs for the lowest DOC solution (2.5 mg/L or 1-in-20 solution). Two salient features are worth noting. First, the absorbance due to this level of color is relatively small, as evidenced by the relatively modest drop-off in the magnitude of the signal. Second, the spectral response in the deep UV region where nitrate is absorbent is strongly evident. Note that higher nitrate spikes transmit less light, as would be expected.

Similar graphs for each of the dilutions (in order of increasing resulting DOC concentration) are shown in Fig. 8-3 through Fig. 8-5. Note two key things. First, the effect of increasing DOC is to dramatically reduce the transmittance throughout the spectrum, but particularly in the deeper UV portion of the spectrum where nitrate is photoreactive. Second, the signal in the region of active nitrate absorbance is increasingly occluded by DOC, such that for the 12.5 mg DOC/L solution, the variation in absorbance among the nitrate spikes is nearly undetectable. The internal SUNA algorithm accounts for the overall transmittance effect by correcting the nitrate estimate based on absorbance in other portions of the spectrum, but it cannot interpret a signal that has been entirely occluded, and we contend that this occurs at or around 12.5 mg DOC/L.

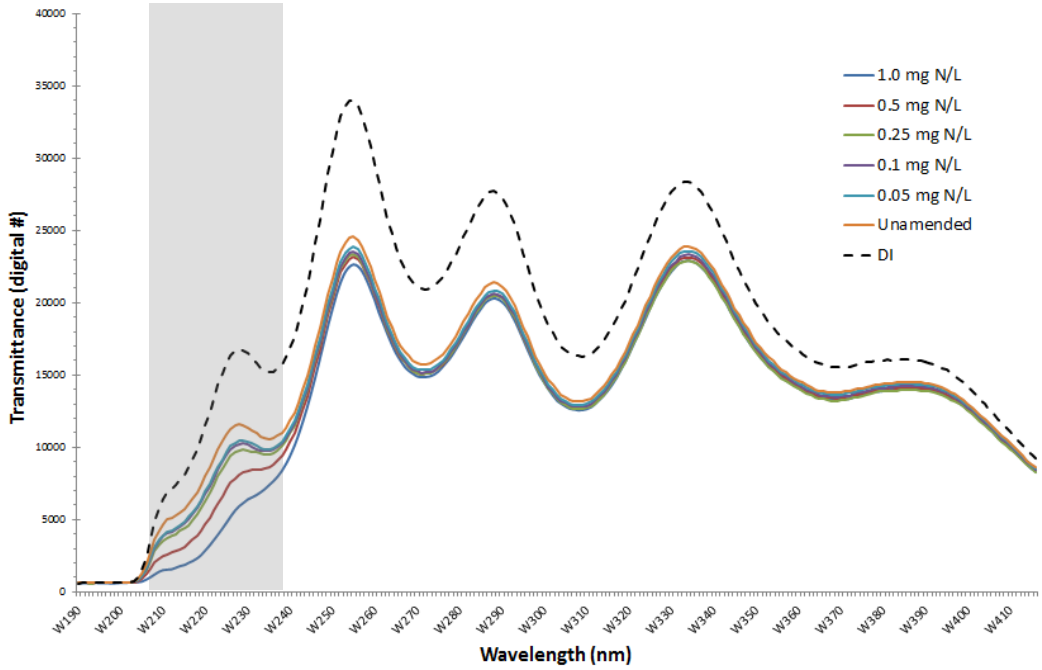

Fig. 8-2 – Transmittance measurements for a 5% solution of Santa Fe River water (ca. 2.5 mg DOC/L) with various nitrate spikes. Transmittance through deionized water shown for comparison (dashed line). Note the variation in the range of 205 to 240 nm, which is where nitrate is UV-absorbent. Grey area denotes spectral region of nitrate absorbance.

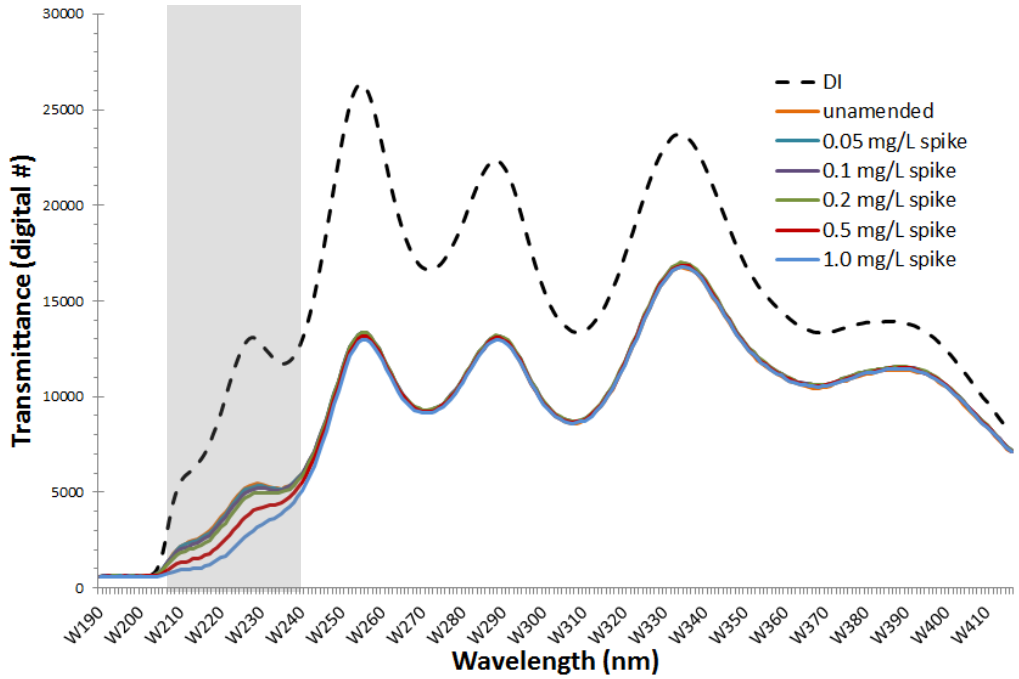

Fig. 8-3 – Transmittance measurements for a 10% solution of Santa Fe River water (ca. 5 mg DOC/L) with various nitrate spikes. Transmittance through deionized water shown for comparison (dashed line). Note the variation in the range of 205 to 240 nm, which is where nitrate is UV-absorbent. Grey area denotes spectral region of nitrate absorbance.

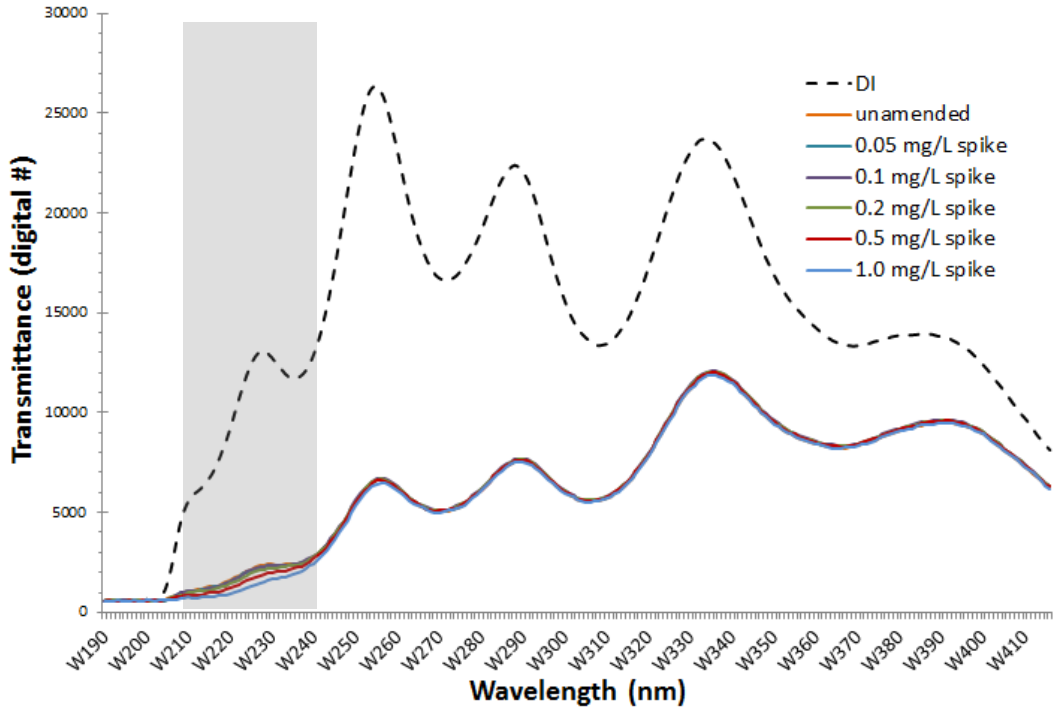

Fig. 8-4 – Transmittance measurements for a 20% solution of Santa Fe River water (ca. 10 mg DOC/L) with various nitrate spikes. Transmittance through deionized water shown for comparison (dashed line). Note muted but still detectable variation between 205 to 240 nm, where nitrate is UV-absorbent. Grey area denotes spectral region of nitrate absorbance.

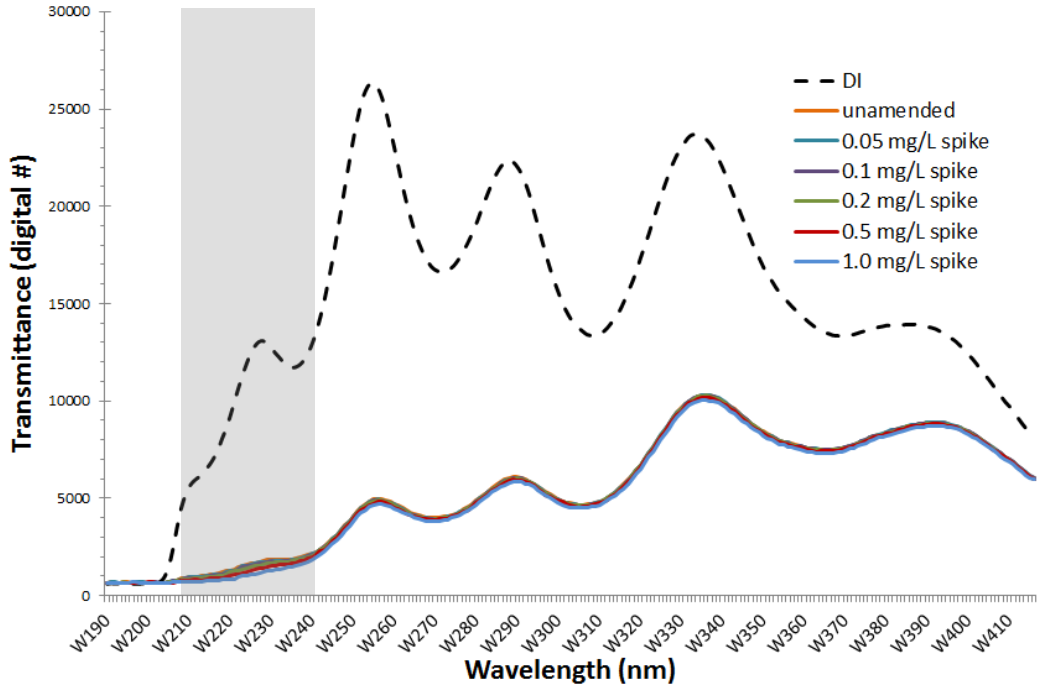

Fig. 8-5– Transmittance measurements for a 25% solution of Santa Fe River water (ca. 12.5 mg DOC/L) with various nitrate spikes. Transmittance through deionized water shown for comparison (dashed line). Note the loss of variation in the range of 205 to 240 nm, which is where nitrate is UV-absorbent. Grey area denotes spectral region of nitrate absorbance.

Based on the SUNA estimates for each dilution and matrix spike, we compared the measured and expected concentrations. Estimated concentrations were adjusted based on the nitrate content of the Santa Fe River water (0.04 mg/L) so the values are not exactly the magnitude of the matrix spike expected concentration. That is, for the 1.0 mg N/L spike, the expected concentration is something slightly higher depending on the sample dilution. For the period of measurement (typically 8-12 minutes) in each sample, we calculate a standard deviation of the estimate, and report that as the error bars in Fig. 8-6 through 8-9. Note that the expected and measured concentrations are are reported on a log-scale to allow clear visual assessment of agreement at the lower concentrations; as such, error bars are assymetrical.

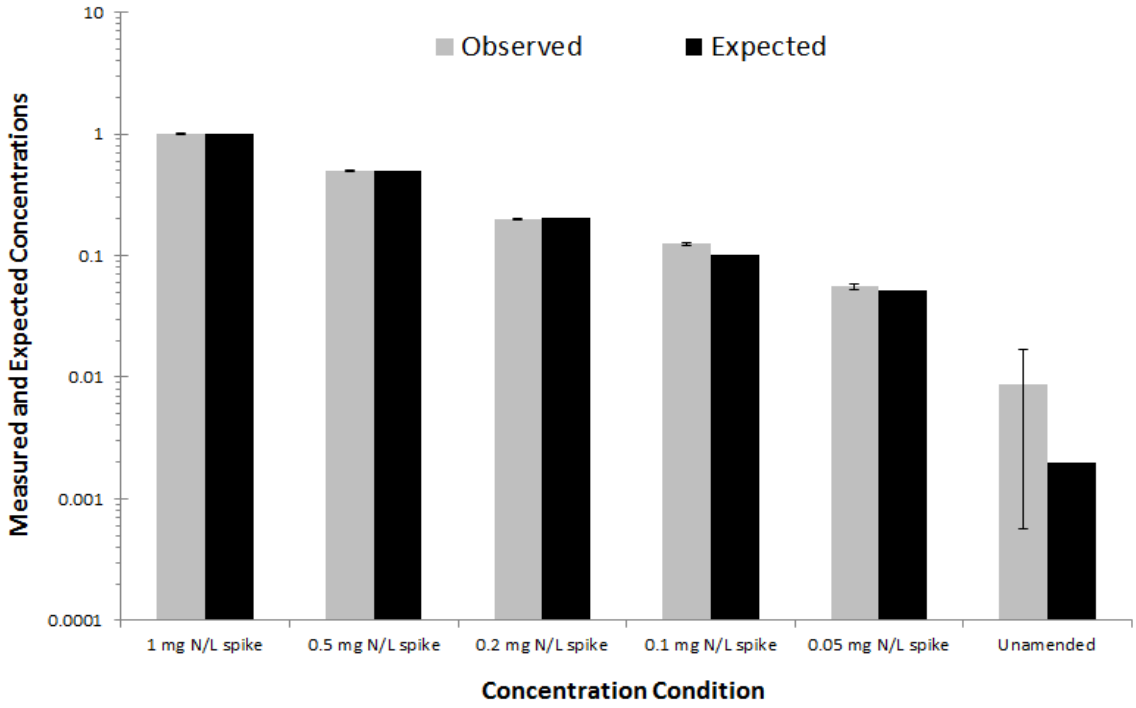

Fig. 8-6 – Expected (grey bars) and observed (black bars) nitrate concentrations for the 5% solution at different matrix spikes, including unamended. Error bars represent 1 standard deviation around the mean for the duration of the sensor installation in each sample.

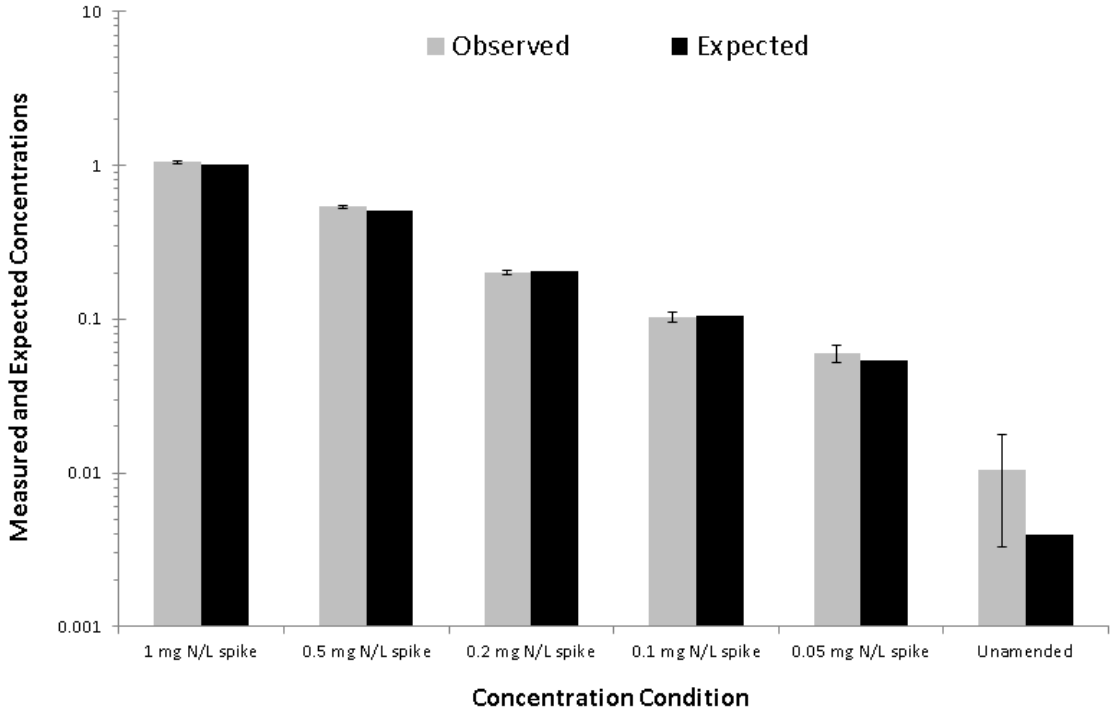

Fig. 8-7 – Expected (grey bars) and observed (black bars) nitrate concentrations for the 10% solution at different matrix spikes, including unamended. Error bars represent 1 standard deviation around the mean for the duration of the sensor installation in each sample.

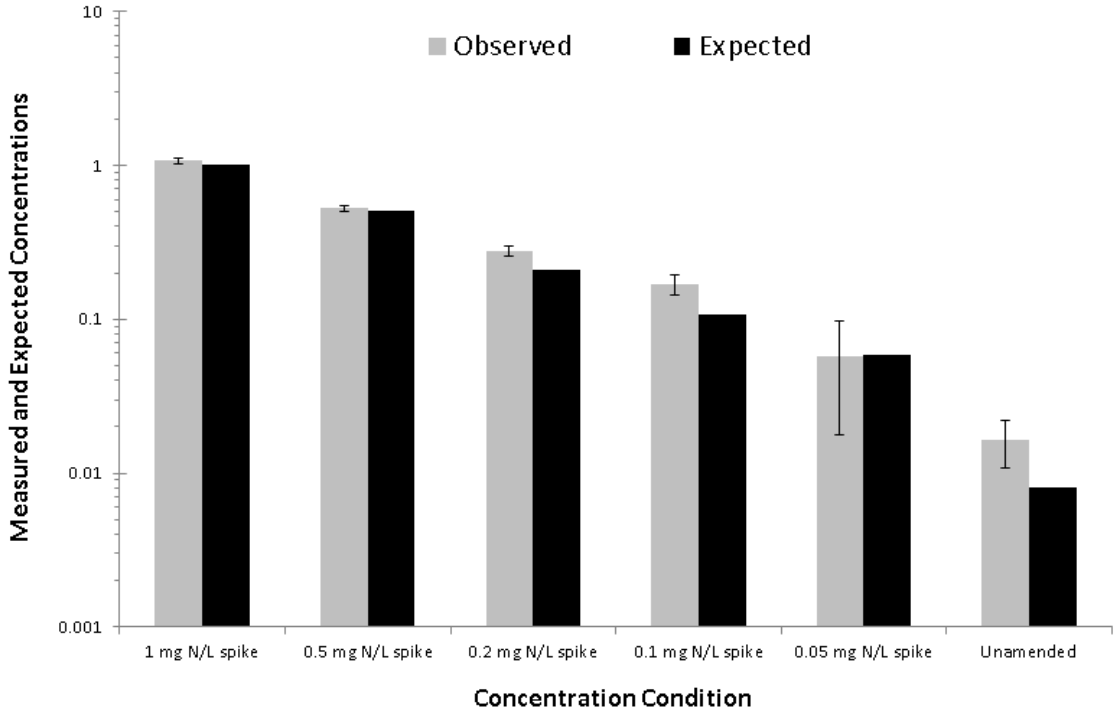

Fig. 8-8– Expected (grey bars) and observed (black bars) nitrate concentrations for the 20% solution at different matrix spikes, including unamended. Error bars represent 1 standard deviation around the mean for the duration of the sensor installation in each sample.

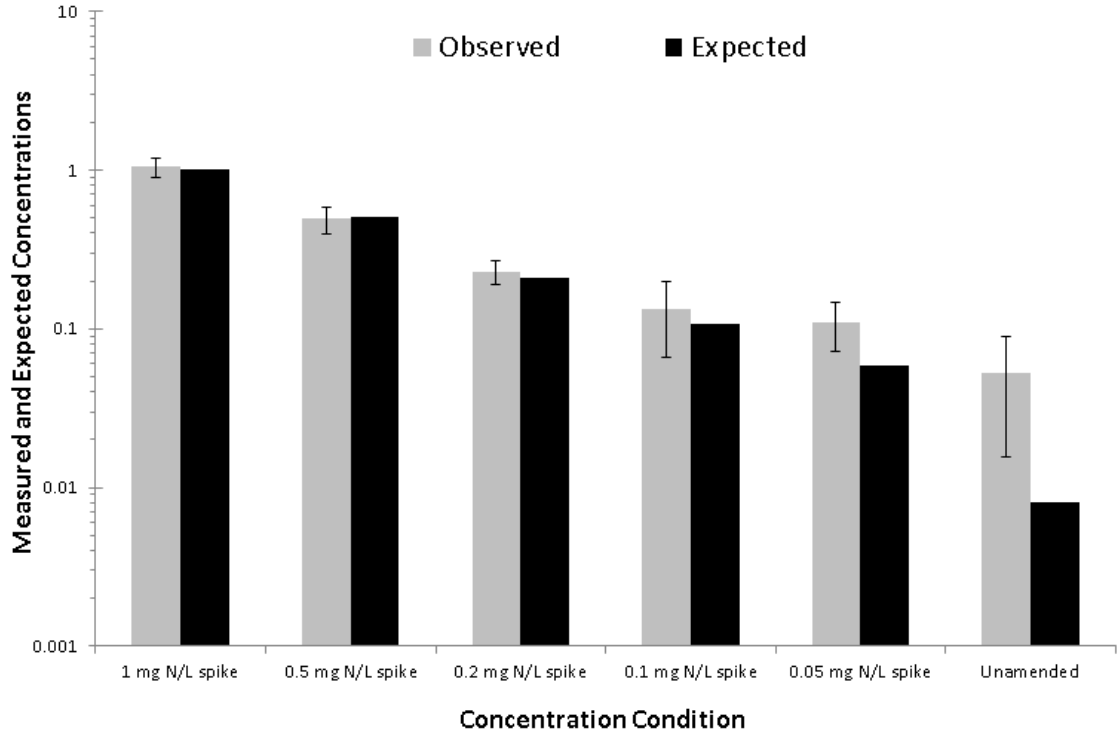

Fig. 8-9 – Expected (grey bars) and observed (black bars) nitrate concentrations for the 25% solution at different matrix spikes, including unamended. Error bars represent 1 standard deviation around the mean for the duration of the sensor installation in each sample.

Finally, we report the standard deviations for each solution (DOC x NO3 concentrations) to assess the precision of each estimate (Fig. 8-10), and the root mean squared error (RMSE) to assess the accuracy of each estimate (Fig. 8-11). The precision is relatively good for the low DOC samples across all matrix spikes, but declines markedly at higher DOC. Note that values at 25 mg DOC/L (the next dilution step) are not presented because no nitrate estimates were obtained (the sensor reported an error related to insufficient light). Note that the error rates for the low DOC samples at low nitrate concentrations are MUCH better than the manufacturer precision specifications of 2 µM or 0.028 mg N/L; values were between 3 and 8 µg/L, or as much as 80% better than was reported. Error rates at higher DOC values were higher

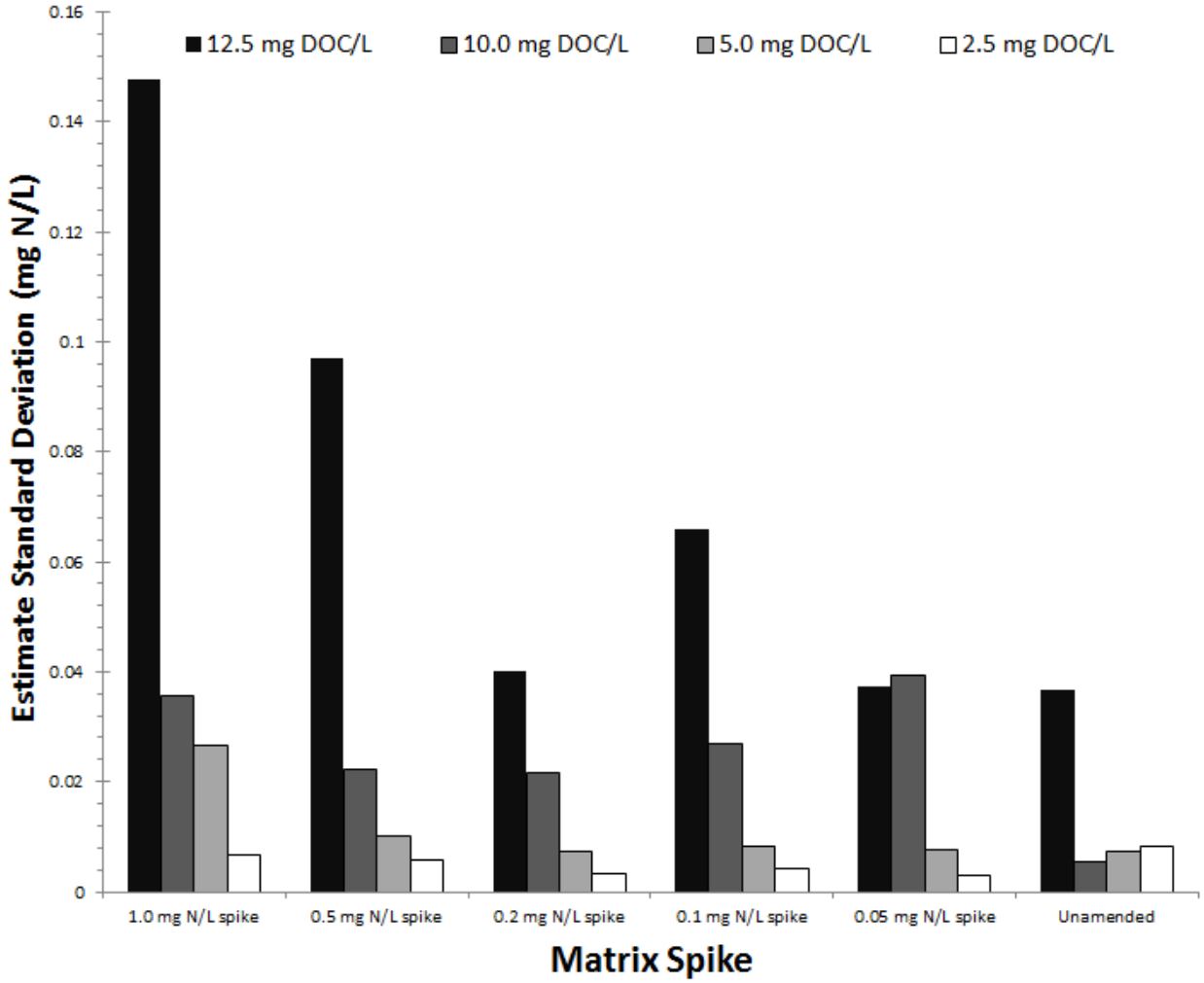

Fig. 8-10 – Standard deviation around the mean of measurements made at 2 second intervals in each solution (DOC x nitrate). Bars represent different DOC concentrations, while different nitrate spikes are shown as categories along the x-axis. The standard deviation (in mg N/L) are the resulting value. Note that the coefficient variation (CV = SD:Mean) is actually lowest for the 1.0 mg N/L spike and highest for the unamended solution.

than the published specifications, sometimes by a significant amount (average = 0.070 mg/L). The striking pattern of higher error at higher DOC concentrations was unexpected, and the reasons for this behavior are unknown.

A similar analysis of DOC interference of accuracy, as measured by the root mean squared error, shows a very similar pattern. Errors were higher for higher DOC, and for higher concentrations. However, several anomalies stood out. Specifically, the accuracy of the 0.2 mg N/L solution as lowest for the 10 mg DOC/L solution rather than the 12.5 mg DOC/L solution, and was nearly worse for 0.1 mg N/L. Low accuracy was seen for the 5 mg DOC/L in only the higher nitrate spikes, which is difficult to understand.

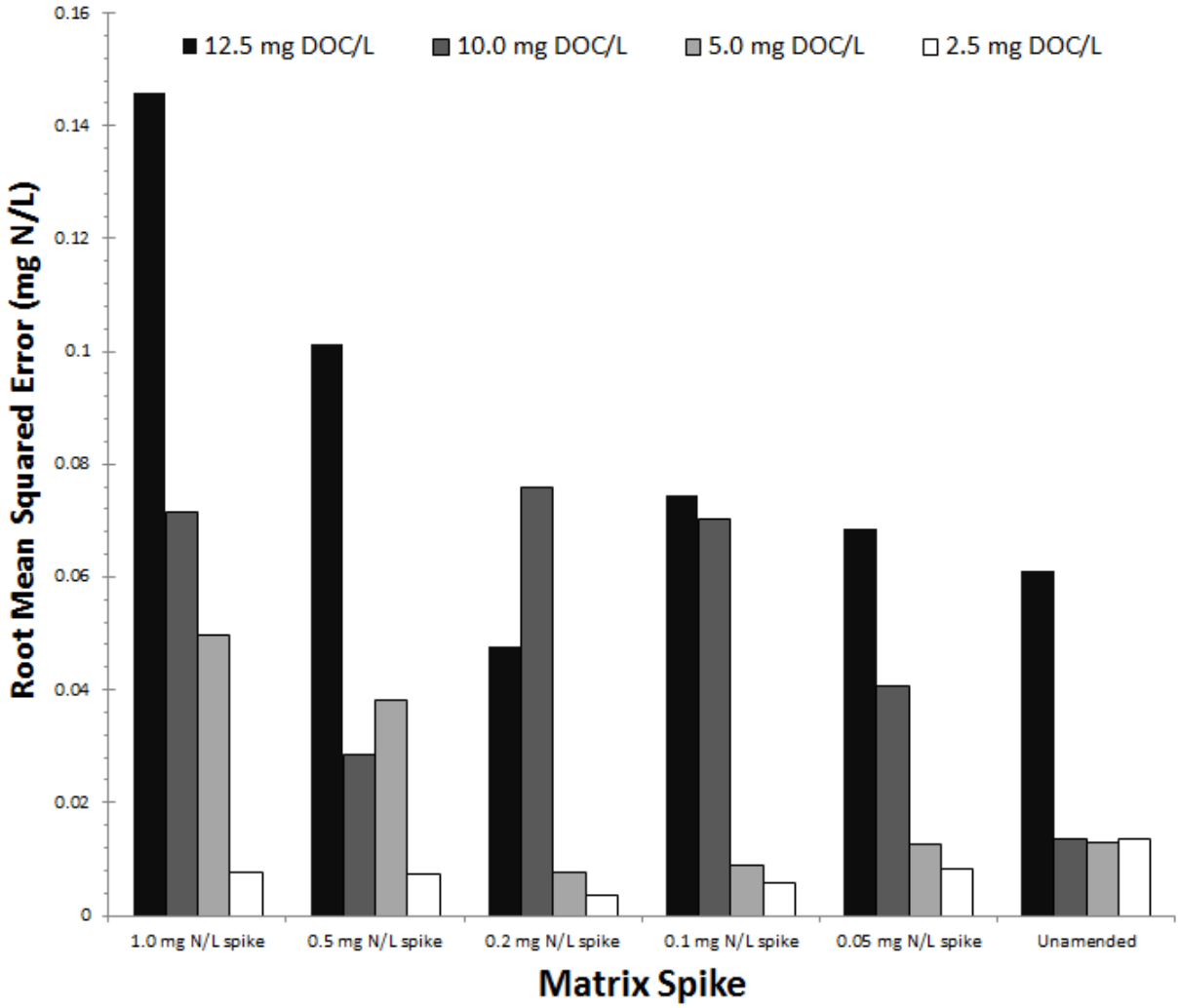

Fig. 8-11 – Root mean squared error of measurements (vis-à-vis the expected concentration) made at 2 second intervals in each solution (DOC x nitrate). Bars represent different DOC concentrations, while different nitrate spikes are shown as categories along the x-axis. The RMSE (in mg N/L) are the resulting value.

Discussion

The overall implications of these data are that the sensors are deployed out of the box (i.e., with no new algorithms or DOC corrective action) are viable for river conditions up to ca. 12.5 mg DOC/L. This level is compatible with most rivers in the country, but NOT the blackwater rivers of the Southeastern Coastal Plain. Applications in those river systems will require additional considerations, including new algorithms that can operate at low signal, new hardware (to increase the transmittance signal, perhaps by adjusting the path length), and techniques for attenuating the absorbance effects of DOC.

The first two approaches are unlikely to be fruitful for extending the utility of these sensors into the range necessary for use in black water rivers. They may expand the range of appropriate settings somewhat, but concentrations 5 or more times those at which signal occlusion was observed are typical in the coastal plain and actually do not contain a nitrate signal any longer because the DOC signal is so strong. As such, techniques for actively removing the DOC interference are required. Ray Thomas (Dept. of Geological Science at the University of Florida) has been working on this problem, and has constructed several promising proto-type approaches that may extend the method utility to black water rivers substantially. Specifically, he has explored the use of oxidation reagents and low level UV irradiation to effectively eliminate the chromophores that lead to UV light absorbance without also creating new nitrate (i.e., via complete oxidation of DOC to mineral constituents).

While these methods may make some SUNA applications possible, they also constrain how the sensors are used. Specifically, the irradiation time is ca. 1 hr, meaning that the temporal sampling resolution is lower. This precludes their use for longitudinal transects, and increases the uncertainty within the diel method. However, the methods presented is this report apply to a broad range of rivers and may permit a significant increase in our understanding of their temporal behavior and process rates, even at lower accuracy and precision.

References Cited

Albertin A. 2009. Nutrient dynamics in Florida Springs and relationships to algal blooms. Ph.D. Dissertation, University of Florida

Albertin, A. R., J.O. Sickman, A. Pinowska, & R.J. Stevenson. 2001. Identification of nitrogen sources and transformations within karst springs using isotope tracers of nitrogen. *Biogeochemistry* **in press**, doi:DOI: 10.1007/s10533-011-9592-0.

Alexander R.B., R.A. Smith and G.E. Schwarz. 2000. Effect of stream channel size on the delivery of nitrogen to the Gulf of Mexico. Nature 403:758-761

APHA, AWWA & WEF. 2005. *Standard Methods for the examination of water and wastewater*. Method 4500-NO_3^- B. 21st edn, American Public Health Association, Washington, DC.

Aravena, R. and W.D. Robertson. 1998. Use of multiple isotopic tracers to evaluate denitrification in ground water: Study of nitrate from a large-flux septic tank system plume. Ground Water 36:975-982

Arthur, J. D., Wood, H. A. R., Baker, A. E., Cichon, J. R. & Raines, G. L. 2007. Development and Implementation of a Bayesian-based Aquifer Vulnerability Assessment in Florida: . *Natural Resources Research, Vol. 16, No. 2, p. 93 - 107* **16**, 93-107.

Bacchus, S. T. and P. J. Barile. 2005. Discriminating sources and flowpaths of anthropogenic nitrogen discharges to Florida springs, streams and lakes. Environmental & Engineering Geoscience 11: 347-369

Battaglin, W.A., C. Kendall, C.C.Y. Chang, S.R. Silva and D.H. Campbell. 2001. Chemical and isotopic evidence of nitrogen transformation in the Mississippi River, 1997-98. Hydrological Processes 15:1285-1300

Bencala, K.E. and R.A. Walters. 1983a. Simulation of solute transport in a mountain pool-and-riffle stream: a transient storage model. Water Resources Research 19:718–724

Bencala, K.E., D.M. McKnight and G.W. Zellweger. 1990. Characterization of transport in an acidic and metal-rich mountain stream based on a lithium tracer injection and simulations of transient storage. Water Resources Research 26:989–100

Bencala, K.E., R.E. Rathbun and A.P. Jackman. 1983b. Rhodamine WT dye losses in a mountain stream environment. Water Resources Bulletin 19:943–950

Boedeltje, G., A. J. P. Smolders, and J. G. M. Roelofs. 2005. Combined effects of water column nitrate enrichment, sediment type and irradiance on growth and foliar nutrient concentrations of Potamogeton alpines. Freshwater Biology 50: 1537-1547.

Böhlke, J. K. 2002. Groundwater recharge and agricultural contamination. *Hydrogeology Journal* **10**, 153-179, doi:10.1007/s10040-001-0183-3

Böhlke, J. K., Wanty, R., Tuttle, M., Delin, G. & Landon, M. 2002. Denitrification in the recharge area and discharge area of a transient agricultural nitrate plume in a glacial outwash sand aquifer, Minnesota. *Water Resources Research* **38**, 1105 doi: 10.1029/2001wr000663.

Böhlke, J.K., J.W. Harvey and M.A. Voytek. 2004. Reach-scale isotope tracer experiment to quantify denitrification and related processes in a nitrate-rich stream, midcontinent United States. Limnology and Oceanography 49:821-838

Bott, T. L. 1996. Primary productivity and community respiration, p. 533-556. *In* F. R. Hauer and G. A. Lamberti [eds.], Methods in stream ecology. Academic Press.

Böttcher, J., O. Strebel, S. Voerkelius and H.L. Schmidt. 1990. Using isotope fractionation of nitrate nitrogen and nitrate oxygen for evaluation of microbial denitrification in a sandy aquifer. Journal of Hydrology 114:413–4

Buchanan, T.J., and W.P Somers. 1969, Discharge measurements at gaging stations: U.S. Geological Survey Techniques of Water-Resources Investigations, Book 3, chap A8, 65 p. (Also available at pubs.usgs.gov/twri/twri3a8/.)

Burgin, A. J. and S.K. Hamilton. 2007. Have we overemphasized the role of denitrification in aquatic ecosystems? A review of nitrate removal pathways. Frontiers in Ecology and the Environment 5, 89-96

Canfield, D. E., and M. V. Hoyer. 1988. Influence of nutrient enrichment and light availability on the abundance of aquatic macrophytes in Florida streams. Canadian Journal of Fisheries and Aquatic Sciences. 45:1467-1472.

Casciotti, K.L., D.M. Sigman, M.G. Hastings, J.K. Böhlke and A. Hilkert. 2002. Measurement of the oxygen isotopic composition of nitrate in seawater and freshwater using the denitrifier method. Analytical Chemistry 74:4905–4912

Castro, N. M., and G. M. Hornberger. 1991. Sub-surface water interactions in an alluviated mountain stream channel. Water Resources Research 27:1613-1621.

Chasar, L., Katz, B. G. & Griffin, D. 2005. Evaluation of nitrate sources in springs of the Santa Fe River basin using natural tracers: geochemical, specific microbiological, and multiple stable isotopic indicators. (Alachua County Environmental Protection Department, Gainesville, FL).

Chen, D.J.Z. and K.T.B. MacQuarrie. 2005. Correlation of $\delta^{15}N$ and $\delta^{18}O$ in NO_3^- during denitrification in groundwater. Journal of Environmental Engineering and Science 4:221-226

Chen, F., G. Jia and J. Chen. 2009. Nitrate sources and watershed denitrification inferred from dual isotopes in the Beijiang River, south China. Biogeochemistry 94:163-174

Choi, J., J.W. Harvey, and M.H. Conklin. 2000. Characterizing multiple timescales of stream and storage zone interaction that affect solute fate and transport in streams. Water Resources Research 36:1511–1518.

Cristensen, P.T., L.P. Nielsen, J. Sørensen, P. Revsbeck. 1990. Dentrification in ntrate-rich streams: Diurnal and seasonal variation related to benthic oxygen metabolism. Limnology and Oceanography 35(3):640-651.

D'Angelo, D.J., J. R. Webster, S. V. Gregory and J. L. Meyer. 1993. Transient storage in Appalachian and Cascade mountain streams as related to hydraulic characteristics. Journal of the North American Benthological Society 12: 223-235.

Davidson, E. A. and S. Seitzinger. 2006. The enigma of progress in denitrification research. Ecological Applications 16:2057-2063

Day, T.J. 1975. Longitudinal dispersion of natural streams. Water Resources Research 11:909–918.

De Brabandere, L., T.K. Frazer and J.P. Montoya. 2007. Stable nitrogen isotope ratios of macrophytes and associated periphyton along a nitrate gradient in two subtropical, spring-fed streams. Freshwater Biology doi:10.1111/j.1365-2427.2007.01788.

De Montety, V., J.B. Martin, M.J. Cohen, C. Foster and M.J. Kurz. 2011. Influence of diel biogeochemical cycles on carbonate equilibrium in a karst river. Chemical Geology doi:10.1016/j.chemgeo.2010.12.025

Deutsch, B., M. Voss and H. Fischer. 2009. Nitrogen transformation processes in the Elbe River: Distinguishing between assimilation and denitrification by means of stable isotope ratios in nitrate. Aquatic Sciences 71:228-237

Dhondt, K., P. Boeckx, O. van Cleemput and H. Hofman. 2003. Quantifying nitrate retention processes in a riparian buffer zone using the natural abundance of ^{15}N in NO_3^-. Rapid Communications in Mass Spectrometry 17:2597-2604

Dodds, W.K. 2006. Eutrophication and trophic state in rivers and streams. Limnology and Oceanography 51:671–680

Duarte, C. M., Y.T. Prairie, T.K. Frazer, M.V. Hoyer, S.K. Notestein, R. Martinez, A. Dorsett and D.E. Canfield. 2010. Rapid accretion of dissolved organic carbon in the springs of Florida: the most organic-poor natural waters. Biogeosciences 7, 4051-4057, doi:10.5194/bg-7-4051-2010

Duarte, C.M., and D.E. Canfield. 1990. Macrophyte standing crop and primary productivity in some Florida spring-runs. Water Resources Bulletin 26:927–934

Elder, J.W. 1959. The Dispersion of marked fluid in turbulent shear flow. Journal of Fluid Mechanics 5:544–560

Elser, J. J., Bracken, M. E. S., Cleland, E. E., Gruner, D. S., Harpole, W. S., Hillebrand, H., Ngai, J. T., Seabloom, E. W., Shurin, J. B., and Smith, J. E. 2007. Global analysis of nitrogen and phosphorus limitation of primary producers in freshwater, marine and terrestrial ecosystems. Ecology Letters, 10:1135-1142.

Ensign, S.H. and M.W. Doyle. 2006. Nutrient spiraling in streams and river networks. Journal of Geophysical Research 111: doi:10.1029/2005JG000114

Evans, R.D. 2001. Physiological mechanisms influencing plant nitrogen isotope composition. Trends in Plant Science 6:121–126.

Eyre, B. D., S. Rysgaard, T. Dalsgaard and P.B. Christensen. 2002. Comparison of isotope pairing and N-2 : Ar methods for measuring sediment-denitrification-assumptions, modifications, and implications. Estuaries 25, 1077-1087

[FSTF] Florida Springs Task Force. 2000. Florida's springs: Strategies for protection and restoration. Florida Department of Environmental Protection, Tallahassee, Florida. 63 pp.

Fogel M.L., and L.A. Cifuentes. 1993. Isotope fractionation during primary production. In Organic Geochemistry, Engel M, Macko S (eds). Plenum Press: New York; 73–98

Fogg, G. E., Rolston, D. E., Decker, D. L., Louie, D. T. & Grismer, M. E. 1998. Spatial variation in nitrogen isotope values beneath nitrate contamination sources. *Ground Water* **36**, 418-426.

Frazer, T. K., S. K. Notestein, and W. E. Pine. 2006. Changes in the physical, chemical and vegetative characteristics of the Homosassa, Chassahowitzka and Weeki Wachee Rivers. Southwest Florida Water Management District, Tampa, Florida, USA.

Fukada, T., K.M. Hiscock, P.F. Dennis and T. Grischek. 2003. A dual isotope approach to identify denitrification in groundwater at a river-bank infiltration site. Water Research 37:3070-3078

Galloway, J.N., F.J. Dentener, D.G. Capone, E.W. Boyer, R.W. Howarth, S.P. Seitzinger, G.P. Asner, C.C. Cleveland, P.A. Green, E.A. Holland, D.M Karl, A.F. Michaels, J.H. Porter, A.R. Townsend and C.J. Vörösmarty. 2004. Nitrogen cycles: past, present and future. Biogeochemistry 70:153-226

Gooseff, M.N., R.O. Hall Jr. and J.L. Tank. 2007. Relating transient storage to channel complexity in streams of varying land use in Jackson Hole, Wyoming. Water Resources Research 43:W01417

Gooseff, M.N., S.M. Wondzell, R. Haggerty and J. Anderson. 2003. Comparing transient storage modeling and residence time distribution (RTD) analysis in geomorphically varied reaches in the Lookout Creek basin, Oregon, USA. Advances in Water Resources 26:925–937

Granger, J, D.M. Sigman, M.F. Lehmann and P.D. Tortell. 2008. Nitrogen and oxygen isotope fractionation during dissimilatory nitrate reduction by denitrifying bacteria. Limnology and Oceanography 53:2533-2545

Granger, J., D.M. Sigman, J.A. Needoba and P.J. Harrison. 2004. Coupled nitrogen and oxygen isotope fractionation of nitrate during assimilation by cultures of marine phytoplankton. Limnology and Oceanography 49: 1763 – 1773

Granger, J., Sigman, D. M., Lehmann, M. F. & Tortell, P. D. 2008.Nitrogen and oxygen isotope fractionation during dissimilatory nitrate reduction by denitrifying bacteria. *Limnology and Oceanography* **53**, 2533-2545.

Green, C. T., L.J. Puckett, J.K. Bohlke, B.A. Bekins, S.P. Phillips, L.J. Kauffman, J.M. Denver, H.M. Johnson Limited occurrence of denitrification in four shallow aquifers in agricultural areas of the United States. 2008. Journal of Environmental Quality 37:994-1009, doi:10.2134/jeq2006.0419

Green, C. T., J. K. Bohlke, B. A. Bekins and S. P. Phillips. 2010. Mixing effects on apparent reaction rates and isotope fractionation during denitrification in a heterogeneous aquifer. Water Resources Research 46, doi:W0852510.1029/2009wr008903

Groffman P. M., M. A. Altabet, J. K. Bohlke, K. Butterbach-Bahl, M. B. David, M. K. Firestone, A. E. Giblin, T. M. Kana, L. P. Nielsen, and M. A. Voytek. 2006. Methods for measuring denitrification: Diverse approaches to a difficult problem. *Ecological Applications* 16:2091-2122.

Guillette, L. J., and T. M. Edwards. 2005. Is nitrate an ecologically relevant endocrine disruptor in vertebrates? Integrative and Comparative Biology 45:19-27.

Gulliver, J. S., J. R. Thene, and A. J. Rindels. 1990. Indexing gas transfer in self-aerated flows. *J. Environ. Engr.* 116:503-523.

Haggerty, R., S.M. Wondzell and M.J. Johnson. 2002. Power-law residence time distribution in the hyporheic zone of a 2nd-order mountain stream. Geophysical Research Letters 29:1640.

Hall R.O. Jr, B.J. Peterson and J.L. Meyer. 1998. Testing a nitrogen-cycling model of a forest stream by using a nitrogen-15 tracer addition. Ecosystems 1: 283–298

Hamilton, S.K., J.L. Tank, D.F. Raikow, W.M. Wollheim, B.J. Peterson, and J.R. Webster. 2001. Nitrogen uptake and transformation in a midwestern U.S. stream: A stable isotope enrichment study. Biogeochemistry 54:297-340

Hamme, R. C. and S. R. Emerson. 2004. The solubility of neon, nitrogen and argon in distilled water and seawater. Deep-Sea Research Part I-Oceanographic Research Papers 51: 1517-1528, doi:10.1016/j.dsr.2004.06.009

Harrington, D., Maddox, G. & Hicks, R. 2010. Florida Springs Initiative Monitoring Network Report and Recognized Sources of Nitrate. 103 (Florida Department of Environmental Protection, Tallahassee, FL).

Harvey, J.W., M.H. Conklin and R.S. Koelsch. 2003. Predicting Changes in Hydrologic Retention in an Evolving Semi-arid Alluvial Stream. Advances in Water Resources 26:939–950

Heffernan, J.B., M.J. Cohen, T.K. Frazer, R.G. Thomas, T.J. Rayfield, J. Gulley, J.B. Martin, J.J. Delfino, and W.D. Graham. 2010a. Hydrologic and biotic influences on nitrate removal in a sub-tropical spring-fed river. Limnology and Oceanography 55:249–263

Heffernan, J., D. Liebowitz, T. Frazer, J. Evans and M.J. Cohen. 2010b. Algal blooms and the nitrogen-enrichment hypothesis in Florida springs: evidence, alternatives, and adaptive management. Ecological Applications 20 816-829

Heffernan, J.B. and M.J. Cohen. 2010. Direct and indirect coupling of primary production and diel nitrate dynamics in a subtropical spring-fed river. Limnology and Oceanography 55:677-688

Hensley, R.T. 2010. Controls and dynamics of solute transport in Florida's Spring-Fed Karst Rivers. MS Thesis, University of Florida, Gainesville FL

Herrman K., V. Bouchard, and R. Moore. 2008. Factors affecting denitrification in agricultural headwater streams in Northeast Ohio, USA. *Hydrobiologia* 598:305-314.

Hoyer, M. V., T. K. Frazer, S. K. Notestein and D. E. Canfield. 2004. Vegetative characteristics of three low-lying Florida coastal rivers in relation to flow, light, salinity and nutrients. Hydrobiologica. 528:31-43.

Kadlec, R.H., and R.L. Knight. 1996 Treatment Wetlands. Lewis Publishers, Boca Raton, Florida, U.S.A.

Kana, T. M*., C.* Darkangelo, J.B. Oldham, G.E. Bennett, J.C. Cornwell*.* 1994. Membrane inlet mass-spectrometer for rapid high-precision determination of N-2, O-2, and Ar in environmental water samples. Analytical Chemistry 66 4166-4170.

Katz, B. G. 2004. Sources of nitrate contamination and age of water in large karstic springs of Florida. *Environmental Geology* **46**, 689-706.

Katz, B. G., Bohlke, J. K. & Hornsby, H. D. 2001. Timescales for nitrate contamination of spring waters, northern Florida, USA. *Chemical Geology* **179**, 167-186.

Katz, B. G., Chelette, A. R. & Pratt, T. R. 2004. Use of chemical and isotopic tracers to assess nitrate contamination and ground-water age, Woodville Karst Plain, USA. *Journal of Hydrology* **289**, 36-61, doi:10.1016/j.hydrol.2003.11.001.

Katz, B. G., Hornsby, H. D., Bohlke, J. F. & Mokray, M. F. 1999. Sources and Chronology of Nitrate Contamination in Spring Waters, Suwannee River Basin, Florida. (US Geological Survey, Reston, VA).

Katz, B.G., A. Sepulveda and R.J. Verdi. 2009. Estimating nitrogen loading to ground water and assessing vulnerability to nitrate contamination in a large karstic springs basin, Florida. Journal of the American Water Resources Association 45:607-627

Kellman, L., and C. Hillaire-Marcel. 1998. Nitrate cycling in streams: Using natural abundances of NO_3^-–$\delta_{15}N$ to measure in-situ denitrification. Biogeochemistry 43:273–92

Kendall, C. & Elliott, E. M. 2007. in *Stable Isotopes in Ecology and Environmental Science* (eds R.H. Michener & K. Lajtha) 375–449 (Wiley – Blackwell Publishing).

Kendall, C. & Grim, E. 1990. Combustion tube method for measurement of nitrogen isotope ratios using calcium-oxide for total removal of carbon dioxide and water. *Analytical Chemistry* **62**, 526-529.

Kendall, C. 1998. Tracing nitrogen sources and cycling in catchments. In: C. Kendall and J.J. McDonnell, editors. Isotope Tracers in Catchment Hydrology. Elsevier Science B.V Amsterdam, The Netherlands.

Kendall, C., E.M. Elliott and S.D. Wankel. 2007. Tracing anthropogenic inputs of nitrogen to ecosystems. In: R.H. Michener and K. Lajtha, editors: Stable Isotopes in Ecology and Environmental Science. pp. 375–449. Wiley – Blackwell Publishing, Malden, MA.

Knight, R. L. 1983. Energy Basis of Ecosystem Control at Silver Springs, Florida. In: T.D. Fontaine and S.M. Bartell, editors: Dynamics of Lotic Ecosystems. pp 161-179. Ann Arbor Science Publishers, Ann Arbor, MI

Knowles, L., Katz, B. G. & Toth, D. J. 2010. Using multiple chemical indicators to characterize and determine the age of groundwater from selected vents of the Silver Springs Group, central Florida, USA. *Hydrogeology Journal* **18**, 1825-1838, doi:10.1007/s10040-010-0669-y.

Laenen, A., and K.E. Bencala. 2001. Transient storage assessment of dye-tracer injections in rivers of the Willamete Basin, Oregon. Journal of the American Water Resources Association. 37:367-377

Laursen A.E. and S.P. Seitzinger. 2004 Diurnal patterns of denitrification, oxygen consumption and nitrous oxide production in rivers measured at the whole-reach scale. Freshwater Biology 49:1448–1458

Laursen, AE, and SB Seitzinger. 2002. Measurement of denitrification in rivers: an integrated, whole system approach. *Hydrobiologia* 485:67-81.

Lehmann, M. F., P. Reichert, S.M. Bernasconi, A.Barbieri, and J. A. McKenzie. 2003. Modeling nitrogen and oxygen isotope fractionation during denitrification in a lacustrine redox transition zone. Geochimica et Cosmochimica Acta 67:2529–2542

Lightbody A.F., and H.M. Nepf. 2006. Prediction of velocity profiles and longitudinal dispersion in emergent salt marsh vegetation. Limnology and Oceanography 51:218–228

Lowrance R, R. Todd. J. Fail Jr., O. Hendrickson Jr. and R. Leonard. 1984. Riparian forests as nutrient filters in agricultural watersheds. BioScience 34:374–7.

Manning, R. 1890. On the flow of water in open channels and pipes. Transactions of the Institute of Civil Engineers of Ireland 20:161–207

Manning, R. 1895. Supplement to on the flow of water in open channels and pipes. Transactions of the Institute of Civil Engineers of Ireland 24:179–207

Mariotti A., A. Landreau, and B. Simon. 1988. ^{15}N isotope biogeochemistry and natural denitrification process in groundwater: application to the chalk aquifer of northern France. Geochimica et Cosmochimica Acta 52:1869–78

Mariotti, A. 1986. Denitrification in groundwaters, principles and methods for its identification – a review. *Journal of Hydrology* **88**, 1-23.

Mariotti, A., J.C. Germon, P. Hubert, P. Kaiser, R. Letolle, A. Tardieux and P. Tardieux. 1981. Experimental determination of nitrogen kinetic isotope fractionation: Some principles; illustration for the denitrification and nitrification processes. Plant and Soil 62:413-430

Martin, J. B. and Dean, R. W. 2001. Exchange of water between conduits and matrix in the Floridan aquifer. Chemical Geology 179:145-165.

Martin, J.B. and S.L. Gordon. 2000. Surface and ground water mixing, flow paths, and temporal variations in chemical compositions of karst springs. In: Sasowsky, I.D., and C. Wicks, editors: Groundwater Flow and Contaminant Transport in Carbonate Aquifers. pp. 65-92. A.A. Balkema, Rotterdam

Mattson, R. A., E. F. Lowe, C. L. Lippincott, J. Di, and L. Battoe. 2006. Wekiva River and Rock Springs Run Pollutant Load Reduction Goals. Florida Department of Environmental Protection, Tallahassee. 69 pp.

McCallum, J. E., Ryan, M. C., Mayer, B. & Rodvang, S. J. 2008. Mixing-induced groundwater denitrification beneath a manured field in southern Alberta, Canada. *Applied Geochemistry* **23**, 2146-2155, doi:10.1016/j.apgeochem.2008.03.018.

McClain, M.E., E.W. Boyer, C.L. Dent, S.E. Gergel, N.B. Grimm, P.M. Groffman, S.C. Hart, J.W. Harvey, C. A Johnston, E. Mayorga, W.H. McDowell and G. Pinay. 2000. Biogeochemical hot spots and hot moments at the interface of terrestrial and aquatic ecosystems. Ecosystems 6:301-312

McCutchan, JH, JF Saunders, AL Pribyl, and WM Lewis. 2003. Open channel estimation of denitrification. *Limnology and Oceanography: Methods* 1:74-81.

Miyajima, T., C. Yoshimizu, Y. Tsuboi, Y. Tanaka, I. Tayasu, T. Nagata and I. Koike. 2009. Longitudinal distribution of nitrate $\delta^{15}N$ and $\delta^{18}O$ in two contrasting tropical rivers: implications for instream nitrogen cycling. Biogeochemistry 95:243-260

Montoya, J.P. and J.J. McCarthy. 1995. Isotopic fractionation during nitrate uptake by phytoplankton grown in continuous culture. Journal of Plankton Research 17:439-464

Mulholland P.J., J.L. Tank, D.M. Sanzone, W.M. Wollheim, B.J. Peterson, J.R. Webster and J.L. Meyer. 2000. Nitrogen cycling in a forest stream determined by a 15N tracer addition. Ecological Monographs 70: 471–493

Mulholland P.J., S.A. Thomas, H.M. Valett, J.R. Webster, and J. Beaulieu. 2006. Effects of light on NO_3 uptake in small forested streams: diurnal and day-to-day variations. Journal of the North American Benthological Society 25:583–595

Mulholland. P.J., A. M. Helton, G. C. Poole, R.O. Hall, S. K. Hamilton, B. J. Peterson, J.L. Tank, L. R. Ashkenas, L. W. Cooper, C. N. Dahm et. al. 2008. Stream denitrification across biomes and its response to anthropogenic nitrate loading. Nature 452:202-205

Nepf, H.M. 1999. Drag, turbulence, and diffusion in flow through emergent vegetation. Water Resources Research 35:479-489

Nepf, H.M., C.G. Mugnier and R.A. Zavistoski. 1997. The Effects of Vegetation on longitudinal dispersion. Estuarine, Coastal and Shelf Science 44:675–684

Newbold, J.D., R.V. O'Neill, J.W. Elwood and W. Van Winkle. 1982. Nutrient spiraling in streams: implications for nutrient limitations and invertebrate activity. The American Naturalist 120:628–652

Odum, H.T. 1956. Primary production in flowing waters. Limnology and Oceanography 1:102-117

Odum, H.T. 1957a. Trophic structure and productivity of Silver Springs, Florida. Ecological Monographs 27:55–112

Odum, H.T. 1957b. Primary production measurements in eleven Florida springs and a marine turtle-grass community. Limnology and Oceanography 2:85–97

Panno, S. V., Hackley, K. C., Kelly, W. R. & Hwang, H. H. 2006. Isotopic evidence of nitrate sources and denitrification in the Mississippi River, Illinois. *Journal of Environmental Quality* **35**, 495-504, doi:10.2134/jeq2005.0012.

Pellerin, B.A., B.D. Downing, C. Kendall, R.A. Dahlgren, T.E.C. Krauss, J.F. Saraceno, R.G.M. Spencer and B.A. Bergamaschi. 2009. Assessing the sources and magnitude of diurnal nitrate variability in the San Joaquin River (California) with an *in situ* optical nitrate sensor and dual nitrate isotopes. Freshwater Biology 54:376-387

Peterson, B. J., W.M. Wollheim, P.J. Mulholland, J.R. Webster, J.L. Meyer, J.L. Tank, E. Martí, W.B. Bowden, H.M. Valett, A.E. Hershey, W.B. McDowell, W.K. Dodds, S.K. Hamilton, S. Gregory, and D.D. Morrall. 2001. Control of nitrogen export from watersheds by headwater streams. Science 292:86–90

Phelps, G. G. 2004. Chemistry of ground water in the Silver Springs basin, Florida, with an emphasis on nitrate. 54 p. (U.S. Geological Survey, Reston, VA).

Phelps, G. G., Walsh, S. J., Gerwig, R. M. & Tate, W. B. 2006. Characterization of the Hydrology,Water Chemistry, and Aquatic Communities of Selected Springs in the St. Johns River Water Management District, Florida, 2004. 51 pp. (US Geological Survey, Reston, VA).

Pittman, J. R., H. H. Hatzell and E. T. Oaksford. 1997. Spring contributions to water quality and nitrate loads in the Suwannee River during Baseflow in July 1995. Water Resources Investigation Report 97-4152 (U. S. Geological Survey, Reston, VA).

Quinlan E.L., E.J. Phlips, K.A. Donnelly, C.H. Jett, P. Sleszynski, and S. Keller. 2008. Primary producers and nutrient loading in Silver Springs, FL, USA. Aquatic Botany 88:247-255.

Ruehl, C.R., A.T. Fisher, M. Los Huertos, S.D. Wankel, C.G. Wheat, C. Kendall, C.E. Hatch and C. Shennan. 2007. Nitrate dynamics within the Pajaro River, a nutrient-rich losing stream. Journal of the North American Benthological Society 26:191-206

Runkel, R.L. 1998. One-dimensional transport with inflow and storage (OTIS): a solute transport model for streams and rivers. USGS Water-Resources Investigations Report 98–4018. U.S. Geological Survey, Denver

Runkel, R.L. 2007. Toward a transport-based analysis of nutrient spiraling and uptake in streams. Limnology and Oceanography 5:50–62

Rysgaard, S., N. Risgaard-Peterson, N.P. Sloth, K. Jensen, L.P. Nielsen. 1994. Oxygen regulation of nitrification and denitrification in sediments. Limnology and Oceanography 39(7):1643-1652.

Sabatini, D.A. and T.A. Austin 1991. Characteristics of rhodamine WT and fluorescein as adsorbing ground-water tracers. Ground Water 29:341–349

Schwientek, M. F. Einsiedl, W. Stichler, A. Stoegbauer, H. Strauss, P. Maloszewski. 2008. Evidence for denitrification regulated by pyrite oxidation in a heterogeneous porous groundwater system. Chemical Geology 255, 60-67, doi:10.1016/j.chemgeo.2008.06.005.

Scott T.M., Means G.H., Meegan R.P., Means R.C., Upchurch S.B., Copeland R.E., Jones J., Roberts T. and A. Willet. 2004. Springs of Florida. Bulletin No. 66, Florida Geological Survey, Tallahassee

Sebilo, M. G. Billen, M. Grably and A. Mariotti. 2003. Isotopic composition of nitrate-nitrogen as a marker of riparian and benthic denitrification at the scale of the whole seine river system. Biogeochemistry 63:35-51

Sebilo, M., G. Billen, B. Mayer, D. Billou, M. Gably, J. Garnier and A. Mariotti. 2006. Assessing nitrification and denitrification in the Seine river and estuary using chemical and isotopic techniques. Ecosystems 9:564-577

Seitzinger S.P., R.V. Styles, B. Boyer, R. Alexander, G. Billen, R. Howarth, B. Mayer and N. van Breeman. 2002. Nitrogen retention in rivers: model development and application to watersheds in the Eastern US. Biogeochemistry 57: 199-237

Seitzinger, S., J.A. Harrison, J.K. Bohlke, J. K.), A.F. Bouwman, R. Lowrance, B. Peterson, B.), C. Tobias, G. Van Drecht, G. 2006. Denitrification across landscapes and waterscapes: A synthesis. Ecological Applications 16: 2064-2090.

Seitzinger, S.P., J.A. Harrison, E. Dumont, A.H. Beusen and A.F. Bouwman. 2005. Sources and delivery of carbon, nitrogen, and phosphorus to the coastal zone: An overview of global nutrient export from 4 watersheds (NEWS) models and their application. Global Biogeochemical Cycles 19:GB4S01.

Sickman, J. O., A. Albertin, M. W. Anderson, A. Pinowska, and R. J. Stevenson. 2009. A Comparison of Internal and External Supply of Nutrients to Algal Mats in Two First Magnitude Springs in Florida. Journal of Aquatic Plant Management 47: 135-144

Sigman D.M., K.L. Casciotti, M. Andreani, C. Barford, M. Galanter, and J.K. Böhlke. 2001. A bacterial method for the nitrogen isotopic analysis of nitrate in seawater and freshwater. Analytical Chemistry 73:4145–53

Simal, J., M. A. Lage, and I. Iglesias. 1985. 2nd derivative ultraviolet spectroscopy and sulfamic acid method for determination of nitrates in water. Journal of the Association of Official Analytical Chemists 68: 962-964

Smart, P.L. and I.M.S. Laidlaw. 1977. An evaluation of some fluorescent dyes for water tracing. Water Resources Research 13:15–33

Smith, V.H. 2006. Responses of estuarine and coastal marine phytoplankton to nitrogen and phosphorus enrichment. Limnology and Oceanography 51:377–384

Solorzano, L. 1969. Determination of ammonia in natural waters by phenolhypochlorite method. Limnology and Oceanography 14: 799.

Søvik, A.K. and P.T. Mørkved. 2008. Use of stable nitrogen isotope fractionation to estimate denitrification in small constructed wetlands treating agricultural runoff. Science of the Total Environment 392:157-165

Stevenson R.J., A. Pinowska, A. Albertin and J.O. Sickman. 2007. Ecological condition of algae and nutrients in Florida springs: The Synthesis Report. Florida Department of Environmental Protection, Tallahassee, Florida.

Stevenson, R., A. Pinowska, and Y. Wang. 2004. Ecological Condition of Algae and Nutrients in Florida Springs. Florida Department of Environmental Protection, Tallahassee.

Stream Solute Workshop (S.S.W.). 1990. Concepts and methods for assessing solute dynamics in stream ecosystems. Journal of the North American Benthological Society 9:95–119

Tank, J.L., E.J. Rosi-Marshall, M.A. Baker, and R.O. Hall, Jr. 2008. Are rivers just big streams? A pulse method to quantify nitrogen demand in a large river. Ecology 89:2935-2945

Taylor, P. G. and Townsend, A. R. 2010. Stoichiometric control of organic carbon-nitrate relationships from soils to the sea. Nature 464: 1178-1181, doi:10.1038/nature08985

Torrento, C., Cama, J., Urmeneta, J., Otero, N. and A. Soler. 2010. Denitrification of groundwater with pyrite and *Thiobacillus denitrificans*. Chemical Geology 278:80-91, doi:10.1016/j.chemgeo.2010.09.003.

Toth, D. J. and B.G. Katz. 2006. Mixing of shallow and deep groundwater as indicated by the chemistry and age of karstic springs. Hydrogeology Journal 14, 827-847, doi:10.1007/s10040-005-0478-x

Townsend, A.R., R.W. Howarth, F.A. Bazzaz, M.S. Booth, C.C. Clevelent, S.K. Collinge, A.P. Dobson, P.R. Epsteitn, E.A. Holland, D.R. Ekkeney, M.A. Mallin, C.A. Rogers, P. Wayne and A.H. Wolfe. 2003. Human health effects of a changing global nitrogen cycle. Frontiers in Ecology and the Environment 1: 240–246

Ulrich, W.R., J. Lazarovà, C.I. Ulrich, F.G. Witt, and P.J. Aparicio. 1998. Nitrate uptake and extracellular alkalinization by the green alga Hydrodictyon reticulatum in blue and red light. Journal of Experimental Botany 49(324):1157-1162.

US Geological Survey. 2003. Nutrients in the upper Mississippi River: Scientific information to support management decisions. Fact Sheet 105-03. 6p.

Van Breeman, N., E.W. Boyer, C.L. Goodale, N.A. Jaworski, K. Paustian,. S.P. Seitzinger, K. Lajtha, B. Mayer, D. Van Dam, R.W. Howarth, K.J. Nadelhoffer, M. Eve and G. Billen. 2002. Where did all the nitrogen go? Fate of nitrogen inputs to large watersheds in the Northeastern U.S.A. Biogeochemistry 57:267-293

Wankel, S.D., C. Kendall, J.T. Pennington, F.P. Chavez and A. Paytan. 2007. Nitrification in the euphotic zone as evidenced by nitrate dual isotopic composition: Observation from Monterey Bay, California. Global Biogeochemical Cycles 21: GB2009, doi:10.1029/2006GB002723

Warwick J.J. 1986. Diel variation of in stream nitrification. Water Research 20:1325–1332.

[WSI] Wetland Solutions, Inc. 2008. Pollutant Load Reduction Goal analysis for the Wekiva River and Rock Springs Run, Florida. Special Publication SJ2008-SP5, St. Johns River Water Management District, Palatka, FL. 101 pp.

[WSI] Wetland Solutions, Inc. 2011. Ichetucknee Springs: Recreational Impairments? Presentation accessed at: waterinstitute.ufl.edu/research/projects/downloads/Ichetucknee/pres-BKnight-Ichetucknee-feb10-mtg.pdf

Wollheim, W. M., C. J. Voosmarty, B. J. Peterson, S. P. Seitzinger, and C. S. Hopkinson. 2006. Relationship between river size and nutrient removal. Geophysical Research Letters 33.

Wood, E.D., F.A.J. Armstrong and F.A. Richards. 1967. Determination of nitrate in sea water by cadmium–copper reduction to nitrite. *J. Marine Biol. Assoc. UK* **47**, 31-43.